REPORT DOCUMENTATION PAGE

Form Approved OMB No. 0704-0188

1. AGENCY USE ONLY (Leave blank)	2. REPORT DATE	3. REPORT TYPE AND DATES COVERED
	31-January -2000	Final Report

4. TITLE AND SUBTITLE

Simulation of Energetic Materials Combustion

5. FUNDING NUMBERS

F61775-99-WE002

6. AUTHOR(S)

Professor Vladimir Zarko

7. PERFORMING ORGANIZATION NAME(S) AND ADDRESS(ES)

Institute of Chemical Kinetics and Combustion
3 Institutskaya St
Novosibirsk 630090
Russia

8. PERFORMING ORGANIZATION REPORT NUMBER

N/A

9. SPONSORING/MONITORING AGENCY NAME(S) AND ADDRESS(ES)

EOARD
PSC 802 BOX 14
FPO 09499-0200

10. SPONSORING/MONITORING AGENCY REPORT NUMBER

SPC 99-4002

11. SUPPLEMENTARY NOTES

12a. DISTRIBUTION/AVAILABILITY STATEMENT

Approved for public release; distribution is unlimited.

12b. DISTRIBUTION CODE

A

13. ABSTRACT (Maximum 200 words)

This report results from a contract tasking Institute of Chemical Kinetics and Combustion as follows: The contractor will investigate mathematical modeling of self-sustaining and transient combustion of energetic materials (e.g. solid propellants, explosives, pyrotechnics). He will perform a critical survey of original materials of authors and papers published in open literature. He will present various approaches for combustion models; and investigate the problems of intrinsic stability of energetic materials combustion in unconfined volume.

14. SUBJECT TERMS

EOARD, Combustion, Energetic Materials, Propellants

15. NUMBER OF PAGES

16. PRICE CODE

N/A

17. SECURITY CLASSIFICATION OF REPORT	18. SECURITY CLASSIFICATION OF THIS PAGE	19, SECURITY CLASSIFICATION OF ABSTRACT	20. LIMITATION OF ABSTRACT
UNCLASSIFIED	UNCLASSIFIED	UNCLASSIFIED	UL

NSN 7540-01-280-5500

Standard Form 298 (Rev. 2-89)
Prescribed by ANSI Std. 239-18
298-102

SIMULATION OF ENERGETIC MATERIALS COMBUSTION

by V.E. Zarko and L.K. Gusachenko
Institute of Chemical Kinetics and Combustion, 630090 Novosibirsk, Russia

CHAPTER 1.

COMBUSTION OF HOMOGENEOUS ENERGETIC MATERIALS

1.1. GENERAL BACKGROUND

Combustion of solid energetic materials (EM) is characterized by simultaneous course of set of processes, connected with intense warm-up of substance and its gasification in a relatively narrow spatial domain. These are various phase transitions, chemical reactions in the condensed and gas phases, the dispersion of the condensed phase and the reactions in the dispersed phase, the processes of mass- and heat transfer, etc. Heat, which evolves in chemical reactions, serves as driving force for combustion of solid EM, and velocity of the combustion wave propagation is determined in essence by kinetics of chemical reactions and heat emissions from combustion zone as it was for the first time shown in works of Ya. B. Zeldovich and D. A. Franck-Kamenetskii [1, 2].

From mathematical point of view a process of propagation of combustion wave is described by the system of equations of heat- and mass transfer with sources of heat and mater. The characteristic feature of the problem is strong nonlinearity of sources. The presence of the terms, which exponentially depend on the temperature, determines specific behavior of the burning EM.

Let us mention briefly several issues related to the existence of self-sustaining combustion waves. Quantitative criteria of realization of the combustion process can be represented on the basis of physical considerations and approximate estimates in the form [3, 4].

$$\beta = RT_* / E << 1, \quad \gamma = \beta c T_* / Q << 1 \tag{1.1}$$

Here T – characteristic temperature of a process; R - universal gas constant; E and Q - energy of activation and the thermal effect of reaction, respectively; c - specific heat.

The physical meaning of inequality (1.1) is the following: the energy of activation of the combustion reaction must be considerably higher than the energy of the thermal agitation of the molecules at a characteristic temperature of process, and the magnitude of exothermic thermal effect must considerably exceed certain scale quantity of heat. It will be shown below that criteria (1.1) give the upper estimation of the necessary conditions for existence of the combustion wave. It is important to note that these criteria do not include direct information about reactions therefore chemical nature of the reactions of combustion can be most different. Actually, together with the classical cases of oxidative exothermal reactions the processes are known of combustion, caused by the reactions of thermal decomposition (combustion of explosives), direct synthesis (combustion of hydrogen with chlorine, bromine), etc.

Let us consider equation of thermal conductivity for the case of one-dimensional propagation of stationary wave of combustion in infinite space of homogeneous medium:

$$\lambda d^2T / dx^2 - mcdT / dx + \Phi(T) = 0 \tag{1.2}$$

Here x - coordinate; λ - thermal conductivity; $\Phi(T)$ - source function of heat release; m - mass burning rate.

Equation (1.2) is written in moving coordinate system attached to the flame front. Natural boundary conditions consist in the fact that on one of end points we will assume the reaction be completed, and on other - not started yet.

$$x \to -\infty, \quad T \to T_0; \quad x \to +\infty, \quad T \to T_m = T_0 + Q/c. \tag{1.3}$$

The value of mass burning rate m plays a role of eigenvalue of the problem (1.2), (1.3). In order to ensure existence of solution of the energy equation (1.2) it must be implemented additionally $\Phi(T_m)=0$ and $\Phi(T_0)=0$. Condition $\Phi(T_m)=0$ is provided by the complete consumption of parent substance. However, condition $\Phi(T_0)=0$ for ordinary initial temperatures T_0 is not satisfied, since from chemical kinetics it follows that $\Phi(T_0) \sim \exp(-E/RT_0) \neq 0$ with $T_0>0$. From the analysis carried out in works [5, 6], it follows that for the uniqueness of the solution of the problem one additional limitation should be superimposed to the source function, namely: $d\Phi(T_0)/dx \leq 0$.

The existence criterion for steady-state solution of the problem (1.2) in the form $\Phi(T_0)= 0$ looks not justified in real conditions ($T_0> 0$). However, due to large energy of activation for the most chemical reactions the values of $\Phi(T)$ and $d\Phi(T)/dT$ are close to zero at $T \to T_0$. Therefore the function $\Phi(T)$ can be artificially modified in the vicinity of T_0, so that condition $\Phi(T) = 0$ is fulfilled. Actually, it is made by equating function $\Phi(T)$ to zero in certain range of the temperature close to T_0:

$$\Phi(T) \equiv 0; \text{ at } T_0 \leq T \leq T_1$$
$$\Phi(T) > 0; \text{ at } T_1 < T < T_m$$

Direct numerical calculation of the dependence of mass burning rate m on T_1 with variation of the latter in the range ($T_0 \div T_m$) has been conducted by A.G.Merzhanov et al. [7]. It turned out that the value of m relatively weakly depends on the choice of T_1 value (if it does not become too close to T_m) provided that the following relationship between parameters γ and β is met:

$$\Gamma = \gamma - \beta = cRT_0T_m/QE < 1 \tag{1.4}$$

The new parameter Γ characterizes the ratio of the reaction rates at the temperatures T_m and T_0: $\Phi(T_m)/\Phi(T_0) = \exp(1/\Gamma)$. When parameter Γ exceeds numerically 0.1, the steady-state combustion wave can not exist. Critical value $\Gamma= 0.1$ corresponds to the value $\Phi(T_m)/\Phi(T_0) \cong 10^4$.

Inequality (1.4) shows the requirements for the heat release source, which should be met in order to provide steady-state combustion. Namely, the activation energy of exothermic reaction has to be much higher the energy of thermal motion of molecules at initial temperature ($E>>RT_0$), and thermal effect of the reaction should be comparable in value with the enthalpy of system at initial temperature ($Q \sim cT_0$, or $Q > cT_0$).

1.2. STAGE COMBUSTION CONCEPT

The aim of the combustion simulation is to calculate the value of the burning rate and its dependencies on variation of external conditions (pressure, temperature, mass forces, etc.). The great variety and complexity of the processes in the combustion wave lead to the necessity of developing the approximate combustion models.

As is already mentioned, the velocity of the combustion wave propagation is closely related with chemical kinetics. Impossibility of the detailed description of chemical and physical phenomena in the combustion wave of real condensed system leads to the approach based on isolation of

particular stages in the combustion wave. Thus, individual (complex) chemical kinetics of the propellant is replaced by the proper dependencies of the heat release rate in the global chemical reactions on concentration and temperature.

Isolation and mathematical description of chemical transformation stages can be easily correlated with the physical sequence of the mater transformations in the combustion wave. One of the natural ways for the stages isolation is their division by the phase states. As a rule, it is assumed that we have one global reaction in the condensed phase and one or two reactions in the gas phase. Upon one-dimensional analysis of the problem these reactions (stages) may proceed in entirely different spatial zones or can be partly overlapped. For example, one may expect that in combustion of energetic materials with well pronounced dispersion of subsurface layer, the reactions in the condensed phase (aerosol particles) and in gaseous flame are spatially overlapped.

In some limiting case it becomes possible to determine so called "rate control" stage in the combustion wave. By definition, the rate control stage determines the burning rate of the system in such a way that its mathematical description provides close to realistic values calculation of the magnitude of the burning rate as well as its dependencies on external conditions without taking into account the variety of the processes outside this stage. Mathematical models of the rate control stage are called (in Russian literature) elementary combustion models (ECM). Their brief analysis and classification are given in Ref. [8].

1.2.1. Interaction of the stages.

Change in ambient conditions for combustion (pressure, temperature, mass forces) can lead to redistribution of the functions of separate stages. The rate control stage can become subordinate, and vice versa.

In this case the dependence of burning rate on environmental factors can be changed, and the propagation of the combustion wave will be described by other EMC. The reason for the change of the rate control stage is different sensitivity of the reaction rates in different stages to variations in the ambient conditions. The works [9-12] and individual chapters [13,14] are devoted to investigation of regimes of reacting in different stages. The attention is concentrated in the analysis of the simplest cases and classification of basic laws governing the phenomenon. Let us examine their basic idea briefly.

Let the combustion wave propagates in homogeneous (gas or condensed) medium with two consecutive reactions $A \rightarrow B \rightarrow C$. The thermal effects of consecutive reactions are designated as Q_1 ($A \rightarrow B$) and Q_2 ($B \rightarrow C$).

Let us assume for certainty $Q_1 > 0$. There is no special requirement for sign of Q_1 but it is necessary that the sum of Q_1 and Q_2 would be positive and higher then the certain limiting value. Then the combustion temperature equals $T_m = T_0 + (Q_1 + Q_2)/c$, and the temperature, which corresponds to the course only of the first reaction, is $T_{10} = T_0 + Q_1/c$. There are also introduced $u_1(T_{10})$ - rate of the propagation of the wave of only first reaction with its thermal effect; $u_1(T_m)$ - rate, which corresponds to the case when the second reaction proceeds very rapidly, so that the combustion temperature already at the end of the first stage is established; $u_2(T_m)$ - rate, which

corresponds to the course of the second reaction at a combustion temperature (first reaction is very fast).

As a result of analytical examination and numerical solution of the problem the authors of cited works established existence of three stage combustion regimes:

2nd stage rate control,
stage detachment, and
stage merging.

In all cases the corresponding mass flow rates of the first and second stages must be identical and equal to the mass burning rate m. It is convenient to examine the propagation of the combustion wave through the immobile substance. Let us examine case of $Q_1>0$. If in this case $u_1(T_{10})>u_2(T_m)$, the wave of the first stage goes away forward, the second stage virtually does not influence the first, which in this case can be named rate control. This regime is named the regime of detachment.

If $u_2(T_m)>u_1(T_{10})$, the wave of second high-temperature stage will overtake wave of the first stage. In this case in the first stage wave the temperature will increase, and the burning rate will increase too, until with certain finite distance between the zones of the first and second reactions the condition $u_1(T_1) = u_2(T_m)$ is not satisfied. With an accidental increase in the inter-zone distance the first zone is cooled (obtaining less heat feedback from the second) and it is braked, approaching thus the second zone, and vice virsa, so that the process is stable. The temperature at the end of the first zone T_1 no longer is equal to T_{10} and cannot be found from the thermodynamic calculations. This combustion behavior is named the 2nd stage rate control mode. That means that the second stage rules the rate of the first, and $u = u_2(T_m)$.

If equality $u_1(T) = u_2(T_m)$ is not fulfilled up to achievement in the first zone of temperature T_m then the burning rate is limited by the first stage and $u= u_1(T_m) < u_2(T_m)$. This regime is named the stage merging.

Domains of realization of different stage combustion regimes (for the case of $Q_1>0$) can be defined, when taking into account the fact that always $u_2(T_m) > u_2(T_{10})$, in the form:

$$\begin{aligned} &u = u_2(T_m); && u_1(T_m) > u_2(T_m) > u_1(T_{10}) - 2^{nd} \text{ stage rate control} \\ &u = u_1(T_{10}); && u_1(T_m) > u_1(T_{10}) > u_2(T_m) - \text{stage detachment} \\ &u = u_1(T_m); && u_2(T_m) > u_1(T_m) > u_1(T_{10}) - \text{stage merging} \end{aligned} \qquad (1.5)$$

In the case, when parameters of separate stages are such that one of given inequalities is fulfilled, the burning rate of two-stage combustion is close to that, which in this inequality occupies a mid-position.

If the first reaction is endothermic, $Q_1<0$, the following inequalities can be met:

$$u_1(T_m)>u_2(T_m) \quad \text{or} \quad u_2(T_m)>u_1(T_m) \qquad (1.6)$$

In this case true burning rate is close to the single-stage rate, which has minimal value, i.e., conditions are realized for the regimes either of 2nd stage rate control or stage merging.

For the first time one of the possible regimes of stage combustion of condensed systems was theoretically examined by Ya. B. Zel'dovich. This is widely known gas-phase combustion model [15] based on the combustion mechanism of the volatile (secondary) explosives developed by A. F. Belyayev [16]. In [15], the combustion model of volatile explosives has been applied to the combustion of double base propellants.

The hypothetical mechanism of the combustion of double base propellants [15] differs from that for volatile explosives only in terms of the fact that the gasification of the condensed phase occurs as a result of the irreversible endothermic (or weakly-exothermic) chemical reaction. The rich in energy gaseous decomposition products of condensed phase react further in the gas phase releasing basic amount of heat. The part of the heat separated in the gas phase is expended on the gasification of condensed phase and its warm-up from the initial temperature T_0 to the temperature of surface T_1. In this case the distance between the zone of heat evolution in the gaseous phase and the surface of condensed phase is such that the heat flux to the surface of propellant provides the mass flow rate of gasification, exactly equal to the mass flow rate in the gas phase. According to the introduced terminology this combustion is in the 2nd stage rate control mode.

Formula for the mass burning rate is similar to expression for wave propagation velocity of combustion in gas:

$$m^2 = 2n!(cRT_m/QE)^{n+1}(\lambda\rho/c)k_0\, exp(-E/RT_m) \qquad (1.7)$$

Here n - order of reaction; λ, c, ρ - thermal conductivity, specific heat and gas density of gas respectively; k_0 and E - pre-exponent and activation energy; Q - thermal effect of gas-phase reaction; $T_m = T_0' + Q/c$ - maximum combustion temperature; $T_0' = T_0 + Q_1/c_1$ - equivalent initial temperature; T_0 - initial temperature; Q_1 - thermal effect of gasification of condensed phase.

Dependence of the burning rate on pressure p and initial temperature T_0 is characterized by coefficients

$$\nu = d\ln m/d\ln p = n/2, \quad \beta = d\ln m/dT_0 = E/2RT_m^2 .$$

Three-stage model of combustion (one chemical stage occurs in the condensed phase and two - in gas) is proposed by V. N. Vilyunov [17]. The approach presented in his work can be easily applied to an arbitrary number of successive stages; therefore without loss of generality one may examine the simpler case when the reactions proceed in two stages: the first stage in the condensed phase (x<0) and the second - in the gas phase (x>0).

Stationary process of combustion wave propagation is described by the system of equations of mass and energy conservation.

$-\infty<x<0$ (first stage, index 1):

$$\lambda_1 d^2T/dx^2 - c_1 m_1 dT/dx = Q_1 m da_1/dx = -\Phi_1(a_1,T)\cdot Q_1; \qquad (1.8)$$

$$x = -\infty,\ T = T_0,\ a_1 = 1;\ x = 0,\ T = T_s,\ a_1 = 0; \qquad (1.9)$$

$0 < x < \infty$ (second stage, index 2):

$$\lambda_2 d^2T/dx^2 - c_2 m\, dT/dx = Q_2 m da_2/dx - \rho D d^2a_2/dx^2) = -Q_2\Phi_2; \qquad (1.10)$$

boundary conditions

$$x = 0,\ T = T_s,\ \lambda_2 dT/dx = c_1 m(T_s - T_{s1}),\ a_2 = 1, \qquad da_2/dx = -(c_1 m/\lambda_2)(T_s - T_{s1})/(T_1 - T_s);$$

$$x \to \infty,\ T \to T_2,\ a_2 \to 0.$$

Here T_0 - initial temperature; $T_{s1} = T_0+Q_1/c_1$ – the temperature of the condensed phase surface, which corresponds to the course only of first reaction; Q - thermal effect; c, λ - specific heat and thermal conductivity; a - concentration; ρ - density; D - diffusion coefficient.

It is assumed for the condensed phase ρ_1 = const, $D_1 = 0$ and for the gas-phase reaction $Q_2 > 0$. There are no limitations to the sign of the thermal effect of reaction in the condensed phase. It is also proposed that the reaction rate in the condensed phase Φ_1 does not depend on pressure. The temperature of surface T_s in the boundary condition at $x = 0$ has to be determined. Boundary condition for the heat flux at $x = 0$ is obtained on the basis of the following computations. Integrating equations for a_1 and a_2 from $x = -\infty$ to $x = \infty$, one obtains the relationship

$$\int_{-\infty}^{\infty} \Phi_1(a_1,T)dx = \int_{-\infty}^{\infty} \Phi_2(a_2,T)dx = m$$

Integrating further the first of the equations (1.10), we obtain

$$\lambda_2\left(\frac{dT}{dx}\right)_{x=0} = q_1 = Q_2\int_0^{\infty}\Phi_2(a_2,T)dx - c_2m(T_2-T_s) \cong Q_2\int_{-\infty}^{\infty}\Phi_2(a_2,T)dx - c_2m(T_2-T_s)$$

Taking into account preceding relationship and expression for T_{s1}, it can be written expression for q_1 in the form

$$q_1 = m(c_2T_s-c_1T_{s1}) \cong mc(T_s-T_{s1}) \qquad \text{at } c_1 \cong c_2 = c.$$

Boundary condition for da_2/dx is written in approximation of the similarity of the fields of temperatures and concentrations.

Approximations for the chemical reaction rates in the condensed and gas phases take form

$$m_1^2 = 2\rho_1\kappa_1(2T_s - T_{s1} - T_0)^{-1}(RT_s^2/E_1)k_{01}\exp(-E_1/RT_s), \tag{1.11}$$

$$m_2^2 = (2n!\, z\lambda_2/c)(RT_2^2/E_2)^{n+1}(T_2 - T_{s1})^{-1}(T_2 - T_s)^{-n}\exp(-E_2/RT_2) \tag{1.12}$$

Here $z = k_{02}\mu(p/RT_2)^n$; μ - molar mass; p - pressure; R - universal gas constant; n - order of reaction; E and k_0 - activation energy and pre-exponent in Arrhenius's law for the reaction rate; $\kappa_1 = \lambda_1/c\rho_1$.

In expressions for m_1 and m_2 the unknown value is T_s but since during stationary combustion $m_1 = m_2 = m$, relationships (1.11) and (1.12) can he considered as the system for two unknowns, m and T_s. Thus, for example, during the combustion in the regime of stage detachment the burning rate is determined by the reactions in the condensed phase (which is the rate control stage) and is calculated on the basis of (1.11) when $T_s = T_{s1}$ ($Q_1>0$).

1.2.2. Determination of the rate control stage.

Analysis of numerical solution of the problem on the stage flame propagation in homogeneous gaseous medium showed [10] that change of combustion behavior occurs in relatively narrow range of parameters variation. The conclusion is made that for such conditions it is possible to establish the control stage. The procedure to choose the control stage is described above: actual burning rate is close in the value to the value of the rate, calculated according to the relationships for the separate stage and occupying the intermediate position between the minimum and maximum burning rate values.

Upon transfer to modeling the processes of condensed systems combustion question of the choice of the control stage becomes more complex and less clear than in the case of combustion of gases. The specific difficulties appear, connected with the correct description of the chemical transformations simultaneously elapsing in the combustion wave and change in the physical state of the substance: solid - gas-saturated subsurface layer - gas phase

According to available data, in combustion of double base and composite propellants chemical reactions start in the condensed phase and are continued in dispersed particles of solid propellant. Furthermore, chemical reactions occur in the gas bubbles within the surface layer of the condensed phase and then in the flame. With a variation in the ambient conditions for combustion the relative role of reactions in one or the other spatial zones can be changed. For example, it is possible situation when the completeness of chemical transformations of gaseous decomposition products of solid propellant increases with pressure within the limits of condensed phase. In this case one has to assign heat evolution from these reactions not to the adjacent gas zone, but to the gas-saturated surface layer of solid propellant.

In existing analytical models of solid propellant combustion chemical stage nature, as a rule, is unambiguously linked with physical stage nature of transformation of substance in the combustion wave. Unfortunately, these data are hardly available and restricted in volume. There are no reliable experimental proofs of existence at the elevated pressures of developed foamy zone on the surface of solid propellant or of the intense dispersion of the surface layers of condensed phase in the literature. It is necessary also to pay attention to the fact that the particle concentration in the flow of combustion products typically is relatively low. This is due to a significant increase in the volume of the products of combustion upon conversion of substance from the condensed state to the gas: medium density is changed by tens and hundreds of times. Consequently, in the one dimensional description of combustion in the two phase flow of combustion products it is necessary to carefully perform the procedures of the averaging of the hydrodynamic parameters and the function of heat release.

In simplest version, if we do not consider reactions of dispersed particles of condensed phase in the smoke-gas zone above the burning surface when modeling combustion of EM, one may examine following two cases.

Let in the condensed phase the reactions proceed with the summary zero thermal effect (or endothermic). It is obvious that this excludes, the combustion regime with the rate control stage in the condensed phase, but there may exist regimes with the rate control stage in the gaseous phase, when gas-phase reactions at a temperature of flame T_2 determine the burning rate as well as regime with the stage merging when reactions in the condensed phase occur at a temperature close to T_2. For simplicity it is assumed here that the reactions in the gas occur into one stage, though, as it follows from that stated above, this approach is easily generalized to an arbitrary number of stages.

In the second case the exothermic transformations occur also in the condensed phase. Then in addition to already named the regime of stage detachment should be added, when reactions in the gas have finite duration of the induction period. Let us note, however, that in both cases the re-

gime of stage merging is hardly expected. For real gasified EM the examples are unknown when on the surface of condensed phase so high temperature has been realized.

It should be noted that existing theoretical models in majority of cases are based on the concepts of narrow zones of chemical transformations, whereas in the combustion of series of EM (nitroesters, nitramines, mixture compositions on their basis) typically the wide zones are realized, for which theoretical analysis of stage combustion were not fully conducted.

When searching the rate control stages in the combustion wave of EM it is useful to take into account qualitative considerations about dependence of degree of the control effect of one or an other spatial zone on its distance from the burning surface. On the basis of intuitive ideas the concept has been introduced [18] about the "influence zone" as the spatial domain, for which the processes beyond its bounds do not affect the burning rate. From the equation of thermal conductivity, written for the heat flux in the gas phase under the natural boundary condition at infinity ($x \to -\infty$, $q = 0$), we obtain expression for the heat flux into the condensed phase ($\Phi(x)$ is the heat release in the gas phase):

$$q_s = \int_0^\infty \Phi(x) \exp(-c\rho u x / \lambda) dx \qquad (1.13)$$

In accordance with expression (1.13) the "efficiency" of heat feed back from different zones of heat release in gas is lower, the further this zone locates from the burning surface. This fact is noted also in [24].

The search of the rate control stage for real EM was sometimes conducted on the basis of intuitive physical considerations. In this case the quantitative analysis of governing the combustion laws was not always consecutively conducted, mainly the qualitative characteristics of the process were analysed: the dependence of burning rate on p and T_0. As a result the situations appeared when for the same type of EM the different authors treated the mechanism of combustion from the diametrically opposite positions. Thus, according to [19-21], the rate control stage during the combustion of nitroglycerin powders under the pressures up to 100 atm is in the gas phase. However, in accordance with [22, 23] it is in the condensed phase. At the same time there is a sufficiently substantiated opinion that during the combustion of these compositions it is impossible in this pressure range to define the rate control stage and both gas and condensed phase should be taken into consideration [21].

Summarizing, the above indicates that theoretical approach for determination of the rate control stages in combustion of condensed EM is considerably less developed, than in the case of combustion of gas systems. It is especially difficult to do this in the description of the combustion of heterogeneous EM. Therefore, the concept of the rate control stage in the combustion of EM can be used mainly in the course of the qualitative analysis of the process, but the quantitative models of combustion of EM must be built with possible taking into account all essential factors characterizing the phenomenon under study.

1.3. SINGLE-STAGE COMBUSTION MODELS

Greatest difficulties in modeling of the EM combustion within the framework of thermal theory appear in description of different physical processes, which accompany transformation of solid

into gas. They include vaporization of EM, the foaming of substance as a result of its softening and volumetric gas evolution, dissolution and diffusion of reaction gases, dispersion of the material of a reaction layer. For different EM these processes may play different role with variation in combustion conditions. The transformation of the physical state of EM in the combustion wave leads to a change in its properties (density, thermal conductivity, heat capacity) and this can be accompanied by thermal effects. The dispersion of surface layers of EM leads to the fact that certain fraction of condensed phase is decomposed in the gas zone. Accordingly, this changes the thermal effect of reactions in the condensed phase per unit of mass of parent substance. Finally, it makes changes in the wave structure of combustion and, consequently, in the burning rate.

Historically, in modeling of the EM combustion the approach, which postulated the governing role of the condensed phase exothermal reaction, has been most widely used. A mathematical problem is usually formulated for the half-space filled with the condensed phase. In the coordinate system attached to the surface of condensed phase, the equations of heat- and of mass transfer take form [25]:

$$\lambda d^2T/dx^2 - cmdT/dx + \rho Qf(\eta)k_0 \exp(-E/RT) = 0 \tag{1.14}$$

$$m d\eta/dx - \rho f(\eta) k_0 \exp(-E/RT) = 0 \tag{1.15}$$

$$x \to -\infty,\ \eta \to 0,\ T \to T_0; \qquad x = 0,\ \eta = \eta_s,\ T = T_s \tag{1.16}$$

Here η - degree of conversion of the condensed substance into the gas depletion extent; ρ - density of condensed phase; Q - thermal effect of reaction in the condensed phase; $f(\eta)$ - kinetic function, which considers the dependence of reaction rate on the concentration of the non-consumed substance; T_s - surface temperature - unknown value, which has to be determined during computations. Index s corresponds to the values of parameters on the surface.

From (1.14) the first integral follows

$$\lambda dT/dx = q_s + m[Q(\eta_s - \eta) - c(T_s - T)] \tag{1.17}$$

Here $q_s = \lambda(dT/dx)_{x=0}$ - heat flux from gas to the surface of condensed phase.

Assuming T and η independent variables, let us exclude x from equations (1.15), (1.17) and integrate relationship obtained within limits, which correspond to change x from $-\infty$ to 0:

$$\frac{\lambda \rho k_0}{m} \int_{T_o}^{T_s} \exp(-E/RT)dT = \int_0^{\eta_s} [q_s + mQ(\eta_s - \eta) - cm(T_s - T)] \frac{d\eta}{f(\eta)} \tag{1.18}$$

If $E/RT_s >> 1$, the preheat layer is much wider than the reaction zone, i.e. the noticeable change in concentration η occurs in a subsurface layer, where temperature is close to T_s. Therefore without significant error it is possible to assume $T_s - T = 0$, under the integral sign in the right hand side of (1.18), and the left integral approximately to take in the form:

$$\int_0^{T_s} exp(-E/RT)dT \cong (RT_s^2/E)exp(-E/RT_s) \tag{1.19}$$

Now from (1.18) it follows

$$m^2 = (\rho\lambda/QJ_0)(RT_s^2/E)k_0 exp(-E/RT_s) \tag{1.20}$$

$$J_0 = (q_s/mQ)\int_0^{\eta_s}(d\eta/f(\eta)) + \int_0^{\eta_s}(\eta_s - \eta)(d\eta/f(\eta))$$

If $f(\eta) = 1-\eta$, then $J_0 = \eta_s + [1-\eta_s - g_s/mQ]\ln(1-\eta_s)$; and if $f(\eta) = 1$, then $J_0 = (g_s\eta_s/mQ) + \eta_s^2/2$.

In (1.20) m is expressed through T_s and η_s. For determining their values the additional relationships are necessary. One of them is the balance of heat obtained from (1.17) with $x \to -\infty$ ($\eta \to 0$, $T \to T_0$):

$$T_s = T_0 + (Q\eta_s/c) + q_s/mc \qquad (I.21)$$

Another relationship must reflect physical mechanism of formation of the surface. In general case it can be written in the form [14]

$$f(\eta_s, T_s, m) = 0 \qquad (1.22)$$

Determination of the concrete form of the function f is one of the basic problems of the combustion modeling.

Value of heat flux q_s entering equations for T_s and J_0 within the framework of single-stage models is not determined, and for its finding it is necessary to examine processes in gas. From equation (1.13) it is evident that the problem of calculating the heat flux q_s is reduced to finding the expression for function of heat evolution $\Phi(x)$ in the gas zone. Two theoretical approaches to description of $\Phi(x)$ are most widely used. These are the model of narrow reaction zone and model with uniform heat-source distribution in the gas.

In the case of the narrow reaction zone in gas it is possible approximately to express $\Phi(x)$ through Dirak δ-function:

$$\Phi(x) = \Phi^0\delta(x - x^*) \qquad (1.23)$$

where x* - distance between surface of EM and zone of flame.

Equation (1.23), as shown by D. B. Spalding [26], is sufficiently accurate approximation for $\Phi(x)$ with high values of energy of activation.

Substituting (1.23) in (1.13), one obtains

$$q_s = Qm \exp(-mcx^*/\lambda) \qquad (1.24)$$

Equations of type (1.24) are frequently used in combustion model of composite solid propellants. For determining the value of x* C.E. Hermance [27] proposed to use the expression

$$x^* = v_g\tau = \frac{m}{\rho_g(T_g)}\tau = \frac{m}{[\rho_g(T_g)^n k_0 \exp(-E/RT_g)} \qquad (1.25)$$

where v_g - velocity of the motion of gas (linear), τ - characteristic reaction time. Then (1.24) gives

$$q_s = Qm\exp[-(m^2c/\lambda k_0)(RT_g/\mu p)^n \exp(E/RT_g)] \qquad (1.26)$$

Spatial variation in function of heat evolution $\Phi(x)$ is determined mainly by competition between reduced concentration of the reagent and increased reaction rate constant. In [28, 29] an assumption has been made that the resulting reaction rate in this case is approximately constant up to a certain distance of $x_1 >> \lambda/mc$, measured from the burning surface EM. Then from (1.13) it follows

$$q_s \approx \lambda\Phi(0)/mc = (\lambda Q/mc)(\mu p/RT_s)^n k_0 \exp(-E/RT_s) \qquad (1.27)$$

Joint examination of equations (1.20), (1.22) and (1.27) makes it possible to compute mass burning rate m. Below we discuss particular models of combustion based on different concepts about character of physical transformations in the combustion wave.

1.3.1. Foamy surface reaction zone with unlimited expansion.

Preheating in the combustion wave for majority of solid EM is accompanied by melting or softening (for amorphous substances) of their surface layer. Even during the combustion of the typical representative of nonvolatile nitroesters - nitrocellulose, according to the observations of a number of the authors, the burning surface is covered with a liquid layer. The chemical reactions of gasification in the liquefied reaction layer can lead to the foaming and as the result of this, to a change of the actual concentration of substance in the reaction zone. Simultaneously in this case a thermal conductivity of solid is changed also. The presence of the gas bubbles in a reaction layer in combustion of different EM indicated a number of the authors, see for RDX- [30], for DINA - [31]. In monopropellants on the basis of nitrocellulose a foamy structure is reliably observed only under the conditions of thermal decomposition [32] and upon the combustion in vacuum [33].

Combustion model of substances with foamy reaction layer has been described in works of E. I. Maximov and A. G. Merzhanov [34, 35]. Similar problems have been examined also in [19, 36].

Let us consider somewhat simplified in comparison with [34] the formulation of problem. It involves exothermic conversion of solid EM starting within the condensed phase and continuing in two phase flow. The basic assumptions are: heat capacities for condensed and gas phase are equal to each other; chemical reaction proceeds in one stage and has the first order on the concentration of parent substance; the characteristic size of the cells in dispersed medium is much lower than the width of the heat evolution zone, so that the dispersed zone can be considered quasi-homogeneous; from the initial depths of decomposition the parent substance and reaction gases move with the identical rates; the solubility of gaseous products in the condensed phase is negligible.

When making these assumptions, we have

$$d^2T\lambda/dx^2 - cmdT/dx + \overline{\rho}(1-\eta)Qk_0\exp(-E/RT) = 0 \qquad (1.28)$$

$$md\eta/dx + \overline{\rho}(1-\eta)k_0\,exp(-E/RT) = 0 \qquad (1.29)$$

Here η - degree of conversion of condensed phase, connected with the mean density of substance $\overline{\rho}$ in the wave of combustion via relationship $\eta = (\rho_g/\overline{\rho}) - (\rho_g/\rho_c)$, which is valid if $\rho_c/\rho_g >> 1$ (indices c and g relate to the condensed and gas phases, respectively); λ - thermal conductivity of two-phase medium, defined in [34] as "weighted mean" value on λ_c and λ_g in accordance with their volume fractions; k_0, E - pre-exponent and energy of the activation of the reaction of gasification of the condensed phase; Q - its thermal effect.

Within the framework of the assumptions made a mechanism of formation of dispersed medium is not examined and expenditures of energy for formation of bubbles (in the case of foam) or interface (in the case of dispersion) are disregarded.

From physical formulation of the problem it is clear that boundary conditions must be assigned only at $\pm\infty$:

$$x \to -\infty,\ T \to T_0,\ \eta \to 0; \quad x \to \infty,\ T \to T_m,\ \eta \to 1. \tag{1.30}$$

Expression for the burning rate, obtained by classical approximate method (according to Zeldovich, Franck-Kamenetskii), takes form:

$$m^2 = \frac{2\lambda_g p \mu T_m}{QE} k_0 \exp(-\frac{E}{RT_m}) \tag{1.31}$$

Here $T_m = T_0+Q/c$ - combustion temperature in the absence of gas-phase reactions; p - pressure; μ - molar mass.

Dependence of the burning rate on pressure ν = dlnm/dlnp=0.5 and on initial temperature β = $dlnm/dT_0 = E/2RT_m^2$.

For testing the validity of adopted assumptions and analysis of structure of the combustion wave the numerical solution of the problem (1.28)-(1.30) has been carried out [34]. The important result of numerical calculations became the conclusion that basic heat evolution occurs at the very low density of substance, equal to $\overline{\rho} = 2.5\rho_g$.

1.3.2. Finite scale foamy reaction layer.

In contrast to preceding model with unlimited foaming of condensed phase let us introduce into examination the burning surface which is defined as the end of the zone with sharp change of density. The dimension of the zone is much smaller than the width of the chemical reaction zone. Thereby we take into account the fact that there is a certain limit of the foaming, on achievement of which the small bubbles disintegrate. Let us allow also that there is sufficiently high number of small bubbles in a reaction layer. Then it is possible to consider that through the foamy stage virtually entire substance is passed. It is known that the opening of small bubbles, on the surface of liquid does not lead to the generation of a significant quantity of drops [37, 38]; therefore let us disregard the formation of dispersed phase.

Let us examine, as in [34, 35], combustion of a hard volatilizing substance under conditions when the gas-phase reactions either are very fast or occur in regime of spontaneous ignition. The system of equations, describing the propagation of the combustion wave is similar to that given in [34]:

$$(cmdT/dx - \lambda d^2T/dx^2)/Q = -md\eta/dx = \Phi \tag{1.32}$$

$$\Phi = \rho_c(1-\eta)[1+\eta(\rho_c/\rho_g)-\eta]^{-1}k_0 \exp(-E/RT) \tag{1 33}$$

$$x \to -\infty,\ \eta = 0,\ T = T_0; \quad x = o,\ \eta = \eta_s = 1,\ T = T_s. \tag{1.34}$$

Condition $\eta_s = 1$ indicates complete transformation of condensed phase into gas, i.e., the absence of dispersion, so that we will consider the interface between foam and gas as a burning surface. Its temperature T_s is unknown and is a subject to determination.

From the first integral of equation of thermal conductivity (1.32)

$$T_s = T_0 + Q\eta_s/c = T_0 + Q/c \tag{1.35}$$

it follows that within the framework of the model under consideration the value Q must be variable (in more detail we discuss experimental proofs of variability of the value Q during combustion in section 2.7) and depend at least on pressure. Let us formulate this dependence in general form

$$f(Q, T_s, m) = 0 \tag{1.36}$$

Solution of the system (1.32) and (1.33) under the conditions (1.34)

$$m^2 = (2\lambda\rho / Q)(RT_s^2 / E)k_0 \exp(-E / RT_s) \tag{1.37}$$

Joint examination of (1.35)-(1.37) makes it possible to determine Q, T_s and m. Function f in (1.36) corresponds to a certain physical condition at the surface and must be determined independently.

Process of disruption of small bubbles on the surface of liquid can be described mainly qualitatively [38, 39], but it is possible to state that bubble collapse occurs upon achievement of the equality of forces, which destroy (F_p) and stabilize (F_c) small bubble. The gas pressure applied to the "external" surface of bubble's wall plays a role of destroying force: $F_p \approx p_b d_s^2$ (pressure on the "internal" wall applied to the side of liquid, is compensated by the reaction of liquid; kinetic energy of small bubble we disregard). As stabilizing we consider the force of surface tension $F_s \sim \sigma d_s'$. Here $p_b = p_\infty + 4\sigma/d_s$ - gas pressure in the small bubble; p_∞ - external pressure; d_s' and d_s - the outer and inner diameters of small bubble (Fig. 1.1); σ - coefficient of surface tension.

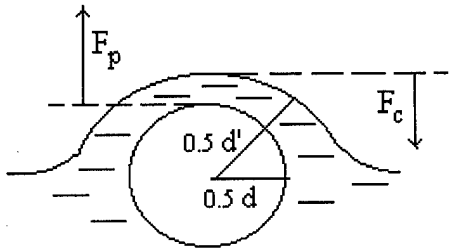

Fig. 1.1. Small bubble on the liquid surface.

Taking into account the fact that the thickness of wall $0.5(d_s' - d_s)$ is usually much less than diameter of small bubble [39], condition of the surface equilibrium can be written in approximate form [40]:

$$F_p / F_c \approx p_b d_s / \sigma \approx p_\infty d_s / \sigma = const \tag{1.38}$$

Relationship (1.38) can be written in another way:

$$p_\infty^{3/\gamma}[m(T_s - T_0)]^{-1} = const \tag{I.39}$$

Actually, diameter of separate small bubble d with given degree of the EM conversion depends on the number of small bubbles N in section with this coordinate. This gives $d \sim N^{-1/3}$. A change in external pressure P_∞ leads to a change in the burning rate m and value of the heat flux q in the zone of foaming. From the theory of phase transformations it is known that during boiling of liquids a number of embryos of the gaseous phase initial spots depends [37] on the value of heat flux to a certain extent γ : $N \sim q^\gamma$. Taking into account this fact and also relationship $q \cong cm(T_s - T_0)$ makes it possible to reduce (1.38) to the form (1.39). When writing (1.39) it is also assumed that in the real range of variation of T_s we consider $\sigma = const$. For the majority of organic liquids the temperature dependence of the coefficient of surface tension is low in value ($\sim 10^{-4}$ J/(m^{2}K)), and with change of T to tens of degrees σ is changed in the hundredths.

The dependence of burning rate on ambient conditions can be obtained by differentiating (1.37) taking into account (1.35) and (1.39). For m(p) it follows (with $E/RT_s>>1$ and $E(T_s-T_0)/RT_s^2 + 2(T_s-T_0)/T_s>>1$):

$$\nu = d\ln m / d\ln p \approx 3/\gamma$$

According to data [41, 42], γ is close to 3; therefore $\nu \cong 1$. For $m(T_0)$, when making reasonable simplifications, it follows

$$\beta = (E/RT_s^2)/[1+(E/RT_s^2)(T_s - T_0)] \cong 1/(T_s - T_0)$$

Expression (1.39) is similar to formula for η_s obtained in [43] (see also section 2.7) upon examination a model with dispersion of a solid reaction layer:

$$\eta_s = \xi' p / mT_s, \quad \xi' = const \tag{1.40}$$

ter multiplying (1.40) by Q′ (in [43] Q′ = const) and designating $Q'\eta_s = Q = c(T_s-T_0)$, we obtain that when T_s = const and $\gamma = 3$ expression (1.40) coincides with (1.39). Expressions for ν and β in the model in question and model [43] are also identical. This shows similarity of the effects of dispersion and foaming on the rate of combustion. At the same time it is necessary to note that the expression (1.39) serves only as the particular relationship, which combines heat evolution in condensed phase $Q \sim (T_s-T_0)$, pressure p and burning rate m without specific relations between variables.

1.3.3. Dispersion of a liquid reaction layer.

The term dispersion of EM designates a phenomenon of mechanical destruction of a surface reaction layer with subsequent transfer of particles into gas zone. Volumetric gas evolution in a reaction surface layer of the condensed phase serves driving force for dispersion of homogeneous EM. From the physical considerations it follows that for EM with exothermal reactions in the condensed phase dispersion must lead to the decrease in heat evolution at the surface reaction zone. According to theoretical analysis [44], the scale of dispersion can determine in significant extent the level of the burning rate, while the dependence of the burning rate on the external conditions can be caused by the character of a change in the degree of dispersion.

In principle, there are possible two different mechanisms of formation of the drops of liquid during combustion of EM: 1) as a result of opening on surface of separate gas bubbles and 2) as a result of aerodynamic interaction of gas with the liquid layer during gas jet outflow from the surface layer.

Opening of the gas bubbles on a surface, apparently, can not lead to significant dispersion of the EM. Thus, according to the analysis [38] of experimental data on the yield of drops from the layer of liquid, blown by gas, no more than 10^{-4} g of the drops fits to each gram of blowing gas. The drops form as a result of the break of the shells of small bubbles.

Another picture is observed in the case of jet stream of gas blowing through the layer of liquid. In this case the mass flow rate of the liquid drops can become commensurate in the value with the mass flow rate of gas. We will call this dispersion regime as pneumatic regime.

From physical considerations it is possible to state that the fluid element, which is located in the surface reaction layer, with finite probability passes pattern of chemical transformation (condensed phase - gaseous products of pyrolysis) as well as pattern of mechanical destruction (con-

densed phase – aerosol). The degree of dispersion (mechanical destruction) must be the higher, the faster surface layer destruction and the slower chemical transformation. With this qualitative formulation it is possible to give appropriate quantitative form of description.

We use expression for degree of dispersion in the form [45, 46]

$$\eta_d = j_d /(\rho_c u_{ch} + j_d) \tag{1.41}$$

Numerator in (1.41) represents the mass flow rate of aerosol, which is generated by the burning surface; denominator represents an overall consumption of mass from the unit of surface; u_{ch} - component of the "observed" linear burning rate u due to the chemical decomposition; ρ_c - density of the condensed phase. After dividing numerator and denominator of (1.41) by the characteristic size of the chemical reaction zone δ (the zone of the aerosol generation) and the effective density of substance ρ we obtain expression for η_d through the characteristic times of the processes (τ_d correspond to dispersion and τ_{ch} - to chemical decomposition):

$$\eta_d = \tau_d^{-1} /(\tau_{ch}^{-1} + \tau_d^{-1}) \tag{1.42}$$

Dispersion of the layer δ is connected with conditions for development of instability in liquid, which, in turn, are determined by the forces of surface tension, and by characteristic size of fluid element, involved in dispersion, as well as by inertia factors and time of dynamic interaction between gas and liquid. In the case of the dispersion of the EM reaction layer a significant role, apparently, can play the effect of collective interaction of gas jets, since on the same fluid element the disturbances from different micro-jets of gas can be applied.

Let us assume that an ultimate strain in the reaction layer, on achievement of which the liquid peptizes, is provided, in essence, as a result of effect of aerodynamic forces. In this case the time of the achievement of ultimate strain, or the time of dispersion τ_d is equal to [47]

$$\tau_d = \xi'(\delta/\overline{u}_g)\sqrt{\rho_c/\overline{\rho}_g}$$

Here ξ'=const; $\overline{u}_g$ - mean relative gas velocity in a reaction layer of thickness δ; $\overline{\rho}_g$ - mean density of gas. Taking into account $\tau_{ch} \sim (\delta/u_{ch}) \approx (\delta/\overline{u}_g)[\rho_c/\rho_g(T_s)]$, let us rewrite (1.42) in the form

$$\eta_d = (1+\xi\sqrt{\rho_g(T_s)/\rho_c})^{-1}, \quad \xi = const \tag{1.43}$$

From (1.43) one may derive a dependence of η_d on p

$$\eta_d \approx 1/(1+\xi''\sqrt{\rho_g}), \quad \xi'' = const$$

Qualitatively similar expression for dependence $\eta_d(p)$ can be obtained also from the examination of the balance of mechanical energy in a reaction layer. With the consumption of portion $(1-\eta_d)$ of the propellant sample with an initial mass m_0, the formed gases acquire kinetic energy $W = (1-\eta_d)m_0 u_g^2/2$ which partially can be spent on the creation of the new interface, i.e. for the dispersion. The work of the formation of surface with area Σ is equal to $W_\Sigma = \sigma\Sigma$, where σ - surface tension. Assuming that the energy of gases issued from the reaction zone is spent on the dispersion with a certain efficiency φ, it is possible to write

$$\sigma\Sigma = \varphi(1-\eta_d)m_0 u_g^2/2 \tag{1.44}$$

Here Σ - summary area of the particles formed from the propellant mass $\eta_d m_0$. It is easy to show that η_d size of particles d_0, m and Σ are connected as follows:

$$\eta_d = \rho_c d_0 \Sigma / 6m_0 \tag{1.45}$$

From (1.44) and (1.45) we obtain

$$1/\eta_d = 1 + (a/\varphi d_0)p^{2(1-\nu)},$$
$$a = [M/(\rho_c T_s R u_0)]^2 12\sigma/\rho_c, \quad u_0 = up^{-\nu} = const \tag{1.46}$$

From (1.46) it is evident that when $d_0 \to 0$, the dispersion degree $\eta_d \to 0$. This means that the energy of the gases released from a reaction layer is insufficient to form a significant number of particles of very small sizes.

Experimental observations show that upon abrupt deradiation or depressurization the subsurface layer of DB propellants may destroy with formation of the net of bubbles and small size particles. Theoretical estimate for the pressure drop δP, which may cause dispersion of liquid layer in stationary and transient conditions (e.g., under oscillating pressure) has been made in Ref. [48].

1.3.4. Dispersion of a solid reaction layer.

Let us examine combustion of EM with solid reaction layer in the condensed phase. The diagram of the substance conversion in the combustion wave takes a form (14]

$$\begin{array}{ccc} & \nearrow & A_1^d \longrightarrow A_2 \\ A_1^c & \longrightarrow & A_2 \end{array} \tag{1.47}$$

Here A_1^c - initial condensed substance; A_1^d - the same substance in the disperse state; A_2 - gaseous product of the reaction. According to diagram (1.47) the chemical decomposition occurs in one stage ($A_1 \to A_2$), which proceeds in two spatially divided zones: condensed ($A_1^c \to A_2$) and disperse ($A_1^d \to A_2$)

Laws of conservation of energy and substances, written in the coordinate system attached to the surface of condensed phase, take the form:

$$\lambda d^2T/dx^2 - cm(1+\Delta)dT/dx + Qmd\eta/dx = 0 \tag{1.48}$$
$$v_c\, d\eta/dx - k_0(1-\eta)\exp(-E/RT) = 0 \tag{1.49}$$

Here $\Delta = z_0\rho_0/\rho_c(1-z_0)$; z - volume fraction of gas per unit of volume of porous (or disperse) medium; z_0 - porosity of initial specimen; ρ_c - density of the condensed substance; $\rho_0 = \mu p/RT_0$ - density of inert gas in the pores in the initial state; T_0 - initial temperature; v_c - rate of the motion of the condensed phase; $v_c = v_0$ for unreacted part of specimen; η - degree of conversion of condensed substance. Additional relationships should be also met:

$$z\rho v_g + \rho_c(1-z)v_c = m(1+\Delta) \tag{1.50}$$
$$\rho_c(1-z)v_c = (1-\eta)m \tag{I.51}$$
$$(\pi d^3/6)\rho_c v_c dv_c/dx = 3\mu_0 d_p(v_g - v_c), \quad x>0 \tag{1.52}$$
$$-k_\Phi dp/dx = z(v_g - v_0), \quad x<0 \tag{1.53}$$

Here ρ - gas density; v_g –gas velocity; d_p - diameter of the dispersed particle; μ_0 - viscosity of gas; k_Φ - filtration factor of the gas through the porous medium.

Relationships (1.48)-(1.53) compose system of five equations (when x>0 one should exclude equation (1.53), and when x<0 – to exclude equation (1.52)) for six unknowns: T, η, v_c, v_g, z, m.

Boundary conditions to system (1.48)-(1.53) have a form

$$X \to -\infty,\ T=T_0,\ \eta = 0,\ v_g = v_c = v_0;$$

$$X \to \infty,\ dT/dx = 0,\ \eta = 1,\ z = 1. \tag{I.54}$$

First integral of system (1.48)-(1.49) makes it possible to determine combustion temperature T_g, and to build relation between q, T and η:

$$q = \lambda dT/dx = cm(1+\Delta)[(T-T_0)-\eta(T_g-T_0)],$$

$$T_g = T_0 + Q/[c(1+\Delta)].$$

For closing the problem it is sufficient to formulate equation, which determines conditions on the interface separating disperse zone and condensed phase.

We will consider that on the interface the equality of forces is reached, which act on the particles from gas flow, F_d and provide cohesion between particles the in reaction zone of condensed phase, F_c. If dispersion is caused by destruction of condensed phase by the gas flow with small Re numbers, i.e. when $Re = (\rho v_g d/\mu_0)_{x=0} < 1$, then at x=0

$$F_d = F_c = [(\pi d^3/6)/(1-z)][(z/k_\Phi)(v_g - v_0)] \tag{1.55}$$

Here the first factor, isolated with square brackets, is the volume of a single particle; the second factor is the force, which acts upon unit volume of porous medium of reaction zone.

Since values F_c, z, d and k_Φ, depend on degree of conversion η, condition of dispersion take the form

$$m\eta_s \approx \rho_s f(\eta_s),\quad f(\eta_s) = (6/\pi d^3)(1-z)k_\Phi F_c \tag{1.56}$$

The inequality $z_0\rho_0 << (1-z_0)\rho_c$, $v_0 << (v_g)_s$ is taken here into consideration. From the qualitative analysis of problem (1.48)-(1.54) and (1.56), carried out in [14], it follows that it is possible to find such a value of degree of conversion η_s^0, that with $\eta_s < \eta_s^0$ the laws governing the combustion are determined by the reactions in the disperse zone (rate control stage in the disperse zone) and when $\eta_s > \eta_s^0$, they are determined by the reactions in the condensed phase of EM (stage detachment regime).

Dependence $m(p,T_0)$ is determined by the form of function $f(\eta_s)$ in (1.56) and by the value of η_s. Assuming $f(\eta_s) = f_0 = \text{const}$ and $\eta_s > \eta_s^0$, one obtains

$$m \cong (p\mu f_0/RT_s)[Q/c(T_s - T_0)],\quad T_s \neq T_s(T_0)$$

$$T_s \cong (E/2R)/ln[(QR)^{3/2}(\lambda_{ks}\rho_c k_0)^{1/2}/(4p\mu f_0 c^2\sqrt{E})],$$

$$\nu = d\ln m/d\ln p \cong 1-(2RT_s^2/E)/(T_s - T_0), \tag{1.57}$$

$$\beta = d\ln m/dT_0 \cong 1/(T_s - T_0).$$

If $f(\eta_s) = f_0 = \text{const}$ and $\eta_s < \eta_s^0$, itt follows

$$m = m_d\sqrt{1+(\rho_s f_0/m_d)^2},$$

$$\nu = \frac{1}{2}(1+\eta_s^2),\quad \eta_s \cong \rho_s f_0/\sqrt{(f_0\rho_s)^2 + m_d^2},$$

$$\beta = (1-\eta_s^2)E/RT_g^2.$$

Here m_d is the rate of single-stage combustion of easily dispersed EM (see section 1.31).

If $f(\eta_s) \neq$ const, then for the most important case $\eta_s > \eta_s^0$ the burning rate is calculated as before by (1.57). The surface temperature T_s grows with increase of T_0, when $d\ln f/d\eta_s < 0$, and vice versa:

$$\partial T_s / \partial T_0 \cong -(2cRT_s^2 / EQ) d\ln f / d\eta_s$$

The dependencies of the burning rate on pressure and initial temperature are as follows:

$$\nu = 1 - (2RT_s^2 / E)\beta; \quad \beta \cong (T_s - T_0)^{-1} - (c/Q) d\ln f / d\eta_s$$

Dispersion process can be considered in more detail by taking into account the possibility of solid material destruction under action of deformations due to strains and stresses in EM. The deformations in EM can be caused by the steep gradient thermal wave propagation into the bulk of material. When solving the conjugated problem of the thermal and mechanical waves propagation, one may study the effects of dispersion and stresses on the ignition and combustion characteristics of EM [49-51]

CHAPTER 1 - REFERENCES .

1. **Ya. B. Zeldovich, D. A. Franck-Kamenetskii**. Theory of thermal flame propagation. *Journal of Physical Chemistry (Russian)*, 1938, Vol. 12, pp. 100-105.

2. **Ya. B. Zeldovich, D. A. Franck-Kamenetskii**. To the theory of uniform flame propagation. *Reports of the USSR Academy of Sciences*, 1938, Vol. 19, pp. 693-69B. (R)

3. **A. G. Merzhanov**. Processes of combustion in the chemical technology. Chernogolovka, 1978. *Preprint, Institute of Chemical Physics, USSR Academy of Sciences*. (R)

4. **S. I. Khudyayev**. Mathematical theory of combustion and explosion. Chernogolovka,- 1980. *Preprint, Institute of Chemical Physics, USSR Academy of Sciences*. (R)

5. **A. H. Kolmogorov, I. G. Petrovskiy, N. S. Piskunov**. Study of the equation of diffusion, connected with the increase of substance, and its application to one biological problem. *Bull. of the Moscow State University,* 1937, Vol. 1, Ser. A. Iss. B. (R)

6. **Ya. B. Zeldovich**. Flame propagation theory. *Journal of Physical Chemistry (Russian)*, 1948, Vol. 22, pp. 27-49.

7. **A. G. Merzhanov**. Thermal waves in chemistry. Chernogolovka, 1978. *Preprint, Institute of Chemical Physics, USSR Academy of Sciences* (R)

8. **A. G. Merzhanov**. Theory of the stationary homogeneous combustion of the condensed substances. Chernogolovka, 1968. *Preprint, Institute of Chemical Physics, USSR Academy of Sciences*. (R)

9. **B. I. Khaikin, E. N. Rumanov**. To the Problem of Regimes of Exothermal Reaction in the One-Dimensional Gas Flow. *Combustion, Explosion, and Shock Waves,* 1975, Vol. 11, pp. (R) 671-678.

10. **B. I. Khaikin, A. K. Filonenko, S. I. Khudyayev**. Flame Propagation in Gas with Proceeding of Two Consecutive Reactions. *Combustion, Explosion, and Shock Waves,* 1968, Vol. 4, pp.(R) 591-599.

11. **B. I. Khaikin, A. G. Merzhanov**. On the combustion of substances with a solid reaction layer. *Reports of the USSR Academy of Sciences*, 1967, Vol. 173, pp. 1382-1385. .(R)

12. **A. G. Merzhanov, E. N. Rumanov, B. I. Khaikin**. Multizone combustion of the condensed systems. *Journal of Applied Mechanics and Technical Physics (Russian)*, 1972, Vol. 6, pp. 99-105. .(R)

13. **A. K. Filonenko**. Author's abstract of PhD Thesis. Chernogolovka, Institute of Chemical Physics, USSR Academy of Sciences, 1970. .(R)

14. **B. I. Khaikin**. Author's abstract of Dr. Sci. Thesis. Moscow, Institute of Chemical Physics, USSR Academy of Sciences, 1975. (R)
15. **Ya. B. Zeldovich**. In the book: Theory of the combustion of propellants and explosives. M.: Nauka, 1982, pp. 49-86. .(R)
16. A. **F. Belyayev**. In the book: Theory of the combustion of propellants and explosives. M.: Nauka, 1982, pp. 35-43. (R)
17. **V. N. Vilyunov**. To the mathematical theory of stationary combustion of the condensed substance. *Reports of the USSR Academy of Sciences*, 1961, Vol. 136, pp. 136-139. .(R)
18. **A. F. Belyayev, N. N. Bakhman**. Theory of the combustion of powders and solid rocket propellants. . *Combustion, Explosion, and Shock Waves,*, 1966, Vol. 2, pp.(R) 3-18.
19. **Rice D. K, Ginell R. J**. Theory of the Burning of Double-Base Propellants. Rocket Powders.- *Phys. Coll. Chem.*, 1950, V.54, pp. 885 - 917.
20. **K. K. Andreyev, A. F. Belyayev**. Theory of Explosives. Moscow, Oborongiz, 1960. (R)
21. **I. Aoki, N. Kubota**. Structure of the Combustion Zone of High and Low-Energy Double-Base Propellants. *Express-information. Astronautics and rocket dynamics. VINITI* [Institute of Scientific and Technical Information], 1981, No. 38-123. (R)
22. **P. F. Pokhil, 0. I. Nefedova, A. D. Margolin**. On the anomalous dependence of rate of combustion of propellant on the initial temperature. *Reports of the USSR Academy of Sciences*, 1962, Vol. 145, pp. 860-862. (R)
23. **E. V. Konev, S. S. Khlevnoy**. On the combustion of propellant in the presence of luminous radiation. *Combustion, Explosion, and Shock Waves*, 1966, Vol. 2, pp.(R) 33-41.
24. **V. D. Barsukov, V. P. Nelayev**. On the thermal effect of the zones of chemical transformation on rate of combustion of the condensed system. *Journal of Engineering Physics*, 1975, Vol. 29, pp. 989-993. (R)
25. **V. A. Strunin**. On the condensed combustion zone of explosives. *Journal of Physical Chemistry (Russian)*, 1965, Vol. 39, pp. 433-435. (R)
26. **Spalding D. B**. *Combustion and Flame*. I957. V. 1, pp. 296-300
27. **C. E. Hermance**, A Model of Composite Propellant Combustion Including Surface Heterogeneity and Heat Generation, *AIAA Journal*, V. 4, 1966, pp. 1629-1637.
28. **Milller M.S. and Coffee T. P**. On the Numerical Accuracy of Homogeneous Solid Propellant Combustion Model. *Combustion and Flame* I983, v.50,. pp. 75-88.
29. **Milller M.S.,** In Search of an Idealized Model of Homogeneous Solid Propellant Combustion, *Combustion and Flame*, 1982. v. 46, p. 5l - 73.
30. **E. I. Maksimov, A. G. Merzhanov, Yu. R. Kolesov**. Density distribution of substance in the combustion zone of the condensed systems. *Reports of the USSR Academy of Sciences*, 1965, Vol. 162, pp. 1115-1118. (R)
31 R. K. Tukhtayev. Author's abstract of PhD Thesis. Novosibirsk: IFKhIMS, Siberian Division of the Academy of Sciences of the USSR, 1970. (R)
32. **V. V. Aleksandrov**. Author's abstract of PhD Thesis. Novosibirsk, Institute of Chemical Kinetics and Combustion, Siberian Division of the Academy of Sciences of the SSSR, 1970.
33. **P. F. Pokhil**. Author's abstract of Dr. Sc. Thesis. Moscow, Institute of Chemical Physics, USSR Academy of Sciences, 1954, see also in the book: Theory of the combustion of propellants and explosives. M., Science, 1982, pp. 117-140. (R)
34. **E. I. Maksimov, A. G. Merzhanov**. To the theory of the combustion of condensed substances. *Combustion, Explosion, and Shock Waves*, 1966, Vol. 2, pp.(R) 47-58.

35. **E. I. Maksimov, A. G. Merzhanov**. On one model of the combustion of nonvolatile explosives. *Reports of the USSR Academy of Sciences*, 1964, Vol. 157, pp. 412-415. (R):
36. **Crawford B. L, Hugget C, McBrady J. J**. Mechanism of the Burning of Double-Base Propellant - *J. Phys. Coll. Chem*, 1950. v. 54. pp. 854 - 862
37. **E. I. Nesis**. Boiling of liquids. M.: Nauka, 1973. (R)
38. **S. S. Kutateladze, M. A. Styrikovich**. Hydrodynamics of gas-liquid systems. Moscow, Energiya, 1976. (R)
39. **V. G. Gleim, I. K. Shelomov, B. R. Shidlovsky**. On the processes, which lead to the generation of drops with the break of blisters on the interface liquid - gas. *ZhPKh*, 1959, Vol. 32, pp.218-222 (R)
40. **V. Ya Zyryanov**. Author's abstracts of PhD thesis. Novosibirsk: Institute of Chemical Kinetics and Combustion, Siberian Division of the Academy of Sciences of the SSSR, 1980. (R)
41. **R. Gertner, D. Westuener**. Problems of physics of boiling. M.: Mir, 1964. (R)
42. **Nishikawa K., Jamagata K**. *Int. J. Heat Mass Transfer*, 1960, v. 1. p. 219.
43. **B. I. Khaykin, A. G. Merzhanov**. On the combustion of substances with a solid reaction layer. *Reports of the USSR Academy of Sciences*, 1967, Vol. 173, pp. 1382-1385. (R)
44. **A. G. Merzhanov**. On the role of dispersion during the combustion of propellants. *Reports of the USSR Academy of Sciences*, 1960, Vol. 135, pp. 1439-1441. (R)
45. **Zarko V. E., Zyryanov V. Ya.**, "Surface Layer Destruction During Combustion of Homogeneous Powders", *Progress in Astronautics and Aeronautics, AIAA*, Vol. 88, 1983, pp. 220-227
46. **V.E. Zarko, V.Ya. Zyryanov, and V.V. Chertischev**, "Dispersion of the Surface Layer during Combustion of Homogeneous Propellants", *AIAA Paper* 96-0814 (34th Aerospace Sciences Meeting, Reno, 1996)
47. "Physical Background of the Working Process in the Combustion Chambers of Ramjet Engine". **B.V. Rauschenbach, S. A. Belyi, I. V. Bespalov, et al.** Moscow, Mashinostroyeniye, 1964. (R)
48. **Gusachenko L.K**. Dispersion under nonstationary combustion of solid propellants. *Combustion, Explosion, and Shock Waves* 1991, Vol. 27, No. 1, pp. 63-66.
49. **A.G. Knyazeva**. "Front velocity of the simplest solid-phase chemical reaction and internal mechanism stresses". *Combustion, Explosion, and Shock Waves*, 1994, Vol. 30, No. 1
50. **V.E. Zarko, and A.G. Knyazeva**. "Simulation of Ignition Transients for Two-Component Solid Propellants under Irradiation", *Journal of Propulsion and Powers*, 1995, N 4.
51. **A.G. Knyazeva, E.A. Dyukarev**. "A model for the autowave propagation of solid-phase low – temperature chlorination of butil chloride", *Combustion, Explosion, and Shock Waves*, 1998, Vol. 34, No. 5.

CHAPTER 2

SIMULATION OF MONO- AND DOUBLE BASE PROPELLANTS COMBUSTION

In this chapter the results are given of modeling the combustion processes of real homogeneous substances, which are either individual chemical compounds - monopropellants (ammonium perchlorate, nitramines, etc.) or more complex objects like double base propellants (DB), which consist of mixture of individual substances. Selection of the objects is caused, on the one hand, by their practical value for the contemporary technology, and on the other hand, by the presence of the vast material of investigations available in the scientific literature.

2.1. PROBLEMS OF THE MODELING THE REACTION ZONE IN THE CONDENSED PHASE

Most of homogeneous energetic materials (EM) of practical interest transform upon combustion from initial solid into liquid and then final gaseous products. Therefore, the combustion model of such EM consists typically of several parts. The simplest physical pattern, including one-dimensional laminar motion with heat transfer, diffusion and chemical reactions, and the greatest progress in its mathematical simulation (e.g., use of the increasingly complex kinetics) hold for the gaseous part of the process. More complex processes occur in the solid phase where in the preheat zone some changes in the crystalline modification of a substance are likely along with the cracking caused by thermoelastic stresses. These processes are sure to have effect on the nonstationary characteristics of EM combustion. However, in steady-state conditions their role is, probably, small assuming a thermal combustion mechanism. There is evidence for the low intensity of solid-phase chemical reactions as compared with the liquid-phase ones for the most widespread EM: ammonium perchlorate [1], octogen and hexogen [2]. The rate control role in the thermal mechanism of EM combustion belongs to the processes occurring in the zone providing the greatest portion of heat to "satisfy the needs" of the condensed phase, i.e. heating to the surface temperature and all phase transitions. The authors [1] assume that at 20...100 atm the above zone is (for ammonium perchlorate) the zone of liquid-phase reactions in which about 70% of the needed heat is released. Conclusion on the rate control role of the gas flame zone at pressures below 5 atm and that of liquid-phase reactions at 70-90 atm has been made on the basis of thermocouple measurements of the temperature profiles in the combustion wave hexogen and octogen [3]. The contributions from both zones become comparable at 20 atm. The same (comparability of contributions) holds for DINA (dinitroxydiethyl nitramine) at atmospheric pressure [4]. Thus, in a series of the practically important EM, the effective simulation of their combustion is impossible without describing the processes occurring in the zone of liquid-phase reactions.

The importance of purity of original EM

The initial substance purity can be of importance in studying EM combustion. Impurities, inevitable upon production, and introduced at times on purpose, behave themselves differently than the basic EM component creating thus a specific inhomogeneity of composition in the combustion wave of the initially homogeneous EM. It is known that upon combustion of double-base propellants their surface zone is depleted of nitroglycerin, which vaporizes and decomposes earlier than other components. On the contrary, the nonvolatile and almost inert impurities (catalysts, soot) amounting to 1-2% of the mass of initial EM can form almost solid cover on its

burning surface. For information on the similar observations for a series of individual and double-base EM, see [5, 6]. Known is the fact of metal accumulation on the burning surface of many metal-containing compositions. When studying hexogen combustion it should be taken in consideration that depending on technology hexogen can contain up to 10% of octogen. It is expected that even a smaller portion contained in the initial hexogen sample will be sufficient for the burning surface to be covered with a liquid layer of more thermostable (as compared with hexogen [7]) octogen. To prove that, one has to perform chemical analysis of the surface layer of the extinguished sample. The steady-state combustion rate can be almost insensitive to such impurities if the rate control role belongs to the gas phase. However, it is expected that the nonstationary combustion characteristics may substantially depend on the fraction of impurity in the initial substance.

Density in two-phase zone

For nonvolatile energetic materials a model of steady-state combustion with the rate control stage in the foam zone was proposed [8] in which the liquid transforms into gas due to the first-order exothermic reaction and both of the phases move with the same velocity. No special conditions were imposed for the foam-aerosol interface. The density, transversely averaged to the motion, continuously changes from solid to gas magnitude. The model proposed in [9-11] is based on general equations for one-dimensional motion of the two-phase medium (and also with the "smeared" burning surface). Additional account is taken in [9] (as compared with [8]) of the possible relative motion of phases owing to the Marangoni effect, which drives bubbles "entering" the burning surface. The interaction of two phases and the character of their motion should be determined in each case by the user. In particular, two variants are proposed in [10].

In the first case, the mass flow rate m^*=idem holds over the entire two-phase region without averaging, i.e., for both of the phases separately, so that $u_c\rho_c = u_g\rho_g = m^*$. Since the liquid density ρ_c does not change, u_c = idem holds, i.e., the liquid moves in a quasi-solid manner. With approach to the interface, the gas density ρ_g decreases owing to heating, and the gas velocity increases. This variant corresponds to the jet model of gas outflow where the system of "longitudinal" pores passing to the surface is realized. The "transverse" diffusion instantaneously supplies the pores with the gaseous products of liquid decomposition. In the case of fairly small and numerous pores, we can neglect the "transverse" components of liquid velocity. Note that this case is the more probable, the higher is the viscosity and the closer is the liquid to the solid. In the second variant [8] the viscosity completely suppresses the relative motion of phases. The condition $u_g=u_c=m^*/\rho$ is fulfilled, where $\rho = \rho_g\alpha+\rho_c(1-\alpha)$ is the density of the two-phase mixture and α is its porosity (volumetric gas fraction). It is reported [10] that for nitramines it is much easier to bring the experimental data into agreement with the calculations performed in terms of the first-variant model. The experimental data [12] confirm the possibility of the jet regime of gas removal from the reacting layer at the surface of some DB propellants at low pressures. It is noteworthy that this effect could be favored by a carbon carcass on their surface.

The intermediate case can be described by a semi-empirical method [10] using "floating" parameter s: $u_c = (1- s\alpha)\, m^*/\rho_c$, $u_g = (1- s\alpha+s)\, m^*/\rho_g$. In particular, with $s\to\infty$, the limiting case of the spontaneous "longitudinal" removal of the gas from liquid to surface is realized. A very fast removal of dissolved gas is possible not only by bubbles, but also by diffusion from a fairly thin liquid film. In this extreme case, we get $u_g\to\infty$. Since the mass gas flow is of finite value

and at depth x it is equal to $\rho_g u_g \alpha = \int_x^\infty w dx$ (w being the mass velocity of gas formation in liquid), $\alpha \to 0$. Thus, we get $\rho = \rho_c$. Note that the linear liquid velocity in this case decreases with approach to the surface. In the stationary case, we have $\rho_c u_c = m^* - \int_x^\infty w dx$. In [13,14] the problem statement corresponds to the case where the gaseous products of liquid decomposition are dissolved in liquid and transferred without changing its density. These concepts hold only for the small degrees of decomposition.

Subsurface vaporization

Studying combustion of vaporizing EM, one should take into account phase transitions over all interfaces including those of bubbles and droplets. In [10] for a droplet zone and in [15, 16] for the entire two-phase zone the equation is used for the non-equilibrium mass velocity of vaporization from the unit area of interface

$$m^* = \rho_g . u^{\downarrow} [p_v(T)/p - n_v] \qquad (2.1)$$

where $\rho_g . u^{\downarrow}$ is the mass flow rate of the vapor molecules per unit area of interface, $p_v(T)$ is the equilibrium pressure of saturated vapor, n_v is the mole fraction of vapor above the surface. Using of (2.1) at temperature close to the boiling point is methodically incorrect. Indeed, since $u^{\downarrow}$ is of the order of sound velocity, the deviation of the relative partial pressure from its equilibrium value $p_v(T)/p - n_v = m^*/\rho_g u^{\downarrow}$ is of the order of the Mach number. In deflagration problems, this value is much smaller than unity and thus, the vapor pressure can be considered to be equilibrium. Taking into account this small deviation may cause only small changes in the model. In other words, in the calculation procedure, Eq. (2.1) should not play the role of the key relation for calculating m* (the equation "resists" this by giving a great error at small relative errors in substituted values). As in the case of neglecting this correction, the equation should relate the values T, p, and n_v. To this end, it should be used in the form: $p_v(T)/p = n_v + m^*/\rho_g u^{\downarrow}$.

The peculiarities of heat transfer through the bubbles

In all available papers, heat transfer in the foam is considered using the expression for the "effective" coefficient of thermal conductivity constructed in terms of additivity similarly to the expression for density and capacity: $\lambda = (1- \alpha)\, \lambda_c + \alpha\, \lambda_g$. It holds for the λ_c value comparable or exceeding λ_g. However, in the case of strong vaporization into bubbles, the heat transfer does not follow the Fourier mechanism. It can be demonstrated that each bubble with strong vaporization into it is a miniature heat tube. According to [17,18], the effective thermal conductivity of heat tubes with vaporization and condensation can be 1000 times greater than that of gold. In this case more suitable is the "relay-race" model of thermal conductivity of mechanical mixture $1/\lambda = (1- \alpha)/\lambda_c + \alpha/\lambda_b$. Here λ_b is the effective thermal conductivity of bubble. Assuming that $\lambda_b >> \lambda_c$, we get $\lambda \approx \lambda_c/(1- \alpha)$.

Account of a solubility of gaseous decomposition products

Probably, this effect has been first taken into account in the model of homogeneous EM combustion [19]. According to the existing at that time notions of the high degree of burning EM dispersion, it was assumed that the burning surface (actually, dispersion surface) is located at the place where the solubility limit of the gaseous products of liquid decomposition is reached. Attainment

of an equilibrium-like condition at the burning surface as a possible triggering event for dispersion was later stated in Ref. 20.

Let us consider the appearance of the gas bubbles in a reaction layer of the condensed phase during EM combustion as sufficient condition to form the burning surface. In order to analyze the effect of solubility in the "pure" form, we also assume that the rate control stage is located in the reaction zone of condensed phase. After designating concentration of dissolved gases as a, the condition of the surface forming can be written in the form x = 0, a = a_s, where a_s - maximum (under given conditions) solubility. Heat released during decomposition of the condensed phase is consumed on the warm-up of the fresh EM from initial temperature T_0 to the surface temperature T_s. In Ref. [19], the analysis of the laws governing the combustion is carried out under the assumption that

$$c(T_s - T_0) = \varepsilon a_s \tag{2.2}$$

where a_s depends exponentially on T_s and linearly on pressure p:

$$a_s \approx p \; exp\,(L/RT_s) \tag{2.3}$$

Here L - heat of solution; ε- proportionality factor.

Substituting (2.3) in (2.2), we obtain equation for T_s

$$\pi\, c(T_s - T_0) = p\, exp(L/RT_s), \quad \pi = const.$$

Value of the surface temperature T_s uniquely determines the burning rate in the combustion model with the rate controlling condensed phase reactions. In this case

$$v = d\ln u / d\ln p = \beta(T_s - T_0), \quad \beta = d\ln u / d\ln T_0 = (E/2RT_s^2)/(1+A),$$
$$A = (L/RT_s^2)(T_s - T_0) \tag{2.4}$$
$$If \quad A >> 1, \quad then \quad v = E/2L, \quad \beta = v/(T_s - T_0).$$

In more general formulation of the problem the effect of solubility of gaseous products on the laws governing combustion was investigated by numerical method [21]. The location of the rate control zone was not preliminary assigned in this case. From the results of the numerical analysis of the problem it followed that approach presented above is valid only with a comparatively high solubility and the high magnitude of the heat of solution (L ≥ E/2, E - energy of activation of the decomposition of the condensed phase). In all remaining cases a two-phase zone (aerosol or foam) is the burning rate control stage. More precise consideration should take into account the possibility of liquid super-saturation by dissolved gas at high speed of the increase of its concentration. The nonstationary variant of the model was also discussed [22].

Necessity of considering the dissolved products diffusion.

It is expected that in some region of variations in EM parameters and external conditions, the combustion regimes are possible in which the gaseous product of liquid decomposition dissolved in the liquid is removed to the burning surface by molecular diffusion without forming any bubbles so that the product concentration profile is formed with a maximum inside the liquid layer. It is known that in liquids, the diffusion coefficient D_c positively depends on temperature. In this particular case, D_c is very small and diffusion provides the effective removal of dissolved gas only from a fairly thin liquid film. In experiment [23] no bubbles were observed to form in the polymer film on the surface of the metallic disc heated to 430°C if the film thickness did not exceed 10-20 μ. Since the zone thickness of the liquid-phase reactions of burning EM can be of this order of magnitude, the combustion regime with the diffusion removal of gas is quite possible. In

[23], for the bubble nuclei, it is assumed that $d \approx 30A^{\circ}$. The dissolved gas molecules have $d \approx 3\text{-}5$ A° [24]. Therefore, the molecules diffuse and are removed from the surface much more rapidly than the bubbles. In other words, a sufficiently effective diffusion does not remove bubble nuclei from the film. It just eliminates the cause of their appearance.

Let us find out how the above possible absence of bubbles in the liquid-phase zone with thickness x^* depends on pressure. The time of the diffusion removal (with diffusion coefficient D) of the dissolved gaseous reaction products $(x^*)^2/D$ must be shorter than the residence time of reacting liquid in this zone (x^*/u_c). So that the condition for the absence of bubbles is $D(T_s) > x^*u_c$. Let us estimate the pressure-dependence of both of the inequality sides. We use the above $D(T) \sim \exp(-E_D/RT)$ and the Clayperon-Clausius relation on the surface $\exp(-\mu L/RT_s) \sim p$, where μL is the thermal effect of vaporization, cal/(mol K). Then, we get $D(T_s) \sim p^a$, $a = E_D/\mu L$. For EM of the hexogen and octogen type, $\mu L \sim (20\text{-}30)\ 10^3$ cal/mol. The E_D value was experimentally obtained to be about 14500 cal/mol for oxygen diffusion in polyvinylacetate [24]. Since size d of the molecules of the gaseous products of initial decomposition is greater than that of oxygen and the condition $E_D \sim d^2$ is satisfied, it is stated that $D(T_s)$ has the exponential positive dependence on P with index $a > 0.5$. It can be shown that the u_cx^* value logarithmically depends on pressure. Since the exponential dependence at large arguments is stronger, it is concluded that no bubbles can be observed at fairly high pressure.

Bubbles, their evolution and interaction

When the dissolved product concentration exceeds the limiting one, the gas bubbles arise within the liquid-phase reaction zone that violates the one-dimensionality pattern. Owing to the inevitable concentration inhomogeneities, the nuclei appear discretely rather than uniformly on some plane. In this case, the diffusion carries away the dissolved intermediate product to the bubble, decreasing thus the saturation degree and preventing the appearance of close neighbours.

Let us discuss the evolution of bubbles and the possibility and ways of local averaging of variables over space and time. In the burning foam there is a size-distribution of bubbles, because the appearance of large bubbles is followed by the appearance of the small ones. The initial reason for both of the processes is gasification (chemical decomposition of liquid and its vaporization). Examining the liquid element with bubbles, it is easily envisioned that the bubbles grow with gasification conserving their shape and number until coming into contact with the neighbouring bubbles. Thereafter, the two-phase medium becomes the multiple foam. The further ingress of gas with conservation of the number of bubbles causes their elongation along the normal to the burning surface, which contradicts the principle of surface energy minimum. This principle makes the bubbles join. Appearance of the new small bubbles between the large ones is related to the rise in temperature of the foam element approaching the surface. The temperature rises due to exothermic reaction and heat supply from the flame. In this case, the gas formation rate increases in the "Plateau channels", i.e., the most thick liquid formations between the bubbles. Their thickness, which at smaller reaction rate allowed one to remove the gaseous reaction products by diffusion to the neighboring bubbles, is now excessive and the new bubbles arise in the "channels". The above arguments assume the foam motion and swelling according to [8] without pronounced interface movements, which is typical of the "true" multi-layer foam with a relatively small temperature drop on each bubble. When the bubble size is comparable with that of the entire reaction

zone, this distorts the bubble form and becomes one of the reasons for the relative motion of phases. The matter is that the liquid viscosity μ and surface tension σ are temperature-dependent. The Marangoni effect is known, i.e., the motion of a bubble toward decreasing σ. When σ does not noticeably change along the bubble surface, this motion can occur without changing its form. In the case of a change, the bubble will become pear-shaped in accordance with the Laplace formula. When μ also noticeably changes along the bubble surface, it will expand toward lower viscosity with further ingress of gas, i.e., the elongated end of the "pear" will move faster to the burning surface. This case resembles the jet regime and differs from it by the impulsive behavior of the elongated bursting bubbles.

Bubble-induced mixing

At the "hot" boundary of the foam, each bubble is eventually destroyed. This is followed by the liquid pulsations, i.e. fast local movements of the environment occupying under surface tension a free place with a scale of the order of the diameter of the burst bubble. Thus, the bursting bubbles can mix the foam. The second reason for mixing is the motion of bubbles to the surface under the Marangoni effect (see [25]) and the Archimedes force. In this case, the presence of bubbles of different size considerably enhances the mixing which sharply intensifies the heat- and mass-transfer. In particular, the convective diffusion can remove the liquid-dissolved gas from the reaction zone more effectively that restricts the bubble formation and growth. The above arguments are concerned with a homogeneous monopropellant. Similarly to [26], it is established that the passage of any inhomogeneity to the melting surface favors either the appearance or intensification of turbulence in the liquid-phase reaction zone. The visual observations [6] have revealed convection in the melted layer of the burning DINA, namely the laminar one in the transparent part of the layer close to the solid phase and the turbulent one in its nontransparent subsurface part. In [6], the bubble size was smaller than the size of mixing zones and thus, the use of the continual approach became possible. Transition to more infusible EM (octogen) and high pressures allows one to eliminate the dependence of combustion characteristics on the orientation of the burning surface relative to gravity. In this case, however, there are some problems with simulation due to poor foundation of the continual approach. An increase in pressure leads to a substantial decrease in bubble size R_b because the size of the liquid-phase reaction zones decreases by an order of magnitude upon transition to pressures of tens of atm. As R_b decreases, the components of bubble velocity also decrease under the Marangoni ($\sim R_b$) and Archimedes ($\sim R_b^2$) forces. Since the intensity of bubble removal relative to the liquid decreases near the surface, the bubbles just grow and burst. The case is realized where the linear velocity of bubble increase is much higher than that of burning (the velocities of bubble transfer by liquid in the system connected to the burning surface) so that no followers are formed during bubble lifetime; the "one-layer" foam is realized. In this case, the greatest bubble size is of the order of the reaction zone thickness and the question arises of the validity of the continual approach. In a similar case for AP, it was used, with certain limitations, the one-dimensional stationary approach and was obtained the efficient combustion model neglecting even bubbles. The same was realized in [10]: a one-dimensional model was used mentioning, however, that the bubble size can be of the order of the two-phase zone thickness.

Estimation of mixing

Let us assume that the general pattern on the surface differs in different sites only by a shift in time from that on a particular region (circle, square) with a typical size equal to the diameter of a

bursting bubble. It is suggested that for above reasons, this bubble has grown only toward the burning surface so that the babble diameter coincides with distance x from the burning surface to the place of bubble origin. In this case, we have neglected the relative size of the bubble part "protruding" above the surface. Since the diffusion coefficient can be interpreted as a ratio of pulsation size square and its period, we get $D_c \sim \bar{x}^2/\bar{t}$. The pulsation frequency $\bar{t}^{-1}$ is given as a ratio of the second volumetric gas flow rate through the region under study (area $\sim\bar{x}^2$) to the bubble volume $\sim\bar{x}^3$, $\bar{t}^{-1} \sim \bar{x}^2\bar{V}/\bar{x}^3 \sim \bar{V}/\bar{x}$, where $\bar{V}$ is the volumetric gas flow rate (bubbles) per 1 cm^2 of the surface, cm/s. Consequently, we get $D_c \sim \bar{x}\ \bar{V}$. The dependence of D_c on the coordinate can be taken into account by introducing, e.g., a decrease of D_c to 0 at a distance $\bar{x}$. It is interesting to compare the convective additive to the D_c transfer coefficient with the "molecular" temperature diffusivity of the liquid phase $(\lambda/c\rho)_c \approx 0.001$ cm^2/s. When the reaction is effective enough, the V value is the product of the linear velocity of gas flow from the surface by the depth of subsurface decomposition. According to [11], for hexogen or octogen, this can give several tens of cm/s at atmospheric pressure. If in this case, thickness $\bar{x}$ is of the order of 10 μm, then on the surface the convective thermal conductivity caused by bursting bubbles, is tens times more effective than the molecular thermal conductivity. However, as the pressure rises, $\bar{x}$ and $\bar{V}$ decrease with the efficiency of heat removal from the zone of liquid-phase reactions. As a result, at high pressures, the temperature maximum is likely to arise in the liquid-phase reaction zone, which causes instability [14].

Equilibrium conditions on the surface.
In the case of multicomponent mixture of liquid components the equality takes place on the surface of the chemical potentials or the fugacity f of the both phases for each component [28].

$$f_{i,g} = \varphi_i x_{i,g} p = f_{i,liq}; \quad f_{i,liq} = \gamma_i x_{i,liq} p_{i,liq}; \quad \sum x_{i,g} = 1; \quad \sum x_{i,liq} = 1 \qquad (2.5)$$

Here $x_{i,g}$ and $x_{i,liq}$ are the molar fractions of components near interface from the side of gas and liquid, respectively; φ and γ are the coefficients of fugacity and activity related to the non-ideality of gas mixtures and solutions. Deviation of the values for coefficients φ and γ of unity can be essential under conditions of high pressures and low temperatures. For simplicity, one may take $\varphi = \gamma = 1$. Further, one may also assume that the pressure in the liquid approximately equals the pressure of saturated vapor of its component and can be calculated by $p_{i,liq} \sim B_i \exp(L_i/RT)$. It means that we neglect the energy expenses on formation of gas nuclei in a liquid layer as well as contribution of the recoil force applied to the liquid surface. The equation of mechanical equilibrium for the liquid surface is derived from Eq.2.5:

$$\sum x_{i,g} \left(p_{i,liq}\right)^{-1} = p^{-1} \qquad 2.6$$

Strong dependence of $p_{i,liq}$ on temperature makes it possible to neglect by all terms in the left hand side of expression 2.6, excepting the main one that corresponds to the component with the highest boiling temperature. Note that when pressure changes, the boiling temperature changes as well. Regarding the pressure dependence, the component's temperature order may change by places. Therefore, changing pressure can lead to changing the component in the liquid mixture, which determines the mixture boiling point.

Let we demonstrate how to use expression (2.5) in the case of two-component system. If the closed vessel is partially filled with two-component mixture having molar fractions $x_{1,liq}$ and $x_{2,liq} = 1-x_{1,liq}$, the gas phase easily reaches equilibrium in the form:

$$x_{1,g}\, p = x_{1,liq}\, p_{1,liq}, \quad x_{2,g}\, p = x_{2,liq}\, p_{2,liq}, \tag{2.5'}$$

Further, let the vessel becomes open and the gas mixture with another parameters p', $x'_{1,g}$ and $x'_{2,g}$ starts to flow above the liquid surface. Obviously, the parameters of the components inside thin subsurface liquid layer begin to adjust to the gas parameters and process of re-arrangement of temperature and concentration profiles will propagate into the bulk of liquid. The speed of this process can be significantly enhanced by the convection. During the process an "excessive" component is delivered to the surface and evaporated while "deficient" one is condensed from the gas phase and transported into the bulk of the material. It has been proposed in Ref. [29] that above mechanism provides decrease in the volume content of easy volatile components in subsurface layer of multi-component liquid drops suspended in the hot gas stream. This leads to overheating the central core of drop that may cause experimentally observed burst of drops in gas streams.

Similar phenomena can occur in combustion of molten energetic materials but in this case stationary waves of the liquid parameters variation can be observed. Here in the contrast with above case the reason for permanent difference between parameters of gas and liquid component on different sides of interface is the flame reactions and corresponding heat and mass feedback to the burning surface. Note that for some easily melted energetic materials the processes in thick liquid layer can be accompanied by macro-scale convection [4].

It should be underlined that expression (2.5) can be also written in different of relation (2.6) form, namely [30]:

$$\sum x_{i,liq}\, p_{i,liq} = p \tag{2.7}$$

It is convenient to use that expression when the values of $x_{i,liq}$ are a priori known, e.g., if there is no reactions and diffusion in subsurface layer. However, it is doubtful using (2.7) in real situation with the presence of chemical and physical processes. In addition, use of (2.7) is difficult in the case of mixture with most easy volatile components. In calculations it leads to uncertainty of $0 \times \infty$ type resulting in large computational error. Note that the use of expression (2.6) instead of (2.7) gives advantage in case of rate control gas phase reactions when the reactions within the liquid diffusion zone $(0, z_d)$ can be neglected. If one assumes additionally that this zone is relatively thin (diffusion relaxation time $t_d = z_d/u$ less than the thermal relaxation time $t_{th}=\lambda_c/c\rho_c u^2$), the processes in the condensed phase can be treated without taking into account change in the heat and species fluxes across the liquid diffusion zone. In the gas phase, the values of $x_{i,g}$ can be found from the solution of the problem describing reactions, diffusion and heat propagation in the region $z < 0$. As the boundary conditions one may use the heat balance at the surface ($z = 0$)

$$-\lambda_g \frac{\partial T_g}{\partial z}(-0) = -\lambda \frac{\partial T_c}{\partial z}(+0) + m\sum_i x_{i,liq}(+0) Q_i \tag{2.8}$$

and mass fluxes balance ($z = 0$)

$$-m x_{i,g}(-0) - D_g \frac{\partial x_{i,g}}{\partial z}(-0) = -m x_{i,liq}(+0) \tag{2.9}$$

Here m is the mass flow rate and Q_i is the heat of gasification, which is closed to the experimental value of evaporation heat. Detailed expressions in the form of (2.5) are not needed now because in the thin liquid diffusion zone the components ratio practically does not change and to close the problem formulation one needs only to calculate the vapor pressure for component with the highest boiling temperature.

Equations (2.8) and (2.9) do not include terms with heterogeneous heat release and multicomponent diffusion, which may become important for the gas mixture with strong difference in component's molecular mass. In the condensed phase, the problem is considered for the heat propagation without diffusion. If it turns out that the effects of the reactions and thermal relaxation in a liquid diffusion layer could not be neglected, the problem formulation has to be extended. In this case equation (2.9) takes the form

$$-mx_{i,g}(-0) - D_g \frac{\partial x_{i,g}}{z}(-0) = -mx_{i,liq}(+0) - D_{liq} \frac{\partial x_{i,liq}}{\partial z}(+0) \qquad (2.10)$$

and expression (2.5) should be included in the problem formulation.

2.1 – REFERENCES

1. **C. Guirao, F.A. Williams**. "A model for ammonium perchlorate deflagration between 20 and 100 atm", *AIAA Journal*, 1971, No.7, 1345-1356.
2. **Yu.Ya.Maksimov**, *Trudy MKhTI*, Proceedings of the Moscow Chemical Technology Institute, Moscow, 53,73, 1967 (R).
3. **A.A Zenin**. "HMX and RDX: combustion mechanism and influence on modern double-base propellant combustion". *Journal of Propulsion and Power*, 1995, V.11, No.4, 752-758.
4. **V.V.Aleksandrov, A.V.Boldyreva, V.V.Boldyrev and R.K.Tukhtaev**," DINA combustion at atmospheric pressure", *Combustion, Explosion, and Shock Waves*,1973, No.1, pp. (R) 140-142.
5. **A.G.Arkhipov and A.P.Denisyuk**,"Influence of catalysts on temperature coefficient...", *Combustion, Explosion, and Shock Waves*, 1990, No. 5, pp. (R) 65-69.
6. **R.K.Tukhtaev**,"Study of the mechanism of the action of acatlytic additives...". Candidate Thesis, Novosibirsk, IKhTIMS, 1976 (R).
7. **E.Yu.Orlova**, Chemistry and tecnology of high explosives. L.,"Khimiya", 1973 (R).
8. **E.I.Maksimov and A.G.Merzhanov**, "On the theory of condensed substance combustion". *Combustion, Explosion, and Shock Waves*, 1966, No.1, pp. (R) 47-58.
9. **S.B. Margolis, F.A. Williams, R.C. Armstrong**. "Influences of two-phase flow in the deflagration of homogeneous solids". *Combustion and flame*, 1987, V.67, No.3, 249 -- 258.
10. **S.C. Li, F.A. Williams, S.B. Margolis**. "Effects of two-phase flow in a model for nitramine deflagration". *Combustion and flame*, 1990, V.80, No.3, 329 -- 349.
11. **S.B. Margolis, F.A. Williams**. "Effect of two-phase flow on the deflagration of porous energetic materials", *Journal of propulsion and power*, 1995, V.11, No.4, 759-768.
12. **V.E.Zarko, V.Ya.Zyryanov and K.P.Koutzenogii**. *Arvhivium combustionis*, 1984, t.4, No.2.
13. **V.E. Zarko, L.K. Gusachenko, A.D. Rychkov**. "Simulation of combustion of melting energetic materials", *Defense Science Journal* (India),1996, V.46,No.5, pp.425-433.

14. **L.K.Gusatchenko, V.E.Zarko and A.D.Rychkov**, Instability of combustion model with vaporization on the surface and overheating in the condensed phase. *Combustion, Explosion, and Shock Waves*, 1997, 1.
15. **Y.--C. Liau, V. Yang**. "Analysis of RDX monopropellant combustion with two--phase subsurface reactions". *Journal of propulsion and power*, 1995, V.11, No.4, 729-739.
16. **J. Davidson and M. Beckstead**. "Improvements to RDX combustion modeling", *AIAA 96-0885*.
17. **P.Dan and D. Ray.** Heat tubes, M., 1979.
18. Physical encyclopedic dictionary. M., Sovetskaya Entziklopediya, 1983, p.745 (R).
19 **A. D. Margolin, P. F. Pokhil**. Effect of pressure on the rate of processes in a reaction lay r of the condensed phase of the burning propellant. *Reports of the USSR Academy of Sciences,* 1963, Vol. 150, pp. 1304-2306 (R).
20. **F.A. Williams,** Combustion Theory, 2nd Edition. The Benjamin/Cummings Publishing Company, Inc., 1985.
21. **O.B.Yakusheva, E.I.Maksimov, and A.G.Merzhanov**, The influence of the solubility of gaseous decomposition products on the regularities of condensed substance combustion", *Combustion, Explosion, and Shock Waves*, 1966, No.3, pp. (R) 125-129.
22. **L.K.Gusachenko**. On the problem of nonsteady-state combustion rate. *IFZh*, 1966, V. 11, No. 4 (R).
23. **O.F.Shlenskii and D.N.Yundev**. The effect of a decrease in the intensity of nucleus formation in thin liquid films and its application for studying the properties of overheated substances". *TVT*, 1994, V.32, No.1, 139-141 (R).
24. **D.W. Van Krevelen**. Properties of polymers correlations with chemical structure. Elsevier, 1972.
25. **L.K. Gusachenko and V.E. Zarko**. The Marangoni effect upon combustion of energetic materials with a liquid layer on the surface". *Combustion, Explosion, and Shock Waves*, 1996, No.2, pp. (R) 141-142.
26. **V.Ya.Zyryanov, V.M.Bolvanenko**, O.G.Glotov, and Y.M.Gurenko."Turbulent model of solid propellant combustion". *Combustion, Explosion, and Shock Waves*, 1988, No.6, pp. (R) 17-26.
27. **V.E. Zarko, L.K. Gusachenko, A.D. Rychkov**. The effect of phase transitions on combustion stability of melted energetic materials. In: Combustion and Detonation (proceedings of 28th Int. Annual Conf. of ICT). 1997, Karlsruhe, FRG.
28. M.Kh. Karapet'yants, Chemical Termodynamics, Moscow, Khimiya, 1975, pp. 141-148 (R)
29. **C.K. Law,** "Internal Boiling and Superheating in Vaporizing Multicomponent Droplets, *AIChE Journal*, V.24, No. 4, 1978.
30. **L.K. Gusachenko, V.E. Zarko, V.Ya. Zyryanov et al.**, Modeling the Combustion Processes Processes of Solid Propellants, Novosibirsk, Nauka, 1985, pp. 60-63 (R).

2.2 COMBUSTION OF NITRAMINES

2.2.1 Thermal decomposition kinetics.

Nitramines have been used as explosives in mining, artillery, and engineering over a long period of time. In the last two decades, considerable interest in nitramines has been expressed by the developers of propellant compositions for gun systems and rocket motors, i.e. solid propellants (SP). As SP component, nitramines have a number of useful properties, such as high density, high combustion temperature, and weak radiation absorption by the combustion products. Because of new practical demands, recent studies have been directed to the detailed mechanism of thermal decomposition at various heating rates, including rates comparable with the heating rate of a substance in a combustion wave. This required a serious effort to develop effective methods of kinetic studies. As a result, considerable progress toward an understanding of the chemical mechanism of nitramine decomposition and combustion has been achieved. It should be mentioned that the relative simplicity of the chemical structure of nitramines compared with other monopropellants (substances that are capable of burning independently in an inert medium) was a reason for the considerable interest in the basic investigation of their chemical transformations. However, because of significant technical difficulties, the thermal decomposition of nitramines has not yet been clearly understood, and the work along this line is underway.

The great body of available information requires generalization and analysis. Such work was partially carried out in [1-3]. However, since the publication of these papers, a considerable body of new data has been obtained. Therefore, it is justified an attempt to give a survey of the state-of-the-art in studies of the thermal-decomposition kinetics of nitramines. As the subject, we chose the cyclic nitramines that have been most widely used in practice: RDX (cyclotrimethylenetrinitramine) and HMX (cyclotetramethylenetetranitramine).

Physical properties

Table 2.1 gives thermophysical characteristics taken from different literature sources [4-10].

Table 2.1. Thermophysical characteristics of RDX and HMX.

Matter	ΔH^0_f	Q_m	T_m	ρ_{20}	$C_{p,l}$	$C_{p,s}$	λ_s
RDX	20.1 [4] 21.3 [5] 14.71[9,10]	8.52 [6] --- ---	478 [5] 477 [3] ---	1.816 [5] 1.806 [2] ---	0.45 [4] --- ---	0.32-0.45 [4] --- ---	0.0004 [7] --- ---
HMX	17.9 [4] 17.1-17.92 [5] 17.96 [9] 11.3 [10]	11.4 [6] --- --- ---	554 [4] 553 [8] --- ---	1.91 [4] 1.92 [8] --- ---	--- --- --- ---	0.43 [4] --- --- ---	0.0009 [7] --- --- ---

Note. The reference numbers are enclosed in square brackets.

Here ΔH^0_f is the enthalpy of formation at 298 K, kcal/mol; Q_m is the heat of melting, kcal/mole; T_m is the melting point (melting with decomposition), K; ρ_{20} is the density at 20 °C, g/cm^3; $c_{p,l}$ is the heat capacity of the liquid phase, cal/(g K); $c_{p,s}$ - heat capacity of the condensed phase, cal/(g K); and λ_s is the thermal conductivity of the condensed phase, cal/(cm sec K). Evidently,

the enthalpies of formation have the widest scattering, since their determination requires very accurate measurements.

Temperature dependencies for the heat capacities of the condensed and liquid phases of RDX are given: $c_{p,s}$ = 0.0389 + 0.0007 T [11], $c_{p,s}$ = 0.235 + 0.00068(T-273) [12]; $c_{p,l}$ = 0.258 + 0.00086(T-273) [12].

We assume that the surface evaporation of pure nitramine obeys the Clausius--Clapeyron law in the form log p_s = A - L/(4.575 T_s), where A = const , p_s is the equilibrium vapor pressure above the surface of the substance, L is the latent heat of sublimation (or evaporation at $T_s > T_m$), and T_s is the surface temperature. The phase-transition temperatures are related by [13]

$$L_{subl} = L_m + L_{vap} \qquad (2.11)$$

Experimental determination of p_s over a wide temperature range involves fundamental technical difficulties because of the intense decomposition of nitramines at elevated temperature. The quantity L_{subl} can be determined most reliably, and the quantity L_{vap} can be estimated by Eq. (2.11). In this case, one should bear in mind that, at a high surface temperature, the thermal-decomposition products dissolved in the melted layer decrease the nitramine-vapor pressure. Hence it follows that the heat of evaporation at temperatures close to the boiling point cannot be determined with high accuracy, and this is actually evidenced by the data in Table 2.2.

Note that one of the world's first studies [14] on determination of the heats of evaporation of explosives was reported by A. F. Belyaev in 1940. In a more recent paper [15], he reported that the most probable heat of evaporation and boiling point (p = 1 atm) for RDX are equal to 26 kcal/mol and 340 °C, respectively, but remarked that these data are not sufficiently reliable. In the accurately performed investigation of Maksimov et al. [16], it was established that T_b = 664 ± 33 K (T_b is the boiling point) and L_{vap} = 22.5 ± 0.5 kcal/mol for RDX and T_b = 744 ± 37 K and L_{vap} = 27.6 ± 1 kcal/mol for HMX.

HMX is known to have four polymorphic solid-state modifications: α, β, γ, and δ [2], which are stable at T= 115 - 156, 20 - 115, ≈ 156, and 170 – 279 °C, respectively. The densities of the corresponding HMX modifications are given in Table 2.3.

Table 2.2. Parameters of the evaporation law $p_s = A - L/4.575T_s$ (p, Torr)

Matter	T_s, K	A	L, kcal/mol	Regime	Ref.
RDX	329-413	14.4	31.5	Subl.	[15]
	329-413	14.4±0.6	31.5±0.5	>>	[17]
	328-371	14.2	31.1	>>	[19]
	<470	14.9	32.0	>>	[3]
	505-520	10.6	20.3	Evap.	[18]
	>478	10.3±0.6	22.5±0.5	>>	[16]
HMX	<550	14.9	38.4	Subl.	[3]
	370-487	17.6	44.3	>>	[15]
	370-402	16/2	41.9	>>	[19]
	370-487	17.6±1.9	44.3±0.7	>>	[17]
	>555	13.9	27.9	Evap.	[20]
	>553	11.1±1.9	27.6±1	>>	[16]

Table 2.3. Density of different polymorphic modifications of HMX

Phase	β	α	γ	δ
ρ, g/cm^3 [2]	1.903	1.87	1.82	1.78
ρ, g/cm^3 [8]	1.92	1.87	1.82	1.76

The thermodynamic parameters of the phase transition of HMX $\beta \rightarrow \delta$ at T = 175 – 200 °C and p = 0.1 – 6.9 MPa are as follows: enthalpy $\Delta H_{\beta\rightarrow\delta}$ = 2.41 kcal/mol and entropy $\Delta S_{\beta\rightarrow\delta}$ = 5.59 cal/mol. The p - T phase diagram for the liquid and condensed phases of RDX (α, β, and γ modifications) is given in [21]. According to [21], at p < 30000 atm the α modification is the main for condensed phase of RDX. Its density at room temperature is equal to 1.806 g/cm^3.

Condensed-phase thermal decomposition of nitramines at the temperatures below the boiling point.

Suryanarayana et al. [22] studied, at T = 230, 254, and 285 °C, the thermal decomposition of HMX whose NO_2 groups contained 99 % nitrogen isotope N^{15}. Using mass spectroscopy at T = 230°, they obtained the following main components: N_2O (40 %), NO (9.9 %), N_2 (9.6 %), HCN (4.5 %), CH_2O (22.9 %), CO_2 (8.5 %), and CO (4.1 %). The nitrogen-containing compounds were primarily in the form $^{14}N\,^{15}NO$, ^{15}NO, $^{14}N\,^{15}N$, and $HC\,^{14}N$.

The composition of the decomposition products of "labeled" (i.e. containing ^{15}N atoms) HMX and RDX is given in [23]. The thermal decomposition was performed in a reactor with a volume of 380 cm^3 in argon at T = 230 – 285 °C and at p = 40 torr. The sample weight was 50 mg. The content of compounds with the given types of nitrogen atom in the decomposition products [23] is given in Table 2.4. From the experimental data of Suryanarayana et al. [22, 23] the following conclusions can be drawn: the break of the C—N bond dominates over the break of the N—N bond, NO is formed from the nitrogen of the nitrogroup (NO_2), almost all N_2O and N_2 species are formed without break of the nitramine N—N bond, and HCN is formed from the "ring" nitrogen.

Table 2.4. Content of compounds, containing ^{15}N, in decomposition products of nitramines

Matter	T, °C	$^{14}N^{15}NO$	$^{14}N^{15}NO$	^{15}NO	$HC^{14}N$
HMX	230	98	93-100	93-100	100
HMX	254	98	92	95-100	100
HMX	285	98	95	95-100	100
RDX	190	99	99	95-100	100

The decomposition mechanism of HMX proposed in [22] includes the break of four C—N bonds with the formation of four CH_2NNO_2 molecules, which then decompose into CH_2O and N_2O. Goshgarian [24] studied the decomposition of HMX and RDX at temperatures lower and higher than the melting point in vacuum and in a flow reactor in a hot helium stream at p = 1 atm. In the thermal decomposition of HMX in a flow reactor at T = 240 – 290 °C, a mass spectrometer recorded intense peaks with m/e = 30 (CH_2O, NO), 44 (N_2O, CO_2, CH_2NO), 28 (N_2, CO, H_2CN), 27 (HCN), 18 (H_2O), and 46 (NO_2), while peaks with m/e = 70 (C_2H_2NNO, $C_2H_2N_2O$) and 75

(CH_2NHNO_2, CH_3NNO_2, CH_2NNO_2H) were recorded only at T = 270 – 290 °C. Fragments with large molecular masses were also observed: M = 120 ($CH_2N_3O_4$), 128 ($C_3H_4N_4H_2$), and 148 ($C_2H_4N_2N_2O_4$). The appearance of these fragments was associated with the possible formation of HNO_2. The peaks with m/e = 175, 128, and 81 indicate the possibility of elimination of HONO from RDX and from the HMX fragment with M = 222. The formation of the fragment with M = 128 from the fragment with M = 222 is postulated in [24].

Goshgarian [24] proposed several schemes of nitramine decomposition. The HMX decomposition at low temperatures leads to the elimination of CH_2NH_2 and NO_2 (which gives M = 176). At high temperatures, the elimination of CH_2NNO_2 dominates, and the spectrum is similar to that of the RDX. For RDX, it is postulated that the elimination of NO_2 proceeds at low temperatures and the scission of the ring with elimination of CH_2NNO_2 (this gives M = 148) proceeds at high temperatures. Schroeder [25] examined the scheme of decomposition of RDX that included scission of the bond N-NO_2 with formation of NO_2 and fragment of RDX followed by decomposition of fragment with formation of CH_2N^* and $H_2C{=}N\text{-}NO_2$

Farber and Srivastava [26, 27] studied the thermal decomposition and sublimation of nitramines at p = 10^{-5} – 10^{-3} atm. In the thermal decomposition of RDX at 220 °C, peaks with m/e = 28, 30, 40, 44, 46, 56, 74, 82, 83, 102, 120, 128, 132, and 148 were observed. The peaks with m/e = 74 and 148 were assigned to the initial fragmentation of RDX with the formation of CH_2NNO_2. The peaks with m/e = 128, 82, and 83 were attributed to a competing process involving elimination of NO_2 and H from the RDX molecule (HONO formation). The peaks with m/e = 102 and 56 are associated with the subsequent elimination of NO_2 from the fragment with M = 148, whereas the migration of NO_2 in this fragment causes elimination of CH_2N and explains the formation of the peak with m/e = 120. One of the major products of HMX decomposition at 175 – 275 °C was a $C_2H_4N_4O_4$ molecule (M = 148). Components were also recorded at m/e = 222, 128, 120, 102, 74, 56, 46, 32, 30, 28, and 18.

The peaks with m/e = 120 ($CH_2N_3O_4$) and 128 can also be attributed to reactions of gaseous products with the condensed phase. Farber and Srivastava [27] also detected peaks with m/e= 249 and 250 and concluded that nitrous acid NHO or NO_2 should also form.

The peak with m/e = 120 was postulated previously [28] to be the result of migration of the NO_2 group in the molecule with saturated bonds (fragment of division of HMX by two equal parts with m/e 148). Morgan and Bayer [29], using electron spin resonance (ESR), detected large amounts of H_2CN^* and NO_2 radicals in the HMX pyrolysis products at 260 °C. As the temperature increased to the melting point, the H_2CN^* concentration decreased abruptly.

The effect of experimental conditions on the results of kinetic studies has been widely discussed in the literature on thermal decomposition. The differences in mass and geometrical dimensions of samples and reactions on the walls and in the volume of a vessel lead to the so-called "compensation effect," i.e., for a given substance, the activation energies and pre-exponents determined by different investigators are in direct relation: the higher the activation energy, the higher the preexponent. An example of the kinetic compensation effect for the homolytic decomposition of dimethylnitramine is given in [30]. No theoretical ground for this effect is available. Note only that in experimental studies within a comparatively narrow temperature range, one can determine

reliably only the average reaction-rate constant. Extrapolation of the kinetic data beyond the narrow temperature range leads to significant errors in the calculation of the chemical reaction rate.

Oxley et al. [31] undertook an attempt to eliminate side effects in nitramine decomposition. Isothermal decomposition was studied at 189 – 289 °C (HMX) and 200 – 240 °C (RDX) in an acetone solution at a concentration of the substances not higher than 1 %. These conditions prevented intermediate radical reactions and auto catalysis. For comparison, experiments were performed on the decomposition of 0.2 g samples of the powdered pure substances at 200 – 250 °C (RDX) and 230 – 270 °C (HMX). Interestingly, in nitramine decomposition in low-concentration solutions, the number of moles of the gaseous products formed was 3--4.5 times smaller than in the decomposition of the powdered substances. Special experiments showed that the primary decomposition of the RDX condensed phase is described by a first-order equation, and the decomposition rates for the powder and solution are approximately the same at fixed temperature. The significant difference in composition and amount between the decomposition products is due to the different reaction pathways. In particular, in the decomposition in solution, the observed amount of the mononitroso derivative of RDX is 3--4 times larger than that in the decomposition of the powdered substance. Analysis of the kinetic data and the composition of the decomposition product led to the conclusion that the initial step of the decomposition of RDX and HMX involves homolytic break of the N-NO_2 bond. In addition, the important role of the intramolecular transition of hydrogen is noted. The joint progress of these reaction steps leads to dissociation of the ring structure of the nitramines.

It is interesting to note that Oxley et al. [31] did not detect NO and NO_2 traces in the products of complete decomposition of RDX and HMX, whereas these traces were recorded in [32--34]. Rauch and Fanelli [32] proposed an original treatment of the decomposition mechanism of RDX. They detected small amounts of nitrogen dioxide NO_2 in the decomposition of molten RDX at 212 °C. The NO_2 yield did not depend on the sample weight and increased in proportion to the reactor volume. The yield of the remaining products did not depend on the sample weight and the reaction volume. This indicates that NO_2 is formed in the gas-phase decomposition, and the remaining products are formed primarily in the liquid phase. The authors conclude that the scission of the N—NO_2 bond proceeds exclusively in the gas phase.

It is of interest to compare the data of different authors for the composition of the gaseous products of nitramine decomposition in the liquid phase. This comparison is given in Table 2.5. It follows from Table 2.5 that the amount of gaseous products increases with increase in the degree of decomposition of the starting substance in going over from RDX to HMX. The difference in the qualitative composition of the products can be attributed to the temperature effect, and also to the difference in sample weight (recall that minimum weighted samples were used in [31]) and in geometrical dimensions of the vessels.

Table 2.6 gives the composition of the products from the thermal decomposition of RDX at 195 °C determined experimentally in [35]. In these cases, NO_3, NO_2, and H_2O are also presented.

In studies of the reaction rate, it was found that a change in sample volume by a factor of 10 does not change the decomposition rate for a constant reactor volume. However, the decomposition

rate is directly proportional to the reactor volume. It is concluded that the gas-phase decomposition of RDX is of significance in the initial stage.

Table 2.5. Composition of gaseous decomposition products in moles per 1 mole of decomposed nitramine.

Matter	α, %	T,°C	Composition									Ref.
			N_2	N_2O	NO	H_2CO	CO	CO_2	HCN	NO_2	Sum	
RDX	100	206	1	0.95	0.98	trace	0.76	0.89	0.23	---	4.81	[34]
	19	212	1.08	1.22	0.23	trace	0.41	0.54	0.03	trace	3.51	[32]
	93	212	0.99	1.36	0.45	0.97	0.52	0.61	---	trace	4.9	[32]
	100	240	1.37	1.24	---	---	0.88	0.86	---	---	4.35	[31]
	100*	240	0.49	0.04	---	---	0.26	0.15	---	---	0.94	[31]
	30*	240	0.39	0.13	---	---	0.22	0.13	---	---	0.87	[31]
HMX	100	285	0.93	1.6	1.2	0.86	0.42	0.3	---	---	5.31	[23]
	100	300	0.8	1.72	2.4	1.44	0.24	0.16	---	---	6.76	[33]

Note. α corresponds to the degree of nitramine depletion; the asterisk denotes a 0.75 % solution of RDX in acetone.

Table 2.6.Composition of gaseous decomposition products of RDX at 195 ^{0}C in dependence of the vessel volume V and depletion degree α.

V, cm^3	α, %	Composition, mol/mol									
		N_2	N_2O	NO	H_2CO	CO	CO_2	HCN	NH_3	HCOOH	Sum
150	5	0.83	1.4	0.86	1.1	0.2	0.5	trace	0.83	0.93	6.65
868	9	0.65	0.92	1.3	1.2	0.16	0.3	trace	0.69	0.6	5.82
150	92	1.26	1.08	0.51	1.04	0.36	0.7	trace	0.34	0.37	5.66

Cosgrove and Owen [36] studied the effect of the composition of the gas medium on the decomposition rate of RDX. N_2, N_2O, CO, and H_2O turned out to inhibit the decomposition of RDX. An NO additive decelerates the decomposition as compared with other gases, and CH_2O accelerates the decomposition.

Robertson [37] measured the decomposition products of liquid RDX at 225 and 267 ^{o} in nitrogen (a pressure of 60 torr was used to inhibit the evaporation process). N_2, N_2O, NO, CO_2, CO, and H_2 in descending order, and also significant unmeasured amounts of CH_2O and H_2O were detected. The same products were found for HMX at 280 °C. NO_2 formation was not observed. The large amounts of CH_2O and N_2O are evidence in favor of the mechanism including transfer of an O atom to the neighboring CH_2 group with the subsequent elimination of CH_2O.

High-temperature pyrolysis of nitramines

Rocchio and Juhasz [38] detected N_2 (17.4), N_2O (17.1), NO (23.1), CO (3.6), CO_2 (4.2), HCN (19.2), and H_2O (15.4) in the products of HMX pyrolysis on a heated block at T = 271 – 800 °C. The relative percent composition of the gas mixture at a block temperature of 350 °C is indicated in the parentheses.

Axworthy et al. [33] studied the high-temperature pyrolysis of HMX and RDX in a hot helium stream at a temperature of 300 to 1000 °C. The yield of CH_2O, N_2O, NO, N_2, HCN, CO, and CO_2 with variation of temperature was analyzed. At T ≈ 300 °C, N_2O and CH_2O were the main pyrolysis products. The N_2O and CH_2O contributions decreased, and the NO and HCN contributions increased with a rise in temperature. At T = 600 °C, the N_2O, NO, and HCN contributions were approximately equal (≈ 20 – 30 %), and the CH_2O contribution was about 5 %. At T = 800 °C, the HCN contribution was ≈ 25 %. Axworthy et al. [33] explained the small CH_2O yield at high temperatures by the following factors:

--- smaller amount of CH_2O formed in the primary products of pyrolysis,
--- proceeding the secondary reactions involving CH_2O, and
--- thermal decomposition of CH_2O.

Flanigan and Stokes [39] studied the decomposition products of HMX and RDX using rapid heating of a copper (platinum) wire. Both NO_2 and N_2O were detected. Since the HMX and RDX spectra turned out to be similar, a unified five-stage mechanism similar to that suggested by Schroeder [25] was proposed for nitramine decomposition, :

(1) Formation of a free NO_2 radical;
(2) Rapid fragmentation of the ring;
(3) Formation of methylene nitramine $CH_2{=}N{-}NO_2$ and CH_2N^* radical;
(4) Conversion of unstable CH_2NNO_2 species to CH_2O and N_2O;
(5) Reactions of NO_2 and N_2O with CH_2O to form CO, CO_2, N_2, H_2O, and NO. Reactions of CH_2N^* with the other products produce HCN.

Fifer [3] proposed the generalized scheme of nitramine decomposition taking into account the data of various investigators. According to Fifer [3], the fragment with M = 222 formed from HMX does not necessarily correspond to RDX and the components with M = 148 and 102 cannot be pictured cyclically. The proposed scheme does not include bimolecular reactions between large fragments, and also between the products NO_2, HCN, CH_2O, etc.

One should take into account that NO_2 has relatively high reactivity. There is no clear understanding of HONO formation, since nitrous acid is rapidly expended by the route 2 HONO = $NO + NO_2 + H_2O$ to form NO_2. Therefore, the presence or absence of NO_2 cannot confirm scission of the $N{-}NO_2$ bond.

The presence of NO_2 is only indicative of the possibility of scission of the $N{-}NO_2$ bond or HONO elimination. Evidently, the C—N bond energy is greater than the $N{-}NO_2$ bond energy. Thus, according to the estimate of Shaw and Walker [40], the $N{-}NO_2$ bond energy is E(N-N) =66 kcal/mol for RDX, and it is E(N-N) =46.2 kcal/mol for HMX. The C—N bond energy is estimated as 85 kcal/mol for RDX and as 60 kcal/mol for HMX. Hence, it is assumed that in the thermal decomposition of nitramines, either NO_2 (or HONO) is first split out with immediate elimination of CH_2N from the nitramine molecule or HCN is first split out with the subsequent loss of one or more CH_2NNO_2 molecules.

The studies performed in 1990's [41-47] made a significant contribution to the understanding of the thermal-decomposition mechanism of nitramines at low heating rates and under isothermal

conditions at temperatures lower or somewhat higher than the melting point. Technically, these studies were very complex, and this was a peculiar cost for the uniqueness of the experimental data obtained. Thus, for example, these studies widely used simultaneous high-sensitive thermogravimetric gas-beam modulated mass spectroscopy, methods of isotope mixing, and measurements of the deuterium kinetic isotope effect.

Experiments with both the original nitramines and their complete analogs containing labeled ^{2}H, ^{13}C, ^{15}N, and ^{18}O atoms were performed to study the decomposition kinetics, to elucidate the reaction pathways, and to identify the reaction products. The results obtained are summarized by Bulusu and Behrens [47]. It was found that the primary steps of decomposition (scission of the N—NO_2 bond and formation of HONO) and secondary reactions between the starting nitramines and its decomposition products result in the formation of H_2O, N_2O, CH_2O, NO, CO, HCN, NO_2, NH_2CHO, and CH_3NHCHO molecules, which are common for the decompositions of RDX and HMX. At the same time, $C_3H_3H_3O$ (M = 97) and $C_3H_6H_6O_5$ (M = 206, ONDNTA) are formed only in the decomposition of RDX, and $(CH_3)_2N$—NO (M = 74) and $C_4N_8H_8O_7$ (M = 280, ONTNTA) are formed only in the decomposition of HMX. Experiments on isotope mixing of the starting compounds and nitramines with the nitrogen atoms entirely replaced by ^{15}N atoms showed that the mononitroso compounds ONDNTA and ONTNTA are produced via the formation of the N—NO bond in place of the scission N—NO_2 bond. Both ONDNTA and ONTNTA then decompose into low-molecular products, thus ensuring the low average molecular mass of the thermal decomposition products of nitramines.

The most detailed results are reported for the thermal decomposition of RDX. In particular, Bulusi and Behrens [47] proposed the following generalized scheme [47] of the reaction pathways for RDX at 200 – 215 °C (in the liquid phase):

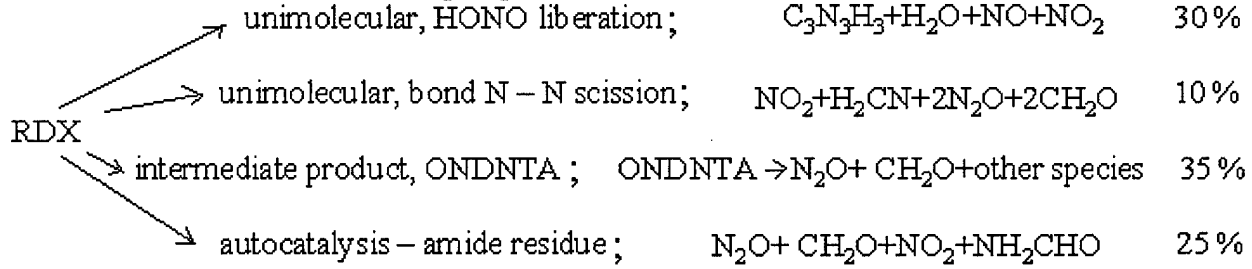

Here the numbers in percent correspond to the fraction of the starting RDX that decomposes by the given reaction pathway. The authors note that the latter autocatalytic pathway can be realized via the decomposition of both the starting substance and its mononitrose analog, the intermediate product ONDNTA.

Because of the lack of quantitative experimental data, it is impossible to formulate a similar scheme for the decomposition of molten HMX. One can only speak on the qualitative similarity of the initial steps of the decompositions, but the higher melting point and, accordingly, the higher degree of the condensed-phase decomposition can introduce significant corrections into the real picture of the process.

Note that the above experimental data correspond primarily to the results of studies of low-temperature decomposition of nitramines or decomposition under slow-heating conditions. Obviously, it is difficult to extrapolate these data to the conditions of combustion or explosion waves

because of the great difference in heating rates and temperatures in the reaction zones. In particular, Fifer [3] noted that it is important to find direct evidence for what the first step of the thermal decomposition is: the scission of the N—N bond (elimination of NO_2 or HONO) or the scission of the C—N bond (elimination of $CHNNO_2$). It is not clear whether the first step is the gas-, liquid-, or condensed-phase decomposition.

Over the last decade, great success has been achieved in developing dynamic high-sensitive methods of recording gaseous products of the thermal decomposition of nitramines under isothermic and nonisothemic conditions [48]. The goal was to bring the conditions of experiments on thermal decomposition as close as possible to the conditions of residence of substances in a combustion wave at elevated pressures.

Oyumi and Brill [49] studied the thermal decomposition of RDX and HMX samples with a mass of 1 mg at various heating rates (8 – 200 K/sec) of a Nichrome wire and at nitrogen pressures of 0.003 - 68 atm using a high-speed infrared spectrometer with a Fourier transform. Temporal records of NO_2, N_2O, CH_2O, HCN, NO, CO_2, HONO, and CO concentrations were obtained. HNCO in small amounts (by estimates, < 5 %) was detected. In the decomposition of RDX in nitrogen at a = 1 atm in the vicinity of the melting point (T ≈ 75 K), the major decomposition products are NO_2, N_2O, CH_2O, and HCN, and NO, CO, HONO, and CO form in small amounts. With time, the CH_2O and N_2O concentrations decrease, and the NO concentration increases. This is attributed to the progress of the reaction between CH_2O and NO_2. The formation of CH_2O and NO_2 is explained by the decomposition of RDX into CH_2HHO_2 followed by the decomposition into CH_2O and NO_2.

The decomposition of HMX in nitrogen at a = 1 atm yields the same products, but the initial HCN concentrations are higher than the CH_2O concentrations at all heating rates (in the decomposition of RDX, this is observed only at high heating rates). The composition of the products formed in the decomposition of nitramines at various nitrogen pressures is given in Table 2.7. In this case, the Nichrome wire was initially heated at a rate of 140 K/sec, and the wire temperature was then maintained at this level. The components H_2O, H_2, and O_2, which are not detected by this method, and also HNCO, CO, and nitramine aerosols are not included in Table 2.7.

Table 2.7. Gaseous products of RDX and HMX decomposition at different pressures.

Matter	p, atm	t, s	T, K	CO_2	N_2O	NO	CH_2O	NO_2	HCN	HONO
RDX	1	9.6	645	4	22	5	15	32	14	8
RDX	68	9.8	630	16	24	13	29	18	---	---
HMX	1	9.85	645	3	19	7	19	21	25	6
HMX	68	8.7	630	9	26	19	19	4	25	---

According to experimental data of Oyumi and Brill [49], NO_2 is one of the major initial products of the decomposition of RDX, and the decomposition of HMX yields primarily HCN and N_2O. The NO_2 concentration decreases rapidly in secondary reactions, and the NO concentration is initially small and increases rapidly in secondary reactions. Nitrous acid HONO is found in the initial stage of the process. With decrease in pressure, the NO_2 fraction in the products of RDX decomposition increases. Thus, at a nitrogen pressure of 50 torr and a heating rate of 110 K/sec,

the NO_2 fraction ≅ 50 %, HCN ≅ 20 %, CH_2O ≅ 10 %, and N_2O ≅ 10 %. Oyumi and Brill [49] draw the following conclusions:

1. The formation of NO_2 dominates in the rapid RDX pyrolysis (the heating rate is 8—200 K sec^{-1}) at atmospheric pressure. This indicates the predominant break of the N—NO_2 bond in the initial stage of decomposition of RDX.
2. The initial NO concentration is close to zero.
3. CH_2O and N_2O are important initial products of RDX pyrolysis near the melting point, possibly because the break of the C—N bond occurs in the condensed phase. When the temperature of the wire considerably exceeds the RDX melting point, the HCN and NO_2 concentrations become significant, and this points to the gas-phase decomposition of RDX.
4. At all temperatures, RDX pyrolysis is accompanied by the formation of nitrous acid HONO, but nitrous acid is unstable, and, hence, sensitive recording methods are required.
5. At low pressures and high heating rates, RDX sublimation makes a great contribution. High pressures and heating rates decrease the NO_2 yield, prevent the formation of HCN and HONO, and increase the yield of NO, CO_2, and CH_2O.
6. CH_2O and N_2O, along with HCN and NO_2, are the major products of HMX decomposition in the vicinity of the melting point. With increase in temperature and heating rate, HCN and NO_2 dominate, and CH_2O and N_2O play a less significant role.
7. HONO is the product of HMX pyrolysis at subatmospheric pressures and heating rates of 40 – 145 K sec^{-1}.
8. With increase in pressure from 0.003 to 68 atm, the role of reactions in the HMX condensed phase increases relative to gas-phase reactions.

Palopoli and Brill [50] reported data on the thermal decomposition of HMX on a Nichrome ribbon at atmospheric pressure in different gases and under heating rates of 40, 90, 140, and 180 K/sec. The final temperature of the ribbon was 600, 780, and 1000 K. At all heating rates at the initial moment the H_2CO yield is about two times higher than the yield of HCN ≈ NO ≈ NO_2 ≈ N_2O, and it is a factor of 6--8 higher than the HONO yield. In [50], the formation of CHO and N_2O is explained as follows:
--- transfer of an O atom from the NHO_2 group to the CH_2 group followed by scission of the C—N bond [40],
--- dissociation of H_2CNNO_2 via a similar process,
--- bimolecular decomposition of H_2CNNO_2 catalyzed by the OH radical [51]:

$$H_2CNNO_2 + OH = H_2CO + N_2O + OH.$$

The effect of the composition of the gas mixture on the thermal decomposition of HMX was studied [50] at atmospheric pressure and a heating rate of 140 K/sec in gas mixtures of the following partial compositions: (380 torr H_2)/(380 torr Ar, CO, O_2, NO); (25 torr NO_2)/(735 torr Ar); (380 torr NH_3)/(380 torr Ar). The final temperature was 900 K. The initial formation of the products (t ≅ 2 sec) occurred at T ≈ 550 K, which is close to the melting point. The addition of NO_2 and NH_3 exerted the most significant effect on the decomposition. The addition of NO_2 leads to a sudden decrease in the H_2CO yield and increase in the NO yield. The HCN concentration increases only slightly, and this is attributed to the reaction $H_2CN + NO_2 \rightarrow HCN + HONO$,

which increases the HONO yield. The decomposition of HONO is an effective source of OH radicals, which are responsible for fast dissociation of H_2CO.

With the addition of HN_3, isocyanic acid HNCO, which is observed in all the other experiments, is absent. H_2CO is present in small amounts and is rapidly expended, and HONO is absent. Cyanic acid HCN and nitrogen dioxide NO_2 are rapidly consumed and the N_2O concentration rapidly increases. Palopoli and Brill [50] explain this by the common mechanism of NH_3 oxidation. In particular, the decomposition of NO_2 and the formation of N_2O are associated with the reaction $NH_2 + NO_2 \rightarrow N_2O + H_2O$, and the rapid decomposition of HCN is associated with significant production of OH radicals. It is concluded that NH_x and NO_2 can exert a significant effect on the burning rate of nitramine-based propellants.

The purely gas-phase decomposition of RDX was studied in [52], where a molecular beam of RDX vapors was irradiated by CO_2-laser pulses. The pulse duration was 600 nsec, and the repetition frequency was 30 or 100 Hz. RDX vapors were produced by sublimation of the substance in a vacuum furnace at 130 °C (vapor pressure 0.1 torr); He at a pressure of 50 torr was used as a carrier gas. A beam of RDX molecules moving at an average speed of 10 m/sec was irradiated by a CO_2-laser pulse, which led to multiphoton dissociation and the subsequent decomposition of RDX molecules. The products were then analyzed by means of a time-of-flight mass-spectrometer. A detailed consideration of the time history of the amplitudes of signals at chosen values of m/e and analysis of the composition of the decomposition products led Zhao et al. [52] to the conclusion that the primary step of gas-phase decomposition of RDX proceeds predominantly by instantaneous division of the ring into three identical fragments with mass 74 (CH_2NNO_2). The subsequent secondary dissociation of CH_2NNO_2 yields HCN, H_2CO, HONO, and N_2O. Energy estimates show that under irradiation by a CO_2-laser pulse, RDX molecules acquire a fairly large store of internal energy, and this leads to scission of the C—N bond, although the scission of the N—N bond is more thermodynamically favorable.

An attempt to study the primary step of condensed-phase decomposition of RDX was undertaken by Botcher and Wight [53]. In this study, a thin RDX film produced by vacuum deposition on a massive substrate, which was transparent to infrared radiation, was irradiated by a short (35 μ sec) pulse of a CO_2 laser under vacuum and cooling to 77 K. According to simple estimates of thermal balance ignoring evaporation, a film 10 – 15 μm thick should be heated instantaneously to 1000 – 1200 K. After that, rapid cooling to about 400 K due to heat transfer to the substrate should occur for 0.003 sec. The authors note that this estimate is rather rough, and they did not attempt to measure the rate constants of the chemical reactions. Obviously, allowance for the finite transparency of the film and substrate materials, as well as allowance for the evaporation of the film leads to a decrease in the film temperature. Note that the features of evaporation of materials at a heating rate higher than 10^7 K/sec are completely unknown, and this introduces additional difficulties into the treatment of the temperature conditions in the object studied. But this does not affect the reliability of the qualitative data of this paper related to the finding and identification of the primary products of condensed-phase decomposition of RDX.

In the experiment with pulsed irradiation, about a third of the mass of the film has been evaporated during the heating—cooling period, and the remaining part of the condensed phase was analyzed using infrared spectroscopy to study the composition of the decomposition products.

Under the action of a pulse with a minimum power, that ensured the appearance of initial decomposition products, only dimers of nitrogen dioxide (N_2O_4) were recorded in the condensed phase. This can be treated as the result of scission of the N—N bond and NO_2 formation in the primary step of RDX decomposition. When irradiation was performed using a more powerful pulse and a cover glass, which prevents dispersion of the evaporating substance and decomposition products, NO, HCN, N_2O, and CO_2 were additionally recorded. The other possible decomposition products were not identified because their spectra were overlapped by the spectrum of the starting RDX. However, the number of the NO_2 species formed in the decomposition of one RDX molecule remained to be established, although the number of RDX molecules that had decomposed indicated indirectly the formation of one NO_2 species in the primary step. In the subsequent investigation of the same authors [54], which was performed using RDX in which ^{14}N nitrogen atoms were completely replaced by ^{15}N atoms, Botcher and Wight obtained direct evidence for the formation of one NO_2 radical in the primary step of condensed-phase decomposition of RDX. It was expected that if both the NO_2 molecules forming a dimer are produced by the decomposition of the same RDX molecule, only dimers such as $^{14,14}N_2O_4$ and $^{15,15}N_2O_4$ have to be observed. Otherwise, formation of dimers such as $^{14,15}N_2O_4$ was also expected. Under pulsed irradiation of a film consisting of a mixture of the starting and "labeled" RDX, N_2O_4 molecules were detected with a statistically uniform distribution of ^{14}N and ^{15}N, and this unambiguously indicates the formation of one NO_2 species in the high-temperature condensed-phase decomposition of RDX.

Formal kinetic parameters of thermal decompositon of nitramines

The rate constants $k = B \exp(-E/RT)$ of the thermal condensed- and gas-phase decomposition of RDX and HMX are given in Tables 2.8 and 2.9.

Table 2.8. RDX data (T_{melt}= 478 K)

Phase	T, K	Log B (B in sec^{-1})	E, kcal/mol	k, s^{-1} at 473 K	Ref.
Solid	423-460	19.1	52.0	$1.2\ 10^{-5}$	[55]
Solution *	433-473	14.3	39.7	$9.0\ 10^{-5}$	[55]
Solid	423-473	---	---	$< 10^{-6}$	[3]
Solid	---	14.5	41.5	$2.1\ 10^{-5}$	[58]
Gas	443-463	11.7	30.0	$6.88\ 10^{-3}$	[56]
Gas	443-473	13.5	35.0	$1.9\ 10^{-3}$	[57]
Gas	480-531	13.5	34.1	$5.5\ 10^{-3}$	[59]
Gas	543-474	16.0	40.4	$2.15\ 10^{-3}$	[17]
Liquid	480-525	18.8	48.2	$3.37\ 10^{-4}$	[60]
Liquid	505-520	18.3	47.1	$3.4\ 10^{-4}$	[59]
Liquid	486-572	18.5	47.5	$3.55\ 10^{-4}$	[37]
Liquid	473-523	14.3	37.8	$6.8\ 10^{-4}$	[31]
Solution 0.7% in acetone	473-513	17.9	45.4	$8.34\ 10^{-4}$	[31]

Note.

In Tables 2.8 and 2.9, the asterisk denotes a solution of nitramine in m-dinitrobenzene.

It follows from the tables that the rate of the low-temperature gas-phase decomposition (at 200 °C) of RDX is a factor of several hundreds higher than that of the solid-state decomposition, and it is a factor of several tens higher than the decomposition in the liquid state; the rate of the solid-state decomposition of HMX is lower than the rate of decomposition of RDX.

Table 2.9. HMX data (T_{melt} = 553 K)

Phase	T, K	Log B (B in sec^{-1})	E, kcal/mol	k, s^{-1} at 500 K	Ref.
Solid	456-503	11.2	37.9	$4.28\ 10^{-6}$	[55]
Solution *	444-488	15.0	44.9	$2.36\ 10^{-5}$	[55]
Solid	453-513	---	---	$< 10^{-7}$	[3]
Solid	---	10.8	39.0	$5.64\ 10^{-7}$	[58]
Gas	478-553	14.2	39.5	$7.70\ 10^{-4}$	[57]
Gas	503-523	13.2	32.0	0.257	[56]
Gas	518-548	12.5	38.0	$7.74\ 10^{-5}$	[17]
Gas	546-560	20.2	52.9	$1.18\ 10^{-3}$	[37]
Gas	521-656	12.8	32.5	$3.9\ 10^{-2}$	[61]
Liquid	544-587	19.7	52.7	$4.59\ 10^{-4}$	[37]
Liquid	544-558	18.8	51.3	$2.37\ 10^{-4}$	[62]

The rate constants of nitramine decomposition versus temperature are given in Figs. 2.1 and 2.2. As follows from the figures, the literature data on the decomposition of RDX agree satisfactorily for both the gas and liquid phase; the data for HMX decomposition are characterized by a significant scattering.

The above materials cannot claim to be a thorough review of the data available on the thermal decomposition of RDX and HMX, because these data are very extensive and are not easily accessible. Nevertheless, they provide a clear understanding of the complex decomposition mechanism of cyclic nitramines and its dependence on various factors.

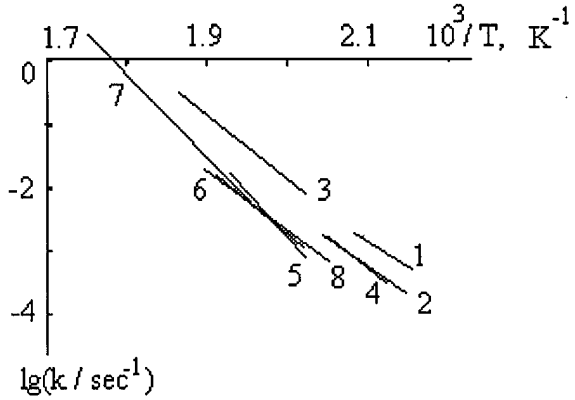

Fig. 2.1. Rate constants of gas-phase (curves 1--4) and liquid-phase (curves 5--8) decompositions of RDX versus temperature: the data of [56] (1), the data of [57] (2), [59] (3), [17] (4), [60] (5), [59] (6), [7] (7), and [31] (8).

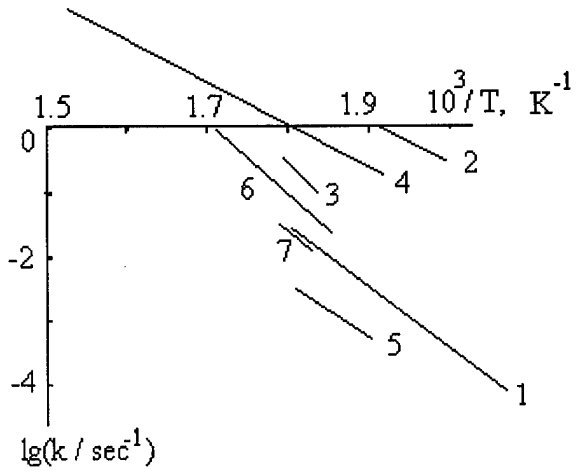

Fig. 2.2. Rate constants of gas-phase (curves 1--5) and liquid-phase (curves 6 and 7) decompositions of HMX versus temperature: the data of [57] (1), [56] (2), [37] (3), [61] (4), [17] (5), and [37] (6).

Summary of decomposition studies.

The nitramines studied, as well as the majority of energetic materials, are capable of both condensed-phase and gas-phase chemical transformations. In this case, depending on the heating rate, sample dimensions, and also on the composition of the ambient medium, both primary and secondary chemical reactions can occur, and this is responsible for the great variety of decomposition products and rates of the global reactions.

Apparently, the primary step of gas-phase decomposition of nitramine vapors can be studied in the most pure form if the interaction between the decomposition products is effectively inhibited. An example of such a study is given in [52], where the decomposition of a molecular beam of RDX vapors under the action of a short laser pulse was studied.

The primary step of condensed-phase decomposition is difficult to study separately. An interesting experimental approach was formulated in [54], where a thin RDX film was irradiated by a laser pulse under deep vacuum and deep preliminary cooling of the substrate. The further improvement of this approach is associated with the use of recording methods with a high time resolution to realize the possibility of observing the formation kinetics of primary and secondary decomposition products under programmed heating (at a varied rate) of thin films.

It also seems promising to study nitramine decomposition in low-concentration solutions, in which secondary chemical reactions can be effectively inhibited [31]. In this case too, dynamic methods of recording the new compounds formed in the thermal decomposition are required. This will make it possible to observe the evolution of the chemical composition of reaction products. Note, in particular, that Oxley et al. did not detect nitrogen oxides NO and N_2O (see Table 5), although NO_2 formation in the early stage of decomposition was postulated to be the primary step. It is expected that the high-speed techniques of recording infrared spectra will clarify this feature of the process.

At present, the speed of response of commercial devices for recording infrared spectra is tens and hundreds scans per second. Such devices make it possible [30] to study in detail the temporal evolution of the gaseous chemical compounds formed in the thermal decomposition of nitramines under heating rates of tens and hundreds of degrees per second or at moderately high temperatures (several tens of degrees below the calculated boiling point). Note once more the fundamental difficulties in detecting the products of the primary step of the thermal decomposition. If these products are formed in the condensed phase, they should diffuse to the surface and desorb to the gas phase. Even at small thickness of the film, the time of diffusion in the condensed phase is finite, and this is responsible for the finite degree of conversion for the secondary reactions. This interaction of the products can continue in the gas phase unless rapid dilution of the products by inert gases is ensured. Thus, if one seeks to reach a considerable decrease in geometrical dimensions of specimens of the substances studied, it is necessary to increase considerably the sensitivity and speed of response of the recording techniques. In reality, the available recording techniques do not permit one to determine reliably the composition of the primary products of the high-temperature liquid-phase decomposition of nitramines. They provide only indirect evidence for the existence of the global mechanism of the reaction [30].

Botcher and Wight [54] proposed a plausible mechanism for the condensed-phase thermal decomposition of RDX. It is based on the ideas formulated by Melius [51]. The theoretical calculations of Melius [51] showed that the scission of the N—N bond and the subsequent decomposition of the ring structure of the nitramine is much more thermodynamically favorable than the scission of the C—N bond (and, of course, more favorable than the simultaneous scission of three C—N bonds, as was shown in [52] for the gas-phase decomposition of RDX). Thus, according to [54], the primary step of the thermal decomposition of RDX produces, as in the Shroeder scheme [25], an NO_2 radical and an organic radical, which then decomposes to form HCN, OH, and a new organic radical. The interaction of the latter with OH gives rise to N_2O, H_2O, HCN, NO, and CH_2O. This scheme allows one, in particular, to explain the nonsimultaneous appearance of NO_2 and N_2O in the experiments of [30] on high-speed heating of RDX films.

To conclude this brief survey of data on the thermal decomposition of nitramines, it should be noted that there are real causes for the difference between the thermal-decomposition mechanisms under different experimental conditions. At high heating rates, the reactions proceed at high temperatures and by a monomolecular mechanism. These kinetic data are related to the combustion and explosion process. At low heating rates, the reactions can proceed by a bimolecular mechanism involving primary products of decomposition. The data obtained in such experiments are related to thermal explosion and thermal decomposition during the storage and processing of energetic materials. To propose and verify theoretical mechanisms for the chemical transformations of energetic materials, it is necessary to use experimental data obtained under special model conditions. The theoretical models should then be used with allowance for the effects of spatial and temporal factors on the progress of the chemical transformations. Such a task will require further improvement of experimental and theoretical methods.

2.2.2 Modeling of Cyclic-Nitramine Combustion

The combustion of cyclic nitramines has been extensively studied in the last three decades, when nitramines, as an addition to the explosives "profession", have found practical use as components of modern rocket propellants. Basic research of nitramines is also important, since they are the simplest monopropellants and there is hope that a detailed physicochemical mechanism for transformations in the combustion wave can be formulated and a theoretical correlation between the chemical composition of the material and its combustion characteristics will be established. It should be noted that this problem is still far from being solved, and a likely explanation of the similarities and differences in combustion characteristics even for cyclic nitramines that are similar in composition RDX and HMX is presently not available.

The combustion of most modern high-energy materials is characterized by melting of the material at a temperature below the burning surface temperature and the possibility of simultaneous processes of thermal decomposition and vaporization in the surface layer. In early studies of combustion of melted explosives, it was assumed that, since the activation energies of thermal-decomposition reactions could exceed several fold the latent heat of vaporization (for example, according to Belyaev [63], they can differ by a factor of 2 or 3), such materials burn without appreciable heat release in the condensed phase, and an endothermal vaporization process dominates on the surface. Accordingly, the combustion of melted materials has been mostly interpreted in terms of a gas-phase mechanism. Subsequently, new experimental data were obtained on the kinetics of thermal decomposition and vaporization and inconsistency with classical concepts were revealed. For example, Aleksandrov et al. [64] demonstrated experimentally for the first time that fairly intense exothermic reactions proceed in the combustion of DINA in the condensed phase. The gas products of the thermal decomposition are responsible for the bubble-like structure of the surface layer of the condensed phase. However, it is important to note that obtaining objective information on the parameters of the combustion of energetic materials involves significant technical difficulties because of the narrow spatial regions, high temperature, and hostile environment. This limits the possibilities of studying the processes to a considerable extent. For example, high temperature gradients hampers use of classical optical methods, and in thermocouple measurements, the presence of a liquid layer introduces uncertainty in the determined values of surface temperature and heat flux from the gas to the condensed phase because of possible adherence of the liquid to the thermocouple junction. Note that video recording of combustion at atmospheric pressure and examination of extinguished specimens of nitramines indicate the presence of bubbles in the subsurface layer.

However, earlier studies showed that formal analysis of extinguished specimens and data of low-speed movie records can lead to incorrect results. For example, it was established [65, 66] that the presence of developed foam on the surface of extinguished specimens of double-base propellants is a consequence of residual gas liberation in cooling. At the same time, high-speed movie records make it possible to detect, on a burning surface, only single short-lived bubbles that occupy less than 10% of the specimen surface. Similar observations made by U.S. researchers, showed that the "foam layer" appears when a low-speed camera is used but disappears with high-speed photography [67].

Considerable advances have been made in the description of the chemical mechanism of gas-phase transformations in nitramine combustion, but the essence and relative contribution of con-

densed-phase reactions still remain in question. For better understanding of the mechanism of physicochemical transformations in the combustion wave, adequate physicomathematical models of nitramine combustion must be constructed on the basis of a critical analysis of the available information and a combination of experimental and theoretical approaches. Literature data on the thermal decomposition of nitramines that are of interest for studying chemical processes in the combustion wave were reviewed elsewhere [68].

In thethis section, we attempt to generalize the available experimental data on the macrokinetic characteristics of RDX and HMX combustion waves and their chemical structures. A brief review of the available mathematical models is presented and reduction of the mechanism of combustion reactions in cyclic-nitramine flames is discussed later.

Physical parameters of the combustion wave

As follows from the results of numerous studies, the nitramine-combustion wave includes several regions: a solid nonreactive substance, a melted subsurface layer, a narrow zone of chemical reactions beneath the burning surface, which is partially filled with gas bubbles, a zone of primary gas-phase reactions, an induction (dark) zone, and a zone of secondary gas-phase reactions. In addition, small liquid droplets can be formed as a result of bursting the bubbles on the burning surface. The efforts of experimenters are usually directed toward studying the temperature profile and burning rate of the materials in question.

One of the first attempts at a detailed study of the combustion wave of pressed nitramine specimens was undertaken by Mal'tsev and Pokhil [69]. An optical method was used to measure the temperature distribution as a function of pressure at various distances from the burning surface (Table 2.10). The attenuation of radiation in flame with height above the burning surface of RDX was measured at pressures p = 20, 40, and 60 atm.

Table 2.10. Spatial temperature distribution in flame of RDX.

p, atm	T, K at H, mm			T_f, K	Ref.
	0.04	0.06	0.10		
1	900	1020	1270	1970	[70]
	1000	1100	1300	2800	[71]
5	1400	1830	2270	2770	[70]
20	1600	2560	3140	---	[7]
	1960	2460	2770	2970	[70]
40	2400	3000	---	---	[69]
60	2800	3200	---	---	[69]
90	2270	2580	2830	3070	[70]

Note. *H is the distance from the burning surface (in millimeters); the temperature values are taken from graphs and rounded to 50°; T_f is the flame temperature.*

Table 2.11. Parameters of the RDX combustion wave.

p, atm	u, cm/s	T_s, °C	Q_c, cal/g	Q_g, cal/g	ρ, g/cm^3	Ref.
1		320	-84	190	1.56	[70]
	0.039	---	---	---	---	[71]
	0.035	---	---	---	1.75	[72]
5	0.17	360	-61	176	1.66	[70]
20	---	380	15	129	1.67	[69]
	0.50	420	58	84	1.66	[70]
	0.48	---	---	---	1.75	[72]
	0.46	---	---	---	1.75	[73]
40	---	420	14	146	---	[69]
60	1.05	---	---	---	1.75	[72]
	---	440	12	156	1.67	[69]
	0.95	---	---	---	1.75	[73]
90	1.80	490	140	27	1.66	[70]
	1.6	---	---	---	1.75	[73]

Note. *T_s is the surface temperature.*

The burning-surface temperature was determined [69] by extrapolation of the temperature profile data. In addition, temperature profiles were used to estimate the heat Q_c released in the condensed phase, and the heat feed back to the condensed phase from the gas (Table 2.11):

$$Q_g = \frac{1}{\rho u}\left(\lambda \frac{\partial T}{\partial x}\right)_s$$

Here and below, ρ is the specimen density, u is the linear burning rate, T is the temperature, λ is the thermal conductivity of the gas phase, x is the space coordinate, and the subscripts c and s correspond to parameters in the condensed phase and on the burning surface, respectively. The obtained estimates of heat release indicate that the condensed-phase decomposition is endothermal.

The temperature profile in the combustion wave of pressed RDX specimens was measured [70] at p = 1 - 90 atm by tungsten - rhenium thermocouples inserted into the specimens. The temperature profile was used to determine the burning-surface temperature, the heat release in the condensed and gas phases, the heat flux from the gas phase into the condensed phase, and the thickness of the melted layer. It was found that the heat release in the condensed phase was negative at p < 5 - 10 atm and positive at p > 10 atm. Based on this, it was concluded that vaporization is dominant at low pressures while thermal decomposition with positive heat release is dominant at high pressures.

Analysis of the data presented in Tables 2.10 and 2.11 indicates that the numerical values of the parameters corresponding to the specified combustion conditions differ considerably. Unfortunately, as in many other studies of the combustion of energetic materials, the authors do not re-

port estimates of the confidence intervals of the measured quantities, and this makes objective comparison of the analyzed results difficult. It is obvious that, along with procedural errors, such factors as the density, phase composition, and purity (presence of impurities) of the materials studied make a substantial contribution to the spread in the measured values. It is possible, therefore, that energetic materials produced at different times and in different places will have different combustion parameters, which are essential in discussing fine details of the combustion-wave structure.

Note that the conventional methods for measuring the mean burning rate do not allow recording local (in time) pulsations of the rate of motion of the condensed-phase surface. However, observations of the nature of flame luminescence and dynamic measurements of the reactive force of the combustion products show that, at least at atmospheric pressure, RDX burns with chaotic pulsations at a frequency exceeding 500 Hz [74]. The nature of these pulsations has not been reliably established, nor has the scale of their effect on the measured mean burning rate.

In the case of HMX combustion, a characteristic feature associated with the existence of various stable crystalline modifications of the material should be noted. It is customary to assume that commercial HMX consists entirely of the β-modification, which is stable from room temperature to 376 K. It was shown [75], however, that when the β-modification is heated to a temperature exceeding 435 K (162°C and above), the δ - modification forms which is capable of existing for several hours at normal temperature. This means that occasionally or specially heated and subsequently cooled specimens of HMX could contain a considerable fraction of the δ-modification. The latter has increased sensitivity to impact, which increases the danger of technological operations with that material, and an increased burning rate, which can affect the overall burning rate of the mixture of crystals. The results of measurements of the burning rates of the β - and δ-modifications of HMX [75] are presented in Table 2.12 along with the data of other researchers on combustion-wave parameters at p = 1 - 70 atm. The large satter of the data on the burning rates of HMX at atmospheric pressure is noteworthy. It should be borne in mind, however, that at this pressure HMX is capable of burning in a strikingly expressed self-oscillating mode [74], and this can affect the measured pseudo stationary burning rate.

The data in Tables 2.11 and 2.12 contain inconsistent information on the relative role of the contributions of exothermic transformations in the condensed and gas phases to the energy balance on the burning surface. According to [70], for both RDX and HMX at relatively low pressures (p = 1 - 5 atm), endothermal processes take place in the condensed phase, and the combustion wave is maintained chiefly by heat release in the flame. At p > 50 atm, however, heat release in the condensed phase becomes dominant. At the same time, there are data for RDX [69] and for HMX [77] that do not agree with the tendency indicated above. Obviously, the limited set of experimental data does not permit one to arrive at final conclusions on the mechanism of nitramine combustion over a wide pressure range.

In general, despite the relative similarity of the mechanism of RDX and HMX combustion, i.e., the small difference in the combustion laws $\log u = \text{const} + \nu \log p$, there are serious differences in their responses to variations of initial temperature and dynamic oscillations of the external heat flux. For example, according to [79], for RDX at p = 10 - 100 atm, the temperature sensitivity of the burning rate $\beta = (\partial \ln u / \partial T_0)_p$ is extremely low and equals (1 - 2) 10^{-3} K^{-1}, while for HMX,

$\beta \approx 5\ 10^{-3}\ K^{-1}$ at low pressure (p = 10 atm) and drops to $10^{-3}\ K^{-1}$ at p = 50 - 100 atm. It is important to bear in mind that exact measurements of β at a level of $10^{-3}\ K^{-1}$ are difficult to perform; the relative error rises to 100% or more.

Table 2.12. Parameters of the HVX combustion wave.

p, atm	u, cm/s	T_s, °C	Q_c, cal/g	Q_g, cal/g	ρ, g/cm^3	T_f, °C	ref.
1	0.041	320	-41.6	112	1.7	2100	[76]
	0.053	---	---	---	β(1.89)	---	[75]
	0.075	---	---	---	δ(1.78)	---	[75]
	0.05	400	64.9	53.6	1.7	---	[77]
5	0.12	---	---	---	1.72	---	[72]
	0.13	410	76.6	68.4	1.7	---	[77]
	0.15	400	20	110	1.7	2300	[70]
	0.16	380	61	58	1.7	2300	[76]
	0.13	---	---	---	β(1.89)	---	[75]
	0.17	---	---	---	δ(1.78)	---	[75]
10	0.28	420	93	44	1.7	2500	[76]
	0.24	---	---	---	β(1.89)	---	[75]
	0.35	---	---	---	δ(1.78)	---	[75]
	0.235	---	---	---	1.72	---	[72]
	0.25	---	---	---	1.72	---	[73]
20	0.40	460	100	53	1.7	2600	[70]
	0.41	450	110	41	1.7	2700	[76]
	0.42	---	---	---	1.72	---	[73]
	0.48	---	---	---	1.72	---	[72]
40	0.76	560	---	---	---	---	[78]
60	0.94	500	152	25	1.7	2750	[76]
70	1.0	490	128	35	1.7	2750	[70]
	1.2	---	---	---	1.72	---	[73]
	1.15	---	---	---	1.72	---	[72]

Notes. *The values of T_s in [77] correspond to the initial temperature of intense condensed-phase decomposition [discontinuity in profile of T (x)]. The values of Q_c in [70] where calculated by the equation $Q_c = c\ (T_s - T_0) - Q_g + Q_m - Q_{rad}$, where $Q_g = (\lambda / \rho u)(\partial T/\partial x)_s$, and Q_m and Q_{rad} are the heat expenditures for melting and heat feedback due to the emission from the flame, respectively. The values of Q_c in [77] were calculated by a similar equation for $(Q_m - Q_g) = 0$.*

The burning rate (reactive force) response at atmospheric pressure to perturbations of the radiation flux for RDX has a weakly expressed resonance character (f_{res} = 6 Hz), while HMX is capable of burning in a self-sustained regime with regular nonlinear burning-rate oscillations with a frequency of 3 – 5 Hz. An important characteristic of RDX combustion in air is an anomalously wide melt zone, which can be recorded by a thermocouple method. In theoretical modeling of stationary combustion, this effect is sometimes described using a higher value of thermal conductivity for the melted layer than for the crystalline phase. It seems that this approach is inconsistent with the experimentally observed bubble formation in the liquid layer, which can only re-

duce the effective thermal conductivity. A decrease in the average density of the condensed phase of RDX as the burning surface is approached from the cold end was recorded by exposure of the specimen with x-rays [80]. This information does not yet have independent confirmation; experimental research must be continued to substantiate the data on the density of burning nitramines. For example, it can be expected that for the combustion of HMX, whose melting point is almost 80 K higher than that of RDX and whose melt zone is correspondingly narrower, the effects of gas liberation in the liquid layer must be relatively insignificant.

Flame chemical structure

Data on flame chemical structure are extremely important from the point of view of verification and substantiation of model theoretical concepts, which at present make it possible to calculate the concentration profiles of a large number of gas components. Here one should always bear in mind the difficulties of objective comparison with the results of laboratory experiments performed on specimens with finite dimensions under conditions of various kinds of boundary effects and heat transfer. The task of the experimenter, therefore, is to make the experimental conditions as close as possible to the one-dimensional conditions that are usually adopted in theory.

Spectroscopic and mass-spectrometric methods are traditionally employed to study flame chemical structure. Probably, the simplest method for recording gas components in flame is the one of measuring their luminescence intensities. However, problems with interpretation of the experimental data can arise in this case, since chemical reactions in flames produce molecules in a nonequilibrium state. As noted in [81], chemical luminescence is usually caused by excited electronic states formed in secondary reactions that do not correspond to the main energy mechanism of flame reactions. The possible effects of chemical luminescence must be analyzed with allowance for the characteristics of specific flames. In particular, this effect does not permit the effective concentration of the OH radical in the ground state to be determined in solid-propellant flames [81]. At the same time, in a nitromethane flame the emission of the OH and NH radicals has a purely thermal nature, but the emission of the CN radical clearly demonstrates a chemical nature (the vibrational temperature exceeds the rotational by a factor of 2) [82]. Planar laser-induced fluorescence (PLIF) appears very effective but fairly complicated to implement. A pulsed "laser sheet" (a flat beam 100 – 200 μm thick) excites the gas components in the flame of a burning specimen, and a high-resolution video camera records the emission intensity of the excited ground states of the gas species. The maximum resolution on the camera screen ($\approx$ 5 μm) allows the PLIF method to be used successfully to study the flames of various materials, including nitramines. A simpler optical method based on measurement of selective absorption is widely used along with PLIF. Here, however, it is necessary to take into account the contributions from flame zones with different temperatures, and this is an independent difficult problem.

Unlike contactless optical methods, mass spectrometry is based on sampling of the gas with subsequent analysis of its composition. An important advantage of mass spectrometry over spectroscopy is the possibility of analysis of a wider range of substances. At the same time, the contact nature of the method causes serious difficulties in recording highly reactive components (atoms and radicals) and in correcting for the disturbing action of the probe.

One of the first studies of flame chemical structure was published in 1973 [83]. The relative emission intensities of OH, C_2, CN, CH, H_2, O_2, and N_2 were measured along the height of an

RDX flame burning at p = 30 atm. It was found that the intensity of OH emission rose sharply near the surface (at a distance of ≈ 100 μm) and then was held at nearly a constant level in the flame. The intensity of CN and CH luminescence rises gradually and then remains at an almost constant level in the flame. The maximum measured flame temperature, which was 2500 K, was achieved at a height of 0.3 mm from the burning surface. In the regions of 5200 - 6000 and 3400 – 4500 Å, continuous spectra were recorded which are attributed to the reactions $NO + O \rightarrow NO_2 + h\nu$ and $CO + O \rightarrow CO_2 + h\nu$, respectively ($h\nu$ is the quantum energy).

The further development of spectrometric methods has considerably increased the reliability and information content of experimental data. Results of studies of RDX flames in air are presented in [81]. Pressed pellets (with a density of 95 – 98 % of the crystal density) were burned in a self-sustained regime and under the action of a CO_2 laser. In the latter case, combustion was considerably nonuniform over the surface, owing to the bell-shaped cross-sectional energy distribution of the laser beam, and the temperature profile was characterized by the presence of a "plateau", i.e., a flame structure with two temperature zones was formed.

In the self-sustaining combustion regime, the PLIF method was used to measure the relative NO, OH, CN, and NH concentrations at various distances from the burning surface. Absolute values of the concentrations were obtained by absorption measurements in the ultraviolet and visible regions of the spectrum. The concentrations were 310 and 260 ppm for CN and NH, 17 and 3.6 % for NO and OH, and less than 1 % for H_2CO and HONO. The NO_2 concentration could not be measured because of the rapid disappearance of this component near the burning surface. The temperature profile was obtained by a combined method: in the condensed phase and at a height of 0.3 mm above the surface by means of 5-μm thermocouples; and in the gas phase up to the maximum temperature by processing the rotational-temperature profile of the OH radical. Processing of temperature and concentration profiles of the gas components showed that maximum heat release in the flame correlates well with the maximum CN concentration (this is confirmed by observations of other flames). This allows the CN concentration profile to be invoked to determine the "flame stand off distance" — an approximate quantitative characteristic used to compare the energy intensities of different flames and in semi-empirical burning rate calculations. According to the data of [81], the flame standoff distance increases under CO_2 laser radiation, which is absorbed in a narrow surface layer of RDX. This results in the appearance of a dark zone near the surface and the formation of more extended zones of NO_2 and NO concentration variation. Hanson-Parr and Parr [81] believe that large quantities of NO and NO_2 indicate the dominant role of breaking the N—NO_2 bond in the RDX molecules. In addition, the fact that the maximum NO_2 concentration is established at a finite distance from the burning surface is interpreted as evidence of the presence of RDX vapors above the burning surface.

Spectroscopic flame measurements permit only indirect evaluation of condensed-phase reactions, which are largely masked by fast gas-phase reactions near the burning surface. An original attempt to determine the primary products of condensed-phase decomposition by absorption-spectrum recording was made by Wormhoudt et al. [84]. Fiber light guides transparent at wavelengths of 2 – 5 μm were inserted into an opening parallel to the specimen surface to be ignited at a distance of a few millimeters from it. As the burning surface approached the opening, the intensity of N_2O absorption was continuously recorded. Simultaneously, the temperature near the opening was measured by a thermocouple made of Chromel--Alumel wire 127 μm in diameter.

The link to the temperature profile was rather approximate because of uncertainty of the location of the thermocouples and their large diameter. A sharp rise in the N_2O concentration is observed at relatively low temperatures (100 – 150 °C), at which the onset of intense reactions in the condensed phase is hardly possible. It is concluded that N_2O is formed in the more-heated layers of the condensed phase as a result of secondary gas reactions in bubbles. The disrupture of bubbles toward the cold end can occur when the specimen have cracks, which the authors observed in a visual study of longitudinal sections of starting specimens. It is intended to continue the work on the designed installation by performing simultaneous measurements of the NO_2 and NO concentrations.

Mass spectrometry was used for the first time to study nitramine flames at the end of the 1960s. Bernecker and Smith [23] studied the products of RDX and HMX combustion at p = 0.1 - 12 MPa. It was established that the principal final combustion products were in practically the same ratio for both materials (N_2 : CO: CO_2 : H_2 : H_2O = 3:2:1:1:2), which changes little at p > 2.5 MPa. NO, N_2O, and HCN were detected in small amounts. Formaldehyde CH_2O was not found in RDX combustion and was detected only in minor amounts in HMX combustion at atmospheric pressure.

Considerably more complete information on the chemical structure of the zone of gas-phase reactions in nitramine flames was obtained later [86-88] by time-of-flight mass spectrometry. Use of miniature quartz conical probes with a 0.1-mm opening and a tip outside diameter of 0.3 mm permitted the detailed study of the transformation zone of intermediate products of condensed-phase decomposition. The space distribution of concentrations for the gas components was measured when the burning specimen was moved toward the probe. The data corresponding to small (less than 0.1 mm) distances from the probe end to the burning surface were not analyzed because of the uncertainty of exact location of the probe end and because of the possibility that droplets of the melted material could strike the probe.

The results of mass-spectrometric studies of RDX flames are summarized in [87, 88]. RDX specimens 10 mm in diameter and 20 mm long were compressed from 50-μm particles to a density of 1.8 g/cm^3. Combustion was produced in argon at p = 0.05 MPa. Combustion was stable with a rate of 0.25 mm/sec. The burning surface of the specimens, which were extinguished by fast depressurization, was fairly smooth: the unevenness in an area 8 mm in diameter did not exceed 0.1 mm. A peak at m/e = 75 (RDX, fragmentary) was recorded at distances x < 0.1 mm from the burning surface. This could be due to vapor or liquid RDX that was sucked into the probe (m/e is the ratio of the molar mass of the species to the degree of ionization). From an analysis of the experimental data, Korobeinichev et al. [87] and Kuibida [88] concluded that the RDX flame, as asserted earlier [89], consists of two zones. The narrow cold flame region adjacent to the burning surface (x < 0.1 mm, estimated from the width of the decomposition zone of RDX vapor) has a temperature of ≈ 1100 K. Because of its smallness and the imposition of the process of probe interaction with the liquid surface layer of RDX, this region was not studied. After the first is a wide (≈ 2 mm) reaction zone of the intermediate products formed in reactions in the narrow zone. The following peaks were recorded in this wide luminescent flame region: I_{14} (N_2, NO_2, NO, N_2O, HCN), I_{28} (CO, N_2, N_2O, CO_2, CH_2O), I_{30} (NO, NO_2, N_2O, CH_2O), I_{29} (CH_2O), I_{27} (HCN), I_{44} (N_2O, CO_2), I_{46} (NO_2), I_{43} (HNCO), I_{42} (NCO), I_{18} (H_2O), and I_2 (H_2). Molecules from which ions of the given mass could be formed are shown in parentheses. The

component with m/e = 43 can exist in three forms: HCNO, HNCO, and HOCN. It is shown [35] that only HNCO exists in the gas phase at room temperature.

According to [25, 26], the main products of the cold flame zone are not NO_2 and CH_2O, as was assumed in [27, 29, 30], but NO and HCN, and the subsequent reactions of the latter determine the chemical structure of the luminescent zone of the RDX flame.

The combustion of pressed RDX pellets in argon at p = 1 atm assisted by CO_2-laser radiation with an intensity of 400 W/cm^2 was studied by Litzinger et al. [92]. Concentration profiles of the stable components were obtained by a mass-spectrometric method in the gas phase. The space resolution of the method using a quartz probe with a 30-μm opening was estimated by the authors at 100 – 150 μm. During the experiment, the specimen was moved toward the probe at a controlled speed by means of a mechanical drive. The distance from the burning surface to the probe tip was monitored by a video camera. The standoff distance of the luminescent (violet) flame in laser-assisted combustion was ≈ 5 mm with oscillations of 1 mm about the mean position. On the burning surface, bubbles were recorded that were considerably smaller (≈ 100 μm) than in combustion with weak heat supply or in pyrolysis in vacuum.

Quantitative data were presented on the gas-species concentrations at heights of 0 - 5 mm above the burning surface. Substances typical of RDX thermal decomposition were detected: NO_2, NO, N_2O, HCN, H_2O, N_2, CO, CO_2, and H_2. The appearance of a peak corresponding to m/e = 29 was initially explained by CH_2O decomposition in the ion source. However, experiments with a triple quadruple mass spectrometer showed that an ion with that mass is formed by another substance. In addition, according to spectroscopic measurements [81], the CH_2O concentration in the flame is very low. Therefore, data on the CH_2O concentration were not given in [92]. Nor do Litzinger et al. [92] consider correction of the measured values in the immediate vicinity of the burning surface, just as in the distant zones of the flame. Comparison with the NO and N_2O concentration profiles obtained under the same combustion conditions by the PLIF method [81] showed fair qualitative and quantitative agreement between independent experimental data. According to [92], in a narrow zone on the order of 0.5 mm above the surface, the NO_2 and HCN concentrations drop rapidly, the NO and H_2O concentrations rise, and the CO and N_2O concentrations vary extremely weakly. The CO_2 concentration at the surface is vanishingly small and becomes appreciable only at a height of 1.5 - 2 mm. It should be emphasized that all these data were obtained under combustion conditions with a powerful external heat supply and correspond to a combustion wave with the flame greatly removed from the surface. Moreover, laser radiation leads to uncontrollable heating of the probe and, as a consequence, to additional perturbation of the flame-zone structure. For this reason, comparisons of the experimental data of [92] even with the data of spectroscopic studies under similar combustion conditions [81] should be performed with caution, and comparisons with the data on self-sustained combustion [87, 88] are simply not valid, due to great differences in the experimental conditions. Attempts to bring about a relative mass balance (the total ratio of atoms in the measured components) have not been successful. In this connection, Litzinger et al. [92] correctly note that good quantitative agreement of the obtained experimental data with the results of theoretical calculations should not be expected.

A spectroscopic study of the chemical structure of a HMX flame at atmospheric and higher pressures was performed [71] using the PLIF method. It was found that self-sustained combustion at

p = 1 atm has a fluctuating nature and above the burning surface there is a zone containing droplets of liquid HMX (the mechanism of droplet formation was not investigated). Measurement of the NO concentration in this zone is impossible because of spectrum overlap. Time fluctuations did not permit measuring the space distribution of the component concentrations in the flame, but their maximum values were obtained: ≈ 6.5 % for H_2CO and NO_2, 3.6 % for OH, and 210 ppm for CN. HMX combustion under the action of a continuous CO_2 laser flux (400 W/cm^2) proceeds in a regime with a distant secondary flame. The flame stand off distance measured by CN luminescence varies from 4 to ≈ 0.2 mm as the pressure increases from 1 to 12 atm. The flame "thickness" varies from 4.5 to 0.5 mm in this case.

Mass-spectrometric probing of HMX flames at nitrogen pressures of 0.05 and 0.1 MPa was performed by Korobeinichev et al. [86] and Kuibida [88]. The burning rates of the specimens were 0.2 and 0.45 mm/sec, and their density was 1.76 g/cm^3. At lower pressures, fluctuations of the intensities of the recorded peaks were observed. At p = 0.1 MPa, peaks with m/e = 2 (H_2), 18 (H_2O), 27 (HCN), 28 (N_2, CO), 29 (CH_2O), 30 (NO, N_2O, NO_2, H_2CO), 43 (HNCO), 44 (N_2O, CO_2), 46 (NO_2), and 75 (HMX, fragmentary) were measured as a function of the distance x to the burning surface. The CH_2O and NO_2 concentrations drop to zero with an increase in x. The intensity of the HCN peak reaches a maximum at x = 0.6 (the point at which CH_2O and NO_2 disappear) and then drops to zero at x=1.2 mm. The presence of a peak with m/e = 42 (NCO) suggests the presence of molecules of isocyanic acid HN=C=O in the flame. The peak with m/e = 75 was recorded at a distance of a few tens of micrometers from the burning surface.

According to the experimental data of [22, 50, 86-88, 93], the main products of nitramine decomposition are CH_2O, NO_2, NO, N_2O, and HCN. Therefore, efforts have been directed toward studying the reactions

$NO_2 + CH_2O$ (I); $N_2O + CH_2O$ (II); $NO_2 + HCN$ (III).

Studies [91, 94, 95] were performed by spectroscopic methods in shock waves. This limited the volume of obtained information. Experimental results were interpreted in terms of a simple unbranched reaction. The rates of decrease in NO_2 and N_2O were used to determine the rate constants of the global stages (I - III). Results of a calculation performed on the basis of a multistage mechanism [91] indicate that reaction III proceeds in two steps. The first step involves consumption of NO_2 and an increase in the molar fraction of NO, and the second involves a reaction of NO with HCN. More complete data were obtained in the experiments of [96, 97] with a flat burner. The combustion of an HCN/NO_2 mixture at p = 25 torr and a mass flow rate of 0.0013 g/(cm^2 sec) was studied. The main combustion products, as detected by the FTIR method (infrared spectrometry with Fourier transform), were NO, CO, CO_2, and H_2O. The CO concentration was measured as a function of the distance from the burner edge. The temperature profile in the flame was determined from the CO vibrational temperature. The flame thickness, as determined by the criterion dT/dx > 0, was ≈ 6 mm. Based on processing of experimental data and analysis of the chemical mechanism, a reaction scheme was proposed that was recommended by Thorne and Melius [97] as a submechanism for the study of nitramine flames.

Mathematical modeling

One of the first studies on the modeling of combustion processes of melted or liquid volatile energetic substances was carried out more than 60 years ago at the Institute of Chemical Physics, Moscow [63]. A distinguishing feature of this and numerous subsequent studies was the assumption of a single global exothermic reaction that determined the rate of heat release and, accordingly, the burning rate. Based on general, often qualitative, physical considerations, the location of this reaction was specified in the combustion wave, and this determined whether burning rate controlling stage is in the gas or liquid phase. The required kinetic parameters were selected on the basis of *a priori* considerations, the structure of the molecules, and the global chemical equations of the reaction, or by solving inverse problems of the thermal theories of ignition and combustion.

At the present time, it is known [98, 99] that agreement between calculated and measured burning rates can be achieved even on the basis of fundamentally different theoretical premises, since combustion models contain a large number of matching parameters, primarily the coefficients of global chemical reactions. Therefore, the problem is one of direct experimental substantiation of the assumptions made. Moreover, it is stated [100] that comparison with experimental data must be performed not only for the burning rate and its dependence on pressure, but also for its dependence on the initial temperature, which is more sensitive to the parameters of the problem, and for the space distributions of the temperature and component concentrations in the combustion wave.

Early models did not show a deep understanding of the physical processes in the combustion waves of melted energetic substances. In pioneering studies [63, 101], a fundamental concept of the combustion mechanism of volatile energetic materials at low and moderate pressures was formulated according to which vaporization of the substances occurs with a considerably higher probability than the condensed-phase reaction, and the mass rate of vaporization under steady conditions is equal to the mass rate of vapor combustion. The latter can be calculated from formulas of the theory of combustion in gases [102]. In particular, if it is assumed that vaporization of a liquid energetic material occurs on the surface while a mono-molecular reaction proceeds in the gas phase, for the mass burning rate ρu we obtain [63] formula

$$\rho u = 2\frac{RT_{\max}^2}{E_g}\sqrt{\frac{(\lambda\rho A)_g}{Q(T_{\max}-T_0)}\exp\left(-\frac{E_g}{RT_{\max}}\right)} \qquad (2.12)$$

Here $T_{max} = T_0 + Q/c_g$ is the maximum temperature in the gas, and the total thermal effect Q includes the latent heat of vaporization of the energetic material; A_g and E_g are the pre-exponent and activation energy of a reaction in the gas; ρ_g, λ_g, and c_g are the density, thermal conductivity, and specific heat of the gas at $T = T_{max}$. The boiling point of the liquid energetic material does not enter in formula (2.12), since it is not the determining parameters of the problem in the case of a rate controlling gas phase. The same paper, with a reference to Ya. B. Zeldovich, who published a derivation and analysis of the formula 4 years later [103]), gives a formula for combustion of liquid energetic materials at elevated pressures, at which the probability of an exothermic reaction in the condensed phase can become considerably higher owing to an increase in the boiling point T_b:

$$\rho u = \frac{T_b}{c_c (T_b - T_0)} \sqrt{\frac{2QR(\lambda A)_c}{E_c} \exp\left(-\frac{E_c}{RT_b}\right)} \qquad (2.13)$$

Formula (2.13) defines an exponential dependence of the burning rate on the boiling point T_b and predicts a strong dependence on pressure: $d\ln\rho u / d\ln p = E_c/2L$, where L is the latent heat of vaporization. We note that [103] contains a warning about the use of the expression (E_c/2L) with L = const for high pressures, close to critical ones for the existence of a liquid phase. The simple formula for the vapor pressure above the surface of a heated liquid in the form p = const exp(-L/R T) should also be used with caution, since the value of L is reduced as the liquid temperature is increased.

Various models for the combustion of melted energetic materials with a global single-stage chemical mechanism have been published [104--106], in which particular regularities of the process have been refined. The further development of the concepts of the combustion of energetic materials based on experimental results has led to studies of multistage chemical transformations in combustion waves. The pioneering work in this area, which is characterized by an expanded global mechanism of chemical reactions, was performed by V. N. Vilyunov [107]. He proposed a three-stage scheme for the reaction of energetic materials in combustion waves: the initial transformation takes place in the condensed phase and is followed by a transformation of intermediate products from the condensed-phase decomposition and the final transformation of the intermediate compounds into combustion products. The burning rate was calculated analytically by the approximate Zeldovich - Frank-Kamenetskii method. Subsequently, the idea of multistage chemical transformations was used successfully [108] for the more complex case of the combustion of energetic materials with a phase transition on the surface (vaporization, sublimation). It was assumed that independent global chemical reactions of the first order proceeded in the condensed and gas phases. In the pores of decomposing material, vapor is formed by an equilibrium mechanism with subsequent exothermic transformation of the vapor into final combustion products. The vaporized energetic material in the flame above the surface undergoes a similar transformation. The condensed-phase reaction also leads to formation of final combustion products. The problem was solved numerically. It was found that, depending on the numerical values of the determining parameters, there are combustion regimes with rate controlling reactions (which determine the burning rate almost completely) in both the condensed and gas phases. Moreover, calculations showed that there is also a mixed combustion regime, in which the burning rate is approximately equal to the sum (with an error not more than 15 %) of the rates of purely solid-phase and gas-phase combustion. The pressure exponent in the burning-rate law in the mixed regime is equal to the half-sum of the exponents in the laws for the solid-phase and gas-phase regimes, and the initial temperature burning rate coefficient takes an intermediate value for single-zone combustion regimes.

Simultaneously with [108], a model of RDX combustion based on a global mechanism of two successive chemical reactions was published [89]. It involves partial decomposition in the liquid phase and simultaneous vaporization of the remaining initial RDX from the burning surface. The intermediate decomposition products react in the gas phase to the final combustion products. RDX decomposition in both the liquid and gas phases is described by the first-order reaction

$$RDX \rightarrow 1.5\ N_2 + N_2O + NO_2 + 3\ CH_2O \qquad (2.14)$$

with the following kinetic parameters for each phase:

$k_{3,\,liq} = 3\ 10^{18} \exp(-41500/RT)\ \ sec^{-1}$ [37]; $k_{3,\,gas} = 3.16\ 10^{15} \exp(-41500/RT)\ \ sec^{-1}$ [59]
The secondary reaction between the decomposition products is described as

$$5/7\ CH_2O + NO_2 \rightarrow NO + 2/7\ CO_2 + 3/7\ CO + 5/7\ H_2O \qquad (2.15)$$

Two sets of constants were examined for reaction (4):
$k_4 = 10^9 \exp(-19000/RT)$, liter/(mol sec) which was obtained in [109] for $T \approx 430$ K, and
$k_4 = 1.26\ 10^{10} \exp(-26700/RT)$, liter/(mol sec) which was obtained in shock-tube experiments at T=970 – 1470 K.

Estimates of the characteristic times for gas-phase chemical reactions (2.14) and (2.15) have shown that the reaction of RDX-vapor decomposition is completed about 100 times faster than the reaction to the final products. Accordingly, the chemical structure of the gas-phase flame consists of internal and external zones. The internal zone exerts a real effect on the heat feed back to the burning surface, especially at relatively low pressures. For example, in calculations in which the rate of the secondary reaction was artificially reduced by a factor of 10, the total heat flux from the flame changed by 7, 11, and 16 % at p = 10, 20, and 40 atm, respectively. Therefore, primary attention in numerical modeling was given to a calculation of the combustion-wave parameters in the internal (adjacent to the surface) zone of the flame.

For the kinetic constants used in the calculations, it was found that the width of the RDX-vapor decomposition zone above the surface at p = 10 – 40 atm was only 5 – 2 μm, and the temperature of the internal flame zone varied within 1100 – 1200 K. The degree of decomposition of the initial RDX on the burning surface was 7 – 13 %. The increase in the degree of RDX decomposition in the condensed phase with rise in pressure is due to the increase in the liquid-phase reaction rate with increase in the surface temperature, which obeys the law of equilibrium vaporization (Clausius--Clapeyron equation). The effect of temperature is stronger than that of a reduction of residence time.

A similar chemical-reaction scheme was used by the same authors to describe the HMX combustion wave [110]. The calculation results are strikingly similar: at p = 20 - 40 atm, the zone of HMX-vapor decomposition is 4 – 2 μm, and the temperature in the internal flame zone rises to approximately 1100 K. The mass fraction of HMX vapor near the burning surface is 30 %. Proceeding from the assumption of a two-zone structure of the HMX flame [110, 90], Cohen et al. [111] proposed a more detailed scheme of global chemical reactions. It includes three liquid-phase decomposition reactions of the substance and five or six gas-phase reactions, depending on the selected reaction path, for example, through formation of CH_2O or HCN. The alternative choice of a path is a result of insufficient knowledge of the true mechanism. Nevertheless, the results of calculation of the combustion-wave parameters were close. When the pressure changes from 20 to 100 atm, the amount of HMX that reacts in the condensed phase varies from 2 to 8 %, which indicates the dominant effect of exothermal vapor-phase transformations, even at p = 100 atm. The calculated temperature profile has a clearly expressed two-stage nature with an almost zero gradient in the interval between the primary (vapor decomposition) and secondary (reaction between vapor-decomposition products) flames. The width of the primary-flame zone is reduced by approximately a factor of 2 or 3 when the pressure is increased from 20 to 100 atm; the temperature of this zone is 1030 - 1080 K. The calculation data led to the important conclusion that it is practically impossible to increase the burning rates for HMX by means of catalysts. This

goal can be accomplished by acting on the chemical mechanism of the process to increase the heat release near the surface.

Note that a "plateau" on the temperature profile was not observed in later experimental studies [70, 71]. The conclusions of [110, 111] that condensed-phase chemical transformation of nitramines are insignificant are based exclusively on theoretical estimates of an a priori character, since it is very difficult to measure that quantity experimentally. Nevertheless, an indirect estimate can be made by a temperature-profile analysis, which indicates an appreciable contribution of exothermic reactions in the condensed phase to the heat balance on the burning surface [70, 76, 78]. Of interest in this connection are the results of modeling in [78], based on an examination of intense reactions in a liquid surface layer as well as in vapors of vaporized substance near the burning surface. As an indirect basis for their approach, Mitani and Williams [78] note that the power law of the burning rate versus pressure does not undergo appreciable changes at nearly atmospheric pressures and in the range of 70 – 100 atm, but the experimental data indicate flameless combustion at p = 1 atm and a change in flame color from blue to bright orange with passage through the pressure level of 70 – 100 atm.

Analytical solutions and estimates made on their basis [78] attest to a gradual increase with pressure of the relative contribution of the heat flux from the gas flame q_s to the heat balance on the burning surface (the mass fraction of vaporized material η increases from 0.65 to 0.75 with an increase in pressure from 1 to 100 atm):

$$q_s + \rho u Q(1 - \eta) - \rho u L \eta = c \rho u (T_s - T_0). \qquad (2.16)$$

A combination of independently determined kinetic parameters with selected values of the order and pre-exponent for the gas-phase reaction, yields fairly good agreement of the calculated and experimental data on the dependencies of the burning rate on pressure and initial temperature. It was found that at the lower limit of combustion with respect to pressure (≈ 0.2 atm), the heat flux from the gas phase is close to zero. According to the combustion theory [78], this must lead to diffusion thermal instability, which is actually observed in experiments.

The fairly deep transformation of the condensed-phase (tens of percent) predicted by a number of models makes it necessary to seek methods for the adequate description of this process. The first such description was presented in [112], which dealt with the combustion of polyvinyl nitrate. It was hypothesized that the gases formed in the liquid layer moved simultaneously with the burning surface. In this case, the density of the material in the combustion wave decreases monotonically to the gas density. Another limiting case was considered in [113], where it was actually hypothesized that gas jets emerged at increased velocity from the depth of the liquid layer. The approach of [113] was studied in detail in [114, 115] as applied to nitramines. The law of conservation of mass is written as

$$(\rho u)_c(1 - \alpha) + (\rho u)_g \alpha = dm/dt = \text{const} \qquad (2.17)$$

where α is the volume fraction of gas in a given combustion-wave cross section. It was proposed that $u_c \neq u_g$ be calculated using an additional parameter s, which characterizes the relative effect of the surface-tension forces (Marangoni effect) and liquid viscosity. Then,

$$u_c = [(dm/dt)/\rho_c](1 - s\alpha), \quad u_g = [(dm/dt)/\rho_g](1 - s\alpha + s).$$

Unfortunately, the lack of reliable experimental data on the surface-tension coefficient does not permit one to estimate s reliably. In [115], for example, calculations were performed for s = 0.

As noted above, models with an extended global mechanism have made it possible to explain rather successfully the observed dependencies of the burning rate on pressure and initial temperature, but they are incapable of explaining the actual behavior of the gas-component concentrations in a flame. This problem can be solved only on the basis of a detailed chemical mechanism of reactions in a flame, that includes a large set of elementary steps. In one of the first studies in this area, devoted to RDX combustion [116], the experimental data of [87] were used to formulate a multistage kinetic mechanism that included 23 components and 90 reversible elementary steps. The problem was solved for the secondary flame zone under the assumption that the primary zone (vapor-decomposition zone) generates NO and HCN rather than NO_2 and CH_2O, as was assumed by a number of authors. Calculations made it possible to distinguish the leading (in the sense of component production) steps of the process and to refine the rate constants of little-studied reactions. As a result, fairly good agreement with measured [87] component-concentration profiles was obtained in [116-118], but the absence of experimental data on the temperature profile did not permit additional estimate of the rate constants to be obtained. An attempt was undertaken to model the chemical processes over the entire flame zone using a detailed kinetic mechanism supplemented by a single-stage reaction of RDX-vapor decomposition. Along with other components, the molar fraction of vapor on the burning surface was varied in the calculations. When the law of conservation of energy for the condensed and gas phases was satisfied, the mass flow rate of vapor was overestimated in the calculations, and this could be a consequence of the adopted values of the rate constants for the little-studied steps. Nevertheless, as numerous subsequent calculations have shown, the assumptions of a monotonic rise of temperature (single-zone structure), the leading role of the interaction of HCN and NO, and the multi-step nature of RDX-vapor decomposition were valid.

After [116-118], similar studies were published abroad. HMX combustion was modeled in [119] on the basis of a kinetic mechanism containing 26 components and 77 reversible elementary reactions. The effect of the composition of the condensed-phase decomposition products on the burning rate was examined by calculations. When the single decomposition pathway

$$HMX \rightarrow 4\,H + HCN + NO_2 \qquad (2.18)$$

was selected, the calculated burning rate was lower than the experimental. It is emphasized that HCN and NO are the main reacting components in this case and the source of NO is the reaction

$$H + NO_2 \rightarrow NO + OH.$$

Attempts to describe the decomposition process strictly through the reaction

$$HMX \rightarrow 4\,(CH_2O + N_2O) \qquad (2.19)$$

led to a divergence in the computation process. When the decomposition channels were combined and the fraction of decomposition through channel (2.19) was increased, the calculated burning rate rose greatly. Therefore, both decomposition branches were combined to obtain the required burning rate. In [51, 120], an attempt was made to combine a detailed description of the chemical reactions in a RDX flame with a global description of condensed-phase reactions. The total mechanism [51] included a detailed kinetic scheme of RDX-vapor decomposition and comprised 38 components and 158 stages. RDX decomposition in the liquid phase was modeled by the first-order reaction RDX $\rightarrow$ 3 CH_2O +3 N_2O with rate constant $K = 4.66 \cdot 10^{18}$ exp(-47800/RT) [sec^{-1}]. According to calculations performed for p = 0.5, 1, 17, and 20 atm, about 93 % of the RDX is vaporized from the burning surface, and the burning rate is chiefly governed by the heat feed from the flame. At p = 0.5 atm, the calculated concentration profiles are in satisfactory agreement with experiment [87].

The approach of [51, 120] was further developed by American researchers. For example, a substantially detailed description of liquid-phase processes can be found in [121]. The formation of bubbles in the liquid phase and the reaction in them of 18 gaseous components were taken into account. In the liquid phase, reactions between five liquid components and seven gaseous components dissolved in the liquid components were allowed for. The refined kinetic mechanism from [51] was used in the gas phase. The problem of unsteady RDX combustion formulated in [121] requires knowledge of numerous constants that are presently unavailable. Examples of calculations of combustion-wave parameters are not presented in [121]. A description of processes in a foamed liquid layer that was simpler and more realizable in practical calculations was proposed in [122]. The calculations employed two detailed chemical flame mechanisms: according to [51] and [123]. The temperature distribution and the concentration profiles of the main components were well reproduced. In combustion under normal conditions ($p = 1$ atm and $T_0 = 20\ ^{\circ}C$), the degree of condensed-phase decomposition on the surface is 50 %, and the volume fraction of the gas phase reaches 40 %. It is interesting to note that in a combustion wave at $p = 90$ atm the parameter values are similar (degree of decomposition 50 % and volumetric fraction of bubbles 35 %). However, the thickness of the chemical-reaction zone in the condensed phase is reduced approximately from 90 μ to 1.5 μm in this case. It must be borne in mind that condensed-phase transformations are described in the model by an integrated method - by both the chemical reaction of the starting liquid RDX and the reaction of the products of RDX-vapor decomposition in the bubbles. The equation of conservation of mass (2.17) is solved in [122] assuming that $(u\rho)_g = (u\rho)_c$. In fact, this means that the gases escape from the burning surface in a jet mode (the scheme described in [113]), and it is difficult to expect that a foam layer will be formed on the surface. Consequently, the residence time of the gaseous components in the liquid layer must be extremely short, at least at low pressures. Therefore, an integrated description of heat release in the condensed phase with allowance for gas-phase reactions in bubbles and jets is unjustified.

Formulations of the problem similar to [122] have been carefully analyzed in [100, 124] from the point of view of the selection of input data for model calculations and to explain the observed temperature profile. It was found that the weak points in the full-scale modeling of combustion waves were in the description of the condensed-phase decomposition processes and the liquid-to-gas transition. All researchers have to use a simplified global description of the condensed-phase reactions that includes two or three parallel stages. The choice of kinetic parameters for these reactions is rather arbitrary. The vaporization process is described approximately, often using kinetic constants that correspond to sublimation experiments. Nevertheless, with a proper selection of input data, calculations permit mainly successful matching with available experimental results for the burning rates of RDX and HMX, their temperature sensitivities, and the temperature and concentration profiles. Some questions remain concerning the concentration profiles of NO_2 and NO, which could be a result of experimental errors or incorrect specification of the input parameters for the calculation. Moreover, the detailed kinetics of nitramine-vapor decomposition remains little studied both theoretically and experimentally.

In [51, 122, 124], the mass burning rate is calculated as the difference between the mass fluxes of molecules that have left and returned to the liquid. The ratio of the mass burning rate to the fluxes is small ($\approx 0.001 - 0.0001$ [125]), and this can lead to instability of the computation process. In addition, the coefficient of accommodation (sticking) of liquid molecules is usually un-

known, and in most calculations it is assumed *a priori* to be equal to unity. To avoid this, it was proposed [125] that the law of equilibrium vaporization be used as a condition at the liquid--gas interface (as in [89]) and the burning rate be determined as an eigenvalue of a boundary-value problem.

In modeling the RDX combustion wave, Prasad et al. described [125] the process of liquid-phase decomposition by the stages

$$RDX \rightarrow 3\ CH_2O + 3\ N_2O,$$
$$RDX \rightarrow 3\ H_2CN + 3\ NO_2,$$
$$CH_2O + NO_2 \rightarrow CO + NO + H_2O$$

This implies that the gases are dissolved in the liquid and leave it by diffusion and that a foam layer does not exist. Flame reactions are described by a chemical mechanism based on 228 elementary stages and 44 reagents. The basis of the mechanism was borrowed from [51], and additions were taken from [126, 127]. The calculations gave an exponent of the burning-rate law equal to 0.76, which correlates with the experimental dependence fairly well. Satisfactory agreement was also obtained with the experimentally measured temperature profile and burning rate temperature sensitivity. It is pointed out that the process of RDX melting in fact occurs not suddenly at a given temperature but is "spread" over a certain temperature interval. It is also noted that the use of classical concepts of vaporization and condensation of molecules under strong temperature gradients in the liquid, which correspond to combustion in the presence of a powerful external heat supply, can lead to substantial errors.

It should be noted that the overwhelming majority of efforts to model the combustion of energetic materials and nitramines, in particular, have been devoted to the description of steady processes. This is due to the great difficulties in the numerical realization of such problems (analytic approaches do not work because of the strong nonlinearity of the equations) and the absence of physical concepts of the dynamic behavior of the reacting system. As applied to nitramines, Zarko et al. [128, 129] formulated the problem of the unsteady combustion of melted energetic material with an exothermic transformation in the liquid phase (one global reaction of the first order) and the gas phase (a global reaction of the first order for vapor decomposition and a global reaction of the second order for the interaction of the decomposition products). A boundary condition at the interface was formulated in the form of the Clausius--Clapeyron equilibrium vaporization law. Despite the simplified formulation, the model allowed a number of important observations to be explained. It was shown that, depending on the choice of kinetic parameters, ignition can occur as a result of heat release in the condensed or gas phase. However, when intense pulsed heating of the gas near the surface is simulated (by means of a wire or electric spark), a flame can be ignited at a short distance from the burning surface. This theoretical prediction was verified at the Institute of Chemical Kinetics and Combustion in laboratory experiments at atmospheric pressure. Ignition of pressed RDX by an ND/YAG laser led to flameless gasification of the specimen, which became flame combustion when a local flame from a gas burner was introduced into the stream of decomposition products.

Intrinsic instability of combustion with vaporization on the surface in the presence of appreciable heat release in the condensed phase and with comparatively weak heat release from the gas was revealed by calculations [130]. The instability is caused by the formation of a temperature

maximum in the liquid layer due to the heat sink on the surface as a result of endothermal vaporization process.

It is interesting to note that the unsteady combustion mechanism is sensitive to energy stimulus with comparatively small contributions. In particular, this pertains to the melting heat, which is less than 3 – 4 % of the total heat effect of combustion. It was established [131] that allowance for melting narrows the stability region of steady combustion for semi-transparent materials. For opaque energetic materials, there is a region of stable combustion under radiation, which is bounded by upper and lower critical values of radiant flux. The greater the melting heat, the wider the region of stable combustion under radiation.

Erikson and Beckstead [132] undertook an attempt to construct a numerical model of unsteady RDX combustion within the framework of a detailed chemical mechanism that included two global chemical stages in the condensed phase and 120 elementary steps (43 components) in the gas phase. The behavior of the RDX burning rate under periodic action of laser radiation was modeled. Satisfactory quantitative agreement with experimentally measured [133] amplitudes of the burning-rate response was achieved, and the behavior of the phase shift of the burning rate was reproduced qualitatively. It must be noted, however, that along with a comparatively detailed description of the chemical mechanism, Erikson and Beckstead [132] used a very approximate relation between the instantaneous burning rate and the surface temperature T_s in the form of the pyrolysis law $u = \text{const} \exp(-E_v/R\ T_s)$, where E_v is the activation energy of vaporization. Neither the structure of this relation nor the choice of an activation-energy value is justified, and this casts doubt on the reliability of information obtained in such calculations.

It is interesting to note that when global kinetics was used, calculations [129] showed the possibility of obtaining qualitatively different forms of the burning-rate response function for the periodic action of laser radiation. One of these forms, which coincides with the classical form [133, 134], is obtained under conditions of flameless gasification, which approximately corresponds to the specification of a pyrolysis law for the burning rate. Another, which is distinguished by the asymptotic convergence of the response function on a finite value (instead of zero level, as in the classical case), occurs when the rate controlling zone is located in the gas phase.

It is obvious that a great deal of efforts must be applied to construct an adequate description of unsteady combustion even for comparatively simple monopropellants such as nitramines. One aspect of this work involves the construction of reduced global schemes that follow from detailed chemical mechanisms. Successful examples of such schemes are known (see, e.g., [135]) but for nitramine flames they are not available.

Reduction of a detailed chemical mechanism is aimed primarily at reducing the volume of computations. At the same time, selection of rate controlling stages, which is an important aspect of this work, facilitates a deeper understanding of the chemistry of the combustion process.
According to the aforesaid, a two-stage chemical process occurs in the gas phase of a nitramine combustion wave. The complexity of the chemical process and the lack of many kinetic parameters cause complicates the theoretical description of the process. In particular, the abovementioned detailed kinetic mechanisms differ considerably in the number of steps as well as in the rate constants of the elementary steps. In experiments, along with stable components, optical

methods yield a distribution of active species (atoms and radicals) [71, 81], and, therefore, allowance for steps in which these species participate is important in identification of the kinetic mechanism. However, the energy contributions of species with small molar fractions are small, the roles of active species in the chemical process differ, and some of them can often be ignored in calculations in technical applications. For processes in RDX flames, the rate controlling stages were studied in [116--118] (23 components and 90 steps) in the luminous zone of the flame, while in [51] (38 components and 158 steps) and [123] (44 components and 228 steps) they were studied in the entire flame zone. Series of calculations of the chemical structure of the RDX flame we performed to find the rate controlling steps and components. The calculations were performed [136] for p = 0.5 – 90 atm. As input data for the calculations, experimental values were specified of the burning rate and burning-surface temperature as well as initial molar fractions of components typical of RDX combustion under self-deflagration conditions and under the influence of laser radiation. The kinetic mechanism included reactions from the mechanisms of [51, 125] and contained 265 steps and 43 components. The selection was performed using various sets of elementary-reaction rate constants. Preliminarily, kinetic mechanisms were obtained consisting of 80-100 stages and 31-35 components (C_2N_2, HCNO, CNO, H_2CNO, H_2CNH, H_2O_2, NO_3, HNO_3, NCN, HO_2, HOCN, and NH_3 were excluded).

Concluding remarks

As already noted, the problem of constructing an adequate physicochemical mechanism of nitramine combustion has been stated, among others. It is apparent from the above material that the concept of "adequacy" itself has evolved over time. In particular, use of extended schemes of global reactions instead of schemes with a single global reaction has greatly increased the "flexibility" of mathematical description, which has considerably improved the agreement with experiment. However, the selection of kinetic parameters for any global chemical stage contained in the complex mechanism of transformations in the combustion wave cannot be based on *a priori* assumptions. This is a fundamental difficulty in formulation of global chemical mechanisms.

So far, experiments have played a decisive role in the understanding of the nitramine-combustion mechanism. Recent studies have provided important information on the structure of the combustion wave. It has been found that the temperature distribution in a self-sustained combustion wave has a single-zone structure, but the chemical stages of vapor decomposition and the formation of final combustion products are separated in space. Under the influence of a powerful radiant flux, the temperature distribution also becomes two-zone, the zones are broadened, and this provides new fundamental possibilities for studying the combustion mechanism, since the composition of the gasification products, which under these conditions is more easily determined, carries information on the chemical transformations in the condensed phase. The need to develop new experimental approaches to studying the structure and dynamic behavior of the combustion wave retains its importance. In particular, it remains unknown how a two-phase medium is formed in a liquid layer, how gas is liberated from a condensed substance, and what conditions characterize processes on a burning surface.

Theoretical description of nitramine combustion has gained considerable development in the past decade. However, it can be said that it still depends to a considerable extent on the intuition and individual "skill " of the researcher. Impressive advances have been made in the description of nitramine flames. It has become clear that the lack of reliable information on the concentration

profiles in real flames is limiting at the present time, but theoretical calculations make it fairly easy to explain new experimental data. At the same time, the description of condensed-phase processes has been implemented at a very approximate level, and, as has been emphasized above, the choice of global reactions and kinetic parameters does not have a reliable basis.

Studies of the unsteady combustion of nitramines are of significance as a source of important additional information on the combustion mechanism. On the one hand, the problem is one of obtaining reliable experimental information on the unsteady burning rate and on the behavior of the temperature and concentration profiles. On the other hand, considerable efforts are required to construct adequate mathematical models and methods for their solution. It is obvious that unsteady processes contain an enormous volume of information, which cannot be obtained and processed over a reasonable period of time. Both approaches must therefore be combined to increase the effectiveness of research.

2.2. - REFERENCES

1. **F. I. Dubovitskii and B. L. Korsunskii**, "Kinetics of the thermal decomposition of n-nitrocompounds," Usp. Khim., 1981, v. 50, No.10, pp.1828-1871.
2. **T.L.Boggs**, "The thermal behavior of cyclotrimethylenetrinitramine (RDX) and cyclotetramethylenetetranitramine (HMX)," in: K.Kuo and M.Summerfield (eds). Fundamentals of Solid-Propellant Combustion, AIAA, New York, 1984, pp.121-175. (Progress in Astronaut. and Aeronaut, 90).
3. **R.A.Fifer,** "Chemistry of nitrate ester and nitramine propellants," ibid., pp. 177-237.
4. **M.Ben-Reuven and L.M. Caveny,** "Nitramine monopropellant deflagration and general nonsteady reacting rocket chamber flows'', MAE Report, 1980, No.1455. Princeton Univ.
5. **E. Yu. Orlova**, Chemistry and technology of brisant explosives [in Russian], Khimiya, Leningrad, 1973.
6. **P.G.Hall**, "Thermal decomposition and phase transitions in solid nitramines," Trans. Faraday Soc., 1971, v. 67, Part 2, pp. 556-562.
7. **K. K. Andreev**, "Thermal decomposition and combustion of explosives"[in Russian], Nauka, Moscow, 1966.
8. Chemical Encyclopedia, Moscow, Great Russian Encyclopedia, 1992, v .3, p.369.
9. **A.E.Fogelzang**, "Combustion and explosives data base flame", Version 2.4, Mendeleev Technol. Univ., Moscow, 1995.
10. **H.Bathelt**, "Data base of thermochemical data," 3nd edition. Pfinztal, Inst. Chem. Technol., Germany, 1996.
11. **R.L.Shoemaker, J.A.Stark, and R.E.Taylor**, "Thermophysical properties of propellants," in: High Temp.-High Pressures, ETPC Proc., 1985, v. 17, pp.429-435.
12. **L. Ya. Kashporov**, "Thermal analysis of RDX combustion," Fiz. Goreniya Vzryva, 1994, v. 30, No.3, pp. **20-28.**
13. **F. Daniels and R.A. Alberti,** Physical Chemistry, 2nd ed., John Wiley and Sons, New York-London, 1961.
14. **A. F. Belyaev**, "On combustion of boiling explosives," Dokl. Akad. Nauk SSSR, 1939, v 24, p. 253.
15. **A. F. Belyaev**, "Boiling point and evaporation heat for several secondary explosives," Zh. Fiz. Khim., 1948, v. 222, No.1, pp. 91-101.

16. **Yu. A. Maksimov**, "The boiling point and enthalpy of evaporation of liquid RDX and HMX," Zh. Fiz. Khim., 1992, v. 66, No.2, pp. 540-542.
17. **Yu. A. Maksimov, V. N. Apal'kova, O. V. Braverman, and A. I. Solov'ev**, "Kinetics of thermal gas-phase decomposition of cyclotrimethylenetrinitramine and cyclotetramethylene-trinitramine", Zh. Fiz. Khim, 1985, v. 59, No.2, pp. 342-345.
18. **R.N.Rodgers**, "Determination of condensed phase kinetic constants, note," Thermochim. Acta, 1974, No.9, pp.444-446.
19. **J.M. Rosen and C. Dickinson**, "Vapor pressures and heats of sublimation of some high melting organic explosives," J. Chem. Eng. Data, 1969, v. 14, No.1, pp. 120-124
20. **N.S. Cohen, G.A. Lo, and J. Crowley**, "Model and chemistry of HMX combustion," AIAA J., 1985, v. 23, No.2, pp. 276-282.
21. **P.J. Miller, S. Block, and G.J. Piermarini**, "Effects of pressure on the thermal decomposition kinetics, chemical reactivity and phase behavior of RDX," Combust. Flame, 1991, v. 83, No. 1 and 2, pp. 174-184.
22. **B. Suryanarayana, R.J. Graybush, and J.R. Autera,** "Thermal degradation of secondary nitramines: a nitrogen-15 tracer study of HMX," Chem. Ind., London, 1967, v. 52, pp. 2177-2178.
23. **B. Suryanarayana, J.R. Autera, and R.J. Graybush**, "Mechanism of thermal decomposition of HMX," in: Proc. 1968 Army Sci. Conf. (OCRD), West Point, New York, 1968, v. 2, p.423.
24. **B.B. Goshgarian**, "The thermal decomposition of RDX and HMX," AFRPL-TR-78-76, Oct. 1978.
25. **M. Schroeder**, "Critical analysis of nitramine decomposition results: some comments on the chemical mechanism," in: 16th JANNAF Combust. Meeting, CPIA Publ. 308, December 1979, v .2, pp.17-34.
26. **M. Farber and R.D. Srivastava**, "Mass spectrometric investigation of the thermal decomposition of RDX," Chem. Phys. Lett., 1979, v. 64, pp. 307-309.
27. **M. Farber and R.D. Srivastava**, "Thermal decomposition of HMX," in: 16th JANNAF Combust. Meeting, CPIA Publ. 308, December 1979, v. 2, pp.59-71.
28. **J. Stals**, "Chemistry of aliphatic unconjugated nitramines. Pt. 7: interrelations between the thermal, photochemical and mass spectral fragmentation of RDX," Trans. Faraday Soc. 1971, v. 67, pp. 1768-1775.
29. **C.V. Morgan and R.A. Bayer**, "Electron-spin-resonance studies of pyrolysis products," Combust. Flame, 1979, v. 36, pp. 99-101.
30. **T.B.Brill,** "Multiphase chemistry consideration at the surface of burning nitramine monopropellants," J. Propuls. Power, 1995, v. 11, No.4, pp. 740-751.
31. **J.C. Oxley, A.B. Kooh, R. Szekeres, and W. Zhang,** "Mechanism of nitramine thermolysis," J. Phys. Chem., 1994, v. 98, pp. 7004-7008.
32. **F.C. Rauch and A.J. Fanelli**, "The thermal decomposition kinetics of hexahydro-1, 3, 5-trinitro-1, 3, 5-triazine above the melting point: evidence for both a gas and liquid phase decomposition," J. Phys. Chem., 1969, v. 73, No.5, pp. 1604-1608.
33. **A.E. Axworthy, J.E. Flanagan, and D.E. Woolery**, "High temperature pyrolysis studies of HMX, RDX and TAGN," in: 15th JANNAF Combust. Meeting, CPIA Publ. 297, February 1979, pp. 253-265.
34. **G.K. Adams** "The thermal decomposition of RDX," SAC Rept. 5766. February 1944.

35. **J.D. Cosgrove and A.J. Owen**, "The thermal decomposition of 1, 3, 5-trinitrohexahydro-1, 3, 5-triazine (RDX). Part I: The products and physical parameters," Combust. Flame, 1974, v. 22, No.1, pp. 13-18.
36. **J.D. Cosgrove and A.J. Owen**, "The thermal decomposition of 1, 3, 5-trinitrohexahydro-1, 3, 5-triazine (RDX). Part II: The effects of products," ibid, pp. 19-22.
37. **A.J.B. Robertson**, "The thermal decomposition of explosives. Part II: cyclotrimethylene-trinitramine and cyclotetramethylenetetranitramine," Trans. Faraday Soc., 1949, No.45, pp. 85-93
38. **J.J. Rocchio and A.A .Juhasz**, "HMX thermal decomposition chemistry and its relations to HMX-composite propellant combustion," in: 11th JANNAF Combust. Meeting, CPIA Publ., December 1974, pp.247-265.
39. **D.A. Flanigan and B.B. Stokes**, "HMX deflagration and flame characterization. V. 1, phase II: Nitramine decomposition and deflagration characterization," AFRPL-TR-79-94. October 1980.
40. **R. Shaw and F. Walker**, "Estimated kinetics and thermochemistry of some initial unimolecular reactions in the thermal decomposition of 1, 3, 5, 7-tetranitro-1, 3, 5, 7-tetraazacyclooctane in the gas phase," J. Phys. Chem., 1977, v. 81, No. 25, pp. 2572-2576.
41. **R. Behrens (Jr.),** "Thermal decomposition of energetic materials: temporal behaviors of the rates of formation of the gaseous pyrolysis products from condensed phase decomposition of octahydro-1, 3, 5, 7-tetranitro-1, 3, 5, 7-tetrazocine," J. Phys. Chem. 1990, v. 94, No. 17, pp. 6706-6718.
42. **R. Behrens (Jr.) and S. Bulusu**, "Thermal decomposition of energetic materials. 2. Deuterium isotope effect and isotope scrambling in condensed-phase decomposition of octahydro-1, 3, 5, 7-tetranitro-1, 3, 5, 7-tetrazocine," J. Phys. Chem. 1991, v. 95, No.15, pp. 5838-5845.
43. **R. Behrens (Jr.) and S. Bulusu**, "Thermal decomposition of energetic materials. 3. Temporal behaviors of the rates of formation of the gaseous pyrolysis products from condensed phase decomposition of 1, 3, 5-trinitrohexahydro-s-triazine," J. Phys. Chem., 1992, v. 96, No. 22, pp.8877-8891.
44. **R Behrens (Jr.) and S. Bulusu**, "Thermal decomposition of energetic materials. 4. Deuterium isotope effect and isotopic scrambling (H/D, $^{13}C^{18}O$, and $^{14}N^{15}N$) in condensed phase decomposition of 1, 3, 5-trinitrohexahydro-s-triazine," ibid, pp. 8891-8897.
45. **R. Behrens (Jr.),** "Identification of octahydro-1, 3, 5, 7-tetranitro-1, 3, 5, 7-tetrazocine (HMX) pyrolysis products by simultaneous thermogravimetric modulated beam mass-spectrometry and time-of-flight velocity-spectra measurements," Int. J. Chem. Kinet., 1990, v. 22, No. 2, pp. 135-157.
46. **R. Behrens (Jr.),** "Determination of the rates of formation of gaseous products from the pyrolysis of octahydro-1, 3, 5, 7-tetranitro-1, 3, 5, 7-tetrazocine (HMX) by simultaneous thermogravimetric modulated beam mass spectrometry," ibid, pp. 159-173.
47. **S. Bulusu and R. Behrens**, "A review of the thermal decomposition pathways in RDX, HMX and other closely related cyclic nitramines," Defence Sci. J., 1996, v. 46, No.5, pp. 347-360.
48. **T.B. Brill**, "Connecting the chemical composition of a material to its combustion characteristics," Progr. Energ. Combust. Sci. 1992, v. 18, pp. 91-116.
49. **Y. Oyumi and T.B. Brill**, "Thermal decomposition of energetic materials. 3. A high-rate, in situ, FTIR study of the thermolysis of RDX and HMX with pressure and heating rate as variables," Combust. Flame, 1985, v. 62, pp. 213-224.

50. **S.F. Palopoli and T.B. Brill**, "Thermal decomposition of energetic materials. 52. On the foam zone and surface chemistry of rapidly decomposing HMX," Combust. Flame, 1991, v. 87, No. 1, pp. 45-60.
51. **C.F. Melius**, "Thermochemical modeling. II: Application to ignition and combustion of energetic materials," in: S. Bulusu (ed.) Chemistry and Physics of Molecular Processes in Energetic Materials, Kluwer, Boston, 1990, pp. 51-78.
52. **X. Zhao, E.J. Hintsa, and Y.T. Lee**, "Infrared multiphoton dissociation of RDX in a molecular beam," J. Chem. Phys., 1988, v. 88, No. 2, pp. 801-810.
53. **T.R. Botcher and C.A. Wight,** "Transient thin film laser pyrolysis of RDX," J. Phys. Chem., 1993, v. 97, pp. 9149-9153.
54. **T.R. Botcher and C.A. Wight,** "Explosive thermal decomposition of RDX," J. Phys. Chem., 1994, v. 98, pp. 5441-5444.
55. **Yu. Ya. Maksimov**, "The thermal decomposition of RDX and HMX," in: Theory of Explosives (Proc. of Mendeleev Moscow Chem. Technol. Inst.) [in Russian], No.53, Vysshaya Shkola, Moscow, 1967, pp. 73-84.
56. **M. S. Belyaeva, G. K. Klimenko, L. T. Babaitseva, and P. N. Stolyarov**, "Factors responsible for the thermal stability of cyclic nitramines in the crystalline state," in: Chemical Physics of Combustion and Explosion. Kinetics of Chemical Reactions [in Russian], Chernogolovka 1977, pp. 47-52.
57. **Yu. M. Burov and G. M. Nazin**, "Effect of the structure on the gas-phase decomposition rate of secondary nitramines, " Kinet. Katal., 1982, v. 23, No.1, pp. 12-17.
58. **G. K. Klimenko**, "Thermal stability and chemical structure of polynitro- and nitrocompounds," in: Combustion and Explosion: Materials of the 4th All-Union Symp. on Combustion and Explosion [in Russian], Nauka, Moscow, 1977, pp. 585-593.
59. **R.N. Rogers, G.W. Daub,** "Scanning calorimetric determination of vapor phase kinetic data," Anal. Chem. 1973, v. 45, No. 3, pp.596-600.
60. **R.N. Rogers, L.C. Smith**, "Application of scanning calorimetry to the study of chemical kinetics", 1970, No.1, pp. 1-9.
61. **D.F. Mc. Millan, J.R. Barker, K.E. Lewis, et al**,"Mechanism of nitramine decomposition: very low-pressure pyrolysis of HMX and dimetlhylnitramine," SRI International, June 1979.
62. **R.N. Rogers**, "Differential scanning calorimetric determination of kinetic constants of systems that melt with decomposition," Thermochim. Acta. 1972, No. 3 pp. 437-447.
63. **A. F. Belyaev**, "On combustion of explosive materials" Zh. Fiz. Khim., 1938, v. 12, p. 93.
64. **V. V. Aleksandrov, A.V. Boldyreva, V. V. Boldyrev, and R. K. Tukhtaev**, "Combustion of DINA at atmospheric pressure," Fiz. Goreniya Vzryva, 1973, v. 9, No. 1, pp. 140-142.
65. **V. E. Zarko, V. N. Simonenko, and A. B. Kiskin**, "Radiation-driven transient burning: experimental results," in: L. DeLuca, E. W. Price, and M. Summerfield (eds.), Progress in Astronautics and Aeronautics, 1992, v. 143, ch. 10.
66. **V. E. Zarko, V. Ya. Zyranov, and V. V. Chertischev,** "Dispersion of the surface layer during combustion of homogeneous propellants," AIAA, Reno, 1996, Paper No. 96-0814.
67. **C. L. Thompson, Jr., and N. P. Suh**, "Gas phase reactions near the solid-gas interface of deflagrating double-base propellant strand," AIAA J. 1971, No.1, pp. 154-159.
68. **N. E. Ermolin and V. E. Zarko**, "Mechanism and kinetics of the chemical decomposition of cyclic nitramines," Fiz. Goreniya Vzryva, 1997, v. 33, No. 3, pp. 10-31.

69. **V. M. Mal'tsev and P. F. Pokhil,** "Estimation of the thermal effect of the initial stage of combustion of solid propellants and explosives," Prikl. Mekh. Tekh. Fiz., 1963, No. 2, pp. 173-174.
70. **A. Zenin**, "HMX and RDX: combustion mechanism and influence on modern double-base propellant combustion," Journal of Propulsion and Power, 1995, v. 11, No. 4, pp. 752-758.
71. **T. P. Parr and D. M. Hanson-Parr**, "Solid propellant flame structure," in: T. Brill, T. Russell, W. Tao, et al. (eds.), Decomposition, Combustion, and Detonation of Energetic Materials, (Symposium held Nov. 27--30, 1995, Boston), Pittsburgh, 1996, pp. 207-219.
72. **A. E. Fogelzang,** "Flame," Combustion of Explosives and Propellants Database, Version 2.43, Mendeleev Chemical Technology Univ., Moscow, 1996.
73. **A. L. Atwood, T. L. Boggs, P. O. Curran, et al.,** "Burn rate temperature and pressure sensitivity of solid-propellant ingredients," in: Combustion Instability of Solid Propellants and Rocket Motors, Politechnico di Milano, Milan, 16-18 June 1997.
74. **V. N. Simonenko, A. B. Kiskin, V. E. Zarko, and A. G. Svit**, "Characteristics of self-sustaining nitramine combustion at atmospheric pressure," Fiz. Goreniya Vzryva, 1997, v. 33, No. 6, pp. 68-71.
75. **M. Herrmann, W. Engel, and N. Eisenreich**, "Thermal expansion, transitions, sensitivities, and burning rates of HMX," in: Propellants, Explosives, Pyrotechnics, 1992, v. 17, pp. 190-195.
76. **A. A. Zenin, V. M. Puchkov, and S. V. Finyakov,** "Characteristics of HMX combustion waves at various pressures and initial temperatures," Fiz. Goreniya Vzryva, 1998, v. 34, No.2, pp. 59-66.
77. **N. Kubota and S. Sakamoto**, "Combustion mechanism of HMX," Propellants, Explosives, Pyrotechnics, 1989, v. 14, pp. 6-11.
78. **T. Mitani and F. A. Williams**, "A model for the deflagration of nitramines," in: 21st Symp. (Int.) on Combustion, The Combustion Inst., Pittsburgh, 1986, pp.1965-1974.
79. **A. L. Atwood, T. L. Boggs, P. O. Curran, et al.,** "The determination of burn rate temperature sensitivity of solid-propellant ingredients," in: Combustion Instability of Solid Propellants and Rocket Motors, Politechnico di Milano, Milan, 16-18 June 1997.
80. **E. I. Maksimov, A. G. Merzhanov, and Yu. R. Kolesov,** "On the distribution of material density in the combustion zone of condensed systems," Dokl. Akad. Nauk SSSR, 1965, v. 162, No. 5, pp. 1115-1118.
81. **D. Hanson-Parr and T. Parr**, "RDX flame structure and chemistry," in: 30th JANNAF Combustion Subcommittee Meeting, Monterey, CA, Nov., 1993.
82. **W. Eckl, V. Weiser, M. Weindel, et al.,** "Spectroscopic investigation of nitromethane flames," Propellants, Explosives, Pyrotechnics, 1997, No.3, pp. 180-183.
83. **V. M. Mal'tsev, A. G. Stasenko, V. A. Seleznev, and P. F. Pokhil**, "Spectroscopic studies of the flame zones of condensed systems," Fiz. Goreniya Vzryva, 1973, v. 9, No. 2, pp. 220-225
84. **J. Wormhoudt, P. L. Kebabian, and C. E. Kolb**, 'Infrared fiber-optic diagnostic observations of solid-propellant combustion," Combust. Flame, 1997, v. 108, pp. 43-60.
85. **R. R. Bernecker and L. C. Smith**, "On the products formed in the combustion of explosives. Freeze-out of the water—gas reaction," J. Phys. Chem., 1967, v. 71, pp. 2381-2390.
86. **O. P. Korobeinichev, L. V. Kuibida, and V. Zh. Madirbaev**, "Investigation of the chemical structure of HMX flames," Fiz. Goreniya Vzryva, 1984, v. 20, No. 3, 43-46.

87. **O. P. Korobeinichev, L. V. Kuibida, et al.,** "Study of the flame structure and kinetics of chemical reactions in flames by mass spectrometry," in: Mass Spectrometry and Chemical Kinetics [in Russian], Nauka, Moscow, 1985, pp.73-93.
88. **L. V. Kuibida**, "Investigation of nitramine flame structure by molecular-beam mass spectrometry," Candidate's Dissertation in Phys.-Math. Sci., Institute of Chemical Kinetics and Combustion, Novosibirsk, 1988.
89. **M. Ben-Reuven, L. H. Caveny, et al.,** "Flame-zone subsurface reaction model for RDX deflagration," in: 16th Symp. (Int.) on Combustion, The Combustion Inst., Pittsburgh, 1977, pp. 1223-1233.
90. **M. Ben-Reuven and L. H. Caveny,** "Nitramine flame chemistry and deflagration interpreted in terms of a flame model," AIAA~J., 1981, v. 19, No. 10, pp. 1276-1285.
91. **R. A. Fifer and H. E. Holmes**, "Kinetics of the HCN + NO_2 reaction behind shock waves," J. Phys. Chem., 1982, v. 86, pp. 2935-2944.
92. **T. A. Litzinger, B. L. Fetherolf, Y. Lee, and C. Tang,** "Study of the gas-phase chemistry of RDX: Experiment and modeling," J. Propulsion Power, 1995, v. 11, No. 4, pp. 698-703.
93. **Y. Oyumi and T. B. Brill,** "Thermal decomposition of energetic material. 3. A high-rate, in situ, FTIR study of the thermolysis of RDX and HMX with pressure and heating rate as variables," Combust. Flame, 1985, v. 62, pp. 213-224.
94. **R. A. Fifer**, "A shock tube study of the high-temperature kinetics and mechanisms of nitrogen dioxide-aldehyde reactions," in: G. Kamimoto (ed.), Proc. of the Tenth International Shock Tube Symposium Shock Tube Research Society, 1975, pp. 613-620.
95. **R. A. Fifer and H. E. Holmes**, "Kinetics of nitramine flame reactions," in: 16th JANNAF Combustion Meeting, CPIA Publ. 308, v..2, Dec. 1979, pp.35-50.
96. **L. R. Thorne and C. F. Melius**, "The structure of hydrogen cyanide-nitrogen dioxide premixed flames," in: 26th JANNAF Combustion Meeting, Oct. 1989, p. 10.
97. **L. R. Thorne and C. F. Melius,** "The structure of hydrogen cyanide--nitrogen dioxide premixed flames," in: 23rd Symp. (Int.) on Combustion, The Combustion Institute, Pittsburgh, 1990, pp. 397-403.
98. **M. S. Miller**, "In search of an idealized model of homogeneous solid propellant combustion," Combust. Flame, 1982, v. 46, pp. 51-73.
99. **L. K. Gusachenko, V. E. Zarko, et al.,** "Modeling of solid-propellant combustion processes" [in Russian], Nauka, Novosibirsk, 1985. Translation FTD-ID(RS)T-0211-88, micrifishe FTD-88-C-000338L
100. **M. W. Beckstead, J. E. Davidson, and Q. Jing,** "A comparison of solid monopropellant combustion," in: Challenges in Propellants and Combustion, 100 Years After Nobel, Ed. K.K. Kuo, Begell House, Inc, New York, Wallingford (UK), 1997, pp.1116-1132.
101. **A. F. Belyaev**, "On combustion of glycol dinitrate," Zh. Fiz. Khim., 1940, v. 14, p.1009.
102. **Ya. B. Zel'dovich and D. A. Frank-Kamenetskii**, "Theory of thermal propagation of the flame," Zh. Fiz. Khim., 1938, v. 12, No. 1, pp. 100-105.
103. **Ya. B. Zel'dovich**, "To the theory of combustion of powders and explosives," Zh. Eksp. Teor. Fiz., 1942, v. 12, p. 498.
104. **K. K. Andreev and M. S. Plyasunov,** "On the dependence of the burning rate of explosives on initial temperature," in: Theory of Explosives [in Russian], Nauka, Moscow, 1967, pp. 263-288.
105. **K. K. Andreev**, "Thermal decomposition and combustion of explosives," [in Russian], Nauka, Moscow, 1966.

106. **A. A. Koval'skii, E. V. Konev, and B. V. Krasil'nikov**, "On the combustion of nitroglycerin powder," Fiz. Goreniya Vzryva, 1967, v. 3, No. 4, pp. 547-554.
107. **V. N. Vilyunov**, "Mathematical theory of steady combustion of condensed materials," Dokl. Akad. Nauk SSSR, 1961, v. 136, No. 1, pp. 136-139.
108. **V. A. Strunin, A. N. Firsov, K. G. Shkadinskii, et al.**, "Steady-state combustion of decomposing and vaporizing condensed materials," Fiz. Goreniya Vzryva, 1977, v. 13, No. 1, pp. 3-16. [See also **V. A. Strunin and G. B. Manelis**, "Analysis of elementary models for the steady-state combustion of solid propellants," J. Propulsion Power, 1995, v. 11, No. 4, pp. 666-676].
109. **F. H. Pollard and R. M. H. Wyatt,** ``Reaction between formaldehyde and nitrogen dioxide. Part~1. The kinetics of the slow reaction," Trans. Faraday Soc., 1949, v. 45, pp. 760-767.
110. **M. Ben-Reuven and L. H. Caveny**, "Nitramine flame chemistry and deflagration interpreted in terms of a flame model," AIAA J., 1981, v. 19, No. 10, pp. 1276-1285.
111. **N. S. Cohen, G. A. Lo, and J. C. Crowley**, "Model and chemistry of HMX combustion," AIAA~J., 1985, v. 23, No. 2, pp. 276-282.
112. E. I. Maksimov and A. G. Merzhanov, "To the theory of combustion of condensed materials," Fiz. Goreniya Vzryva, 1966, v. 2, No. 1, pp. 47-58.
113. **R. L. Hatch**, Chemical kinetics combustion model of the NG/binder system," in: 23rd JANNAF Combustion Meeting, CPIA Publ. 457, Oct. 1986, v. 1, pp. 157-165.
114. **S. B. Margolis, F. A. Williams, and R. C. Armstrong,** "Influences of two-phase flow in the deflagration of homogeneous solids," Combust. Flame, 1987, v. 67, No. 3, pp. 249-258.
115. **S. C. Li, F. A. Williams, and S. B. Margoils**, "Effects of two-phase flow in a model for nitramine deflagration," Combust. Flame, 1990, v. 80, No. 3, pp. 329-349.
116. **N. E. Ermolin, O. P. Korobeinichev, L. V. Kuibida, and V. M. Fomin**, "Kinetics and mechanism of chemical reactions in RDX flames," Fiz. Goreniya Vzryva, 1986, v. 22, No. 5, pp. 54-64.
117. **N. E. Ermolin, O. P. Korobeinichev, L. V. Kuibida, and V. M. Fomin**," Analysis of chemical processes in RDX flames," Fiz. Goreniya Vzryva, 1988, v. 24, No. 4, pp. 21-29.
118. **N. E. Ermolin, O. P. Korobeinichev, L. V. Kuibida, and V. M. Fomin**, "Chemical structure and model of RDX flame," in: Structure of Gas-Phase Flames, Materials of Int. Seminar on the Structure of Gas-Phase Flames (Novosibirsk, June 27-31, 1986) [in Russian], Part 2, Inst. of Theor., and Appl. Phys., Sib. Div., Russian Acad. of Sci., Novosibirsk, 1988, pp. 267-279.
119. **R. L. Hatch,** "Chemical kinetics modeling of HMX combustion," in: 24th JANNAF Combustion Meeting, CPIA Publ., 476, 1987, v. 1, pp. 383-391.
120. **C. F. Melius**, "The gas-phase flame chemistry of nitramine combustion," in: 25th JANNAF Combustion Meeting, CPIA Publ., 498, 1988, v. 2, pp. 155-162.
121. **K. K. Kuo and Y. C. Ling,** "Modeling of physicochemical processes of burning RDX monopropellants," in: Proc. 20th Int. Pyrotechnics Seminar, 1994, pp. 583-600.
122. **Y. C. Liau and V. Yang,** "Analysis of RDX monopropellant combustion with two-phase subsurface reactions," J. Propulsion Power, 1995, v. 11, No. 4, pp. 729-739.
123. **R. A. Yetter, F. L. Dryer, M. T. Allen, and J. L. Gatto,** "Development of gas-phase reaction mechanisms for nitramine combustion," J. Propulsion Power, 1995, v. 11, No. 4, pp. 683-697.

124. **J. Davidson and M. Beckstead,** "Improvements to RDX combustion modeling," AIAA Paper, No. 96-0885, Reno, Jan. 1996.
125. **K. Prasad, R. A. Yetter, and M. D. Smooke**, "An eigenvalue method for computing the burning rates of RDX propellants," AIAA Paper No. 96-0880, Reno, Jan. 1996.
126. **W. Tsang and J. T. Herron**, "Chemical kinetic data base for propellant combustion. I. Reactions involving NO, NO_2, HNO, HONO, HCN, and N_2," J. Phys. Chem. Ref. Data, 1991, v. 20, p. 609.
127. **W. Tsang**, "Chemical kinetic data base for propellant combustion. II. Reactions involving CN, NCO, and HNCO," J. Phys. Chem. Ref. Data, 1992, v. 21, p. 753.
128. **V. E. Zarko, L. K. Gusachenko, and A. D. Rychkov**, "Simulation of combustion of melting energetic materials," Defense Sci. J., India, 1996, v. 46, No.5, 425-433.
129. **V. E. Zarko, L. K. Gusachenko, and A. D. Rychkov,** "Modeling of transient combustion regimes of energetic materials with surface evaporation," in: Challenges in Propellants and Combustion, 100 Years After Nobel, (K.K. Kuo, Ed.), Begell House, Inc, New York, Wallingford (UK), 1997, pp.1014-1025.
130. **L. K. Gusachenko, V. E. Zarko, and A. D. Rychkov**, "Instability of combustion model with vaporization on the surface and overheating in the condensed phase," Fiz. Goreniya Vzryva, 1997, v. 33, No. 1, pp. 43-50.
131. **V. E. Zarko, L. K. Gusachenko, and A. D. Rychkov,** "Effect of melting on stability of steady-state and transient combustion regimes," in: "Combustion Instability of Solid Propellants and Rocket Motors," Politechnico di Milano, Milan, 16-18 June 1997.
132. **B. Erikson and M. W. Beckstead,** "A numerical model of monopropellant deflagration under unsteady conditions," AIAA Paper No. 96-0652, Reno, Jan. 1996.
133. **J. C. Finlinson, T. Parr, and D. Hanson-Parr,** "Laser recoil, plume emission, and flame height combustion response of HMX and RDX at atmospheric pressure," in: 25th Symp. (Int.) on Combustion, The Combustion Inst., Pittsburgh, 1994, p. 483.
134. **B. V. Novozhilov,** "Unsteady Combustion of Solid Rocket Propellants" [in Russian], Nauka, Moscow, 1973, 176 pp.
135. "Reduced kinetic mechanisms and asymptotic approximations for air-methane flames," M. D. Smooke (Ed.), Springer, Berlin—Heidelberg, 1991.
136. **N.E. Ermolin, and V.E. Zarko,** "Combustion modeling of cyclic nitramines", *Combustion, Explosion, and Shock Waves*, 1998, V. 34, No. 5, pp. 3-22.

2.3. COMBUSTION OF GAP

Glyzidyl Azide Polymer (GAP) is one of the most perspective candidates for the next generation of fuel-binders for high energy composite propellants. Its advantages are relatively high density, high burning rate, and high energy release in thermal decomposition.

Chemical formula of the GAP prepolymer is $C_3H_5ON_3$. It is seen that GAP is deficient in the oxygen needed for complete combustion. The energetics of the GAP combustion is provided by the scission of N-N_2 bond, which produces gaseous N_2. The thermo-physical and kinetic properties of the GAP polymer can depend on degree and method of curing and cross-linking. Usually, the cured GAP, below we call it as GAP propellant [1,2], consist of 81-85% of the GAP monomer, 16-12% of curing agent (isophorone diisocyanate, IPDI, or hexamethylene diisocyanate, HMDI), and 3% of curing agent (trimethylopropane, TMP). There can be also used catalyst for the curing reaction, e.g., di-n-butylin dilaurate (DBTDL). The molecular mass of the GAP prepolymer is 1980 g/mol [1], density is 1.3 g/cm^3 and heat of formation ΔH_f = 229cal/g [1], or 280 cal/g [3]. The calculations of combustion products of the GAP prepolymer by equilibrium code give at pressure 50 atm the following mole fractions of components [1]:

N_2	CO	CO_2	CH_4	H_2	H_2O	C (solid)
22.34	13.95	0.13	2.15	32.19	0.71	28.47

If the same calculations are made with preventing the formation of solid carbon, the mole fraction of H_2 decreases by about 1% while content of N_2, CO, and CH_4 increases by 12% each. Small amounts (ca. 2-3%) of naphthelene, benzene, and HCN may exist in the combustion products in the last case.

An existence of a carbon residue on the burning surface of GAP was reported in [1,2,4,5]. However, there are some doubts in formation of solid carbon in combustion wave of GAP (see [6,7]). In fact, relatively strong heat release in the condensed phase of the GAP propellant that gives rise in the burning surface temperature up to 700-800 K and provides burning rate about 1 cm/s at pressure 40 atm, leads to relatively high speed of gaseous decomposition products moving from the condensed phase. This means that the residence time for these products in the gas flame is relatively small and one may expect great difference between adiabatic flame temperature (calculated by equilibrium program) and experimentally measured one. The experimental data on the temperature profile measurements are shown in Figs. 2.3 and 2.4.

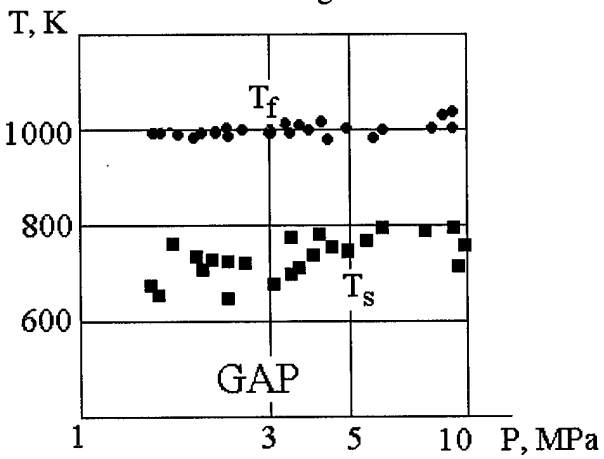

Fig. 2.3. T_f and T_s vs pressure data [2].

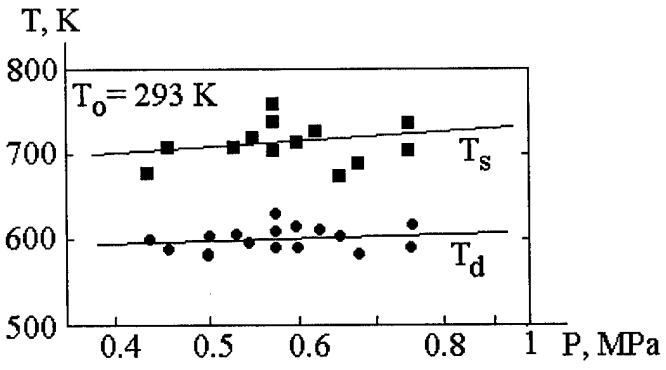

Fig. 2.4. T_s and T_d vs pressure data [1].

Here T_s is the surface temperature, T_f is the maximum flame temperature, and T_d is the decomposition temperature corresponding to the beginning of decomposition reactions in the condensed phase. It is seen that the measured value of T_f is far from thermodynamically determined (ca. 1000 K instead of ca. 1400 K at 50 atm).

2.3.1. Experimental observations.

The first detailed data on the GAP decomposition and combustion has been reported in [1]. Thermochemical analysis with use of DTA and TG techniques showed that when heated at the rate 10 K/min the GAP propellant, cured with HMDI, starts to decompose exothermically at about 475 K and finishes at 537 K. This is accompanied with 42% weight loss. In the second stage of decomposition the weigt-loss continues slowly but heat does not liberate (within the experimental method accuracy). These data were confirmed with more complicated techniques using differential scanning calorimeter and mass spectrometer. It was revealed that heat release in the condensed phase actually terminates when reaching weight-loss about 41%. The amount of nitrogen atoms, evolved from the GAP propellant at this moment, equals 68% and the rest of nitrogen is released during the second stage of decomposition. Analysis of infrared spectra of the GAP propellant samples recorded before and after thermal degradation by 41% exhibited the break of the nitrogene tripple bond ($-N_3$). At the same time the presence of hydrogen atoms in decomposition products with linearly increasing concentration versus decomposition degree gave background for assumption that molecular structure of the GAP may convert under heating from $-CH_2-N=N_2$ into $-C\equiv N$ with simultaneous release of (N_2+H_2). Latest studies of different authors showed that most probably the first step of decomposition consists of the breaking off of N_2 from the azide to form the nitrene [8,9]:

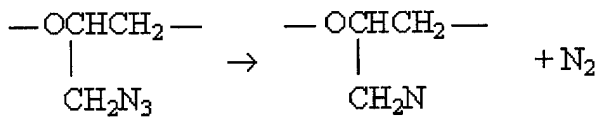

According to the findings of Ref. [9], the further decomposition of nitrene involves two decomposition paths preceding with migration of n-atom inside nitrene molecule. The first path produces NCN, CO and methane while the second path leads to formation of ethylene, acetylene and CO. Unfortunately, there is still no reliable evidences of predomination of any particular path in the GAP decomposition.

Some interesting observations, related to the mechanism of decomposition in combustion conditions, were made via examination with scanning electrone microscope of quenched burning samples of the GAP propellant. First of all, on the top-view of cooled by liquid nitrogen the GAP propellant quenched samples a number of holes of some tens of micron size has been recognized. This shows that subsurface layer is softened during combustion and gases release through it. Microscopic examination of knife-edge cuttings showed existence of cavities in subsurface layer with sizes of the order of several microns. Just below the bubble generating zone the surface of cutted sample is smooth that means that polymer melts at the temperature close to the burning surface temperature.

According to the data of Ref. [1], the pressure exponent of the GAP propellant in the pressure range 10-100 atm equals 0.44 at different initial temperatures. The burning rate temperature sensitivity $\sigma_p = (\partial \ln r_b / \partial T_0)_p$ equals 0.01 K^{-1} in this pressure range. The number of published data on the burning rate behavior is very limited. It has been reported in Ref. [2] that the burning law for the GAP propellant at pressures below 23 atm is similar to that reported in Ref. [1]. At higher pressures the pressure exponent noticeably decreases. In addition to the mentioned values of pressure exponent there have been reported values of 0.28 [10], 0.63 [5], 0.69 [11]. It was also reported rather low value of the burning rate temperature sensitivity equal to 0.002 K^{-1} [2], which seems to be dependent on the type of the curing agent used.

2.3.2. Burning rate simulation.

The first attempt to correlate the burning rate with measured values of the burning surface temperature was undertaken in Ref. [1]. Assuming an Arrenius-type decomposition of GAP propellant in the combustion wave, the burning rate equation was presented in the form:

$$r_b(m/s) = 9{,}160 \exp(-8.7 \cdot 10^4 / RT_s)$$

Based on this expression, the relationship for the value of the surface temperature sensitivity was derived as follows:

$$(\partial T_s / \partial T_0)_p = \sigma_p R T_s^2 / E_s$$

With E_s=20.8 Kcal/mol and experimental values of T_s and σ_p, the magnitude of $(\partial T_s / \partial T_0)_p$ has been determined to be 0.48 at P=50 atm. It should be noted that reported values of σ_p = 0.01 K^{-1} and $(\partial T_s / \partial T_0)_p$ correspond to the domain of very developed unstable combustion. Indeed, according to phenomenological approach [12] the limiting value of $(\partial T_s / \partial T_0)_p$ corresponding to oscillating combustion boundary, has to no less than $[\sigma_p(T_s-T_0)-1]^2/[\sigma_p(T_s-T_0)+1]$. However, with σ_p=0.01K^{-1} and $(T_s-T_0) \geq 350K$ the estimated value of $(\partial T_s / \partial T_0)_p$ exceeds 1.3 which is large 0.48. There is no experimental data on unstable combustion of GAP propellant in studied range of pressures.

A simplified version of the combustion model for the GAP propellant has been presented in Ref. [2]. It was assumed that the N_2 liberation in the melt layer of the condensed phase may play rate

control role. Solution for steady-state one-dimensional combustion wave with negligible heat feedback from gas flame was obtained using an asymptotic analysis:

$$M \sim (T_s / \sqrt{Q_1}) \exp(-E_1 / 2T_s) \tag{2.21}$$

Here M is the dimensionless mass burning rate, and T_s, Q_1 and E_1 are the dimensionless surface temperature, heat of reaction in the melt layer and energy of activation for this reaction, respectively. The relationship obtained is very similar to that developed for the rate control stage in the condensed phase [13]. The dependence of mass burning rate on the surface temperature is the most pronounced due to exponential term. However, the method for calculation of T_s is not reported in [2], thus its value should be determined experimentally. Knowing the values of T_s allows to obtain estimate for E_1.

Actually, relationship (2.21) gives very limited possibilities for describing the GAP combustion law, especially in term of its pressure and temperature sensitivities. This is because of simplified representation of the processes in the condensed phase and practical neglecting the processes in the gas phase. More advanced approach in the modeling of the GAP combustion behavior has been developed in [6].

In accordance with this last approach the combustion wave is divided into 3 regions: 1) the solid non-reacting material, 2) the two-phase decomposition zone, 3) the gas flame. The details of the mathematical formulation of the problem have been described by authors earlier [14]. Briefly, region 1 is described by the energy equation without any source terms. Region 2 involves integration of the energy and species equations in x coordinate until all condensed material has disappeared. The results of integration (temperature and species mass fluxes) are used as boundary conditions for region 3. Region 3 involves integration of energy and species equations in the gas phase. The burning rate is determined from the condition of heat balance at the interface between region 2 and region 3.

The peculiarities of the GAP combustion modeling result from uncertainties in phase transitions with polymer. Instead of true melting, as in the case of crystalline materials, the polymer GAP has no distinctive melting point. Thus, the choice of boundary of region 2 is somewhat arbitrary. It corresponds some temperature value "below a temperature where decomposition is occurring at any significant rate". Again, in the contrary with a case of crystalline materials, it is assumed that the evaporation plays insignificant role. Therefore, the burning surface is defined as the point corresponding to 99.999% conversion of the condensed phase material into gaseous species.

The reaction scheme for the region 2 was constructed on the basis of the very restricted data on the species detected by mass spectrometry in decomposition studies. Three different global mechanisms, involving each 4 steps, were proposed. As mentioned earlier in this section, the first step in every mechanism consists of liberation of N_2. For simplicity, 80% of N_2 is liberated during the first step, the rest of N_2 is liberated in subsequent steps. The difference between mechanisms is that they vary formation of some key components like H_2CN, CN, H_2O, CH_2, CNO, C_2H_3 and C (solid). Products of the condensed phase decomposition react later in the gas phase. A mechanism of the gas phase reactions is composed of several mechanisms used in the literature for

RDX, AP and hydrocarbon gas combustion. Resulting reaction scheme contains 58 species and involves 292 reactions. No reduction of that mechanism was performed.

The calculations were conducted in several successive steps. First, adjusting the species produced and kinetic constants was made in order to set the value of burning rate to the experimental value at fixed pressure, and to match the heat fluxes at the interface between regions 2 and 3. The series of calculations were performed in order to compare the theoretical results with experimental data at different initial temperatures and pressures. It was found that the mechanisms proposed reproduce fairly well the experimental burning law for the GAP propellant in the range of 10-70 atm. Adiabatic flame temperature was compared with thermal-equilibrium temperature computed by thermodynamic code. As is shown in Fig.2.5, mechanisms A and B exhibit rather good agreement at pressures higher than 20 atm but mechanism C gives much lower constant flame temperature. The burning rate temperature sensitivity, measured in Ref. [1], is well reproduced by mechanisms A and B but shows some different behavior in the case of mechanism C.

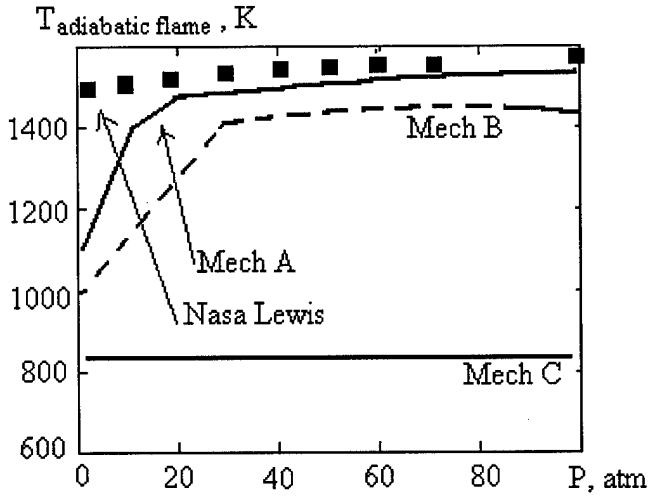

Fig. 2.5. Comparison [6] the theoretical results with experimental data.

It is interesting to note that the difference in mechanisms A and C is mainly in the amount of carbon in solid state produced in the condensed phase decomposition and in the value of heat released during this decomposition. In the case of mechanism C the fraction of solid carbon is negligible and the heat released in the condensed phase is significantly higher (ca. 105 cal/g against 18 cal/g of mechanism A).

When comparing between different mechanisms simulating the GAP combustion behavior, one has to consult with available experimental data. Unfortunately, the volume of these data is extremely small and there exists urgent need in obtaining new experimental information. It regards the quantitative data on species concentrations, temperature profile, burning rate sensitivities. At present time it seems incorrect to compare calculated by particular reaction scheme flame temperature with thermal-equilibrium temperature because there are experimental evidences that the flame temperature in the GAP combustion wave is surprisingly low. At the same time a comparison with very high burning rate temperature sensitivity data, reported in Ref. [1], looks nonjustified because expected from transient combustion theory [15] behavior of this propellant is

very unstable (the modeling concerns only steady-state regimes). Surprisingly, there is only one observation in available literature [3] about self-extinquishment of the GAP propellant at atmospheric pressure.

2.3 REFERENCES

1. **Kubota N., Sonobe T.**, "Combustion mechanism of azide polymer", Propellants, Explosives, Pyrotechnics, vol.13, 172-177,1988.
2. **Hory K., and Kimura M.**, "Combustion mechanism of glycidyl azide polymer", Propellants, Explosives, v.21, 160-165,1996.
3. **Frankel M.B., Grant L.R., and Flanagan J.E.,** "Historical Development of glycidyl azide polymer", Journal of Propulsion and Power, v.8, No.3, 1992.
4. **Lengelle G., Fourest B., Godon J.C., and Guin C.** "Condensed phase behavior and ablation rate of fuels for hybrid propulsion", 29th Joint Propulsion Conference, AIAA 93-2413, 1993.
5. **Yuan L.Y., Liu T.K., and Cheng S.S.**, "The combustion characteristics of GAP gumstock propellants", 32nd Joint Propulsion Conference, AIAA 96-3235, 1996.
6. **Davidson J. and Beckstead M.**, "A mechanism and model for GAP combustion", 35th Aerospace Sciences Meeting and Exhibit, AIAA 07-0592, 1997.
7. **Flanagan J., Woolery D., and Kistner R.**, "Fundamental studies of azide decomposition and combustion", AFRPL TR-96-094, Dec. 1986. (cited by [6]).
8. **Chem J.K., and Brill T.B.**, "Thermal decomposition of energetic materials 54. Kinetics and near-surface products of azide polymers AMMO, BAMO and GAP in simulated combustion", Combustion and Flame, v.87, pp. 157-168, 1991.
9. **Haas J., Eliahu, Yeshadyahy B., and Welner S.**, "Infrared laser-induced decomposition of GAP", Combustion and Flame, v.96, pp.212-220, 1994.
10. **Kubota N., Sonobe T., Jamamoto A., and Shimizu H.**, "Burning rate characteristics of GAP propellants", J. Propulsion and Power, v.6, No. 6, 686-689, 1990.
11. **Simmons R.L.**, "Unusual combustion behavior of nitramines and azides", 4th International Symposium on Special Topics on Chemical Propulsion, Stockholm, Sweden, 1986.
12. . **Novozhilov B.V.** Nonsteady combustion of solid rocket propellants. "Nauka", Moscow, 1973 (R).
13. **Merzhanjv A.G. and Dubovitskii F.I.** "On the theory of steady state monopropellant combustion", Proceedings of USSR Academy of Sciense, 1959, V. 129, No. 1, pp. 153-156 (R).
14. **Davidson J.E., and Beckstead M.W.**, "A three-phase combustion model of HMX", 26th International Symposium on Combustion, The Combustion Institute, Naples, Italy, 1996.

2.4. COMBUSTION OF HNF.

Hydrazinium nitroformate $N_2H_4C(NO_2)_3$, (HNF) is one of the promising candidates for replacement of ammonium perchlorate as an oxidizer in propellant formulations. First publications about the use of HNF in SP appeared in the 60's and 70's in the United States [1,2]. Some later the Russian researchers published the results of HNF thermal decomposition studies [3]. It was stated in one of the earliest papers [4] that HNF is not compatible with the double bonds in the binders like HTPB. Fortunately, the latest studies [5], conducted in Netherlands, revealed good compatibility of HNF with new energetic binders like GAP or BAMO. This gave great impact to investigation of combustion mechanism of neat HNF and HNF containing propellants.

Physicochemical properties.
Neat HNF consists of the needle-like crystals with density of 1.86 g/cm^3 and melting temperature 124^{0}C.Its thermal diffusivity equals 1.63 10^{-3} cm^2/s at room temperature [6].

In the first experiments [1], NO_2 was detected as one of the major decomposition products of HNF. It was assumed that NO_2 reacts with HNF generating again NO_2. Thermocouple measurements [2] have shown 3 zones in the combustion wave: first heating up to 120^{0}C, then development of the bubble zone in the range 120-260^{0}C, and subsequent gasification above 260^{0}C. Thermal decomposition under fast heating (T-jump technique) revealed below 260^{0}C the first stage [7] as endothermal degradation of HNF to hydrazine and nitroform. With increase in the temperature of HNF only small molecules, like H_2, H_2O, N_2, NO and CO_2, were detected.

The neat HNF burning rate is relatively fast. It equals ca. 6.5 mm/s at 10 atm and ca. 30 mm/s at 70 atm. The burning rate pressure exponent equals about 0.83 and burning rate temperature sensitivity equals 0.0012K^{-1} [8]. Detailed measurements of burning rate revealed change in the pressure dependence at moderate pressures: a slope breaks around 20 atm changing from n = 0.95 at law to n = 0.85 at higher pressures [9].

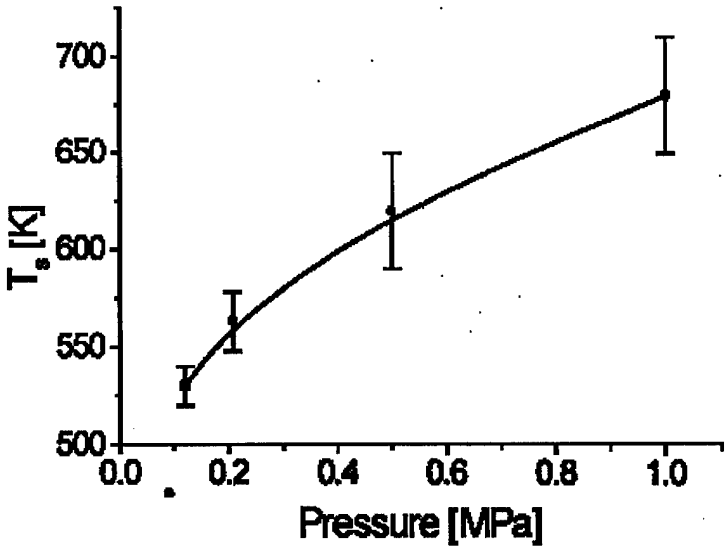

Fig. 2.6. The burning rate versus pressure data [8,9].

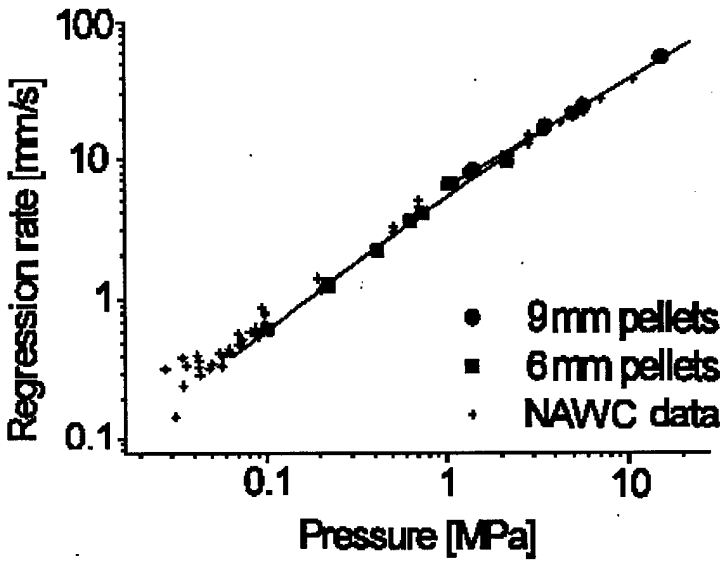

Fig. 2.7. The burning surface temperature versus pressure data [8,9].

This is seen in Fig. 2.6 where burning rate versus pressure data [8,9] are presented. The burning surface temperature increases with pressure. It equals 530K at atmospheric pressure and reaches approximately 675K [9] at P = 10 atm (Fig. 2.7). The addition of small amount of solid carbon (graphite) to the neat HNF leads to slight increase in the burning rate at moderate pressures. In this pressure range (self sustaining combustion regime of HNF exists starting from pressure 0.3 atm) the pressure exponent decreases up to n = 0.81 for HNF/5% graphite mixture [9]. The addition of paraffin (10-20%) leads to decrease in a burning rate by about 2 times at moderate pressures (1-20 atm).

Combustion simulation.

Because of the lack of knowledge of the physical mechanism of HNF combustion and relatively short history of its studying the number of works devoted to mathematical modeling is very restricted. One of the first models of HNF stationary combustion has been presented in Ref. 10. Its further development and extension is made in Ref. 11. In the model, the condensed phase is described in one-dimensional formulation with single endothermal global decomposition reaction of zero-order. The products of condensed phase decomposition react further in the gas phase according to bimolecular irreversible global reaction:

$$B + M \rightarrow C + M$$

Here B represents unstable intermidiate species of condensed phase decomposition such as NO_2, HONO, N_2O, etc. Species M may represent unstable species such as N, H and OH, or any gas species. It is assumed that the gas phase reaction is highly exothermic and can be described in two ways: low-activation-energy limit [12] and classical high-activation-energy limit [13]. In the case of low activation limit the species M are treated as unspecified chain carriers, whose mass fraction is constant and negligibly small as compared to the main species B and C. Therefore gas phase reaction is second-order overall and first order with respect to B. In the case of high activation limit the gas phase reaction is treated in terms of classical thermal decomposition.

The model is formulated on the basis of several simplified assumptions: equality of the molecular weights for all species, constant thermophysical coefficients, equality of the Lewis number to unity. The condensed phase surface is illuminated by external laser flux with radiative energy $Q_r(W/m^2)$. Radiative energy absorbs in the bulk of material according to Beer's law with absorption coefficient K_a.

Solution of the energy equation for the condensed phase gives expression for the mass burning rate m in the form [14,15]:

$$m^2 = \frac{A_c R T_s^2 \lambda_c \rho_c \exp(-E_c / RT_s)}{E_c [C_c (T_s - T_0) - Q_c / 2 - f_r Q_r / m]} \qquad (2.22)$$

Here A_c and E_c are pre-exponent and activation energy, λ_c is the thermal conductivity. Q_c is the heat of reaction, f_r is the fraction of Q_r absorbed below the surface reaction zone. In particular case of HNF Q_c = -7.2 cal/g, i.e. the reaction is endothermal, and E_c = 18000 cal/mol.

Heat balance at the interface gives expression for calculation of the burning surface temperature:

$$T_s = T_0 + Q_c / c_p + [\lambda_g (\partial T / \partial x)_{x=0} + Q_r](mc_p)^{-1}$$

To calculate the term $\lambda_g (\partial T/\partial x)_{x=0}$, the equations of energy and species conservation in the gas phase under assumption of low activation energy, $E_g \rightarrow 0$, have to be solved. Finally, one obtains

$$T_s = T_0 + Q_c + \frac{Q_c}{c_p} + \frac{Q_g}{c_p(1 + \kappa_g c_p m / \lambda_g)} ,$$

where κ_g is the characteristic reaction zone width in the gas phase.

In the case of high activation energy gas phase reactions ($E_g \rightarrow \infty$) the burning rate is given by expression [15]:

$$m^2 = \frac{2\lambda_g B_g M^2 P^2 c_p T_f^4}{E_g^2 Q_g^2} \exp(-E_g / RT_f) . \qquad (2.23)$$

The flame temperature T_f is calculated from the total heat balance:

$$T_f = T_0 + \frac{Q_c + Q_g + Q_r / m}{c_p} .$$

When taking E_g =40000 cal/mol and Q_g = 583 cal/g, the authors [11] calculated the burning rate versus pressure dependence and compared with similar calculations for the case $E_g \rightarrow 0$. The latter calculations gave better agreement with experimental data. It turned out that the model with $E_g \rightarrow 0$ gave also better agreement with experimental values of the burning rate initial temperature coefficient and burning surface temperature in dependence of pressure. The conclusion is made that simplified model with low activation energy of gas phase reactions may provide good description of experimental observations.

The attempt to construct transient combustion model for neat HNF is presented in Ref.16. The model is formulated within the framework of QSHOD approach (quasi-steady gas phase, homogeneous, one-dimensional). Heat propagation in the condensed phase is described by one-dimensional thermal conductivity equation with heat release term for zero-order reaction. The boundary condition for energy equation at the burning surface is written in the simple form of equality of heat fluxes at the interface.

Heat propagation in the gas phase is described by KTSS-type model [17] with constant heat release uniformly distributed over the reaction zone attached to the burning surface. To match the floating coefficients, the values at atmospheric pressure of the burning rate 0.68 mm/s and surface temperature 553 K were used. Calculations by the model agree well with experimental data on stationary self-sustaining and laser-assisted combustion. The response to perturbations of external radiant flux turned out over predicted at high frequencies when compared with laser recoil experiment [18]. However, agreement becomes better if experimental data are corrected on the constancy of radiation power.

Critical comments.
Despite demonstration of good correlation between theoretical predictions and experimental findings there is a strong need in further investigation of the details of the HNF combustion mechanism, both experimentally and theoretically. Indeed, the fact of melting at relatively low temperature means that subsurface layer of HNF is in a liquid state and one may expect the presence of HNF vapors above the burning surface. This is very probable event because of (according to [16]) endothermal reactions in the condensed phase. In the case of evaporation, the mathematical model has to be supplemented with appropriate term in the heat balance at the surface as well with additional condition on the value of the burning surface. The latter, if taken in the form of the Clausius-Clapeyron type equation, may provide convenient tool to calculate the burning surface temperature in dependence on pressure. It should be also underlined the need in the proper accounting for every phase transition in the combustion model. In particular, the calculations of the burning rate response to perturbations of the external heat flux, if made without taking into account the effect of melting, lead to wrong theoretical predictions [19]. Therefore the results, presented in Ref. [16] should be thoroughly checked on this matter.

2.4. REFERENCES

1. **G. von Elbe, R. Friedman, J.B. Levy and S.J. Adams,** "Research on Combustion in Solid Rocket Propellants: Hydrazine as a Propellant Ingredient", Atlantic Research Corp., Techn. Rep. DA-36-034-AMC-0091R, July 21, 1964.
2. **E.T. McHale and G. Von Elbe**, "The Deflagration of Solid Propellant Oxidizers", *Comb. Science Techn.* 2, 227-237, 1970.
3. **V.A. Koroban, T.I. Smirnova, T.N. Bashirova and B.S. Svetlov,** "Kinetics and Mechanisms of the Thermal Decomposition of Hydrazinium Trinitromethane, Tr.-Mosk. Khim.-Tekhnol. Inst., 104, 38-44, 1979.
4. **G.M. Low**, "Hydrazinium Nitroformate Propellant with Saturated Polymeric Hydrocarbon Binder", U.S.Patent 3,708,359, Jan 2, 1973.
5. **J.M. Mul, P.A.O.G. Korting, and H.F.R. Schöyer**, "Search for New Storable High Performance Propellants", AIAA Paper 88-3354, Boston, Massachusetts, 1988.
6. **D.M. Hanson-Parr and T.P. Parr,** "Measurements of Solid Rocket Propellant Oxidizers and Binder Materials as a Function of Temperature", submitted to J. Energ. Mat., 1997.
7. **G.K. Williams and T.B. Brill**, "Thermal Decomposition of Energetic Materials 67. Hydrazinium Nitroformate (HNF) Rates and Pathways under Combustionlike Conditions", Comb. Flame 102, 418-426, 1995.

8. **J.C. Finlinson and A.I. Atwood**, "HNF Burnrate, Temperature Sensitivity, and Laser Recoil Response from 1 to 6 atm", 34th JANNAF Comb. Meeting, West Palm Beach, Florida, 27-31 Oct. 1997.
9. **J. Louwers, G.M.H.J.L. Galiot, M. Versluis et al.**, "Combustion of Hydrazinium Nitroformate Based Compositions," 34th AIAA/ASME/SAE/ASEE Joint Propulsion Conference and Exhibit, July 1998, AIAA Paper 98-3385.
10. **J. Louwers, G.M.H.J.L. Gadiot, M.Q. Brewster, S.F. Son,** "Model for steady-state HNF combustion," Intern. Workshop on Combustion Instability of Solid Propellants and Rocket Motors, Politecnico di Milano, 16-19 June 1997.
11. **J. Louwers, G.M.H.J.L, Gadiot, M.Q. Brewster et al.**, "Steady-state HNF combustion modeling," J. of Propulsion and Power, in press.
12. **M.Q. Brewster, M.J. Ward, and S.F. Son**, "New paradigm for simplified combustion modeling of energetic solids: branched chain gas reactions," AIAA Paper 97-3333, 1997.
13. **M.R. Denison, and E. Baum**, "A simplified model of unstable burning in solid propellants," ARS Journal, 1961, v. 31, pp 1112-1122.
14. **G. Lengelle**, "Thermal degradation kinetics and surface pyrolysis of vinyl polymers," AIAA Journal, 1970, v. 8, pp. 1989-1998.
15. **M.M. Ibiricu, and F.A. Williams**, "Influence of externally applied thermal radiation on the burning rates of homogeneous solid propellants," *Combustion and Flame*, 1975, v. 24, pp. 185-198.
16. **J. Lowers, G. Gadiot, M. Versluis, et al.,** "Measurement of steady and non-steady regression rates of hydrazinium nitroformate with ultrasound," Intern. Workshop on Measurement of Thermophysical and Ballistic Properties of Energetic Materials, Politecnico di Milano, Italy, June 1998.
17. **H. Krier, J.S. T'ien, W.A. Sirgnano, and M. Summerfield,** "Nonsteady burning phenomena of solid propellants: theory and experiments, *AIAA J.*, 1968, v.6, p. 278.
18. **J.C. Finlinson**, "Laser recoil combustion response of HNF, oxidizer from 1 to 6 atm, AIAA, 1997, 97-334
19. **V. E. Zarko, L. K. Gusachenko, A. D. Rychkov**, Effect of melting on dynamic combustion behavior of energetic material, *Journal of Propulsion and Power*, No. 6, 1999.

2.5. COMBUSTION OF ADN

Ammonium salt of dinitramide, $NH_4N(NO_2)_2$ (ADN), is another promising candidate for use in solid propellants as an effective chlorine-free oxidizer.

Physicochemical properties.
ADN density equals 1.82 g/cm^3 and melting temperature equals 92^{0}C. The combustion temperature of neat ADN is of moderate value and reaches 2060 K at pressure 70 atm. The temperature profile in the combustion wave exhibits at low pressures 3 distinctive extended zones (see Fig. 2.8) with very weak heat feedback from the gas flame.

Experimentally, it was established [1] that the neat ADN burns steadily in the pressure range 2-20 atm and above 100 atm. At pressures below 2 atm combustion of thoroughly purified neat ADN does not exist but mixture of ADN and 0.2% paraffin burns steadily starting at least from 0.2 atm. Self sustaining combustion of thovoughly purified ADN was observed at atmospheric pressure only under heating of the pressed samples up to the temperature 100^{0}C. It is interesting to note that self sustaining combustion of pressed ADN samples was observed in [2] under atmospheric pressure at initial temperature 25^0 C. The reason for such differences in combustion behavior of different ADN samples might be different degree of purification of the ADN powder [3]. Measurement of the burning surface temperature at relatively high burning rates represents difficult technical task. Therefore, experimental data are available only for low pressures. According to Ref. [1], T_s equals ca. 320^{0}C at P=2 atm and about 380^{0}C at P=5 atm. According to Ref. [2], the burning surface temperature equals 400^{0}C at P=3 atm.

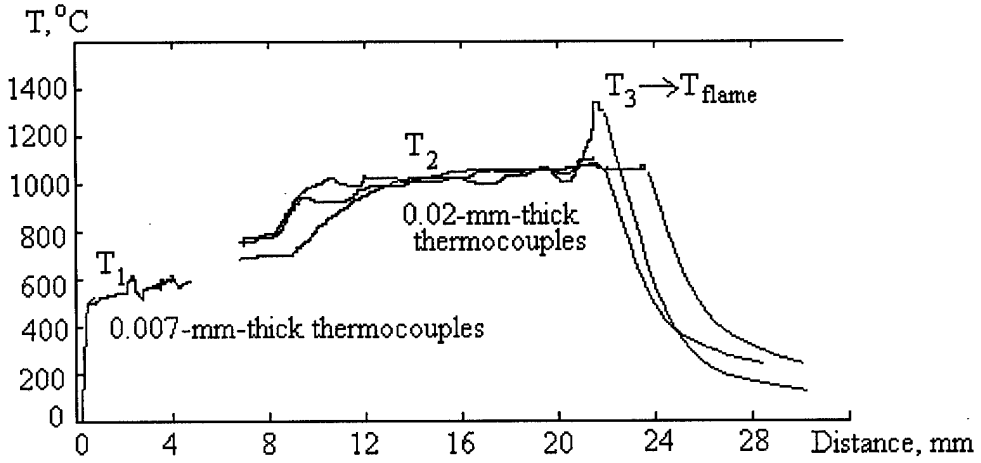

Fig. 2.8. The temperature profile in the combustion wave [1].

Thermal decomposition of ADN in conditions of slow heating rate (2 K/min) exhibits onset of exothermic reactions at 127^{0}C with heat of decomposition about 61 Kcal/mol [4]. It was proposed that the decomposition is initiated by dissociation of ADN in the melt layer to ammonia NH_3 and hydrogen dinitramide $HN(NO_2)_2$ [4,5] followed by exothermal decomposition of $HN(NO_2)_2$ producing N_2O and HNO_3.

In the experiments with fast (2000 K/sec) heating of thin ADN film on a platinum filament to 260^0C and subsequent keeping filament at this temperature it was found [6] that at the beginning ADN decomposes to NH_3, HNO_3 and N_2O, which form in comparable amounts as detected by FTIR method. However, this is mildly endothermic reaction and does not account for major heat release. Therefore it was proposed that under rapid thermolysis conditions dissociation of ADN, producing NH_3 and $HN(NO_2)_2$, dominates. Subsequent interaction between NH_3 and NO_2 may provide high exothermicity in the bubbling surface layer or in the gas phase near the surface.

In addition, it was proposed theoretically [7] and confirmed by experimental findings [8] direct evaporation of ADN at high temperatures with subsequent degradation in the gas phase onto NH_3 and $HN(NO_2)_2$. The experiments were conducted with tiny amount (10^{-4} g) of ADN heated on the metal ribbon with the rate of 90 K/s or in the regime of electrical discharge (heating time 0.01 s). Decomposition products were recorded with a time-of-flight mass-spectrometer. It was found [8] that under vacuum conditions ($P=10^{-6}$ Torr) the mass-spectrum of decomposed ADN differs significantly of that under subatmospheric and atmospheric pressure. It was suggested that this was caused by adsorption of gaseous ADN and its decomposition products on the walls of the vacuum chamber. The experiments under pressure 1-6 Torr showed that unlike other ammonia salts, ADN evaporates into gas phase as whole molecule and decomposition on ammonia and hydrogen dinitramide occurs later at higher gas temperatures.

Combustion simulation.

It follows from the measurements of thermal profile that at pressures below 3 atm ADN burns without luminous flame [1,2]. Examination of the temperature distribution shows that at moderate pressures (below 10 atm) the heat feedback from the gas phase is negligible in the heat balance on the burning surface and the burning rate is controlled by the condensed phase reactions. Mass-spectra of gas samples, taken near the burning surface of ADN at 3 atm, show the presence of gaseous ADN and hydrogen dinitramide [8]. With the pressure increase up to 6 atm the second high temperature zone appears at the height of 6-8 mm above the burning surface. The main reaction in this zone is supposed to be ammonia oxidation by nitric acid.

Qualitative description of the ADN combustion mechanism has been presented in the following way [1]. It is assumed that in the melt layer at the surface the ADN decomposes to form condensed ammonium nitrate and gaseous N_2O. Bubbling of the surface layer leads at low pressures to formation of ejected drops of condensed material consisting of ADN and ammonium nitrate with ADN content decreasing sharply with pressure. The burning surface temperature is determined by dissociation of ammonium nitrate. The temperature in the second flame zone is controlled by oxidation of ammonia (1000-1200^0C). Partially unreacted N_2O decomposes in the third flame zone observed at pressures above 10 MPa. Unstable combustion of ADN in the range of 20-100 atm is caused by overheating in the subsurface melted layer due to excessive heat release in the condensed phase. At higher than 100 atm pressures the gas-phase reactions are likely to play a dominant role in ADN combustion. Similar conclusions about the combustion mechanism of different dinitramide salts were made in Ref.[9].

Quantitative description of the gas flame mechanism in ADN combustion has been presented in Ref. [10]. The system of equations for one-dimensional nonstationary flow of reacting gas mixture was solved with the method of the problem solution given in [11]. Kinetic mechanism of the flame reactions includes high temperature submechanism for the mixture $NH_3/N_2O/NO/NO_2/HNO_3/H_2O/N_2$ with addition of stages that involve vapor of ADN, $HN(NO_2)_2$ and NH_2NO_2. Total number of stages equals 203.

To obtain stationary solution of the problem, boundary conditions at the fixed coordinate near the burning surface were set according to experimental data [8]. Boundary conditions downstream of the gas flow corresponded to equilibrium terms. An example of the gas composition at the beginning of the space coordinate is shown below in mole percentages:

NH_3	H_2O	N_2	NO	N_2O	HNO_3	ADN_{vap}
8	30	8	19	24	8	3

In calculations, the surface temperature was taken equal to 400^0C and mass flow rate at P=3 atm equal to 1.97 g/cm^{2}s. Comparison with experimental data on species concentrations in flameless combustion regime (temperature does not exceed 800 K) showed good agreement except spatial species distribution for NH_3. Better agreement was achieved with zero concentration of ADN vapor in the boundary condition.

Chemical structure of the second flame zone (maximal temperature 1500K) was calculated for the pressure 6 atm. Temperature and species concentration profiles turned out to be in a good agreement with experimental data. The third flame zone is realized theoretically at the distance of 8000 mm from the burning surface with final temperature of about 2200 K. The results of calculations demonstrate the urgent need in more detailed experimental data on species concentrations, especially in the vicinity of the burning surface. In fact, there is no available in the literature of reliable evidences of quantified measures of the ADN vapors, which is very difficult to detect. Precise measurement of the mole fraction of NH_3 close to the burning surface would give important information for substantiation of the calculations by detailed chemistry mechanism.

2.5. - REFERENCES.

1. A.E Fogelzang, V. P. Sinditskii, V. Y. Egorshev et.al., Combustion behavior and Flame structure of Ammonium Dinitramide. Combustion and Detonation. 28th International Annual Conference of ICT, June 24 - June 27, 1997, Karlsruhe, Federal Rederal republic of Germany, pp. 99.1-99.14.

2. O. P. Korobeinichev, A. G. Shmakov, A. A. Paletsky, Thermal decomposition of ammonium dinitramide and ammonium nitrate. Combustion and Detonation. 28th International Annual Conference of ICT, June 24 – June 27, 1997, Karlsruhe, Federal Republic of Germany, pp.41.1-41.11.

3. A.E.Fogelzang. Personal communication, June 1997.

4. S. Lobbecke, H. Krause, A. Pfeil, Thermal decomposition and stabilization of ammonium dinitramide (ADN). Combustion and Detonation. 28th International Annual Conference of ICT, June 24 – June 27, 1997, Karlsruhe, Federal Republic of germany, pp. 112.1-112.8.
5. G. B. Manelis, Thermal decomposition of dinitramide ammonium salt. 26th Int. Annual Conference of ICT, 04.07 – 07 – 07. 1995, "Pyrotechnics Basic Principles. Technology, Application", 15.1-15.15.
6. T. B. Brill, P. J. Brush, and D. G. Patil, Thermal Decomposition of Energetic Materials 58. Chemistry of Ammonium Nitrate and Ammonium Dinitramide Near the Burning Surface Temperature. Comb. And El., 1993, v. 92, No.1,2, pp. 178-186.
7. M. Mebel, M. C. Lin, K. Morokuma, and C.F. Melius, Theoretical study of the gas-phase structure, thermochemistry, and decomposition mechanisms of NH_4NO_2 and $NH_4N(NO_2)_2$. J. Phys. Chem. 1995, v.99, No.18, pp. 6842-6848.
8. O. P. Korobeinichev, L. V. Kuibida, A. A. Paletsky, A.G. Shmakov, "Molecular-Beam Mass-Spectrometry to Ammonium Dinitramide Combustion Chemistry Studies", J. of Propulsion and Rower, 1998, v. 14, No. 6, pp. 991-1000.
9. V. P. Sinditskii, A. E. Fogelzang, A.I. Levshenkov, et al., "Combustion Behavior of Dinitramide Salts", 36th Aerospace Sciences Meeting and Exhibit, Jan. 1998, Reno, AIAA Paper 98-0808.
10. N. E. Ermolin, "Modeling of chemical processes in ammonium dinitramide flame", in press.
11. N.E. Ermolin, O.P. Korobeinichev, A.G. Tereschenko et al., "Modeling of kinetics and mechanism of chemical reactions in the flame of ammonium perchlorate", Chemical Physics (Russian), No. 12, 1982, pp. 1711-1717.

2.6. COMBUSTION OF AMMONIUM PERCHLORATE

Ammonium perchlorate (AP) relates to the compounds with large excess of oxygen. This provides possibilities for its wide application as an oxidizer in various composite propellants. Beginning to the systematic studies of mechanism and combustion law of AP has been established by the work of Friedman with co-workers [1], in which the existence of the lower and upper pressure limits of combustion was discovered. The numerous investigations, carried out in the recent decades, made it possible to get more details of the AP combustion behavior over a wide range of pressure and initial temperatures. Thus, it was revealed that the pressure upper limit of combustion (~270 atm, according to [1]) in many respects was obliged to heat losses from the combustion wave. Later it was established that even under conditions, when the heat losses were reduced to the minimum (large diameter of sample, shell of thermal insulation material), the dependence of the burning rate on pressure remained anomalous.

The plot of dependence of AP burning rate on pressure can be conditionally divided [2] into four characteristic domains (Fig. 2.9.). Combustion in domains 1, 2 and 4 is stable and characterized by the positive value of the derivative *dm/dp*. Combustion in domain 3 has an unstable (pulsating) character. The deepest decrease in the burning rate (domain 3) has been observed for single AP crystals [2]. In the case of the combustion of pressed tablets of AP in the combustible or thermal insulation shells the depth of this minimum is reduced, and in certain cases it is substituted by plateau [2].

Location of boundaries of chosen domain depends on initial temperature of the AP samples. The lower pressure limit of AP combustion is ~ 20 atm at 20 ^{0}C [3] and ~ 15 atm at T_0 = 50 ^{0}C. Unstable combustion behavior begins with p = 140-150 atm and it changes again into stable with p = 280-300 atm.

Boundary between 1 and 2 domains (p = 56-70 atm, [39]) separates combustion regime with constant pressure exponent ν in the burning law, $m \sim p^{\nu}$ (ν = 0.77 [2] in domain 1) and regime with variable ν, which is gradually decreased in value with the pressure increase. The microscopic study of the extinguished crystals of AP [2] revealed that structure of the burning surface in the above regimes is different. In the domain 1 the surface of AP is covered with small bubbles and foam while in the domain 2 it is porous.

On the surface of samples, which burned in domain 3, according to [3], separate pockets are observed with needle-like formations, concentrated in the regions of the greatest burn out of surface. With further increase in pressure (domain 4) needles cover the entire surface.

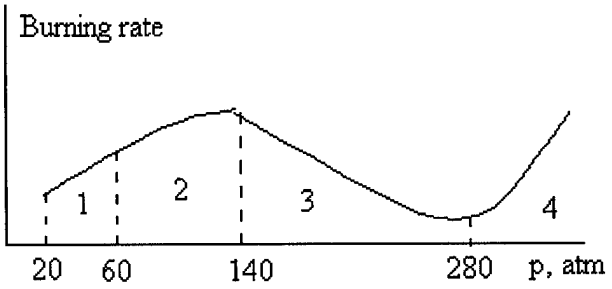

Fig. 2.9. Dependence of the burning rate of AP on pressure [2].

Character of dependence of the burning rate on pressure and examination of a fine structure of the surface layer testify for complexity of processes, which occur in the wave of AP combustion. The vast studies of the mechanism of AP thermal decomposition both in the low-temperature (at T<300 ^{0}C) and high-temperature (at T>380 ^{0}C) regimes demonstrated [4], that the examination of the condensed phase decomposition of AP within the framework of the concept of the single rate control stage does not make it possible to explain entire set of experimental results. Nevertheless the majority of researchers came to the conclusion about the important role of AP dissociation in the condensed phase on ammonia and perchloric acid with their subsequent vaporization.

Developing the model of AP combustion, V. A. Strunin and G. B. Manelis have used a concept of the rate control role of exothermal reactions in the condensed phase. According to [5, 6], decomposition of AP occurs in the wave of combustion via following routes:

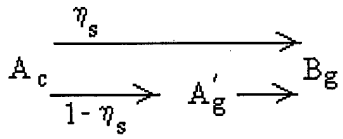

(2.24)

Mass fraction η_s of the parent substance A_c is decomposed in the condensed phase to final products B_g and remaining part $(1-\eta_s)$ dissociates to ammonia and perchloric acid (A_g') and then vaporizes and produces finally B_g.

Complete system of equations, which describes course of global reactions according to diagram (2.24), is given in [6]. From the numerical analysis of the problem it follows that depending on the particular values of the input parameters (thermal effects of stages and kinetic constants), as in the case of the consecutive reactions (see Section 1.2.2), different combustion regimes can realize. These are regimes with the rate control reactions in the condensed or in the gas phase. In the combustion regime with the rate control condensed phase reactions equation (1.20) is valid for the mass burning rate m [5]:

$$m^2 = (\rho\lambda / J_0 Q)(RT_s^2 / E)k_0 \exp(-E / RT_s) \qquad (2.25)$$

Here for the zero-order reactions

$$J_0 = 0.5\,\eta_s^2$$

And for the first-order reactions:

$$J_0 = \eta_s + [1-\eta_s - q_s /(mQ)]\ln(1-\eta_s)$$

where $q_s = \lambda(dT/dx)_{x=0} \approx 0$ (gas-phase reactions proceed in the regime of stage detachment); Q - thermal effect of decomposition upon stage $A_c \rightarrow B$.

In (2.25), the value of m depends on the surface temperature T_s and on the value of η_s, which determines shared contribution of two competing stages $A_c \rightarrow A_g'$ and $A_c \rightarrow B_g$ in gasification of parent substance. In [5,6] for closing the problem the two additional relationships are used: equation of the balance of heat at the burning surface

$$c(T_s - T_0) = Q\eta_s - L(1-\eta_s) \qquad (2.26)$$

and the relationship for the partial pressures of the products of sublimation p_s and decomposition products of the condensed phase $(p-p_s)$

$$(p-p_s)/p_s = (r_d/r_s)\eta_s/(1-\eta_s) \qquad (2.27)$$

Here p - external pressure; r_d and r_s - number of moles, which are generated during decomposition and sublimation of one mole of parent substance, respectively. Relationship (2.27) is written under assumption on the insignificant dilution of gas in the adjusting to the burning surface zone by the gas-phase reaction products. The law of vaporization is taken in the form of Clausius-Clapeyron equation

$$p_s = B \exp(-L/RT_s) \qquad (2.28)$$

System of equations (2.25)-(2.28) makes it possible to compute the burning rate of combustion depending on the external parameters in the combustion regime with the rate control condensed phase reactions.

For the burning rate temperature coefficient the formula is obtained, which has the form [7]:

$$\beta = \partial \ln m/\partial T_0 = (E/2L)(T_m-T_s)^{-1}+(T_s-T_0)^{-1} \qquad (2.29)$$

The formula is valid for moderate pressure when $L(T_m-T_s)/RT_s^2 >> 1$. Here T_m is the maximum combustion temperature.

At low pressures the variation of β is determined mainly by the second term in (2.29), which is reduced with increase in p. At higher pressures the first term, which grows with increase in p, is responsible for the variation of β. Thus, dependence $\beta(p)$ in the wide pressure range is depicted by the curve with minimum. Calculation of dependence $\beta(p)$ for AP, carried out in Ref. [7], is satisfactorily agreed with the experimental data. This may serve indirect evidence of the validity of the proposed model for AP combustion with the rate control condensed phase reactions. However, the results of calculation of the burning rate pressure sensitivity do not allow making optimistic conclusion. Indeed, the formula for coefficient ν has the form:

$$\nu = d \ln m/d \ln p \approx E/2L, \quad \text{if } \alpha L/RT_s^2 >> 1.$$

Here E - energy of the activation for transition A→B in diagram (2.24), $\alpha = (1-\eta_s)[\eta_s+(1-\eta_s)\, r_s / r_d]\, (Q-L)/c$. With an increase in the pressure the sublimation is depressed, and ν is weakly reduced. In the extreme case, when $p \to \infty$, then $\eta_s \to 1$ and $\nu \to 0$ ($m \to$ const).

Such behavior of m(p) does not meet with experimental observations and, by the opinion of authors [6], is the consequence of excessive idealization of the processes in the condensed phase of burning AP. In [8, 9], more detailed diagram of AP combustion has been examined:

$$
\begin{array}{c}
\text{(decomposition products) gas} \\
\uparrow 2 \qquad \uparrow 3 \\
(NH_4ClO_4)_c \xrightarrow{1} (NH_3 + HClO_4)_c \\
\downarrow 4 \qquad \downarrow 5 \\
(NH_3)_g(HClO_4)_g \\
\downarrow 6 \qquad \downarrow 7 \\
\text{(decomposition products) gas}
\end{array}
\tag{2.30}
$$

According to (2.30), stage 1 - dissociation of initial substance; 2, 3 - condensed phase decomposition of dissociation products; 4, 5 - sublimation of dissociation products; 6, 7 - gas-phase decomposition of sublimated ammonia and perchloric acid; indices c and g designate condensed and gas phases, correspondingly.

In mathematical description of diagram (2.30) the solubility of ammonia and perchloric acid in parent substance are taken into consideration through equilibrium constant $K_1 = [NH_3]_c[HClO_4]_c$. In addition, equations of mass conservation during dissolution and sublimation are included.

Under the assumption that exothermic condensed phase reactions (stages 6, 7 occur in regime of stage detachment) still remain rate controlling in AP combustion, approximate equation for the burning rate was obtained [8, 9].

$$
m^2 = \frac{2\lambda(RT_s^2/E)k_0 \exp(-E/RT_s)}{\eta_s^2 Q} K_1 \frac{K_{HClO_4}}{K_{NH_3}} \frac{1+apK_{NH_3}}{1+apK_{HClO_4}} \tag{2.31}
$$

Here K_{HClO4} and K_{NH3} - constants of the solubility for corresponding substances; $\alpha = 1/\rho r_d$, ρ - density of AP, η_s – fraction of AP, which decomposes by stages 2 and 3 with the thermal effect of Q.

For ν and β the following expressions has been obtained [9]:

$$
\nu = \frac{(T_m - T_s)E}{2RT_s^2}\left[1+\frac{(T_m-T_s)L}{2RT_s^2}\right]^{-1} - \frac{a(K_{HClO_4}-K_{NH_3})p}{2(1+aK_{NH_3}p)(1+aK_{HClO_4}p)}, \tag{2.32}
$$

$$
\beta = \left(\frac{E}{2RT_s^2} + \frac{T_m - T_s}{T_s - T_0}\frac{L}{RT_s^2}\right)\left[1+\frac{(T_m-T_s)L}{RT_s^2}\right]^{-1} \tag{2.33}
$$

On the basis of data stating greater pressure of the ammonia vapors in comparison with the pressure of perchloric acid vapors, the conclusion was made that in AP combustion the solubility of perchloric acid in the condensed phase is relatively higher, i.e., $K_{HClO_4} > K_{NH_3}$. Because of this with the pressure increase, in accordance with to (2.32) and (2.33) the drop in the burning rate must occur. Possible formation within the condensed phase of the intermediate products, which displace equilibrium in favor of NH_3 (for example, it can be water) even more strengthens this drop in the rate. Thus, according to the data [3], at pressure ~150 atm the temperature on the

burning surface of AP (~320 ^{0}C) approximately corresponds to the boiling point of water (~360 ^{0}C). Beginning from this pressure, the burning rate of AP is reduced and the character of combustion becomes unstable.

Combustion stability of AP within the framework of the above model has been analyzed in [9, 10]. It was shown that the account of the temperature dependence of the heat of sublimation L leads to the fact that when the initial temperature increases the criterion of intrinsic combustion stability (with respect to B. V. Novozhilov [11]) ceases to be fulfilled. Moreover, the intermediate combustion instability pressure domain may exist. Combustion in this domain is unstable, but out of the domain it is stable. The form of the calculated domain of unsteady combustion qualitatively agrees with the experimental data for the number of organic amine perchlorate.

It is to be noted that the detailed mechanism of decomposition and combustion of AP still remains unclear despite intense research work during last more than three decades. Especially it regards to description of the condensed phase reactions. In addition to described above global kinetic mechanism several attempts to develop more comprehensive reaction schemes were undertaken. One of the first one was made in 1971 [12] with single global reaction in the condensed phase and 14 gas phase reactions. In fact, it was extended semi-global mechanism and its background was not well justified. Subsequent works by Ermolin et al. [13 – 16], published in 1982 - 1995, gave rather detailed and substantiated scheme of gas phase reactions but did not concern any details of the condensed phase reactions. Only recently new experimental data became available that gave more insight into condensed phase decomposition reactions [17]. Based on these and other available data the AP condensed phase 4 step mechanism was formulated in [18]. It was suggested that due to high pressure existing in the bubbles inside subsurface liquid layer of AP, the reactions in the condensed phase go to completion and produce final products according to equation

$$4AP \rightarrow 3.25\ HCl + 5.875\ H_2O + 1.146\ O_2 + 1.833\ N_2O + 0.375\ Cl_2 + 0.33\ NH_3$$

The calculations of the AP burning rate were performed [18] with use of mentioned 4 step condensed phase mechanism and slightly modified Ermolin's 79 step gas phase mechanism. The results of calculations exhibited good agreement with experimental data [13] on temperature and species space distribution in combustion of AP at subatmospheric pressure 0.6 atm. Comparison with available experimental data on burning rate and its temperature sensitivity in the pressure range 30-110 atm showed important role of condensed phase reactions in getting better agreement with calculation results [18]. As in a previous work of the same group [19], the conclusion can be made about urgent need for more precise and detailed experimental data on combustion characteristics of AP in order to substantiate contemporary most comprehensive mathematical description of the combustion mechanism.

2.6 REFERENCES

1. **R. Friedman, R. G. Nugeut, K. E. Rumbel, A. C. Scurlock**, "Deflagration of ammonium perchlorate,"- 6th Symp. (Intern.) on Combustion, Reinhold, 1957, pp.612-619.
2. **T. L. Boggs**. " Deflagration rate, surface structure and subsurface profile of self-deflagrating single crystals of ammonium perchlorate," AIAA Journal, 1970, No 5, pp. 867-873.
3. **A. P. Glazkova**, Catalysis of explosive combustion. M.: Nauka, 1976 (R).

4. "Mechanism of thermal decomposition of ammonium perchlorate," Institute of Chemical Physics, USSR Academy of Sciences, Chernogolovka, 1981 (R).
5. **V. A. Strunin, G. V. Manelis, A. N. Ponomarev, V. L. Tal'roze**, "Effect of the lowering emission on the combustion of ammonium perchlorate and mixture systems on its basis," *Combustion, explosion, and shock waves*, 1968, Vol. 4, pp. (R) 584-590.
6. **V. A. Strunin, A. N. Firsov, K. G. Shkadinskiy, G. V. Manelis**, "Stationary combustion of the decomposed and evaporating condensed substances," *Combustion, explosion, and shock waves*, 1977, Vol. 13, pp. (R) 3-9.
7. **V. A. Strunin, G. V. Manelis**, "On the burning rate temperature coefficient of the condensed substances," *Combustion, Explosion and Shock Waves*, 1975, Vol. 11, pp. (R) 797-799.
8. **G. B. Manelis, V. A. Strunin**, "The mechanism of ammonium perchlorate burning," *Combustion and Flame"*, 1971, v. 11, pp. 69 - 77.
9. **G. V. Manelis, V. A. Strunin**, Mechanism of the combustion of ammonia and hydrazonia salts," In: Combustion and explosion. Proceedings of the III All-Union symposium on combustion and explosion, M.: Nauka, 1972, pp. 53-57 (R).
10. **V. A. Strunin, G. V. Manelis**, "On the stability of the stationary process of VV combustion, limited by reaction in the condensed phase," *Combustion, Explosion and Shock Waves*, 1971, Vol. 7, pp. (R) 498-501.
11. **B.V Novozhilov**, "Unsteady combustion of solid rocket propellants," Moscow, Nauka, 1973, pp. 176 (R).
12 **C. Guirao, F.A. Williams**, "A Model for Ammonium Perchlorate Deflagration between 20 – 100 atm", *AIAA Journal*, V. 9, No. 7, pp. 1345-1356, 1971
13. **N. E. Ermolin, O. P. Korobeinichev, A. G. Tereschenko and V. M. Fomin**, "Measurement of the concentration profiles of reacting components and temperature in an ammonium perchlorate flame", *Combustion, Explosion and Shock Waves,* 1982, Vol.18, No. 1, pp.46-49 (R).
14. **N. E. Ermolin, O. P. Korobeinichev, A. G. Tereschenko and V. M. Fomin**, "Kinetic calculations and mechanism definition for reactions in an ammonium perchlorate flame", *Combustion, Explosion and Shock Waves,* 1982, Vol. 18, No. 2, pp. (R) 61-70.
15. **N. E. Ermolin, O. P. Korobeinichev, A. G. Tereschenko and V. M. Fomin**, "Simulation of kinetics and chemical reaction mechanism of ammonium perchlorate burning", *J Chem. Phys.,* 1984, Vol. 1(2) (R).
16. **N.E. Ermolin**, "Model for chemical reaction kinetics in perchloric acid-ammonia flames", *Combustion, Explosion and Shock Waves,* 1995, Vol. 31, pp. (R) 58-69.
17. **R. Behrens and L. Minier**, "Thermal decomposition behavior of ammonium perchlorate and of an ammonium perchlorate based composite propellant", *33rd JANNAF Combustion Meeting,* 1966, Vol. 1, CPIA #476.
18 **Q. Jing, M. W. Beckstead and M. Jeppson**, "Influence of AP solid phase decomposition on temperature profile and sensitivity", *AIAA 98-0448, 36th Aerospace Sciences Meeting and Exhibit,* Jan. 12-15, 1998, Reno, NV.
19. **M. Tanaka, M. W. Beckstead**, "A three phase combustion model of ammonium perchlorate", *AIAA 98-0448, 32nd AIAA/ASME/SAE/ASEE Joint Propulsion Conference*, July 1-3, 1996, Lake Buena Vista, FL.

2.7. COMBUSTION OF DOUBLE BASE PROPELLANTS

P. F. Pokhil and his coworkers of the (Semenov) Institute of Chemical Physics, Moscow conducted in 50's systematic experimental studies of mechanism and laws governing stationary combustion of DB propellants in broad ranges of pressure and initial temperatures. In the course of the study of the combustion mechanism two experimental findings of fundamental value were obtained [1]: a) the chemical reactions of gasification of the condensed phase of DB propellant are summary exothermic; b) the process of gasification is accompanied by the dispersion of a significant part of the condensed phase.

The value of these findings for subsequent development of the combustion theory of propellants is difficult to overestimate. They became the basis of contemporary concepts about the mechanism of DB propellant combustion and initiated number of theoretical and experimental works.

In existing theoretical works the concepts of multi stage structure of the combustion wave are extensively used. According to Refs. [1-4], exothermic reactions during combustion of DB propellants occur in a subsurface layer of the condensed phase, in the particles belonging the disperse zone, and in the gaseous decomposition products of the condensed phase.

In [1, 5-8] approximate estimates were given for contribution of different stages to the heat balance on the burning surface of DB propellants. It was found that the heat release in the condensed phase of DB propellant, which represents a relatively small portion of the total amount of heat released in the combustion (~7-15% depending on the pressure and initial temperature), gives 70-100% of amount of heat needed for stationary combustion wave propagation. With increase in pressure ($p < 100$ atm) and the initial temperature the role of the condensed phase reactions, according to [1, 6, 9], increases. This fact requires special attention to be paid to studying the processes, which take place in the condensed phase of the burning propellant.

Magnitude of thermal effect of decomposition EM in the condensed phase and temperature on the burning surface T_s are closely related to the scale of dispersion; T_s depends on the consumed portion of EM in the condensed phase. The burning rate depends in turn on the value of T_s. The systematic experimental studies of the dispersion, carried out in 1970-1980s [10, 11], confirmed the data of Pokhil about significant scale of the dispersion of DB propellants in vacuum, but they refuted hypothesis about maintaining dispersion degree by approximately the same level with the pressure increase.

According to the results of [10, 11], during the combustion of DB propellants the degree of dispersion with an increase in the pressure is monotonically reduced from 30-40% at pressure $p<3$ mm Hg to the values, which do not exceed several percents with $p=0.5$ atm. Simultaneously the burning rate is increased by 3-5 times (at the same initial temperature).

The question arises: does observed increase in the burning rate correspond to increase in the thermal effect of the condensed phase decomposition Q as a result of reduction of a dispersion degree? Let us examine this problem in more detail on the example of combustion of DB propellant N (55% nitrocellulose, 26% nitroglycerin, 13% dinitrotoluene, 6% additives).

Let us designate as degree of dispersion the ratio of the mass, which left from the burning surface in dispersed state, to total consumed mass of EM for the same time interval. The decrease of the dispersion degree for the propellant N from $\eta_d \approx 0.35$ at $p \leq 3$ mm Hg to $\eta_d \approx 0$ at $p = 400$ mn Hg is accompanied by an approximately three-fold increase in the burning rate (at $T_0=120^0$C). If we do not consider the specific behavior of the volatile components in the combustion wave of DB propellant (nitroglycerin – NGL, and dinitrotoluene - DNT), then observed decrease η_d must lead to increase T_s by value $\Delta T_s \approx 0.3\ Q_c/c > 100$ K. Mass burning rate m with this increase of T_s must be increased at least by an order of magnitude, since m ~exp(-E/RT$_s$) and E~20000 cal/mol [12].

In works [10,14] it has been shown that significant role in the balance of heat for condensed phase of propellant N play volatile components of the propellant: NGL and DNT. Indeed, the balance energy for the burning surface has the form:

$$c(1-\alpha)(T_s - T_0) + c\alpha(T_b - T_0) + \alpha L + c\alpha\Delta T_b = (1-\alpha)Q_c\eta_s' \qquad (2.34)$$

Here α, T_b, L - mass fraction of volatile components in the propellant formulation correspondingly, their boiling temperature and heat of vaporization (T_c and L for NGL and DNT are approximately equal, according to [15]);$\eta_s' = 1-\eta_s/(1-\alpha)$ – extent of the decomposition of nonvolatile component (nitrocellulose).

The terms in (2.34) reflect the expenditures of heat, liberated upon decomposition of $(1-\alpha)\eta_s'$ portion of propellant, for heating of nonvolatile component from T_0 to T_s plus heating of volatile components to T_b, their subsequent vaporization and warm-up of the vapors by ΔT_b during their escape from condensed phase.

Assuming, according to rough estimates, that $\alpha c\Delta T_b/(1-\alpha)Q_c\eta_s << 1$ (as a result of small magnitude of ΔT_c since vapors of volatile components during the escape produce channels in a reaction layer of condensed phase and residence time of vapors there so little that the warm-up does not exceed value $\Delta T_b \sim 30$°C [10]), we will obtain for the low pressures ($p << 1$ atm):

$$T_s = T_0 + \frac{Q_c\eta_s'}{c} - \frac{\alpha}{1-\alpha}\frac{L}{c} - \frac{\alpha}{1-\alpha}(T_b - T_0) \qquad (2.35)$$

From (2.35), it is evident that T_s depends not only on the degree of dispersion, but also on the boiling point of volatile components T_b. Since with an increase in pressure T_b is increased, heat expenditures for volatile components heating are also increased. This restricts strong increase of T_s and, consequently, of the burning rate.

At pressures where spatially divided fronts of gasification (vaporization and decomposition) exist, propagation of the combustion wave in the coordinate system, connected with the burning surface, can be described by the system of equations:

$$\lambda d^2T/dx^2 - (1-\alpha)cmdT/dx + (1-\alpha)Q_c\Phi = 0 \qquad (2.36)$$

$$md\eta/dx + \Phi = 0, \quad \Phi = \rho_c f(\eta)k_0 exp(-E/RT), \quad x \leq 0, \quad \alpha < 1 \qquad (2.37)$$

Here λ - thermal conductivity; k_0, E and $f(\eta)$ - pre-exponent, energy of activation, and kinetic function, correspondingly.

The terms, connected with the heat expenditures for heating and vaporization of volatile components, are not included in (2.36). The possibility of such treatment is ensured by the fact that the

front of vaporization plays "external" role with respect to the zone of chemical reactions and the presence of volatile components is taken into account under the boundary condition at the "cold" end:

$$X \to -\infty,\ \eta' \to 0,\ T \to T_0^*;\ x = 0, \eta = \eta_s',\ dT/dx = 0.$$

Integration of (2.36), with taking into account of (2.37) and boundary conditions, gives relationship $T_S = T_0^* + Q_c\eta_s'/c$, which coincides with (2.35) when

$$T_0^* = T_0 - \alpha(T_c - T_0^{**})/(1-\alpha),\ T_0^{**} = T_0 - L/c$$

Solution of the system (2.36), (2.37) under assumptions of Zeldovich - Franck-Kamenetskii takes the form (with $f(\eta) = 1$)

$$m^2 = 2\lambda\rho_c(RT_s^2/E)k_0\exp(-E/RT_s)/\eta_s'^2(1-\alpha)Q_c. \qquad (2.38)$$

For closing the problem it is necessary to know dependence of η_s' on internal and external parameters of combustion. It is most simple to use empirical dependence [10] $\eta_s' = \eta_{s1} - B\delta_b$, where δ_b - distance between the fronts of gasification which are caused by chemical reaction and vaporization; B - empirical constant; η_{s1} - degree of conversion at $T_b = T_s$. At $p \geq p_1$, when inequality $|T_s - T_b| \leq RT_s^2/E$ starts to held, the value of η_s' is assumed constant and equal to η_{s1}.

By expressing δ_b through m, T_s, T_b and T_0 the relationship for η_s' can be written in the form

$$\eta_s' = \eta_{s1} - (B\lambda/cm)(1-\alpha)^{-1}\ln[(T_s - T_0^*)/(T_b - T_0^*)] \qquad (2.39)$$

Equations (2.38) and (2.35), taking into account (2.39) and dependence $T_b(p)$ in the form of Clausius-Clapeyron equation

$$T_b = L/R\ln(p_0/p), \qquad p_0 = \text{const}$$

compose algebraic system for finding m, T_s and η_s'.

Dependencies of the burning rate on T_0 and p take the form

$$\nu \cong (E/2L)(T_b/T_s)^2,\quad \beta \cong E/2RT_s^2. \qquad (2.40)$$

Form of expressions for β and ν is similar to those known from literature. However, the dependence on the pressure is the specific feature of the expression for ν. This is because of dependence $T_b = T_b(p)$. With the decrease in pressure T_b is reduced more rapidly than T_s and dependence m(p), according to (1.84), weakens. This character of behavior of ν corresponds to experiments [1].

For DB propellant N satisfactory agreement with the experiment is observed if one takes $E \cong L \cong 20000$ cal/mol. In this case $\beta = 2.5\cdot10^{-2}$ K^{-1} - experiment (p<1 atm), and $\beta \cong 2\cdot10^{-2}$ K^{-1} – calculation, $\nu = 0.3 \div 0.4$ - experiment ($p \leq 10^{-1}$ atm), and $\nu = 0.3$ – calculation, $\nu = 0.6$ - experiment ($10^{-1} < p < 1$ atm), and $\nu \cong 0.5$ – calculation. Thus, the used form of heat balance on the burning surface (1.78) allows even in the case of a significant variation in the degree of dispersion to correlate the calculated and experimental dependencies $u(p, T_0)$.

2.7.1 Combustion model with variable heat release in the condensed phase.

Numerous investigations [1, 5, 6] testify that during burning of nitrocellulose (NC) and powders on its basis the heat release Q_c in the condensed phase depends on p and T_0. This fact was usually explained by assuming the dispersion of the certain fraction of condensed phase η_d into the

smoke-gas zone, so that $Q_c = Q_0 (1-\eta_d)$, where $Q_{0=}$const - heat evolution with the complete gasification of the condensed phase, a η_d is expressed in the form of a certain function of T_s and p [14]. However, for the pressures of $p \geq 1$ atm the concept about the determining effect of the dispersion degree on the value of Q_c contradicts experiment [10, 11].

Let us examine simple model of reaction zone of the condensed phase of DB propellants, explaining variability of Q_c without use of the dispersion concept. It is known that the first elementary act of the thermal decomposition of nitroesters is the endothermal breaking CO-NO_2 bond with the formation of two free radicals: the dioxide of nitrogen and alcoxyl radical [12, 16], which then enter into the secondary chemical oxidation reactions. On the basis of the concept of the multi stage chemical transformation in the combustion of propellants based on NC, A. A. Zenin assumed [12] that a large difference in the kinetic constants of the decomposition of DB propellants, obtained under conditions of low-temperature thermolysis and during the burning, can be explained by the change of the rate control stage. However, it is obvious that the change of the rate control stage must not lead within the framevork of model [12], to a change in summary thermal effect Q_c. One may expect that during the decomposition of such complex chemical compounds as NC and NGL, following the first stage (breakaway of NO_2-groups) another set of series-parallel reactions is realized. Let us divide conditionally all this set into two parallel global competing reactions with different thermal effects Q_2 and Q_3 (for the certainty let us assume $Q_3 > Q_1$). Schematically, the way of transforming the initial propellant A into the reaction gaseous products P_1 and P_2 can be represented in the form [17]

$$A \xrightarrow{K_1, Q_1} B \begin{cases} \xrightarrow{K_2,\ Q_2,\ 1-\eta_s} P_1 \\ \xrightarrow{K_3,\ Q_3,\ \eta_s} P_2 \end{cases} \qquad (2.41)$$

Here K_i (i = 1, 2, 3) - rate constant of the corresponding stage of decomposition; B - intermediate product (denitrated propellant with dissolved NO_2); η_s – fraction of the product B, which reacts by the most calorific way with the thermal effect Q_3 .

Total thermal effect Q_c in this case is determined by the shared contribution of different reactions in the decomposition of propellant to the gaseous products

$$Q_c = Q_1 + Q_2(1-\eta_s) + Q_3\eta_s \qquad (2.42)$$

Here Q_1 - thermal effect of the breakaway of NO_2-groups per unit mass of initial propellant. According to analysis of Zenin [12], stages A→B and B→P in the combustion wave at moderate pressures are spatially divided, so that the reactions B→P start after the virtually entire completion of the first stage of decomposition. Taking this into account, the degree of conversion in the first stage is accepted in (1.86) equal to 1. The summary exothermic character of the decomposition of DB propellant is determined by secondary condensed phase reactions with participation of NO_2 [1]. This is testified by the facts that the maximum thermal effect of the thermal decomposition corresponds to the minimum yield of NO_2 into gaseous products [16], and increase Q_c with increase in pressure is accompanied by decrease in the content of NO_2 in reaction products [1].

Indirect data, which testify for important role of secondary condensed phase reactions with participation of intermediate volatile product, are obtained also in the work [18]. In experiments on the high-temperature pulse calorimetry it was revealed that the specific heat release rates in the thick (12-13 μm) films of NC are higher than in the thin (<3 μm) ones. Within the framework of

the concepts developed this is explained by the fact that the diffusion of NO_2 from the thick NC films is hindered; therefore, secondary reactions run more effectively. The possible important role of the diffusion of volatile intermediate products upon decay of nitro-compounds was also indicated by K. K. Andreev when he analyzed the values of the kinetic constants [19].

Let us assume that the efficiency (depletion degree) of reacting in stage with the thermal effect of Q_3 is determined by the intensity of NO_2 participation in secondary processes in the condensed phase. Reaction with the thermal effect of Q_2 in that case will be the decomposition of the denitrated product. During the burning the degrees of decomposition in terms of each of the ways will be determined by the probability of the NO_2 involvement into the secondary reactions. This probability depends on the conditions of the deletion of the molecules NO_2 from the reaction zone, i.e., from the rates of diffusion and filtration of macro-quantities of NO_2.

Thus, the probability of reaction for NO_2 will be determined by the width of the reaction zone δ, by the coefficient of diffusion D, by the linear burning rate u, and the fraction of the molecules NO_2, which are found in the dissolved state, C/C_0 (where C_0 and C are the concentrations of NO_2 in the initial propellant and in the liquefied reaction layer). Since the probability of the secondary reaction with the participation of $N0_2$ linearly depends on the degree of decomposition in terms of the stage with effect of Q_3, it is possible to write $\eta_s = \eta_s(C/C_0, D, \delta, u, K_3)$. From dimensionality considerations one obtains

$$\eta_s = \xi'(C/C_0)^{n_1}(u\delta/D)^{n_2}(K_3\delta^2/D)^{n_3} = \xi'\pi_1^{n_1}\pi_2^{n_2}\pi_3^{n_3}. \quad (2.43)$$

Exponents n_1, n_2 and n_3 need the independent determination. Assuming the order of the reaction on concentration of NO_2 being equal to unity [12], we immediately obtain $n_1 = 1$. Considering the species of NO_2, entering the chemical reaction, equiprobable throughout entire zone δ, we may assume $\eta_s \sim \delta/l_d$, where l_d - characteristic diffusion length. But $\delta/l_d = \delta/(D\delta/u)^{1/2} = \pi_2^{1/2}$, hence, n_2=0.5. Complex π_3 presents the square of the ratio of the characteristic rates for the chemical reaction and diffusion. Since the yield of two competing processes is proportional to the first degree of the ratio of the rate constants for these processes, $n_3 = 0.5$. Taking further into account that K_3=u/δ, we obtain that $\pi_3 = \pi_2$ and relationship (2.43) takes the form

$$\eta_s = \xi'(C/C_0)(u\delta/D), \quad \xi' = const. \quad (2.44)$$

Taking into account that $\delta \sim T_s^2/u(T_s - T_0)$, and $D \sim T_s/\mu$ and $\mu \sim \exp(E'/RT_s)$, we derive finally

$$\eta_s = \xi pT_s \exp(E'/RT_s)/(T_s - T_0), \quad \xi = const \quad (2.45)$$

When deriving (2.45), it was assumed that the heat of NO_2 solution is close to zero, and solubility is proportional to pressure, i.e., $C \sim p$.

Introduction of the degree of decomposition in the form of (2.44) does not make essential complications in mathematical description of DB propellant combustion. The propagation of the combustion wave is formally described by the ordinary system of equations for the rate control reaction stage in the condensed phase with incomplete transformation of solid substance into the gas on the surface. This will only imply the replacement of complex $Q_0\,\eta_s'$ by $Q_c(\eta_s)$ according to (2.42) and (2.44). Here Q_0=const - thermal effect of the decomposition of condensed phase; $\eta_s' = 1-\eta_d = f(p, T_0, u)$ - degree of conversion of condensed phase into the gas on the surface.

Expression for the burning rate u now takes the form [20]

$$u^2 \sim T_s^2 \exp(-E_3 / RT_s) / Q_c^2 \qquad (2.46)$$

Energies of activation of both simultaneous reactions B $\rightarrow$ P_1 and B $\rightarrow$ P_2 seem to be close. Thus, for the oxidative reactions with participation of NO_2, value E = 19000 cal/mol [12], and for the decomposition of pure cellulose in the range of temperatures 260 to 310 ^{0}C E_2 = 14000-26000 cal/mol [21].

The comparison with experiment for DB propellant N can be performed by examination the following dependencies: $Q_c(T_0.)$, $Q_c(p)$, $u(T_0)$ and $u(p)$.

a) The dependence $Q_c(T_0)$ can be found by differentiating expression (2.42) on T_0 taking into account (2.44) and condition $T_s = T_0+Q_c/c$:

$$\partial Q_c / \partial T_0 = c(1 - E'/RT_s)/[cT_s / \eta_s(Q_3 - Q_2) + E'/RT_s + T_0/(T_s - T_0)]. \qquad (2.47)$$

The value of E' for pure NC is about 28000 cal/mol [22]. And though in the course of the propellant destruction in the wave of combustion the value of E', apparently, is changed, one may expect the retention of E' value on the sufficiently high level, such that $E'/RT_s >> 1$. In this case, as can be seen from (2.46), $\partial Q_c/\partial T_0 < 0$.

Let us evaluate the magnitudes of thermal effects Q_1, Q_2 and Q_3. Greatest thermal effect $Q_{c,max}$ is realized when $\eta_s = 1$. From (2.42) it follows that $Q_{c,max} = Q_1 + Q_3$. Computed value of Q_1 obtained by the summation of energies of CO-NO_2 bonds in the propellant N, is approximately equal to -400 cal/g, and $Q_{c,max}$ = 800 cal/g [16], then Q_3 = 1200 cal/g. If denitrated NC does not essentially differ from regular cellulose, the value of Q_2 seems to be close to zero [23]. Degree of conversion $\eta_s \cong (Q_c - Q_1)/Q_3 = [c(T_s-T_0)-Q_1]/Q_3$ with p$\geq$1 atm is close to 0.5. Then it is fulfilled

$$\partial Q_c / \partial T_0 \approx -c. \qquad (2.48)$$

With increase in T_0, as it follows from analysis of (2.48), the value of Q_c is reduced. Physically this means that an increase in T_0, which simultaneously leads to increasing T_s, leads to an increase in the diffusion removal of the molecules of NO_2 from condensed to the gas phase ($D \sim T_s/\mu$). This is reflected by decrease in η_s.

b) The dependence $Q_c(p)$ is determined by differentiating expressions (1.86) and (1.88) on p taking into account relationship $T_s = T_0 + Q_c/c$. Eliminating derivatives on η_s and T_s,we obtain

$$\partial Q_c / \partial \ln p = (Q_3 - Q_2)\eta_s[1 + (Q_3 - Q_2)\eta_s E'/cRT_s^2]^{-1}. \qquad (2.49)$$

Then, assuming $(E'/RT_s)(Q_3-Q_2)\,\eta_s/cT_s >> 1$, we obtain

$$\partial Q_c / \partial \ln p \cong cRT_s^2 / E'. \qquad (2.50)$$

Figure 2.10 gives diagram of dependence $Q_c(T_0)$ constructed according to expression (2.47). The heat capacity of propellant is taken average in the range of T_0 from -200 to 100^{0}C; E' is assumed equal to 12500 cal/mol. In the same figure the experimental data $Q_c(T_0)$ [5, 6, 24, 25] are plotted. Figure 2.11 shows the dependence $Q_c(p)$ calculated by (2.49). The experimental data [5, 6, 24, 25] are depicted by circles.

c) Using (2.46) with the same approximations we obtain temperature sensitivity of the burning rate

$$\beta = \partial \ln u / \partial T_0 \cong (T_s - T_0)^{-1}(1 + E/E').$$

d) Similarity, the burning rate pressure sensitivity is expressed by

$$\nu = = \frac{\partial \ln u}{\partial \ln p} \cong \frac{E_3 / 2RT_s}{E'/RT_s + cT_s/(Q_3 - Q_2)\eta_s} \cong \frac{E_3}{2E'}.$$

Thus, the model proposed describes with reasonable accuracy the basic burning laws of DB propellant over a wide range of the burning conditions.

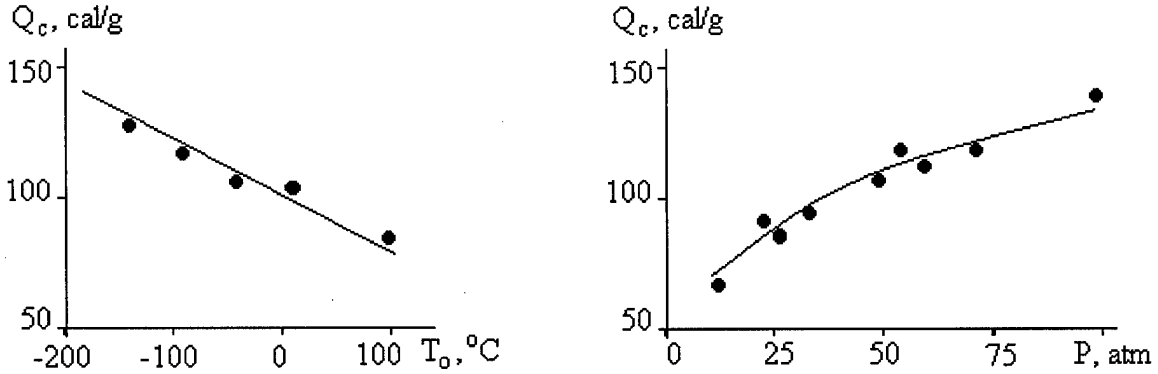

Fig. 2.10. Dependence of the heat evolution in thecondensed phase of DB propellant N on initial temperature at p=20 atm.

Fig. 2.11. Dependence of the heat evolution in the condensed phase of DB propellant N on pressure at T_0=20 ^{0}C.

2.7.2. Effect of the initial temperature on the burning rate.

The question about causes strengthening the dependence of the burning rate of DB propellant N on initial temperature was repeatedly discussed in the literature [24, 26, 27].

According to experimental data [24], the burning rate temperature coefficient $\beta=\partial \ln u/\partial T_0$ at pressure 20 atm increases from ~$0.5\cdot10^{-3}$ K^{-1} at T_0 = -150 ^{0}C to $15\cdot10^{-3}$ K^{-1} at T_0 = 140^{0}C. Similar pattern is observed at other pressures. It is also shown [24] that the dependence of the burning surface temperature T_s on T_0 is strengthened with increase of T_0. Thus, the value of derivative $r = \partial T_s / \partial T_0$ at p = 20 atm varies from ~0.2 at T_0 = (-100, -150)^0 C to ~ 0.5 at T_0 = (100, 140)^{0}C. The variation of r at p=1 atm is still stronger: from 0.1 at T_0 = (-100, -200)^0 C to 1.0 at T_0 = (50, 100)^{0}C.

The concept of unique dependence $u(T_s)$ [25] gives possibility to reduce the problem on the reasons for strengthening dependence $u(T_0)$ to the analysis of dependence $T_s(T_0)$. Further, the use of a heat balance in the form

$$\bar{c}(T_s - T_0) = Q_c = \sum Q_i \qquad (2.51)$$

reduces the problem to the analysis of dependence $Q_c(T_0)$. Here $\bar{c}$ - average over the temperature range (T_0, T_s) specific heat of the propellant; $\Sigma Q_i = Q_{ch} + Q_{th} + Q_r + Q_{alt}$ – amount of heat required for the warm-up of the unit of the propellant mass from T_0 to T_s; Q_{ch} – heat released during the chemical decomposition of the condensed phase; (Q_{th} + Q_r) - heat feedback to the condensed phase via the thermal conductivity from gas (Q_{th}) and the radiation from flame (Q_r); Q_{alt} - other

possible (or alternative) heat sources or sinks. Relationship (2.51) is formulated for the unit of propellant mass and it is accurate in the absence of dispersion, i.e., it has to be considered at p>1 atm.

In Ref. [24] the data are cited on heat evolution $(Q_{ch}+Q_{th}) = Q'_c$ in the condensed phase of DB propellant N, calculated from the difference in heat fluxes Δq on the boundaries of chemical reaction zone: $(Q_{ch}+Q_{th})=\Delta q/\rho_c u$. The account of the fact that for non-metallized propellant the contribution of Q_r to the value of ΣQ_i is relatively low ($Q_r << Q_{ch}+Q_{th}$ [5, 28]) gives the possibility to evaluate the contribution of Q_{alt} via the comparison of values $\overline{c}\,(T_s-T_0)$ and $(Q_{ch}+Q_{th})$. Note that $\overline{c}\,(T_s - T_0)$ and $(Q_{ch}+Q_{th})$ are determined in an independent manner.

Table 2.13 presents the values of $(Q_{ch}+Q_{th})$ calculated according to the experimental data [24] in dependence on T_0. There are also presented data on $\overline{c}\,(T_s - T_0)$ calculated with use of (2.51) according to experimental data $T_s(T_0)$ at p = 20 atm and $\overline{c}$=0.3 cal/(g K) for propellant N. The magnitude of $\overline{c}$ is taken as average value of the heat capacity of DB propellant N in the investigated temperature range (-200, -150)^{0}C according to the data [28-31].

Table 2.13. Parameters of the combustion wave of DB propellant N.

T_0, °C	-150	-100	-50	0	50	100	140
T_s, °C	250	260	270	300	340	360	380
Q'_c, cal/g	150	140	125	110	100	85	75
$\overline{c}\,(T_s-T_o)$,cal/g	120	110	95	90	90	80	75
Q_{alt}, cal/g	-30	-30	-30	-20	-10	-5	0

It follows from Table 2.13 that the values of heat release in the condensed phase of propellant, calculated by (2.51), can be correlated with those directly measured only if one assumes an existence of some endothermal process with thermal effect Q_{alt}, which depends on T_0 in accordance with reported data.

What is the nature of this effect? According to Ref. [28], essential role in the combustion of double base propellant N may play irreversible exothermic "low temperature reactions". Indeed, if one choose proper value of $\overline{c}$ in expression (2.51), the values of $Q_c = \overline{c}\ (T_s-T_0)$ and $Q_c = Q_{ch} + Q_{th}$ can become equal at low temperatures and one receives $Q_{alt} > 0$ at elevated temperatures. However, this is not consistent with observed in [28] combustion behavior of thermally treated propellant N. Actually, the burning rate of propellant N, which was preliminary heated during 1 hour under temperature 130^{0}C, exhibits increased by 7-12% value at the temperature 20^{0}C as compared with fresh propellant. This contradicts hypothesis on essential contribution of "low temperature" exothermic reactions in observed dependence $u(T_0)$ upon assumption on the rate control reactions in the condensed phase. In scope of this approach one may expect only decrease in the burning rate because of reduction by approximately 26 cal/g [28] of summary heat release in the condensed phase.

Investigations carried out for the mixture of nitrocellulose and nitroglycerin [33], showed that this mixture is limitedly compatible and presents true solution only within certain ranges in composition and temperature. The warm-up of the mixture NC and NGL above the so-called lower

critical mixing temperature (LCMT) leads to the separation of the system into two different phases, one of which is depleted by NG, and the other - by NGL. There are also several proofs of the existence of the components separation effect for the propellant N, which contains NC and NGL as the basic components. Since the lamination is accompanied by a change in a number of properties of the propellant, it is of interest to examine its effect on the combustion law parameters.

Let us point out initially the facts, which testify about possibility of components separation in DB propellant N during heating, and estimate the value of LCMT. Extrapolation of data [33] into the domain of the composition, which corresponds to formulation of propellant N, gives the value of LCMT about 60–90 ^{0}C. Since the process of plastification of NC by nitroglycerin proceeds with the heat liberation [34], reverse process (separation) must be accompanied by the heat absorption. For the propellant N this is marked, in particular, by a sharp increase of heat capacity when increasing the ambient temperature above 60°C: from 0.35 cal/(g.K) at 60°C to 0.5 at 92°C [31]. It is necessary to note that the thermal effect of separation depends on the depth of penetration into the domain of incompatibility, so that the effect can be "smeared" in the wide range of temperatures higher than LCMT. This serves as obstacle to the detection of effect in experiments on thermal analysis. Besides, with an increase in the temperature the masking effect of exothermic decomposition reactions begins to develop.

Hysteresis of structural and thermodynamic properties of system upon heating and cooling serves as one of distinctive manifestations of a separation. As has already been indicated, the preliminary heating of DB propellant N at 130^{0}C for 1 hour (with subsequent cooling) leads to an increase in its burning rate by 7 to 11% at 1 atm and 20 ^{0}C. Within the framework of the approach under discussion this can be explained by the fact that when the propellant was kept for a long time at the temperature above LCMT its components were separated rather effectively. When cooling in a relatively short time, a slow solvation process may not be completed entirely and the combustion proceeds with an enhanced rate because there is no need to spend heat for total desolvation of components.

Since the process of separation at T_0> LCMT proceeds essentially by diffusion way, one may expect that the burning rates will differ in samples heated different time. Usually the warm-up time to the required T_0 takes tens of minutes. If the process of separation in the sample for this time takes place at the sufficient degree, it is possible to expect also increase in the burning rate of this sample in comparison with the sample, whose warm-up to the same temperature proceeds rapidly. For example, it can be done via absorption of radiant energy from the external source in the process of combustion. It has been shown [28] that the rates of combustion of samples under the effect of radiant flux of known density are lower than the rate of combustion of the samples, warmed up to equivalent initial temperatures estimated by the known relations (see, for example, [35]). Disagreement between burning rates begins to noticeably exceed an experimental error with heat flux $q_r \geq 3$ cal/(cm^{2}s), which corresponds to the effective initial temperature $T_0 \geq 60$ ^{0}C, which is close to the estimated value of LCMT. Values of the burning rate temperature sensitivity coefficient $\beta = \partial \ln u/\partial T_0$ corresponding certain value of the burning rate reached by different ways, due to variation of a initial temperature $u(T_0)$ in one case and due to variation of a radiant flux $u(q_r)$ in other case, may also differ at T_0>LCMT

$$\beta(T_0) / \beta(q_r) = r(T_0) / r(q_r) \cong 2.5; \qquad r = \partial T_s / \partial T_0 \tag{2.52}$$

To obtain the numerical value of the ratios of burning rate and surface temperature sensitivities the expression (2.51) and data of Table 2.13 were used.

2.7. - REFERENCES

1. **P. F. Pokhil**. Author's abstract of Dr. Sc. Thesis. Moscow, Institute of Chemical Physics, USSR Academy of Sciences, 1954, see also in the book: "Theory of the combustion of propellants and explosives", M., Science, 1982, pp. 117-140. (R)
2. **E. I. Maksimov, A. G. Merzhanov**, "To the theory of the combustion of condensed substances", *Combustion, Explosion, and Shock Waves*, 1966, Vol. 2, pp. 47-58.
3. **E. I. Maksimov, A. G. Merzhanov**, "On one model of the combustion of nonvolatile explosives", *Reports of the USSR Academy of Sciences*, 1964, Vol. 157, pp. 412-415. (R):
4. **B. L. Crawford, C. Hugget, J. J. McBrady**, "Mechanism of the burning of double-base propellant,"- *J. Phys. Coll. Chem*, 1950, Vol. 54, pp. 854 - 862
5. **A. A. Zenin**. Author's abstracts.of PhD. Thesis. Moscow, Institute of Chemical Physics, USSR Academy of Sciences, 1962.
6. **V. M. Maltsev, P. F. Pokhil**, "Evaluation of the thermal effect of initial stage of the combustion of propellants and explosives," *Journal of Applied Mechanics and Technical Physics*, 1963, Vol. 2, pp. 173-174.
7. **P. F. Pokhil**, "On the rate control stage in the combustion of propellants," *Combustion, Explosion, and Shock Waves*, 1969, Vol. 5, pp. 439-440.
8. **G. K. Adams**, "Mechanics and chemistry of solid propellants," Oxford: Pergamon Press, 1967.
9. **V. D. Barsukov, V. P. Nelayev**. On the thermal effect of the zones of chemical transformation on the burning rate of the condensed system. *Journal of Engineering Physics (Russ.)*, 1975, Vol. 29, pp. 989-993. (R)
10. **V. Ya Zyryanov**. Author's abstracts of PhD Thesis. Novosibirsk: Institute of Chemical Kinetics and Combustion, Siberian Division of the Academy of Sciences of the SSSR, 1980.
11. **V. E. Zarko, V. Ya. Zyryanov**, V. V. Chertishchev, Combustion and Explosion. Proceedings of IV All-Union symposium on combustion and explosion, Chernogolovka, 1977, pp. 226-230.
12. **A. A. Zenin**. On one model of a reaction layer in the condensed phase of double base propellant. *Reports of the USSR Academy of Sciences*, 1973, Vol. 213, pp. 1357-1360.
13 **C. Guirao, F.A. Williams**, "A Model for Ammonium Perchlorate Deflagration between 20 – 100 atm", *AIAA Journal*, V. 9, No. 7, pp. 1345-1356, 1971.
14.**V.E. Zarko, V.Ya. Zyryanov, K.P. Koutzenogii**, "Combustion mechanism of double-base propellants at subatmospheric pressures," 16th Intern. Symposium on Combustion Process. Karpacz, 1979, pp. 59-60.
15. **A. F. Belyayev**, "Combustion, detonation and the work of explosion of the condensed systems," M.: Nauka, 1968.
16. **G. V. Manelis, Yu. I. Rubtsov, L. P. Smirnov, F. I. Dubovitskiy**, "Kinetics of the thermal decomposition of pyroxylin", *Kinetics and Catalysis (Russ.)*, 1962, Vol. 3, pp. 42-48.
17. **V. Ya. Zyryanov**, "On the heat evolution in the condensed phase of the burning propellant," *Reports of the USSR Academy of Sciences*, 1980, v. 251, pp. 632-635.

18. **V. V. Aleksandrov**. Author's abstract of PhD Thesis. Novosibirsk, Institute of Chemical Kinetics and Combustion, Siberian Division of the Academy of Sciences of the SSSR, 1970.
19. **K. K Aidreyev**, "Thermal decomposition and combustion of explosives," 2nd Ed. Moscow, Nauka, 1966.
20. **V.A. Strunin**, On the condensed phase zone in combustion of explosives, *Journal of Physical Chemistry (Russ.)*, 1965, Vol.39, pp. 433-435.
21.**G. Janos, F. Sandor**, *Magy. Kem. Fol.*, 1975, Vol. 81, pp. 36-40.
22. **G. A. Grinyute, P. I. Zubov, A. T. Sazharovskiy**, "Effect of temperature on the time dependence of the strength of nitrocellulose films". In the book: The mechanism of the processes of film formation from the polymeric solutions and the dispersions, M.: Nauka, 1966, pp. 165-170.
23. **R.R. Baker**, *J. Therm. Anal.*, 1975, Vol.8, pp. 163-167.
24. **A. A. Zenin, O. I. Nefedova**, "On combustion of double base propellants over a wide range of initial temperatures," *Combustion, Explosion, and Shock Waves*, 1967, Vol. 3, pp. 45-53.
25. **A. A. Zenin, B. V. Novozhilov**, "The unique dependence of the burning surface temperature of double base propellant on the initial temperature," *Combustion, Explosion, and Shock Waves*, 1973, Vol. 9, pp. 246-249.
26. **V. V. Aleksandrov, E. V. Konev, V. F. Mikheyev, S. S. Khlevnoy**, "To a question about temperature of the surface of burning nitroglycerin powder," *Combustion, Explosion, and Shock Waves*, 1966, Vol. 2, pp. 68-73.
27. **A. D. Margolin**, "On the rate control stage of combustion," *Reports of the USSR Academy of Sciences*, 1961, Vol. 141, pp. 1131-1134.
28. **E. V. Konev**. Author's abstract of PhD Thesis. Novosibirsk: Institute of Chemical Kinetics and Combustion, Siberian Division of the Academy of Sciences of the SSSR, 1967.
29. **A. I. Korotkov, O. I. Leypunskiy**, "Dependence of the burning rate temperature coefficient of propellant at atmospheric pressure on the initial temperature," In the book: Physics of explosion, No 2, M.: USSR Academy of Sciences, 1953, pp. 213-224.
30. **V. F. Zhdanov, V. P. Maslov, S. S. Khlevnoy**, "Thermophysical coefficients of nitroglycerin powder at low temperatures," *Combustion, Explosion, and Shock Waves*, 1967, Vol. 3, pp. 40-41.
31. **D. B. Balashov**. *Journal of Physical Chemistry* (Russ.), 1966, Vol. 40, pp. 2937-2940, and pp.3065-3070.
32. **C. Hugget**, "Combustion of solid rocket propellants". In the book: Liquid and solid rocket propellants," M.: Inostrannaya Literatura, 1959, pp. 235-301.
33. **V. A. Golovin, Yu. I. Lotmentsev, R. I. Shneyerson**, "Study of the compatibility of nitroglycerin with nitrocellulose by the static method of measuring the pressure of saturated vapor". *High-molecular Compounds* (Russ.), 1975, Vol. A17, pp. 2351-2354.
34. **A. G. Gorst**, "Propellants and explosives," M.: Mashinostroyeniye, 1972.
35. **Ya. B. Zeldovich, O. I. Leypunskiy, V. V. Librovich**, "Theory of the unsteady combustion of powder", M.: Nauka, 1975, 131 pp.
36. **V. N. Simonenko, V. E. Zarko, K. P. Kutsenogiy,** "The experimental study of the regimes of auto- and induced oscillations of the propellant burning rate". *Combustion, Explosion, and Shock Waves*, 1980, Vol. 16, 60-67.

CHAPTER 3
STATIONARY COMBUSTION OF UNIMODAL HETEROGENEOUS CONDENSED SYSTEMS

3.1. INTRODUCTORY REMARKS

Heterogeneous condensed systems, as it follows from the name, have three-dimensional non-homogeneous physical structure and consist of different chemical components. As typical representatives of such systems serve the solid rocket propellants, in which the particles of powder-like filler (oxidizer, additives of explosives and metallic fuel, catalyst, etc.) are distributed in the matrix of binder performing also the role of fuel. It is necessary to note that the division of solid propellants (SP) into the homogeneous and the heterogeneous to the certain degree is conditional. It depends on the ratio of the scales of the zones of chemical reaction to the size and mixing lengths of components and can vary with a variation in the ambient conditions and the burning rate value.

Components of heterogeneous SP, besides their direct functional designation, can be classified according to their capability for self sustaining combustion. On the burning surface of SP the inert type components, not capable of burning independently, are gasified under the effect of the heat flux, which enters from the flame. The combustion of the particles of active components (some types of oxidizers, additives of explosives, some types of bonding agent) proceeds under the conditions of the effect of additional heat flux from the distant zones of the SP flame. Simultaneously, an interaction due to the mixing and the heat transfer with other propellant components occurs. As a result the burning rate of active energetic component in the SP formulation can prove to be either higher or lower than the rate of its independent combustion.

From theoretical point of view the process of combustion of heterogeneous SP depends not only on thermophysical and kinetic factors, but also on diffusion that characterizes efficiency of mixing the reagents, which enter the reaction zones. Among the parameters that determine the combustion laws an effective size of the particles of the filler appears, and more accurately – a function of mass size distribution for filler particles.

Essential line of the physical picture of heterogeneous SP combustion is heterogeneity and connected with it transience of the components transformation on the burning surface. This is caused by essential difference in the physical and chemical properties of SP components and by the presence of different states of the substance interfaces. The wealth of the forms of transformations and physical states of components in the combustion wave does not make it possible to construct the universal description of the process of SP combustion. Therefore, a more realistic way consists in the choosing the limiting or extreme cases and elaborating the models, which work in the limited range of the parameters variation. Note that the discussion deals first of all with analytical type models, where it is necessary to sufficiently strongly simplify the description of phenomenon in order to obtain approximate solution.

As natural limiting cases there emerge versions of the models with very fine and very coarse grains of filler (kinetic and diffusion combustion behavior according to terminology introduced

by N. N. Bakhman [1]). In the first case components manage to mix before entering the chemical reactions (quasi-homogeneous models); the second case corresponds to situation, when the size of grain exceeds the thickness of preheated layer. In the last case the correct account of diffusion and accurate determination of the components concentration on the burning surface are important. For the grains of intermediate size, compared with the thickness of the preheated layer, the models are developed using different methods for averaging the heterogeneity of the thermal and diffusion wave structure both on the surface of the condensed phase and in the flame. In these models the averaging is performed either over the geometric surface of the burning SP (spatial averaging) or over sufficiently prolonged time interval during the combustion front propagation into the bulk of propellant along the chosen normal direction (time averaging).

3.2. QUASI-HOMOGENEOUS SYSTEMS

We will call quasi-homogeneous such models, in which heterogeneity does not affect processes essential for combustion, so that the burning rate can be calculated using relationships for homogeneous models. Nevertheless the preceding stages may "feel" the mentioned heterogeneity. For example, typical SP based on AP at a sufficiently low pressure has the rate control stage in the gaseous flame (at low pressures AP, as it was noted in Chapter 2, can not independently burn). Gas flame at a low pressure is considerably distant from the surface, and reactions in it proceed in the kinetic regime (combustion of the premixed gas), hence, heterogeneity of SP here in no way is manifested. However, in this case the SP heterogeneity leads to non-uniform character of thermal and other physicochemical processes in a layer of the condensed phase with the thickness of the order of AP particle size.

3.2.1. Compositions with perfectly mixed components on the surface

It is known that many of utilized in SP components are present on the burning surface in the melted form. If both the oxidizer and binder are melted, then it is possible their interaction and mixing. Certainly, it is not completely obvious that such SP burns as homogeneous system: highly reactive oxidizer even before the complete mixing can react with the fuel in the liquid phase creating the non-uniformity of heat evolution. Furthermore, the not completely mixed components, vaporizing by separate streams, can cause non-uniformity in the gas phase. The experiments conducted with containing the nitramine filler SP [2,4] showed that in sufficiently large pressure domain and in a reasonably wide size range of filler particles the combustion of SP only slightly depends on the value of grain size. In Ref. [3], the photographs of SP surface are presented (formulations based on octogen or hexogen with the polyurethane binder) taken before and after the combustion at p=20 atm. On the extinguished surface the uniform fine-grained structure has been observed with grain size much less than in the fresh sample section. This indicates the quasi-homogeneity of composition upon the combustion of SP. It is natural to use in this case the models developed for homogeneous formulation with the rate control stage in the gas phase (as for nitramine, which composes here major part of mass of SP). In Ref. [4], the model developed earlier [5] for homogeneous EM of the type of nitroglycerin powder (see Chapter 2) is examined. The utilization of this model, which causes doubts namely in the case of nitroglycerin powders where the rate control stage can he in the condensed phase, is more substantiated for the SP based on nitramines.

In the model [4], the combustion regime with gas phase rate control stage has been taken for examination. The model was developed for SP containing nitramines and DB propellant as a binder-fuel.

$$u_1(T_s) = u_2(T_2) \tag{3.1}$$

$$u_1(T_s) = A_s \exp(-E_s / RT_s) \tag{3.2}$$

$$u_2(T_2) = p\sqrt{\frac{\lambda_2 Q_2 \varepsilon_2 z_2 \exp(-E/RT_2)}{\rho^2 c[c(T_s - T_0) - Q_1](RT_2)^2}} \tag{3.3}$$

$$c(T_2 - T_0) = Q_1 + Q_2, \quad Q_1 = \alpha Q_{sox} + (1-\alpha)Q_{sDB} \tag{3.4}$$

Here index 2 relates to the gas phase; α - mass fraction of filler (nitramine), $Q_{s,ox}$ and $Q_{s,DB}$ - heat release (cal/g) of nitramine and binder, respectively. For the octogen with the binder of DB propellant type the following values of constants have been used: c = 0.37 cal/(g K); $\lambda_2 = 10^{-4}$ cal/(cm s K); $\rho = 1.54$ g/cm^3; $E_s = 14$ kcal/mol; $z_s = 36000$cm/s; $\varepsilon^2 z_2 = 1.4\ 10^8$ cm^3/(g s); $Q_2 = 330$ cal/g; $Q_{s,DB} = 100$ cal/g; $Q_{s,ox} = 50$ cal/g; T_0=293 K. The value of $Q_{s,ox}$ is used as the matching coefficient because of the lack of reliable data (in more detail about the characteristics of octogen see Chapter 2). Let us note that in expression (3.1) the value u_2, although weakly, depends on T_s, so that (3.1)-(3.4) represent the system of transcendental equations. Dependence of T_2 on the formulation composition is considered only through Q_1, the effect of dilution on Q_2 is not taken into consideration. From (3.1)-(3.4) it is easy to obtain

$$\nu = \partial \ln u / \partial \ln p, \quad \beta = \partial \ln u / \partial T_0:$$

$$\nu = \left(1 + \frac{1}{2}\frac{T_s}{T_s - T_0 - Q_1/c}\frac{RT_s}{E}\right)^{-1}$$

$$\beta = \left(\frac{RT_s^2}{E} + 2(T_s - T_0 - Q_1/c)\right)^{-1}.$$

3.2.2. Formulations with fine size heterogeneous components.

If size of filler particles is sufficiently small, then even in the absence of melting the process of combustion of heterogeneous composition can be treated as quasi-homogeneous. The combustion model for such compositions was developed in Ref. [6] using following assumptions:

-- the rate control role in the process of combustion belongs to condensed phase reactions;

-- the burning rate is determined by the decomposition of oxidizer;

-- the combustion system is quasi-homogeneous and one-dimensional, i.e., the size of grain of oxidizer is much smaller than the thickness of preheated layer.

The problem formulation takes account of exothermic decomposition of oxidizer (for example, AP), the endothermal decomposition of fuel, the oxidation of fuel by the gaseous decomposition products of oxidizer, the endothermal processes an the surface (sublimation, vaporization, dispersion). Model is described by following equations in the condensed phase $0 \le x < \infty$

$$\lambda d^2T/dx^2 + mcdT/dx + Q_1\omega_1 - Q_2\omega_2 + Q_3\omega_3 = 0 \tag{3.5}$$

$$md\eta_i/dx + \omega_i = 0; \quad i = 1,2,3 \tag{3.6}$$

with the boundary conditions $x \to \infty, \ \eta_i \to 0, \ T \to T_0; \quad x = 0, \ \eta_i = \eta_{si}, \ T = T_s.$

Here η_1 – degree of the decomposition of oxidizer; η_2 – degree of the decomposition of fuel; η_3 – degree of the oxidation of fuel; Q_i, and ω_i - heat and the rate of the corresponding reactions:

$$\omega_1 = \rho k_1 \, exp(-E_1 / RT), \quad \omega_2 = \rho k_2 \, exp(-E_2 / RT) \tag{3.7}$$

$$\omega_3 = s\rho_g \left(\frac{1}{k_k} + \frac{1}{k_D} \right)^{-1}, \quad k_k = k_3 \exp(-E_3 / RT), \quad k_D \sim D \tag{3.8}$$

Here k_i, E_i - pre-exponent and the activation energy, respectively; ρ - density of condensed phase (constant); s - specific (per 1 cm^3 of propellant composition) surface of the oxidizer; ρ_g - gas density of oxidizer; D - diffusion coefficient. The structural state of the gas within the condensed phase (solution, small bubbles) is not defined concretely. The relationship is used, which couples the degree of the vaporization of oxidizer ($1-\eta_{s1}$) on the burning surface with the pressure of saturated vapor (B and L - its parameters) at the given external pressure p:

$$1 - \eta_{s1} = (B / p) exp\,(-L / RT_s) \tag{3.9}$$

The system (3.5)-(3.9) makes it possible to determine $m(p,T_0,s)$. It is obtained by approximate analytical method of Zeldovich [7]

$$m^2 \approx \frac{2\lambda RT_s^2}{E_1 c^2 (T_s - T_0)^2} \left(Q_1 \omega_1(T_s) - Q_2 \omega_2(T_s) + Q_3 \omega_3(T_s) \right) \tag{3.10}$$

From (3.5) and (3.6) it follows

$$\eta_{s1} = \int_0^{\eta_s} \omega_i / \omega_1 d\eta \approx \eta_s \omega_i(T_s) / \omega_1(T_s), \qquad i = 2,3. \tag{3.11}$$

For finding T_s the first integral of (3. 5) is used

$$c(T_s - T_0) = Q_1 \eta_{s1} - Q_2 \eta_{s2} + Q_3 \eta_{s3} \tag{3.12}$$

The system of transcendental equations (3.7)-(3.12) makes it possible to calculate parameters m, T_s, η_{s1}, η_{s2}, η_{s3} as function of p, T_0, s. The model under discussion, in contrast to the above model with melting and the rate control stage in the gas phase, gives essential dependence m(s). Depending on the values of the entering the model coefficients it is possible to obtain different forms of curves for $\nu(p)$, $\beta(p)$, $\nu(T_0)$, $\beta(T_0)$, and also numerical values for stability limits of combustion. This makes it possible to qualitatively explain experimental data for the wide set of solid propellants.

Let us present now the possible ways of generalizing the model by removing some of initial assumptions. To eliminate an assumption about the rate control role of the condensed phase is possible, if one introduces into the examination the intense reactions in the gas phase. It is convenient to use for this the model presented in Chapter 2 for the combustion of homogeneous propellant [8]. According to the model, the burning rate in the wide range of the parameters can be obtained by solving separately the given system of equations for two cases: a) without taking into account heat evolution in the condensed phase; b) without taking into account heat evolution in the gas phase. After that it suffices to compute the sum of the obtained linear burning rates. Solving this problem, one should keep in mind used in [8] assumption about the open porosity of the zone of reactions in the condensed phase.

The possibility to eliminate an assumption about the smallness of the size of the oxidizer grain as compare with the thickness of a preheated layer is examined in Ref [6]. It is noted that only with keeping of this assumption the temperatures of the surface of filler and binder (oxidizer and fuel)

can be considered identical, otherwise it is necessary to consider a difference in their values. The effect of the heterogeneity nature of system in this case is proposed to consider within the framework of quasi-homogeneous approach by the introduction of an effective coefficient of the heat exchange between components, proportional to the specific contact surface. The method of accounting the heterogeneity nature is demonstrated in Ref. [9] on the example of the combustion of homogeneous propellant with inserted disperse component, which can be fuel, catalyst or metal. If the particle size d of the mentioned component is of the order of the thickness of a preheated layer or exceeds it, it is possible to disregard the chemical interaction of this component with the remaining volume of the propellant (the specific surface area of reaction is too small). Then the disperse component plays the role of inert additive, which must be warmed up by heat transfer from the remaining components. In connection with this in the equation of thermal conductivity the function of the heat-sink appears

$$F = -SNq, \tag{3.13}$$

where S - area of the particle; N - number of particles in 1 cm^3; q - heat flux into the particle. It is assumed that $S \sim d^2$, $N \sim \alpha/d^3$, $q \sim \lambda(T-T_0)/d$, where α - mass fraction of the inserted component. Then (3.13) can be rewritten in the form

$$F \sim \lambda\alpha(T - T_0)/d^2 \tag{3.14}$$

Within zone $0 < x < \infty$, where it is possible to disregard the reactions of the decomposed components (preheat zone), the equation of thermal conductivity with included F is linear on T and can be easily solved:

$$T = T_0 + (T_s - T_0)\exp\left[-x\frac{mc}{2\lambda}\left(1+\sqrt{1+\alpha\left(\frac{2\lambda}{mcd}\right)^2}\right)\right] \tag{3.15}$$

Equation for T_s one may obtain from the condition
that on the boundary with the zone of reactions (x = 0) the heat flux into preheat zone $-\lambda dT/dx$, calculated according to (3.15), is equal to the heat flux from the zone of reactions:

$$\frac{mc}{2}(T_s - T_0)\left(1+\sqrt{1+\sqrt{1+\alpha\left(\frac{2\lambda}{mcd}\right)^2}}\right) = mQ\eta_{s1} \tag{3.16}$$

Here Q - thermal effect of decomposition of the propellant, whose formulation does not contain the component in question. The degree of decomposition η_{s1} is connected with p, T_s according to (3.9). It is also used the relationship obtained from the examination of the zone of reactions, where the influence of particles can be disregarded

$$m \sim \exp(-E/2RT_s) \tag{3.17}$$

The system (3.9), (3.16) and (3.17) makes it possible to find m, T and η_{s1}. It is easy to recognize that the approach presented gives for the coarse particles ($2\lambda/(mcd)<1$) the increasing dependence m(d): according to (3.15) and (3.16) the dependence T(x) and value of T_s with increase of d are approaching from below, respectively, to the form and values, which they have without the particles. Physically this corresponds to the decrease of relative heat losses, since with the given α increase of d leads to decrease of specific heat exchange surface between the components. With small d (more accurately, with $2\lambda/(mcd) >> 1$) the approach examined is not valid, in particular, due to the need for the account of heterogeneous reaction on the intercomponent surface. However, the condition $2\lambda/(mcd) >> 1$ makes it possible to neglect the temperature nonuniformity and intercomponent heat exchange. Reactions on the component interface can be taken into account,

for example, according to quasi-homogeneous model presented above [6], which gives decreasing dependence m(d). Thus, the function m(d), decreasing with increase of d in the domain of small d and increasing with the high values of d, has a minimum. Analogous considerations and calculations permit to predict maximum for dependence $\nu(d)$, where $\nu = \partial \ln m / \partial \ln p$. It is interesting to note that similar findings were made in the experiments [9] on the combustion of model SP, which contain 75% AP (<56 μm), 15% of hydrocarbon binder (not capable of the independent combustion) and 10% of carbon with different size d of the particles (fraction ≈1, <70, 100-200, 300-400 μm). Minimum m(d) and maximum $\nu(d)$ have been obtained; with increase of p a minimum of m(d) is shifted to the side of smaller d, which is naturally explained by the decrease of a preheated layer thickness.

3.2.3. Critical assessment of quasi-homogeneous combustion models

Let us discuss in more detail the concepts presented in section 3.2. In order to evaluate a possibility of one-dimensional description of the processes in the zone of condensed phase reaction of composition with components melted on the surface, it is necessary to investigate complex picture of penetration of the melts. Exception presents the case, when the rate control stage is located in the gas phase and the gas jets from separated on the surface components manage to mix prior to the beginning of noticeable reaction, i.e. $x_k > x_D$. Here x_k is the "kinetic length"; $x_k \sim m/p^{\delta}$, where m – mass flow rate and δ - order of reaction, p – pressure; x_D is the "diffusion length" $x_D \sim \rho_g D/m$, where ρ_g – gas density and D – diffusion coefficient. With $\rho_g D = \text{const}$ this regime can be obtained by decrease of p, if $\nu - \delta < -\nu$, $\nu < \delta/2$ (and vice versa – with increase of p, if $\nu > \delta/2$). This regime can also exist, in principle, for SP with infusible on the surface components (see the BDP type models, Sect. 3.3).

Model of Kubota [3,4] is suitable for SP with fixed mass content of melted component α, complete mixing of melt on the surface and rate control stage in the gas phase. However the model does not examine some phenomena, which can occur at a significant variation of the nitramine content in the SP formulation.

1. Model of Kubota does not consider a variation of parameters in the gas phase with mass content of nitramine. It is understandable that to take this into account is much more difficult than in the case of existence of the melt layer on the burning surface, where for calculation of Q_1 a hypothesis about the independent decomposition of the mixed components is actually used. In the examination of parallel gas-phase reactions in contrast to condensed phase the location of zone with the rate control stage and the degree of depletion for both gas components in this zone are not known in advance. With the change of α the entering in (3.3) heat Q_2 (which determines T_2) can depend on α nonlinearly. In addition the change of the rate control reaction (change E_2) can occur, see [10]. In connection with this the account of dependence of Q_1 on α is useless.

2. If in combustion of double-base propellant, used as a binder, the rate control stage is located not in the gas [11], but in the condensed phase, then with sufficiently low α the rate control stage of the SP combustion will also be in the condensed phase. In this case (with the strong change of α) it is profitable to use more flexible monopropellant model, for example, the model [39]. It is easy to show that this model, which represents a special case of BDP model, predicts the modes of stage detachment, gas phase control and even stage merging (true, but with the unlikely values of the parameters).

Come further to discussion of the combustion model for SP with fine size of oxidizer particles and rate control reactions in condensed phase. It should be underlined that in this case the oxidizer size must be less than a thickness of the reaction zone in condensed phase, not a thickness of preheated layer, as it was stated in Ref. [6]. By integration specifically in the zone of reactions the formulas (3.10) and (3.11) are obtained. Using in this case one-dimensional equations (3.5)-(3.6) within the zone of reactions, we implicitly assume that the size of the heterogeneity, not considered by these equations, is considerably smaller than the thickness of the zone of reactions. Note, that if the size of the oxidizer particles is lower than the thickness of a preheated layer, but exceeds the thickness of a zone of reactions, then the temperature distribution can be considered uniform across a preheated layer (one-dimensional), but only out of the zone of reactions, where the heat evolution creates in homogeneity on temperature profile. The correctness of the derivation of formulae (3.10), (3.11) in this case would be disturbed. The examples of the account of the heterogeneity of the heat evolution see below, in Section 3.3 (UTD-model).

In Ref. [7], evaluation of thickness of zone of reactions $\Delta x_{ch} = (RT_s^2/E)/(dT/dx)$ is given. Here dT/dx – characteristic value of the temperature gradient. In our case it is of the order $u(T_s-T_0)/\kappa$, κ - thermal diffusivity. Let us substitute the values typical for the double-base propellants: E ~ 20 kcal/mol, T ~ 650 K, R=1.96 cal/(mol K), T_0 ~ 300 K, u ~ 0.5 cm/s, x ~ 0.001 cm^2/s; then Δx_{ch} ~ 2 μm. Then the condition of quasi-homogeneity takes the form $D_{ox}<<2$ μm (D_{ox} - size of the oxidizer particles), i.e., model is applicable only to compositions with ultra-dispersed filler. In practice such compositions are used rarely, but the relevant quasi-homogeneous model can he used for describing the combustion of pseudo-propellant, corresponded to the finest fraction of the polydisperse oxidizer (see Chapter 4).

In connection with that stated above it is difficult to agree with the statement of authors [6] about possibility of spreading the model to the range of oxidizer particles sizes $D_o > \kappa/u$ within the framework of homogeneous approach [9]. However, the idea developed in Ref. [9] of the account of intercomponent heat exchange deserves special discussion. It is important to note that investigation [9] is carried out for the initially homogeneous composition with the inserted particles reacting at sufficiently high temperature only on their surface. For this very reason the particles of sufficiently large size d, whose total reacting surface per unit of the burning surface is low, become the heat sinks.

According to Ref. [9] a decreasing dependence m(d) takes place in the domain of small d, where quasi-homogeneous model is valid and with increase of d the specific surface area in the reaction zone decreases. The dependence m(d) becomes increasing with large d, when particles burn in the regime of heat-sink and the specific (per unit volume) power of the heat loss decreases with increase of d. Thus, it follows a basic result, agreeing with the experiment: the existence of minimum in the curve m(d) and its displacement with increase of p into the domain of small d.

Mathematically, the case $d >> \kappa/u$ is examined in [9], although regime of heat-sink begins already with $d > \Delta x_{ch}$. The range of variation of d, which is of great interest, is excluded by this from the examination. It is noteworthy that precisely in this region the averaging for the purpose of obtaining the one-dimensional equation of thermal conductivity is still justified (see Section 2.3).

Finally, assignment of heat flux into particle in the form $q \sim \lambda(T-T_0)/d$ introduces large error: with small d it overestimates heat losses (in particular, for $d \to 0$ they become according to this formula infinite, in this case $T_s \to T_0$) and for large d it underestimates them. According to the used dependence in this case $q \to 0$, but actually $q \sim mc(T_s-T_0)$, since in large particle a preheated layer is forming with the thickness of the same order of magnitude, as in the interlayer space with the equality of the thermal constants of the material of interlayer and particles.

3.3. HETEROGENEOUS SYSTEMS WITH UNIFORM TEMPERATURE DISTRIBUTION IN A PREHEAT ZONE (UTD – MODELS)

Let us assume that the size of the oxidizer particles is greater than the thickness of the reaction zone in the condensed phase, but it is considerably smaller than the thickness of preheated layer, i.e., $\Delta x_{ch} < D_o << \kappa/u$. In this case the preheated layer can be considered uniform in temperature, but in the reaction zone of the condensed phase one should take into consideration the non-uniformity of the heat evolution and caused by it temperature non-uniformity in the gas phase, as well as transient character of gas release from the burning surface with the time scale of order of burnout time for the oxidizer grain. In order to use upon the derivation of the heat balance an assumption on one-dimensionality of the temperature profile in a preheated layer, the heat flux into the condensed phase has to be averaged over the surface of SP. For UTD-models this averaging simulates the real physical process of the leveling of heat fluxes, which occur under the SP surface in the layer with a thickness of $\sim D_0$. It is possible to consider the averaging, which is characteristic for the UTD-models, of the mass burning rate m over the surface of SP as a natural addition to the averaging of heat evolution.

3.3.1. Reaction at the surface of binder around the oxidizer grains

C. E. Hermance [12] developed the model for the case, when particle size exceeds thickness of a reaction zone. It was later established that the field of the model application is very limited; however, it was used as a basis for developing many subsequent versions of the UTD-models. The problem is formulated for SP containing oxidizer with mass fraction α and particle size D_0. Actually a polydisperse SP is examined. The following processes of chemical nature are considered:

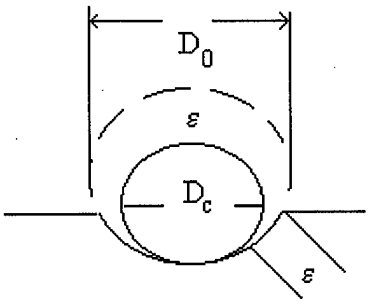

Fif. 3.1. Sketch of the burning surface element [12]

a) the endothermal decomposition of fuel-binder (with a mass flow rate m_f and thermal effect Q_f) on the flat part s_f of the cross-section surface s_0 of the sample;

b) the two-stage exothermic decomposition of oxidizer with summary heat release ($Q_{gp} - Q_L$);
c) the exothermic heterogeneous reaction (with a mass flow rate $m_{\varepsilon f}$) of the decomposition products of solid oxidizer on the curve surface $s_{\varepsilon f}$ of binder, contacted with the recess around the crystals (Fig. 3.1).

In the gas flame the reaction products of the stages a), b) and c) interact with thermal effect Q_F. It is assumed that these products have sufficient time for mixing, and gas flame can be considered one-dimensional. The temperature of the burning surface is assumed identical over entire section of SP sample. The one-dimensional equation of thermal conductivity in a preheated layer of the condensed phase is used. It is valid, as it was noted above, with satisfaction of condition $D_0<\kappa/u$. The decomposition (pyrolysis) of binder is described by equation

$$m_f \sim \exp\left(-E_f / RT_s\right) \tag{3.18}$$

Heterogeneous reaction is described by:

$$m_{\varepsilon f} \sim C\exp\left(-E_\varepsilon / RT_s\right) \tag{3.19}$$

Here C - concentration of oxidizer in the annular gap (recess with the depth ε around the crystal of oxidizer). It is assumed that this concentration corresponds to the equilibrium partial pressure above crystal of the oxidizer:

$$C \sim \exp\left(-E_{ox} / RT_s\right) \tag{3.20}$$

Such supposition is justified in the case of rather narrow gap around crystal and moderate rate heterogeneous reaction. As far as oxidizer is concerned, it is assumed that its combustion will "adjust" to the combustion behavior of binder in the gap and over the flat region. Thus, the total mass burning rate becomes proportional to the consumption rate of binder:

$$ms_0(1-\alpha) = s_f m_f + s_{\varepsilon f} m_{\varepsilon f} \tag{3.21}$$

It is also assumed that the combustion of binder in gaps makes a negligible effect on the flat surface s_f of binder as compared with its value for the fresh cut of the propellant sample. Therefore, it is taken $s_f = (1-\alpha)s_0$ and mass balance takes the form

$$m = m_f + (s_{\varepsilon f} / s_0)m_{\varepsilon f} /(1-\alpha) \tag{3.22}$$

In order to find $s_{\varepsilon f}$ it is necessary to examine surface of gap around single spherical crystal, which is equal approximately to $\pi D_c \varepsilon$ (see Fig. 3.1). Here D_c is the diameter of cross section of burning crystal by the binder plane. With chaotic distribution of oxidizer particles in the bulk of SP, the burning surface contains different value D_c and $\varepsilon(D_c)$ corresponding to different locations of particles:

$$s_{\varepsilon f} = \sum_{i=1}^{N} \pi D_{ci} \varepsilon\left(D_{ci}\right) = \pi N\left(D_c \varepsilon\right)_{av} \tag{3.23}$$

Here N - number of particles, whose sections are located on the cut plane of sample. In particular, if we assume $\varepsilon(D_c) \sim D_c$ then it is possible to use statement, known in stereometry, that in the multi-component mixture with disordered structure the components are represented on the sufficiently large plane cross section in the same ratio, as in the bulk of the mixture: $\sum \pi D_{ci}^2 / 4 = \zeta s_0$, where ζ - volume fraction of oxidizer.

On the other hand, on the cross section of sample we can fix only those particles, whose centers are misaligned not more than by $\pm D_0/2$ from this section and, consequently, they all are located

in the volume $v=s_0D_0$. Thus, for the N particles and for the mean cross-sectional area of particle we obtain the relationships:

$$N = \zeta v/\left(\pi D_0^3/6\right) = 6\zeta s_0/\pi D_0^3,$$
$$\sum \pi D_{ci}^2/4 = \zeta s_0 = N\pi\left(D_c^2\right)_{av}/4 = (3/2)\zeta s_0\left(D_c^2\right)_{av}/D_0^2 \quad ,$$
$$\left(D_c^2\right)_{av} = \frac{2}{3}D_0^2 \tag{3.24}$$

With $\varepsilon(D_c) \sim D_c$ the relationship (3.23) takes the form

$$s_{\varepsilon f}/s_0 = 4\zeta\varepsilon/D_c \tag{3.25}$$

Actually $\varepsilon/D_c \neq$ const, but in view of the complexity of computing the entering in (3.33) sums it is proposed in [12] to approximately calculate $s_{\varepsilon f}/s_0$ by (3. 25), computing there value $\varepsilon(D_c)/D_c$ when $D_c = D_0\sqrt{2/3}$.

It is assumed that the depth of gap ε is equal to the size of burned out part of initial sphere of AP from the top along the axis of symmetry:

$$\varepsilon = D_0 - D = u_{ox}\left(t_c - t_{ign}\right), \quad u_{ox} \sim p^{\delta}, \quad t_{ign} \sim D_0^{n+1}/p^k,$$
$$t_c \sim L/u, \quad L = D_o\left(1+1/\sqrt{3}\right)/2, \quad u_f = m_f/\rho_f \tag{3.26}$$

Here u_{ox} and u_f - linear burning rates of oxidizer and binder; t_{ign} - ignition time of oxidizer; t_c - time of reaching by the flat binder surface of the point, where the section of the virgin particle of oxidizer would have a diameter of $D_c = D_0\sqrt{2/3}$. Constants δ, k, n and proportionality factors in (3.26) are taken from the experimental investigations of other authors.

On the burning surface the balance of heat for 1g of SP is written:

$$c\left(T_s - T_0\right) = -\alpha Q_L + \left(\alpha - m_{\varepsilon f}s_{\varepsilon f}/ms_0\right)Q_{gp} +$$
$$Q_{\varepsilon f}m_{\varepsilon f}s_{\varepsilon f}/ms_0 - \left(m_f s_f/ms_0\right)Q_f + Q_F\exp\left(-\xi^*\right) \tag{3.27}$$

In this equation the first term in the right hand side determines heat expenditures for the first (endothermal) stage of the oxidizer decomposition. The second term indicates heat evolution in the second stage of decomposition reaction, which is realized in immediate proximity of the oxidizer surface. In this case it is considered that in the reactions of this stage the oxidizer, which has already reacted in the gap with the binder, does not participate. Remaining terms correspond to the heat evolution in the gap, heat expenditures for the pyrolysis of binder on the flat part of its surface and the heat feedback from the gas phase. The multiplier $\exp(-\xi^*)$ designates the reaching the burning surface fraction of the heat, which was released in the flame. For the second-order reaction the relationships are used

$$\xi^* = mcx^*/\lambda, \quad x^* = m\tau/\rho_F, \quad 1/\tau \approx \rho_g\, exp\left(-E/RT_F\right) \tag{3.28}$$

Thermal effect Q_F of the gas flame is assumed as not depending on p and T_0. The variability of the flame temperature, hence, automatically follows from the relationship

$$c\left(T_F - T_0\right) = Q_F + Q_s \tag{3.29}$$

For simplicity, the magnitudes of the heat capacity for the condensed phase and gas are taken identical, that does not introduce large error since they are actually close in value. The value Q_s in (3.29) marks total heat release on the surface, i.e., it is equal to the right side (3.27) without the

last term. It is evident that this expression, generally speaking, depends on pressure and initial temperature.

The above equations form a closed system and permit to calculate numerically $m(p, T_0, \alpha, D_0)$. It must be noted that the model was created specifically for SP with AP as an oxidizer. For the compositions, which contain AP and polysulfide binder, calculations were carried out, which showed a good accord with experiment on dependence m(p) in the wide interval of pressures (to 1000 atm) and considerably worse accord on the temperature sensitivity. In initial work [12] the weak places for model were noted, the main thing from which - the absence of the proofs of the existence of heterogeneous reactions on the binder and resulting finite value gaps around crystals of AP. Actually, subsequently it was revealed ([17, 18], see also Section 3.4), that during AP combustion in the SP formulation recesses around the crystals are not formed, and this questions the fitness of the model for describing the combustion of SP on AP.

Concepts, developed in [12], can nevertheless be useful, in particular, when studying combustion of SP based on oxidizer not capable of independent combustion, for example, $KC10_4$.

3.3.2. Competing flames (Beckstead-Derr-Price) model

Experimental observations [17], according to which during combustion of real SP the gaps around AP particles, as a rule, are not formed, were used as a basis for developing model of competing flames
[13], called as BDP model for surnames of authors: Beckstead, Derr, Price.

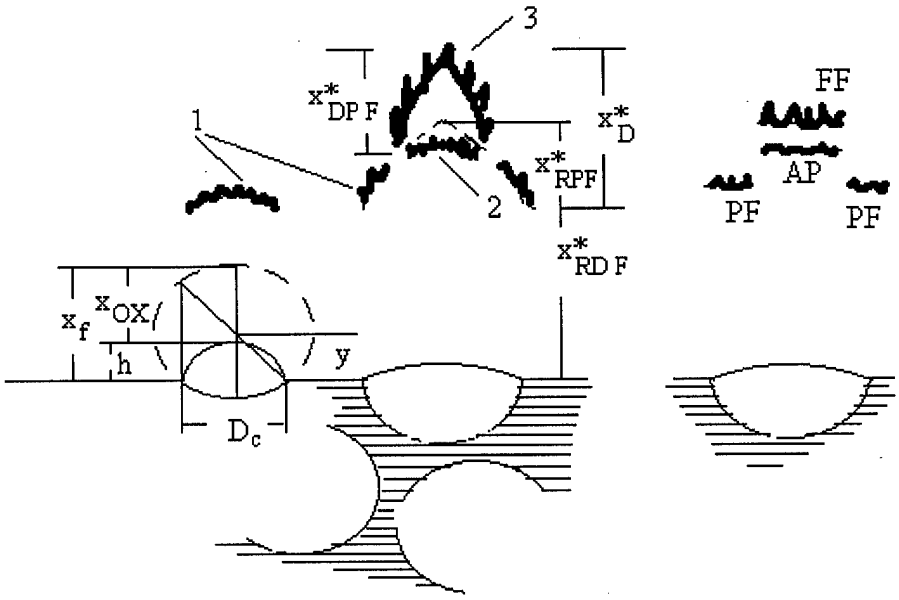

Fig. 3.2. Diagram of flames in BDP model.

In contrast to the Hermance model [12], in BDP model it is assumed that binder plays passive role, and rate of its burn out (pyrolysis) is adjusted to the rate of burn out of oxidizer. The new diagram of the flames is postulated (see Fig. 3.2): it is assumed that the reaction between the fuel and oxidizer occurs not on the surface of the ring recess around the AP particle, but in the diffusion flame. The two-stage decomposition reaction of AP is divided in space. The first stage is re-

alized in the zone of the reactions in condensed phase and, in the contrast to [12], it is considered exothermic, since besides the dissociative sublimation of some part of AP it includes solid-phase decomposition of approximately 70% AP to the end products. The second stage, where the oxidation of ammonia by perchloric acid is considered the main step, is realized in purely kinetic "natural flame" of AP. In the place of the contact of natural flame 2 (AP) with the diffusion one the latter is divided into two parts: primary flame 1 (PF) and final diffusion flame 3 (FF). In contrast to the model of Hermance, the temperature T_F of the final flame is calculated thermodynamically on the basis of SP formulation and therefore weakly depends on pressure

Thus, a non-uniformity of the heat evolution is taken into consideration on the surface of SP (heat liberation on AP and heat absorption on binder) and in the gas phase where for determining the form of flame it is necessary to solve two-dimensional problem of heat propagation and species diffusion. The versions of its solution are given in Section 3.4.2. Let us only note that in accordance with the version of solution of the Burke-Schumann problem, used in [13], the flame overhangs the oxidizer or fuel depending on what component in SP is in excess as compared with the stoichiometric ratio. As a rule, the fuel in excess and the flame is sloped to the side of AP, although in the combustion of polydisperse compositions for the largest in size fractions of AP the opposite situation is possible. It is considered that the primary flame begins at certain "kinetic" height x^*_{RPF} above the line of contact of AP with the fuel.

It is assumed that the surface of binder is plane and vaporization occurs with heat expenditure Q_f. The expressions for the pyrolysis law for the surface of oxidizer and the total balance of heat on the surface of SP are taken in the form:

$$m_{ox\equiv} = A_{ox}\ \exp(-E_{ox}/RT) \tag{3.30}$$

$$s_o m_T c(T_s - T_0) = -m_{ox} s_{ox} Q_L - m_f s_f Q_f + \beta_F Q_{PF} m_T s_0 \times \tag{2.31}$$

$$\times \exp(-x^*_{PF} c m_T/\lambda) + (1-\beta_F) m_{ox} s_{ox} [Q_{AP} \exp(-x^*_{AP} c m_{ox}/\lambda) + Q_{FF} \exp(-x^*_{FF} c m_{ox}/\lambda)]$$

It is necessary to find m_T and T_s as functions of p, T_0, D_0, α. Here m_{ox} and m_f - mass burning rates (g/cm^2s) of oxidizer and binder, respectively; T_s - surface temperature, which, as in [12], is assumed to be identical for the entire surface. Since the role of binder is considered secondary and it is not necessary to use for it the strongly depending on T_s expression of type (3.30), assumption about uniform distribution of T_s over the surface does not introduce significant error.

In expression (3.31) the value $s_o = s_{ox} + s_f$ corresponds to the burning surface of sample; s_{ox} and s_f – correspond to the surfaces of oxidizer and binder, respectively. Note, that the surface of oxidizer is bent (see Fig. 3.2) due to the fact that crystal of AP projects above binder (or is lowered) to the height h. In Ref. [13] the derivation is given of expressions for h/D_o and $s_{ox}/s_o = f(\zeta, h/D_o)$, where ζ - relative volume fraction of AP in the propellant; D_o - particle size. The AP crystal shape is considered in the form of a spherical segment. The values of $s_o m_T$, $s_{ox} m_{ox}$ and $s_f m_f$ are the total mass flow from the burning surface of SP and the mass flows of the products of gasification of AP and binder, respectively. The relationships are hold

$$m_{ox} s_{ox} = \alpha s_o m_T, \qquad m_f s_f = (1-\alpha) s_o m_T \tag{3.32}$$

where α - relative mass fraction of AP in the propellant. The relation between m_T and mean linear burning rate of SP is discussed at the end of this Section. Taking into account (3.32) relationship (3.31) takes the form

$$c(T_s - T_0) = -\alpha Q_L - (1-\alpha)Q_f + \beta_F Q_{PF} \exp(-x^*_{PF} cm_T / \lambda) +$$
$$+ \alpha(1-\beta_F)[Q_{AP} \exp(-x^*_{AP} cm_{ox} / \lambda) + Q_{FF} \exp(-x^*_{FF} cm_{ox} / \lambda)] \quad (3.33)$$

The left hand side of expression (3.33) stands for the heat required for heating the unit mass of the propellant from T_0 to T_s. In the right hand side of expression (3.33) the values - αQ_L and $(1-\alpha)Q_f$ stand for amounts of heat necessary for the conversion into the gaseous state of oxidizer and binder with their appropriate mass fractions α and $(1-\alpha)$. Remaining terms correspond to the heat feedback to the burning surface from different flames (see Fig. 3.2). Here Q_{PF}, Q_{AP}, Q_{FF} - thermal effects of flames 1, 2 and 3. Value of Q_{PF} is calculated per 1g of reaction products in flame 1, Q_{AP} and Q_{FF} – per 1g of AP consumed in these flames. Therefore the terms in (3.33), which correspond to the flames 2 and 3, are multiplied by α. Value β_F is the portion of AP, which burns out in flame 1; $(1-\beta_F)$ is the portion of AP, which reacts in the flame 2 and then is finally in flame 3. The heat capacities of solid and gaseous oxidizer and fuel are considered identical. Exponential multipliers in (3.33) show what portion of the heat, which is liberated in the appropriate flame at a distance of x* from the burning surface, reaches this surface. Relationship of type (1.13), valid for the delta-like distribution of the heat sources, actually is used. For x_{AP}* expression (3.34) is used, which corresponds to the model of the flat gas flame with the order δ of the reaction in the rate control stage

$$x^*_{AP} = m_{ox} / \left(k_{AP} \cdot p^{\delta}\right); \quad \delta = 1.8; \quad k_{AP} = 1.12 \left(cm^3 \cdot s \cdot atm^{\delta}\right)^{-1} \quad (3.34)$$

Values of k_{AP} and δ are found experimentally. Flames 1, 3 are close in the shape to parabolic ones. Referring to the results of own calculations, the authors of the BDP model reported that in terms of the total heat flux into the condensed phase the parabolic flame with a height of x_D* is equivalent to the flat flame with the same summary heat evolution, which has the same projected area on the surface of SP and height $\bar{x}^*_D$ (distance from the base of parabolic flame):

$$\bar{x}^*_D = A_{sh} x^*_D, \quad A_{sh} \approx 0.3 \quad (3.35)$$

As far as entering in (3.35) height $\bar{x}^*_D$ of parabolic flame is concerned, from the analysis of the solution of Burke-Schumann (see Section 3.4.2) the conclusion is made that the height of parabolic is close to the diameter of its base, i.e., to the diameter D_c of section of the AP particle with the plane of the binder (see Fig. 3.2). The parabolic flames on the right side of the diagram, depicted in Fig. 3.2, are substituted by the "effective" flat flames. Their height is calculated from the formulas

$$x^*_{FF} = x^*_{AP} + 0.3 x^*_{DFF}, \quad x^*_{PF} = x^*_{RPF} + A_{sh} x^*_{DPF} \quad (3.36)$$

Here x^*_{RPF} - kinetic" height of primary flame. For x^*_{RPF} the formula of type (3.34) is used:

$$x^*_{RPF} = m_T / \left(k_{PF} \cdot p^{\delta_{PF}}\right) \quad (3.37)$$

As reported in Ref. 19, in the subsequent versions of the BDP model the dependencies were taken into account of multipliers k_{AP}, k_{PF} in (3.34, 3.37) on the temperature of the corresponding flames:

$$k \sim \exp\left(-E / RT\right) \quad (3.38)$$

Values of the temperature of primary and final diffusion flames are calculated thermodynamically on the basis of the propellant formulation and, consequently, they depend on the fuel/oxidizer (f/ox) ratio in the propellant, i.e. $k_{PF} = k_{PF}$(f/ox). Taking into account (3.38), the value k_{AP} depends on (f/ox) and on the particle size, since T_{AP} is somewhat increased due to the heating from the final flame. Thus, when presenting in Ref.19 the modified BDP model, the expression for T_{AP} is given in the form

$$T_{AP} = T_F - \frac{Q_{FF}}{c}\left(1 - e^{(x^*_{FF} - x^*_{AP})cm_{ox}/\lambda}\right) \tag{3.39}$$

Entering in (3.36) the diffusion lengths x^*_{DFF}, x^*_{DPF} (height of "paraboloids", see Fig. 3.2) can be determined with the help of the solution of Burke-Schumann (detail see in Section 3.4.2). Let us note here that according to this solution the height of the "parabolic" diffusion flame depends mainly on the diameter of its base and (in less extent) on the f/ox ratio for the gaseous mixture and other parameters. In particular, in Fig. 3.2 broken line on the top of diagram shows the part of diffusion flame, which would be realized in the absence of inherent flame of AP. In the real case, passing through the flame front of AP, gaseous mixture changes its f/ox ratio, becoming more fuel rich, that also leads to the elongation of the final diffusion flame.

In the BDP model, it is proposed to use the fact that for sufficiently low values of the product mD_0 (with $mD_0<10^{-3}$ g/(cm s), see derivation in Section 3.4.2) the height of "parabolic" flame according to the solution of Burke-Schumann can he taken equal to the diameter of its base. In this case, assuming the form of the diffusion flames parabolic, it is easy to find the unknown heights by geometric method. Value of A_{sh} in the second formula (3.36) is not specified in Ref. [13], but from the "geometric" evaluations it is clear that it is changed from 0.3 when x^*_{AP}-$x^*_{RPF} \geq x^*_{DPF}$ (value, obtained in [13] for the first formula (3 36)) to 0.5 ($x^*_{RPF} + x^*_{AP}/x^*_{DPF}$ when x^*_{AP} - $x^*_{RPF} << x^*_{DPF}$.

Fraction β_F of oxidizer, reacting in the primary flame, is determined as the ratio of area of the ring projection of primary flame on the base of parabolic to the total base area:

$$\beta_F = \left(x^*_{AP} - x^*_{RPF}\right)/x^*_{DPF} \tag{3.40}$$

From Fig. 3.2 it is evident that even for particles of AP of the same size there is a wide range of values of areas of the burning surfaces at each moment of time. Since (3.33) is obtained by averaging over the entire surface of sample, the last terms, in which p_F, x^*_{PF}, x_{FF} depend on diameter of the base of parabolic, are written for certain effective diameter D_c of particle. It is clear that it would be more accurate to use summation of individual particle sections over surface. However, this is rather complicated, and as D_c the BPD model uses introduced earlier by Hermance [12] value $D_c = D_0\sqrt{2/3}$.

Below the derivation of several relationships of BPD model is given.

1. Thermal effects in the flames are determined in (3.33) by

$$Q_{AP} = c\left(T_{AP} - T_0\right) + Q_L \tag{3.41}$$

$$Q_{PF} = c\left(T_F - T_0\right) + \alpha Q_L + \left(1-\alpha\right)Q_f \tag{3.42}$$

$$Q_{PF}/\alpha = Q_{AP} + Q_{FF} \tag{3.43}$$

Heat capacity of gas and solid propellant is assumed to be identical –c ~ 0.3 cal/(g C). Relationship (3.41) indicates that the heat release of AP combustion is expended on its heating from T_o = 300 K to T_{AP} ~ 1400^{0}C and on dissociative sublimation with the heat 480 cal/g. Thus, total heat release is equal to 0.3 (1400-300)+480 = 810 cal/g. However, part of this heat is liberated within and on the surface of AP. Authors [13] considered that this part composes 75% and it does not depend on pressure and initial temperature (in [20] it was assumed 70%), then Q_{AP} = 210 cal/g, Q_L = 480-0.75 810 = -120 cal/g.

Relationship (3.42) means that the heat liberation in a primary flame is spent for heating of reagents from T_o to T_F. T_F is considered as temperature of the final products of the propellant combustion) and for spending on the effects, connected with transformations of reagents on the burning surface. In this case it is considered that reagents enter into flame 1 in the same (in the general case - nonstoichiometric) ratio $(1-\alpha)/\alpha$, in which they are contained in the propellant. Namely for this ratio the calculation of $T_F(\alpha)$ is conducted.

Relationship (3.43) means that with combustion of 1g of AP in the flame (left side of (3.43)) or in the flames 2+3 (right side of (3.43)) the identical amount of heat is liberated.

One should keep in mind that in many instances the role of flame 3 is small. In Ref. [21] Beckstead does not consider its contribution into the balance of heat on the burning surface, but considers the effect on x^*_{AP} through T^*_{AP} according to (3.34, 3.39).

2. Expression (3.31) contains parameter m_T, which can be replaced using (3.32) by $m_T = m_{ox}$-$s_{ox}/\alpha s_0$. Let us examine the derivation of expression for s_{ox}/s_0. Convex or concave area of the AP particle is considered either spherical, see Fig. 3.2. Diameters of section of all AP particles with plane surface of binder are considered identical:

$$D_c = D_0\sqrt{2/3} \tag{3.44}$$

In this case the area $s_{p\,ox}$ of such identical plane sections coincides with real area of summary surface, formed by different sections by binder plane of arbitrarily distributed in propellant AP particles. Start first with calculation of relation $s_f/ s_{p\,ox}$ taking into account that $(s_f + s_{p\,ox})$ is the area of the plane section of sample. Therefore sections of AP and binder are presented there in the same proportion as in the bulk of propellant sample, i.e $s_{p\,ox}/(s_{p\,ox}+ s_f) = \zeta$, where ζ - relative volume fraction of AP. Then

$$s_f/ s_{p\,ox}=(1/\zeta)-1 \tag{3.45}$$

Further, it is known from geometry that for the spherical segment the ratio of the lateral areas and base is equal to

$$s_{ox}/s_{p\,ox}=1+(2h/D_c)^2 \tag{3.46}$$

Combing (3.44), (3.45) and (3.46), we finally obtain

$$s_{ox}/s_0=\zeta[1+6(h/D_0)^2]/[1+6\zeta(h/D_0)^2]. \tag{3.47}$$

Note, that in the survey [19] the value of in (3.47) was calculated by formula $h^2 = 0.5\,(h_+^2 + h_-^2)$. The meanings of h_+ and h_- are explained below (see formula 3.51).

3. For derivation of h/D_0 let us apply theorem about equality of products of the segments of intersecting chords (see Fig. 3.2):

$$(D_c/2)^2 = x_f(D_0 - x_f), \tag{3.48}$$

$$D_c^2 = (2/3)D2_0, \qquad x_f/D_0 = 0{,}5(1 \pm \sqrt{1/3}) \tag{3.49}$$

$$h = x_f - x_{ox};\ x_f = u_f t, x_{ox} = u_{ox}(t - t_{ign});\quad h = x_f(1 - u_{ox}/u_f) + u_{ox}t_{ign} \tag{3.50}$$

Here it is assumed that when the AP particle "appears" at the burning surface, the binder burns with a constant linear velocity u_f in the period t, and AP burns with a constant linear velocity $u_{ox} \neq u_f$ in the period $t - t_{ign}$ (t_{ign} - time of AP ignition). At the moment in question the diameter of the "plane" AP section $D_c = D_o\sqrt{2/3}$. From (3.47) and (3.4) it follows

$$h_{\pm} / D_0 = 0.5(1 \pm 1\sqrt{3})(1 - u_{ox} / u_f) + u_{ox} t_{ign} / D_o \qquad (3.51)$$

Ambiguity of the h-values reflects the fact that one and the same magnitude of diameter D_c can be obtained by two different sections of particle.

Difference in rates u_{ox} and u_f is used in the model only when finding h. For u_f it is used the expression of type (3.30)

$$u_f \rho_f = A_f \exp(-E_f / RT_s), \qquad (3.52)$$

Note that $u_f \rho_f$ in (3.52) does not coincide with m_f (3.32) because m_f is averaged in time value of $u_f \rho_f$ but (3.51) and (3.52) uses instantaneous value of u_f at the moment, when the diameter of the AP particle section with the binder plane (see Fig. 3.2) reaches the value $D_c = D_o\sqrt{2/3}$.

Variation of u_f in time is not considered in the model. As justification serves noted by the BDP model authors weak dependence of calculated values of m_T and T_s on h/D_o and, consequently, on m_{ox}/m_f and t_{ign}. Apparently, without large error it might be possible to assume h=0, $s_{ox}/s_o = \xi$. Specifically, it was made later by Beckstead in relay race model [21] (see Section 3.5.2).

4. Let us examine connection of m_T with the linear burning rate u. In Ref. [13] it was erroneously accepted $m_T = u_p\rho_p$ where ρ_p is the density of propellant (in the subsequent versions of the model the error was corrected). Mass flow rate from the total (not plane) burning surface of sample is designated in [13] as $s_o m_T$. On the other hand, this quantity can be presented with the utilization of plane section ($s_{pox}+s_f$) of the sample:

$$s_o m_T = (s_{pox} + s_f)\, \rho_p u_p, \quad u_p = (m_T/\rho_p) s_o/(s_{pox}+x_f)$$

By combining (3.44), (3.45), (3.46), the relationship between u_p and m_T can be expressed as

$$u_p = (m_T/\rho_p)[1+3\xi(h/D_o)^2] \qquad (3.53)$$

After substitution in (3.33) of relationships (3.32), (3.34-3.37) and (3.40) the system of equations (3.30), (3.33) becomes closed and can be solved by the method of iterations. It was accepted E_{ox} = 22 kcal/mol in (3.30), with A_{ox} being selected in such a way that calculation would coincide with experimental data [22] on $T_s(p)$.However, to get agreement between calculated and experimental data on the dependence $T_s(p)$ became possible only for small sizes of the AP particles. For D_o = 200 μm the calculations gave underestimated values of T_s and m. As a whole, the model gives a good qualitative agreement with the experimental data on the dependencies of m on p, T_0, D_o, α.

In particular the characteristic (with bend) dependence m(p) is obtained, which can he explained as follows. At the low pressures, when $x^*_{PF} < x^*_{AP}$ (see Fig. 3.2), there is only "natural" kinetic flame ($x^*_{RPF} >> A_{sh}x^*_{DPF}$). With an increase in pressure the combustion changes into diffusion control regime ($A_{sh}x^*_{DPF} > x^*_{RPF}$). If in this case $x^*_{PF} < x^*_{AP}$, at the curve m(p) gently sloping section or even plateau appears. Finally, with further pressure increase the inequalities $x^*_{PF} > x^*_{AP}$, $\beta_F < 1$ will be hold and at high pressures the kinetic flame 2 above AP will become the main supplier of heat from the gas phase, and dependence m(p) again becomes steeper. It is easy to see that for this model the gently sloping section in the curve m(p) for the coarser particles is reached at lower pressure than for the fine ones. The same reason causes the characteristic for the models of the BDP type dependence of value $\beta = \partial \ln m/\partial T_o$ on size D_o of AP particles. With small D_o in the diffusion regime $\beta(D_o)$ = const; with increase of D_o the combustion behavior

changes, and $\beta(D_o)$ sharply increases in connection with strengthening of the role of flames 2 of pure AP [44]. All these conclusions qualitatively agree with the experiment.

3.3.3. Effect of the local non-uniformity of the fuel/oxidizer ratio

M. King [15] developed a combustion model on the basis of the BDP model, by preserving idea of competing flames and modifying almost all the remaining elements. Considering that the averaging "according to Hermance" of the parameters over the burning surface introduces the not allowing to simple evaluation error, he took into account temporal changes in the rates of the burn out of oxidizer u_{ox} and adjacent to it binder u_f.

In order to be bounded to the examination of a single particle, it is necessary to make an assumption about the ordered structure of the propellant. The burn out is analyzed of the cell limited by the planes of symmetry in the form of parallelepiped with dimensions of $D_1 \times 0.866D_1 \times 0.82D_1$. To the center of cell a spherical AP particle is placed with diameter D_o (naturally, $D_o < 0.82D_1$). Remaining space is filled with binder. As in the BDP model, temperature T_s of the surface of binder and AP is considered identical, the surface of the binder is plane, and surface of AP is spherical (see Fig. 3.2). The mass burning rates of AP (at the top of particle) and binder are taken in the form

$$m_{ox} = A_{ox}\, exp\left(-E_{ox} / RT_s\right) \tag{3.54}$$

$$m_f = A_f\, exp\left(-E_f / RT_s\right) \tag{3.55}$$

As in the BDP model, for AP and binder the total balance of heat is written in the form (for simplification we assume $c_f = c_{ox} = c$):

$$m^* c\left(s_f + s_{pox}\right)\left(T_s - T_0\right) = -m_{ox} s_{ox} Q'_{ox} - m_f s_f Q'_f + q^* \tag{3.56}$$

$$m^*\left(s_f + s_{pox}\right) = m_f s_f + m_{ox} s_{ox} \tag{3.57}$$

Here m* - total mass flow rate from the burning surface of cell; q* - total heat flux to this surface from the gas phase; Q_{ox} and Q_f - effective values of heat of phase transitions with heat evolution due to reactions in the condensed phase included. From equations (3.54), (3.55) and (3.56) unknown values T_s, m_{ox}, m_f are determined. In the contrast to the BDP model for the total mass flow rate from the surface of cell instantaneous (time dependent) value is used according to (3.54), (3.55) and (3.57).

Let us examine geometry of the SP surface. Area s_f of surface of fuel and area s_{pox} of section of AP by surface (plane) of fuel represent summary cross-sectional area of cell:

$$s_f + s_{pox} = 0.866 D_1^2 = const \tag{3.58}$$

Values D_1 and D_0 are connected through the AP volume fraction:

$$\zeta = \left(\pi D_0^3 / 6\right) / \left(0.866 \cdot 0.82 D_1^3\right) \tag{3.59}$$

As in the BDP model, the following relationships are used (see Fig. 3.2)

$$s_{ox} / s_{pox} = 1 + 4\left(h / D_c\right)^2 \tag{3.60}$$

$$s_{pox} / \pi = D_c^2 / 4 = x_f\left(D_o - x_f\right) \tag{3.61}$$

$$h = x_f - x_{ox} \tag{3.62}$$

whence follows

$$s_{ox}/\pi = D_0 x_f - 2x_f x_{ox} + x_{ox}^2$$
$$s_f = 0.866 D_1^2 - \pi x_f (D_0 - x_f) \tag{3.63}$$

In these relationships (in contrast to the BDP model) it is taken

$$D_c = D_c(t) \neq D_0\sqrt{2/3}$$
$$dx_f dt = u_f\ ,\quad dx_{ox}/dt = u_{ox} \tag{3.64}$$

The delay time of the particle ignition is not considered. At the moment of arrival of the particle apex to the burning surface it is assumed t=0 and $x_f = x_{ox} = 0$. In (3.64) the values $u_f = m_f/p_f$, $u_{ox} = m_{ox}/p_{ox}$ should be taken according to (3.54) and (3.55). As the argument for the numerical calculation it is convenient to take x_f. At each step Δx_1 the system of transcendental equations is solved and all parameters of the problem are determined.

With experiment one should compare the time averaged value of m*. Since the model does not contain the mechanism of the burn out of the binder, in the cases when $x_f < 0$ and $x_f > D_o$, for obtaining the total time of the cell burn out artificial procedures are used. For example, the average rate of the burn out of cell can be taken as equal to the rate of the burn out of AP grain.

The expressions for Q_f' Q_{ox}', in (3.56) are given as follows

$$Q_f' = G_f Q_f \tag{3.65}$$

$$Q_{ox}' = G_{ox} Q_L - (1 - G_{ox}) Q_{EXO} \tag{3.66}$$

Here Q_f - heat of vaporization of binder; Q_L - heat of dissociative sublimation of AP; Q_{EXO} - thermal effect of reactions in the condensed phase, calculated per 1g of AP; G_f and G_{ox} – fractions of binder and oxidizer, which are converted directly into gas phase, (1- G_{ox}) - fraction of AP, which reacts in the condensed phase and on the burning surface.

Instead of used in the BDP model condition G_{ox} = const the following is used

$$1 - G_{ox} = \int_{x=0}^{x'} R_\alpha (dx/u_{ox}) \tag{3.67}$$

where R_α is the fraction of oxidizer, which reacts in the unit of time in the condensed phase; coordinate x = 0 is selected on the burning surface, x = x′ corresponds to the beginning of the region, where the chemical reaction can be neglected. According to [24],

$$R_\alpha = B_{sub}\, exp(-E_{sub}/RT) \tag{3.68}$$

Integral in (3.67) is calculated by iterations, for the first approximation the Michelson temperature profile is used. Products of the AP sublimation, which are generated with the rate of R_α, interact with fuel in the stoichiometric ratio, so that for G_f one has

$$(m_f/m_{ox})(s_f/s_{ox})(1 - G_f)/(1 - G_{ox}) = (f/ox)_{stoich} = const \tag{3.69}$$

Let us examine now derivation of expression for q* in (3.56). The "kinetic" length x^*_{RPF} of primary flame stands for the distance between the burning surface and the beginning of this flame (see Fig. 3.2). To facilitate calculating the total heat flux q* the real two-dimensional picture (see Fig.3.2) is substituted by the idealized one-dimensional one (Fig.3.3).

Assume that the heat evolution of parabolic diffusion flame is "smeared" evenly on the layer with thickness of s^*_D located above the sample of SP. Heat evolution from AP is considered located

within an infinitely thin layer at a height x^*_{AP} above the burning surface which is spread above entire grain of AP. According to the original diagram of flame the inherent AP flame (see Fig. 3.2) becomes narrow in the vicinity of the top of parabolic diffusion flame. Therefore the overall heat evolution in this region is reduced. In the BDP model this phenomenon is considered by multiplier β_F. In King's model (see Fig. 3.3) the area of AP flame does not vary, but the decrease of heat evolution is taken into account by the linear dependence of the intensity of heat evolution on the unit area of the AP flame on the height above the surface (heat evolution becomes zero when $x^*_{AP} = x^*_{RPF} + x^*_D$).

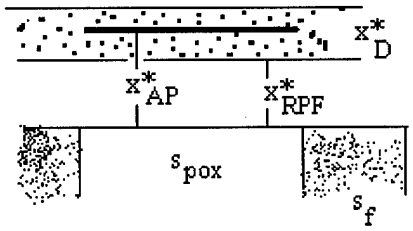

Fig. 3.3. Idealized diagram of flames in King's model.

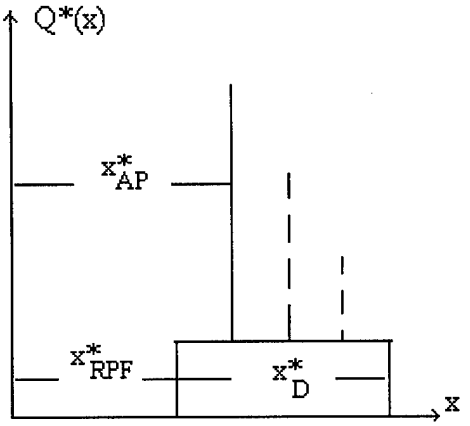

Fig. 3.4. Distributed heat evolution in flame.

It is assumed that the thermal diagram in Fig. 3.3 is approximately described by one-dimensional equation of thermal conductivity

$$\frac{d}{dt}\left(\lambda\frac{dT}{dx} - m^*cT\right) = -Q(x)$$
$$T(0) = T_s, \quad T\Big|_{x=x^*_{RPF}+x^*_D} = T_f \tag{3.70}$$

In line with the assumptions made the graph Q(x) takes the form, depicted in Fig. 3.4. By broken lines the heat evolution of the AP flame for other two values x^*_{AP} is marked.

Solving (3.70), where one should take Q(x) in accordance to Fig. 3.4, it is possible to obtain

$$\frac{\lambda(dT/dx)_{x=0}}{m^*c(T_f - T_s)} = \frac{1 - e^{-z_2}\Delta\Theta'\left[z_2 e^{z_3 - z_2} - \left(1 - e^{-z_2}\right)\right]}{z_2 e^{(z_1 - z_2)} - \left(1 - e^{-z_2}\right)} \tag{3.71}$$

$$z_1 = \frac{m^*c}{\lambda}\left(x^*_{RPF} + x^*_D\right), \quad z_2 = \frac{m^*c}{\lambda}x^*_D, \quad z_3 = z_1 - \frac{m^*c}{\lambda}x^*_{AP},$$
$$\Delta\Theta' = (z_3/z_2)Q_{AP}G_{ox}/\left[c(T_f - T_0)\right].$$

Here $\Delta\Theta'$ is the relative heat evolution in the AP flame; multiplier z_3/z_2 considers the dependence mentioned above on the position of AP flame; Q_{AP} is the heat evolution in the flame of AP as monofuel; $G_{ox}<1$ since part of AP is consumed during decomposition in the solid phase. Using (3.71) it is possible to calculate heat flux q_f to the binder, and when assuming in (3.71) $\Delta\Theta'=0$, to calculate heat flux q_{ox} coming to AP. Finally, one obtains

$$q^* = s_{pox}q_{ox} + s_f q_f \tag{3.72}$$

For "kinetic" length (standoff) distances x^*_{APF} and x^*_{AP} actually the same expressions are used, as in the BDP model. Upon the calculation of the height x^*_D of diffusion flame, by x^*_D is intended the distance, at which the reaction proceeds up to 90%. With such determination the value x^*_D can be computed even with the stoichiometric ratio of the components in SP, when the height of determined by the traditional method (see Section 3.4.2) diffusion flame becomes infinite. Height x^*_D can be found numerically from formula (3.97), which contains also parameter $\nu = \Phi c^2/(1-c^2)$, where $\alpha_T = 1/\Phi$ is the mass ratio (ox/f) in gasification products, divided by the appropriate stoichiometric ratio. As a rule, in typical SP $\alpha_T < 1$ although, for example, at the moment of the passage of maximum $m_{ox}s_{ox}/m_fs_f$ during the burn out of cell, in the model in question it is possible to get $\alpha_T>1$.

Upon calculating α_T it is taking into account in [15] (by multipliers G_f and G_{ox}) the depletion of reagents in the reaction between oxidizer and fuel under the burning surface. The expression for α_T is as follows

$$\alpha_T = 1/\Phi = (f/ox)_{stoich}(su\rho G)_{ox}/(su\rho G)_f \tag{3.73}$$

During the time of the burn out of cell, the value of α_T substantially varies.

In the model, it is proposed to consider decomposed as oxidizer and fuel not entire content of AP and binder, but to consider part of the products of their decomposition inert. In particular, the AP particles were treated as consisted of oxidizer by 96%, and binder as consisted of the fuel by 28%. It was reported in [15] that after appropriate selection of the coefficients the model agrees well with experiment on combustion of SP based on AP (size of particles 5, 20, 200 μm) and hydroxyl terminated polybutadiene binder (HTPB).

3.3.4. "Petite ensemble" model

To take into account a local transience of heterogeneous system combustion is possible not only by examining variation in time of the process in the vicinity of a single chosen particle of oxidizer (as this is done in King's model), but also examining instantaneous picture of combustion of entire sample, i.e. spatial distribution of the parameters at a fixed moment of time. If King's approach is compared with the survey of the motion-picture film about the fate of single particle of oxidizer, then it is appropriate to compare alternative approach with investigation of an instantaneous photograph of the surface of the burning sample. The idea about the processes on the surface can be obtained from the examination of a group of particles, if corresponding to these particles frames form the mentioned film. This group can prove to be relatively small.

Attempt to realize described approach was made in the "Petite ensemble" model [14]. Let us list coincidences and differences in the elements of this model and BDP model. As in the BDP model, the surface temperature T_s is considered as identical in every point of the surface, the surface of binder – plane, the surface of oxidizer, contacting with gas – spherical. Upon calculation of the shape of this surface the burning rates of oxidizer and binder u_{ox} and u_f are considered constant, the dependence of the ignition time t_{ign} on the diameter of the oxidizer particle is neglected. The height of the flame above the surface is determined on the basis of solution of Burke-Schumann. The basic relationships of the BDP model, written in the form (3.30) –(3.32), are used.

However, calculation of the burning rate using these relationships is made with specifically determined values of s_{pox}, s_{ox}, s_o, x^*_{AP} and x^*_{PF}. According to Ref. 14 the averaging of the cross-sectional areas of the AP particles is conducted among the particles, which have been already ignited. The AP burning surface is calculated by separate averaging. If particle burns out relatively fast, before its "cold" (bottom) end is reached by the combustion front of binder, it is assumed for maintaining the quasi-planarity of the propellant burning surface that the generating recess is instantly filled with the melt of binder. And vice versa, if particle did not burn out completely up to this moment, then it flies away. In this case the change of the f/ox ratio in the gases, leaving the burning surface, is considered as well as corresponding change in the temperature of flame. Upon calculation of the height of the diffusion flame several terms of series in the solution of Burke - Schumann are considered.

Let as give example of derivation of expression for s_{ox} and s_{pox}. For calculation s_{ox} let us find initially the burning surface of one particle. If after the arrival of AP particle to the propellant surface the binder around particle is burned-out on x_f, with particle burning out itself to x_{ox}, then

$$s_{ox}(x_f) = \pi(D_0 x_f - 2x_f x_{ox} + x_{ox}^2) \tag{3.74}$$

(just the same as above in King's model equation 3.63). Assuming at the moment of arrival of particle to the propellant surface t=0 and x_f=0, we have

$x_f = u_f t$, $x_{ox} = u_{ox}(t - t_{ign}) = (x_f - x_{ign})u_{ox}/u_f$, $x_{ign} = u_f t_{ign}$.

Here t_{ign} is the time of the particle ignition. Then (3.74) takes the form

$$\begin{aligned} &s_{ox}(x_f)/\pi = x_f^2\omega(\omega-2) + x_f[D_0 + 2\omega(1-\omega)x_{ign}] + (\omega x_{ign})^2, \\ &\omega = u_{ox}/u_f \end{aligned} \tag{3.75}$$

On the burning surface with random particle distribution there are located AP particles with different x_f. In this case for burning particles x_f varies from x_{ign} to $x_{max} = \min(D_0, x_{cr})$, $x_{cr}=x_{ign}+D_0/\omega$. If $x_{cr} > D_0$, the particle on the surface is not able to burn out and flies away, when $x_f = x_{max} = D_0$. If $x_{cr} < D_0$ the particle burns, completely on the surface, leaving after burning a pit (King examines only this case).

Therefore the total area of the burning AP particles is

$$s_{ox} = \int_{x_{ign}}^{x_{max}} s_{ox}(x_f)\,dN \tag{3.76}$$

Here dN - number of AP particles on the surface with the centers of these particles being located from the surface at a distance ($0.5D_0$- x_f) in the zone with a thickness of dx_f. With area of the cross section of the sample s_p the volume of that zone equals $s_p dx_f$ and since in the propellant with the volume fraction of AP equals ζ, the concentration of the centers of particles is $\zeta/(\pi D_0^3/6)$ and the number of particles in this layer is

$$dN = s_p dx_f \zeta/(\pi D_0^3/6) \tag{3.77}$$

From (3.75)-(3.77) it follows

$$\begin{aligned} &(s_{ox}/s_p)/\zeta = \omega(\omega-2)(\chi_m^3 - \chi_i^3) + 3[2\omega(1+\omega)\chi_i + 1]\times \\ &\times(\chi_m^2 - \chi_i^2) + 6(\omega\chi_i)^2(\chi_m - \chi_i), \\ &\chi_m = x_{max}/D_0, \quad \chi_i = x_{ign}/D_0 \end{aligned} \tag{3.78}$$

Let us analogously find entering in (3.47) total cross-sectional area of ignited particles, which are cut with plane of fuel

$$s_{pox} = \int_{x_{ign}}^{x_{max}} s_{pox}(x_f)dN \tag{3.79}$$

Here $s_{pox}(x_f) = \pi x_f(D_0 - x_f)$ (see presented above models of BDP and King), dN should be taken according to (3.77). Then we find

$$(s_{pox}/s_p)/\zeta = 3(\chi_m^2 - \chi_i^2) - 2(\chi_m^3 - \chi_i^3) \tag{3.80}$$

In the particular case $x_{ign} = 0$, $x_{max} = D_0$, when the surface of binder remains plane, from (3.80) it follows common relationship $s_{pox} = \zeta s_p$.

As in the BDP model, the terms corresponding to heat evolution in flame are calculated in balance of heat for certain average size of AP particle section, namely, for arithmetic mean value of cross-sectional areas of ignited particles. Obviously, for its finding it is necessary the value s_{pox} from (3.80) to divide by the total number of the ignited particles N_{ign}:

$$N_{ign} = \int_{x_{ign}}^{x_{max}} dN = 6s_p(\zeta/\pi D_o^2)(\chi_m - \chi_{ign}) \tag{3.81}$$

Further, for the mean cross-sectional area of particle we obtain

$$(\pi/4)\overline{D}_{ign}^2 = s_{pox}/N_{ign} = (\pi D_0^2/6)[3(\chi_m^2 - \chi_i^2) - 2(\chi_m^3 - \chi_i^3)]/(\chi_m - \chi_i) \tag{3.82}$$

In the particular case, when $x_{ign} = 0$, $x_{max} = D_0$, this gives, $\overline{D}^2 = (2/3)D_0^2$.

For calculating parameters of the diffusion flame it is necessary to know effective external radius b of the fuel stream, which surrounds stream of oxidizer. Authors of Ref. [14] assume that the fuel on the propellant surface is divided into equal parts between all being present on it particles of AP, including those not ignited. One may obtain total number of particles on the flat surface, assuming in (3.81) $x_{ign} = 0$ and $x_{max} = D_0$

$$N = 6\zeta s_p/(\pi D_0^2) \tag{3.83}$$

Total surface of fuel $s_f = s_p(1-\zeta)$, and surface per one particle is

$$\Delta s_f = s_f/N = (1-\zeta)(\pi D_0^2/6\zeta) \tag{3.84}$$

For the stream with an effective radius b we have

$$\pi b^2 = \Delta s_f + (\pi/4)\overline{D}_{ign}^2 \tag{3.85}$$

In the case when $x_{max} = D_0$ i.e. when incompletely burned particles fly away from the surface, in relationships (3.84) and (3.85) instead of ζ the value ζ' is used, which considers a change in the components ratio due to the carry-off of the solid oxidizer.

The balance of heat and calculation of the flame temperature are considered with account of the effect of carry-off of oxidizer. Size of remaining AP grains is $h = x_f - x_{ox} = x_f(1-\omega) + x_{ign}\omega$ at $x_f = D_0$ (if in this case h>0). Then mass α' and volume ζ' fractions of the consumed in the condensed phase oxidizer are as follows

$$\alpha'/\alpha = \zeta'/\zeta = 1 - (h(D_0)/D_0)^3 \tag{3.86}$$

In this case for the oxidizer remaining on the surface one has

$$\alpha' m_T s_p = m_{ox} s_{ox},$$

where s_{ox} - surface of burning AP according to (3.78).

Calculations, carried out on the "petite ensemble" model in a wide range of variation of different parameters, gave results sufficiently close to the results of calculations according to the BDP model. Greatest deviation of the results of calculations from that by the BDP model gave an application of formula (3.82) for effective size of the AP particle section. We give according to Ref. [19] relative change in the calculated burning rate (in comparison with the BDP model) caused by the differences in the procedure of averaging. Calculation was carried out with the values of the parameters α, D_0 typical for the SP combustion.

P,atm	3.6	6.4	11	20	36	65	115
$U_{(pet.ens)}/u_{(BDP)}$	0.981	0.976	0.943	0.896	0.852	0.796	0.728

3.3.5. Account of difference in the temperature of oxidizer and fuel at the burning surface

In UTD-models presented above an assumption about equality of the temperatures T_s and T_{sf} of oxidizer and fuel on the burning surface was essentially used. At the same time there are experimental data, according to which T_s and T_{sf} can noticeably be distinguished ([23], see also Section 3.5). Another weak point in the models with the uniform temperature distribution, based on the concepts of BDP, is the complete absence of the heat supply into the binder from the gas phase in the case when diffusion flame hangs above the binder. An attempt to eliminate these two deficiencies in the models of the BDP type has been undertaken in Ref. [16], after developing the approach, which was conditionally named "improved model".

For describing combustion of oxidizer AP a simplified version of the BDP model was used. The corresponding equations take the form:

$$\begin{aligned} m_{ox} &= A_{ox}\, exp\left(-E_{ox}/RT_s\right) \\ c_s(T_s - T_o) + \Delta H_s + Q_L &= \\ = \beta_{ox}[(\beta_F/\alpha)Q_{PF}\exp(-\zeta_{PF}) + (1-\beta_F)Q_{ox}\exp(-\xi_{ox})], & \\ Q_{ox} = \beta_p\left[c_g(T_{ox}-298) - c_s(T_0-298) + \Delta H_{ev}\right], & \\ Q_L = Q_{ox} - Q_F, \quad Q_F = c_g(T_{ox}-298) - c_s(T_0-298) + \Delta H_g, & \\ m_{ox}(1-\beta_p) = A_s\exp(-E_s/RT_s) & \end{aligned} \tag{3.87}$$

Here β_p=1-β_s is the AP fraction which is decomposed in the gas phase. Multiplier $\beta_{ox} < 1$ considers that the part of the heat is transferred into the fuel, even if the flame is located only above the oxidizer.

As in the BDP model, value β_F indicates the fraction of AP located under the primary flame; α - mass fraction of AP in the propellant.

The process of the fuel pyrolysis is described by equations

$$\begin{aligned} m_f &= A_f\, exp(-E_f/RT_{sf}), \\ c_f(T_{sf}-T_0) + Q_f &= (1-\beta_{ox})\frac{Q_{PF}}{1-\alpha}exp(-\xi_{PFf}) \end{aligned} \tag{3.88}$$

Experimental values of A_f and E_f for different binders are taken from [23] (see Section 3.5.1). The dimensionless height ξ_{PFf} of flame above the binder does not coincide with the height ξ_{PF} of the flame above AP:

$$\xi_{PF} = \frac{c_g m}{\lambda_g}\left(A_{fh}x_D + \frac{m}{k_{PF}\cdot p^{\delta_{PF}}}\right),$$
$$\xi_{PFf} = \frac{c_g m}{\lambda_g}\left(B_{fh}x_D + \frac{m}{k_{PF}\cdot p^{\delta_{PF}}}\right) \qquad (3.89)$$

Here the first terms in the parentheses represent the "diffusion height" and the second terms – the "kinetic height" of the flame (compare with 3.36 and 3.37). The value of the coefficient B_{fh} in (3.89) is accepted as $B_{fh} \approx A_{sh}/8$. Because of the multiplier 1/8 in the second equality (3.89) the first term in the parenthesis has smaller weight than in the first equality. The examination of the calculated form of flame, obtained from the solution of Burke-Schumman [27] (Fig. 3.5a), has given a basis for the introduction of multiplier 1/8. This multiplier taken into account the low height of "hanging" above the fuel part of the flame near its base. In the original BDP model -with the excess of fuel, typical for SP, it was accepted that the heat flux from the gas enters only into the oxidizer, but according to the equation of the total balance of heat (2.31) the part of the heat feedback is expended on heating and vaporizing the fuel (heat exchange occurs through the condensed phase).

Mass flows of oxidizer and fuel are connected with relationship

$$m_{ox}s_{ox} / m_f s_f = \alpha(1-\alpha) \qquad (3.90)$$

This relationship makes it possible to determine during the solution of entire system of equations the value of the coefficient β_{ox} describing distribution of heat feedback from the gas between the fuel and oxidizer. Areas s_{ox}, s_f and entire geometry of the burning surface are taken according to the BDP model.

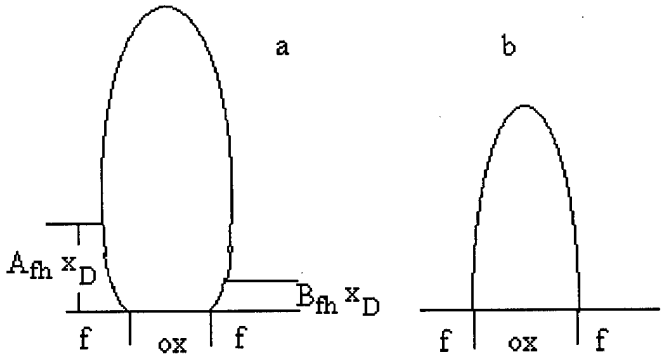

Fig. 3.5. Typical form of the burner flame according to Burke-Schumann. a) flat flame; b) axisymmetric flame.

The model was checked by calculations for conditions of experiment, described in Ref. [15] (propellant AP + polybutadiene binder, α = 0.73 and 0.77; D_o = 5, 20, 200 μm; p = 7...120 atm), and showed fair agreement with experiment in the whole range of pressures and AP grain sizes.

3.3.6. Critical discussion of the UTD-models

1. When using UTD-models, a typical shortcoming consists in their incorrect application with oxidizer particle size $D_o > \kappa/u$. Let us show this mistake on the example of the BPD model. We will examine the balance of heat (3.31) for the real nonhomogeneous surface of SP. Thus far the thickness of the preheated layer in the condensed phase is more than the size of heterogeneity ($\kappa/u > D_o$), such form of equation is justified, since the redistribution occurs in the bulk of a preheated layer of nonuniform heat flux entering from the surface. But with an increase in the size of AP particles (with p = const) the picture of heat exchange changes and global averaging becomes meaningless, since its physical basis is absent, namely, redistribution of heat flux from the surface. Oxidizer and binder start to burn "individually", this leads to the bending of surface. With a very large difference in the rates of the oxidizer and binder burn out (SP with nitramines or with AP at elevated pressures, see also the "sequential" model of Beckstead, Section 3.5.2) the form of dependence m(p) can be determined by the slowly burning component (binder). Consequently, the used in the BDP model assumption that the burning rate of SP is determined by the burning rate of combustion of AP, with $D_o > \kappa/u$ can lead to the erroneous conclusions.

In Ref. [19], the attention was focused on sharply underestimated in comparison with experiment, values of the rate of combustion, which give calculations the BDP model for propellant with coarse AP particles (for example, 200 μm). This fact was also noted by the authors of the BDP model. Modification of BDP model proposed in Ref. [19] for the propellant with the polybutadiene binder exhibited a good agreement with experiment in the case of AP particles size 5 and 20 μm but computed more than twice lowered in comparison with experiment burning rate in the case of the particles with size of 200 μm. The same has been demonstrated for this propellant by "unsteady" model of King [15], also based on the BDP model. King correlated better theory with experiment by using selected values of the coefficients, with which the heat liberation in the solid phase depended on pressure. As it was stated in Ref. 19, this way can be considered as correct. Assuming that for coarse AP particles the inherent flame of AP becomes the main supplier of heat from the gas phase (since there is reduced portion β_F of AP, which burns in the primary flame), it is proposed [19] to improve the model of AP combustion by considering completely probable the dependence of heat evolution, mentioned above, on the pressure. At the same time, according to experimental data [20], in the pressure range of 20-100 atm) this dependence is absent (see also Section 1.4.2).

However, noted above disagreement between theory and experiment can be explained in another way. Let us discuss theoretical and experimental data presented in Table 3.1.

Table 3.1. Comparison of calculated and experimental burning rates (cm/s) at pressure 20 atm

Propellant	$U_{exp.}$	$U_{calc.}$	Refer.
AP	0.3	-	[20]
70% AP(200μm)+PS	0.5	0.3	[13]
73%AP(200μm) +HTPB	0.3	0.15	[19]

Binders: PS - polysulfide, HTPB – hydroxyl terminated polybutadiene.

It is known that polysulfide propellant "is hot", the temperature of flame $T_f = 2545K$ [13, 23]. The heat feedback from the gas goes to the coarse ($D_o = 200$ μm) AP crystals mainly from the inherent flame, and they have to burn with actual rate of ~0.3 cm/s. Hot primary flame heats up only part of binder and the thin zone of AP adjacent to the binder layer. With $\kappa/u < D_0$, it is possible to disregard heat exchange between this region and the bulk of the crystal of AP.

In this case one may expect the higher rate of AP burn out, which is confirmed by visual observations [17] of extinguished surface of the polysulfide formulation: at p = 20 atm the majority of AP crystals protrudes above SP surface. Apparently, obtained in the experiment the burning rate of polysulfide propellant, equal to 0.5 cm/s, is close to the average burning rate of the sections, situated under the primary flame.

At the same time the calculations [13] that considered, as in the BDP model, the rate control role of AP gave 0.3 cm/s. Why this result was obtained, it is easy to comprehend by examining the balance of heat (3.31). For coarse AP crystals $\beta_F << 1$, and in the total balance heat feedback from the primary flame can be neglected. The portion of the heat, which enters from the diffusion flame, due to the high value of the stand off distance flame $x^*_{FF} \sim D_o$ is also low. Thus, binder is presented in (3.31) only by the term $(msQ)_f$. In calculation in question authors of [13] used for Q_f a value of 50 cal/g, which is 10 times less than the value, found experimentally in the later work [12]. Therefore term $(msQ)_f$ proved to be low, and the heat balance (3.31) actually coincided with the balance for pure AP. Naturally, the calculation gave $u \cong u_{ox} \cong 0.3$ cm/s.

Let we discuss another example. Polybutadiene propellant is "cold": according to Ref. [23], with $\alpha = 0.7$ the value $T_f \cong 1450K$. In the more accurate examination it is necessary to take into account that $T_f \sim 1450K$ is the mean temperature of products, and the primary flame is hotter. However, with such high values of the f/ox ratio (~1.4) it is shifted from the interface to the side of oxidizer, and binder obtains little heat (see comments on the solution of Burke - Schumann in Section 3.4.2). Apparently, in this case the rate of the burn out of binder is somewhat less than the burning rate of AP, or it is close to it. The latter determines overall rate of SP combustion r~0.3 cm/s observed in the experiment.

In calculation performed in accordance with the BDP model in the balance of heat (3.31) it is possible, as before, to neglect by heat feedback from the primary and diffusion flames, but it is necessary to consider heat expenditure for vaporization of binder $(msQ)_f$, where $Q_f = 433$ cal/g [23]. Part of these heat losses, according to the model, falls on AP, lowering thus the temperature of its surface and rate of combustion, and consequently, overall burning rate. It is no surprising therefore that calculation gave value of u = 0.15 cm/s, i.e.- much less than it was obtained in the experiment.

Thus, in two cases examined above the disagreement between calculation and experiment for formulations with coarse AP particles can be explained not by variation of fraction G of oxidizer, which is decomposed in the condensed phase, as it was proposed in Ref. 19, but by the fact that for coarse AP particles assumptions placed into model about redistribution of heat within a preheated layer and about rate control role of AP decomposition are not met.

2. Ignoring or insufficient account of local non-uniform and transient combustion behavior, caused by heterogeneity of heat release, is an overall deficiency in known today UTD-models and as a whole all models of combustion of heterogeneous SP.

Thus, in Hermance's model the gas flame above surface of SP is considered plane, i.e. non-uniform character of heat release is excluded completely. In the BDP model and in all based on it models the heterogeneity in the gas phase is considered by the bending of flame according to the solution of Burke-Schumann. However, boundary conditions, for which solution [27] and its modification [19] were obtained, do not completely correspond to the SP combustion, that in many instances can substantially influence the results (about this in detail see in Section 3.4.2). Furthermore, the form of flame obtained by the solution of Burke- Schumann is usually oversimplified: the bent flame is substituted by the equivalent (equal to the total heat flux in SP) flat flame. In this case a possibility is lost to calculate heat flux from the gas to the hinder for the case, when flame is located strictly above the crystal of oxidizer.

In connection with above mentioned the attempts to make more precise version of the Burke-Schumann solution with retention of mentioned crude assumptions are useless. Nevertheless such attempts are undertaken in a series of works. Thus, in the petite ensemble model [14] the increased number of terms of series is taken in the solution of Burke-Schumann. In King's model [15] localized above oxidizer infinitely thin curved flame is substituted without reasonable basis by the flat flame of finite thickness above the selected cell of propellant (oxidizer + binder).

Finally, in improved combustion model [16] the author's combine a detailed description of the form of flame according to Burke-Schumann with the rough simplification of this form: in order to calculate the heat flux into the binder for the case, when diffusion flame is closed above the oxidizer, they consider the partial overhang of this flame above the binder according to Fig. 3.5a.

In the BDP model such specific details were not considered, binder in this situation obtained the heat necessary for the gasification directly from the oxidizer by thermal conductivity through the condensed phase. In model [16] there is no such way, since for the oxidizer and the binder the separate balances of heat are written, without interaction within condensed phase. Therefore an attempt was made to take into account some heat feedback from the gas phase, with reference to the form of the flame. This reference, however, was incorrect: according to Ref. [27], Fig. 3.5a relates to the flat flame burner, and for the cylindrical burner simulating combustion of SP Fig. 3.5b is given in [27] without the overhang of the flame base above the peripheral part.

In models examined gas-dynamic non-uniform behavior, caused by curvature of burning surface is not considered, the need for this account was discussed by the Soviet authors even in the 60's, when the terms "frozen turbulence" and "permanent transience" [25, 43] were introduced.

The account of peripheral component of velocity of gas near the surface of SP might give possibility, for example, to calculate convection heat transfer to the binder for the case, when flame is closed above the crystal of oxidizer.

3. Account of transience is closely related to the correctness of averaging upon calculation of mass burning rate m. If we come back to analogy with movie film about the life of single particle (see the beginning of Section 3.3.4), then one may state that in all UTD-models, except King's model, one frozen frame of mentioned film is examined only, and information, which is contained in remaining frames, in no way is used. In this particular case the burning rate is calculated of the sample, on the surface of which all particles with different residence time are substituted to the identical, that correspond to the selected frame, i.e., to the specific residence time on the surface.

In models of Hermance, BDP and "improved model" as such chosen particle the one is used with diameter of section $D_c = D_0 2/3$. In this case as a result of the averaging the summary area of the plane sections of particles on the surface of sample is retained. There is no, however, evidence for considering that simultaneously the summary heat flux into the sample is retained, provided that the flux from each particle is not proportional to the area of its section, i.e., $\sim D_c^2$.

Neither in the model of Hermance nor in the BDP model there is no such proportionality. It should be noted a certain inconsistency, which was shown upon the development of the model of Hermance. Introduced in it the averaging of heat flux into the sample in accordance with the particle sizes for the polydisperse composition (see Chapter 4) can be naturally spread, for any composition (including monodisperse one) if one average the heat fluxes, according to sizes of the particle sections with the plane of binder. However, Hermance's model in the case of unimodal composition averages section of the particles but not heat fluxes from them into the sample.

Authors of the BDP model noncritically adopted this methodology, although in their model it can lead to more serious errors in view of strong (exponential) dependence of heat flux from gas phase on D_c. As far as the "improved model" [16] is concerned, upon the calculation of heat flux into the sample, besides the noted deficiency in all models of the BDP type, it involves new one: there is no serious background for using separate heat balances for the oxidizer and binder, while it is not considered the heat exchange between them by thermal conductivity through condensed phase. As it was already noted above, to use "one-dimensional" balance of heat in the condensed phase is possible only for UTD-models under condition $D_0 < \kappa/u$. It is clear that the inter-component heat exchange in this case is unavoidable.

Let us describe an approach for more correct averaging the heat flux over the surface to derive balance of heat (3.31). Let we designate through f(D) the heat flux, obtained from the gas phase by particle (with diameter of section D by the plane surface of the binder) and "attached" to it binder. The total flux to the surface of sample is equal to $\int f(D)dN$. Let us introduce now the shift y of the center of particle relative to the surface of SP. On the surface, the particles are located, for which $|y| < D_0/2$. Their total number according to (3.83) equal

$N_0=\zeta D_0 s_p/(\pi D_0^3/6)$ and the number of particles with the centers in the layer by comprises $dN = N_0 dy/D_0$. From Fig. 2.2 it follows $(2y)^2+D^2=L_0^2$ then

$$dy = \frac{\pm DdD}{2\sqrt{D_0^2 - D^2}}, \quad \int_0^{N_0} f(D)dN = 2\frac{N_0}{D_0}\int_0^{D_0/2} f(D)\frac{DdD}{2\sqrt{D_0^2 - D^2}} \tag{3.91}$$

In the petite ensemble model instead of $D_c = D_0\sqrt{2/3}$ as the effective the diameter is taken such one, which upon the replacement of all particles on the sample surface by the "effective" particle with given diameter ensures the retention of summary cross-sectional area of the ignited particles. In a certain sense this selection of the effective diameter of the section of particle takes into account the unsteady effects (ignition) on the surface. However, only the total cross-sectional area of the burning particles is determined accurately in this case, but not the connected with them mean heat flux. These calculations can be made more precise. Note, that according to the model, it should be considered the presence on the surface of the non-ignited particles and empty places (pits) after the burn out of ignited particles. In other words, in the petite ensemble model the connected to the given particle heat flux depends on the section of particle D, an it is more correct to take it in the form $f(D(y))= f_1(y)$, so that instead of (3.91) one obtains

$$\int_0^{N_0} f_1(y)dN = \int_{-D_0/2}^{+D_0/2} f_1(y)\frac{N_0 dy}{D_0} = \frac{s_p\zeta}{\pi D_0^3/6}\int_{-D_0/2}^{+D_0/2} f_1(y)dy \tag{3.92}$$

If one calculates only heat flux from the gas and does not consider it in the cases of non-ignited and already burned out (with the pits) sections of the SP surface, then

$$\int_0^{N_0} f_1(y)dN = \frac{s_p\zeta}{\pi D_0^3/6}\int_{-(D_0/2)+y_{ign}}^{y_{max}} f(D(y))dy, \tag{3.93}$$

$$D(y) = \sqrt{D_0^2 - 4y^2}.$$

Here y_{ign} is the height of the apex of the particle above the surface of binder at the moment of ignition, and y_{max} can be less than $D_0/2$, if particle sufficiently rapidly burns out and leaves a pit.

Let us note additional difficulty connected with averaging of the heat flux from the gas phase. When trying to use the relationships (3.91) and (3.93) we face with the need for assigning the distribution of the binder area between the oxidizer particles on the SP surface. In the petite ensemble model upon the calculation of the heat flux from the "effective" burning particle it is accepted that the binder is divided into equal parts between all (including not yet burning) particles at the surface.

Here the authors manifest inconsistency: when formulating the polydisperse version of the model (see Chapter 4) they proposed the nonuniform distribution of the binder between the original particles of different sizes. It would be natural to disseminate this non-uniformity, to

the distribution of the binder between the burning particles, which have different sections by the plane of binder even with the same initial size of D_0.

The discussed deficiencies in theory, connected with averaging and transience, do not relate to King's model, where one particle is examined only, but averaging is conducted according to time. It is the only model, where an attempt is done of the "direct" account of transience. Unfortunately, in this model the interaction of particle with its neighbors over the burning surface of SP is not taken into consideration. Without such interaction it is impossible in any able way to describe the burn out of binder before and after the burning of the oxidizer particle. Interaction "disappeared" (adiabatic planes of symmetry were introduced to bound the cell with the particle) resulting from the assumption about the ordered arrangement of the particles in the SP. Loss of the randomness in the model became the cost for mathematical simplicity, essential for physics of process (see about the role of randomness [43]). Specifically, the randomness ensures at any moment at time the presence on the SP surface of the set of the hot spots, heat from which is propagated (for example, by thermal conductivity through the condensed phase) both to the binder and to the yet not ignited particles of the oxidizer. The specimen of SP with the regular arrangement of the oxidizer particles has anisotropic properties and in some directions can not burn at all. Namely this case is modeled in Ref. [15]: particles of AP form the cubic lattice in the SP, the specimen is ignited on the plane parallel to one of the symmetry planes. After the burn out of the first layer of particles it remains no ore focus of heat evolution on the surface, and burning must be interrupted. Thus, the attempt within the framework of UTD-models to forego natural for these models averaging over the burning surface led to the failure.

Critical discussion of the surface geometry description let us conduct only for the petite ensemble model, for which geometry considerations are developed in the greatest detail. First of all, the correctness of the account of the departing AP particles causes doubt. Actually, calculation of carry-off of AP in the model with clearly assigned by geometry surface is formally feasible.

It is known, however, that the assumption about the "quasi-planar" surface of fuel is introduced only for simplicity. In fact, the surface of binder has deviations from the mean level of the order of D_o. The binder in the zone of contact with AP obtains an entirely different quantity of heat than on the middle of the interlayer between two grains. This unavoidably causes the bending of the surface of fuel.

Further, under the assumption about "quasi-planarity" an account of carry-off of particles is made with errors. When $x_{max} = D_o$, it is incorrect to use in (3.84) the value ζ', which considers the carry-off of AP particles, instead of ζ. In this case, with the carry-off of AP particles the surface of binder in the model remains plane without additional assumptions about the behavior of melt. In this case the expressions are valid for N and Δs_f written in the form (3.83), (3.84). To illustrate let us imagine that the surface of fuel moves with a speed of u_f, and the AP does not burn. Therefore entire oxidizer flies away from the burning surface. This does not prevent us from deriving formula (3.84) for the area of fuel, belonging to one AP particle (line of reasoning it remains previous). It is a different fact that in this case the heat balance is changed, since the temperature of the adjacent flame is lowered.

And on the other hand, in the case $x_{cr} < D_o$, when pits appear on the surface, relation (3.84) becomes invalid, which, apparently, remained unnoticed. When on the surface instead of some particles depressions appear, it is impossible after that to use expression $s_f/s_p = 1 - \zeta$. This relation is correct only for the section of initial specimen by plane. The filling of pit with the melt of the binder nothing varies: in this case there is lack of AP, but not the binder. One may assume that the pit is not filled with melt and does not burn. In this case it will vanish completely after a certain time, and surface will become a plane, see Fig. 3.6. Then on the surface it is fulfilled $s_p/s_f = 1 - \zeta$, where s_f stands for the surface of the gasified binder. But for calculating the total number N of AP particles on the surface an expression (3.81) should be used with $x_{ign} = 0$, $x_{max} < D_o$. So that expression Δs_f in (3.84) acquires multiplier D_o / x_{max}.

Let us note that in Ref. 21 (see also Section 3.5.2) the "spherical" geometry of the AP particles on the burning surface has been rejected, referring to the results of experimental observations of the burning surface.

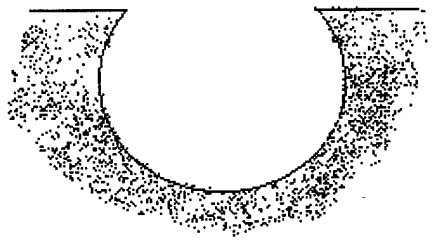

Fig. 3.6. Possible version of account of pits on the burning surface.

Let us consider used in the UTD-models the concepts about burning behavior of AP in combustion of SP. Below, in Section 3.4.2, it will be shown that with some (completely real) parameters of combustion the arrangement of the flames, assumed as the basis of the BDP model, can substantially be changed because of the ballasting effect of the binder in the gas phase. This effect is not considered by the BDP model.

The concept about the burning behavior of AP developed in King's in model causes criticism. Examining the original text and considering the value $Q_{AP} = 810$ take into account cal/g presented in the table of constants, one may come to the conclusion that Ref. [15] does not take into account the heat release in the condensed phase of AP as monofuel. Entire heat release under the burning surface of composite propellant is considered occurring due to the reactions of AP with binder, according to [24]. It follows from calculations that the portion of the propellant, which is decomposed under the surface, depends on the burning rate and comprises from 25 to 50% (according to the BDP model it is decomposed under the surface 75% of AP). Sufficiently convincing arguments in favor of expression $1 - Q_{ox} \approx \text{const} = 0.7$, given in [20] for pure AP, cannot be disproved by reference only to the fact that for the composite propellants the BDP model poorly corresponds to some experiments. As for the relationship (2.68) for the sub-surface reactions, considered in King's model between the AP and binder, it does not include a dependence on the AP grain size, which is completely unrealistic.

Thus, time t_{ign} from the arrival of particle to the surface to its ignition is taken as equal to zero [15], or depending on pressure [13,14], or from pressure and size of particle of AP [12]. Actually, the ignition time must depend on all these parameters, as well as on the nature of binder and its thermal characteristics.

3.4. COARSE OXIDIZER CONDENSED SYSTEMS

3.4.1. Effect of capability of oxidizer for self-sustaining burning.

Let we consider as coarse the oxidizer grains with dimension of D_{ox} significantly greater of thickness κ/u of the preheated layer. For the case of the combustion of fine oxidizer grains there are sufficiently in detail developed models (see Sections 3.2 and 3.3). As far as the SP with coarse oxidizer grains is concerned, the situation is much more complex. Beginning from the 60's theoretically and experimentally it was developed idea about the determining rate control role of "tips" - foremost sectors of the combustion front, which are propagated along the contact surface of fuel and oxidizer [25, 1]. It was subsequently explained [26] that most widely used solid oxidizer (AP) does not form "tips" in the conditions, when it is capable of the independent burning. It was reported [26] that the "tips" were discovered in the case, when the catalyst was put onto the contact surface of AP with the fuel.

Experiments, carried out by Price with coworkers [18], are most informative. The laminated specimens were used, which consist each of two plates of pressed AP with wedge-shaped gap filled with fuel-binder. As the binder there were used: polybutadiene with the terminal groups of hydroxyl (HTPB) and carboxyl (CTPB), copolymer of butadiene with acrylic acid (PBAA) or with acrylic acid and acrylonitrile (PBAN) and thiokol (PSF). Samples were combusted in the manometer bomb in the nitrogen under pressures from 14 to 140 atm.

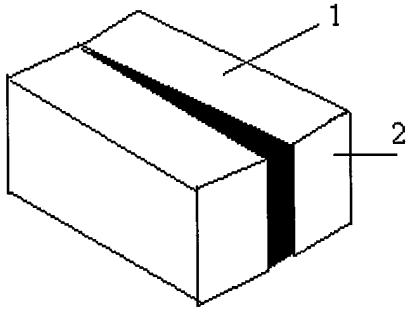

Fig. 3.7. Diagram of laminated specimen.

Extinction of the burning samples was made by fast depressurization. Samples were usually ignited from the upper end (face 1 in Fig. 3.7). In some experiments with $p<21$ atm the specimens were ignited from the front (face 2 in Fig. 3.7). Pressure in this case did not decrease, and extinction occurred due to the heat losses, when the interlayer of fuel on the surface became too thin for maintaining the AP combustion (with $p<21$ atm pure AP is not capable to independently burn). The extinguished surface was studied under an electron scanning microscope. The methodology described makes it possible to investigate burning with the very thin (up to 10 μm) interlayers of binder, characteristic of typical SP.

The profiles of the extinguished burning surface are schematically shown in Fig. 3.8 and very similar for all four investigated types of binder. It is evident that at all pressures and sizes of

the interlayer of binder the AP surface in the immediate proximity of the binder is elevated that indicates that the rate of AP burn out reduced there. At a high pressure (140 atm) and thick interlayers of the binder (more than 70 μm) on the specimens with binders PBAN and PSF near the interface with the binder the surface AP has even the plane sections. Apparently, they did not burn before the moment of quenching.

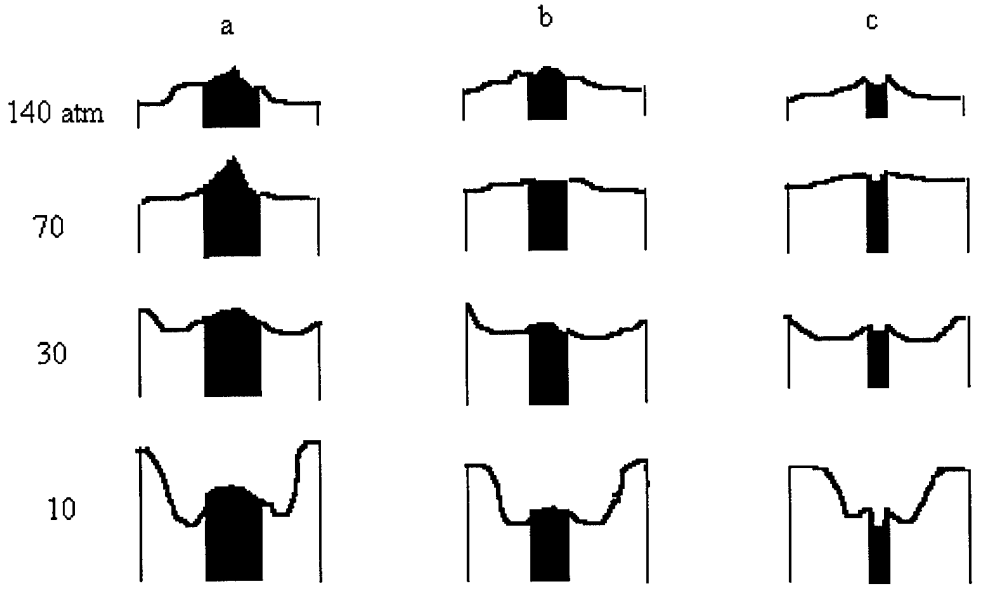

Fig. 3.8. Effect of pressure and thickness of binder interlayer on profile of the burning surface [18]. Thickness of interlayer, μm: a) 150, b) 70, c) 30.

In the specimens with thick interlayers the binder protrudes above the surface of the AP and even (except binder PSF) spreads in the form of melt over it. With a small thickness of interlayer (30 μm) and at all pressures the surface of binder is also fused, but it is located below the level of AP in the "groove". The walls of "groove" are parallel, and they are formed by the AP without traces of burning. At relatively low pressures ($p< 30$ atm) the profile of surface for all sizes of interlayer has depressions, in which, obviously, there was the maximum speed of burning. Under the conditions, when AP independently does not burn ($p<21$ atm), on the extinguished surface the binder is located on the bottom of the heavy cut (having nevertheless small increase in the middle), while with the thickness of the binder layer < 20μm there is no burning generally. It was also noticed that the strips with a reduced rate of the AP burn out, situated on both sides from the binder interlayer under all conditions for experiment, have the smooth surface, which differs from other AP surface. There was no such strip and, respectively, underspeeds of AP burning in the control experiment, where instead of the binder mica was inserted into the specimen. And vice versa, analogous strip (on the AP along the interface with the binder) is observed on the photograph [18] of the extinguished surface of SP, which contained AP in the grain form and binder UTPB and burned at $p\approx 10$ atm.

Authors of [18] stated that the lowering of AP burning rate in the vicinity of contact with binder can not be explained only by the binder spreading. Actually, in thin interlayers binder was in "grooves", and in thick interlayers the binder PSF did not spread, which is evident from

photographs. As a possible cause for suppressing AP burning the convection cooling is proposed of its surface by the cold products of the pyrolysis of binder. On the other hand, let us note that besides the convection, whose role is reduced when examining the thinner interlayers, the decelerating effect of AP burning near the binder one may explain by the diffusion dilution of the products of gasification of AP by the products of the binder pyrolysis. In this case the location of point, where the stoichiometric ratio of the mixture is reached (and, consequently, the maximum of burning rate) can be shifted to the side of AP. The details of such combustion behavior are given below (see next Section).

Let us also pay attention to the fact [18] (see Fig. 3.8) that at pressures 70 and 140 atm there is "pedestal" on the AP surface, connected with deceleration of burning, but there is no minimum, connected with the effect of primary flame. This means that in the points of reaching the stoichiometric ratio in the gaseous mixture the burning surface obtains less heat feedback from the gas than in the points far from the interlayer, where only AP burns. Using concepts of the BDP model, it is possible to claim that the following inequality takes place

$$Q_{stoich} \exp(-\xi^*_{stoich}) < Q_{AP} \exp(-\xi^*_{AP}), \quad p=70 \text{ atm}, \tag{3.94}$$

in spite of the fact that the "primary" flame is hotter, i.e., $Q_{stoich}>Q_{AP}$. Because of the different flame kinetics the values ζ^*_{stoch} and ζ^*_{AP} differently depend on pressure. In the BDP model for the composition AP+PSF the orders of reaction for the stoichiometric mixture ("primary flame") and the inherent AP flame are assumed to be 1.5 and 1.8, respectively. Then, according to (3.89) the right side of (3.94) more strongly depends on pressure, and with lowering in the pressure the sign of inequality in (3.94) will be changed. And indeed, with p=30 atm we see in Fig. 3.8 the profiles with minimum.

Nevertheless, it should be noted that in the pressure range 70-140 atm the results of experiments described above do not entirely correlate with the widely used diagram of flames, proposed in the BDP model. For better understanding of the combustion mechanism one may consider finding of Ref. [23], according to which the binder surface temperature in most cases exceeds the AP surface temperature. In connection with this the existence of "grooves" in experiments [18] for the thin interlayers requires explanation: either conclusions [23] are incorrect or grooves were formed in the process of quenching. However, the picture of surface was identical after quenching by the pressure drop and spontaneous extinction with p = const, when depicted in Fig. 3.7 specimen burned from face 2. Therefore it is impossible to explain the formation of grooves by the fact that with the pressure drop the binder was thrown out by the released gas.

One additional possibility remains unstudied. Grooves can be formed provided that the binder is capable of the relatively slow low-temperature decomposition during a certain time after disappearance of flame, but for the AP there is no such capability. If in this way a layer of binder with characteristic size of the thickness of the preheated layer is decomposed, then groove is formed in the case when the thickness of interlayer is less or of the same order of magnitude as the thickness of a preheated layer. However, for the thick interlayers the projections has to be preserved. The expressed doubts do not relate to the correctness of treatment of the AP surface profile in Fig. 3.8: since the walls of "grooves" are parallel, the AP was not decomposed there. Even if it was decomposed on the surface within the time of quenching at the depth of the order of magnitude of a preheated layer thickness, this would not change the gen-

eral view of the profiles in Fig. 3.8, since their characteristic dimensions, for example, the distance of minimum from the interface between AP and binder, are much greater than the thickness of a preheated layer.

3.4.2. Correct formulation of the diffusion flame problem (Burke – Schumann solution). The known solution of Burke- Schumann [27,28] for the form of the gas burner diffusion flame was used for description of SP combustion in the BDP model [13] and other models created on its basis (see survey [19] and [29]).

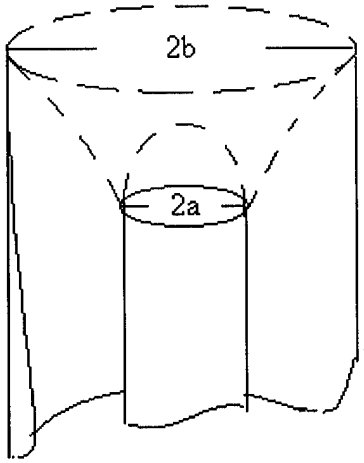

Fig. 3.9. Diagram of the gas burner.

In [27,28], the form of laminar diffusion flame has been analytically found for the burner, into which the gaseous oxidizer and fuel enter via coaxial tubes (Fig. 3.9). The version of the "flat flame" burner was also examined. According to Fig.3.9 the flame begins at the edge of the wall of the core tube and is finished on the axis of flow or on the wall of external tube. This depends on which reagent from those coming through the internal or through the external tube, is in the deficiency. Solution is obtained for the extended ("long") flames, with parameter $\psi=\rho D/mb<<1$. Here ρ, D and m - density, diffusion coefficient, and mass flow of gases, respectively; b - radius of external tube. With $\psi<<1$ it is possible to neglect without large error the "cross heterogeneity" of value m and the non-uniform character of flow, caused by the heat evolution in flame and non-uniformity of mass supply in the pipes. Flame form and length, computed according to the solution of Burke-Schumann, are close to experimentally measured on the gas burners.

The problem formulation [27] has been used in BDP model [13] for modeling the SP combustion. The element of the plane burning surface in the form of a circle $r \leq a$ of oxidizer and surrounding interlayer $a<r<b$ of fuel was examined. In this case it was necessary to generalize solution to the characteristic for SP the case of "short" flames, $\psi \geq 1$. However, in [13] and in all subsequent works it was not taken into consideration that with assumption $\psi \approx 1$ the boundary condition on plane z=0 (on the SP surface), used in Ref. [27], is not correct. Due to this the form of flame can be radically changed, which is shown below.

Let us assume that the mass burning rate over entire SP surface is identical and equal to m. The mass flow rate in the gas also is everywhere identical, equal to m of and is directed along axis z from the surface. The relative concentrations equal to α_1 for oxidizer and α_2 for fuel. The mass transfer proceeds according to the Fick law with the coefficient of diffusion D. It is assumed that everywhere ρD = idem. The gas-impermeable baffle is installed at x = ± b. This phenomenon is mathematically described as follows:

$$\begin{gathered} m\partial\alpha_i/\partial z = \rho D\nabla^2\alpha_i - w_i, \quad i=1,2; \\ b \geq x \geq 0, \quad z \geq 0 \\ x=0, \quad x=b, \quad \partial\alpha_i/\partial x = 0; \\ z=0, \quad m\alpha_{1,2} - \rho D\partial\alpha_{1,2}/\partial z = \begin{cases} m,0 & at \quad x<a \\ 0,m & at \quad a<x<b \end{cases} \end{gathered} \tag{3.95}$$

Depending on the form of the Laplace operator ∇^2, the problem (3.95) can describe the plane or axisynmetric case. It is assumed that oxidizer A_1 and fuel A_2 react according to the reaction scheme:

$$\nu_1 A_1 + \nu_2 A_2 \rightarrow \nu_3 A_3$$

Obviously, the reaction rates w_1, w_2 are connected with the relationship

$$w_1/(\nu_1\mu_1) = w_2/(\nu_2\mu_2)$$

Here μ_1, μ_2 - molar masses. Expressions for the reaction rates can be excluded from the examination, if instead of α_1 and α_2 we will seek their combination $\beta=\alpha_1-\nu\alpha_2$ where $\nu^{-1}=(\nu_2\mu_2)/(\nu_1\mu_1)$ is the stoichiometric mass ratio (f/ox) for the examined composition oxidizer-fuel. In terms of β the problem takes the form

$$\begin{gathered} (m/\rho D)\,\partial\beta/\partial z = \nabla^2\beta \\ x=0, \quad x=b, \quad \partial\beta/\partial x = 0 \\ z=0, \quad \beta - \frac{\rho D}{m}\frac{\partial\beta}{\partial z} = \begin{cases} 1 & at \quad x<a \\ -\nu & at \quad a<x<b \end{cases} \end{gathered} \tag{3.96}$$

For axisymmetric case (x≡r) we introduce dimensionless variables $\rho D/mb=\psi$, $r/b=\xi$, $z/b=\eta$, a/b = c and give the solution of the problem (3.96)

$$\beta = (1+\nu)c^2 - \nu + 2c(1+\nu)\sum_{k=1}^{\infty}\frac{J_1(\varphi_k c)J_0(\varphi_k\xi)}{\varphi_k J_0^2(\varphi_k)} \times \frac{2\exp\left(-(\eta/2\psi)(\sqrt{1+(2\varphi_k\psi)^2}-1)\right)}{1+\sqrt{1+(2\varphi_k\psi)^2}}, \tag{3.97}$$

$$J_1(\varphi_k) = 0$$

In the "plane" case (ξ=x/b) the solution of (3.96) takes the form

$$\delta = \frac{2\beta+(\nu-1)}{\nu+1} = 2c - 1 + \frac{4}{\pi}\sum_{k=1}^{\infty}\frac{1}{k}\frac{\sin(k\pi c)}{1+\psi m_k}\exp(-m_k\eta)\cos(k\pi\xi), \tag{3.98}$$

$$m_k = \left[(k\pi)^2 + (1/2\psi)^2\right]^{1/2} - (1/2\psi).$$

For the calculations it is convenient to represent (3.98) in the form

$$\delta - 2c + 1 = f(c-\xi) + f(c+\xi),$$

$$f(x) = \frac{4}{\pi}\sum_{k=1}^{\infty}\frac{\sin(k\pi c)\exp(-m_k\eta)}{k\left(1+\sqrt{1+(2k\pi\psi)^2}\right)}.$$

To simulate the conditions of the described above experiment [18] with a thin layer of fuel (with thickness 2h) between thick layers of oxidizer one should assume b $\rightarrow \infty$ and take in (3.96) boundary condition in the form

$$z = o, \quad \beta - \frac{\rho D}{m}\frac{\partial\beta}{\partial z} = \begin{cases} -\nu & at \quad 0 < x < h \\ 1 & at \quad x > h \end{cases}$$

Designating $2(\beta-1)/(\nu+1)=\gamma$, $x/h = \xi$, $y/h = \eta$, $\rho D/mh = \psi_h$ and using a cos-transform of Fourier on ξ, it is possible to obtain

$$\gamma = -\frac{4}{\pi}\int_0^{\infty}\frac{\exp\left[(-\eta/\psi_h)\left(\sqrt{0.25+(\omega\psi_h)^2}-0.5\right)\right]}{\sqrt{0.25+(\omega\psi_h)^2}+0.5}\times\frac{\sin\omega\cos(\omega\xi)}{\omega}d\omega \tag{3.99}$$

or in the more convenient for the numerical calculation form

$$-\frac{4}{\pi}\gamma = J\left(\frac{\eta}{2\psi_h},\frac{1-\xi}{2\psi_h}\right)+J\left(\frac{\eta}{2\psi_h},\frac{1+\xi}{2\psi_h}\right),$$

$$J(x,y) = \int_0^1 e^{-y\frac{1-z}{z}}\sin\left(x\frac{\sqrt{1-z^2}}{z}\right)\frac{dz}{(1+z)^2(1-z)}$$

Analogous axisymmetric problem (strand of the fuel with diameter 2h, pressed into the large specimen of oxidizer) has a solution

$$\gamma = -4\int_0^{\infty}J_1(s)J_0\left(\frac{sr}{h}\right)\frac{exp\left[(-\eta/\psi_h)\left(\sqrt{0.25+(\omega\psi_h)^2}-0.5\right)\right]}{\sqrt{1+(2\psi_h s)^2}+1}ds \tag{3-99a}$$

By comparing expression (3.97) with solutions [27, 28] in the form

$$\beta = (1+\nu)c^2 - \nu + 2c(1+\nu)\sum_{k=1}^{\infty}\frac{J_1(\varphi_k^c)J_0(\varphi_k^{\xi})}{\varphi_k J_0^2(\varphi_k)}\exp(-\eta\psi\varphi_k^{\xi})$$

we recognize that in latter instead of complex (3.100)

$$f(\psi,\eta,k) = \left[2/\left(\sqrt{1+(2\varphi_k\psi)^2}+1\right)\right]exp\left[-\frac{\eta}{2\psi}\left(\sqrt{1+(2\varphi_k\psi)^2}-1\right)\right] \tag{3.100}$$

the factor $\exp(-\eta\psi\varphi_k^2)$ enters, which can be obtained from $f(\psi,\eta,k)$ at $\psi<<1$.

Of course, this result was obtained in [27,28] not by simplification of expression (3.97), but by solving the problem simplified in comparison with (3.96). In particular, the index in exponential term was changed as a result of neglecting by the term $\partial^2\beta/\partial z^2$ in the equation of diffusion (3.96). However, the multiplier before the exponential term in (3.100) was degenerated into unity due to neglecting in boundary condition (3.96) by diffusion flux $-\psi\partial\beta/\partial(z/b)$. It means the following for was used

$$z = 0, \quad \beta = \begin{cases} 1 & at \quad x < a \\ -\nu & at \quad a < x < b \end{cases} \tag{3.101}$$

Comparing now with (3.97) the solution [13] generalized for the "short" flames (exhibited in the expanded form in [19]), one may recognize that the exponential terms turn out to be equal, since in the equation of diffusion the term $\partial^2\beta/\partial z^2$ is taken into consideration. The multiplier before the exponential term in expression (3.100), in Ref. [19] as well as in [27,28], is degenerated into unity that indicates the utilization of simplified boundary condition of (3.101) type.

Let us show how this solution was used in the models of BDP type. From the definition of β it follows that with $\beta = 0$ the stoichiometric ratio of components is achieved. In particular, if there is a diffusion flame, its front must be localized on the surface $\beta = 0$. In the front of diffusion flame we have $\alpha_1 = \alpha_2 = 0$, and the ratio of components takes all values, including stoichiometric. In order to find the height of the flame, for example, when it is closed above the particle of oxidizer, one should assume $\beta=0$, $\zeta=0$ and express the height $x^*=z=b\eta$ from expression (3.97). Considering only the first term in (3.97), authors [13] expressed η in the form:

$$x^* = z \approx 2b\psi\gamma / \left(\sqrt{1 + (7.64\psi)^2} - 1 \right), \tag{3.102}$$

where γ - logarithmic (supposedly weakly changing) function of ν, c, ψ. Then with $\psi>1$ it is possible to set $x^* \approx 2b \approx 2a = D_c$. In Ref. [14], the value of x^* was determined numerically taking into account few terms of series, in Ref. [21] there were considered 50 and more terms. By numerical calculation and by selection of the constants the expressions were obtained [21] for the "diffusion" height of flame above the oxidizer (if $f/ox < (f/ox)_{stoich}$):

$$x^* \approx 2.02b(f/o)_{stoich}^{0.929} (f/ox)^{1.604} \tag{3.103}$$

and above the binder (if $f/ox < f/ox_{stoich}$)

$$x^* \approx 1.17b(f/ox)_{stoich}^{-0.858} (f/ox)^{1.871} \tag{3.104}$$

Here b – external radius of two- layer oxidizer-fuel gas jet; for SP, as a rule, $2b \approx D_c$.

In King's model [15] attempt was made of recomputation of stream dimension b and ratio b/a taking into account the fact that mass burning rates of oxidizer and can he different, but linear gas velocities approach to leveling due to friction. It was assumed that the velocities leveling occurs on the distance which is considerably smaller than the height of diffusion flame. As it was noted in [19], this assumption is insufficiently substantiated. Indeed, the velocities and concentrations leveling occurs by the same mechanism and approximately for at one time.

Let us examine now, which consequences for the combustion models give neglecting by the diffusion term in the boundary conditions of problem (3.95) that is permissible only with $\psi = \rho D/mb \ll 1$. According to boundary condition (3.101), the surface $\beta = 0$ originates in the place of the contact of the solid oxidizer and fuel on the SP surface. Here $\beta(x, 0)$ has a discontinuity with sign change, i.e., it may have any magnitude in the range from $-\nu$ to 1, including 0.

However, the accurate boundary condition of the problem (3.96) at $z = 0$, $x = a$ contains discontinuity only of the gradient of β value. The value of β itself is continuous and it is not necessarily equal to zero. Surface $\beta = 0$ originates not in the place of the contact of the solid oxidizer and fuel. This displacement becomes greater with increase of $(1-\nu)$ and ψ. Moreover, un-

der some conditions the surface $\beta=0$ and the diffusion flame can not be realized at all. Using expression (3.97) one may find condition, with which this surface is subtended into single point due to the excess of fuel. Let we substitute $\zeta=0$, $\eta=0$, $\beta=0$ in (3.97):

$$\nu_+(\psi,c)=\left[\left(c^2+2c\Sigma\right)^{-1}-1\right]^{-1};$$
$$\Sigma\equiv\sum_{k=1}^{\infty}\frac{J_1(\varphi_k c)}{\varphi_k J_0^2(\varphi_k)}\times\frac{2}{1+\sqrt{1+(2\varphi_k\psi)^2}} \qquad (3.105)$$

Results of calculation by (3.105) are presented (see [29a]) in Fig. 3.10.

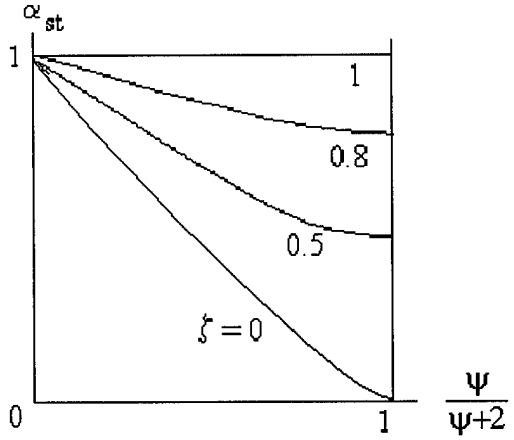

Fig. 3.10. Boundary lines restricting domain of existence (to the left and below appropriate line) of the surface $\beta=0$.

Here $\alpha_{st}=\nu/(1-\nu)$ is the stoichiometric mass fraction of oxidizer, $\xi=c^2$ is the volumetric fraction of oxidizer in the condensed phase. Parameter $\Psi/(\Psi+2)=\rho D/(\rho D+2am)$ characterizes the role of diffusion in mass exchange, $2a=D_c$ - diameter of AP particle cross-section, see Fig. 3.2. With given value ξ the "stoichiometric" surface does not exist in domain to the right and above the appropriate ξ-line in Fig. 3.10. The lines with $\xi=0.5$ and $\xi=0.8$ are obtained by calculation according to relationship (3.105) while the line $\xi=0$ corresponds to approximate solution of equation

$$2\int_0^{\infty}\frac{J_1(s)ds}{1+\sqrt{1+(s\rho D/ma)^2}}=1-\alpha_{st}$$

This equation is equivalent to the condition of transformation into single point of a "stoichiometric" flame surface above single oxidizer crystal situated at the plane surface of fuel gasified with mass flow rate m (the same as for oxidizer). The above equation follows from the equation in generalized form (3.99a) at values $r=\eta=\beta=0$.

In the models [13,14,16] the effect of no-existence of diffusion flames was not taken into consideration. However, these models managed to describe a transition to kinetic combustion regime (premixed flame) with $a\to 0$. This was done using some artificial approach, namely, by representing the heat feedback from the primary flame to the surface of sample S in the form:

$$q = m\, S\, \beta_F\, Q_{PF} \exp(-X_{PF}^*),\ Q_{PF} = c(T_F - T_0) + \alpha\, Q_L + (1 - \alpha)\ Q_f, \qquad (3.106)$$

$$X_{PF}^{*} = X_{RPF}^{*} + 0.6a$$

Here β_F – fraction of oxidizer consumed in the primary flame of decomposition products of oxidizer and fuel; Q_L and Q_f – heat of gasification for oxidizer and fuel, respectively; 0.6a – "diffusion" height, X_{RPF}^{*} - "kinetic" height that depends for given components only on T_F and P; T_F – maximal temperature in the final flame calculated by thermal-equilibrium program.

With $2a \to 0$ and $\beta_F \to 1$, relationships (3.106) give correct estimation for heat feedback to the burning surface from premixed flame with narrow zone of heat release. However, with $2a > 0$ and $\beta_F < 0$ these formulae do not describe the heat feedback from diffusion "primary" flame whose temperature corresponds to stoichiometric ratio of the components and does not depend on α. Namely such value of T_F was postulated in Ref. [21]. But when taking T_F, corresponding to stoichiometric flame value, the relationships (3.106) loose the possibility to describe "kinetic" combustion regime for premixed gas at $2a \to 0$. These difficulties can be overcome in a formal way if one takes T_f changing from "kinetic" to "diffusion" value upon changing the value of $(0.6a/X_{RPF}^{*})$ from 0 to ∞. More justified approach has to take into consideration simultaneous existence of the "cap" of diffusion flame above the top of oxidizer grain of finite size and some cooler flame of premixed gas above the rest of the oxidizer surface and binder.

Let us evaluate a possibility of disappearing the diffusion flame above the oxidizer particles (Fig. 3.10) in typical combustion conditions. According to Ref. [13], $\rho D \approx 1.6\ 10^{-4}$ (g/cm s); $(T/T_o)^{3/2}$; T_o=300K; $T \approx 2545$K; and $\rho D \approx 0.8.10^{-3}$ g/(cm s). Let also $m \approx 0.5$ g/(cm^2 s), $2a \approx 20$ μm, where value 2a approximately corresponds to the size of the oxidizer particle. Then $\psi \sim 1.4$, and $\rho D/(\rho D + 2a\ m) = \Psi/(\Psi+2) = 0.41$. According to graphs in Fig. 3.10 the diffusion flame will not exist at $\alpha_{st} > 0.6$, and such values of α_{st} are reasonable for real SPs, which have typically α_{st} = 0.82-0.88. Actually, the diffusion flame disappears already with smaller α_{st}.

Similar effect of diminishing the area of "stoichiometric" surface can be examined for the case of combustion of laminated ("sandwich"-type) samples – thin layer of binder between thick layer of pressed AP. It follows from (3.99) at $\eta = \beta = 0$ that the distance X from the middle point of the binder lamina to the place of reaching stoichiometric ratio in gas above the sample surface meets the relationship

$$2(1 - \alpha_{st}) = \varphi(\tilde{X} + \tilde{Y}) - \varphi(\tilde{X} - \tilde{Y}),\quad \tilde{X} = 2mX/\rho D,\ \tilde{Y} = 2mL/\rho D, \tag{3.107}$$

$$\varphi(z) = \frac{4}{\pi}\int_0^{\infty} \frac{sin(zt)}{t(1+\sqrt{1+t^2})}\,dt$$

Here 2L is the width of the binder layer. It can be shown that

$$\varphi(z) = 1 - \frac{4}{\pi}\int_0^{1} F(z,t)\,dt,\quad F(z,t) = \sqrt{1-t^2}\ exp(-z/t),\quad z > 0$$

Function F has a maximum F_m at $t=t_m$ with equality $t_m^3/(1-t_m^2) = z$ being held. The function graph can be approximately represented to the right from the maximum by one fourth of ellipse with half axes F_m and $1-t_m$ while to the left from the maximum it is represented by cubic parabola with extremums at t=0 and $t=t_m$. Such parabola divides for equal parts the rectangular

area with the sides equal to F_m and t_m. The error of approximation is close to zero at $t \to 0$ and it is maximal at $t_m=1$. Thus, we have

$$\varphi(z) \approx 1 - (1- t^2_m)^{1/2}[1 - (1-2/\pi)t_m] \exp(-t^2_m/(1- t^2_m)), \quad t^3_m/(1- t^2_m) = z, \quad z > 0, \quad \varphi(-z) = -\varphi(z) \tag{3.108}$$

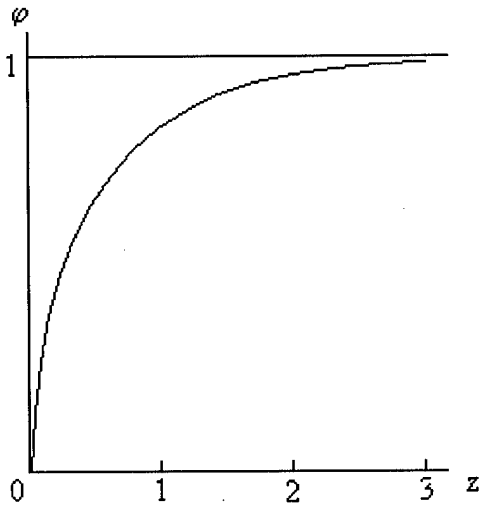

Fig. 3.11. Dependence of φ versus z.

The plot of φ(z) is presented in Fig. 3.11. Let us estimate at which conditions the stoichiometric ratio in the gas phase is reached exactly on the line X = L corresponding to the interface between binder and oxidizer. Assuming in (3.107) $\tilde{X} = \tilde{Y}$, we may take typical value of α_{st} equaled 0.875. Then relationship (3.107) gets the form $\varphi(z) = \varphi(2\tilde{Y}) \approx 0.25$. According to Fig.3.11 it follows that $z = 2\tilde{Y} \approx 0.05$. Finally, assuming $\rho D \cong 0.001 g/cm \cdot s$ and $m \approx 0.5 g/cm^2 \cdot s$ one obtains $2L \approx 5 \cdot 10^{-5} cm = 0.5 \mu m$. Since that in experiments [18] the binder layer width 2L was no less than 10 μm, one may conclude that in most practically meaning cases the experiments with laminated samples combustion lead to the following expressions, which mean that stoichiometric ratio is reached above the oxidizer surface:

$\tilde{X} > \tilde{Y}; \quad X > L.$

Looking on the plot in Fig.3.11 one may conclude that it is convenient to solve the relationship (3.107) by iteration method assuming for the beginning $\tilde{X}_0 \to \infty$:

$$\varphi(\tilde{X}_{i+1} - \tilde{Y}) = \varphi(\tilde{X}_i - \tilde{Y}) - 2(1 - \alpha_{st}) \tag{3.109}$$

The first approximation takes the form:

$$X \approx L + (\rho D/m)\ \text{const} \tag{3.110}$$

Here constant value depends on α_{st} and does not depend on L. Thus, expression (3.110) does not give dependence of (X-L) on L that correlates well with experimental findings. In experi-

ments [18] with sufficiently wide variation of size 2L of the binder layer the maximal burning rate of oxidizer was reached approximately at the same distance from the binder-oxidizer interface. Adjusting to the interface the oxidizer surface burned with lowered rate and had "smooth" shape. Explanation [18] of the low burning rate due to influence of the convective cooling the oxidizer surface by combustible gases does not take into consideration the role of diffusion thermal processes in the gas phase. According to discussed here approach the lowering of the burning rate close to the binder-oxidizer interface can be caused by significant dilution of oxidizer decomposition gases with the fuel decomposition products.

The fact is that on the surface $\beta=0$ the concentration of components is in stoichiometric ratio and concentrations not necessarily equal to zero. They turn into zero (which is characteristic for the diffusion flame) on this surface only at a certain "kinetic" distance from SP. Therefore, with a decrease in the area of the surface $\beta=0$ its "diffusion" part will vanish before than entire surface $\beta=0$ vanishes, see Fig. 3.12.

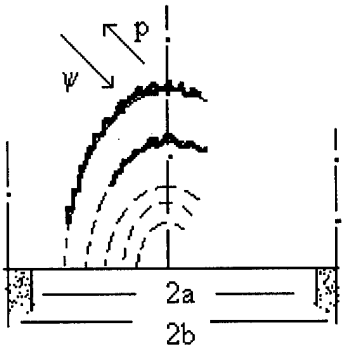

Fig. 3.12. The flame form with taking into account the diffusion in boundary condition.

Let us consider further some results of solution of the problem of Burke-Schumann. If in the described experiment on the combustion of laminated specimens with thin interlayers of binder [18] a deceleration of AP burning is actually caused not by spreading of binder melt, but by the excess of the products of its pyrolysis in the gas phase, then minimum on the surface profile of AP must correspond to the stoichiometric ratio of components in the gas flame above this place. In this case the characteristic value of pressure $p=p_1$, with which the minimum on the AP profile vanishes with increase of p, contains information useful for determining constants entering in the combustion model. Thus, by analogy with (3.94) one obtains

$$Q_{stoich}\exp\left(-\xi^*_{stoich}\right)=Q_{AP}\exp\left(-\xi^*_{AP}\right),\quad p=p_1 \tag{3.111}$$

Here $\xi^*=cmx^*/\lambda$, for calculating x^* the ratios of type (3.37) and (3.38) are used. Expression (3.111) is useful for selection of the constants. In addition, a certain information about the diffusion coefficient can be extracted also from the value of the coordinate of minimum on the profile of quenched AP.

As far as solution of Burke-Schumann discussed above is concerned, despite its oversimplifications there is deserving confidence conclusion about disappearance with sufficiently high values of parameters ψ and Φ of the surface $\beta=0$, where the stoichiometric ratio of components is achieved. This conclusion is based on the form of boundary condition on the surface of SP and may not be changed if under the same condition we take into account the "hydrody-

namic" heterogeneity of problem, caused by heat evolution in the flame and variability along the surface of SP of the mass flow rate of gas formation.

3.5. HETEROGENEOUS SYSTEMS WITH STRONG DIFFERENCE IN THE COMPONENTS BURNING RATE OR IN A SURFACE TEMPERATURE

3.5.1. Effect of non-uniform surface temperature.

Oxidizer and binder can have considerably distinguished temperatures of surface as it was established experimentally, for example, in Ref. [23]. In that work the pyrolysis of seven types of the binder upon radiative heating was performed, with values of the surface temperature and the rate of ablation being measured, and movie film being conducted. Experimental data [23] are presented in Table 3.2. Filming showed that with typical for the combustion of SP heat fluxes the binder on the surface is in a liquid state and contains the coke formations, whose number increases with pressure, and also in the presence of AP. Referring to the low values of value E in the pyrolysis law $m=Aexp(-E/RT_s)$ (see Table 3.2), the authors [23] draw the conclusion that the boiling or degradation of polymers thru the weak bonds takes place.

In Section 3.3.5 we discussed "improved model" [16] that considers difference in temperatures of oxidizer T_s and binder T_f on the burning surface. The contradictory character was noted of the utilization of balances of heat for these components (by averaging heat feedback to the surface of SP, as this was done in models of the BDP type) without taking into account the heat exchange between them in the condensed phase. This contradiction can only be avoided in the more detailed examination of the processes on the surface of SP. If it is possible to neglect spreading of the liquid binder over the SP surface, then the problem is reduced to taking into consideration of the non-uniformities (roughness) surface of SP. Note that the roughness of the burning surface was not considered in Ref. [16] because earlier it was stated [23] that this effect may only slightly change the calculated burning rate. However, "two-temperature models" [30, 31] (see also Ref. [1]) took into account the roughness of the burning surface.

Table 3.2.
Values of physicochemical parameters of typical binders.

Binder	A, $g/cm^2 s$	E, kJ/mol	Q, J/g	M, g/mol	$(ox/f)_{stoich}$	T_F, K	ρ_f, g/cm^3
CTPB	12.8	44	1595	18.5	9.5	1437	0.92
HTPB	299	70.7	1810	18.7	9.3	1451	0.92
PU	49.4	42.7	1090	20.8	6/2	1787	1.01
PBAN	270	70.0	2360	18.9	9.0	1430	0.93
PSF	5.6	36.4	2260	26.2	4.9	2545	1.27
HTPB, saturated	7,3	37.6	3180	18.7	9.3	1446	0.91
Fluoro-Hydro-carbon	2.6	71.1	4200	28.5	1.5	2265	0.60

Note. *A – mass flow rate of pyrolysis, E – energy of activation, Q - heat of decomposition; M - molar mass of the products of pyrolysis; $(ox/f)_{stoich}$ is calculated by taking AP as an oxidizer; T_F is the flame temperature calculated for SP with the ratio AP/Binder equal to 70/30.*

It is believed that the SP combustion behavior may substantially depend on how decomposition products of AP under a layer of the binder are released: whether the blisters or channels are formed or simply the section of binder, located directly above the ignited crystal of AP, is ejected into the gas phase. According to Ref. [32], namely the latter case was observed by the authors of works [33] and [34]: in combustion of SP based on the polybutadiene binder and nitramines (the latter have T_s much lower than that for AP) the binder was shouted in the gas phase in the form of ribbons.

One may also analyze an opposite case (SP based on volatile binder), when the temperature on the surface of binder is lower than that of oxidizer, i.e. $T_{sf} < T_s$. In this case a UTD-model must consider the escape of the oxidizer particles into the gas phase.

Sizes of ejected crystals of AP can be estimated. We will consider that grains of AP are peptized from the burning surface of SP as a result of the loss of contact with the bonding agent due to the gasification of binder under the crystal. For sufficiently large AP particles it is possible to disregard the curvature of their surface and to consider plane isothermal surfaces in the burning crystal. Then it can be to shown that at the moment of reaching the temperature of the binder gasification T_{sf} by the rear boundary of the grain, the remaining thickness of crystal h in the direction of burning is equal to

$$h \approx (\kappa / u) \ln\left[(T_s - T_0)/(T_{sf} - T_0)\right] \qquad (3.112)$$

Here κ, u and T_s –thermal diffusivity, linear burning rate and the temperature of the burning surface of AP crystal. When deriving (3.112) there was not taken into consideration thermal conductivity variation upon crossing interface AP - binder. Partly this is compensated by the fact that for the burning AP the temperature profile is considerably more stretched [41], than computed according to Michelson's equation, used in deriving (3.112).

Diameter of sphere, equivalent by volume to ejected spherical segment, equals $D=(6w/\pi)^{1/3}$, where $w =(\pi h^2/3)[(3/2)D_0-h]$ - volume of segment, D_0 - initial size of AP crystal.

Finally, for the diameter of the ejected particle we obtain

$$D_d = \left[h^2(3D_0 - 2h)\right]^{1/3}$$

where h is calculated by (3.112) with known values u, T_s, T_{sf}.

For functional test of the model presented we carried out experiments on recording via microcinematography of the particle sizes of AP, which are ejected from the burning surface of model SP specimens. As the binder the polymer with known relation $T_{sf} \approx \text{const}_1 \ln(\text{const}_2 / p)$ was used. Samples were prepared with monodisperse powders of AP, which had a mean

counting particle size from 200 to 750 μm. Combustion experiments were conducted at pressures 1 and 33 atm.

Temperature of AP surface was calculated by formula [42]

$$T_{AP} = \left[835^{-1} - \frac{R}{30 \cdot 10^3} \ln \frac{u}{0.3} \right]^{-1}, \; K; \quad [u] = cm/s.$$

It was used in calculations of T_s that u is equal to the linear burning rate u_1 of the SP specimens. The experimental dependence $u_1(p)$ was used. The disagreement of experimental and calculated values of D_d in all cases did not exceed 30%.

3.5.2."Relay race" type models.

If there are evidences for considering the burning rate of oxidizer the known value (for example, sufficiently coarse grains of AP or nitramines may burn as monopropellant) or very large in comparison with the burning rate of binder, then for calculating the burning rate of SP it is convenient to use averaging over time. Returning to the "photographic" concept, we may say that the averaging parameters over the surface of SP, characteristic of the UTD-models, can be identified with the utilization of an instantaneous photograph of the surface (King's approach - with the movie about behavior of a single particle) whereas averaging over time - with sufficiently prolonged filming of region on the burning surface of SP with size of the order of D_o.

Beckstead in Ref. [35] calls this approach by term "successive" when particles of oxidizer fall in the field of view of researcher one after another, in contrast to the "parallel", i.e., simultaneous their examination when averaging over the surface. In the following discussion we will call models with the averaging over time "the relay race" models.

Apparently, Bakhman and Belyayev [1] were the first who applied this approach. They determined mean linear burning rate as the ratio of a certain characteristic distance, taken along the normal to the mean burning surface, to the time of passing that distance by the burning surface. The diameter D_o of the oxidizer grain together with the thickness d_f of relating to this grain layer of binder was selected in Ref. [1] as such distance. If the mean burning rates of oxidizer and binder are equal to u_o and u_f, respectively, then the average rate of SP combustion can be calculated by formula

$$u = \frac{D_0 + d_f}{(D_0 / u_0) + (d_f / u_f)} \tag{3.113}$$

At a high burning rate of oxidizer $u_o >> u_f$, we obtain

$$u \approx u_f (1 + D_0 / d_f) \tag{3.114}$$

i.e., the rate of SP combustion is controlled by the slow burnout of binder. In Ref. [1], the opposite case is examined, when

$$(D_0 / u_0) >> (d_f / u_f), \quad u \approx u_0 (1 + d_f / D_0) \tag{3.115}$$

The relation (3.115) shows, in which case an assumption $u = u_{ox}$, accepted in the models of the BDP type, is justified.

"Relay race" approach for SP based on AP and active, i.e. capable of independent burning, binder was also used by Kubota and Masamoto [36], who proposed analogous (3.113) relationship

$$1/u = (\zeta'/u_{AP}) + (1-\zeta')/u_f \tag{3.116}$$

Here ζ' - the volume fraction of SP, which burns with the rate u_{AP}. It is assumed that not only AP burns with this rate, but also part of the binder, namely, the layer with a thickness of η around each crystal of AP. The dependence of thickness of the layer on size D_o of particle AP is not considered.

If ζ - volume fraction of AP and n - number of AP particles per unit of volume of SP, then for ζ' it is implemented

$$\zeta' = (\pi/6)(D_0 + 2\eta)^3 n = (\pi n D_0^3/6)(1 + 2\eta/D_0)^3 = \zeta(1 + 2\eta/D_0)^3 \tag{3.117}$$

For calculation of u_{AP} the empirical dependence is used

$$u_{AP} = 0.38 p^{0.45}/D_0^{0.15} \tag{3.118}$$

Here we have: [u] = cm/s, [p]=atm, [D_o]= μm. Burning rate of combustion of the remaining part of the binder, excluding layers surrounding the particles of AP, is defined as for the monopropellant (see Section 3.2.1).

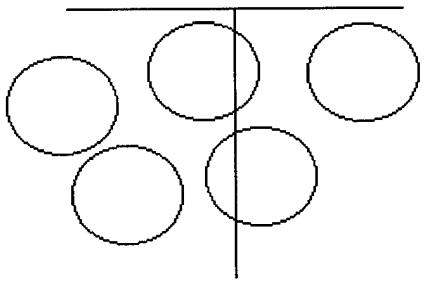

Fig. 3.13. To the method of averaging for the "relay race" model.

An attempt to take into account in more detail an interaction of components within the framework of the relay race model was undertaken in Refs. [21,35]. As in the model of Bakhman and Belyayev [1], the combustion is examined in direction of normal to the mean burning surface in successive intervals of time for different sections of oxidizer and binder, situated along the normal (see Fig. 3.13). It is assumed that in the real case the burning is propagated along the way, which is only slightly deflected from this normal. The time averaged burning rate of sufficiently long, in comparison with the size of particles D_o, specimen length is calculated by:

$$u = \frac{x}{t} = \frac{x}{N\left[T_{ign} + (D/u_0) + \left(f/u_f + (1-f)/u_f^*\right)d\right]} \tag{3.119}$$

Here N - number of the crossed AP particles by the normal; D - average size of this intersection; d - average size of intersection of normal with the binder section; t_{ign} - time of the particle ignition; u_o - rate of its burning; f - fraction of the binder, which burns in the "primary flame" with the oxidizer; u_f - rate of its burn out; u^*_f - rate of the pyrolysis of the remaining binder.

Since with random distribution of particles in the volume of SP the components along straight line are presented in the same ratio as in the bulk of SP, one has:

$$DN/x = \zeta, \quad Nd/x = 1-\zeta \tag{3.120}$$

where ζ - volume fraction of oxidizer. Now (3.119) takes the form

$$1/u = t_{ign}(\zeta/D) + (\zeta/u_0) + (1-\zeta)\left(f/u_f + (1-f)/u_f^*\right) \tag{3.121}$$

For entering in (3.121) average size D of intersection of the particle with normal the authors of [35] accept $D = D_0\sqrt{2/3}$, referring to Hermance [12]. For the ignition time calculation of AP particle the relationship is used

$$t_{ign} = 4.32\frac{C}{cm^{0.7}} D_0^{1.7}/u_0 \tag{3.122}$$

This expression was obtained via treating experiments [37] for AP, but it was also applied in [35, 21] for octogen. Here

$$C = (E_s/E_{ref})(T_{melt} - T_0)/(T_{ref} - T_0) \tag{3.123}$$

where E_s - energy of activation of the surface reaction; T_{melt} - melting point of oxidizer; E_{ref}, T_{ref} - constants. For the rate of pyrolysis u^*_f of the part of binder outside of the "primary flame" an expression is proposed with the reference to the work of Strahle [38]

$$u_f^* \approx u\exp(-u_f d/2\kappa) \tag{3.124}$$

where κ - thermal diffusivity of the condensed phase. For entering into (3.121) rates u_o and u_f the separate balances of heat are written as in the two-temperature "improved model" [16]. Burning rate of oxidizer is determined from the relation of the type of pyrolysis law and equation of the balance of heat, written only for oxidizer. This equation takes the form:

$$c(T_s - T_0) = -Q_L + \beta_p\beta_F(1 + (f/ox)_{stoich})Q_{PF}\exp(-\xi_{PF}) + (1-\beta_F)Q_{ox}\exp(-\xi_{ox}) \tag{3.125}$$

Here T_s - temperature of the burning surface of oxidizer; Q_L - thermal effect of gasification. The second term in the right hand side describes the heat feedback from the "primary flame"; β_p – relating to the oxidizer portion of heat, which comes from the primary flame to the burning surface.

As it has been reported in Ref. [19l regarding the preceding works of Beckstead, for β_p the value of 1/3 or 2/3 was accepted in dependence on whether the mass ratio (f/ox) was larger or smaller than the stoichiometric one. In this case, according to the solution of Burke-Schumann, the diffusion flame is inclined, respectively, to the fuel or to the oxidizer. Fraction of the oxidizer β_F, which burns out in the "primary flame", is calculated geometrically just as in the initial BDP model; $(f/ox)_{stoich}$ -stoichiometric mass ratio of the fuel and oxidizer. If m_{ox} – total mass flow rate from the oxidizer, then $m_{ox}\beta_F[1+(f/ox)_{stoich}]$ is the mass flow rate of the reagents, which burn out in the primary flame; Q_{PF} - heat evolution in the primary flame calculated per unit mass of the combustion products. The value of $\zeta_{PF} = x^*_{PF}\, cm_{ox}/\lambda$ is calculated as in the initial BDP model, see (3.36)-(3.38). By numerical calculations on the basis of the Burke-Schumann solution there are proposed the expressions for the "diffusion" heights of flame above oxidizer and binder (3.103), (3.104). The last term in (3.125) considers the heat feedback from the inherent flame of the oxidizer (see Chapter 1 and Section 3.3.2). The heat feedback from the final flame is not considered. The surface of oxidizer is considered flat.

Rate u_f of burn out of the binder under primary flame is found from relationship (3.88) and the balance of heat:

$$c\left(T_{sf}-T_0\right)=-fQ_f+\left(1-\beta_p\right)\cdot f\left[1+\left(f/ox\right)_{stoich}\right]^{-1}\cdot Q_{PF}\exp\left(-\xi_{PF}\right) \qquad (3.126)$$

Here the first term in the right hand side considers heat consumption on the vaporization of the binder, the second term corresponds to the heat feedback from the primary flame to the binder. For f the "semi-empirical" expression is proposed

$$f=1.2f_F\left(T_0/298\right)exp\left(-\xi_{PF}\right) \qquad (3.127)$$

where f_F - binder,which is needed for the stoichiometric reaction with the oxidizer in the primary flame.

Calculations according to the model presented were performed for SP based on octogen and HTPB binder (polybutadiene with hydroxyl terminal groups). This binder is inert and relatively thermoresistant while octogen, on the contrary, has low melting point and high burning rate. Such conditions are favorable for applying relay race type models. It has been reported [35, 21] that calculations agreed well with experiments described in [33, 34].

3.5.3. Critical discussion of the "relay race" models.

Let us compare materials of Sections 3.4 and 3.5. The characteristic for the "relay race" models the "successive" method of averaging (average over time) does not formally have the explicit advantages over the "parallel" method, i.e., by averaging over the surface. In the "parallel" method the real surface of binder everywhere differs from plane, in the "successive" - the

normal to the burning surface everywhere differs from normal to the plane section of specimen. The errors of the same order of magnitude do not permit to make simple evaluation. However, "successive" averaging can be considered preferable for SP with hardly volatilizing binder or with the fast burning filler, and also with the large size of the filler grains. For example, for the fast burning oxidizer the "relay race" model predicts (see (3.114)) that with small changes in the parameters the general burning rate of SP varies proportional to the rate of the burn out of binder. The "petite ensemble" model predicts the opposite, namely, the determining role of the fast burning component. Contradiction is caused by the fact that with a large difference in the burning rates of components according to the "petite ensemble" model there appears too many "empty pits", and this (see Section 3.3.6) decreases the plausibility of model.

However, developed at the present time "relay race" models are also distant from perfection. Actually, enumerated above conditions, favorable for applying sequential models, simultaneously contribute to manifestation of nonuniform effects connected with bending of surface and with gas-dynamics non-uniform character. The latter even on the flat surface of SP can be caused by a difference in mass burning rates of individual components. Strong non-uniform character of gas flow affects the character of heat feedback from the gas phase and changes it as compared with that, which is postulated in the models of the BDP type. Actually, the heat transfer by convection is supplemented. For the coarse $D_o \geq \kappa/u$ grains of filler the non- uniform character is developed also in the condensed phase: the temperature heterogeneities do not manage to be leveled and the balance of heat with the averaging of heat fluxes over the surface of SP looses correct physical meaning.

In fact, the heat exchange does not manage to level the heterogeneity of the temperature in the condensed phase not only between the components (this fact was taken into account in Ref. [21] by using separate balances of heat for the oxidizer and for the binder), but also even between the center section and the periphery of one large AP particle. Apparently, for sufficiently coarse grains ($D_o >> \kappa/u$) instead of the inherent in BDP type models calculation of the mean mass burning rate of the entire grain it should be found the rate of burn out on its periphery, using in this case the data of experiments of the type [18] with the laminated specimens. Let us note that calculation of the burning rate on the periphery of the filler grain (AP or nitramine) is necessary not only for finding total mass flow rate from this grain or its average burning rate u_o. It is also needed for calculating the rate of the burn out of binder which must depend, in particular, on change in the time of the burning rate of grain. In the sequential model [21], the expressions (3.122) and (3.123) for t_{ign} are obtained by processing experimental data of Shannon and Peterson [37] on the combustion of pressed specimens of AP. Data [37] do not contain dependence of t_{ign} on the compacting pressure P_{comp} although it is evident that when $P_{comp} \to \infty$ the specimen burns as single crystal, but when $P_{comp} \to 0$ (free packing charge) the most possible is convective burning. Furthermore, it causes no doubts that the ignition time of AP particle in SP, besides its inherent characteristics, must depend at least on the thermal physical parameters of binder.

In the model of Bakhman, Belyayev [1] it should be noted limited applicability of relation (3.115), which is fulfilled when $(D_o/u_o) >> (d_f / u_f)$. Actually, inequality $D_o/d_f > 1$ cannot be too strong for monodisperse SP for the purely geometric reasons; therefore fulfillment of $(D_o/u_o) >> (d_f / u_f)$ requires $u_f \geq u_o$. However, if the binder burns two times more faster than the

oxidizer, sequential approach becomes incorrect: burning goes away forward along the binder, unburned oxidizer is ejected into the gas phase. Consequently, the fufillment of (3.115) and applicability of the actually using condition $u \approx u_o$ models of the type of BDP are limited to narrow region $u_f \sim u_o$.

Let us give several critical comments regarding "relay race" model approach [21].
a). The entering in (3.121) value D of average size of intersection of particle with the normal to the burning surface is taken in the form $D=D_o\,(2/3)^{0.5}$, referring to Hermance [12]. It can be shown that this relation is not applicable here. In Fig. 3.13 the straight line intersects those particles, whose centers are located in a cylinder of D_o diameter surrounding straight line. Cylinder's volume is $V = \pi x D^2_o/4$. Concentration of particles equals $n = \zeta/(\pi D^3_o/6)$. Then the number of particles in cylinder equals $N = Vn = 3\zeta x/2D_o$. By equating this expression with (3.120), we obtain $D = (2/3)\,D_o$
b). Expression (3.124) for the pyrolysis rate of binder outside the "primary flame", $u^*_f \sim u \exp(-u_f d/2\kappa)$ does not have concrete physical meaning. It was introduced in [38] simply as an example of nonlinear dependence for $u^*_f(d)$.
c). Finally, by comparing the terms describing heat evolution in the balances of heat (3.125) and (3.126) and taking into account that Q_{PF} relies on the unit of mass of reacting mixture, it is possible to draw conclusion that portion f of binder reacts in "primary flame" in stoichiometric ratio, that contradicts determination of f_F in (3.127).

3.5.4. Effect of heat losses into inclusions.

Let us examine combustion of SP based on energetic binder (it can be also inert binder filled with ultrafine oxidizer) capable of relatively fast self-sustaining burning [45]. In this case coarse particles of filler, e.g., oxidizer, metal, etc. become effectively involved in chemical transformations mostly on a rather far distance from the burning surface where they are heated up to the high enough temperature. At the same time, in the vicinity of the leading edges of the flame, which penetrate into binder layer, the relatively cool heterogeneous inclusions play a role of local heat sinks, retarding the burning rate.

Before examining the system with coarse inclusions it is convenient to consider another extreme situation with inert and very fine additive that makes the system quasi homogeneous. If T_* is the temperature of the rate control zone, the heat expenditure to warm up the inert inclusions, with mass fraction Y and specific heat c_{add}, equals $\Delta Q = c_{add} Y(T_*-T_0)$. From physical considerations the effect of ΔQ on the burning rate is the same as lowering [46] the initial temperature by ΔT_0:

$$c_{add} Y(T_*-T_0) = c\Delta T_0 \qquad (3.128)$$

Here c is the mean specific heat of the system. Further, let we consider the known from experiment the burning rate temperature coefficient $\beta = \partial \ln u/\partial T_0$ for the original system (without additives). Then the ratio of the burning rates for the systems with and without additives can be taken approximately in the form:

$$z=u/u_0 \cong 1 - \beta\Delta T_0 = 1 - \gamma Y; \quad \gamma = (C_{add}/c)(T_* - T_0) \qquad (3.129)$$

According to estimations the value of γ for typical AP based formulations is close to unity.

Analysing now the case with coarse size inclusions one may conclude that equivalent decrease in initial temperature has to be smaller than in the case of fine inclusion particles. This is due to less

effective heat exchange between binder layer and coarse inclusions. Thus, it is proposed [45] similar to above expression for z:

$$Z = 1 - \beta\Delta T, \text{ where } \Delta T = \Delta T_0[1 - \exp(-b\kappa\tau/L^2].$$

Here b is the constant, which depends on the conditions of heat exchange; κ is the thermal diffusivity of binder; L is the half of the binder layer width; $\tau = d/u_0$, where d is the inclusion diameter, u_0 is the burning rate of the system without additives. Based on geometrical considerations, the value of L can be estimated approximately as $L = d(\kappa\xi^{-1/3} - 1)$, where ξ is the volume fraction of the inclusions and κ is the constant of the order of unity magnitude. Combination of the above expressions leads to relationship that can be used for treatment of the experimental data on the burning rate variations:

$$\ln [1 - (1-z) / \gamma Y] = - b\kappa/u_0 d(\kappa\xi^{-1/3} - 1)^2 \qquad (3.130)$$

Experimental results were obtained at atmospheric pressure and processed by expression (3.130). The homogenized matrix consisted of AP with size less than 10 micron, rubber and 8% of catalyst was used as fast burning binder. The burning rate of matrix comprised 7 mm/s. Fairly well fitting of the experimental data by expression (3.130) tells in favor of "workability" of the approach under discussion. Actually, all types of additives to the system with fast burning matrix cause retardation of the burning rate because of the common physics of the process, namely, due to heat losses from the combustion zone for "inert" warming up the inclusions material.

The approach described can be partially improved if one calculates $\tau = d/u_0$ using value of actual burning rate u instead of u_0 that may give possibility to predict the combustion limits for the system. In particular, if one uses simplified relationship for z in the form $u/u_0 \approx \exp(-B\kappa\tau/L^2)$ with $\tau = d/u$, the condition for flame quenching takes the form $z^* = e^{-1}$ (according to the experiment [45] $z^* = 0.3$ that is close to this estimation). In addition, it might be useful to take into consideration the temperature distribution inside inclusions and examine the effect of their thermophysical parameters on the burning rate.

CHAPTER 3 - REFERENCES

1. **N. N. Bakhman, A. F. Belyayev**. Combustion of heterogeneous condensed systems. M.: Nauka, 1967.
2. **E. Cohen-Nir**. Combustion Characteristics of Advanced Nitramine- Based Propellants.- 18th Symp. (Intern.) on Combustion., 1981, pp.195-206.
3. **N Kubota**. Combustion Mechanisms of Nitramine Composite Propellants.- Ibid., pp. 187 – 194.
4. **N. Kubota, T. Masamoto**. Flame Structures and Burning Rate Characteristics of CMDB Propellants.- 16th Symp. (Intern.) on Combustion. 1976, pp. 1201-1210.
5. **N. Kubota, T.J. Ohlemiller, L.H. Caneny, M. Summerfield**, 15th Symp. (Intern.) on Combustion, 1975, pp.529-540.
6. **V. A. Strunin, G. V. Manelis**, "Mechanism of the combustion of mixture solid fuels". *Combustion, Explosion, and Shock Waves*, 1979, v. 15, pp. (R) 24-33.
7. **Ya. B. Zeldovich,** To the theory of the combustion of propellants and explosives. In the book: The theory- of the combustion of propellants and explosives. M.: Nauka, 1982, pp- 49-86 (R).
8. **V. A. Strunin, A. N. Firsov, K. G. Shkadinskiy, G. V. Manelis**, "Steady combustion of decomposed and evaporating condensed substances". *Combustion, Explosion, and Shock Waves*, 1977, v.1, pp. (R) 3-9.

9. **V. A. Strunin, A. P. D'yakov, G. B. Manelis,** "Effect of the dispersion of components on the characteristics of combustion of mixture composition". *Combustion, Explosion, and Shock Waves*, 1981, v. 17, pp. (R) 15-20.
10. **B. I. Khaykin**, Author's abstract of Dr. Sci. Thesiss. M.: OIKhF of the AS USSR, 1975 (R).
11. **I. Aoki, N. Kubota,** "Structure of the combustion zone of high and low-energy double base solid propellant". Express-information: Astronautics and rocket dynamics, Moscow, 1981, v. 38, ref. 123.
12. **C. E. Germance,** "A model of composite propellant combustion including surface heterogeneity and heat generation". *AIAA Journal*, 1966, V. 4, No 9, pp. 1629-11637.
13. **M. W. Beckstead, R. L. Derr, C. F. Price,** "A model of composite solid-propellant combustion based on multiple flames". *AIAA Journal*, 1970, V. 8, No 12, pp. 2200-2207.
14. **R.L. Click, J. A. Condon,** "Statistical Analysis of Polidisperse, Heterogeneous Propellants Combustion: Steady State".-13th JANNAF Comb. Meet, CPIA 281, v. 11, pp.313- 345.
15. **M. K. King**, "Model for Steady State Combustion of Unimodal Composite Solid Propellants".-*AIAA Paper*. 78 - 216.
16. **N. S. Cohen, L. D. Strend,** "An improved model for the combustion of AP composite propellants". *AIAA Paper* 81-1553 and AIAA Journal, 1982, V. 20, No 12, pp. 1739-1746.
17. **T. L. Boggs, R. L. Derr, M. V. Beckstead,** "The surface structure of ammonium perchlorate composite propellants". *AIAA Journal*, 1970, V. 8, No 2, pp. 370-372.
18. **E. W. Price, J. C. Handley, R. R. Panyam, et al.,** "Combustion of Ammonium Perchlorate – Polymer Sandwiches", *AIAA Journal*, v.19, No. 3, 1981, pp. 380-386.
19. **N. S. Cohen,** "Review of composite propellant burn rate modeling", *AIAA Journal,* 1980, V.18, No 3, pp. 277-293.
20. **C. Guirao, F.A. Williams**, "A Model for Ammonium Perchlorate Deflagration between 20 – 100 atm", *AIAA Journal*, V. 9, No. 7, pp. 1345-1356, 1971
21. **Beckstead M.W.**, "A Model for Solid Propellant Combustion".- *18th Symposium (International) on Combustion.*, 1981, p.p 175 - 187.
22. **Powling J.**, "Experiments Relating to the Combustion of Ammonium Perchlorate - Based Propellants".- *11th Intern. Combustion Symp.* 1967, p. 447.
23. **N. S. Cohen, R. V. Fleming, R. Derr,** "Role of binders in solid propellant combustion". - *AIAA Journal*, 1974, V. 12, No 2, pp. 212-218.
24. **R. H. W. Waesche, and J. Wenograd,** "The Effects of Pressure and Additives on the Kinetics of Decomposition of Ammonium Perchlorate". *Western States Section/Combustion Inst. Preprint* No. 67-8, San Diego, April 1967, see also *AIAA Paper* 69-145.
25. **N. N. Bakhman,** "The limiting cases of combustion of mixture systems". *Reports of the AS USSR*, 1959, v. 129, pp. 1079-1081 (R).
26. **N. N. Bakhman,** "Survey of the models for the layer systems combustion". In: Rocket propellants. Ed. by Ya. M Paushkin and A. Z. Chulkov. M.: Mir, 1975, pp. 57-73 (R).
27. **Burke S. P Schumann T. F W.**, "Diffusion Flames".- *I - II International Symposium on Combustion*, 1965, pp. 2- 11.
28. **F. A Williams,** Combustion theory. The fundamental theory of chemically reacting flow systems. Second edition. The Benjamin / Cummings Publishing Company,Inc. 1985.

29. **L. K. Gusachenko**, "On the use of Burke-Schumann solution for diffusion flame by description of condensed matters combustion", *Combustion, Explosion, and Shock Waves*, 1985, v.21, No 2, pp (R) 41-45.
29a. **L. K. Gusachenko**. "The effect of diffusion-thermal washing off of inhomogeneities in gas phase of heterogeneous condensed systems". *Proceedings of Workshop on the Gas Flame Structure (1986), part I*, Ed. V.K. Baev, Novosibirsk, 1988, pp.121-127 (R).
30. **Schultz R., Green L., Penner S.S,** "Studies of the Decomposition Mechanism. Erosive Burning. Sonance and Resonance for Solid Composite Propellants". *–III AGARD Colloquim* , 1058, p.367.
31. **Nachbar W., Gline G. B.**, "The Effect of Particle Size and Nonstoichiometric Composition on the Burning Rates of Composite Solid Propellants".- *V AGARD Colloquium*, p.551.
32. **M. W. Beckstead, K. P. McCarty,** "Modeling calculations for HMX composite propellants". *AIAA Journal,* 1982, V. 20, No 1, pp. 106-115.
33. **McCarty K. P. lsom K. B., Jacox J.I.**, "Effect of Formulation Variables on HMX Propellant Combustion".- *15th JANNAF Combustion Meeting*, v.2, CPIA, 297, 1979, pp. 11-12.
34. **McCarty K. P., Beckstead M. W., Isom K. B., Jacox J. I.**, "RDX propellant Combustion".-*16th JANNAF Meeting,* v.3, CPIA, 308, 1979, pp. 269-288.
35. **Beckstead M. W.**, "A Model for Composite Modified Double Base Propellants".- *AIAA Paper*. 82-0355.
36. **Kubota N., Masamoto T.**, "Flame Structures and Burning Rate Characteristics of CMDB Propellants".-*16th Symp. (Intern.) on Combustion*, 1976, pp.1201-1210.
37. **L. I. Shennon, Ye. Ye. Pitersen,** "Characteristic of the combustion of samples made from ammonium perchlorate". *AIAA Journal*, 1964, No 1.
38. **V. K; Shtrale,** "Some statistical considerations in the burning of composite solid propellants". *AIAA Journal*, 1978, V. 16, No 8, pp. 843-847.
39. **M. W. Beckstead,** "Model of double-base propellant combustion". *AIAA Journal,* 1980, V. 18, No 8, pp. 980-985.
40. **Price C. F Boggs T. L.,** *Letter Memorandum* 388-299-79, U. S. Naval Weapons Center, China Lake, CA (Aug. 1979). Inform. on [6].
41. **A. P. Glazkova,** Catalysis of combustion of explosives. M.: Nauka, 1976 (R).
42. **Lengelle G., Brulard G., Monted H.**, "Combustion Mechanisms of Composite Solid Propellants". *16th Symp. (Intern.) on Combustion*, 1976, pp. 1257-1269.
43. **S. S. Novikov, P. F. Pokhil, Yu. S. Kazantsev, L. A. Sukhanov,** "Model of the "permanent transiency" of the combustion zone of the mixture condensed systems". *Journal of applied mechanics and technical physics* (Russian), 1968, v. 3, pp. 128-133.
44. **N. S. Cohen,** *AIAA Paper*, 84-0286.
45. **S. S. Novikov, V. Yu. Potulov, and S. V. Chuiko**, "On interaction of the combustion front of the condensed system with heterogeneous inclusions", Combustion of Condensed Systems, Chernogolovka, 1977, pp. 56-58.
46. **Ya. B. Zeldovich, O. I. Leipunskii, and V. B. Librovich**, "Theory of nonstationary combustion of powder". Moscow, Nauka (Science), 1967.

Chapter 4.

STATIONARY COMBUSTION OF HETEROGENEOUS SYSTEMS WITH POLYDISPERSE COMPONENTS.

Polydisperse compositions contain particles of filler of different sizes. The developments of the combustion models for polydisperse SP is urgent for two reasons. First, ideally monodisperse compositions do not occur in practice, there are compositions with the more or less narrow fractions of filler. Secondly (and this is main thing), polydisperse compositions possess the important advantage for practice because they make it possible to obtain the highest degree of filler loading needed to approach the stoichiometric ratio between the fuel and the oxidizer in the SP formulation and to obtain the maximum specific impulse in the rocket motor.

Theoretical models of solid propellant combustion describing dependence on of burning rate the oxidizer particles size were developed intensely for period of last there decades by the combustion experts throughout the world. In the original works by Manelis and Strunin (see Chapter 3), by Summerfield [1] and Bakhman and Belyayev [2], the initial set of particles was substituted by the conditionally monodisperse powder with a certain characteristic size, determined using the assigned method. This approach made it possible qualitatively to correctly explain the dependence of burning rate on the oxidizer grain size, in particular, an increase in burning rate with the decrease of particle size and saturation of this dependence with the small and large particle sizes.

Named approach proved to be barely effective in description of the laws governing combustion of contemporary SP, which contain, as a rule, several fractions of oxidizer. The demand arose for the development of the more advanced models, which consider the wide collection of the sizes of the oxidizer particles.

4.1. EXTENSION OF THE UTD-MODEL FOR HETEROGENEOUS MIXTURES

It is natural to take account of the polydisperse size distribution by generalization of the monodisperse models using developed methods of averaging the burning rate. It was shown earlier that for UTD-models the averaging is conveniently conducted through the whole area of the burning surface:

$$ms_p = \sum_i (m\ \Delta s_p)_i ; \quad s_p = \sum_i \Delta s_p \tag{4.1}$$

Here m - mean mass burning rate; s_p - area of the plane section of specimen, $(m\Delta s_p)_i$ – "instantaneous" mass flow rate from the i-th particle of filler and portion of binder that occupy the "related" to this particle area on the SP surface with projection $\Delta s_{p,i}$ on section s_p of the initial specimen. Summation is performed through all particles, represented on the surface. Sum expression in (4.1) can be classified into the narrow fractions ΔD_o of the filler particles (here D_o – original diameter of the filler particle, but not its intersection with s_p:

$$ms_p = \sum_j \left(\sum_n m_n \Delta s_{p,n} \right)_j \tag{4.1'}$$

where j - number of the narrow fraction. For fixed j the values of $\Delta s_{p,n}$ are the areas of sections, connected with different sections of the same size particles (fraction j) arrived on the burning surface of AP. In addition, for the equation of the heat balance in condensed phase it is necessary to know analogous sum for the heat flux q into the condensed phase:

$$qs_p = \sum \left(q\Delta s_p\right)_i = \sum_j \left(\sum_n q_n \Delta s_{p,n} \right) \tag{4.2}$$

In order to switch over to the distribution functions, we may formally use that introduced by Glick and Condon [3] concept of pseudo-propellant. For this end let us call the set of surfaces $\Delta s_{p,n}$ from internal sums (4.1) and (4.2), relating to the j-th narrow fraction of filler, as the surface of the j-th pseudo-propellant:

$$\sum_n \Delta s_{p,n} = \Delta s_{p,n} \tag{4.3}$$

and let us represent internal sums themselves in the form

$$\left(\sum_n m_n \Delta s_{p,n} \right)_j = m_j \Delta s_{p,j}, \tag{4.4}$$

$$\left(\sum_n q_n \Delta s_{p,n} \right)_j = q_j \Delta s_{p,j} \tag{4.4'}$$

Further, let us call values of m_j and q_j as the mass burning rate and heat flux into the condensed phase for the pseudo-propellant related to the narrow filler fraction j.

The prefix "pseudo" indicates, first of all, that the discussion deals with the complex geometry part of SP, mentally isolated in the bulk of the specimen. Besides, one should keep in mind that depending on the method of distributing the binder between the fractions of oxidizer it may happen that some fractions (with largest grains) "obtain" too little binder. When taking such fraction and "related" to this fraction binder, we may not be able to manufacture real solid propellant because of the lack of binder: the SP will contain many voids. Area $\Delta s_{p,j}$ can be presented in the form [3]

$$\Delta s_{p,j} = \Delta s_{p\,ox,j} / \zeta_j,$$

where $\Delta s_{pox,j}$ - area of plane section occupied with the j narrow filler fraction (j pseudo-propellant. The above expression can be rewritten in another form keeping in mind that the "surface" fraction ζ_j equals the volume fraction $\zeta(D_0)$ of oxidizer in pseudo-propellant j

$$\Delta s_{p,j} = \frac{\Delta s_{p\,ox,j}}{s_{p\,ox}} \frac{s_{p\,ox}}{s_p} \frac{s_p}{\zeta_j}$$

where s_{pox} - total cross-sectional area occupied with oxidizer. Similarly, it is possible to replace $s_{pox}/s_p = \zeta$; ζ - volume fraction of oxidizer for entire composition. Assuming chaotic particle distribution one obtains $\Delta s_{pox,j}/s_{pox} = \Delta V_{ox,j}/V_{ox}$ since the "surface" fraction of the j-th oxidizer fraction in the plane section of initial specimen is equal to its volume fraction. If the oxidizer of the same material is used, then the volume fraction is equal to the mass fraction $\Delta M_{ox,j}/M_{ox}$. Then after passage to the limit $\Delta D_0 \rightarrow 0$ it follows from (4.1):

$$\frac{m}{\zeta} = \int_{-\infty}^{+\infty} \frac{m(D_0)}{\zeta(D_0)} F(D_0) d \ln D_0 \tag{4.5}$$

Here $m(D_0)$, $\zeta(D_0)$ - m and ζ for the pseudo-propellant with the size of particles D_0; $F(D_0)$ - distribution function:

$$F(D_0) = \frac{1}{M_{ox}} \frac{dM_{ox}(D_0)}{d \ln D_0} = \frac{1}{v_{ox}} \frac{dv_{ox}(D_0)}{d \ln D_0} \tag{4.6}$$

For the only fraction of oxidizer the function $F(D_0)$, as a rule, is described well by the logarithmically normal distribution function

$$F = \frac{1}{\sigma\sqrt{2\pi}} exp\left[-\frac{1}{2}\left(\frac{\ln D_0 - \overline{\ln D_0}}{\sigma} \right)^2 \right] \tag{4.7}$$

If in the propellant one has several fractions of oxidizer of the same nature $M_{ox} = \sum_k M_{ox,k}$, then

$$F = \sum_k (M_{ox,k} / M_{ox}) F_k \tag{4.8}$$

where F_k is determined by (4. 6) with coefficients σ_k, $\overline{(\ln D_0)}$. To find the entering into (4.5) term $\zeta(D_0)$, let us assume according to [3], that the mean volume of the binder, which burns together with the particles of diameter D_o, is equal to $\Delta v_b = CD_0^n$, where n is taken from experiment ($2 \leq n \leq 3$). Value of C depends on the formulation of the propellant (see below). Then, regarding to definition of $\zeta(D_0)$, one obtains

$$\zeta(D_0) = (\pi D_0^3 / 6) / [(\pi D_0^3 / 6) + CD_0^n] = (1 + (6C / \pi) D_0^{n-3})^{-1} \tag{4.9}$$

Let us find value of C from the condition

$$1 - \zeta = \int \Delta v_b(D_0) dN \tag{4.10}$$

Here $(1-\zeta)$ - the volume of binder in 1 cm^3 of propellant; dN - number of the particles of oxidizer with size in the range between D_0 and D_0+dD_0 in 1cm^3 of propellant, $dN = dv_{ox}/(\pi D_0^3/6)$. The value of dv_{ox} can be taken from (4.6), setting there $v_{ox}=\zeta$ (per unit of volume of propellant). Then

$$1-\zeta=\int_{-\infty}^{+\infty} CD_0^n \frac{F(D_0)}{\pi D_0^3/6} d\ln D_0,$$
$$C=\frac{\pi}{6}\frac{1-\zeta}{\zeta}\left(\int_{-\infty}^{+\infty} D_0^{n-3} F(D_0) d\ln D_0\right)^{-1} \tag{4.11}$$

In the original work of Glick and Condon [3] the total heat balance in condensed phase was not used. Expression for the mean heat flux can be derived similarly to that how it was derived (4.5):

$$\frac{q}{\zeta}=\int_{-\infty}^{+\infty}\frac{q(D_0)}{\zeta(D_0)} F(D_0) d\ln D_0 \tag{4.12}$$

Expressions (4.5) and (4.12) for m and q are obtained without specific assumptions about physics of process (it is postulated only randomness of particle distribution in SP) and therefore are always valid. Since in (4.1) the value $(m\Delta s_p)_i$ has a meaning of the mass flow rate (without indication of the phase state) from the surface of SP, which corresponds to area $\Delta s_{p,i}$ of the plane section of specimen, expression (4.5) remains correct upon the dispersion of the part of the filler and binder.

Let us stress the formal character of definitions (4.4) and (4.4)' for entering in (4.5) and (4.12) the burning rate $m_j = m(D_o)$ and heat flux $q_j = q(D_o)$ for the pseudo-propellant related to the size of particles D_o. The averaging in (4.4), (4.4)' is conducted through surface $\Delta s_{p,j}$ of the j-th pseudo-propellant, which consists of the scattered over section s_p of specimen small aria "patches" $\Delta s_{p,n}$. In fact, the averaging of the heat flux by (4.4) even under conditions of UTD-models ($D<<\kappa u$) does not have its physical analog - the smoothing of the heat fluxes in the condensed phase near the burning surface.

In concrete UTD-models, when describing the polydisperse version, entering in (4.5) and (4.12) values of $m(D_0)$ and $q(D_0)$ are calculated with utilization of monodisperse version.

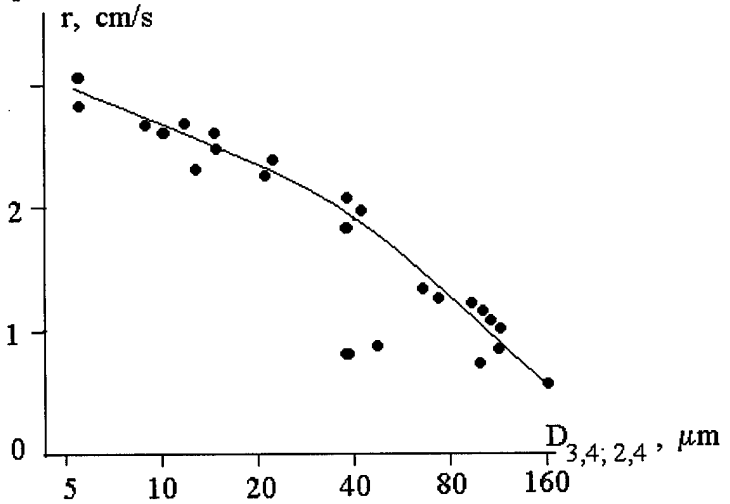

Fig. 4.1. Dependence of burning rate on filler particle size distribution [8].

Most simply account of polydisperse size distribution appears in the Hermance model [4] (monodisperse version see in Section 3.3.1). Connected with one particle of oxidizer the mass flow rate from the condensed phase and the heat feedback from the gas phase according to (3.22), (3.25), (3.27) linearly depend on $D_c\,\varepsilon(D_c)$, where $\varepsilon(D_c)$ - depth of the binder depression near the crystal of the oxidizer (see Fig. 4.1); D_c - diameter of the section of initial crystal (without taking into account its burning) by the plane of binder. Therefore needed for calculation of $m(D_o)$ and $q(D_o)$ averaging by (4.4) and (4.4)' is reduced to the averaging of the value $D_c\,\varepsilon(D_c)$ over the sections of the particles of the pseudo-propellant, related with size of D_o of particles. In Ref. [4] this operation is substituted by the calculation of known function $D_0\,\varepsilon(D_0)$ at $D_c = D_0\sqrt{2/3}$. In this case the use of "polydisperse" expressions (4.5), (4.12) for. m and q is reduced to the fact that the following integral, is substituted into the balances (3.22), (3.27) of mass and heat instead of the average for the oxidizer mono-fraction expression $< D_c\varepsilon(D_c)>$,

$$\overline{\langle D_c \cdot \varepsilon(D_c)\rangle} = \int_{-\infty}^{+\infty} \langle D_c \cdot \varepsilon(D_c)\rangle F(D_0) d\,ln\,D_0 \tag{4.13}$$

In the model of Hermance there is no need to define the method of distributing the binder between the particles of oxidizer. Therefore for the pseudo-propellants it is possible to take, for example, $\zeta(D_0)$= const = ζ, and it becomes clear by what manner the utilization of (4.5) and (4.12) with the linear dependence of $q(D_0)$ and $m(D_0)$ on $< D_c\,\varepsilon(D_c)>$ gives (4.13). In Ref. [4], function $F(D_0)$ is taken in the form close to the expression of (4.8) type for two logarithmically normal distributions, and instead of integral (4.13) two sums are used.

Cohen's survey [5] reported about polydisperse versions of the BDP model. It is assumed that the binder on the entire SP surface has identical temperature T_{sf} and the burning rate m_f. The burning surface of binder is plane. For the oxidizer corresponding values T_{sox} and m_{ox} depend on the size of particles D_0. In this case instead of (4.5) one may use equivalent expression (4.14), which depends only on the burning rate of the oxidizer:

$$\alpha m = \int_{-\infty}^{+\infty} m_{p\,ox}(D_0) F(D_0) d\,ln\,D_0 \tag{4.14}$$

Here α - mass fraction of oxidizer; $m_{p\,ox}= m_{ox}(D_0)s_{ox}(D_0)/s_{pox}(D_0)$ - mean mass flow rate 1 cm^2 of that part of the plane section of specimen, which is occupied with the narrow oxidizer fraction of the particles size D_0. Values of $m_{ox}(D_0)$ and $s_{ox}(D_0)/s_{pox}(D_0)$ are calculated, as in the original BDP model, by (4.30) and (4.47). However, for temperature $T_{sox}(D_0)$, which determines according to (4.30) the value of $m_{ox}(D_0)$ separate balances of heat are used for each narrow oxidizer fraction (and one additional balance of heat for the binder). Total mean heat flux in the form of (4.12) is not used.

Actually, polydisperse versions of the BDP model can be treated as generalization for several oxidizer fractions of two-temperature "improved model" presented in chapter 3. Limited number (3-4) of the narrow fractions is used; therefore, instead of integral (4.14) sums are examined. The

redistribution of heat fluxes between each fraction and binder is considered only in the gas phase, as in the "improved model". The direct interaction of fractions (redistribution of heat fluxes) in the published versions of models is not considered.

If utilization of separate heat balance can be considered as the first step in direction of isolation of pseudo-propellants, then the "petite ensemble" model [3] reached the logical end by postulating complete independence of burning of pseudo-propellants.

For calculating the burning rate it is proposed [3] to use relationship (4.5), calculating the value $\zeta(D_0)$ on the basis of (4.9) and (4.11), and the burning rate of pseudo-propellant $m(D_0)$ - on the basis of presented in Chapter 3 model "petite ensemble" for the monodisperse composition with the size of particles D_0 and the volume fraction of oxidizer $\zeta(D_0)$.As it is reported in survey [5], the model [3] gives reasonable agreement with the experiment only in the case of not too strongly distinguished sixes of the oxidizer grains of different fractions.

4..2. EXTENSION OF THE "RELAY RACE" TYPE MODELS

The combustion model [7] gives example of polydisperse version of the "relay race" approach. We will enumerate here its differences from the described in Chapter 3 monodisperse version. Expression for the burning rate instead of (4.14) takes the form

$$u = x / \Sigma t_i \tag{4.15}$$

where t_i - transit time of the combustion wave passing through the encountered on the way particles of the i-th narrow oxidizer fraction and the "related" to them binder. Correspondingly, expression (3.121) is transformed into the following

$$1/u = \sum_i \left[t_{ign,i} \cdot (\zeta_i / D_i) + (\zeta_i / u_{0i}) + \chi_i \left(f_i / u_g + (1 - f_i) / u_{gi}^* \right) \right] \tag{4.16}$$

Here ζ_i - volume fraction of the propellant, occupied with the binder, "related" to i-th fraction of oxidizer. In all "primary flames" the burning rate of the burn out of binder u_f is assumed as identical. The balance of heat for the i-th fraction of oxidizer differs from "monodisperse" balance (3.125) only in terms of the fact that all the values entering it (except for c, T_0 and $(f/ox)_{stoich}$ obtained index i. The heat balance for the binder takes form (4.17))

$$c(T_{sf} - T_0) = -f_{rb} Q_f + \sum_i (1 - \beta_{pi}) f_i \left(1 + (g/o)_{steih}^{-1}\right) Q_{PFi} \exp(-\xi_{PFi}) \tag{4.17}$$

where $f_{rb} = \sum_i f_i$ - portion of the binder, which reacts in all "primary flames". Model is proposed for a number of the narrow fractions not exceeding three. Limitation is caused by the necessity to solve a bulky system of equations in connection with the utilization of a balance of heat for each narrow fraction.

Let us show that the equation (4.16) can be easily generalized by analogy with [3]. Actually, by examining an increasing number of the narrow fractions, one obtains

$$\zeta_i \to \frac{dv_{ox}(D_0)}{v} = \frac{dv_{ox}(D_0)}{v_{ox}} \frac{v_{ox}}{v} = \zeta F(D_0) d\ln D_0 \tag{4.18}$$

Here v - volume of specimen, the function of particle size distribution $F(D_0)$ is introduced according to (4.6). Analogously, it can be derived

$$\chi_i \to \frac{dv_b(D_0)}{v} = \frac{dv_b(D_0)}{dv_{ox}(D_0)} \frac{dv_{ox}(D_0)}{v},$$
$$\frac{dv_b(D_0)}{dv_{ox}(D_0)} = \frac{CD_0^n}{\pi D_0^3/6} = \frac{6C}{\pi} D_0^{n-3} \tag{4.19}$$

where $dv_b(D_0)$ - volume of binder, "related" to narrow oxidizer fraction with the particle size from D_0 to D_0+dD_0. Multiplier C is calculated by (4.11).

Now expression (4.16) takes the form

$$1/u = \zeta \int_{-\infty}^{+\infty} \left(\frac{1}{u(D_0)} + \frac{t_{ign}(D_0, u(D_0))}{(D_c)_{mean}} \right) F(D_0) d\ln D_0 + (1-\zeta) \left(\frac{f}{u_g} + \frac{1-f}{u_g^*} \right)_{mean},$$
$$(D_c)_{mean} = \frac{2}{3} D_0, \tag{4.20}$$
$$\left(\frac{f}{u_g} + \frac{1-f}{u_g^*} \right)_{mean} = \left[\int_{-\infty}^{+\infty} \left(\frac{f(D_0)}{u_g} + \frac{1-f(D_0)}{u_g^*(D_0)} \right) F(D_0) D_0^{n-3} d\ln D_0 \right] / \int_{-\infty}^{+\infty} F D_0^{n-3} d\ln D_0$$

Calculations according to the "relay race" model showed that with the high degree of SP loading the dependence of burning rate on the granulometric composition (ratio of fine to coarse fractions) becomes weak. It was revealed that the finest fraction of octogen determines the value of the burning rate, if its fraction mass comprises more than 25% of entire oxidizer. It was also noted that the catalysts weakly affect the burning rate. This is explained by the fact that catalysts of the used type accelerate the reactions of primary flame, but for the octogen it is relatively cold in comparison with its mono-fuel flame.

The listed results, obtained by calculation, are confirmed by experiment. It is reported in Ref. [7] that the experiments were conducted for 17 different SP containing octogen and the binder HTPB. The octogen particles with size of 400, 200, 58 and 4 μm in different ratios were introduced in SP formulations. Pressure varied from 28 to 120 atm. Results of calculations qualitatively and quantitatively agreed with the experiments.

4.3 COMBUSTION OF THE MIXTURES WITH DIFFERENT OXIDIZER GRAIN SIZE

The model which considers interaction of oxidizer particles with strongly distinguished sizes. is presented in the appendix to Ref. [6]. In basic part of the work the authors applied for describing the combustion of polydisperse compositions their "improved model", based on the BDP model. In this case the separate balances of heat for the oxidizer and the binder and different surface temperatures for these components were used. The mass burning rate was determined through the

pseudo-propellant according to the "petite ensemble" approach [3]. It was obtained a good agreement with the experiment for the formulation based on bimodal AP (82% of AP, 1μm/7μm = 1/2; 80% of AP, 9μm/90μm = 1/1; 82% of AP, 90μm/200μm = 1/5). However, for the formulation with the very strongly distinguished AP fractions (70% of AP, 0.6μm/400μm = ¾; 18% Al; CTPB binder) calculated burning rate proved to be 3 times higher than experimental one. Aluminum was considered in calculation as an inert additive (heat sink). The authors of [6] noted that the better agreement can be succeeded if in expression for the burning rate to neglect by the contribution of the pseudo-propellant, which corresponds to the fine oxidizer fraction.

Analyzing reasons for disagreement, the authors of [6] conclude that if binder is prorated to the surface areas of corresponding oxidizer fractions (which acknowledges as reasonable assumption), then pseudo-propellants, related to the fine fractions of oxidizer, prove to be enriched by fuel, and those related to the coarse oxidizer fractions - depleted by fuel.

As a result, both pseudo-propellant types have a temperature of flame considerably lower than with the stoichiometric ratio of components, whence follows sharply decreased burning rate of SP. Opposite effect is obtained if we take the proposition of Beckstead [7]: for any ratios of fuel the temperature of flame to consider maximally possible, and namely, the same as for the stoichiometric ratio. The reason for such proposition is that precisely these temperatures are reached at the front of purely diffusion flame. The deviation of the ratio of components from the stoichiometric affects, according to Beckstead, only the height of the flame.

Concerning results of analysis of question about temperature of flame the authors of [6] drew a conclusion about insufficient validity of both approaches and proposed new one. For the formulations containing several narrow fractions of oxidizer, which are sharply distinguished by the particle sixes, the concept of modified pseudo-propellants connected with these fractions is introduced. Pseudo-propellants in Cohen-Strand radically differ from the pseudo-propellants in Glick-Condon. Thus, according to Glick-Condon the SP consists of the system of independently burning pseudo-propellants, but according to Cohen-Strand the SP with fractions of oxidizer strongly distinguished by the particle size is comprised of the series of "those inserted" one in another of pseudo-propellants. In this case for each subsequent pseudo-propellant the preceding one (connected with the finer oxidizer fraction) serves as the active binder. Initial pseudo-propellant consists of oxidizer of the finest fraction and entire binder. (*To be more accurate, almost entire. According to Ref. [6], the binder is divided between the fractions proportional to their surface. For example, in the composition with the fractions of AP 0.6μm/400μm = 3/4 the binder is divided between the fractions in the ratio (3/0.6)/4/400) = 500/1*). The latter pseudo-propellant coincides with the propellant incomplete formulation.

Thus, the pseudo-propellant connected with given fraction of oxidizer can be in complete manufactured, if from the prepared for the mixing components to retract the coarsest (larger than given size) fractions of oxidizer. The temperature of flame for each pseudo-propellant is determined by thermodynamic calculation by its composition. For each of the pseudo-propellants, that comprises finally the SP formulation, the ratio fuel/oxidizer is not less than that for the whole SP (there are no pseudo-propellants with the temperature of flame, which is sharply reduced due to the strong excess of oxidizer).

The interaction of the flames of different pseudo-propellants is considered in the following way. According to the "improved model" with its separate balances of heat for the oxidizer and the binder it is possible to calculate for a given pseudo-propellant which part of the heat from its flame falls to the appropriate active binder, i.e., to the pseudo-propellant of the lower rank.

For the mentioned composition with distribution of AP onto fractions of 0.6μm/400μm = 3/4 the burning rate was calculated according to "improved model" taking into account the fact that the binder and AP fraction of 0.6μm together are active binder for the AP fraction of 400 μm. Calculation demonstrated a good agreement with the experiment.

It should be noted that idea of a pseudo-propellant as an active binder analog has been discussed previously by Bakhman and Belyayev [1]. They examined a possibility of use of the of "relay race" type model (when the burning rate of the oxidizer crystals of coarse fraction is more than the burning rate of active binder). It was also examined the contradictory version, when active binder burns more rapidly. However, their approach did not include interaction between the flames of coarse oxidizer and active binder.

4.4. DISCUSSION OF THE COMBUSTION MODELS FOR HETEROGENEOUS CONDENSED SYSTEM.

Models of combustion of polydisperse SP are constructed on a basis of monodisperse models and therefore they absorb all the complexities and contradictions, noted in preceding Sections. The difficulties can only be aggravated due to strengthening of the heterogeneity of the parameters on the burning surface of SP containing polydisperse filler.

Polydisperse versions of UTD-models and "relay race" type models are discussed below. Presented in survey [5] polydisperse versions of the models of Beckstead and Cohen, and also (especially) the model of Glick and Condon have essential deficiency. Thus, in the models of Beckstead and Cohen different fractions of oxidizer interact only through the gas phase [5].

In this case part of the heat of "primary flames" is delivered to the binder. In the model of Glick and Condon the interaction is not considered at all: the pseudo- propellants, connected with different fractions of oxidizer, burn completely independently.

At the same time these models use balances of heat for different fractions of oxidizer or for different pseudo- propellants, which is admissible only with $D_0 << \kappa/u$, i.e., within the framework of UTD-models. Using in the mentioned balances of heat a concept of mean temperature of surface and mean heat flux, we thereby assume redistribution in the condensed phase (near the surface) of the heat flux, which enters the condensed phase. However, this redistribution between the particles of the chosen narrow fraction or between scattered in the volume of SP pieces of the chosen pseudo-propellant is simply impossible without the interaction in the condensed phase with their other ambient medium.

Obviously, within the framework of UTD-models there is need for account of introduced by the filler polydisperse size distribution the non-uniformity of parameters across the SP surface (temperature, heat flux from gas phase, curvature, etc.). In particular, this can be done as follows: to

separate in the condensed phase near the surface of SP the layer with a thickness of ~ max(D_0), that has the bent interface with the gas phase and plane interface with the remaining volume of sample. On the plane boundary it is possible to use balance of heat total for entire sample taking into account an expression of type of (4.12) for the heat flux. For the chosen layer one must solve complex (multi-dimensional) problem about the redistribution of heat fluxes; however, it is possible to hope that in this case the account of the relatively small thickness of this layer max $D_0 << \kappa/u$ will result in some simplifications.

Coming to discussion of "relay race" model [7], we may note that its polydisperse version does not contain errors, introduced upon consideration of different particle size. It is presented in Section 3.5.2 the monodisperse version the assumption was used about independent burn out of different (including those adjacent) particles of filler and interlayers of binder, which lay on the same normal to the burning surface of sample (see Fig. 3.13). Therefore, the introduction of different particle sizes did not introduce additional contradictions. Only deficiencies in the monodisperse version of the model can be recognized, and the main of them – non-consistency between the method of averaging over time, giving the greatest effect with $D_0>>\kappa/u$, and calculation of "local" burning rate by the BDP model mostly efficient with $D_0<<\kappa/u$.

There are, however, "favorable" circumstances. First of all, the main thing in the Beckstead model is the method of averaging along normal to the surface of combustion. It can be combined with any model of the combustion of single particles, including those with particles interaction. Secondly, the BDP model that was not designed for the application in the case of a thin preheated layer (since it uses the heat balance, based on the averaging of heat fluxes over the surface, to which the real process must correspond of redistributing the heat in a thick preheated layer), may give accurate result because with a thin preheated layer an oxidizer burns with its actual speed. Therefore, at least for thin preheated layers the BDP model is not contradictory.

"Pseudo-propellant" model, proposed by Bakhman, Belyayev [1] and elaborated in detail by Cohen, Strand [6], is extremely useful, although it is applicable mainly to compositions with oxidizer fractions very strongly distinguished by particle size. In the model [6] the main disadvantage in the widespread model of Glick-Condon is reduced, namely, the independence of the combustion of pseudo-propellants. The idea of the "inserted" pseudo-propellants possesses the sufficient generality: the burning rate of each pseudo-propellant can be calculated not compulsorily by the "improved model" or other model of the BDP type with the averaging of burning rate over the surface. It is completely admissible here the application of "relay race" models (especially for the pseudo-propellants, related to the coarsest oxidizer fractions).

Let us demonstrate application of "pseudo-propellant" model [1, 6] for explanation of one experimental finding (Miller's experiments [8].) The burning rate of 29 nonmetalized compositions was determined for seven different pressures (from 0.7 to 200 atm). Nature and overall content of binder and oxidizer (AP) in all compositions were identical, the ratio of AP fractions was changed only. The fractions of particles 400, 200, 90, 50, 20, 6, 2 and 0.7 μm were used.

It was reported that with accuracy not less than 15% the data of experiment coincide with the results of calculation according to the modified BDP model and according to the Glick-Condon model. It proved to be that at fixed pressure all experimental data (for 25 compositions with es-

sentially distinguished distribution of AP) with good accuracy can be fitted by one curve in coordinates u (burning rate) and characteristic size $d_{3,4;2,4}$:

$$d_{3,4;2,4} = \left(\sum_i n_i d_i^{3,4} \right) / \sum_i n_i d_i^{2,4}$$

where n_i – number of particles, which have diameter d_i. Summation is performed over all i-numbers.

However, data on four formulations with coarse AP fraction (400 μm) did not correspond to general dependence (Fig. 4.1). In these formulations the content of coarse fraction comprised more than half of the mass of entire oxidizer, and the ratio of fine fractions was sharply different, so that value $D_{3,4;2,4}$ for these four compositions was substantially different (see Fig. 4.1). Nonetheless the rate of combustion virtually coincided for these four compositions, as if fine AP fractions did not give a contribution to integral (4.5). Miller considers that "the combustion of fine AP fraction was suppressed", and focuses attention on uneven (with the increase of the portion of the coarse AP fraction only by 2%) character of the burning rate behavior. Data of Miller agree with the results calculations by Cohen, Strand [6] (see Section 4.1.3 for SP, containing 70% of AP; 0.6μm/400μm = 3/4; 18% Al, and binder CTPB). The agreement of calculations by the Glick-Condon model with Miller's experiment in this particular case was reached only after disregarding contribution from pseudo-propellant corresponding the finest AP fraction. It was reported in Ref. [7] that SP based on octogen and binder CTPB also exhibit weak dependence of the burning rate on the ration of the filler fractions.

CHAPTER 4 REFERENCES

1. **N. N. Bakhman, A. F. Belyayev,** Combustion of the heterogeneous condensed systems. Moscow, Nauka, 1967.
2. **M. Summerfield, G. S. Suterland, M. J. Webb, et al.**, "The Burning Mechanism of Ammonium Perchlorate Propellants", *ARS Progress in Astronautics and Rocketry*, V.1,: Solid Rocket propellant Research, Academic Press, New York, 1960, pp. 141-182.
3. **Glick R.L., and Condon J. A.**, "Statistical Analysis of Polydisperse, Heterogeneous Propellant Combustion: Steady State".- *13th JANNAF Combustion Meeting*, CPIA. 281, v.11, Dec.1976. p. 313 - 345.
4. **C. E. Hermance**, "A Model of Composite Propellant Combustion Including Surface Heterogeneity and Heat Generation", *AIAA Journal*, V. 4, 1966, pp. 1629-1637.
5. **N. S. Cohen**, "Review of Composite Propellant Burn Rate Modeling", *AIAA Journal*, V. 18, No. 3, 1980, pp. 277-293.
6. **N. S. Cohen, L. D. Strand,** "An improved model for the combustion of AP composite propellants". *AIAA Paper* 81-1553.
7. **M. Beckstead, K. P. McCarthy,** "Modeling calculations for HMX composite propellants", *AIAA Paper* 80-1116
8. **Miller R. R**, "Effects of Particle Size on Reduced Smoke Propellant Ballistics". -*AIAA Paper*, 82-1096.

Chapter 5.

COMBUSTION OF METAL IN SOLID PROPELLANTS

Interest to metals as the potential components of rocket propellants arose at the dawn of rocket era due to the great heat release from the reaction of metal oxidation, which exceeds substantially that of the reaction of usual hydrocarbon fuels. This provides a higher temperature of combustion products and thus a higher SP efficiency in a rocket motor.

According to the pioneer calculations published in Russia in 1929 [1] boron and lithium are most preferable with respect to heat release upon combustion in oxygen. The later investigations performed in the area of chemical thermodynamics showed [2] that more heat is released by combustion of either beryllium in oxygen or lithium in fluorine. Note that the oxygen, interacting with metals, fails to give the maximum heat release. Actually, most effective oxidizers are fluorine monoxide, then fluorine, trifluorine nitrogen, ozone, and only then oxygen. The best fuels are lithium, beryllium, boron as well as aluminum and magnesium (boron belongs to metals by convention). The above sequence of the efficiency of fuels corresponds to the reaction heat per 1 g of metal. The various aspects of metal combustion in rocket propellants have been considered in excellent reviews [4,5], paper collections [6,2] and textbooks [7,8]. Below, the general principles of metallic particle combustion and the problems of combustion of the widely used metals: aluminum, magnesium, and boron are reported. Further the agglomeration of a metal and its transformation upon combustion are also discussed.

5.1. PHYSICAL PRINCIPLES OF METAL COMBUSTION

Unlike liquid droplets of hydrocarbon fuel, the combustion of metallic particles exhibits a great variety of mechanisms because, as a rule, the initial metallic particle is covered with oxide layer. In addition, the various combinations of oxide and metal characteristics, e.g., the temperatures of melting, boiling and solubility determine the variety of combustion mechanisms. A characteristic feature of the series of metals enclosed in the class of metals with nonvolatile oxide (e.g. aluminum, beryllium, titanium, zirconium) is the oxide refractory nature. For these metals the heat of oxide gasification exceeds the chemical energy released by the metal-oxygen reaction [8]

$$\Delta H_{vap\text{-}dissoc} > Q_R - (H^o_{T,vol} - H^o_{298}) = \Delta H_{avail} \qquad (5.1)$$

where $\Delta H_{vap\text{-}dissoc}$ is the evaporation-dissociation heat of metallic oxide; $(H^o_{T,vol} - H^o_{298})$ is the enthalpy spent to heat oxide up to the boiling temperature; Q_R is the heat of metal-oxygen reaction at standard temperature 298 K. Equation (4.1) shows that when the reaction products are in the gaseous state, the oxidation is endothermic and the self-sustaining (stationary) combustion becomes impossible. It is also seen that up to the boiling temperature (dissociation temperature) there is no gaseous metal oxide in the reacting system.

According to Eq. (5.1) the maximum flame temperature for the metals with a refractory oxide is limited to the boiling temperature of oxide. The stationary combustion occurs at lower temperature giving rise to the condensed oxide, which is necessary for the process to occur. The combustion of metals may occur either in the vapor phase or due to heterogeneous oxidation. Obviously,

for the vapor-phase combustion it is necessary to heat the metal to the temperature close to its boiling temperature that is high for many metals. According to Glassman's criterion, "for a metal to burn as a vapor, the oxide volatilization temperature must be greater than the temperature of the metal boiling point"[8]. Account must be taken of the fact that at high temperatures oxide decomposes (partially or completely) and the "boiling point" of the oxide corresponds to the temperature at which the condensed oxide is in equilibrium with the ambient gas containing the products of its decomposition. In this case, the "boiling point" is sure to change with the chemical composition of ambient gas but may be readily calculated for a fixed composition and pressure of the gas. This significant refinement of the concept of "boiling point" for liquid oxide was underlined in [9], criticizing the false claim [10] that the vapor-liquid oxide equilibrium can be calculated neglecting chemical transformations.

The up-to-date classification of the combustion regimes of metals is presented in [5]. As mentioned above, the main distinctive feature used in the classification of the combustion modes of metals is the oxide (oxidation product) volatility. The second property is the volatility of the metal. Finally, the third feature is the oxide solubility in the metal. It is interesting that the three metals analyzed are referred to the different sections of a given classification. Thus, aluminum is characterized as a nonvolatile metal with nonvolatile and insoluble oxide while boron is characterized as the "metal" with volatile and soluble oxide.

It should be taken into account that, in fact, the combustion mechanism may depend not only on the physical properties but also on the geometrical dimensions of metallic particles. It has been shown [5] that the combustion behavior differs for "small" and "large" particles, in particular, for volatile metals. In this case, the size limit is about 50 μm. It is assumed that the small particles are less prone to oxide coating formation and burn mainly in the vapor-phase regime. The relative values of the boiling and melting points of metals and oxides also have effect on the combustion mechanism. Remember that the boiling temperature depends on pressure and gas composition of the environment. In particular, the early melting of metals (most known metals) may lead to either the break or dissolving of oxide skin and the early oxide melting (boron, tungsten) may cause the non-coating of particles which allows oxygen to reach the metal.

Metal heating and oxidation are related to two important parameters, characterizing the protective properties of the oxide skin. The first parameter is the relationship between the coefficients of thermal expansion of solid metal and oxide. When their ratio exceeds unity, the oxide skin cracks upon heating. The second parameter is the relationship between the molar volume of solid oxide and constituent metal, i.e. the oxide skin porosity. This relationship is calculated by the formula below (the Pilling-Bedworth coefficient):

$$\beta = (\rho_{me}/nA_{me})(\rho_{ox}/M_{ox})^{-1}$$

In this case ρ_{me} and ρ_{ox} are the metal and oxide densities, respectively, n is the number of metal atoms in the oxide molecule; A_{me} is the atomic mass of the metal; M_{ox} is the molecular mass of the oxide. It is known that if $\beta<1$, the oxide skin is porous, and the metal interacts with oxygen even at a relatively low temperature. When $\beta >> 1$, e.g., $\beta=3$, the oxide skin is subjected to significant inner stresses, and does not actually prevent metal oxidation. The best protecting properties are observed for oxide skins with $\beta=1.5$ (e.g., for aluminum $\beta=1.45$).

A peculiarity of the combustion of metallic particles in solid propellants lies in the fact that the temperature conditions and their residence time in the combustion wave are induced independently due to the combustion of other propellant components. These conditions are often unfavorable for metal ignition and effective combustion. Indeed, the burning surface temperature of most solid propellants is substantially lower than the melting temperature of the metals used which prevents their ignition and leads to the accumulation of metal on the burning surface. Under these conditions the metallic particles on the burning surface merge to form rather large "agglomerates" that need much time to burn out. Actually, the combustion of metals in solid propellants only starts either on or near the burning surface and ends some time later in the flow of combustion products leading to the effects of distributed combustion.

5.2. COMBUSTION OF METALLIC PARTICLES UNDER FIXED CONDITIONS

Laboratory experiments under well-characterized and controlled conditions with a minimum number of variable factors are of great importance in understanding metallic particle combustion. These experiments involve single metallic particles heated by hot gas, laser or hot plate. Below we give the experimental and theoretical results of a study of combustion of aluminum, magnesium, and boron particles. Most attention is paid to aluminum as it is most studied and is widely used in solid propellants.

5.2.1. Aluminum

Physical properties

As has been mentioned above, Al belongs to the class of nonvolatile metals with a nonvolatile oxide. The physical characteristics of Al and its stoichiometric oxide are listed below in Table 1.

Table 5.1. Physical properties of Al and Al_2O_3.

Property	Al	Al_2O_3
Melting temperature, K	933[4]	2320[4]
Temperature of boiling, dissociation, K	2791[8]	4000[8]
	2750[4]	3253[4]
Latent melting heat, cal/g	96[2]	
Evaporation, dissociation heat, cal/g	3050[2]	4358[8]
Heat of formation, cal/g		-3927[8]

The partial pressure of Al vapor is 5.2×10^{-7} mm Hg for $T = T_{melt.}$(933K) and 1 mm Hg at 2150 K. The aluminum oxide has two crystal modifications: α(corundum) with a rhombohedral lattice and γ(alumina) with a cubic face-centered lattice. The α-Al_2O_3 density is 3.96 g/cm^3, that of γ-Al_2O_3 is 3.42 g/cm^3. The oxide porosity (the Pilling-Bedworth criterion) is 1.45 that determines its high protective properties. Under fast heating of Al to 770 K the amorphous oxide skin is formed on its surface and the heating to higher temperatures gives mixture of amorphous oxide and γ-Al_2O_3.

Peculiarities of the combustion mechanism

In [13-16] the combustion of individual aluminum particles has been studied at atmospheric pressure in the flow of hot oxidative gas with variable composition created either using a gas burner or by combustion of a metal-free propellant charge. The luminosity and image of burning particles were recorded. The analysis of high speed movie data shows that after a corresponding heating the 100-200 μm particles are ignited during 0.2-0.3 ms. At this instant the intensity of particle luminosity increases sharply but the diameter of the luminous zone exceeds negligibly that of the particle. Further, during 1 ms the width of the luminous zone increases either to 2.5-3.5 particle diameters if combustion occurs in the "dry" medium containing no water vapor or to 1.5-2 diameters in the case of combustion in the "wet" medium. When the particle falls behind the gas flow, the luminous tail forms which indicates a tentative occurrence of exothermic reactions. After ignition, the Al particles begin to rotate with a frequency of $10^3 - 10^4$ Hz, which is followed by distortions in their trajectories. This can be caused by nonuniform distribution of oxide over the metal droplet and by the side pulse of the reactive force arising from nonuniform metal evaporation.

In the final stage, the burning Al particle splits up often into several small particles, scattering at different angles with respect to the direction of the initial particle motion. It is reported [13] that the fragmentation of the burning Al droplets in the propane-oxygen-hydrogen flame is observed only in the case where the concentration of oxygen exceeds 28-38% (the lower is the flame temperature, the higher is the necessary oxygen concentration). A similar limit to oxygen content (32%) has been determined for the flame hydrocarbon-oxygen-nitrogen [14]. It is assumed then that the fragmentation of Al particles in the flame depends on the overheating of liquid metal and on intense vapor release.

The combustion of Al particles in the high-temperature flame gives rise to the hollow transparent oxide particles. These hollow particles are often bound to the surface of burning Al particles. The existence of either hydrogen or water vapor in the flame stimulates the formation of hollow spheres. The phase composition of the oxide, forming upon Al combustion in oxygen, depends on the conditions of its formation [2]. The main fraction under usual combustion conditions is composed of α-Al_2O_3 (corundum). This oxide modification is most stable. Combustion either in subatmospheric pressure conditions or upon sharp cooling the products results in the formation of γ-Al_2O_3, which under heating above 1000 K transforms into α-Al_2O_3.

Interesting results have been obtained [17] for the combustion of Al particles in the medium with varying partial oxygen pressure from 0.2 to 1.5 atm. In this case, the method of laser heating, described in [18], was used. The pulse of ruby laser radiation ignited a particle with a diameter of about 50 μm, fastened initially (without glue, only electrostatically) to a silicon thread of 10 μm in diameter. A reflecting mirror was used to irradiate particles uniformly. The ignition and combustion of a freely falling Al particle was recorded with a high-speed camera at a frequency of about 5000 frames/s.

At a given partial oxygen pressure, two ignition regimes have been established. For the low energy laser pulse values, the ignition proceeds slowly and the flame radius increases gradually. The condensed oxide is kept on the particle upon combustion and the flame is nonspherical in shape. When the energy exceeds the threshold value, the ignition is rapid, the oxide is not accu-

mulated on the particle, and the flame is spherical in shape. Thus, combustion is experimentally shown to follow different mechanisms depending on initial conditions.

The qualitative explanation of the results [17] is given additionally in [5]. For simplicity, it is assumed that all combustion products are in the condensed phase. In this case, in the quasistationary combustion regime the net velocity of ambient gas, determined by oxygen diffusion, must be directed towards the metal particle and the oxide particles in the regime of intense combustion (without accumulation of oxide on the metal) must move outward. The motion of the oxide particle outward is provided by a thermophoretic force. In the case of low ignition energies, the surface of metallic particles does not initially become freed of oxide skin and the thermophoretic mechanism of oxide particle motion becomes unstable due to non-sphericity which is sure to lead to the irregular and non spherical combustion of the Al droplet.

This simplified mechanism may be more pronounced for the case of Al combustion in the oxygen-rich medium. In pure oxygen the diffusion control regime of metal combustion is impossible. Indeed, a fast burning of the Al droplet with almost spherical wrinkled flame surface which periodically emits fine oxide, has been experimentally observed when combusting in oxygen [17]. Unfortunately, as shown in [5], the questions of experimental data interpretation find no answer. How is the burning rate of metals controlled? The chemical kinetics with the finite velocities of heterogeneous transformations gives rather overestimated burning rates. What is the contribution of oxygen diffusion through the condensed oxide? Does the spherical flame image observed in [17] represent the liquid oxide skin?

The data of high speed movie of liquid Al droplet combustion [17] show that within the measurement accuracy the law of droplet diameter change with time may be described by either $d^2 = d_0^2 - kt$ or $d = d_0 - kt$. Treating a great body of data, we see that for small particles (smaller than 10 μm), more suitable is the linear law and for the relatively large particles, preferable is the square (d^2) law. It is concluded then [5] that for aluminum and most other metals the combustion of small particles follows the kinetic mechanism and that of large particles follows the diffusion control mechanism.

The method of laser heating of metal particles was used in a number of papers to study the details of combustion mechanism. The Al particles with diameter 230-680 μm, attached to the tip of a thin quartz thread, were ignited using a CO_2-laser in the air and in CO2 and O_2 (P=1 atm)[19]. It has been established that the heating in the air by a low radiant flux (the melting of particle 400 μm in diameter for 0.5 s) gives first micro fractures and then causes the melting of the Al particle which then becomes mirror-shiny. Its diameter was observed [17] to increase by 5%. A subsequent weak heating for 10-15 s fails to cause any changes in the appearance and size of the liquid Al droplet. An increase in the laser heating intensity leads to changes in the qualitative picture of the process. After particle melting and the formation of a bright droplet, a luminous aureole 50 μm wide appears after an interval of 20% of the heating time. Then, after a delay equal to double the time of heating to melting, the flame appears at the local point near the surface of the particle, which propagates further over the surface with a velocity of about 800 mm/s.

In the combustion regime with a developed flame, small spherical particles of 20-80 μm move from the surface of a "parent" particle. In this case, the smallest particles leave the flame zone

and the larger ones return after a time to the particle surface. The luminescence of the hot Al droplet is inhomogeneous. The luminous regions, covering 30% of the total area, are observed to form on the droplet surface. These luminescent spots correspond to oxide "caps". The ignition time of Al particle (400 μm) in the air under these conditions was 270 ms, that of the particles of 230 μm was 100 ms. When CO_2 was used instead of air, the ignition time (flame appearance) increased by 10-15%. Ignition in pure oxygen is much faster (a 400 μm particle is ignited in 110 ms) and transition to combustion is realized during a very short period and cannot be studied in detail with a framing rate of 5000 frame/s.

The data, supplementary to the results [19] for the condensed products of Al particle combustion in air, are given in [20]. The Al particles 250-900 μm in diameter, fastened with an ethanol droplet to the tip of the quartz needle, were ignited by a CO_2-laser and allowed to fall on a thin glass plate. Finally, the "parent" particle and a set of small oxide particles precipitated on the plate. A microscope analysis of this precipitate shows that the smoke particles of 1 μm are uniformly distributed in concentric zones around the parent particles. In this case, the concentration maximum is localized at a distance of 2.5-3 diameters from its surface (initial particles being 900 μm in diameter). The oxide particles with a mean diameter of 10-100 μm have been recorded along with the smoke particles. The larger the initial Al particle, the larger is the oxide particle. The estimated calculation of the total volume of precipitated particles shows that the "mean" oxide particles must be hollow.

An original method to investigate the ignition and combustion of individual metallic particles has been developed in [21]. The pre-charged Al particles with diameter 35-70 μm were supplied through the hole in the upper electrode to a special electrodynamic levitator, holding a particle at the center of the gas cavity between electrodes. Ignition was realized using a CO_2 laser. The burning particle was photographed at a rate of 25-1000 frame/s and recorded using photomultiplier tubes of flame radiation at wavelengths of 488 nm and 514.5 nm, corresponding to strong lines in the radiation range of AlO. Experiments were carried out in air at 1-40 atm. It has been established that the delay in ignition of a 40 μm Al particle is 2.5 ms under laser radiation of a given intensity (a focused CO_2-laser, 20 W) at 1 atm and increases to 5 ms at 40 atm. The total time of ignition measured by the flame radiation signal decreases by about 30% with rising pressure from 1 to 20 atm when combustion occurs without laser radiation at the instant of ignition and by about 100% when combustion occurs under constant radiation. With further pressure rise to 40 atm the combustion time remains almost constant. The dependence of combustion time on diameter for the self-sustaining combustion of the Al particle (the laser being switched off at the instant of ignition) is square, $t \sim d^2$ over the entire pressure range of 1-40 atm.

Qualitatively, a sequence of events in the ignition and combustion of the Al particle is described as follows. The formation of flame upon ignition takes less than 1 ms. In this case, it covers the entire surface of the particle. The luminous flame zone extends gradually and is held at a distance of 2-3 radii of the particle from its surface at 1 atm and of 3-4 radii at 20 atm. The luminosity intensity at 20-40 atm is maximal at the beginning of combustion. Then it remains at a mean level with variations for 50-60% of combustion time and decreases about 3-fold compared to the mean level at the final stage amounting to about 30% of the total time of luminescence. At 1-20 atm the luminosity intensity decreases monotonically with time. A decrease in luminescence level in the final stage of combustion is accompanied by a decrease in the size of the luminous zone and by a

spread of the dark zone over the surface which gradually covers the entire particle. It is assumed then that the dark zone is a cooling oxide skin, which prevents oxide diffusion to the metallic particle. The size of the extinct particle, determined from the cadres of speed shooting, is close to the initial size before ignition. The chemical composition and the material density of the extinct particle are, however, unknown.

Note that the qualitative observations of [21] correlate well with the results obtained in [22,23] concerning the stages of Al particle combustion (luminescence). At the same time, in [22,23] available is an important quantitative information about the parameters of Al particle combustion. Experiments were carried out in air using 85-150 μm particles, produced by means of a pulsed micro-arc discharge by melting a wire aluminum electrode. In experiments with freely falling burning Al particles the color temperature of a metallic droplet was measured by recording radiation at wave lengths of 520, 580, and 458 nm, which did not coincide with the bands in the oxide emission spectrum. In addition, the luminous flame has been shot with 0.5 ms exposure time and the particles extinguished on the glass and metallic plates have been studied.

A comparison with the data obtained in experiments on laser flux ignition [17,18,21] shows that a general character and the time of Al particles burning in air remain almost unchanged despite the difference between the methods of ignition. The visualization and measurements of radiation intensity [23] testify to the existence of three stages of Al particle combustion. In the first stage, the signal of particle (not of flame) radiation is smooth and average in amplitude. The measured metal temperature amounts to 2600-2700°C with variations of 50°C, which exceeds the boiling temperature of pure metal. In the second stage, the radiation intensity increases noticeably and becomes oscillating. The mean temperature drops by 200°C with 100°C variations. Finally, in the third stage, the radiation intensity reaches a comparatively low level (noticeably lower than the initial level) and is also of an oscillating nature. The temperature decreases gradually from 2400°C to 2000°C with 150°C variations, followed by extinction. Excellent agreement observed between the color temperatures determined using two different ratios of the radiation intensities (580/520 nm and 580/458 nm) allows the conclusion [23] that the particle and flame temperatures differ but weakly. The duration of the first period with decreasing diameter of initial particles from 180 μm to 80 μm increases from 25 to 35% of the total combustion time and that of the third period decreases from 60 to 55%.

Extinction by impact on a cold Al plate in various combustion stages allows to measure the time dependence of the burning particle diameter. This dependence appeared to be diameter square fit, $t \sim d^2$. As mentioned in [23], the conventional methods of extinction by "freezing" in inert gas fail to provide the necessary accuracy because such a comparatively slow process gives rise to voids in the metallic particle which is not observed upon extinction on a metallic plate. The usual microscopic investigation of the extinguished particles as well as the pictures made using a scanning electron microscope show that in the first two stages the surface remains clean. Only in the third stage the oxide "caps" are formed whose volume increases with time amounting to more than 50% of the particle volume by the end of its combustion.

The examination of the extinguished metallic particles with electron probe microanalyzer "Cameca SX50" testifies that in the first stage the local atomic content of oxygen in the extinguished particle does not exceed 4% which corresponds to the oxygen concentration in the parent

Al wire. In the second stage the local oxygen concentration varies from 4 to 14% and in the third stage it reaches 55% if the electron beam falls directly on the oxide "cap". The latter is in fair agreement with the theoretical content of oxygen in Al_2O_3.

A detailed X-ray analysis of the cross-sections of the extinguished particles was undertaken in order to check the presence of atoms other than Al and O in the particle interior. Search for nitrogen indicated that the nitrogen atoms are recorded only in the third stage and only in the oxide "cap". At the same time, a small impurity of iron (less than 0.5% atomic), typical of the initial material of the Al wire, is recorded in the metallic part of the extinguished particle and does not exist in the oxide "cap". These data indicate that the oxide "cap" is formed by the material deposition from the flame zone rather than due to the phase transformation of the initial metal on the particle surface.

The mean local oxygen concentration in the surface layer may be explained by analyzing the diagram of the phase equilibrium in the Al-O system. The diagram shows that 14% correspond to the maximum content of oxygen in liquid Al upon nonstationary dissolving of suboxides. In this case, the boiling temperature for the system liquid Al-O solution, liquid Al_2O_3, and gaseous oxides is lower by 220°C than that of liquid pure metal. It is assumed that the transition from the first stage to the second stage occurs due to the saturation of the metal surface layer by dissolved suboxides AlO and Al_2O which may give rise to liquid oxide on the surface of a burning particle. Its gradual accumulation results in transition to the third stage, characterized by the asymmetric growth of the oxide "cap".

Additional experiments with use of a.c. and d.c. electric fields [23] show that the burning Al particles are charged positively and a 165 μm particle burns in the field with a frequency of 10 kHz and strength of 2000 V/cm by 15-20% faster than without the a.c. field. It is supposed then that the eigen electric field of the burning Al particle may have effect on the processes occurring in the flame zone and on the process of oxide "cap" formation.

New information about the temperature field and the concentration distribution upon combustion of a freely falling Al particle was derived using advanced spectroscopic technique combined with electron probe microanalysis of condensed combustion products [24]. Experiments were performed in the quiescent air; the particle size was 210 μm; ignition was realized using either Ar- or CO_2-lasers. Recording of the total burning particle radiation using photodiode shows a three-stage pattern of luminescence (see Fig. 5 1), as described earlier in [21,23]. A changeover from the "smooth" to "intermittent" luminosity regime with the rotation and fragmentation of the burning particle has been explained with respect to the course of the chemical reaction in the particle and the formation of voids filled with gaseous Al suboxides.

To provide the maximum objectivity of interpretation of the spectroscopic data, the PLIF images of Al were recorded in the initial combustion phase in the presence of a symmetric flame around the burning particle. When publishing the first option of experimental results in [24], it was underlined that in order to eliminate the data statistical uncertainty one should use improved experimental technique and advanced mathematical treatment. A Revised Version of the data on AlO profile and temperature distribution around burning Al particle is presented in Fig. 5.2. The radial distribution of both the AlO concentration and vibrational temperature were calculated us-

ing the complex treatment of the induced fluorescence signal. It has been established that the maximum AlO concentration is reached at a distance about 2 radii from the particle center and the maximum flame temperature, equal approximately to 3300K, is reached at a distance of 5 radii. The AlO temperature near the particle surface is equal to 2250°C, i.e., it is substantially lower than that of Al boiling. A micro-X-ray analysis of the condensed combustion residuals, collected in the process of impacting the burning particles on silicon wafers, shows that the maximum concentration of small Al_2O_3 particles is at a distance of 3.5 radii from the particle center (Fig. 5 2).

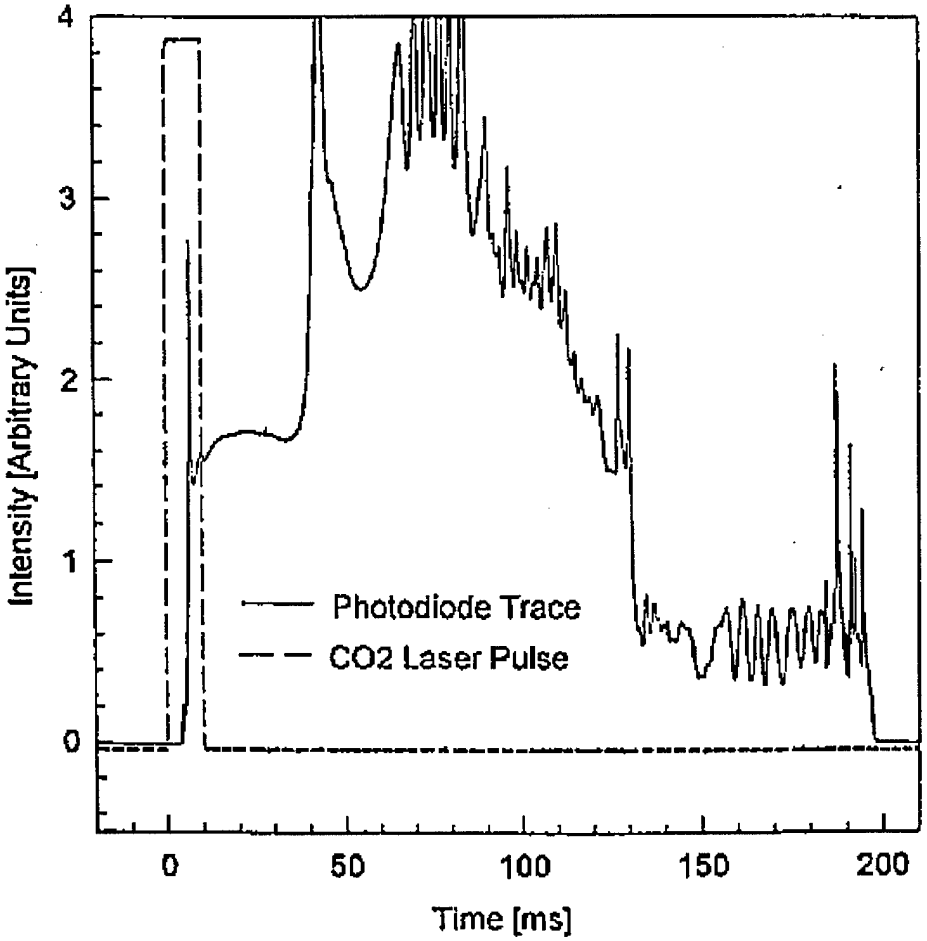

Fig. 5.1. Photo-diode record of burning particle radiation (taken from [21, 23]).

Analyzing the results of the above papers, one may formulate a general picture of the combustion of a single Al particle in the oxygen-containing medium. Heating the particle by external heat flux results in metal melting, followed by an increase in the volume and by the cracking of the oxide skin. In the case of slow heating (about 0.1-10 K/s) the cracks in the oxide skin are healed and no ignition is observed. Under rather fast heating the particles are freed from the initial oxide skin and the metal vapors, reacting with oxygen near the particle, are ignited. Initially, combustion follows the mechanism similar to the classical mechanism of the evaporating hydrocarbon droplet. The peculiarities of the combustion mechanism of metallic combustibles are determined by the behavior of oxidation products. The combustion intermediate, AlO suboxide, is definitely recorded in the gas phase, and is likely to play the key role in the reaction mechanism [24]. In the regime of the developed symmetric flame (initial combustion stage) AlO diffuses towards the

metallic particle and reacts with liquid Al. Nonzero Al concentration near the metal surface [24] indicates that the rate of this reaction is limited by chemical kinetics rather than by diffusion. The temperature of metal surface in the self-sustaining combustion is determined by the data of different authors in the range of 2100-2400°C, i.e. below the boiling temperature of pure aluminum. This is the only indication of overheating of the metal surface [23] that can be attributed to the unsteadiness of the process and should be checked again in future experiments. The surface temperature at the instant of ignition is below the melting temperature of oxide (2040°C).

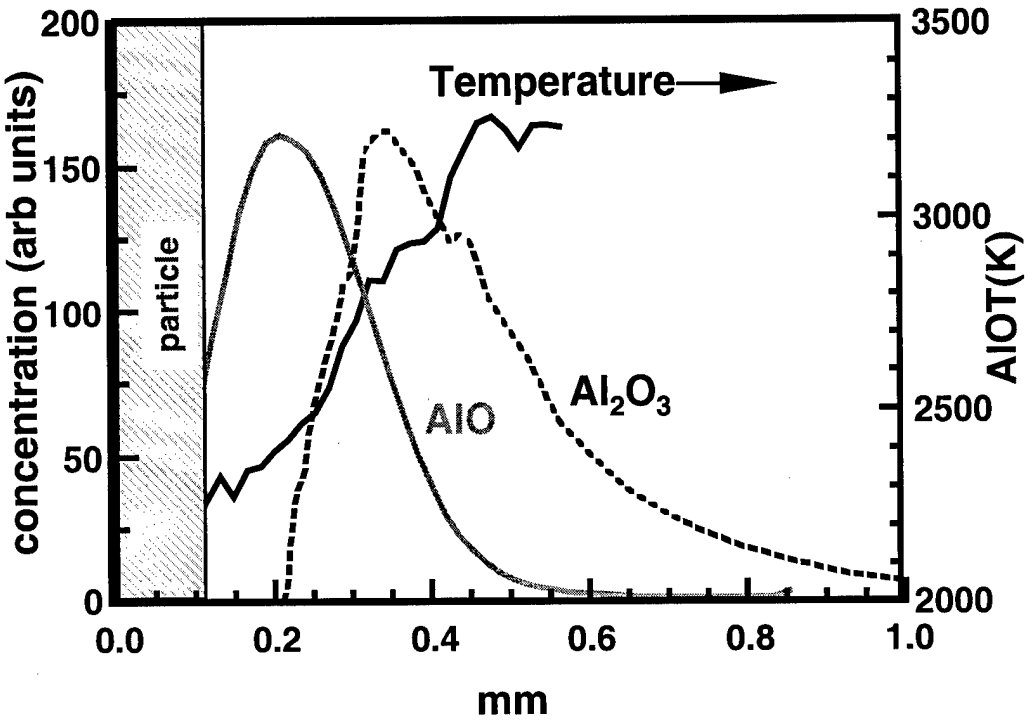

Fig. 5.2. AlO profile and temperature distribution around a burning Al particle.

The above pattern of Al combustion in oxygen coincides mainly with that obtained by the results of a study of Al combustion in pure CO_2 [25]. It has been established that the ignition of preheated cylindrical Al samples (m =2.1 g) in the counter flow CO_2 stream at a relatively low Al temperature causes a slow oxidation of the sample from the surface. When heated above critical temperature, the Al sample is ignited and burns giving a bright green-white flame. The critical ignition temperature is lower than the melting temperature of Al_2O_3. Spectroscopic measurements show that the considerable concentrations of Al and AlO vapors are observed above the burning metal surface. In this case, the peak of AlO concentration is at a finite distance from the surface. It is assumed that AlO diffuses to the sample surface. At the same time, according to the data of shooting, 0.85 s after the beginning of combustion the metal surface remains clean and contains no traces of stoichiometric oxide, Al_2O_3.

Combustion of Al particles in solid propellant

The thermodynamic calculations show that the combustion products of the typical ammonium perchlorate-based solid propellants contain H_2O, CO_2, and CO as the main oxidizer agents. The amounts of other oxidizers (OH, O_2, O, etc) are negligible. Thus, the results of investigations of

Al combustion in oxygen-containing mixtures cannot be directly referred to Al combustion in the products of solid propellant decomposition, in particular, in a quantitative respect. According to [2], the combustion time in the flame of solid propellants of spherical Al particles at 1 atm is proportional to d^2 and at pressures above 30 atm it is proportional to $d^{1.5}$. It is known, that the burning time is approximately in reverse proportion to the total concentration of oxidizers in the flame and the flame temperature and medium pressure practically have no effect on burn out time.

It should be noted that the combustion of the individual (virgin) particles is not typical of the flames of metallized solid propellants. Actually, in the combustion wave of such propellants we observe the coalescence of the initial small size (5-30 μm) aluminum particles, and comparatively large agglomerates (50-300 μm) eject from the surface. The question of metal agglomeration will be discussed later. Now we would like to mention that it is not reasonable to simulate experimentally the ignition and combustion of agglomerates by inserting equivalent large metallic particles to the propellant. Experiment shows that the large individual Al particles (100-200 μm) cannot be ignited at least at low pressures on the reacting surface of solid propellants and they burn out at greater distances from the burning surface than agglomerates [2].

However, the data on the burning times of individual Al particles of small sizes in gas flames whose composition imitates that of the combustion products of solid propellants are of specific interest for treating real combustion processes. In [26] the spherical Al particles of diameter 40-80 μm were burnt out in the combustor of the diffusion flame with a separate supply of CO_2, H_2O, and O_2. The calculated composition of combustion products was varied within the range $(H_2:O_2) \rightarrow (0.89:0.11)$ and $(CO_2:H_2O:O_2) \rightarrow (0.18:0.66:0.16)$. The burning time was calculated by treating the photomultiplier signal measuring the luminescence intensity of the reacting particle. It has been established that the method of treatment introduces substantial errors due to measurements because extinction occurs gradually and the luminescence signal decay has asymptotic nature. The method of treatment by a given minimum level of luminosity, assumed as the end of combustion, was used as most reliable. The dependence of burning time on particle size was in agreement with the square law. Under this condition ($t \sim d^2$), the dependence of burning time on the concentration of the effective oxidizer is exponential with an exponent of -0.85. In this case the effective oxidizer is the sum of molecular concentrations of O_2, H_2O, and CO_2 with the corresponding weights 1, 0.533, and 0.135, determined earlier by the mathematical modeling of Al combustion [27].

Mathematical modeling of Al particle combustion.

The models of Al combustion are qualitatively similar to the classical combustion model of the evaporating droplet but display substantial peculiarities due to consideration of the condensation of oxide and its interaction with the initial metal. There are not less than ten variants of the model differing in both the consideration of various factors and the methods of solution (see, e.g. [27-34]). A brief analysis of the models is given in [27] suggesting the improved variant of the Law model [29]. Improvements concern a reasonable extension of the chemical mechanism of Al reacting and a more detailed consideration of gasdynamic factors and the process of oxide accumulation on the burning metal surface.

The problem of combustion under steady-state conditions is formulated separately for the internal (between metal surface and flame) and external (from flame surface to infinity) zones. Figure 5.3

shows a simplified sketch of the proposed mechanism for Al particle combustion. It is assumed that upon combustion the condensed oxide precipitates first on the surface of a pure spherical metallic particle as a hemisphere, preventing metal from evaporation from this part of particle surface. The calculated amount of precipitated oxide after metal burnout corresponds to oxide particle with diameter about 65% of that of the initial metallic particle.

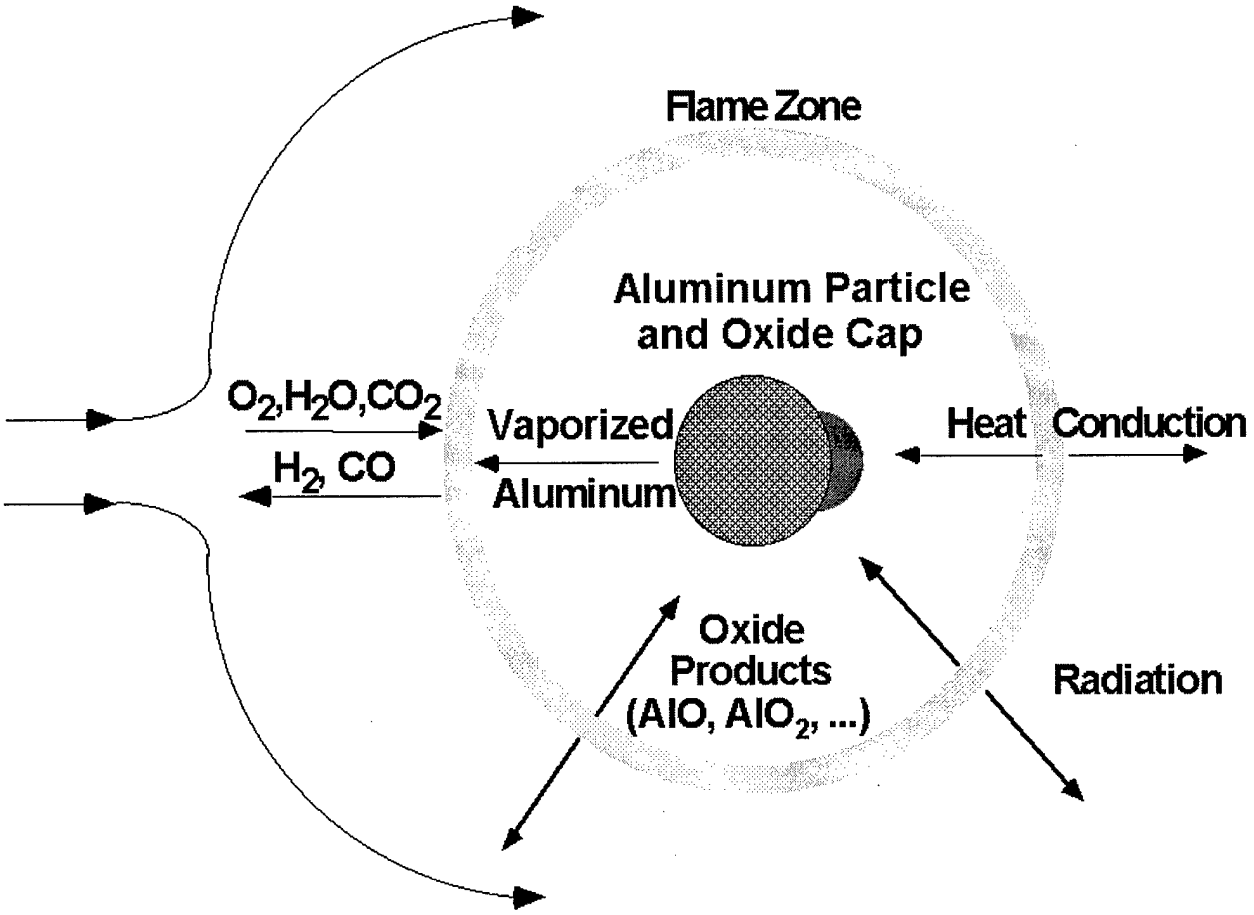

Fig. 5. 3. Schematic of a simplified combustion model for aluminum.

Four potential combustion modes are postulated depending on the ambient temperature and composition. At low gas temperature or oxidizer concentration the ambient gas moves towards flame surface whose temperature is lower than the boiling temperature of oxide. In this case, the fraction of evaporating oxide is zero. As the ambient temperature and oxidizer concentration increase, the flame temperature reaches the boiling temperature of oxide. In this case the fraction of evaporating oxide becomes nonzero and increases gradually and the direction of ambient gas is reversed due to an increase of the diffusion flow of the evaporated oxide. The direction of the total gas flow away from the flame is preserved with further rise in both ambient temperature and oxidizer concentration when it is assumed that 100% of the forming oxide evaporate and the flame temperature becomes higher than that of oxide boiling.

Note that the available experimental data have been obtained within comparatively narrow limits of the variations in medium parameters and it is impossible to verify the existence of all postulated combustion modes. The calculations by model [27] show that the burning depends substan-

tially on the oxide type. Therefore, calculating the effective oxidizer concentration in the flame it is necessary to sum up the mole fractions of reagents with a corresponding weight factor as has been already mentioned in the analysis of experimental data [26] (among the typical oxidizers in the solid propellant flame most effective is oxygen and then water vapor and, at last, CO_2). At the same time, the size of the flame zone is unusually dependent on the type and concentration of components. As the oxygen concentration increases, the flame stand off distance increases from 1.5 to 2.5 radii from the Al particle center. However, as the concentration of water vapor increases, this distance decreases from 2.5 to 2.0 radii and remains almost the same and equal to 2.2 radii with variations in CO_2 concentration.

In the initial variant of the model the temperature on the burning Al surface was taken to equal the boiling temperature of pure metal. It is worthwhile to consider further the boiling which occurs simultaneously with the dissociative reaction between liquid oxide and Al, resulting in gaseous Al, Al_2O, and AlO. The influence of pressure in the model is taken into account only due to a change in the thermophysical parameters of medium and boiling on particle surface. The calculated increase in particle burning velocity is only 20% with pressure rise from 1 to 70 atm. This is substantially higher than the experimental [14] and calls for model improvement. The blocking of a part of evaporating particle surface by condensed oxide causes a decrease in burning velocity by about 25%, neglecting additional heat release due to oxide condensation. Obviously, taking into account this heat in the case where Al suboxides react on the metal surface with each other and with the metal may change considerably the heat balance and affect the calculated results. This points, however, to the necessity of obtaining quantitative information about heterogeneous reactions of Al, its suboxides and oxide. Nevertheless, as a whole, the model [27] describes satisfactorily the experimental data on Al particle combustion at relatively low pressures and with a formal consideration of oxide accumulation under laser heating and in the flames with various compositions. The values of burning velocity predicted for high pressure are substantially lower than that in experiments which makes it necessary to analyze in detail the theoretical concepts to improve the model.

5.2.2. Magnesium

Physical properties

Magnesium belongs to the class of volatile metals with nonvolatile oxide. The physical characteristics of both Mg and its oxide are listed in Table 2.

Table 5.2. Physical properties of Mg and MgO.

Property	Mg	MgO
Density, g/cm^3	1.74	3.07-3.20
Melting temperature, K	923[4]	3080[4]
Temperature of boiling , dissociation , K	1366[8]	3430[8]
	1385[4]	3533-3853[4]
Latent melting heat, cal/g	82.2[2]	
Evaporation, dissociation heat, cal/g	1337[2]	4003[8]
Formation heat, cal/g		-3591[8]

In the dry air or oxygen the oxide forms with a cubic lattice. Its thickness may reach 70 A^{o}. When the temperature does not exceed 700 K, the oxide skin displays protective properties, thus providing a slow oxidation of magnesium according to the parabolic law. As the temperature rises further, the oxide skin becomes thicker and loses its protective properties. Magnesium is oxidized by the linear law.

A noticeable evaporation of magnesium starts at 870 K. The pressure of solid magnesium vapors (below T_{melt}) obeys the formula below [2]:

$$\log P(\text{mm Hg}) = 3.27 + 2.5 \log T - (7636/T)$$

The pressure of Mg vapors above the melting point is 26 mm Hg at 1073 K, 94 mm Hg at 1173 K, and 280 mm Hg at 1273 K.

Combustion of single Mg particles

The combustion of magnesium has been studied in the various types of experimental apparatus including the diffusion flame burners, the electric heating of wires, etc. A detailed investigation of the combustion of Mg particles of 50-200 μm on a laser ignition set-up, used earlier to study the combustion of Al particles [17], has been performed in [35]. Experiments were carried out at atmospheric pressure in the air and in the oxygen/argon mixtures varying a mass fraction of oxygen from 0.03 to 1. The individual particles were ignited accidentally because of their irregular shape (resembling chips) and the absorption of laser radiation energy was dependent on particle orientation. Usually, the ignition occurred during 0.5ms. However, in low oxygen concentration mixtures a gradual ignition without flash was observed in the gas phase. Upon combustion in dilute mixtures the Mg particles are commonly rounded which testifies to the absence of oxide accumulation on their surface. Combustion in air is characterized by the irregular character. In the initial phase the metal jetting is observed. In the final stage fragmentation is quite probable. The surprising thing is that the particles, burning in the air, often preserve their irregular shape with a noticeable nonuniform luminescence over the surface. It is assumed then that upon ignition on these particles the oxide is accumulated which is preserved in the solid state and is, probably, accumulated upon combustion. The irregularly burning particles rotate in flight with a rate of hundreds to thousands R.P.M. The luminous flame size is three-fold that of Mg particles which indicates the existence of the extended diffusion flame zone.

Interesting observations of Mg particle behavior (100-300 micron size) under heating in a glass tube in the air were made in [36]. It has been established that under the heating rate of 10-1000 K/s before reaching melting temperature the Mg particle volume increases about 25-fold. Thereafter the flash is observed to occur for 3 to 80 ms. The combustion products form a hollow coating with a rough outer surface and a smooth inner surface and a negligible amount of white submicron particles of magnesium oxide. Special mass-spectroscopic measurements showed that the melted particle blows up due to the release of hydrogen, which could not have been pre-stored in the metal and must have resulted from decomposition of impurities such as magnesium hydride or magnesium hydroxide. A sharp increase in particle volume causes the cracking of the oxide skin, which allows the oxidizer to move towards the metal, which results in the heterogeneous oxidation of the metal.

Experiments on Mg powders produced by various methods (liquid metal dispersion in the inert medium, electrolysis, the cutting of large metallic pieces, etc.) testify that the effect of blowing

under heating is typical of this metal. It is expected that the particle blowing was also recorded in the works of other researchers and caused both the formation of hollow shells with the sizes exceeding the initial metallic particles [37] and the anomalous combustion of free falling particles [35]. Note, however that as the medium's pressure rises, the effect of blowing is suppressed and the transition to the vapor-phase combustion of magnesium is realized.

The results of a study of Mg particle combustion in the solid propellant flame at high pressures are presented in [38]. To exclude the influence of condensation and coagulation in the high-temperature flame zone, the spherical Mg particles of 11.6 μm were introduced into nitrocellulose in amount of 10% wt. In this case, the precalculated flame temperature did not exceed the melting temperature of Mg oxide. The pressed tablets were combusted at constant pressure of 1-100 atm. The condensed products were divided into fine and coarse particle fractions and analyzed by their size and mass. The fine particle fraction of combustion products (less than 2 μm) consists mainly of cubic crystal subjects. At pressures above 20 atm the combustion products contain fine spherical particles reaching 20-30% in number at 110 atm. Actually, the local temperature in the combustion zone of an individual Mg particle may be higher by 200 K than the calculated equilibrium flame temperature. The mass portion of the fine particle fraction is about 80 % in the pressure range of 20-110 atm. The size d_{30} for small MgO particles varies in this range from 0.36 to 0.60 μm for a cubic crystal and from 1.6 to 0.45 μm for spheres.

A coarse fraction of combustion products in the pressure range of 20-110 atm in which the agglomeration of the initial Mg particles (10% by weight) was observed, consists of spherical particles close in size to the initial particles. Thus, at 85-110 atm the mean size d_{30} of coarse particles in combustion products is 9.2-10.4 μm (at 20-42 atm this size varies from 5 to 8 μm). Irradiation by an electron beam under electron microscope shows that most coarse Mg particles are hollow spheres. It is assumed then that such particles are formed due to both the heterogeneous oxidation of the initial metallic particles and the partial condensation of oxide on their surface during combustion. A decrease in the sizes of particles belonging to the coarse fraction at 20-40 atm may be due to the fragmentation of metallic droplets upon combustion within a given pressure range.

The ignition and combustion of Mg in CO_2 is of specific interest because these processes may be used to produce energy under conditions prevailing in Mars. At the same time, this study is important for explaining Mg combustion in the flame of solid propellants. The cylindrical samples of 0.2-12 mg supplied with a thermocouple and corresponding to the equivalent spherical particles with diameter 0.64-2.36 mm, were heated [39] under conditions of conductive heat transfer from pure CO_2 or ($CO+CO_2$) mixture. The sample temperature, total luminescence intensity, and the emissivity spectrum of flame were measured with varying initial ambient temperature.

The thermocouple measurements show that at contact with hot gas first an increase in sample temperature is observed and then a comparatively long plateau at melting temperature followed by a rather slow linear rise in the sample temperature. Calculations performed by the equation of heat balance using the coefficient of heat exchange determined from the initial heating period produce quite unexpected results. Just before ignition, the rate of chemical heat release was substantially lower than during metal melting, i.e., the oxide skin under heating in CO_2 acquires protective properties. Note that the heating of metal was performed rather slowly. For example,

when using coarse samples (equivalent diameter being 2.3 mm), the duration of heating to ignition temperature was about 27 s (CO_2 temperature being 1030 K), the melting took about 10 s.

The high-speed movie shows that the flame appears at the local points on the sample surface and covers gradually the entire surface to form the diffusion combustion front at the finite distance from the surface. When the sample burns out, condensed residue remains which consists of two concentric shells with a porous substance in the layer between the shells. The inner shell is black due to the presence of pure carbon which is assumed to favor the strengthening of the protective properties of the oxide skin under heating before ignition and only the mechanical destruction by metal vapors with their subsequent inflammation gives rise to the flame. A particular feature of Mg ignition in pure CO_2 is in the fact that the temperature of liquid metal exceeds that of its boiling at a given pressure. For 1-mm particles this difference reaches 300-400 K. It is suggested then that the pressure of metal vapor under the solid oxide skin may be substantially higher than the ambient pressure (according to estimate, up to 10 atm for particle diameter of 1 mm). It is also assumed that the emission of luminous fragments from the surface of Mg particles, burning in CO_2, provides a periodic decrease in pressure within the oxide skin. Experiments in air show the destruction of the burning Mg droplets [40] which is attributed to the appearance of excess pressure under overheating and to the existence of a less solid oxide skin.

Diluting CO_2 by carbon monoxide weakens the combustion intensity. When CO concentration (in the mixture with CO_2) exceeds 25%, the burning time of coarse Mg particles increases 2-3-fold. The spectral measurements show that unlike combustion in CO_2 and in air, in the CO medium there is no radiation zone with a continuum spectrum. The combustion residues contain no fine-disperse products. It is assumed that the combustion in CO occurs mainly in the heterogeneous regime with a distant zone of homogeneous oxidation of metal vapors.

Mathematical modeling of Mg particle combustion.
A simplified model of Mg combustion in oxygen [2] considers a spherical particle with surface temperature equal to that of metal boiling. The evaporated metal reacts with oxygen at some distance from the surface (the internal flame boundary) at temperature exceeding the boiling temperature of oxide. This assumption is based on the exothermicity of the purely gas-phase reaction $Mg(g) + 0.50_2(g) \rightarrow MgO(g)$. A part of the forming gaseous oxide diffuses to the metal surface and is condensed with heat release. The remaining part diffuses outward and is condensed at the outer boundary of the extended flame zone in which the gas temperature drops to that of oxide boiling. The model predicts that the extent of the flame zone (the distance between the inner and outer boundaries) decreases with decreasing oxygen concentration in the medium. This points to a decrease in the oxide deposition intensity on the metallic particle, burning in the diluted medium that is confirmed experimentally. The model also predicts the value of the radius of the external flame zone. However, the times calculated for combustion in air are almost two-fold (and in the diluted media 5-fold) shorter than the experimental ones. It is assumed that this discrepancy is caused by unsatisfactory description of the solid oxide formation on the metal that leads to a change in the heat exchange.

Attempts to describe theoretically the initial phases of Mg particle oxidation and ignition in oxygen were undertaken in [41]. It is reported that at relatively low temperatures the Mg oxidation is mainly heterogeneous but beginning with 600 K the experimentally determined oxidation rate is

in fair agreement with the calculated velocity of metal evaporation. It is concluded then that at high temperature the contribution of heterogeneous reaction to the mass velocity of metal oxidation must be negligible and the ignition is mainly caused by the reaction of vapor oxidation occurring near the metal surface [41].

5.2.3. Boron

Physical properties

Boron exists in two modifications: amorphous (fine-crystalline) brown, and crystalline dark-gray. By combustion mode, the boron may be referred to the class of nonvolatile metals with a volatile oxide. The physical properties of boron and its oxide are listed in Table 3.

Table 5.3. Physical properties of B and B_2O_3.

Property	B	B_2O_3
Density, g/cm^3	2.33	1.84
Melting temperature, K	~2400[4]	728[4]
Temperature of boiling, dissociation , K	4139[8]	2340[8]
	3940[4]	2133-2316[4]
Evaporation, dissociation heat, cal/g	2250[2]	1229[2]
Formation heat, cal/g		-4343[8]

The pressure of boron vapors at 2000K is 10^{-4} atm and at 2400K it is 10^{-2} atm. The amorphous boron is slowly oxidized in the air at room temperature. Being heated to 1100K in the air it is ignited and burns giving a bright flame. The coarse boron crystals are more stable and are difficult to ignite.

Combustion of single B particles.

In early experiments [42,43] on single particles, heated in a flat-flame burner, it has been established that when the boron particles are heated to 1800-2000 K, they are ignited and burn first with flame of moderate luminosity, then fade out and later begin to burn with brighter luminosity. It is usually assumed that boron burns first in the presence of a semiprotective oxide coating, which is removed by reaction and evaporation. In the second the longest phase, the particle burns with the reactions on the pure metal surface and with formation of suboxides, transforming into the final combustion products at a given distance from the surface [44].

Despite extensive investigations, a description of ignition and of the initial stage of B particle combustion is based on quite different approaches. Using general concepts and analyzing the results of investigations of a comparatively slow boron oxidation, it is assumed that oxygen diffusion to metal through liquid oxide skin determines the process characteristics in the initial combustion phase [44,45]. There is, however, another version according to which the most important role belongs to boron dissolving and diffusion in liquid oxide [46,5]. Indeed, according to [46], the liquid oxide has a vitreous state and must not form the fixed molecular bonds. Therefore it was suggested that the oxygen dissolving in the oxide skin is hindered and the skin composition due to the presence of dissolved boron becomes B_2O_x where $x < 3$.

The ideas proposed in [46] were used in [47,48] to interpret theoretically the experimental data on boron particle ignition. According to theoretical notions, the boron dissolving in liquid oxide is followed by the formation of suboxide BO which is attacked by the gaseous molecules O_2 and H_2O at the gas-liquid interface which results in gaseous BO_2 or HOBO and causes the evaporation of B_2O_3 from the surface. Analyzing a theoretical model, one may see that an alternative hypothesis of oxygen dissolving in liquid oxide and of the basic heat release on particle surface [44] results in a continuous growth of oxide skin, temperature decrease under constant laser heating, and the absence of ignition. The latter sharply contradicts experiment. If we assume that the main heat release occurs in the gas phase, we may explain quantitatively and qualitatively the experimental dependence of ignition time on ambient pressure and temperature. It is important to note that unlike true metals, aluminum and magnesium; boron has a very low thermal diffusivity at high temperature ($5x10^{-3}$ cm^2/s at 2000 K). This determines the purely technical difficulties of boron particle ignition. For example, they cannot be ignited by the pulses of laser radiation using a set-up for ignition of the Al and Mg particles.

Important experimental information obtained in [49-51] allows us to substantiate the hypothesis of boron dissolving in liquid oxide in the stages of heating and ignition. The visual observations using an environmental scanning electron microscope show that under heating in the oxygen-containing medium on a ceramic substrate to 1213 K, a series of small boron crystals with initial size of 2-3 μm melt and coalesce into a droplet. The boron content in the crystals was 93%. The 3 μm particles of amorphous boron with 99.9% purity demonstrated a similar behavior under similar conditions. Additional experiments on heating in Ar have confirmed the fact of B particles melting at 1213 K, and the experiments performed in H_2O vapors gave an even lower temperature (ca.1100 K) of complete liquefaction. To elucidate the nature of melted particles, measurements were performed by the method of X-ray diffraction. Note that the liquefaction temperature is almost twice that of pure boron melting (ca.2400K, [49]). The X-ray analysis showed that the liquefied material has amorphous structure. According to the literature data it is assumed that this material is a boron monoxide polymer, $(BO)_n$ which is indirectly confirmed not only by the amorphous structure but also the brown color, water and methanol insolubility, fragility and hardness of the cooled materials.

Analyzing the available experimental data and the theoretical concepts, a mathematical model, describing two successive stages of boron combustion, was formulated [49]. In the first stage it takes into account not only the formation of liquid $(BO)_n$ but also the dissociative evaporation of the oxide skin with B_2O_2 formation as well as the heterogeneous reactions of the suboxides substance with $O_2(g)$ and $H_2O(g)$ generating $BO_2(g)$ and HOBO(g), respectively. The duration of the first stage was taken as the sum of the time necessary for the complete removal of the B_2O_3 coating, and the time required to reach the melting point of boron. A comparison between the calculated and experimental times shows a satisfactory agreement. As the ambient temperature and pressure or oxidizer concentration rise, the duration of the first stage decreases. There is also a fair agreement between experiment and calculations of the duration of the second combustion stage, performed for two limiting cases, respectively: diffusion and kinetic control combustion mechanisms. It has been shown that if $P \cdot d << 75$ atm·μm, the combustion of boron particles follows mainly the kinetic control mechanism. On the contrary, if $P \cdot d >> 75$ atm·μm, the combustion is limited by oxygen diffusion.

5.3. METAL POWDER AGGLOMERATION AT THE BURNING SURFACE OF SOLID PROPELLANT

The distinctive features of metallic particle properties compared to other propellant components, such as a low volatility at the temperature of combustion surface and the existence of a protective oxide coating which determines relatively low metal reactivity, lead to the accumulation of metal on the surface and to the formation of the so-called agglomerates. An additional reason for metal accumulation on the burning surface is also the effect of a decrease in transient burning rate caused by the metal, which serves as a heat sink in the combustion wave. Note that the structure of heterogeneous propellants determines the formation of the aggregates of small metallic particles at weight concentrations of 16-22%, which are quite typical of solid propellants. Below, it will be shown that in this case each particle has several contacts with the neighboring ones. Therefore, under corresponding conditions, the agglomerates on the burning surface within the limits of a conventional "pocket" in solid propellant represent a joining of several hundreds or thousands of virgin metallic particles.

Concerning the practical use of metallized solid propellants, agglomeration is an unfavorable phenomenon, which leads to the losses of chemical and mechanical energies in a rocket motor due to the metal combustion incompleteness and the nonequilibrium state of two-phase flow. Thus, experimental and theoretical studies of agglomeration are carried out for understanding the mechanism of this phenomenon and for developing the methods of influence on the size distribution of the condensed combustion products. These investigations have been under way from the beginning of the 60s [52,53]. A great body of information has been extracted although the problem is still far from being solved.

In the Soviet literature this phenomenon is for the first time recorded in the works, devoted to the study of combustion of homogeneous SP with the additives of metal, carried out in the beginning of the 60's under P.F. Pokhil's supervision [52]. Approximately at this time analogous investigations were performed in the West. During the prolonged period the accumulations of the qualitative information occurred, on the basis of which original concepts were build about the agglomerating process. Thus, in the early work of American scientists the hypothesis was formulated about the formation of coarse Al particles on the burning surface due to the accidental rendezvous of the moving over the surface original particles of metal [54].

Then this hypothesis has been strongly criticized and there were first formulated [55] qualitative concepts about the formation of agglomerates due to merging the particles of the metal, which are situated within the "pockets" of binder between the coarse grains of oxidizer. During the subsequent years considerable attention was paid to the study of the behavior of metallic particles in the process of rapid heating [56,57]. It should be also noted the contribution of French researchers [58], whose results were not widely known in combustion community and were repeated in other works.

Note that the early investigations have been performed using solid propellants, containing mainly ammonium perchlorate and "inert" fuel-binders of similar composition (polybutadiene, polyurethane, etc.). These propellants demonstrate similar characteristics of agglomeration which makes one think that the phenomenon is studied. The latter two decades are characterized by a consider-

able growth in the number of used components of solid propellants: the application of nitramines and ADN (ammonium dinintramide) instead of ammonium perchlorate and various "active" binders instead of inert polymers. Obviously, the available concept of the mechanism of metal combustion in solid propellants fails to predict the composition of combustion products and the completeness of metal transformation.

According to general notions, in the surface layer of the burning solid propellant there occur the heating of metallic particles and a partial decomposition of a binder. In many cases, the metallic particles are inside the "carcass", consisting of the residues of the decomposing binder, and sinter to form the ill defined "accumulates". At low pressures the burning surface temperature is lower than that of metal melting. At high pressures the metal melts just on the burning surface and then starts to react heterogeneously and/or in a vapor-phase with the oxidizer. The further heating of metallic particles due to both heat exchange with flame and chemical heat release leads to the coalescence of separate particles into a large droplet and to agglomerate ignition. This sequence of events is shown in detail in Figs.5.4 and 5.5 on examples of "poorly" and "readily" agglomerating propellants, correspondingly.

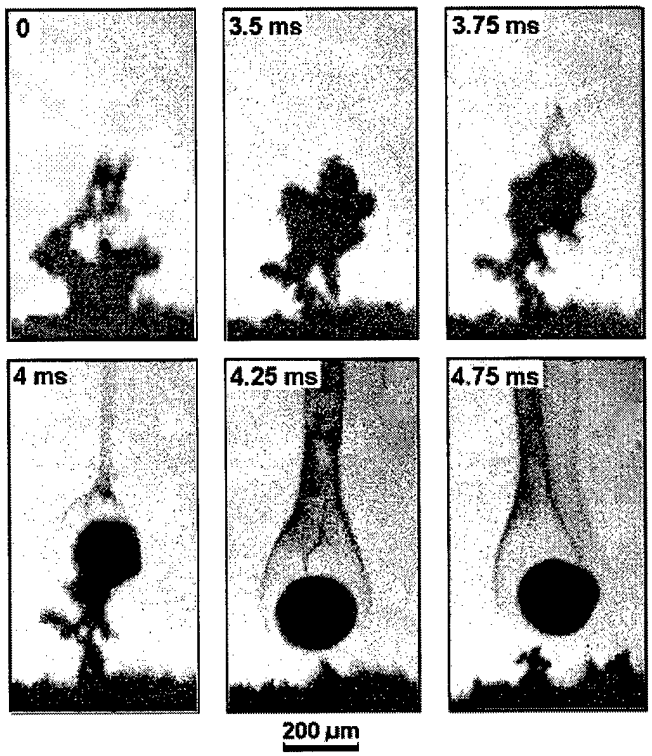

Fig. 5.4. Sequence of events in a "poor" agglomeration process.

The observations were made via high speed movie performed with propellants burning at atmospheric pressure under backlit illumination. Obviously, the behavior of metallic particle aggregates depends on the propellant type. In the poorly agglomerating propellants the formation of particle filigrees on the burning surface is followed by ignition of the top and by coalescence of particles into a large droplet (Fig. 4). For the readily agglomerating propellants the particle coalescence and ignition occur within the limits of the surface layer (Fig.5). Besides, the intermediate case may be realized where the separating nonburning metallic aggregate coalesces into a droplet at a

comparatively large distance from the burning surface and is ignited to form a closed aureole which is then destroyed and transforms into a typical "smoke" tail. It is assumed then that the closed aureole corresponds to a thin liquid oxide coating, existing during a short period of time and which is difficult to shoot. An exact explanation of this phenomenon is still unavailable.

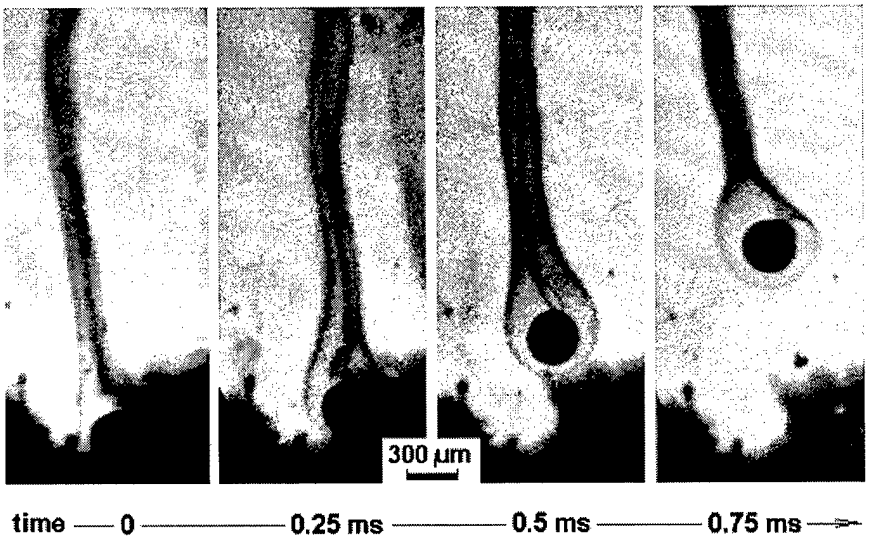

Fig. 5.5. Sequence of events in a "ready" agglomeration process.

The Al agglomerate, separating from the surface, burns usually to form the oxide cap and rotates upon motion in the flame. The agglomerate is surrounded by the zone of luminous flame and of stoichiometric oxide condensation. The suboxide AlO in a gaseous form has been recorded in the flame zone [24], which indicates that the agglomerate combustion is similar in principle to that of a coarse Al particle. However, the prehistory of agglomerate formation leaves the imprint on its inner composition and on the combustion law. In particular, the extinguished agglomerates very often exhibit complex structure with small individual Al particles inside covering oxide shell.

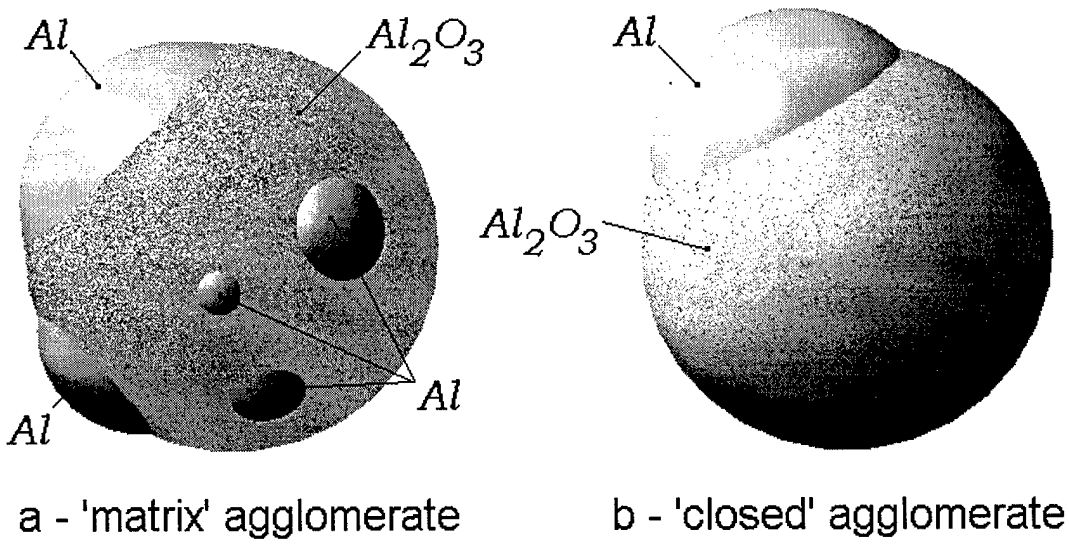

Fig. 5.6. Typical view of combustion residues of Al agglomerates.

A study of agglomerates, collected from the extinguished surface of solid propellant [59] and in the residues of the condensed combustion products [60], shows that agglomerates exist not only in the form of large metallic particles with an oxide cap but also as coarse particles of a "matrix" type, existing at relatively low pressures (see Fig.5.6 with typical view of combustion residues). The latter consist mainly of Al_2O_3 with inclusions of pure metal. They are assumed to form in the case where the propellant surface has a gas-permeable carbon carcass whose temperature exceeds the ignition temperature of metallic particles. Thus, the metallic particles that have not yet separated from the burning propellant are ignited within the carcass and react to an essential degree of consumption. The agglomerates of extra large size are formed upon combustion under the action of mass forces. Under acceleration, directed to the burning surface, the agglomerates cannot separate and are accumulated on the surface to form at relatively high accelerations (50-100 g) particles of several mm in size. With prolonged acceleration, a solid layer of melted aluminum and its oxide may appear on the surface [61].

The problem of coarse agglomerate formation upon combustion in the acceleration field is related to the practical problem of slag formation in rotating rocket motors [62]. This problem should be solved under rigid restrictions on the burning rate to satisfy the given technical requirements. Therefore, of interest are the data on a change in the agglomeration degree with varying propellant composition at almost unchanged burning rate. In particular, it has been established [62] that the introduction of a fine-disperse oxidizer (tri-modal size distribution instead of the bimodal one) reduces the agglomerate size and the substitution of HMX by RDX leads to an increase in agglomerate size. Below, we report briefly on the influence of various factors on metal agglomeration.

5.3.1. Influence of various factors on agglomerate size.

The data on agglomerate dispersion are convenient to compare using a general approach such as the calculation of a function of particle size distribution and the characteristic D_{mn} sizes on its basis:

$$D_{mn} = (\sum D_i^m N_i / \sum D_i^n N_i)^{1/(m-n)}$$

In this case D_i is the middle of size interval in the histogram; N_i is the number of particles in a given size interval. In addition, the results of a granulometric analysis can be represented as an integral distribution function with determination of the size, corresponding to a given per cent (e.g. D_{50}, 50%) of the number of particles or to their total mass.

The size of initial metallic particles has effect on the agglomeration degree in the combustion wave. It is known [2] that the metal powder is agglomerated at a threshold concentration. For example, for the Al particles with size 1 μm the threshold concentration is 1% by weight; for the 10 μm particles it amounts to 2-3% by weight; for the 50-70 μm ones it is 5-7% by weight and the 160 m particles are not agglomerated up to 10% concentrations. These figures may vary depending on the properties of the oxide layer, metal purity, and the quality of propellant mass mixing. They reflect, however, the main tendency: the smaller are the metallic particles, the lower is the threshold. Note that in our experiments when using the ultrafine Al particles ALEX (Al particle size being less than 0.5 μm, the content in propellant equals 18% by weight) the combustion of traditional propellants based on ammonium perchlorate and the inert binder in air resulted in the formation of 10-30 μm agglomerates.

The influence of pressure is determined by two factors: a rise in the burning surface temperature (and in flame) as well as in the burning rate. The temperature factors intensify agglomeration due to a stronger reaction of metal in the surface layer. However, an increase in the burning rate leads to a decrease in the residence time of particles in the heating zone. The empirical facts testify mainly to a decrease of agglomerate sizes with rising pressure.

The size of the oxidizer particles determines a geometrical structure of solid propellants and the coarse oxidizer particles are directly related to the size of the binder "pocket" containing small metallic particles. A general tendency is in the fact that the larger are the coarse oxidizer particles, the larger are the forming agglomerates. Note that for given oxidizers size the size of agglomerates depends on the quality of propellant mass mixing. In particular, using "gelatinization" instead of mechanical mixing to prepare model propellant with 7% of Al weight has caused a substantial (about 1.5-fold) decrease in agglomerate size [2].

The properties of the metal exhibit their effect through a complex of the characteristics of pure metal, its oxide, and foreign impurities. Practically all metals tend to agglomerate in the combustion wave. Experiments on the pressed samples AP/polyformaldehyde/20% Metal burning out at 30 atm showed [2] that the Al particles (<1μm) reach the size of D_{50}=22 μm and the Mg particles (< 1.5 μm) reach only 16 μm size. In this case, however, the burning rate of Mg containing samples is higher which may also cause a decrease in agglomerate size. It is reported [38] that at a relatively low content of Mg in the propellant (10% of weight) the agglomerates, forming at pressures up to 20 atm, are the accumulates consisting of the partially burning initial (11.6 μm) metallic particles. The sampled accumulates can be readily destroyed under ultrasonic treatment.

The high speed movie of the combustion of the pressed sodium nitrate/magnesium (70/30 by weight) mixtures in the air shows interesting peculiarities of both metal agglomeration and burning surface destruction [63]. The Mg particle size was 10-60 μm, sodium nitrate was used as either coarse (125-230 μm) or fine (< 40 μm) fraction. Note that with the volume content of metal in a given mixture of about 40%, the metallic particles form a continuous interconnected structure. Nevertheless, in the samples containing a coarse grain oxidizer we assume the formation of the so-called "pockets" with the metal that fills the gaps between oxidizer particles. The movie shows that in the gas phase above the surface there is a great number of nonluminous particles and a smaller number of the luminous ones. The latter are, as a rule, larger and are observed in the form of the burning magnesium agglomerates. Upon combustion of samples with a fine grain oxidizer we record the relatively coarse particles detached from the surface. Later, they are ignited in the flame. The majority of nonluminous particles are, presumably, the liquid droplets of the products of sodium nitrate thermal decomposition. Their characteristic size is D_{50}=52 μm for the propellants with coarse oxidizer and D_{50}=55 μm for those with a fine oxidizer with a more "smeared" size distribution function of particles. The characteristic size of burning agglomerates for the sample with a coarse oxidizer is D_3 =125 μm. It should be noted that when the burning rate equals 1-2 mm/s the coarse sodium nitrate particles, passing to the burning surface, are assumed not to have enough time to melt completely if they do not stay on the burning surface. It is suggested that the heating of the oxidizer surface layer due to heat transfer through the metallic carcass leads to the partial decomposition of sodium nitrate and to the emission of partially liquefied particles into the flame.

The formation of coarse agglomerates was recorded upon combustion of pressed samples with a high content of Mg (40-70% of weight) and sodium nitrate as the oxidizer [64]. The initial 50 μm Mg particles coarsened in the combustion wave at 10 atm to 150-550 μm. The data on agglomerate structure were not reported [64].

The boron agglomeration in solid propellant combustion has been observed in a number of works [2,44,45]. The quantitative information is, however, rather scarce. Therefore, of great interest are the data [65] on a comparative study of agglomeration upon combustion of propellants with pure aluminum, pure boron, and their mixture. Experiments were carried out at pressures from 1 to 100 atm. The residence time of condensed particles in the flame was 3-10ms. The condensed combustion products were collected in water and then analyzed by their sizes and the content of pure metal. Upon combustion of propellants containing 70% of AP (400 μm, 200 μm, 20 μm), 20% of nitro-binder (polyethylene glycol elasticized with butanetriol trinitrate) and 10% of B (6.8 μm crystals) it has been established that the combustion efficiency of boron in agglomerates increases with pressure from 10% (1 atm) to 65% (100 atm). In this case, the median volume diameter of agglomerates increases from 28 μm to 36 μm. Substituting 30% of crystalline boron by amorphous boron (1.3 μm) leads to doubling of the combustion efficiency at 1 atm but has actually no effect at 100 atm. The microscopic studies show that the condensed combustion products have irregular shape at low pressures and become spherical at high pressures. An increase in agglomerate size with pressure is explained in [65] in terms of the possible agglomeration in the gas flame in which the high temperature is realized. Using experimental data on gaseous combustion products, testifying to the high (compared with equilibrium) CO_2 concentration, the conclusion has been drawn on the advantageous oxidation of hydrocarbons in the flame near the propellant surface that causes oxygen deficit for boron oxidation. Thus, a relatively low rate of boron oxidation is the reason for the impossibility of reaching equilibrium and determines low combustion efficiency of boron.

Making special coating over metallic particles may solve the problem of ignition promotion. The theoretical estimates for boron particles are described in [44]. Zirconium, titanium, and lithium fluoride are proposed as coatings. It is assumed that the oxidation of coating makes the temperature rise to the level at which B_2O_3 boils. The former must free the boron surface of oxide and lead to ignition. According to calculations, the boron particles of 2-10 μm may be ignited at atmospheric pressure in a gas medium at 1900K and partial pressure of oxygen of 0.1 atm and of water vapor of 0.1 atm by spreading either the layer of titanium amounting to 11% or of zirconium amounting to 8% of the weight of the boron particle. It should be noted that at this ambient temperature there is no ignition of pure boron particles. The layer of lithium fluoride, according to [44], may also provide the ignition of boron particles at 1900 K.

Experimental data are available on the influence of coating on the agglomeration of Al particles [65] upon combustion of solid propellants. Copper, nickel, and iron were used as coating in order to increase the melting temperature of a particle and thus to prevent the coalescence of particles within the burning surface. The coating of about 0.1 μm was spread by chemical precipitation from the solution of corresponding salts. The experiments on combustion in air of the pressed mixtures AP/PMMA+2%Al with a nickel coating show that the sizes of Al agglomerates decrease 1.5-fold, the ignition of Al particles occurs at a smaller distance from the burning surface.

Similar data were obtained for copper and iron coatings. Note, however, that the quantitative results on agglomeration [65] were obtained only on the basis of indirect data on the luminescence intensity of the two-phase flow of combustion products (the number of luminescent tracks).

Interesting are the results [66] on a study of the inflammation in air of the cloud of Al particles covered by a thin nickel layer (1-3% of particle weight, thickness being 50-180 Å). With the optimal thickness of the coating the protecting nickel layer prevents aluminum from oxidation in the initial heating stage. However, when the melting temperature of aluminum is reached, the nickel layer cracks due to a double difference in the coefficients of volumetric expansion and is removed which bares the surface of pure aluminum and makes it to react with an oxidizer. The maximum effect is provided by the nickel coating with a thickness of about 100 Å. In this case, the flame propagation velocity over the Al powder cloud with volume median size D_{30}=10 μm increases 1.5-4 times depending on the oxidizer content in the gas medium.

The influence of the binder and oxidizer nature, i.e. the chemical composition of the propellant, is the most difficult problem for studying and analyzing. Obviously, the variations in chemical composition may substantially change the characteristic temperatures in the combustion wave, the residence times and the physicochemical properties of components. Besides, the results are often difficult to compare due to the difference in the particle sizes of components and the methods of selection and analysis of the condensed phase.

A comparative study of Al agglomeration upon combustion in the pressure range 5-40 atm of the pressed AP/fuel mixtures has been performed in [67]. Polymethylmethacrylate (PMMA), polyformaldehyde (PFA), naphthalene, and carbon with added 0.5% paraffin were used as fuels. The tendency to agglomeration, estimated by the characteristic size D_{50}, increases in the series PFA/PMMA/naphthalene/carbon. Actually, the agglomeration for the mixtures with PMMA and PFA was almost the same and less pronounced. The introduction of naphthalene and carbon caused a considerable increase in the size of agglomerates. Thus, with P=40 atm for the AP+PFA+20%Al mixture D_{50}=42 μm and for AP+PMMA+20%Al D_{50}=46 μm, and for the AP+naphthalene+20%Al mixture D_{50}=180 μm in air m and for AP+C+20%Al D_{50}=200 μm. Substituting ammonium perchlorate by potassium perchlorate made the above sequence of fuels unchanged with respect to agglomeration. In this case, however, the size of agglomerates decreased by about 20-30%.

Attempts to study the influence of the binder on the formation of the condensed residues of the combustion of aluminized propellants were made in [68]. Experiments were performed using three propellants containing 17.5% weight of Al and differing in the binder type. Two binders were inert: polybutadiene with carboxy terminated groups (CTPB) and tri-functional polypropylene glycol (TPE); the third binder was energetic, polyethylene glycol with energetic plasticizer bis (2-fluoro-2,2-dinitroethyl) formal, PEG/FEFO.

The preliminary experiments on thermal decomposition of binders in argon with a heating rate of 50 K/min show that CTPB decomposes completely at 485°C and evaporates without bubbles. TPE is fully liquefied at 300°C and under further heating it evaporates with moderate gas and bubble formation. The active binder PEG/FEFO is liquefied at 220°C and boils to form gas bubbles. At 240°C it converts into the brown liquid. When AP is introduced into the binder, CTPB

decomposes, interacting negligibly with AP. At 303 C the character of TPE decomposition changes and the gas release of the TPE+AP system increases. The interaction between AP and PEG/FEFO is actually negligible. The liquid state of the binder transforms, however, into the solid state at about 300°C. These experiments provide a qualitative concept of the binder behavior under slow heating. Remember, however, that in the combustion wave the rate of temperature rise is of 3-4 order of magnitude higher. Thus, it is difficult to predict the binder behavior in solid propellant combustion and it is necessary to perform special experiments on the thermal decomposition of propellant mixtures under fast heating.

The samples of propellants were burnt out in a window bomb at 21.6 atm and in the pipe bomb at 25 atm. The burning rates for propellants with the inert binder were almost identical (ca. 0.8 cm/s) and for the propellant with the active binder they were higher by a factor of two. The filming shows that the propellant with CTPB gives much smoke. The other propellants burnt with clear flame. An analysis of the condensed combustion products gave the same value of D_{50} (88 μm) for both of the propellants with the inert binder. However, for the propellant with the active binder D_{50} was 68 μm. In this case the value of D_{50} characterizes particles whose size exceeds 37 μm. The total mass of these particles for all three propellants was about 5% of the total mass of precipitated particles. The 5-37 μm particles amounted to 7-8% of the mass of the condensed residue for the propellants containing CTPB and active binder and for the propellants with the TPE-binder their fraction was 12.5%. The data on the size-distribution of fine particles were used to estimate the damping rates of sound oscillations in the combustion chamber. Conclusion has been drawn on a considerable influence of the binder on the character of metallized propellant burning. However, it is rather problematic to use the results of a given paper for future estimations because there is no data on size distribution of components as well as for the completeness of aluminum burning-out in agglomerates.

Since it is difficult to interpret the multi-factor experiment on metal agglomeration, it is necessary to perform experiment under rigidly characterized and fixed conditions. Such an attempt was made in [69,70], where the samples of solid propellants with variable composition were prepared using heterogeneous components of the same size, which resulted in a similar geometrical structure of the propellant. The burning velocity was also equalized by means of catalysts. In this case, the initial aim was reached, i.e. the equal capacity of the binder "pockets", filled with metal, and the similar residence times in the surface propellant layer. The model propellants contained 17-20% of Al powder with particle size of 5-30 μm, pure AP, and AP+HMX mixture, inert and active binders. The samples were burnt out in a flow bomb with the downward directed flame. The condensed combustion products were collected in the lower part of the bomb using metallic grids stack and aerosol filter (the minimum captured particle size being 0.5 μm). The products were then analyzed by their sizes and by the content of active aluminum.

The high-speed movie was performed for propellants, burning at atmospheric pressure under backlit illumination. Obviously, the behavior of metallic particle aggregates depends on the propellant type. In the poorly agglomerating propellants the formation of particle filigrees on the burning surface is followed by ignition of the top and by coalescence of particles into a large droplet. For the strongly agglomerating propellants the particle coalescence and ignition occur within the limits of the surface layer. Besides, the intermediate case may be realized where the separating nonburning aggregate coalesces into a droplet at a comparatively large distance from

the burning surface and is ignited to form a closed aureole which is then destroyed and transforms into a typical "smoke" tail. It is assumed then that the closed aureole corresponds to a thin liquid oxide coating, existing during a short period of time and which is difficult to shoot. An exact explanation of this phenomenon is still unavailable.

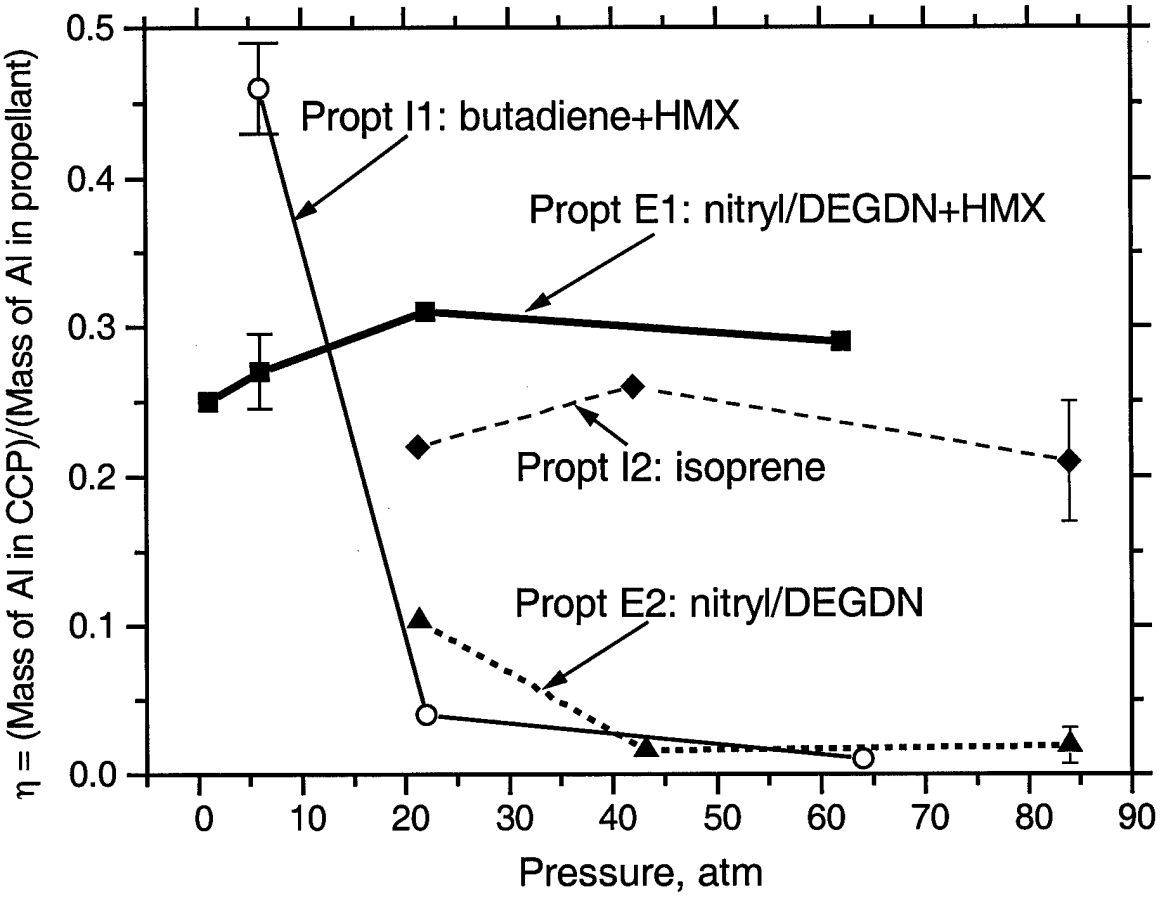

Fig. 5.7. Relative content of unburned Al in condensed combustion products vs. pressure for AP-based propellants with different binders.

Treating the data on aluminum combustion efficiency in the flame with varying pressure from 1 to 80 atm, the following three conclusions have been drawn:

1.A rise in pressure is followed not only by a typical tendency to an increase in the completeness of metal burning-out (propellants I1 and E2) but also by a tendency to the conservation of a high degree of combustion incompleteness (propellants I2 and E1). The latter may be attributed to the effective metal capsulation by oxide. However, the reasons for this change in the agglomerate structure are still unknown. Note that the experiments were carried out under the weak argon blowing of propellants, and the metal was extinguished after mixing with inert gas. It is not yet validated to apply these results to the conditions of a rocket motor. They, however, demonstrate an important feature of the initial phase of agglomerate motion in the flame, which should be taken into account in mathematical models.

2. The phenomenon of capsulation is observed upon propellant combustion with both inert and active binders. Thus, a high reactivity of the binder fails to provide a high efficiency of metal burning-out.
3. A comparison between inert binders shows substantial difference in the influence on the completeness of metal combustion, i.e. at high pressures polybutadiene provides better efficiency of Al combustion than isoprene. Additional information is necessary about the thermal destruction and the adhesion properties of binders at high temperatures to interpret these facts.

The data on particle sizes and a relative content of a coarse fraction are in agreement with the above tendencies in metal combustion efficiency. Note that the fine particles (less than 30-50 m) contain, as a rule, not more than 1% of pure metal whereas the coarse ones contain up to 20-30% (in the capsulated agglomerates). It turns out that for the weakly agglomerating propellants I1, E2 the fraction of fine particles in the total mass of condensed residues varies from 80 to 98% and for the strongly agglomerating particles it amounts only to 45-65%.

5.3.2. The burning time of agglomerates.

As has been mentioned, the burning time of single aluminum particles in oxygen-containing media depends on the diameter to the first power for fine and to the second power for coarse initial particles. The question of agglomerate combustion law has been studied to a smaller degree but we may give some recommended correlations. The empirical relationship below

$$T_b = \text{const}\, D^n/\alpha^m$$

is used in most published papers. In this case, t_b is the time of particle burning; D is the diameter of the initial particle; α is the mole fraction of oxidizing components in the gas medium. Earlier it was assumed that the main oxidizing reagents in the combustion products of solid propellants, H_2O and CO_2, act equivalently, and α equals the arithmetic sum of their mole fractions. According to [2,4], m=0.9 whereas n=1.5 [2] and n=1.75 [4]. A more complex expression for the burning time of agglomerates in the rocket motor chamber has been derived in [71]

$$t_b = \text{const}\, D^{1.8}/R_c P^{0.27}\alpha^{0.9},$$

where R_c is the matching coefficient, taking into account the difference between the burning conditions in the rocket motor chamber and in the bomb; P is the pressure in the chamber. Note that the minor differences in the calculation formulas may result from the differences in experimental conditions, initial components, and the methods of treatment of experimental data.

5.3.3. Mathematical modeling of agglomeration.

A complete model of metal agglomeration in the combustion wave of solid propellants must describe a sequence of stages beginning in the surface layer and continuing on the burning surface. It is necessary to consider the processes of metallic particle heating, the formation of a primary contact, coalescence, partial reacting and ignition. Attempts to create agglomeration models have being under way from the 60s.

One of the first models [54] is based on the idea of collision and coalescence of the melted metallic particles on the burning surface. The model assumes that the residence time of a particle on

the burning surface is equal to the time necessary for the wave to cover the distance equal to the metallic particle diameter. Expressions have been obtained for the critical size of metallic particles. The particles of this size tend to agglomeration. The model, however, fails to predict both upper limit size of agglomerated particles and the size of agglomerates.

Another model has been proposed [72] that is based on the idea of metallic particle accumulation in the liquid-viscous surface layer due to surface tension. The excess of particle ignition time over the time of particle accumulation (complete filling of the liquid-viscous layer) is taken as a criterion for agglomeration. Thus, if the metallic particle is ignited faster than the layer is filled, agglomeration fails: the particle is ejected into the gas phase.

A detailed model of agglomeration as applied to the highly metallized two-component mixtures with a melting oxidizer has been developed in [73,74]. The time of agglomeration has been estimated as a sum of the times of contact and of complete particle coalescence. Special experiments on coalescence under isothermal conditions show that the coalescence of particles obeys the law below

$$(x/2R)^n = tK(T)/R^m,$$

where x is the radius of contact surface between particles with radius R; K(T) is a power function of temperature; t is the time. The indices n and m depend on the mechanism of sintering. In the case of surface diffusion for aluminum n=8 and m=4 and for magnesium n=7.2 and m=4.8. For a viscous flow for Al n=1.4 and m=1, and for Mg n=1.9 and m=1.1.

It is interesting that during Al sintering the process in the initial stage first follows the mechanism of surface diffusion and then the mechanism of viscous flow. The final stage follows the mechanism of volume diffusion (n=4.6 and m=3). The time of Mg particle sintering is 1000-fold longer than that of Al particle sintering. For magnesium the sintering first follows the mechanism of viscous flow and then the mechanism of surface diffusion. If sintering occurs in the active medium, e.g. in the air, the local inflammation of magnesium is realized at a fairly high substrate temperature in the zone of a contact "neck". Thereafter the flame spreads over the particles.

The model [74] gives a qualitatively correct explanation of the experimentally observed dependencies, e.g. the existence of a minimum in the curves of the dependence of the enlargement degree of initial metallic particle size on pressure with varying initial particle size and on the relative density of the pressed sample. The model predicts the ranges of parameters (surface tension of liquid surface layer, particle size, the velocity of gas flow from the surface) in which either the initial metallic particles or the particle agglomerates are dispersed or the carcass is formed after sample burn out.

A relatively simple model of Al agglomeration upon combustion of conventional (up to 20%) solid propellants is proposed in [75]. The model is based on the qualitative concepts of a geometrical structure of composite propellants, characterized by the binder "pockets" filled with metallic particles [53]. The problem reduces to the determination of the "effective pocket" determined as a local minimum volume in which the Al "capsulation" by AP particles is reached and the flame temperature exceeds that of aluminum inflammation. It is assumed that at lower flame tempera-

tures, aluminum cannot be ignited and leaves the burning surface. According to [75], a temperature of 1400 K is taken as that of aluminum inflammation in the gaseous combustion products of solid propellants. It is interesting that calculations for model propellants based on polybutadiene binder (10% of weight), Al (20% of weight) and AP (70% of weight) show a substantial dependence of flame temperature on the particle size of a fine AP fraction. It was assumed then that AP consists of three fractions: fine, medium, and coarse in a 1:6:3 ratio. The flame temperature rises from 1250K to 2000K with varying size of fine particles from 5 to 100 μm. Accordingly, a temperature of 1400K is realized only for the mixtures with fine AP particles large than 50 μm in size. Thus, actually, leads to the formation of fairly large agglomerates despite the existence of fine AP particles in solid propellants. The calculated results are in fair agreement with the available experimental data. It was recommended to reduce the agglomeration intensity in propellants with a three-model oxidizer by increasing the concentration of medium AP particles.

Attempts were made [76] to give in detail the agglomeration model to take into account the influence of pressure and of the physicochemical parameters of propellant components. It is assumed that the ensemble of initial metallic particles within the elementary cell (pocket) melts on the burning surface and coalesces into a single droplet that may move over the surface due to the nonuniform gas flow. The coalescence of single metallic droplets is accompanied by their heating by flame due to the heat release of heterogeneous oxidation reactions. Agglomerates are ignited instantaneously when the critical temperature is reached. As a result, the connection with the burning surface is failed and the agglomerate is carried out by the gas flow. The critical temperature and size of the forming agglomerate are calculated from the equations of heat balance and by the chemical reaction for a reacting metallic droplet. The agglomerate heat exchange with the gas phase on the burning surface is calculated by solving the additional problem on the diffusion flame of oxidizer and binder decomposition products. Giving the reasonable values for kinetic and thermophysical parameters, the calculations in terms of model [76] give the results that are in qualitative agreement with available experimental data. In particular, the increasing dependence of the median agglomerate size on the oxidizer particle size is well reproduced for P=20 atm [77].

It is shown that the characteristic agglomerate size may both decrease and increase with varying both the constants of the global chemical reaction in the gas flame and the mass oxidizer fraction in the propellant, and may even display a maximum with rising pressure as verified by some experiments. In this case, the flame temperature and the dependence of burning rate on pressure vary within a wide range that causes large variations in the intensity of heat exchange with agglomerate on the burning surface. Agglomeration increases with either growing distance of flame stand off or dropping flame temperature.

It is correctly reasoned [76] that the hypothesis of separation of the ignited Al particles from the burning surface which is a basis of the model, fails for the combustion of propellants with a low temperature of either flame or burning surface. Besides, a quantitative use of the model [76] assumes a reliable knowledge of a great body of kinetic and thermophysical parameters which is now impossible. Thus, actual is one of the first calculation models of metal agglomeration [78] based on the analysis of the geometrical structure of heterogeneous propellants. This "pocket model" suggests that the temperature-time conditions in the combustion wave of solid propellants provide, in most cases, the sintering and subsequent melting of metallic particles on the burning

surface. Further behavior of the resulting aggregate of particles in the model is neglected. The conditions for agglomerate ignition are indirectly assumed to be fulfilled. Therefore the calculated values of agglomerates should be considered as predicted with all conditions satisfied. The contacts between metallic particles in the «pocket», consisting of the coarse oxidizer particles, are considered necessary for agglomeration.

It might be easily shown on the basis of geometrical considerations that when the volume content of metal in the pocket is 20% and more, which is typical of conventional solid propellants, the number of contacts per one metallic particle exceeds 1.6. This stimulates the formation of the infinitely long chain of contacting metallic particles and creates the necessary condition for the sintering of metallic particles ensemble. Further, using stereology, the effective pocket size D is calculated and the expected agglomerate size is estimated using the formula

$$D_{ag} = (\beta^{1/3})D,$$

where β corresponds to the volume content of aluminum in the "pocket". Thus

$$\beta = (\beta_{Al})(1 - \Sigma\beta_{ox})^{-1},$$

where β_{Al} and $\Sigma\beta_{ox}$ are the aluminum and oxidizer volume fractions in solid propellants. The effective size D is calculated from the relationship below

$$D = 4(1 - \beta_{ox})/S_{ox}, \quad S_{ox} = (6/D_{ox})(\beta_{ox} - 1)\ln(1 - \beta_{ox}),$$

where β_{ox} and S_{ox} are the volume fraction and specific surface of coarse oxidizer particles in the propellant, D_{ox} is the mean size of coarse oxidizer particles.

The theoretical concepts of [78] were used to analyze the results of a study of agglomeration upon combustion of the pressed pyrotechnic metal-oxidizer mixtures [63]. In this case, the metal first fills the empty gaps between oxidizer grains and then is pressed. The mass fraction of metal ε in the mixture (the oxidizer fraction being $1-\varepsilon$) and the free packed mixture ρ_f are known. Using these values, the expression for calculating the mean-volume agglomerate diameter has the form

$$D_{ag} = 2/3 \cdot D_{ox}[\beta_{Me}/(\beta_{ox}-1)]^{1/3}/\ln(1-\beta_{ox}) \qquad (5.2)$$

Here $\beta_{Me} = \varepsilon\,\rho_f/\rho_{Me}$, $\beta_{ox} = (1-\varepsilon)\rho_f/\rho_{ox}$. This formula gives the value of D_{ag}=140 μm and the experimentally determined value turns out 125 μm.

The existence of AP fine and coarse fractions at a time leads to the widening of the size distribution function of agglomerates with a weak effect on the value of the predicted effective agglomerate size. Let us give some results of such calculations [79]. The bimodal system of the oxidizer particles can be characterized by the mean size $\overline{D}$ and mean free distance $\overline{l} = \overline{R} - \overline{D}$ between the particles, where $\overline{R}$ - mean distance between centers of particles.

Let us assume further that the particles are distributed in the volume according to the Poisson law. Then calculation according to the formula

$$E(D_{aggl}) = \sqrt[3]{\frac{\beta_M}{1-\beta_{ox}}} \cdot \overline{D} \cdot \overline{E}_n \qquad (5.3)$$

gives value of mathematical expectation E of the size of agglomerate. Here

$$\overline{E}_n = \frac{1}{14}\sum_{n=1}^{14} E_n(R_n), \quad E_n = \frac{1}{2}\sqrt[3]{\frac{\overline{D}^3}{\beta_{ox}(\overline{D})^3}}\frac{\Gamma(n+1/3,\alpha)}{\Gamma(n,\alpha)}$$

where E_n - mathematical expectation of value $l_n / \overline{D}$; $\Gamma(x,\alpha)$ - reduced Gamma function.

Comparison of the numerical values of the coefficients E_n and $(2/3)/\ln(1-\beta_{ox})$ in formulas (5.2) and (5.3) at $\overline{D}^3 / (\overline{D} \equiv 1)$, i.e. for monodisperse oxidizer, has shown [79] that the difference between coefficients equals 18% at β_{ox}=0.33 and only 6% at β_{ox}=0.37. Consequently, approximate formula (5.3) with reasonable accuracy makes it possible to calculate average distances between the particles.

It has to be underlined that the model examined is based on substantially simplified picture of the phenomenon of agglomeration. One of the basic assumptions of the model is the possibility of isolation (conditional) in the uninterrupted binder matrix of the cell with the assigned content of powder-like metal. It is difficult to justify by any theoretical method this assumption. Thereby it was important to compare the results of calculations with the data of experimental observations [79] made in combustion of the model SP, which contained the particles of aluminum with the size of 5-50 μm and ammonium perchlorate with the size of 100-300 μm. It followed from these observations that the formation of agglomerates in many instances was preceded with the appearance on the burning surface of aggregates consisted of partially sintered particles. During certain residence time on the surface the aggregates melted and merge into the drop of liquid metal. Only rarely individual aggregates ejected into the gas phase, without having been completely fused. With pressure increase these events could proceed within the limits of the reaction layer of condensed phase. In this case, as a rule, the already formed agglomerates appeared at the burning surface, whose ignition occurred in the limits of the condensed phase.

In the case when SP contains the oxidizer and metal particles identical with respect to sizes, the residence time of metal on the burning surface proves to be insufficient. The non-ignited particles are ejected from the surface and ignited at comparatively large distances downstream. The detailed comparison of the expected sizes of agglomerates with those recorded in experiments with the model propellants showed rather fair efficiency of the model proposed and calculation method.

Experiments were conducted at atmospheric pressure with the specially prepared samples of SP, which contained the narrow fractions of oxidizer. The measurement of the sizes of agglomerates ejected from the burning surface was conducted by high-speed macro cinematography method with the intense pulse back illumination.

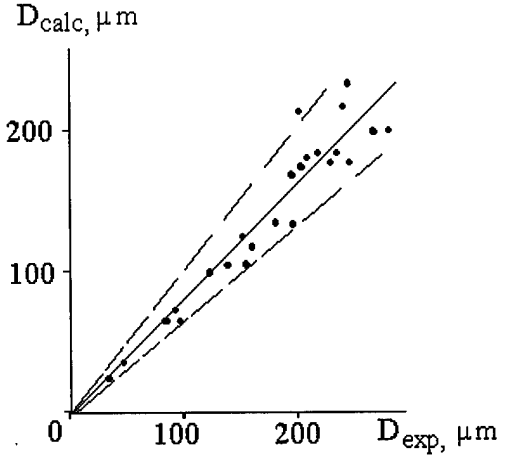

Fig. 5.8. Comparison of calculated sizes of agglomerates on the SP burning surface.

The sizes of the particles of the metal varied in these experiments from 5 to 50 μm, the polybutadiene type binder has been used. As can be seen from Fig. 5.8, with variation in the size of the oxidizer particles from 100 to 300 μm the disagreement of experimental and theoretical results does not exceed 10-15%.

5.4. EFFECT OF AL ON THE BURNING RATE OF A SOLID PROPELLANT.

5.4.1. Mathematical modeling of the combustion of metallized solid propellant.

In Ref. [52] a vast experimental material has been reported, from which it was evident that addition of aluminum powder can both increase and decrease the burning rate of SP. Two approximate analytical combustion models have been formulated in Russia [80, 81] for two-component system with easily gasified oxidizer and hardly gasified fuel. The former is randomly distributed in disperse form throughout the system. The models were intended for describing the combustion of a black powder, but with some stipulations they can be applied to the metallized compositions simulation. By analogy with the combustion model for volatile monopropellant a quasi-homogeneous model with the rate control stage in the smoke-gas phase was examined. Under the assumption about the diffusion combustion regime of ejected from the surface particles the following expression for volume heat evolution rate Φ in the smoke-gas mixture can be written: $\Phi \sim s|\nabla C|$, where $s \sim p/d$ - specific (per unit volume of mixture) area of the particles; $|\nabla C| \sim 1/d$ - concentration gradient of oxidizer near the particle; P - pressure and d - particle size. Then

$$m \sim \sqrt{\Phi_{max}} \sim \sqrt{p}/d \qquad (5.4)$$

If in the zone of maximum heat evolution the particles become detached from the gas, it is fulfilled $m \sim p^{1/3}/d$. The above relationships can be modified in the case of combustion of SP with addition of aluminum. When taking into account an intrinsic heat evolution Φ_0 of the gaseous flame, one obtains

$$\Phi = \Phi_o + \Phi_{Al}, \quad m_0 \sim \sqrt{\Phi_0}, \quad \Phi_0 \sim m_0^2 \sim p^{2\nu_0}, \quad \Phi_{Al} \sim p/d^2,$$

$$m/m_0 = \sqrt{\Phi/\Phi_0} = \sqrt{1 + Bp^{1-2\nu_0}/d^2}, \quad B = const$$

Here m_0 – burning rate of metal-free composition. An expression of such type first was obtained in Ref. [82]. Specifically, it was made with taking into consideration a possibility of the existence of different temperatures for particles and surrounding gas, so that the result of [82] had the form

$$m/m_0 \sim \sqrt{A + Bp^{1-2\nu_0}}, \quad A = const, \quad B = const \tag{5.5}$$

It was reported [52, 82] that qualitatively expression (5.5) agreed well with the experiment: with $\nu_o<0.5$ the ratio of m/m_o has positive dependence on the pressure, and with $\nu_o>0.5$ - negative. It should be noted that upon derivation of (5.5), as in (5.4), the assumptions about the rate control role of smoke-gas zone and about the quasi-homogeneity of the combustion model have been actually used.

More detailed combustion model for aluminized SP without fixing the rate control stage was developed in Ref. [57]. The model effectively used the concepts of "petite ensemble" approach (see Section 3.3.3). There were considered melting the particles of aluminum, their motion in the flame, ignition, combustion and heat supply from the combustion zone of metal to the propellant surface. Calculated burning rate and the pressure exponent for SP with aluminum and without it was compared with reported in Ref. [57] Miller's experimental data. The experiments have been carried out at p=68 atm for 25 SP formulations, which contained in the different ratios eight AP fractions. The numerous parameters, entering the "petite ensemble" model (for SP without metal), were selected for the best agreement with experiments, and then were used without change in the model taking into account aluminum. Thus, the complication of the model did not involve the appearance of new floating coefficients. Since in the majority of experiments the effect of aluminum on the value of the burning rate turned out to be negative (metal acted only as heat-sink in the condensed phase), for the application the simplified version of the model was proposed which did not take into account the combustion of aluminum.

It was assumed that each pseudo-propellant (part of SP, which contains one narrow fraction of oxidizer) contains the same mass fraction of aluminum as entire propellant. The balance of heat for the pseudo-propellant takes the form:

$$\begin{aligned} c(T_s - T_0) = {} & \beta_F Q_{PF} e^{-\xi_{PF}} - \alpha Q_L - (1 - \alpha - \beta) Q_f + \\ & \alpha(1 - \beta_F)\left(Q_{FF} e^{-\xi_{FF}} + Q_{AP} e^{-\xi_{AP}}\right) - \beta Q_{mAl} - \beta c_{Al}(T_f - T_s) \end{aligned} \tag{5.6}$$

Designations are the same as in the BDP model presented earlier (Section 3.3.2). Additionally, here entered: β - mass fraction of aluminum in propellant; Q_{mAl} - heat of Al melting. The right hand side in (5.6) takes into consideration also the heat consumed for melting of metal and heating of ejected particles from T_s to T_f. The size of the particles of the metal is not considered.

Heat balance (5.6) does not include yet the term (see below (5.12)) responsible for the heat feedback to the SP surface from metallic particles burning in the gas flow. All the ejected Al particles according to the model are of the same size, i.e. agglomeration is not considered. It is assumed that on the SP surface the particles have a temperature close to T_s and after detachment from the surface they are ignited after time t_{ign}, according to [2]

$$t_{ign} = 10^{-6}(D_{Al}/70)^2 \exp(32000/RT_f) \tag{5.7}$$

Here D_{Al} - particle size in μm, t_{ign} – ignition time in ms. Equation of particle motion is as follow:

$$\frac{1}{2}\rho_g c_D (v_g - v_p)^2 \frac{\pi}{4} D_{Al}^2 = \rho_{Al} \frac{\pi}{6} D_{Al}^3 \left(\frac{dv_p}{dt} + j \right) \tag{5.8}$$

Here V_g and V_p - gas and particle velocities, respectively; j - directed toward the burning surface acceleration of mass forces (if it exists),

$$c_D = \begin{cases} 28\,Re^{-0.85} & at\ Re < 10 \\ 12.5\,Re^{-0.5} & 10 < Re < 1000, \quad Re = (v_g - v_p)\dfrac{D_{Al}}{\mu}\rho_g, \\ 0.4 & Re > 1000 \end{cases} \tag{5.9}$$

where μ - viscosity of gas. After ignition the diameter of particle in the equation of motion becomes variable, and expression for c_D is multiplied by ~2.5. For D_{Al} the following dependence is used:

$$D_{Al}^{\delta} = D_{Al,0}^{\delta} - \beta_c t, \quad 1.5 < \delta < 2, \quad 0.002 < \beta_c < 0.004\ cm^{\delta}/s \tag{5.10}$$

It is similar to that given in [2]. With known size $D_{Al}(t)$ one may calculate rate of change in the mass of Al particle, dm/dt and heat release rate, dQ_{Al}/dt:

$$\frac{dQ_{Al}}{dt} = \frac{dm}{dt}\frac{dQ_{Al}}{dm}, \frac{kcal}{s}; \quad \frac{dQ_{Al}}{dm} = 7.5\,\frac{kcal}{g}. \tag{5.11}$$

Then the heat feedback to the burning surface from one Al particle can be represented in the form

$$Q_{Al} = \int_{t_{ign}}^{t_c} \frac{dQ_{Al}}{dt} exp\,(-\xi(t))\,dt \tag{5.12}$$

Here t=0 - moment of the particle ejection from the surface; $t_c = D^{\delta}_{Al,0}/\beta_c$ - moment of the particle complete burn out. Since the balance of heat (5.6) is applied for the mass unit of SP, the term supplemented to the right hand side of (5.6) that considers the heat feedback from the combustion of metal in the flame must take form Q_{Al} n, where Q_{Al} is calculated by (5.12) and n - number of particles of the metal in the mass unit of SP, $n=\beta/(\rho_{Al}\pi D^3_{Al,0}/6)$. Let us note that upon taking into consideration the Al agglomeration (i.e., the fact that the SP surface generates metal particles of the amalgamated sizes} instead of product Q_{Al} n one has to compute the corresponding integral.

Results of calculations [82] showed that the heat feedback from burning aluminum to the propellant is noticeable, if combustion occurs within the zone with $\xi = xcm/\lambda_g \leq 1$, i.e., at small distance from the surface. This is realized with the small sizes of particles ejected from the surface and at the low burning rate of SP (for example, for the pseudo-propellant with the coarse oxidizer). The calculated dependence of the thermal contribution of aluminum on the size of the oxidizer parti-

cles is shown in Fig. 5.9, in terms of the portions of different flames in the overall heat flux to the burning surface.

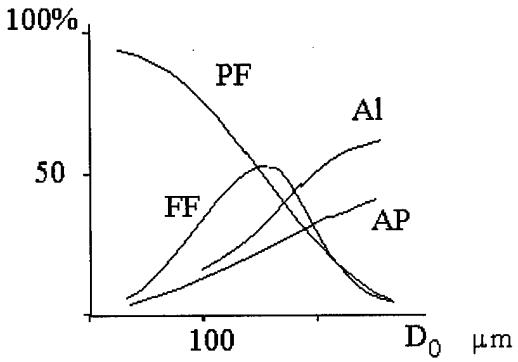

Fig. 5.9. Relative contributions of different flames to the total heat flux to the surface of condensed phase vs the oxidizer grain size.[82].

Comparison with Miller's experiments showed that the model with heat-sink (without taking into account the combustion of particles) overestimates the burning rate for compositions, which contain simultaneously coarse and fine AP fractions, and somewhat underestimates it for formulations, which contain only coarse and medium AP fractions. For the latter formulation the calculations with taking into account contribution from the burning Al particles gave better agreement with experiment.

5.4.2. Discussion of the metal combustion models.

Actually, the models presented contain elements that require refinement or modifications. The validity of assumption about uniform distribution of aluminum among pseudo-propellants [57] (for each of them the mass fraction of metal is the same as for entire propellant) causes doubt. It would be more natural to consider aluminum as distributed evenly over the binder, whereas the binder between the pseudo-propellants is distributed unevenly [83, 84].

Such considerations find confirmation in experimental data [57] for SP, which contained only extreme size AP particles: coarse (400μm) and fine (0.7; 2; 6 μm). The calculations predicted a comparatively small decrease in the burning rate due to introduction of the metal. For SP with overall content of AP decreased from 88 to 70%, the introduction of 18% of aluminum with the particle size of 6 μm, as expected by calculations, had to lower the burning rate from 20-23 to 15-17 mm/s. In the experiment, the burning rate reduced to ~8 mm/s. This significant decrease can be explained by the fact that the particles of metal were localized in the gaps between the AP particles of fraction 400 μm and served as heat-sink for located there small particles of AP with size of 0.7; 2 and 6 μm, which in the absence of aluminum provided high burning rate of these SP. Obviously, the agreement with experiment for these compositions can be improved, if one considers the metal distributed evenly over the binder. In this case the related to fine AP fractions amount of binder will turn out larger than for coarse AP fraction.

Apparently, additional investigations are needed on ignition of Al particles in the flame of SP. It is clear that the combustion of metal would affect the burning rate of propellant only in the case

when the noticeable portion of heat from the burning aluminum particles returns on the burning surface. This means that the distance to the flame of metal must be of the same order of magnitude as the distances of other flames from the burning surface. But in this case heating of aluminum up to its ignition proceeds in the gas flame with the high temperature gradient. Its value does not enter into formula (5.7), obtained by processing the experiment on the combustion of tablets of aluminized SP [2].

Further, it looks unjustified an inclusion in the heat balance (5.6) of term for taking account of heating the Al particle from T_s to T_f. Note that (5.6) has the meaning of heat supply and consumption on the surface. However, the heat balance (5.6) is written in such a way, as if metal on the surface, which has mean temperature T_s, reaches temperature T_f. This statement could not be accepted completely. Actually, liquid Al particles in the f lame are heated by gas, and this can be taken into account, for example, by the decrease in thermal effects Q_{PF}, Q_{FF}, Q_{AP} or by an increase in distances ζ_{PF}, ζ_{FF}, ζ_{AP}. Authors of [57] reported about the inclusion of expenditures for heating of metal in expressions for Q_{PF}, Q_{FF}, Q_{AP} but details of that were not given. Therefore the retention of term $\beta_{Al}(T_f - T_s)$ in (5.6) causes a quandary.

Let us consider defects common for the discussed combustion models. In these models the heat evolution due to the heterogeneous oxidation of the metal in the condensed phase, where about 3-4% of aluminum is consumed [52], is not included. In addition, there is not given background for the assumption on quasi-homogeneity of the combustion zone of the particles of metal in the gas flow.

The last issue can be discussed in more detail. In Refs. [80-82] the burning rate is calculated by the Zeldovich formula for gas phase zone, i.e. the rate control role of this zone and its quasi-homogeneity are assumed. For model [57], which is a model of the BDP type, the heterogeneity of the gas phase can prove to be unessential, if the rate control stage is located in the condensed phase. However, the BDP type model can have the rate control stage in the gas phase, e.g., under low pressures where AP does not burn independently. In such a case the condition of quasi-homogeneity becomes essential for formulating one-dimensional problem.

Let us estimate the size of Al particles necessary to meet the condition of quasi-homogeneity of the gas phase zone. From the common physical considerations it can be stated that the distance between Al particles in the gas has to be smaller than the length of the preheat zone Δx in the gaseous flame. In this case one may expect that the temperature distribution in the gas phase is sufficiently uniform. Thus, the above condition can be formulated in the form: $y < \Delta x$, where y is the distance between Al particles in the gas phase. In accordance with mass conservation law $y=\delta \rho_b/\rho_g$, where δ - mean distance between Al particles in the condensed phase, ρ_b and ρ_g are the binder and gas densities, respectively. The length of the pre heat zone equals
$\Delta x=\lambda_g$ cm, where c – specific heat, and m – mass burning rate.

Similarly to how this was done in the "relay race" model (see Section 3.5.2), let us replace the ratio of the average dimensions of two components (here metal and binder) with the ratio of their volume fractions in the SP:

$$\delta / D_{Al} = [(1-\alpha-\beta)/\rho_c]/(\beta/\rho_{Al}),$$

where β and $(1-\alpha-\beta)$ are the mass fractions of metal and binder in SP.

Finally estimation for D_{Al} takes the form

$$D_{Al} < \frac{\rho_g}{\rho_{Al}} \frac{\beta}{1-\alpha-\beta} \frac{\lambda_g}{cm} \tag{5.13}$$

Note that this relationship is obtained under the assumption about localization of the Al particles in the binder, so that $1-\alpha-\beta \neq 0$. For the typical values of the SP parameters $\rho_g/\rho_{Al} \approx 0.007$, $\beta=0.2$, $\alpha=0.7$, $\lambda_g=3\ 10^{-4}$ cal/(cm s K), c=0.3 cal/(g K), m=1.5g/(g/cm^{2}s). According to the condition (5.13) it is required $D_{Al} < 10^{-5}$ cm = 0.1μm. Certainly, estimation (5.13) needs the refinement: it should be taken into account the hydrodynamic lag of particles in the gas flow, the possibility of convective heat exchange between particles and gas, and the effect of the transversal heat exchange between particles.

Discrete character of the heat evolution in the gas phase makes it necessary to doubt validity of expression (5.12). Let us consider under which assumptions it is possible to use (5.12). For this one can examine the model problem about the heat transfer with δ-type (in time and space) heat evolution in uniform gas flow, m = const. The gas flow goes out from the condensed phase, which occupies half-space with the temperature of interface being T_s = const. It is assumed that the local flash in gas (δ-type heat evolution) does not make disturbances into the flow hydrodynamics, condition m = const is retained everywhere. Then it can be shown that from the total amount of heat released by flash-type oxidation of the Al particle the condensed phase receives portion of heat exp(-cmz*/λ), where z* - distance of the place of Al particle flash from the burning surface of SP.

5.5. COMBUSTION OF AL IN A ROCKET MOTOR

The previous Sections were mainly devoted to the problems of metallic particle behavior under heating in the condensed phase and in the reactions in the flame, i.e. at distances not more than several centimeters from the burning surface. When these data are applied to combustion conditions in a rocket motor, it is necessary to take into account the scale factors, in particular, for the motors, being several meters in length. Actually, the results of laboratory investigations may serve the initial data for mathematical modeling of metal transformation into oxide particles in the rocket motors. It is noteworthy that the completeness of metal combustion and the size-distribution of condensed product particles affect the various characteristics of the rocket motors, i.e. the value of the specific impulse, nozzle wear, combustor stability, the thermal radiation from the plume, environmental effects.

It is highly difficult to perform experimental investigations inside rocket motors. Some easier is to take measurements on motor plumes. However, extrapolation of these results to the area inside the motor is not easy task. Using several complementary methods for recording the condensed phase parameters, the authors [85] have got important information about the evolution of combustion products upon passage of the two-phase flow through the micromotor nozzle. The multi-

ple wavelength extinction measurements were performed together with the measurements of the velocities and sizes of single particles. These measurements gave a characteristic particle diameter D_{32} and the radiation absorption coefficient for the particles. A qualitative information about size and geometric form of particles in motor plume has been obtained by means of SEM studies on the precipitate of condensed combustion products, collected on copper plates, exposed during 0.5 s in the plume. The data on the size distribution of particles in the chamber and in the motor plume were obtained using Malvern systems, measuring the forward scattered light from particles with size of 0.5 μm and larger near the burning surface, as well as at the nozzle entrance and in the motor plume. In experiments a study was made of the model solid propellants with 2% and 5% Al and standard propellant with 16% Al used in Shuttle boosters (14% polybutadiene binder, 69.7% AP).

It is interesting that the experiments using all three types of propellants showed a similar form of the size distribution function of particles, obtained from measurements in the micromotor near the nozzle entrance. The bimodal distribution was recorded with the first mode within the range 1-4 μm and with the second mode within the range 5-8 μm. A characteristic size D_{32} calculated by these distribution functions is in the range 4-17 μm which testifies to the absence of coarse particles (agglomerates) in the combustion products at the nozzle entrance. At the same time, measurements of the size of condensed particles made in the flame 2 cm above the burning surface gave D_{32}=132 μm for the propellant with 16% Al (Shuttle). This size is predicted by estimates obtained from the correlation relationships. The 200 μm particles were also recorded. However, there is a mechanism, which causes substantial decrease in particle size upon motion from the burning surface to the nozzle. The calculated residence time of agglomerates in the flow does not exceed 40 ms and it is hardly probable that they have time to burn out by 90-99%. It is assumed then that the coarse metallic droplets may destroy under the gas flow action although this is also hardly probable in the case where the end burning samples are used and the Mach number is substantially lower than unity.

The optical measurements in the micromotor plume near the nozzle exit showed a change in the form of the size distribution function of particles: modes of 1-4 μm and 5-8 μm were observed together with a pronounced mode between 10-14 μm. Nevertheless, the existence of a great number of particles with sizes smaller than 1-2 μm leads to a decrease in the typical size D_{32} to 2-2.5 μm. The measurements also show that relatively coarse particles are localized at the center line of the plume and the smaller ones (D_{32}=0.2-0.3 μm) are observed in the periphery.
Note that all results [85] were obtained using 25 cm long micromotors with the residence time of gas equal to 30-50 ms. Actually, this is intermediate between the combustion in a laboratory bomb and in the full-scale motor. A fairly developed approach is available for describing the size distribution of the condensed phase particles [86]. Calculations performed within the framework of this approach show that the bimodal size distribution of particles, recorded in the laboratory experiments on particle extinction, is sure to transform into the monomodal one in the nozzle due to collisions of coarse and fine particles. Obviously, it is necessary to verify these predictions for large motors. Actually, however, just few experiments were performed on large motors because of the great technical difficulties. Thus, the results of condensed phase investigations upon solid propellant combustion in the real Shuttle motor and in its reduced copy (18.3%) are of great interest [87]. For the reference, we may note that the critical throat diameter in a micromotor was 0.5 cm, in the Shuttle motor it was 136.8 cm and in its reduced copy it was 25.4 cm.

Known is the empirical Hermsen correlation [88] widely used to calculate the characteristic size D_{43} of the solid rocket motor plume particulates at the nozzle exit plane

$$D_{43}(\mu) = 3.6304 D_t^{0.293}[1.0 - \exp(-0.0008163 \xi_c P_c \tau)] , \qquad (5.14)$$

where D_t is the critical nozzle throat diameter in inches; ξ_c is the Al_2O_3 concentration inside the chamber in gmole/100 g; P_C is the pressure in the chamber in psia per square inch; τ is the mean residence time in the chamber (350 ms for Shuttle motors and 120 ms for its reduced copy).

Formula (5.14) exhibits a good agreement with numerous published data on small and medium size motors. Indeed, the measurement results for the size of particles collected in the motor plume of a small Shuttle copy, coincide to the accuracy of 20% with calculations by formula (5.14). The predicted value of d_{43}=7.717 μm was much lower than the measured values of d_{43}=8-9 μm. However, due to the absence of experimental data, this formula was never tested for the applicability under experimental conditions for gigantic Shuttle motors. Treating the measurement results for the sizes of particles collected for the first time from the motor plume of the Shuttle rocket motor it was shown that the particle distribution is well described by a unimodal function with d_{43}=13.7-11.6 μm. In this case, it was revealed that among 4000 particles only 2-5 ones are larger than 23 μm. According to X-ray microanalysis, the coarse particles have impurities of silicon and calcium, brought from the Earth by a high-temperature flow. On elimination of both the particles larger than 23 μm and all irregularly-shaped ones, the experimentally measured size appears to be 11.2-11.0 μm which is by 0.4-0.6% smaller than that calculated by the Hermsen formula (d_{43}=11.7 μm). These results are assumed to be indirect evidence for the hypothesis of the collision and coalescence of fine particles moving through the nozzle which leads to the transformation of the initial bimodal particle size distribution in the chamber into the monomodal one in the nozzle due to substantial decrease in the fraction of fine particles (smoke).

5.6. CONCLUDING REMARKS

As has been already mentioned, metals are used as components of solid propellants due to both their high heat release upon oxidation and their high density. The thermodynamic calculations show a substantial increase in the specific impulse for metallized solid propellants. In most cases, however, the peculiarities of metallic powders combustion are ignored. This regards to the difficulties of the metal ignition in the combustion wave and to the formation of large agglomerates with volume, being hundreds and thousands times larger that of single particles. In fact, the real combustion of metallic particles in the rocket motor chamber with finite dimensions may be incomplete (chemical losses) and the condensed combustion products may cause two-phase losses (micron particles) and even the formation of slag.

The aim of the specialists in combustion is to study the behavior of metallic particles upon combustion to construct the adequate models for calculating the characteristics of solid propellant performance. Unfortunately, at the present time the information about metallic particle behavior under heating with a rate of several hundred or thousand degrees per second in various oxidative media is rather scarce. Interesting results are available for the ignition of single particles under laser radiation in a purely gaseous medium. However, there is no sense in applying directly these

results to the conditions of metal ignition on solid propellant surface because the time and temperature conditions are quite different.

Note that most problems of the influence of various factors on agglomerate ignition and formation and of the potential role of metallic ingredients on the burning rate and energetic efficiency of solid propellants, put forward in the review of E. Price [4] more than ten years ago, are still open to argument. Moreover, the recent investigations of modern propellants, containing nitramines and energetic binders, add new problems. In particular, the questions arise: what does determine Al "capsulation" in coarse agglomerates upon combustion of some propellants when even after a significant residence time of agglomerates in the flame not less than 20% of initial metal remain unburned? What is the role of the energetic binder in the metal agglomeration and ignition?

Thus, of importance is the role of the correct statement and adequate interpretation of experimental studies. It is necessary to take into account the technical limitations of the available methods for recording condensed particles, which may have substantial effect on the presence of the data, obtained by a concrete method. Thus, it is necessary to combine the independent methods of recording to get objective information. Note that regarding the data on the burning rate of solid propellants there are semi empirical correlations for substituting the values obtained in laboratory conditions by those, corresponding to the conditions of rocket motors. Similar approach to analyze the data on agglomeration although the scale effect is sure to exist.

Finally, note that the synthesis of new components offers new possibilities for creating novel formulations of solid propellants. Thus, e.g. the use of ultrafine powders (the so-called ALEX etc.) may have substantial effect on the characteristics of metal ignition and agglomeration in the combustion wave. Most promising, however, is the approach based on the novel oxidizers having extremely high enthalpy of formation [89]. Calculations show that in propellants with energetic binders the substitution of AP (formation enthalpy –602 cal/g) by a hypothetical oxidizer with the formation enthalpy exceeding 1000 cal/g and higher causes a 40-60 seconds increase in specific impulse. In this case, there is no need to use metal as a propellant component because this reduces the impulse. The propellant of the future may have additional advantages due to the absence of chemical and two-phase losses in the specific impulse as well as due to the absence of environmentally dangerous chlorine-containing combustion products.

CHAPTER 5 REFERENCES

1. **Kondratyuk, Yu.V.**, "The Conquest of the Interplanetary Space", Novosibirsk (Russia), 1929.
2. **Pochil, P.F., Belyaev, A.F., Frolov, Yu.v., et al.**, "Combustion of Powdered Metals in Active Environment", Moscow, Nauka, 1972.
3. **Sakovich, G.V.**, "Design Principles of Advanced Solid Propellants", *Journal of Propulsion and Power*, Vol. 11, No. 4, 1995, pp.830-837.
4. **Price, E.W.**, "Combustion of metallized Propellants", Fundamentals of Solid- Propellant Combustion (Ed. by K.K.Kuo and M.Summerfield), *Progress in Astronautics and Aeronautics*, Vol. 90, Ch. 9, 1984, pp. 479-513.

5. **Williams, F.A.**, "Some Aspects of Metal Particle Combustion", Physical and Chemical Aspects of Combustion, A Tribute to Irvin Glassman (Ed. by F.L.Dryer and R.F.Sawyer), Gordon and Breach Sci.Publ., Ch.11, 1997, pp.267-288.
6. "Heterogeneous Combustion", *AIAA Progress in Astronautics and Aeronautics*, (Ed. by **Wolfgard, H.G., Glassman, I, and Gveen, L.Jr.**), Vol. 15, Academic Press, New York, 1964.
7. **Williams, F.A.**, "Combustion Theory", 2nd edition, Addison-Wesley, Menlo Park, CA, 1985.
8. **Glassman, I.**, "Combustion", 3rd edition, Academic Press, San Diego, London, 1996.
9. **Glassman, I.**, "Comment on "The Combustion Phase of Burning Metals" by Steinberg T.A., Wilson D.B., and Benz F", *Combustion and Flame*, Vol. 93, 1993, pp. 338-342.
10. **Steinberg, T.A., Wilson, D.B., and Benz, F.**, "The Combustion Phase of Burning Metals", *Combustion and Flame*, Vol. 91, 1992, pp. 200-208.
11. **Brzustowsky, T.A., Glassman, I.**, "Spectroscopic Investigation of Metal Combustion", Heterogeneous Combustion, *AIAA Progress in Astronautics and Aeronautics*, (Ed. by Wolfgard, H.G., Glassman, I, and Gveen, L.Jr.), Vol. 15, Academic Press, New York, 1964, pp.41-73.
12. **Pilling, N.B., and Bedworth, R.E.**, "The Oxidation of Metals at High Temperatures", *Journal of the Institute of Metals*, Vol.29, 1923, p.529.
13. **Friedman R., Macek A.,** "Ignition and Combustion of Aluminum Particles in Hot Ambient Gas", *Combustion and Flame*, Vol. 6, 1962, pp.9-20.
14. **Davis, A.**, "Solid Propellants: the Combustion of Particles of Metal Ingredients", *Combustion and Flame,* Vol. 7, 1963, pp.359-367.
15. **Fedoseev, V.A.,** "On Combustion of Mg and Al in Various Media," Kiev State University, *Physics of Aerodispersed Systems*, No. 3, 1970, p. 61-72 (Russian).
16. **Von Grosse, A., and Conway, J.B.**, "Combustion of Metals in Oxygen", *Industrial Engineering Chemistry*, Vol. 50, 1958, pp.663-672.
17. **Wilson, R.P., and Williams, F.A.**, "Experimental Study of the Combustion of Single Aluminum Particles in O_2/Ar," *13th Symposium (International) on Combustion*, Pittsburgh, PA, 1971, pp.833-845.
18. **Prentice, J.L.**, "Combustion of Pulse Heated Single Particles of Aluminum and Beryllium", *Combustion Science and Technology*, No. 1, 1970, p. 385.
19. **Razdobreev, A.A., Skorik, A.I., and Frolov, Yu.V.**, "On Mechanism of Ignition and Combustion of Spherical Particles of Aluminum", *Combustion, Explosion, and Shock Waves*, Vol. 12, No. 2, 1976, pp. (Russian) 203-208.
20. **Arkhipov, V.A., Ermakov, V.A., and Razdobreev, A.A.**, "Dispersion of Condensed Combustion Products of Aluminum Drop", *Combustion, Explosion, and Shock Waves*, Vol. 18, No. 2, 1982, pp. (Russian) 16-19.
21. **Marion, M., Chauveau, C., and Gokalp, I.**, "Studies on the Ignition and Burning of Levitated Aluminum Particles", *Combustion Science and Technology*, Vol. 115, 1996, pp. 369-390.
22. **Dreizin, E.L. and Trunov, M.A.**, "Surface Phenomena in Aluminum Combustion", *Combustion and Flame*, vol.101, 1995, pp. 378-382.
23. **Dreizin, E.L.,** "Experimental Study of Stages in Aluminum Particle Combustion in Air", *Combustion and Flame*, Vol. 105, 1996, pp. 541-556.
24. **Bucher, P., Yetter, R.A., Dryer, F.L., et al**, "Flame Structure Measurement of Single, Isolated Aluminum Particles Burning in Air", *26th Symposium (International) on Combustion*/The Combustion Institute, 1996, pp.1899-1908.

25. **Juasa, S., Sogo, S., and Isoda, H.**, "Ignition and Combustion of Aluminum in Carbon Dioxide Streams," *24th Symposium (international) on Combustion/* The Combustion Institute, 1992, pp. 1817-1825.
26. **Olsen, S.E., and Beckstead**, "Burn Time Measurements of Single Aluminum Particles in Steam and CO_2 Mixtures," *Journal of Propulsion and Power*, Vol. 12, No.4, 1996, pp. 662-671.
27. **Brooks, K.P., and Beckstead, M.W.**, "Dynamics of Aluminum Combustion", *Journal of Propulsion and Power*, Vol. 11, No. 4, 1995, pp.769-780.
28. **Brzustowski, T.A., and Glassman I.,** "Vapor-Phase Diffusion Flames in the Combustion of Magnesium and Aluminum. I. Analytical Developments", Heterogeneous Combustion, *Progress in Astronautics and Aeronautics*, AIAA, Vol. 15, New York, 1964, pp.75-115.
29. **Law, C.K.**, "A Simplified Theoretical Model for the Vapor-Phase Combustion of Metal Particles", *Combustion Science and Technology*, Vol. 7, 1973, pp. 197-212.
30. **King , M.K.**, "Modeling of Single Particle Aluminum Combustion in CO_2-N_2 Atmospheres," *17th Symposium (International) on Combustion*, The Combustion Institute, Pittsburgh, PA, 1977, pp. 1317-1328.
31. **Micheli, P.L., and Schmidt, W.G.**, "Behavior of Aluminum in Solid Rocket Motors," Aerojet Solid Propulsion Co., *AFRPL-TR*-76-58, Sacramento, CA, Jan. 1977.
32. **Kudryavtsev, V.M., Sukhov, A.V., Voronetskii, A.V., and Shpara, A.P.**, "High Pressure Combustion of Metals (Three-Zone Model)," *Combustion, Explosion, and Shock Waves*, Vol. 15, No. 6, 1982, pp. 731-737 (Russian)
33. **Gremyachkin, V.M., Istratov, A.G., and Leipunskii, O.I.**, "Effect of Immersion in a Flow on Metal-Drop" *Combustion, Combustion, Explosion, and Shock Waves*, Vol. 15, No. 1, 1979, pp. (Russian) 26-29.
34. **Turns, S.R., Wong, S.C., and Ryba, E.,** "Combustion of Aluminum-Base Slurry Agglomerates," *Combustion Science and Technology*, Vol. 54, Nos. 1-6, 1987, pp. 299—318.
35. **Law, C., and Williams, F.A.**, "Combustion of Magnesium Particles in Oxygen-Inert Atmospheres," *Combustion and Flame*, Vol. 22, 1974, pp. 383-405.
36. **Shevtsov V.I., Fursev V.P., and Stesik, L.N.**, "Burning Mechanism of the Single Magnesium Particles," *Combustion, Explosion, and Shock Waves*, Vol. 12, No. 6, 1976, pp. (Russian) 859-865
37. **Cassel, H.M., Liebman, J.**, "Combustion of Magnesium Particles I," *Combustion and Flame*, Vol. 6, 1962, pp. 153-156.
38. **Gusachenko, E.I., Stesik, L.N., Fursov , V.P., and Shevtsov, V.I.**, "Study of Condensed Products of Burning of Magnesium Powders. Dependence on Pressure," *Combustion, Explosion, and Shock Waves*, Vol. 10, No. 4, 1974, pp. (Russian) 548-554.
39. **Shafirovich, E.Ya., and Goldshleger, U.I.**, "Ignition and Combustion of Magnesium in Carbon Dioxide," *Combustion, Explosion, and Shock Waves*, Vol. 26, No. 1, 1990, pp. (Russian) 3-10.
40. **Derevyaga, M.E., Stesik, L.N., Fedorin, E.A.**, "Combustion Regimes of Magnesium," *Combustion, Explosion, and Shock Waves*, Vol. 14, No. 5, 1978, p. (Russian) 3.
41. **Fursov, V.P., Shevtsov , V.I., Gusachenko, E.I., and Stesik, L.N.**, "A Role of Evaporation Process of Readily Evaporating Metals in Mechanism of Their High Temperature Oxidation and Ignition ," *Combustion, Explosion, and Shock Waves*, Vol. 16, No. 3, 1980, p. (Russian) 3-12.

42. **Macek, A.**, "Combustion of Boron Particles at Atmospheric Pressure," *Combustion Science and Technology*, Vol. 1, 1969, pp. 181-191.
43. **Macek, A.**, "Combustion of Boron Particles: Experiment and Theory," *14th International Symposium on Combustion*, The Combustion Institute, Pittsburgh, PA, 1972, p.1401.
44. **King, M.K.**, "A Review of Studies of Boron Ignition and Combustion Phenomena at Atlantic Research Corporation over the Past Decade," Combustion of Boron-Based Propellants and Solid Fuels, Edited by Kuo, K.K., and Pein, R., Begell House Publishing Co. and CRC Press, Inc., 1993, pp. 1-80.
45. **King, M.K.**, "Ignition and Combustion of Boron Particles and Clouds," *Journal of Spacecraft and Rockets*, Vol. 19, 1982, p. 294.
46. **Glassman, I., Williams, F.A., and Antaki, P.**, "A Physical and Chemical Interpretation of Boron Particle Combustion," *20th International Symposium on Combustion*, The Combustion Institute, Pittsburgh, PA, 1984, pp. 2057-2063.
47. **Li, S.C., Williams, F.A., and Takahashi, F.**, An Investigation of Combustion of Boron Suspensions", *22nd International Symposium on Combustion*, The Combustion Institute, Pittsburgh, PA, 1989, pp. 1951-1960.
48. **Li, S.C., and Williams, F.A.** "Ignition and Combustion of Boron Particles," Combustion of Boron-Based Solid Propellants and Solid Fuels, Edited by Kuo, K.K., and Pein, R., CRC Press, Boca Raton, FL, 1993, pp. 248-271.
49. **Yeh, C.L., and K.K. Kuo**, "Theoretical Model Development and Verification of Diffusion/Reaction Mechanisms of Boron Particle Combustion," *Transport Phenomena in Combustion*, Vol. I, edited by S. H. Chan, Taylor & Francis, Washington, DC, 1996, pp. 45-63.
50. **Yeh, C.L., and K.K. Kuo**, "Experimental Studies of Boron Particle Combustion," *Transport Phenomena in Combustion*, Vol. II, edited by S. H. Chan, Taylor & Francis, Washington, DC, 1996, pp. 1461-1472.
51. **Yeh, C.L. and K.K. Kuo**, "Ignition and Combustion of Boron Particles," *Progress in Energy and Combustion Science*, Vol. 22, 1996, pp. 511-541.
52. **Pokhil, P.F., Logachev, V.S., Maltsev, V.M., et al.**, "Combustion of Metallized Condensed Systems," Moscow, Institute of Chemical Physics, 1962, 140 pp. (Russian).
53. **Crump, J.E.**, "Photographic Survey of Aluminum Combustion in Solid Propellants," *Proccedings of the 1st ICRPG Combustion Instability Conference*, Vol. 1, Chemical Propulsion Information Agency, Laurel, MD, CPIA Pub. 68, 1965, pp. 367-370.
54. **Povinelli, L.A., and Rosenstein, R.A.,** "Alumina Size Distributions from High-Pressure Composite Solid Propellant Combustion," *AIAA Journal*, Vol. 2, No. 10, 1964, pp.1754-1760.
55. **E.W. Price, J. Crump, G. Christensen, R. Sigal,** Commentary to the article "Alumina Size Distributions from High-Pressure Composite Solid Propellant Combustion "., *AIAA Journal*, 1965, No 9,
56. **Crump J. E., Prentice J. L., Kraeutle K. J.** "Role of Scanning Electron Microscope in the Study of Solid Propellant Combustion. 2.Behavior of Metal Additives". *Comb. Sci. Techn.*, v.1, No. 3, 1969, p.205-223.
57. **Renie J. P., Osborn J. P.** "Combustion Modeling of Aluminized Propellants", *AIAA Paper* 79-1131.
58. **Brulard G.,** "Contribution to the Study of the Combustion of Aluminum Particles", *Recherche Aerospatiale*, 1967, v.118, p. 25-49.
59. **Babuk, V.A., Belov, V.P., Khodosov, V.V., et al.**, "Study of System Containing Aluminum," *Combustion, Explosion, and Shock Waves*, Vol. 24, No. 5, 1988, pp. (Russian) 52-57.

60.**Glotov, O. G., Zyryanov, V. Ya.**, "The Effect of Pressure on Characteristics of Condensed Combustion Products of Aluminized Solid Propellant", *Archivum Combustionis*, Vol. 11, No. 3-4, 1991, pp. 251-262.
61.**Willoughby, P.G., Baker, K.L., Hermsen, R.W.**, "Photographic Study of Solid Propellants Burning in an Acceleration Environment," *13th Symposium (International) on Combustion*, The Combustion Institute, Pittsburgh, PA, 1971, pp. 1033-1043.
62.**Brundige, W.N., and Caveny, L.H.**, "Low Burning Rate Aluminized Propellants in Acceleration Fields," *AIAA Journal*, Vol.22, No. 5, 1984, pp. 638-646.
63.**Zarko, V.E., Karasev, V.V., Silin, N.A., et al**, "Studies on Destruction of the Reacting Surface During Pyrotechnic Combustion" *Proceedings of the 8th International Pyrotechnics Seminar*, 12-18 July 1982, IIT Research Institute, Chicago, Illinois, pp. 728-735.
64.**Rao, R.B., Rao, P.S. and Singh Harihar**, "Agglomeration of Magnesium Particles in Magnesium-Sodium Nitrate Combustion", *Propellants Explosives, Pyrotechnics*, Vol. 21, 1996, pp. 319-324.
65.**Breiter, A.L., Maltsev, V.M., and Popov, E.I.**, "Modification Ways of Condensed Systems Metal Fuels," *Combustion, Explosion, and Shock Waves*, Vol. 26, No. 1, 1990, pp. (Russian) 97-103.
66.**Yagodnikov, D.A., Voronetskii, A.V.**, "Experimental and Theoretical Studies of Ignition and Combustion of Capsulated Aluminum-Particle Combustion", *Combustion, Explosion, and Shock Waves*, Vol. 33, No. 1, 1997, pp. (Russian) 60-68.
67.**Pokhil, P.F., Logachev, V.S., and Maltsev, V.M.**, "The Study of Metallic Particles Confluence in Burning of Metalized Double-Base Propellants and Fuel-Oxidizer Mixtures", *Combustion, Explosion, and Shock Waves*, Vol. 6, No. 1, 1970, pp. (Russian) 80-92.
68.**Kraeutle, K.J., Reed, R.Jr., Atwood, A.I., et al**, "Effect of Binder Type on Aluminum Combustion and Aluminum Oxide Formation", CPIA Publication 308, *16th JANNAF Combustion Meeting*, Vol. II, 1979, pp.225-236.
69.**Glotov, O.G.,Zarko, V.E., and Karasev, V.V.**, "Effect of Binder on the Formation and Evolution of Condensed Combustion Product of Metalized Solid Propellants", Combustion and Detonation, *28th International Annual Conference of ICT*, Karlsruhe, Germany, June 1997, pp.(75-1)-(75-14).
70.*Glotov, O. G., Zarko, V. E., Karasev, V. V., and Beckstead, M. W.*, "Condensed Combustion Products of Metalized Propellants of Variable Formulation", *AIAA PAPER*, No. 98-0449, 1998.
71.**Hermsen, R.W.**, "Aluminum Combustion Efficiency in Solid Rocket Motors", *AIAA Paper* 81-0038, 1981.
72. **Gany, A., Caveny, L.**, "Agglomeration and Ignition Mechanism of Aluminum Particles in Solid Propellants", *17th Symposium (International) on Combustion*, The Combustion Institute, Pittsburgh, PA, 1979, pp.
73.**Gladun, V.D., Frolov, Yu.V., and Kashporov, L.Ya.**, "Model of an Alienation of a Condensed Particle out of the Combustion surface", *Combustion, Explosion, and Shock Waves*, Vol., No. 2, 1976, pp. (Russian) 191-197.
74.**Gladun, V.D., Frolov, Yu.V., and Kashporov, L.Ya.**, "The Mechanism of Agglomeration in Combustion of Metalized Condensed Systems", Division of the Institute of Chemical Physics, Chernogolovka, 1977, 41 pp.
75.**Cohen, N.S.**, "A Pocket Model for Aluminum Agglomeration in Composite Propellants", *AIAA Journal*, Vol. 21, No. 5, 1983, pp. 720-725.

76.**Kovalev, O.B.**, "Physico-Mathematical Modelling of Aluminum Agglomeration by Combustion of Mixed Condensed Systems", *Combustion, Explosion, and Shock Waves*, Vol. 25, No. 1, 1989, pp. (Russian) 39-48.
77.**Grigoriev, V.G., Zarko, V.E., and Kutsenogii, K.P.**, "Experimental Study of Aluminum Particles Agglomeration by Combustion of Condensed Systems," *Combustion, Explosion, and Shock Waves*, Vol. 17, No. 3, 1981, pp. (Russian) 3-10.
78.**Grigoriev, V.G., Koutsenogii, K.P., and Zarko, V.E.**, "A Model of Aluminum Agglomeration by Combustion of Mixed Compositions", *Combustion, Explosion, and Shock Waves*, Vol. 17, No. 4, 1981, pp. (Russian) 9-17.
79 **V. G. Grigor'yev, V. E. Zarko, K. P. Kutsenogii, et al.** "Model of agglomeration of powder-like metal during the combustion of composite formulations", *Reports of the USSR Academy Sciences*, v.259, 1981, p.881-885.
80.**Leypunskii O.I.**. "On dependence on pressure of the black powder burning rate". *Journal of Physical Chemistry* (Russian), Vol. 34, 1960, pp. 177-181.
81.**Novozhilov B. V.**, "The burning rate of a model two-component composite propellant". *Reports of the USSR Academy Science*, Vol. 191, 1970, pp. 1400-1403 (Russian).
82.**N. N. Bachman, Yu. A. Kondrashkov**. "Expression for the burning rate under simultaneous course of homogeneous and heterogeneous reactions", *Reports of the USSR Academy Science*, Vol. 168, 1966, pp- 844-845 (Russian).
83.**Glick R.L., and Condon J. A.**, "Statistical Analysis of Polydisperse, Heterogeneous Propellant Combustion: Steady State".- *Proceedings of 13th JANNAF Combustion Meeting*, CPIA. 281, v.11, Dec.1976. p. 313 - 345.
84.**N. S. Cohen**, "Review of Composite Propellant Burn Rate Modeling", *AIAA Journal*, V. 18, No. 3, 1980, pp. 277-293.
85.**Laredo, D., McCrorie II, J.D., Vaughn, J.K., and Netzer, D.W.**, "Motor and Plume Particle Size Measurements in Solid Propellant Micromotors", *Journal of Propulsion and Power*, Vol. 10, No. 3, 1994, pp.410-418.
86. **Salita, M.**, "Implementation and Validation of the One Dimensional Gas/Particle Flow Code OD3P", *25th JANNAF Combustion Meeting*, Chemical Propulsion Information Agency Publication 498, Oct. 1988, pp.69-82.
87. **Sambamurthi, J.K.**, "Al_2O_3 Collection and Sizing from Solid Rocket Motor Plumes", *Journal of Propulsion and Power*, Vol. 12, No. 3, 1996, pp.598-604.
88. **Hermsen, R.W.**, "Aluminum Oxide Particle Size for Solid Rocket Motor Performance Prediction", *Journal of Spacecraft and Rockets*, Vol. 18, No. 6, 1981, pp. 483-490.
89. **Komarov, V.F., and Shandakov, V.A.**, "Solid Propellants: Specific Features and Application Fields", *Combustion, Explosion, and Shock Waves*, (in press).

CHAPTER 6
TRANSIENT COMBUSTION OF SOLID PROPELLANTS

Transient combustion of solid propellants is of great importance for both technical applications and scientific knowledge. In fact, in solid rocket motor technology and applications there is a urgent need to provide the correct calculations of transitions burning rate during ignition and extinction as well as to estimate the stability of combustion and transients from one combustion regime to another.

It is interesting to note that the fundamental Ya.B. Zeldovich work [I], published in 1942, appeared due to the practical needs of solid rocket motor development. The first Russian field missile M8 (commonly called "Katyusha" in 1940's) used double-base propellant, which experienced unstable combustion. The Zeldovich work [1] gave a start for the further development of approaches in solids combustion and for a long time served a basis for numerous combustion study works in Russia.

Unfortunately, the Zeldovich ideas only became available in the West much later. Nevertheless, they made an important impact on the development of the combustion theory throughout the world.

6.1. PHYSICAL BACKGROUND OF MODELING IN NONSTATIONARY COMBUSTION OF SOLID PROPELLANTS

Development of universal mechanisms and mathematical models for the nonstationary combustion of solid propellants is problematic because of the great variety and complexity of physical and chemical phenomena occurring in the combustion wave. Hence it is necessary to explore the combustion of particular types of solid propellants and develop generalized approaches [2].

The first and most extensively employed model of nonstationary combustion [1] dealt with homogeneous solid propellants, wherein a global exothermic reactions proceeded in the gas and/or in the condensed phase. This model was initially used for description of combustion processes in nitroglycerin powders; then, however, a similar model [3] was applied to the combustion of heterogeneous solid propellants. At the same time, experiment and detailed analysis of the problem show that the simplest model cannot be employed even in the case of homogeneous solid propellants if they have components with different physico-chemical properties. Thus, abrupt switch-off of a sufficiently intense external radiant flux results in instantaneous formation of a net of gas bubbles on the burning surface of nitroglycerin powder. A similar phenomenon is detected at a sharp decrease in the pressure. In this case, a high dispersion of the surface layer can be accompanied, in addition to the abovementioned effects, by phenomena related with temporal and spatial variations of local concentrations of propellant components on the burning surface and with corresponding changes in local burning rates.

It is obvious that more comprehensive and detailed models for nonstationary solid propellant combustion should be developed, which would allow to describe in a realistic way the behavior of

a burning propellant. At first, however, it is reasonable to formulate, according to Ref. [4], a rational approach to studying the given problem. This approach involves the sequence of the following steps:

1. Determination of restricted domains in the space of determining parameters and development of an idealized concept of the physics and chemistry of the process for each domain.
2. Formulation of the mathematical model for the process in the chosen domains of the parameters.
3. Substantiation of the applicability limits for the model, development of a system of test experiments and criteria for domain identification;
4. Designing the interpolation relations, integration of particular models into a system.

It should be noted that the complete realization of this approach is at present impossible since the collection of initial data on the first three steps of the problem is not finished. Meanwhile existing nonstationary combustion models can be divided into two groups.

GROUP 1 - modifications of the classical model for homogeneous solid propellant combustion with one global reaction (following references, as a rule, correspond to primary works and quotations may be incomplete).

1.1. Basic model (taking into account a finite response time only for the thermal layer in the condensed phase) [1-3].
1.2. Pressure dependence of equilibrium component contents and gaseous products temperature [5].
1.3. Change in the flame temperature due to nonstationary heat feedback to condensed phase [6].
1.4. Surface layer dispersion at variable pressure [7].
1.5. Finite response time delay in the preheated layer of the gas phase [8].

GROUP 2 - combustion models for multicomponent and heterogeneous solid propellants.

2.1. Local concentration changes due to accumulation of components on the burning surface [9].
2.2. Spatial separation of the zones of component gasification in the condensed phase of homogeneous and heterogeneous solid propellants [10, 11, 11 a].
2.3. Changes in the temperature profiles in the combustion wave of solid propellants with fine and coarse inclusions [12, 13].
2.4. Time synchronization of a local binder layer regression rate under pressure variation [14].

It is evident that this set of models does not present an exhaustive pattern of the nonstationary combustion of solid propellants and a lot of work is to be done in order to make it sufficiently complete. In particular, a model is to be developed corresponding to the combustion of a solid propellant with large deviation from a stoichiometric mixture formulation (a practically important case - fuel enriched solid propellants).

Experiments show that self-sustaining combustion of such solid propellants is accompanied by local extinction and it can be assumed that nonstationary combustion of these solid propellants would become particularly unstable. Problems of synchronization of local changes in the reaction rate on the burning surface, leading to integral effects, such as extinction or resonance response, should be considered in more detail. Moreover, the models are to be improved in order to describe two- and three-dimensional structures and take into account changes in the shape of the burning surface under the action of various external factors.

In the case when solid propellant burns in a semi-closed volume, in addition to the mass and lin-

ear burning rate, of great importance is the volume rate of gas release. The latter depends on the completeness of chemical reactions, which is in turn a function of mixing and reactant residence time in the reaction volume. One has also to consider the burning law for particles of the condensed phase ejected from the surface, including metal particles.

Mathematical description and background of the applicability of particular models in solid propellant nonstationary combustion require special attention. Because of the complexity of the phenomenon, its description involves, as a rule, some a priori assumptions and includes matching coefficients. At the same time, technical difficulties restrict the possibilities of a detailed experimental study of the process and results are often obtained by primitive techniques. It is obvious that such data do not allow one to reliably establish whether a description corresponds to the assumptions made as well as to determine correctly the applicability limits of a model. Hence, it appears that test experiments should be formulated with the measurement of space and time-resolved characteristics of the nonstationary combustion of solid propellant.

Analysis of particular models of nonstationary burning taking into account specific properties of a chosen type of solid propellant makes it possible to get certain qualitative conclusions. Thus, the account of a finite time of a reaction in the gas phase or a subsurface volatile component release leads to changes in unstable combustion domain boundaries and in the burning rate auto-oscillation frequencies; the account of the effects of ejected particles burning and incompleteness of gas-phase reactions allows one to determine more correctly the boundaries of stable operations of combustion chambers. On the basis of these results one can start to solve the problems of the fourth step - the development of a system of particular models and design of interpolation relations for description of the phenomenon in intermediate regions of determining parameters.

6.2. NONSTATIONARY COMBUSTION OF QUASI-HOMOGENEOUS ENERGETIC MATERIALS WITH QUASI-STEADY GAS PHASE

6.2.1. Development of transient combustion theory in Russia.

Fundamentals of approach by Zeldovich and Novozhilov. In 1942, the model of transient combustion of solid propellants was by Ya.B. Zeldovich [1] based on the following assumptions proposed:

The characteristic thermal relaxation time in the gas phase is much less than that in the condensed phase (the gas phase processes are quasi-steady),

The temperature at the burning surface is constant at given pressure (T_{s0} = const).

There are no chemical reactions in the condensed phase. The burning rate is totally determined by the reactions in the gas phase.

Obviously, the last two assumptions have been made following existing concepts of liquid explosives combustion [15]. Later, 1975, Zeldovich observed [16] that for real propellants the conditions at the burning surface seem to be very different of that proposed above and concluded that his model should be applied for very particular compositions. Based on the main assumption of quasi-steady gas phase behavior the key statement of the dependence of instantaneous burning rate on the current values of pressure and surface temperature gradient was formulated [1]:

$$r_b(t) = r(P(t), \varphi(t)) \qquad (6.1)$$

Here $\varphi = (\partial T / \partial x)_{x=o} = r_b (T_s - T_i) / a$ is assumed to be valid both in steady state and transient conditions; a – thermal diffusivity in the condensed phase.

As the expression (6.1) is true for steady-state combustion it was convenient to determine experimental data on $r_b(f)$ from the dependence of burning rate on initial temperature. This approach where the unknown chemistry of combustion is included in the empirical information has been called the "phenomenological" approach.

Attempts to construct models of transient combustion with non-zero dependence of surface temperature on initial temperature were undertaken later in [17,18] with particular assumptions concerning heat release function. Finally, in 1965 B.V. Novozhilov proposed [19] an extended version of the phenomenological approach now called in the literature the Zeldovich-Novozhilov (ZN) approach. This approach is described in details in an excellent book [20] published in 1973.

According to the ZN approach the exothermic chemical reactions may proceed both in the gas and condensed phases. However, the space extension of the reaction zone in condensed phase due to the high activation energy of chemical reactions is assumed to be very thin compared with the preheated layer of the propellant. Therefore, in addition to the assumption of quasi-steady gas phase, it is assumed that the thermal relaxation time of condensed phase reaction zone is much less than the relaxation time of the propellant thermal layer. Consequently, the problem of transient combustion is formulated in a very simple form which includes the thermal conductivity equation for an inert condensed phase with the closing "phenomenological" correlation and boundary conditions [20]:

$$\partial T / \partial t + r_b (\partial T / \partial x) = a (\partial^2 T / \partial x^2) \qquad (6.2)$$

$$\varphi = \varphi[r_b(t), P(t)] \qquad (6.3)$$

$$T(x,0) = T(x); \; T(0,t) = Ts (\varphi, P); \; T(\infty, t) = T_i \qquad (6.4)$$

It should be noted that the quasi steady gas phase assumption becomes invalid at high pressures.

Stability of the steady-state combustion. In his original paper Zeldovich [1] introduced an additional assumption which concerned the initial temperature dependence of burning rate. He proposed [1] that $\sigma_p = \partial \ln r_{b0}(T_i) / \partial T_i = \text{const}$ that corresponds to an exponential or linear $r_{b0}(T_i)$ dependence. Analyzing the expression for the first integral of the thermal conductivity equation it was determined that the function $\varphi(T_i)$ must have a maximum and the burning rate has 2 values at $\varphi < \varphi_{max}$. The maximum value of the surface temperature gradient is determined by the condition $d\varphi/dT_i = 0$.

From this condition one can derive $\sigma_p(T_{s0} - T_i) = k = 1$ and Zeldovich concluded that it corresponds to the limit of combustion. It followed from this analysis that decreasing T_i leads to increasing surface temperature gradient and the combustion limit (k = l) corresponds to the minimum value $T_{i,\,min} = T_{s0} - 1/\sigma_p$.

The path of the loss of stability was not analyzed in [I]. Later, in the analysis of small perturbations, made by Novozhilov [19,20], it was shown that the steady-state combustion wave is unstable at $k > 1$ when the parameter $r_N = (\partial T_{s0} / \partial T_i)_p$ is less than the critical value $r_N^* = (k-1)^2/(k+1)$. If $r_N = r_N^*$, the burning rate manifests non-damping oscillating behavior with frequency of oscillations $\Omega = k^{0.5}/ r_N$; at $r_N < r_N^*$ the oscillations grow in amplitude and, finally, at $r_N < r_N^{**} = k+l-2k^{0.5}$ the burning rate perturbations grow exponentially in time. Classical analysis [20] was

further developed in several subsequent works. For example, it was shown in [21] that the stability domain becomes less if the preheated layer is narrower than the thermal layer in stationary combustion wave. The presence of the external radiant flux makes the stability domain broader in the case of the opaque propellant, and vice versa [22].

A comparison with experimental results could only be made on the basis of steady-state combustion data [20]. It is interesting to note that there are controversial points of view in the literature on the role of initial temperature in loss of combustion stability for double base propellants. The detailed study of the temperature profiles, performed by Zenin in the 1960's, showed that the real dependence of burning rate on surface temperature gradient is exactly opposite to that assumed by Zeldovich in 1940's: the higher the burning rate, the higher surface temperature gradient [23]. Also, the initial temperature burning rate dependence was found to be so strong that it occurred, in contradiction with [1] , that $k < 1$ at low initial temperatures, but $k > 1$ at high initial temperatures [23,24]. It followed from these findings that at high ambient temperature one could observe unstable combustion of double base propellants. Recently, reliable proof of the combustion stability loss at high ambient temperatures was found [25,26] in experiments with dynamic measurement of the propellant recoil force which is proportional to the square of the regression rate. It was observed that after cutting off of the radiant flux the self-sustaining combustion of double base catalyzed lead oxide propellant at atmospheric pressure and ambient temperatures 100-120 $^{\circ}C$ proceeds with regular non-attenuating oscillations of the burning rate. At lower ambient temperatures, the amplitude of burning rate oscillations after deradiation decreases in time due to the damping effect. This observation provides direct evidence of the loss of combustion stability at elevated initial temperatures for double base propellants with high burning rate temperature dependence.

The above conclusion is in apparent contradiction with experimental observation of pulsating temperature profiles at low initial temperatures but smooth temperature records at high initial temperatures [23]. It has given in the past the reason for several authors to consider lowering the initial temperature as a cause of loss of combustion stability [16,20,23]. However, visualization of double-base propellant combustion at atmospheric pressure shows the existence of macroscopic active reaction spots on the burning surface which become most pronounced at low ambient temperatures [27]. Therefore, the pulsations of the temperature at these operating conditions are of local character. In fact, they characterize a non-uniform (two-dimensional) regression of the surface layer but not the loss of combustion stability in terms of the one-dimensional quasi-steady approach.

Time-dependent combustion. Transient burning occurs due to finite disturbances of the combustion environment, such as time-dependent pressure, blowing gas flow, radiant flux, etc. The question arises, what are the critical values of external parameters which could induce a catastrophic decrease of the burning rate? The first estimate of the critical values was made by Zeldovich [I]. His analysis was based on the assumption of extremely high surface temperature gradients (erroneously attributed to the very low initial temperatures) which could cause the extinction of the propellant.

The Zeldovich concept of extinction can be called "static" as it predicted a cessation of combus-

tion immediately after reaching a critical value of surface temperature gradient. A static concept became very attractive due to its great simplicity and was used in the numerous subsequent works [28-31]. When combined with Novozhilov's stability analysis, the concept meant that the combustion ceases at the boundary of oscillating combustion. The concept of an extinction boundary was formulated in [32,20] but it was doubted later by Frost and Yumashev [33,21]. They discovered, through computer aided simulation of propellant combustion under depressurization, that one needs no special hypothesis about critical conditions in order to characterize the extinction phenomenon. The extinction occurs due to progressive cooling of the condensed phase surface layer that manifests itself in the appearance of an inflection point on the temperature profile in the bulk of the propellant. They also revealed that in the course of transient combustion the parameters of the burning system may temporarily correspond to an unstable combustion domain but it does not serve sufficient condition for extinction.

These findings gave a background for the development of a "dynamic" extinction concept based on examining the dynamic behavior of burning rate. According to this concept, the extinction is determined not only by the instantaneous parameters of the system at the given moment of time, but also by the prehistory of heating and the dynamic properties of the system (temperature sensitivity of the burning rate). Further, the most significant contribution in the development of the dynamic concept was made in the works of De Luca [34].

The problem, which has not yet a clear answer, is how to predict the very low values of burning rate? The formal way is to use extrapolated at low temperatures the expressions for the burning rate versus initial temperature dependence. However, sometimes it takes introducing (for small burning rate) negative values of absolute temperature that has no physical sense. In addition, it corresponds to very low magnitudes of the surface temperature in accordance with the pyrolysis law.

It was proposed in [20] to terminate the dependence $r_b(f)$ at certain low value of the surface temperature gradient. However, the proposal was not specified. Another approach is to check the duration of transient processes and to qualify transients with too long duration as an extinction [35]. But in this case one should justify the extrapolation of experimental dependencies when using classical phenomenological approach.

Ignition to combustion transitions. Ignition transients are a classical example of nonstationary combustion of a propellant with arbitrary initial temperature distribution in a solid. However, when describing the phenomenon, it should be taken into account the absence of developed chemical reactions in the gas phase until the inflammation that makes doubtful the application [32] of the ZN method for calculating the burning rate during the initial stage of combustion.

Based on energetic considerations, Zeldovich proposed [1] that for successful ignition one should simultaneously provide two conditions: reaching the steady-state combustion surface temperature with the surface temperature gradient being less than the critical (maximum) value. It is easy to recognize that this statement is well justified for heating regimes similar to those in a quasi-stationary combustion. However, the static concept gives a wrong prediction when applied to arbitrary heating history.

For example, if the heat flux is high at the initial stage and low enough at the final heating stage the above conditions can be met at a certain moment of time but with abnormally low heat storage in the condensed phase. Obviously, the ignition transient will depend in this case on a number of factors and could not be predicted a priori. This comment refers, in particular, the well-known paper by Librovich [36], (see also [16, Ch. 5, sect.3]) where the ignition delay time was computed for a propellant with a boiling surface temperature. It was stated [36] that in the case of relatively high heat fluxes the energy source should be kept for a certain time after reaching the boiling temperature in order to diminish, due to the latent heat losses, below the critical value the net heat flux penetrating into the bulk of propellant. However, it is clear that after removal of the intense external heat source the condensed phase enthalpy excess will be less than that in stationary combustion wave, and will lead to a drastic decrease in the burning rate. The expected result of the following transient is extinction.

A static concept could not be applied to the most realistic problems of transient combustion due to the great complexity and coupling the physical and chemical processes in a combustion wave. As an illustration, one may consider the ignition by propagating combustion wave passing through the interface of solid propellant samples in contact. Depending on the physicochemical parameters of both samples, various initial temperature profiles in the ignited propellant can be realized. When doing numerical simulation within the framework of the ZN approach, it was revealed [38,39] that the extinction boundary can be expressed in terms of the ratio of steady-state combustion wave parameters for igniting and ignited propellants. In particular, the higher the ratio of the enthalpy excess, the more stable the combustion wave propagation through the contact surface at a given ratio of surface temperature gradients. If one fixes the igniting propellant parameters the high stability of transition is provided with a large thermal relaxation time in the ignited propellant (high thermal diffusivity or small burning rate). The critical values of parameters corresponding to an extinction boundary were found to depend on the chosen values of activation energy in the pyrolysis law and burning rate temperature sensitivity. Simple expressions for the critical conditions of extinction could not be derived and it requires special computational work to characterize transient combustion for a chosen pair of propellant.

6.2.2. Review of western combustion response modeling

Fundamental western approach. This section deals with the approaches to the problems of transient combustion in the western world. This is a very broad area of technical work. Therefore, this section will mainly focus on the approaches used within the US, and primarily on the relationship of acoustic interaction with transient combustion. This is a significant difference in the approaches between the Russian work and that of the US. In the US approach there has been an emphasis on acoustic combustion instability whereas the Russian approach seems to have been broader, applying a fundamental transient combustion approach (i.e. the ZN approach) to a wide variety of applications such as extinguishment, ignition, spontaneous oscillatory combustion, etc. Within the US different models and theories have been applied to each different type of application.

The basis for what can be considered as the foundations of what has become the modem US approach to evaluating combustion instability was established in [40, 3]. Early work on combustion

instability began in the 1940's. This was followed with studies by several workers [41 - 43]. The work of the Hart and McClure group at the Applied Physics Laboratory [40] and the subsequent paper by Denison and Baum [3] focused attention on the acoustic interaction with transient combustion. A result of these works was a concise equation describing the transient response function (i.e. the response of the burning rate to a pressure perturbations). In parallel with their work, experimental work was being performed [44,45] at the NOTS at China Lake, California developing the T-burner. The T-burner provided experimental measurements of pressure response functions for comparison with theory, giving additional emphasis to the focus on acoustic applications. This approach provided a philosophical basis for a majority of subsequent studies. Since that time many theoretical studies have compared their results with T-burner data.

The original Hart and McClure paper allowed for a transient gas phase, but subsequent paper [46] made the simplifying assumption of a quasi steady state (QSS) gas phase. The Denison and Baum paper also assumed a QSS gas phase. In 1968 Culick [47] reviewed the various models that had been published to that time (in the western literature). His review was very significant as he summarized the various papers into a common format. He concluded that all the models that assumed a quasi steady flame reduced to a common numerical form. The form of the response function that he used is

$$R = (m' / m_0)/(p'/ p_0) = nAB / [\lambda+(A/\lambda)-(1+A)+AB] \qquad (6.5)$$

where the parameters A and B are defined as

$$A = (E/RT_{s0})\,(1 - T_i / T_{s0}) \quad \text{and} \quad B = 1 / [\sigma_p(T_{s0} - T_i)],$$

Ω is the non-dimensional frequency and $\lambda(\Omega)$ is a complex function of frequency.

Some models included a second term in the numerator representing a heterogeneous, pressure dependent surface reaction. Most models and subsequent work have dropped that term as not being physically realistic. This is consistent with Russian work. Zenin and Novozhilov [48] showed that the surface temperature of double base propellant is a function of burning rate only (not pressure), allowing them to set the parameter δ_p to zero in the ZN theory. The resulting ZN response function is then equivalent to the form used by Culick and adopted through most of the western literature.

The equivalence of the quasi steady-state gas flame approaches. In 1971 Summerfield, et al. published the first work in the US based on the Russian ZN approach [32]. This started another debate about which approach was better or more correct. In his 1973 monograph [20], Novozhilov recognized that the approaches were identical and that the results should be equivalent. Indeed, the stability boundary presented by Denison and Baum coincides with that of the ZN model [20]. However, this was not realized in the west for some time. Several papers were published by Osborn and his students "comparing" the results of the two methods [49,50]. They apparently made some error in their interpretation of the two approaches as they calculated significantly different results between the two. Eventually it was realized that the approaches were equivalent [51].

The Russian work can be related to western work by comparing response function equations. The ZN response can be stated as (see Novozhilov [20], and Zarko, et al. [52])

$$\Psi = (\Delta r_b/r_{b0}) / (\Delta P/P_0) = (\nu_p + z\,\delta_p) / [1 - k + z\,(r_N - ik / \Omega)] \qquad (6.6)$$

Here $z = iY + 0.5\,(\Omega - Y) / Y$; $Y = (1/8)^{0.5}\,[(1 + 16\Omega^2)^{0.5} - 1]^{0.5}$; $\delta_p = \nu_p r_N - \mu_p k$.

Comparing the parameters, within the two models, the following equivalence can be made between the ZN model and western models.

Western notation		Russian notation
$n = (\partial \ln m_0 / \partial \ln P_0)_{Ti}$	=	$\nu_p = (\partial \ln r_{b0} / (\partial \ln p_0)_{Ti}$;
$A = (Es/RTso)(1-Ti/Tso)$	=	$k/r_N = (Tso - Ti)\,(\partial \ln r_b / \partial Ti)_p / (\partial Tso / \partial Ti)_p$
$B = 1/[\sigma_p\,(Tso-Ti)]$	=	$1 / k = 1 / [(Tso - Ti)\,(\partial \ln r_b / \partial Ti)_p]$

Therefore, with $\delta_p = 0$ the two approaches are numerically equivalent.

Calculation of Combustion Instability Parameters for Response Calculations. During the mid 1970' there was a significant effort of modeling steady state combustion with the development of the PEM version [49] of the BDP model and the extension of the BDP model by Beckstead to apply to a variety of different propellant types [53,54]. It was recognized [49,53] that the calculated steady state combustion parameters could be used to calculate the unsteady parameters of the Denison and Baum (DB) model which is somewhat analogous to the ZN approach. The surface activation energy and the solid thermal diffusivity are input parameters to the models. The models then calculate the burning rate, surface temperature and temperature sensitivity all as a function of pressure and the pressure exponent is also calculated. These are all of the values needed for a calculation of the response function. An inherent assumption in the unsteady analysis is that the propellant is homogeneous and that the flame is premixed. For a composite propellant it is recognized that the solid is not homogeneous and that the combustion controlling mechanism is usually the primary diffusion flame. In the various applications to composite propellants, it is recognized that there is an additional assumption that the parameters calculated in the steady state model, average the heterogeneity and diffusional aspects of the propellant sufficiently to allow the use of either the ZN or DB model. This is recognized as a significant assumption of questionable validity. However, with these inherent assumptions this approach has been applied to a wide variety of AP/HTPB composite propellants [49,50,53], to simple double base propellants [54,55], to AP/HMX containing double base propellants [54], and more recently to advanced propellants [56]. In all cases the validation of this approach has been difficult due to the lack of quantitative data for the various propellant types.

In a parallel effort, Cohen was developing a model to account for the heterogeneity of composite propellants [e.g., 57,58]. His basic premise was that there should be a "layer frequency" associated with the oxidizer particle size of composite propellants. This concept had been postulated early both in the US [59] and in Russia [60]. Cohen combined the ideas of a layer frequency with the two parameter DB type of model to develop a model that would exhibit multiple response peaks. He has published a very useful review [61] of the models used in modeling the unstable response of composite propellants. He has continued to publish a variety of papers [e.g., 62,63]

where he has modeled the effect of oxidizer particle size on the combustion response function. The validation of his concepts has been difficult due to the lack of quantitative data showing this specific effect. Only recently there were published experimental results showing the lack of direct correlation between the oxidizer size and maximum combustion response frequency [64].

Recent work. Several recent papers have by published by Margolis, et al. [65-67]. They have used a large activation energy asymptotic approach to model monopropellant (or homogeneous propellant) combustion. They have looked at intrinsic instability rather than the acoustic coupling problem, and in this sense their work is somewhat analogous to corresponding Russian studies. Deur and Price have published two papers [68,69] trying to incorporate the effects of a diffusion flame into the standard DB type of model. They postulate that the leading edge of a diffusion flame can be kinetically controlled and thus could have a profound influence on a propellant's instability characteristics. They assume a linear relationship between the diffusion flame perturbations and the normal premixed flame response. Their calculations indicate a lower but broader response curve for a typical composite propellant.

Both Clavin, et al. [70] and Micci, et al. [71] have recently published models relaxing the QSS gas phase assumption. Clavin et al. apply a large activation energy asymptotic approach and calculate an extended, high response for higher frequencies, which intuitively seems correct. However, the results of calculating non dimensional maximum response frequency should be carefully checked as their numbers are an order of magnitude higher than those typically calculated by others. Micci's approach is based on a three step kinetics model for the flame which gives the classical two stage flame observed for double base propellants including the dark zone. Micci's results also show a higher amplification at higher frequencies, and their frequency numbers are consistent with previous studies. These results look very promising.

Yang, et al. [72] have also published recent work relaxing the global kinetics assumption that most authors have made in the past. They use the same three step kinetic mechanism for the gas phase that Micci, et al. used, but they also use a three step mechanism for the condensed phase. They do not report any actual response function calculations, as their calculations are coupled to a fluid dynamics model for a rocket motor.

Totally transient combustion problem formulation. Based on the contemporary knowledge of combustion theory [73,74], the governing equations for solid propellant transient combustion can be written. However, keeping in mind a variety of physical and chemical processes involved in solids combustion, there is an important question how to formulate boundary conditions. The main shortcomings are connected at the present time with the treatment of the processes in the condensed phase. For example, it is difficult to describe in details the behavior of subsurface layer (phase changes, bubbles formation and destruction, overall chemical mechanism of condensed phase reactions, etc.) in transient conditions when the temperature and residence time change in very broad range. There are no substantiated solutions of the listed problems so far. Therefore, one may treat existing approaches as only approximate and preliminary attempts to solve the exact transient problem.

There are significant difficulties in analytical solving this problem due to the strong non linearity

of the governing equations. However, a recent attempt has been made by Novozhilov [8] who received a very interesting result concerning the combustion behavior of propellant at small magnitudes of parameter r_N. Based on the Belyayev model of explosives combustion [15] with melting and boiling at the burning surface and considering nonstationary gas phase processes, the total characteristic time of thermal relaxation of the burning system becomes dependable on the complex $t_g^{2/3}\ t_c^{1/3}$ [8], where tg and tc are the characteristic thermal relaxation times for the gas and condensed phases, correspondingly, and $t_c \gg t_g$.

One of the first examples of fully transient propellant combustion problem formulation was made 30 years ago by Vilyunov, et al. [75]. They assumed that the gas phase did not exchange heat with the condensed phase (adiabatic condition) and that the reactions in the condensed phase obeyed a first order law and proceeded to a fixed degree. During ignition transients, damping oscillations of burning rate were discovered. It was later recognized [76,77] that the burning rate oscillations during transition to self-sustaining combustion are not a unique feature of transient combustion but depend on the kinetic parameters of particular type of solid propellant.

A more detailed description of gas phase reactions but with a heterogeneous reaction on the propellant surface was introduced by Armstrong and Koszykowski [78]. They analyzed the temporal behavior of the temperature and reactant mass fraction for the cases of "weak" and "strong" gas phase reaction. It was found that for a stationary burning solid propellant with a detached flame ("weak" gas phase reaction) the thermal profile behavior after cutting off relatively high strength external energy source is the same as that which would be obtained without taking into account exothermic reaction in the gas phase. The reason for this is a small heat content in a gas phase comparatively with a larger one in the condensed phase.

It is interesting to note that the role of gas phase reactions appears to be more important in ignition transients [79]. It was found that the "peninsula" of stable ignition transients is larger in the case of coupled gas and condensed phase reactions as compared with the case of pure condensed reactions.

A more sophisticated approach taking into consideration 2 condensed phase and 2 gas phase reactions has been proposed by Price and Boggs [80]. However, to simplify the problem, a flow reactor scheme was chosen for the gas phase reactions and time-dependent heat feedback to the solid interface was written in terms of flame standoff distance. The model has described the ignition delay and steady-state burning rate for several homogeneous propellants on the basis of a given set of identical parameters for both transient and stationary conditions. The kinetic parameters are determined by comparison with burning rate and ignition data.

Recently, theoretical approach was developed by Knyazeva and Zarko [81] who considered two first order reactions in the condensed phase and one second order reaction in the gas phase. The stability of ignition transients to self-sustaining combustion after removal the external energy source was found to depend on the choice of ignition (extinction) criteria. It was also confirmed once more(see [78,82]) that at least for relatively weak gas-phase reactions the heating of the propellant by powerful heat source (higher than intrinsic heat source in the combustion wave) inevitably leads to extinction after fast removal of the external heat source. This behavior has been ex-

perimentally observed in the experiments with double base propellants ignited by radiant fluxes [83,84].

6.2.3. Intrinsic difficulties and challenges in use of quasi-steady-state approaches.

QSS approaches could be used after making the appropriate estimates of thermal relaxation times in condensed and gas phases. It is difficult to do these estimates because we know very little about the fundamental mechanism and kinetics of the condensed phase chemical reactions. It becomes most questionable for propellant formulations with components that melt and decompose at relatively low temperatures.

QSS approaches should be applied in the ranges of parameters where the dependencies $r_{bo}(T_i)$ and $r_{bo}(T_{so})$ are reliably known experimentally or theoretically. Consequently, without special substantiation it is impossible to use the approaches for simulation of transient combustion in extreme burning conditions like ignition and extinction .

When applying the ZN approach, one needs precise data on $r_{bo}(T_i)$ and T_{so} (T_i) dependencies and their derivatives σ_p and r_N. There are obvious technical difficulties in obtaining these data. For example, to obtain the value $r_N \sim 0.5$ with an accuracy of ~ 20% the value of T_{so} should be measured with an absolute error of no more than 1-2 K if the initial temperature interval is 10-20 K. These limits are not possible in real experiments where the accuracy of T_{so} measurement is no better than ~ 10-20 K [23, 24, 83]. Determining σ_p values it is also difficult to provide accepted accuracy with weak $r_{bo}(T_i)$ dependencies. When $\sigma_p \sim 10^{-2}$ and $\Delta T_o \sim 20$K the σ_p 10% accuracy requires an accuracy of the r_{bo} measurement of ~ 2% which is possible, but could not be improved significantly. Therefore it is practically impossible to obtain the values of $\sigma_p < 10^{-2}$ with an accuracy better than 20-40%.

Application of the ZN approach becomes questionable at very low r_N parameter values. In accordance with the classical version of the approach [20], at the boundary of the loss of combustion stability the predicted frequency of burning rate oscillations $\Omega \sim 1/r_N$. Therefore, at $r_N << 1$ one has value $\Omega >> 1$ and the assumption of quasi-steadiness of gas phase would not be satisfied. More detailed analysis of the range of applicability of the ZN approach is presented in [37].

Historically, transient combustion models were formulated on the basis of simplified versions of steady-state combustion models. The reasons were both the difficulties of analytical and numerical solution and the lack of physical/chemical background for non-stationary models. As a result, theoretical predictions have been rather approximate and weakly substantiated. At the same time, there are urgent practical needs to improve the mathematical simulation of transient combustion processes in order to reliably predict the combustion dynamics in newly designed energetic and propulsion systems. This task can be solved on the basis of improvement of existing quasi-steady approaches as well as elaboration of novel comprehensive transient combustion models.

There are some particular problems which should be solved for further development of transient combustion theory. One of the most important is the identification and definition of the condensed phase chemical reactions. The extent of condensed phase reaction can vary during transient combustion and one needs to have theoretical or experimental information to define the time

varying extent of reaction properly. It is recognized that a unique set of global kinetic parameters will not be able to describe both steady and transient combustion. Multi-step kinetic mechanisms have been used successfully in describing the gas phase combustion of monopropellants. However, to describe the condensed phase, the knowledge of accurate multi-step kinetic mechanisms is not available at this time.

A significant area of future research will be determining detailed kinetic steps in the condensed phase process. Another problem will be the determination of reduced kinetic parameters for describing both condensed and gas phase chemical reactions, which will adequately describe steady and transient combustion. Special kinetic studies should be conducted to determine appropriate parameters for transient and self-sustaining combustion.

Highly accurate values of surface temperature and burning rate are required to be determined in time and labor consuming stationary experiments in order to use the data in the ZN approach. However, it provides only approximate values of the parameters, which one needs to use for transient combustion modeling. One should keep in mind that strictly speaking the problem formulation (6.2-6.4) is written for the bulk propellant and the values of T_s and f should be taken at the back side of the condensed phase reaction zone. Therefore it seems more justified to obtain needed empirical information from the experiments on nonstationary combustion (that is also not so easy to do).

The example of such an approach can be found in [26] where the data on resonant frequencies of oscillatory combustion were used to derive effective values of $T_{so}(T_i)$ and the parameters r_N and k. In the case of weakly sounded resonant response of burning system the regimes with programmed external heating or other well characterized transient combustion regimes could be used for determining experimental information which one needs to use in the ZN approach.

The development of modem, fully transient combustion models needs detailed insight into mechanism of chemical reactions in both the condensed and gas phases as well as information on physical processes occuring in the combustion wave. For example, the processes of solid melting and dissolution of gaseous decomposition products has to be taken into account. The simple idea [15] of pure liquid boiling at the burning surface should be extended to multicomponent mixture boiling with the presence of chemical reactions. To explore the chemical mechanisms of combustion it is promising to use non-intrusive time-resolved spectroscopic methods [86] in conjunction with measuring the instantaneous burning rate. Obviously, it has to be done first on the simplest monopropellants like nitramines. Further it could be extended to double base and composite solid propellants. It is clear that the development of modern transient combustion models takes significant theoretical efforts and essential investments in experimental techniques.

It should be noted that the experimental study of ignition and combustion transients needs to be continued. At present, there are no ways to describe a priory (on the basis of theoretical knowledge only) the physical and chemical processes in the nonstationary combustion wave. Previous work on nonstationary combustion has dealt primarily with specified parameters or critical events: ignition delay, extinction due to strong disturbance of combustion process, etc. In order to get the most reliable knowledge in transient combustion the results of theoretical simulations

should be compared directly with experimental observations of temporal behavior of the parameters in the combustion wave: temperature and species concentration distributions, and burning rate or combustion recoil magnitudes.

6.2.4. Intrinsic stability of self-sustaining combustion of melted energetic materials

When studying intrinsic stability of EM self-sustaining combustion [20], the phase transition in the EM combustion wave has been neglected. However, the problem may be easily formulated to take account of phase transition within the framework of the main idea of phenomenological approach [20].

Simple consideration of all existing phase transitions in EM leads to very cumbersome expressions. Let us take advantage of the fact that for some widely used EM (such as RDX, HMX) the thermal effect of melting is several times higher than the sum of the effects due to change in the structure, and neglect the latter. In this case, similarly to classical approach [20], one may determine the limit of combustion stability at constant pressure in dependence on parameters k and r. The stability limit is a function of the $\bar{Q}$, $\bar{\lambda}$ and ϑ_m parameters. Convenient definitions are:

$$k = (T_s - T_o)\,(\partial\, ln r_b/\partial T_o)_p; \qquad r = (\partial T_s/\partial T_o)_p;$$

$$\bar{Q}_m = Q_m/c(T_s - T_o); \quad \bar{\lambda} = \lambda_{sol}/\lambda_{liq}; \quad \bar{\vartheta}_m = (T_m - T_o)/(T_s - T_o)$$

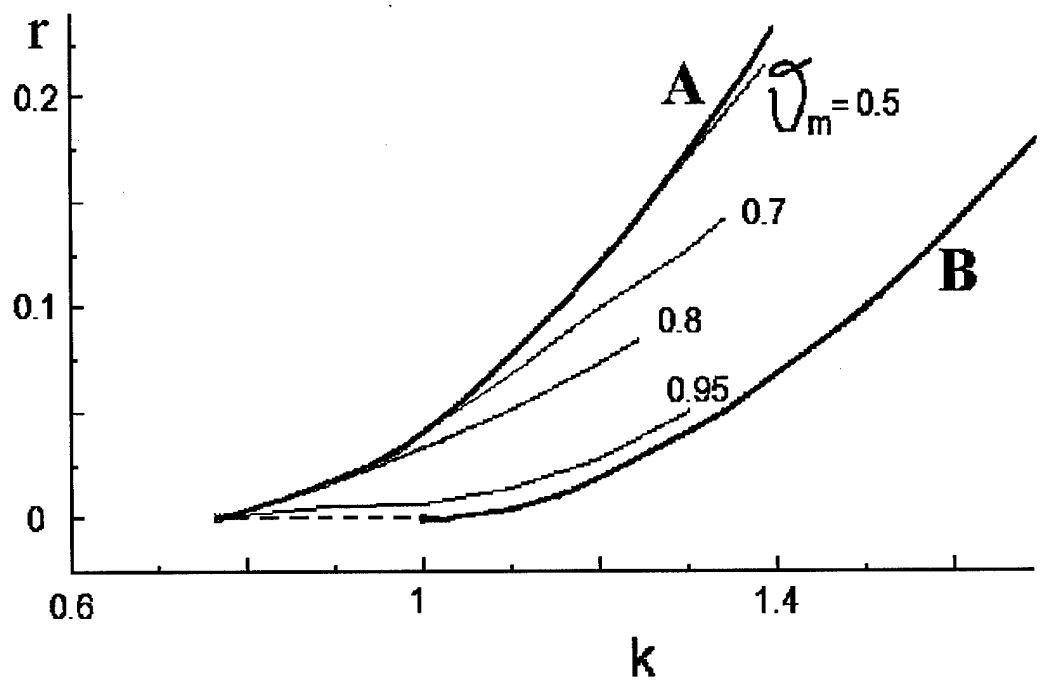

Fig. 6.1. Combustion stability limit at $\bar{\lambda}$=1, $\bar{Q}_m = 0.3$ for different values of ϑ_m

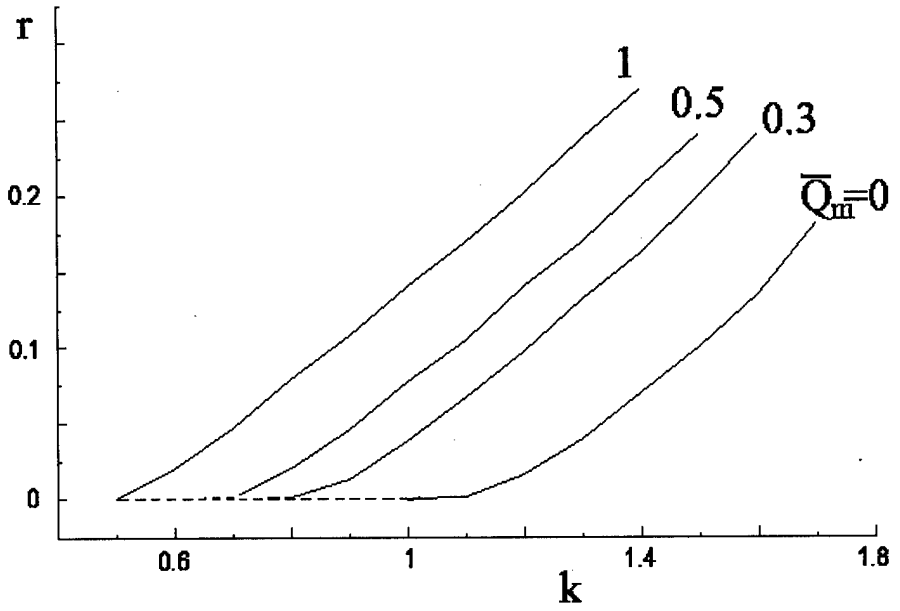

Fig. 6.2. Combustion stability limit at $\bar{\lambda} = 1$, $\vartheta m = 0.7$ for various values of $\bar{Q}_m$.

Figure 6.1 shows the stability limit at $\bar{\lambda}=1$, $\bar{Q}_m = 0.3$ for different values of ϑ_m. Stability domain locates above the solid line. The calculated stability boundaries are between two "limiting" curves A and B for all k values. When this result is compared with that of the "classical" approach [20] stating limit at $r = (k-1)^2/(k+1)$, it becomes obvious that melting decreases stability.

The result obtained for relatively small values of k and r is important. It shows the possibility of combustion instability for melted EM at $k<1$. Note that according to Ref. 20 the combustion without melting is unambiguously stable at $k<1$.

Figure 6.2 shows the stability limit at $\bar{\lambda} = 1$, $\vartheta m = 0.7$ for various values of $\bar{Q}_m$. = 0.7. It is seen that when $\bar{Q}_m$ increases, the stability boundary shifts to the left of basic line ($Q_m = 0$) that means that a domain of stable combustion becomes smaller in size.

A general character of the dependence of the stability limit position on the $\bar{Q}_m$ and $\bar{\vartheta}_m$ parameters is shown in Fig. 6.3 in coordinates k* and r, where $k^* = (T_s - T_o + Q_m/c)\, \partial \ln r_b/\partial T_o = k(1+ \bar{Q}_m)$.

With this coordinate transformation all curves originate from the point (1, 0). It is seen that the smaller the ϑ_m value on the line examined, the larger the distance between the origin of coordinates and branching from the basic line $r=(k^*- 1)^2/(k^*+1)$. The magnitude of curve r(k*) deviation from the basic line has a positive dependence on $\bar{Q}_m$.

The observed behavior of curves has a simple physical meaning. Note that the temperature profile in the bulk of condensed phase displays peculiarity due to phase transition only starting from the distance x_m from the burning surface. When $0<x<x_m$, the Mikhelson profile is realized in the steady-state regime which coincides with that for EM without phase transitions but with reduced initial temperature $T_o^* = T_o - Q_m/c$. It is easy to calculate that $x_m = [\lambda_{liq}/(r_b\, c_{liq}\rho_{liq})]\ln[(1+Q_m)/(\vartheta_m + Q_m)]$ Note also that the harmonic thermal perturbations propagating with a frequency f_0 in the

bulk of EM practically decay at a distance $x_{tf} \propto (f_0)^{0.5}$.

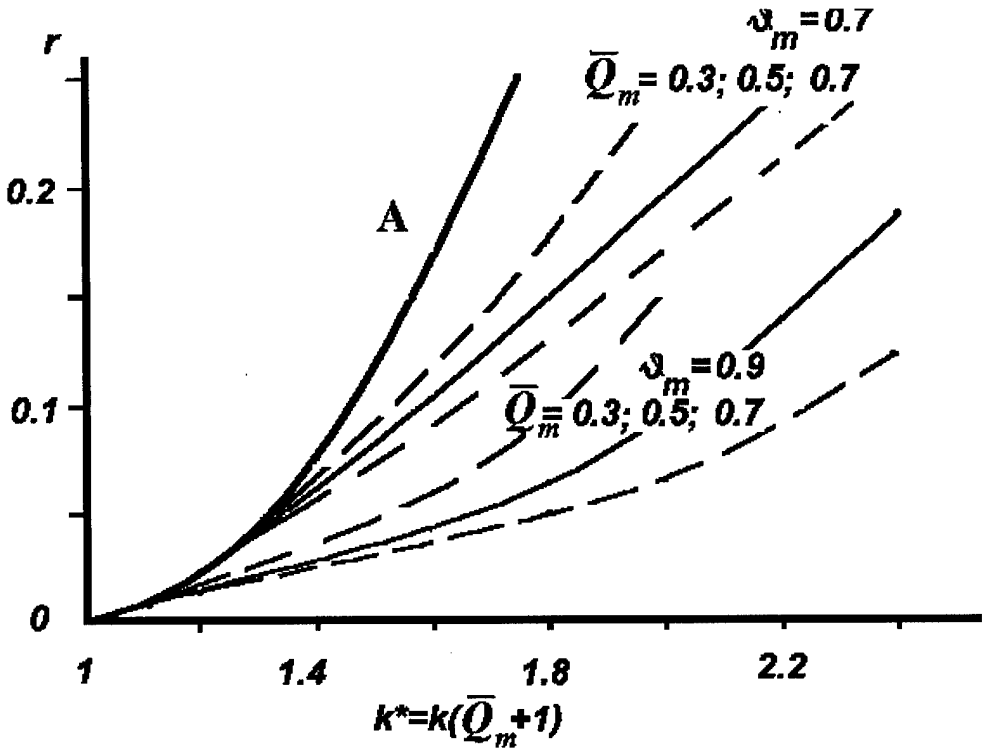

Fig. 6.3. Combustion stability limits in modified coordinates. Curve A: $r = (k^*-1)^2/(k^*+1)$

Obviously, with $x_{tf}<x_m$ the model is "insensitive" to phase transitions. For EM without phase transitions the results of Ref. 20 are hold. Therefore, with $x_{tf}<x_m$ the stability limit coincides with $r=(k^*-1)^2/(k^*+1)$. As the melting temperature decreases, the thickness of the melted layer x_m increases. To preserve the equality $x_m = x_{tf}$, the branching point must be shifted along the basic line towards the lower frequencies (i.e. far from the origin of coordinates).

Consider now the case of fairly low perturbation frequencies when the characteristic distance of thermal wave decay x_{tf} becomes larger than the thickness of melted layer x_m. It means that perturbations reach the surface of phase transition. According to the Le Chatelier principle this must strengthen the decay of perturbations the stronger, the larger is the heat of the phase transition. As a result, it leads to increase of stability domain at ϑ_m = const in coordinates r and $k^*= k(1 + \bar{Q}_m)$. This result reflects a dual nature of the effect of melting heat on the combustion stability. First of all, the finite value melting heat leads, at arbitrary melting temperature, to decrease of stability domain caused by effective decrease of initial temperature. One may recognize this effect in Figs.6.1 and 6.2, when analyzing the position of the beginning (r=0) of curves A. At the same time, with the given value of melting temperature, when the temperature profile oscillations reach the liquid-solid interface, the melting heat acts as a damper and plays positive role in increasing combustion stability in plane r - k* (see Fig. 6.3). However, this does not change overall conclusion about total negative effect of melting heat on the combustion stability because of predominant influence of the first factor. Note that calculations at $r \longrightarrow 0$ (the region of high frequencies,

see Figs. 6.1-6.3) require special analysis in order to take into account finite transition times in the gas phase and in the condensed phase reaction zone [87].

6.2.5.Analysis of different phenomenological models.

Account of the effect of irradiation. The simplest generalization [1,20] is made for the problem statement with respect to condensed phase transparency. Light absorption is given by the Beer law and a corresponding term is added to the equation of condensed phase thermal conductivity. Then, the procedure is performed as described in [1,20]. In [87-89] the nonsteady-state combustion of transparent SP under the action of radiant flux has been studied theoretically and experimentally. Under real conditions of SP combustion it is difficult to determine a portion of radiation absorbed on the surface. Nevertheless, such investigations are very important. The available SP components include the substances that have a strong nonstationary effect determined by their transparency. For instance, according to [90], this it tetryl whose inherent flame heats the condensed phase at $p > 8$ atm for a depth exceeding by 20 times the size of the Michelson preheat layer.

Account of the response of the reaction zone in the condensed phase. In some papers an attempt was made to take into account the characteristic time of the reaction zone in the condensed phase. Indeed, for many compositions the experimentally measured temperature profile in the condensed phase differs noticeably from the Michelson one, probably, due to relatively wide reaction zones existing in the condensed phase [91]. It has been shown [92] that this effect may be taken into account by introducing finite value delay time into the model [20]. A comparison is made with the model, allowing the analytical solution in which the heat release is uniformly distributed over some subsurface layer of the condensed phase. The method can be applied to real SP when using one nonstationary experiment to calculate the needed delay time and applying it to other (arbitrary) laws of the external stimul temporal variations.

In the similar approach papers [93,94] an approximate (in the framework of small perturbations it is nonstationary) solution was found in the zone of chemical reactions of the condensed phase to the temperature and concentration of nonreacting substance. The difference between papers [93,94] is in the fact that the former uses more precise approximate solution to the linearized problem and the necessary amount of boundary conditions (in [93] the problem is overdetermined). Both of the works have two shortcomings. Firstly, they omit one of the parameters determining the solution in the zone of quasistationary processes (and the value of the nonstationary combustion rate). Quasistationary are the processes occurring in the gas phase and in the thin subsurface zone of the condensed phase ($-s < x < 0$) in which the problem could not be reduced to heat propagation and to the global reaction with the Arrhenius dependence of its rate W on temperature T. It is assumed [93,94] that the mass burning rate $m=m(p, \varphi, \beta_s)$, where φ, β_s are the temperature gradient and the portion of consumed condensed phase with $x=-s$. This relationship holds only for the reaction running without any changes in volume. More probable is the assumption of the gaseous reaction products, escaping from the condensed phase through the system of pores resulting from the consumption of the portion of condensed phase volume by reaction. In this case, the total gas flow through the surface $x = -s$

$$\rho_{gs} v_{gs} = \int_{-\infty}^{-s} W dx \qquad (6.7)$$

coincides with the value of m(1- β_s) only under steady-state conditions, which follows from the equation for β

$$W = -\rho_c \frac{d\beta}{dt} = -\rho_c \left(\frac{\partial \beta}{\partial t} + u \frac{\partial \beta}{\partial x} \right), \quad \int_{-\infty}^{-s} W dx = -\rho_c \int_{-\infty}^{-s} \frac{\partial \beta}{\partial t} dx + m(1 - \beta_s)$$

Thus, one should take into account the dependence of the processes in the quasistationary zone not only on the (1- β_s) value (the porosity at the surface) but also on the parameter $\beta_g = \rho_{gs} v_{gs}/m$ which can not be reduced to (1 - β_s) and is the gas portion in the total mass flow through the surface x = -s. Non-identity of β_g and (1- β_s) is the main effect observed for the transience of the condensed phase reaction zone. Taking this into account, we get

$$m = m(p, \varphi, \beta_s, \beta_g) \tag{6.8}$$

This theory flow also takes place in [11,12].

The second shortcoming is the incorrect use of the method for estimating the nonstationary burning rate from the "stationary" empirical dependencies. The method was formally applied as described in [1,20]. The correct application must involve the following logical constructions: the values φ, β_s, β_g in (6.8) may be obtained by solving the nonstationary problem [95,96]. Thereafter, one should choose the m value from the empirical dependencies, i.e. find the "stationary experiment" in which the calculated φ, β_s, β_g could be realized. In other words,

$$m_o(T_o, p, var1, var2) = m(p, \varphi, \beta_s, \beta_g) \tag{6.9}$$

The arguments of the function in the right-hand side are the functions of those in the left-hand side derived for the steady-state regime either experimentally or theoretically, as, for example

$$\lambda\varphi = cm^\circ(T_s^\circ - T_o), \tag{6.10}$$

where the dependencies of m° and T_s° on the same parameters are considered known. Actually, the validness of expression (6.9) takes the equal number of arguments in functions on both sides of equality. Let us assume that we have managed to develop the method for measuring the values below

$$\beta_s = \beta_s(T_o, p, var1, var2), \qquad \beta_g = \beta_g(T_o, p, var1, var2) \tag{6.11}$$

in the steady-state regime. To find m using the calculated values of φ, β_s and β_g from (6.9), it is necessary to know the values of the arguments of the right-hand side of (3) which may be determined by solving the system of three equations (6.9), (6.11) with three unknowns T_o, var1, var2. If it is assumed that the dependence of β_g in (6.9) is insignificant and the error due to neglecting this parameter in [93,94] is not large, the two remaining independent equations must correspond to two unknowns T_o, var1. Using in [93,94] only one unknown T_o indicates a silent recognition of the dependence between φ and β_s and "spoils" the problem definition.

To solve the problem formulated in [93,94] correctly, it is necessary to give various values not only to p and T_o in the "stationary" experiment on measurement of m, T_s, β_s, β_g but also to two other (arbitrary) parameters var1 and var2. Varying these values (either separately or simultaneously or even in combination with T_o), we can obtain any value for β_s, β_g from some two-dimensional domain of the variations in these parameters. It is difficult to name the changes in SP (composition, technology) which should be introduced at p = const and φ = const to alter β_s and not to distort the pattern of phenomena on the surface and the form of function (6.9). Besides, it is impossible to vary β_g with β_s = const because in the steady-state regime $\beta_g + \beta_s = 1$.

Thus, taking into account the characteristic time of the condensed phase reaction zone and preserving the logical scheme [1,20], gives a number of errors.

Account of the finite response time in the gas phase. Some works [92, 8, 70, 71, 98-103] were performed to estimate the influence of the heat propagation characteristic time in the gas phase. An effort was made [98] to take into account the eigenvalue time of the preheat zone in the gas phase by solving the problem without additional (compared to [1,20]) assumptions on surface processes. A case has been studied where the unknown processes in the zones of gas reactions and gasification (vaporization) of the condensed phase near the burning surface (two quasistationary "black boxes") may be considered quasistationary. The times of temperature redistribution in the condensed and gas phases are taken into account.

The empirical dependence of the stationary combustion rate m_o on pressure p, initial temperature T_o, and heat flux q_s absorbed on the SP surface is assumed to be known. It is shown that the mass flow rates at the interface m_s and in the zone of gas reactions m_g must depend on p, φ, q_s and p, φ_g, ψ, respectively, where φ and q_s/λ are the temperature gradients at the "cold" and "hot" ends of the condensed phase reaction zone; φ_g and ψ are the temperature and concentration gradients of the active component in the reaction zone of the gas phase. The φ, q_s, φ_g, ψ values may be determined solving corresponding nonstationary problems in the zones in which no reactions occur. The dependences of m_s and m_g on these parameters which are also hold for the nonsteady-state regime, should be obtained similarly to [1,20], by taking from the empirical data for each set of parameters the steady-state regime that has needed (from calculations) φ, q_s, φ_g, ψ values. This is impossible in a given approach even if we assume that in the "stationary experiment" q_s was changed using additional thermal sources (e.g., laser). The case is that the "stationary experiment" is sure to give $m_s = m_g$ and it is impossible to obtain a pair of m_s and m_g values in the steady-state regime at any T_o and q_s which could be equal to that in the nonsteady-state regime.

Nevertheless, the idea proposed in [98] seems helpful and may be realized in a reduced form if one refuses to describe phenomenologically reaction zone in the gas phase (to give a complete mathematical description of the gas phase as in, e.g., [8, 70, 71, 99-103]). In this case only the subsurface condensed phase zone with the most complex and almost unknown processes is described phenomenologically. If one assumes that the gas phase has a purely thermal influence on this zone (without heterogeneous reactions), then the relationship from [98] will be valid

$$m_s = m_s(p, \varphi, q_s) \qquad (6.12)$$

(otherwise, the expression includes the concentration of the active gas component near the surface). The φ value (as in [8]) may be determined solving the nonstationary problems of heat propagation and diffusion, and the quasistationary dependence (6.9) may be found from experiments with varying T_o and q_s. Some difficulties can be connected with the development of the technique for q_s identification in these experiments because it is difficult to exclude contribution of heat flux from the flame of the combustion products.

6.3. NONSTATIONARY COMBUSTION OF MELTED QUASI-HOMOGENEOUS MATERIALS WITH FULLY TRANSIENT GAS PHASE.

It is known fact that many energetic materials (EM) melt in a combustion wave and have a liquid

layer on the burning surface. In addition, the EM may change their crystal structure at relatively low temperature. Typically, in stationary combustion modeling the effects of phase changes can be taken into account in a very simple way by introducing the effective initial temperature calculated on the basis of heat balance at the burning surface [104, 105].

However, when modeling transient combustion, it is not clear "a priori" if the effect of phase changes can be explained in such a simple way. One may expect that transient combustion behavior of EM, at least near the limits of the combustion stability, depends on the heat and temperature of phase transitions. Obviously, the highest effect is produced by evaporation which is localized at the surface of the condensed phase and has, as a rule, largest magnitude of the latent heat. In the past, mainly the evaporation was considered in combustion modeling. Nevertheless, it seemed that the effect of another phase transitions should also be studied and attempts to explore this problem have been undertaken in recent works. It was shown that melting or phase transition, whose latent heat is considerably less than that of evaporation, may play specific role in radiation-driven combustion [106] as well as in intrinsic stability of EM combustion [107, 108].

The above works had deal mainly with analytical approach and it is of interest to investigate numerically the combustion behavior of melted EM in transient regimes using comprehensive mathematical model. Below we present a description of the mathematical model along with the results of computations.

6.3.1. Mathematical model

General description. A model is intended to describe combustion of melted and evaporated EM with chemical transformations in the condensed and gas phases. Typical representatives of such EM are nitramines, as well as newly synthesized oxidizers like ADN, HNF, etc.

In the condensed phase the model considers heat propagation in solid and liquid states (heat capacity and density are taken the same for both of the states while thermal conductivity coefficients for solid and liquid are assumed different); melting at temperature T_m with endothermal effect Q_m; global exothermic reaction of decomposition of a 1st order in the liquid phase with thermal effect Q_{liq}; radiation absorption in the bulk of condensed phase according to the Beer law, $q_r \alpha \exp(-\alpha x)$. The absorption coefficient α is taken the same for solid and liquid material. The interface between solid and liquid states moves through condensed phase with velocity V_m.

In the gas phase the model takes into account heat propagation, diffusion and two global reactions with thermal effects Q_i, $i = 1, 2$. The products of the first reaction (vapor decomposition via a N_1 order kinetics, mainly of a first order) are assumed to coincide in their composition with the products of decomposition of the liquid phase. The second reaction generates final combustion products via a N_2 order kinetics. Reaction routes of the combustion process are presented by the scheme:

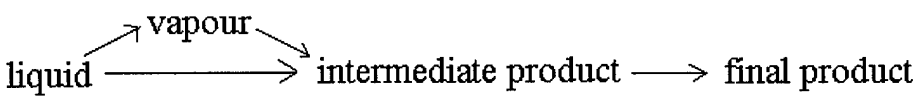

The choice of proper reaction scheme is a very complicated task and still has no sufficient background. This especially concerns the reactions in the condensed phase. Attempts were made to formulate reaction scheme consisting of several (up to 7) global reactions [109, 110] but there is

still no real justification for that. Evidently, when using global reaction approach one has to describe the method for experimental determination of kinetic parameters.

In present work the constants for condensed phase reaction were estimated on the basis of literature data for thermal decomposition of nitramines [111]. In fact, this is a very crude estimate because of great difference in heating rate for combustion and thermal decomposition conditions. In the future it is planning to get needed data from experiments on ignition in special conditions that provide elimination of possible effects of gas phase reactions.

In the literature several detailed schemes for flame reactions in nitramines combustion [112-115], containing more than 40 species and more than 200 steps, can be found. Using of such schemes allows in principle to calculate temperature and concentration profiles in flame. Unfortunately, use of detailed reaction schemes causes difficulties in calculation of transient regimes and it is reasonable to derive reduced kinetic schemes for studying dynamic combustion behavior. This is a task for future work. At the same time the global kinetic parameters can be derived from treatment of experimental data of combustion of melted EM in well characterized conditions. In order to do that, a set of calculations on the basis of model should be performed. As a first estimate, the data for thermal decomposition of nitramines vapor and reaction between their products were used in the present work to specify magnitude of global kinetic parameters for gas phase reactions.

Physical state of the condensed phase. Before formulation of the mathematical model, it is important to discuss physical aspects regarding the processes in the bulk and on the surface of condensed phase. Proceeding of chemical reactions in the bulk of condensed phase raises questions on effective density of liquid EM and on evolution of gas through the subsurface layer. It is naturally to assume that gaseous decomposition products first dissolve in the liquid layer [116]. However, if one takes into consideration an equilibrium solution of gas in the liquid material this corresponds to negligibly small extent of EM decomposition in the condensed phase [117]. At finite decomposition extent one may assume that the gas bubbles form in the liquid layer. Their behavior can be described in several ways.

First description was suggested in 1966 [118] when it was assumed that the velocities of gas and liquid are the same, $V = V_{liq} = m^*\rho_c$. Here $\rho_c = (1-\beta)\rho_{liq} + \beta\rho$ is the effective density of condensed phase. More detailed analyses of two-phase subsurface layer were reported in [119-121]. In particular, semi-empirical expressions were suggested [120] in general case for linear velocity of gas motion $V = (1-s\beta + s)\, m^*/\rho$ and liquid motion $V_{liq} = (1-s\beta)\, m^*/\rho_{liq}$, respectively. Here s is the matching parameter varying in the range from zero to infinity that allows to describe extreme cases of gas release from subsurface layer.

In the present model we consider the simplest case of constant density over the liquid layer. This corresponds to the case of gases dissolved in liquid without formation of bubbles or the case of instantaneous ($V \to \infty$ and $s \to \infty$) removal of gas out of the liquid layer. It should be mentioned that for very thin layers diffusion is also able to provide fast removal of gas from liquid. To estimate, let us assume that gaseous products start to evolve in the bulk of EM at the distance from the surface equal to the length of reaction zone, $l_{ch} \approx 0.1\, (\lambda / C\rho)_{liq}/r_b$. If the residence time for

liquid in the reaction zone, l_{ch}/r_b is greater than the diffusion time $(l_{ch})^2/D$, where D is the diffusion coefficient, the bubbles will not form. The above condition is formulated as $D(T_s) > r_b\, l_{ch} = 0.1\ (\lambda\ /\ C\rho)_{liq}$. A simple estimate shows that the condition is approximately hold for typical melted EM with $D \geq 10^{-4}$ cm^2/s and $(\lambda\ /\ C\rho)_{liq} = 0.001$ cm^2/s.

Detailed consideration of the effect of bubbles on the heat transfer across the liquid layer due to internal evaporation within the bubbles and of the Marangoni and Archimed effects was not made here. The matter is that there is still no reliable observations of foam in subsurface liquid layer of burning melted EM. Quite the contrary, the observations were reported [122] of practical absence of developed foam at the burning surface of double base propellants at atmospheric and elevated pressures despite the presence of foam at the surface of extinguished samples. Thus, introduction of bubbles formation into comprehensive combustion models has to be justified by unambiguous experimental findings. One of the ways to get such information is to perform high speed movie studies of EM combustion with use of soft X-ray radiation source.

Surface evaporation condition. As already mentioned, according to the model conversion of condensed phase into gas proceeds by the way of chemical reaction and evaporation. The latter can be precisely described in terms of gas-kinetic theory if one calculates the mass flow rates of evaporation and condensation. Under non equilibrium conditions, corresponding to the combustion process, the difference between two rates gives mass burning rate. Such approach has been employed in several works [112-114, 120], however, it is rather difficult to use this approach in real calculations. First of all, there is no reliable knowledge of sticking coefficient which characterizes sticking of vapor molecules colliding the liquid/gas interface. Secondly, and most important, the difference between two rates represents difference of two large quantities and small error in their calculation leads to large error in the mass burning rate.

Therefore, in the present model we use another description based on the fact that deviation of partial pressure of vapor from its equilibrium value is of the order of the Mach number for combustion products with magnitude of this number being much less than unity. Consequently, as it was suggested in [123], one may approximately attribute the real magnitude of the vapor pressure to its equilibrium value that can be easily calculated on the basis of Clausius-Clapeyron equation in the form:

$$(M\ /M_1)y_{1s}\ p \approx \text{const}\ \exp(-L/RT_s)$$

Here $(M\ /M_1)y_{1s}$ is the mole fraction of vapor above the surface and p is the ambient pressure. Use of this equation provides better opportunity for convergence of iteration process in numerical modeling. Note that in the gas-kinetic approach the equation of Clausius-Clapeyron is also used for calculating the equilibrium pressure of vapor. An accuracy of these calculations directly depends on the accuracy of the value of the latent heat of vaporization. Unfortunately, this value is known for real EMs with rather low accuracy because of partial decomposition of EMs at relatively high temperatures. The heat of vaporization can be calculated [124] on the basis of semi-empirical expressions or determined by extrapolation of data of surface temperature measurement.

Problem formulation. Let us choose a movable coordinate system (x,t) attached to the burning surface (positive x-axis is directed in the bulk of condensed material) and derive the system of

equations describing physicochemical processes in the condensed phase:

a) solid state $(x_m(t) \le x \le x_R)$

$$C_{sol}\rho_{sol}\left(\frac{\partial T_{sol}}{\partial t} - r_b\frac{\partial T_{sol}}{\partial x}\right) = \lambda_{sol}\frac{\partial^2 T_{sol}}{\partial x^2} + q(t)\alpha\exp(-\alpha x)$$

$$T_{sol}(x,0) = T_0, \quad T_{sol}(x_m,t) = T_m, \quad \left(\frac{\partial T_{sol}}{\partial x}\right)_{x=x_R} = 0$$

b) liquid state $(0 \le x \le x_m)$

$$C_{liq}\rho_{liq}\left(\frac{\partial T_{liq}}{\partial t} - r_b\frac{\partial T_{liq}}{\partial x}\right) = \lambda_{liq}\frac{\partial^2 T_{liq}}{\partial x^2} + \Phi_{liq} + q_r(t)\alpha\exp(-\alpha x)$$

$$\rho_{liq}\left(\frac{\partial y_{liq}}{\partial t} - r_b\frac{\partial y_{liq}}{\partial x}\right) = -\omega_{liq}$$

$$\Phi_{liq} = Q_{liq}\omega_{liq}, \quad \omega_{liq} = A_{liq}\rho_{liq}y_{liq}\exp(-E_{liq}/RT_{liq})$$

$$y_{liq}(x_m,t) = 1, \quad T_{liq}(x,0) = T_0, \quad T_{liq}(x_m,t) = T_m, \quad -\lambda_{liq}\left(\frac{\partial T_{liq}}{\partial x}\right)_{x=x_m-0} = -\lambda_{sol}\left(\frac{\partial T_{sol}}{\partial x}\right)_{x=x_m+0} + Q_m r_m \rho_{liq}$$

The condensed phase generates vapor and a combustible gas. Thus, there are 3 components in the gas phase: vapor, intermediate decomposition product, and final combustion product. The temperature of the components is uniform at the given point of space. The system of equations for the gas phase is as follows $(x_L \le x \le 0)$:

$$C_p\rho\left(\frac{\partial T}{\partial t} - (V - r_b - \sum_{i=1}^{3}\frac{C_{pi}}{C_p}D_i\frac{\partial y_i}{\partial x})\frac{\partial T}{\partial x}\right) = \frac{\partial}{\partial x}(\lambda\frac{\partial T}{\partial x}) + \Phi_1 + \Phi_2$$

$$\rho\left(\frac{\partial y_1}{\partial t} + (V - r_b)\frac{\partial y_1}{\partial x}\right) = \frac{\partial}{\partial x}(\rho D_1\frac{\partial y_1}{\partial x}) - \omega_1$$

$$\rho\left(\frac{\partial y_2}{\partial t} + (V - r_b)\frac{\partial y_2}{\partial x}\right) = \frac{\partial}{\partial x}(\rho D_2\frac{\partial y_2}{\partial x}) - \omega_2 + \omega_1$$

$$\frac{\partial \rho}{\partial t} - r_b\frac{\partial \rho}{\partial x} + \frac{\partial(\rho V)}{\partial x} = 0$$

$$p = R\rho T/M$$

$$\frac{1}{M} = \left(\frac{y_1}{M_1} + \frac{y_2}{M_2} + \frac{y_3}{M_3}\right), \quad \Phi_1 = Q_1\omega_1, \quad \Phi_2 = Q_2\omega_2$$

$$\omega_1 = A_{g1}(\rho\, y_1)^{N_1}\exp(-E_1/RT), \quad \omega_2 = A_{g2}(\rho\, y_2)^{N_2}\exp(-E_2/RT),$$

$$T(x,0) = T_0, \quad y_1(x,0) = y_2(x,0) = 0; \quad at\ x = x_L \quad \frac{\partial T}{\partial x} = \frac{\partial y_1}{\partial x} = \frac{\partial y_2}{\partial x} = 0$$

Boundary conditions at x = 0 are taken in the form:

$$\lambda\left(\frac{\partial T}{\partial x}\right)_{x=-0} = \lambda_{liq}\left(\frac{\partial T_{liq}}{\partial x}\right)_{x=+0} - y_{liq,s}\rho_{liq}r_b L$$

$$-\rho(V-r_b)y_{1s}+D_1\rho\frac{\partial y_1}{\partial x}=\rho_{liq}r_b y_{liq,s}$$

$$-\rho(V-r_b)y_{2s}+D_1\rho\frac{\partial y_2}{\partial x}=\rho_{liq}r_b(1-y_{liq,s})$$

$$-\rho(V-r_b)=-\rho_c r_b,\quad \frac{p}{p_o}y_1=\frac{M_1}{M}\exp\left[-\frac{LM_1}{R}\left(\frac{1}{T_s}-\frac{1}{T_b}\right)\right]$$

In the case of opaque material ($\alpha\to\infty$) the term with q_r must be withdrawn from thermal conductivity equations for solid and liquid phases and boundary condition for heat fluxes should be written in the form:

$$\lambda\left(\frac{\partial T}{\partial x}\right)_{x=-0}=\lambda_{liq}\left(\frac{\partial T_{liq}}{\partial x}\right)_{x=+0}-y_{liq,s}\rho_{liq}r_b L+q_r$$

$$y_1+y_2+y_3+1,\quad D_1\frac{\partial y_1}{\partial x}+D_2\frac{\partial y_2}{\partial x}+D_3\frac{\partial y_3}{\partial x}=0$$

Numerical method. The equations of energy and species concentrations in the gas phase include convective and diffusive terms. It is known that there exist computational difficulties in their solution when using central-difference schemes for convective term. Another difficulty is the stiffness of equations. To overcome difficulties a quasi monotonous difference scheme of second-order accuracy has been developed that effectively operates on real difference grids. Its essence may be explained taking as an example the model nonlinear equation for a scalar function ϕ in the domain $\{0 \le x \le 1;\ 0 \le t \le T\}$.

$$\partial\phi/\partial t + u\partial\phi/\partial x = a\,\partial^2\phi/\partial x^2 + f(\phi, t) \qquad (6.13)$$

where u is the velocity; a is the constant, $f(\phi, t)$ is the source term. The use of approximation $\partial\phi/\partial x \approx (\phi_{i+1}^{n+1} - \phi_{i-1}^{n+1})/(2h)$ for the convective term leads to the fact that the nonphysical oscillations appear in the numerical solution in the range of sharp change of value ϕ. For a given class of problems this corresponds usually to the reaction zone where the temperature and concentration gradients are high enough. To eliminate these oscillations one may apply a difference scheme based on "hyperbolic" approximation. To this end we wrote the left-hand side of Eq. (6.13) along line dx/dt = u that is conventionally called the characteristic line and constructed the following nonlinear two-step difference scheme with using backward Tailor-series expansion of term $f(\phi, t)$ in time:

$$\left(\tilde{\phi}_i^{n+1}-\phi_*^n\right)/\tau = a_*^n\left(\frac{\partial^2\tilde{\phi}}{\partial x^2}\right)_i^{n+1}+f\left(\tilde{\phi},t+\tau\right)_i^{n+1} \qquad (6.14)$$

$$\left(\phi_i^{n+1}-\phi_*^n\right)/\tau = 0.5\times\left[a_i^n\left(\frac{\partial^2\phi}{\partial x^2}\right)_i^{n+1}+a_*^n\left(\frac{\partial^2\phi}{\partial x^2}\right)_*^n\right]+f\left(\phi,t+\tau\right)_i^{n+1}\left[1+\frac{\tau}{2}\left(\frac{\partial f}{\partial\phi}\right)_i^{n+1}\right] \qquad (6.15)$$

Here τ, h are the grid steps over spatial and time variables so that $t = n\tau$; $x = ih$; $n = 0,..., 1/h$; $i=0,..., T/\tau$. The values with subscript * are calculated using appropriate interpolations at the cross-points of the characteristic lines starting from the point (n+1,i) with the straight lines forming the difference grid (with the horizontal ones at $h/\tau > u$ and with the vertical ones at $h/\tau < u$).

The nonlinear difference scheme (6.14)-(6.15) can be easily solved by the Newton method.

Coming back to the solution of original problem formulation, the following procedure has been used. The surface temperature T_s and the burning rate r_b were found via inner iteration procedure at each time-marching step. For a given initial guess of T_s and r_b the equations for species concentrations were solved. Then values y_{1s}, y_{2s} and $y_{liq,s}$ were used to determine the boundary conditions for the energy equations in the gas and condensed phase. After solution of the energy equations new values of T_s and r_b were found from boundary conditions. The inner loop was repeated down to the convergence of T_s and r_b. A variable step grid condensed in vicinity of the liquid/gas interface was used to get the results with 0.1% accuracy.

In order to solve numerically the problem with closing initial and boundary conditions a spatial domain $x_L < x < x_R$ has to be chosen on the basis of physical considerations or numerical experiment. The domain size should allow to establish zero gradients of temperature and species concentrations on the boundaries. For the gaseous mixture (vapor, intermediate and final products, indices 1, 2, and 3 respectively) the corresponding diffusion coefficients were calculated using the Wilke formula $1/D_i = y_1/D_{i1} + y_2/D_{i2} + y_3/D_{i3}$. Values of D_{ik} were calculated using the Lennard-Jones potential with $(\varepsilon/k)_1 = 436$ K, $(\varepsilon/k)_2 = = 244$ K, $(\varepsilon/k)_3 = 97$ K; $\sigma_1 = 6$ Å, $\sigma_2 = 3.7$ Å, $\sigma_3 = 3.6$ Å. The thermal conductivity and specific heat of gaseous mixture were calculated by the formulas $\lambda = \lambda_1 y_1 + \lambda_2 y_2 + \lambda_3 (1-y_1-y_2)$, $c = c_1 y_1 + c_2 y_2 + c3(1 - y_1 - y_2)$, $\lambda_i = A_{\lambda i} + B_{\lambda i} T$, $c_i = A_{ci} + B_{ci} T$, $A_{\lambda i} =$ $5\ 10^{-5}$, $8\ 10^{-5}$, $9\ 10^{-5}$ cal/(cm s K); $B_{\lambda i} = 10^{-8}$, $2.5\ 10^{-8}$, $5\ 10^{-8}$ cal/(cm s K^2); $A_{ci} = 0.2, 0.25, 0.3$ cal/g K; $B_{ci} = 10^{-5}$, $5\ 10^{-5}$, $9\ 10^{-5}$ cal/ (g K^2).

6.3.2. Burning rate response to variations in pressure.

It is important from a practical point of view to predict the EM combustion behavior under pressure variations in order to estimate the possible growth of acoustic oscillations in the combustion chamber. The burning rate responses have been calculated for reference parameters selected according to published data [109-112] and with provision of coincidence with experimental data on RDX burning rate over the pressure range 1-90 atm. The reference parameters are listed in Table below.

Table. Reference Parameters for EM Physicochemical Properties.

==========

thermal conductivity, $\lambda_{liq} = \lambda_{sol} = 0.00055$ cal/ (cm s K),
specific heat of condensed phase, $C_{sol} = C_{liq} = 0.3$ cal/ g K,
density of condensed phase, $\rho_{sol} = \rho_{liq} = 1.72$ g/cm^3,
latent heat of evaporation, L=112 cal/g,
latent melting heat, $Q_m = 38$ (or 60) cal/g,
melting temperature, $T_m = 480$ (or 580) K,
boiling temperature at atmospheric pressure, $T_b = 613$ K ,
initial temperature, $T_0 = 300$ K ,
condensed phase Arrhenius activation energy, $E_{liq} = 47100$ cal/mol,
condensed phase reaction heat, $Q_{liq} = 613$ cal/g,
gas phase Arrhenius activation energy, $E_1 = 15500$ cal/mol and E_2=50000 cal/mol,
gas phase reaction heat, $Q_1 = 725$ cal/g and $Q_2 = 235$ cal/g,
gas reaction order, $N_1 = N_2 = 1.6$,

pre-exponential factor, $A_{liq} = 10^{18.3}$ 1/s, $A_{g1}=10^{10.2}$ g/(cm^{3}s atm^{N_1}), $A_{g2} = 10^{10.2}$ g/(cm^{3}s atm^{N_2}),
molecular mass of vapor, $M_1 = 222$ g/mol,
molecular mass of decomposition products, $M_2 = 35$ g/mol,
molecular mass of combustion products, $M_3 = 30$ g/mol,

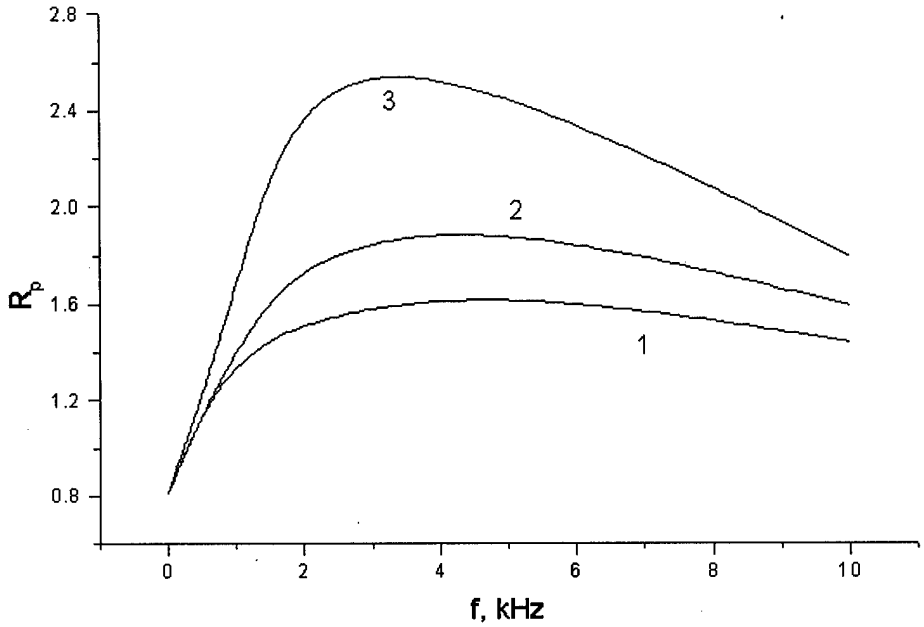

Fig. 6.4. Response function R_p vs frequency of pressure oscillations (p = 70 atm, Δ/p = 0.02$).
1 -- T_m=580 K, Q_m = 38 cal/g; 2 -- T_m=480 K, Q_m = 38 cal/g; 3 -- T_m=480 K, Q_m = 60 ~cal/g.

The calculated results for $R_p = (\Delta r_b / r_b) / (\Delta p/p)$ at pressure 70 atm are presented in Fig 6.4. It is seen that the magnitude of maximum of pressure driven burning rate response function decreases with increase of melting temperature and corresponding decrease of the melted layer width. Qualitative explanation of such behavior can be done in a following way. According to the Le Chatelier principle a phase transition (melting) diminishes an amplitude of oscillations of thermal profile but it works only at frequencies not exceeding certain limiting value. The lower the melting temperature, the wider melted layer and the lower limiting frequency. The reason why the curve 1 in Fig 6.4 has relatively small maximum is that the melted layer is very narrow at T_m = 580 K.

Comparison of curves 2 and 3 indicates that increase of melting heat leads to the loss of combustion stability that is in agreement with the results of analysis of intrinsic combustion stability.

Analyzing Fig. 6.4 one may recognize that behavior of burning rate response function at high frequencies does not follow classical pattern with diminishing the response function magnitude to infinitely small value. Instead, it is seen that response function reaches at high frequencies some finite magnitude. Similar result was reported earlier in Ref. 125 for the common case when one

does not use an assumption of existence of unambiguous correlation between surface temperature and burning rate. Simple qualitative explanation of the result discussed follows from the theory of heat propagation that states that the amplitude of oscillations of surface temperature diminishes to zero at high frequencies of oscillating heat feedback to the solid. In the case when the relationship $r_b = r_b(T_s)$ is hold, this leads to diminishing the amplitude of oscillations of burning rate. However, in common case when such correlation does not exist the finite amplitude oscillations of r_b at high frequencies are possible.

6.3.3. Stability of radiation driven gasification regimes

Gasification is externally stimulated combustion under thermal radiation when the absorbed radiant heat flux is much greater than the heat feed back to the surface from the gas phase. The gasification regimes are rather uncommon for EM application but they can be effectively used for studying combustion mechanism. Strong irradiation leads to high gasification velocity and to detachment of gas flame from surface. The gas flame can be completely eliminated (e.g., in presence of heat sink in the gas phase) so that the process of combustion results from the interaction between radiation and physicochemical conversion of the condensed phase. In this case the determining factors are the radiation absorption, thermal conductivity, melting, the exothermic reaction of decomposition, and evaporation. This process is easier to describe than the complete model which includes the gas flame. The gasification regimes make it possible to get information on the global chemical reactions in the condensed phase. This information may be obtained by comparing experimental and calculated data on the specific behavior of the process, in particular, the regression pattern in critical conditions. We consider below the numerical data which testify to the existence of critical gasification conditions in the form of the lower and upper (in terms of the magnitude of radiant flux qr) limits of existence of steady-state gasification regimes.

Reference data for calculations: p = 1 atm, Q_m = 25 and 60 cal/g, T_m = 480 K, λ_{liq}= 0.00095 cal/(cm s K). The other parameter values are the same as listed in section 6.3.2.

The above parameters correspond to the literature data on the RDX condensed phase. Calculations have shown that for the given value of radiation absorption coefficient α and for fixed other parameters the steady-state gasification regimes exist in the limited (on both sides) range of q_r variations, i.e. there are low and upper limits for q_r which depend on the value of Q_m (see Fig.6.5).

The domain of stable gasification is situated above the corresponding curve Q_m = const. An increase in melting heat Q_m extends the domain of stability. The cause is that instability is due to thermal explosion but increasing of Q_m magnitude (equal to decreasing of T_0) hinders the thermal explosion. The simple theory for the left branches is given in [125], for the right branches it is given below.

Let us prove analytically the existence of the upper gasification limit for $(RT_s^2/E)\lambda /q_r<1/\alpha$. For simplicity, we consider only the case where $Q_m = 0$. The method of the matched asymptotic expansions is applied according to which the "internal" problem (upon neglection by nonstationary and convective terms in the energy conservation equation) takes the form:

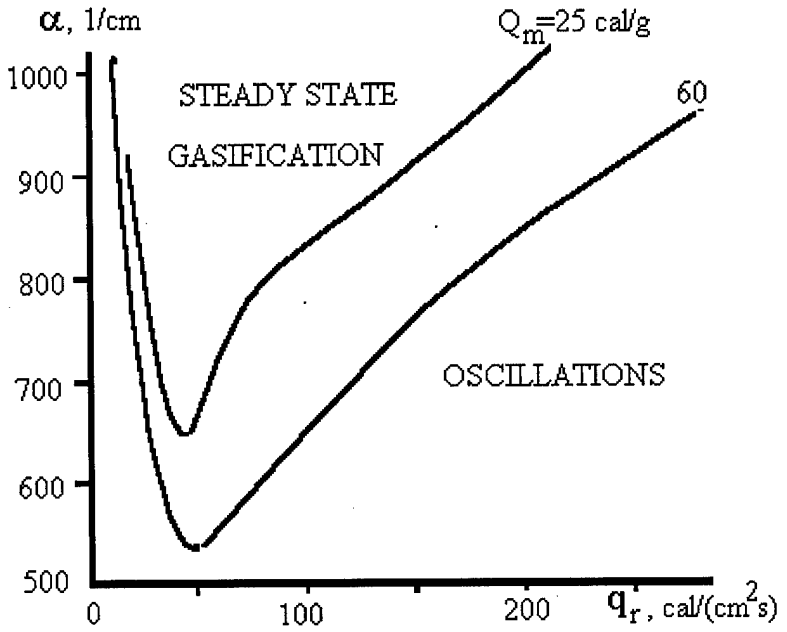

Fig.6.5. Map of the existence of stationary gasification regimes

$$\lambda\, d^2T/dx^2 + \alpha\, q_r \exp(-\alpha x) + k\rho Q_c \exp(-E/RT_s)\exp(\vartheta) = 0;$$
$$\text{at } x=0 \quad T = T_s,\ \lambda\, dT/dx = Lm \tag{6.16}$$

Here $x > 0$, $\vartheta = (T-Ts)\,E/(RT_s^2)$, at $x = 0$ $dT/dx > 0$. Equation (6.16) has no simple analytical solution. To get approximate solution the temperature profile is represented in parabolic form

$$T \approx T_{max} - (T_{max} - T_s)(1 - x/x_{max})^2 \quad \text{or} \quad \vartheta = \vartheta_{max}\,[1 - (1 - x/x_{max})^2]$$

T_{max} is unknown, x_{max} is assumed to be coincided with the maximal overheating point in the "inert" problem. In this problem:

$$\tau = [(1 - \alpha_1)\exp(-\xi) - (L_1 + 1)\exp(-\alpha_1\xi)] / (\alpha_1 - 1) \tag{6.17}$$

$$\xi = x\, mc / \lambda,\ \alpha_1 = \alpha\lambda / (mc),\ \tau = (T - T_0) / (T_s - T_0),\ L_1 = L / [c(T_s - T_0)],\ m = q_r / [c(T_s - T_0)+L]$$

The temperature has a maximum:

$$\tau_{max} = (1 + L_1 / \alpha_1)\,[\alpha_1 (1 + L_1) /(\alpha_1 + L_1)]^{-1/(\alpha_1 - 1)}$$

at $\xi = (\alpha_1 - 1)^{-1} \ln[\alpha_1 (1 + L_1) /(\alpha_1 + L_1)]$

If $\alpha_1 >> 1$, then $x_{max} \approx \alpha_1^{-1} \ln(\alpha_1 + 1)$, $T_{max} - T_s \approx (q_r / \alpha\lambda)\,(L_1 - \ln(L_1 + 1)) / (L_1 + 1)$.

From (6.16) (by integrating) we have

$$\lambda T' - \lambda T'_s + q_r (1 - e^{-\alpha x}) + B_1 e^{\vartheta_{max}} \int_0^{x/x_{max}} \exp\left[\vartheta_{max} (1 - x/x_{max})^2\right] d(x/x_{max}) = 0$$

Here $T' = dT/dx$, $B_1 = x_{max} Q_c k\rho \exp(-E/RT_s)$. At the "cold" boundary (matching point x*)

$$q_+ - q_- = 0 \qquad (6.18)$$

$$q_+ = q_r + B_1 \sqrt{\pi} \frac{1 + erfc\left(\sqrt{\vartheta_{max}}\right)}{2\sqrt{\vartheta_{max}}} e^{\vartheta_{max}}, \quad q_- = \lambda T'_s - \lambda (T')^*.$$

The "outer" problem (upon neglection by chemical heat release and radiation absorption) gives in a steady-state case

$$\lambda (T')^* = - mc (T_s - T_0)$$

Taking into account $m = \lambda T'_s / L$; from used parabolic approximation

$$\lambda T'_s \approx \vartheta_{max} (2\lambda / x_{max}) (RT_s^2 / E). \qquad (6.19)$$

Using (6.19), $q_- = B_2 \vartheta_{max}$, $B_2 = [1 + c (T_s - T_0) / L] (2\lambda / x_{max}) (RT_s^2 / E)$.

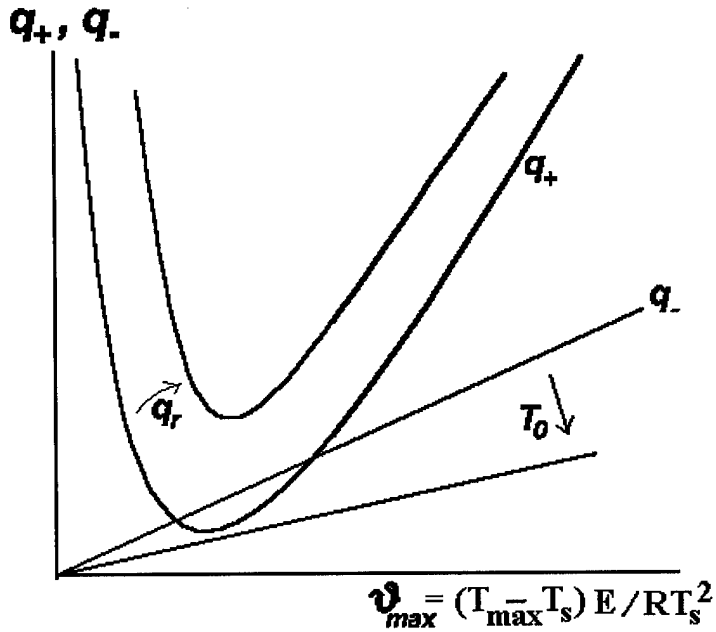

Fig.6.6. Heat release and loss in the reaction zone in the condensed phase of semi-transparent EM

In Fig. 6.6 the $q_+(\vartheta_{max})$ and $q_-(\vartheta_{max})$ lines, corresponding to relations (6.19), illustrate a typical thermal explosion. The existence of a minimum in the $q_+(\vartheta_{max})$ lines is confirmed by the analysis of expression (6.18) for q_+: with $\vartheta_{max} \to 0$ tends to infinity so as $\sim \vartheta_{max}^{-1/2}$; with $\vartheta_{max} \to \infty$, it tends to infinity so as $\sim \exp(\vartheta_{max})$. The term $(1+\text{erfc}(\vartheta_{max}^{1/2}))/2$ may vary only from 1/2 to 1 and in the range of variation of our parameters it is close to unity. Thus, within the range $0 < \vartheta_{max} <$

∞, a minimum must exist. A critical condition for the thermal explosion corresponds to the contact of lines $q_+(\vartheta_{max})$ and $q_-(\vartheta_{max})$ described by the conditions $q_+ = q_-$ and $dq_+ / d(\vartheta_{max}) = dq_- / d(\vartheta_{max})$. In dependence on the values of q_r and other parameters the lines q_+ and q_- may have 2 points of interrection. At high values of initial temperature and q_r there is no interrection point and there is no steady state gasification regime.

6.3.4. Stability of transient combustion under pressure drop and pulse of radiant flux.
The EM combustion behavior have been studied upon transition from the regime at given constant pressure p_1 to that at lower constant pressure p_2. The pressure change occurs during time interval Δt (which, in particular, may be assumed equal zero) with pressure being linearly dependent on time. The values of EM parameters in these calculations were chosen the same as in the calculations of burning rate response to p variations. For fairly low levels of final pressure p_2 and/or short Δt one may observe extinction rather than transition to a new combustion regime.

The extinction boundary was obtained (Fig.6.7) at a given p_1 in the Δt and p_2 coordinates by a series of calculations. Transition to a new combustion regime is realized above this curve and extinction occurs below it. The calculations indicate that the transition stability decreases (and finally one may reach extinction) either with decreasing melting temperature T_m or with increasing thermal effect of phase transitions Q_m.

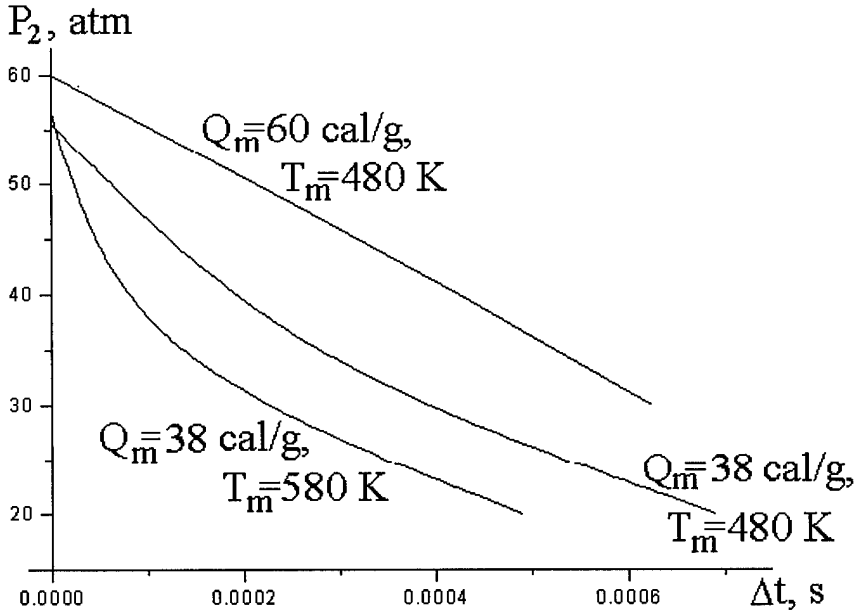

Fig.6.7. Extinction boundary at $p_1 = 100$ atm with different T_m and Q_m values

Burning rate response to the pulse of radiant flux was studied without taking into account reactions in the condensed phase and with gas phase exothermic reactions controlling the EM burning rate. The input parameters were chosen as follows: p=1atm, $A_{g1}=10^{8.85}$ g/(cm^{3}s atm$^{1.6}$), $A_{g2} = 10^{10}$ g/(cm^{3}s atm$^{1.5}$), D=0.15 cm^2/s, $\lambda_{gas} = 0.0002$ cal/(cm s K). Other parameters were taken as listed in section 6.3.2. The burning surface was irradiated during 0.1 s with heat flux 10 cal/(cm^{2}s). Figure 6.8 gives the calculated results which show that the stability of transient combustion depends on the melting heat magnitude.

It is seen from Figs. 6.8 (a, b, c) that increase in melting heat up to rather moderate value 20 cal/g leads to drastical change in combustion behavior of EM subjected to pulsed irradiation. Note that the magnitudes of the parameter $k = (T_s - T_o)\,(\partial\, lnr_b/\partial T_o)_p$, corresponding to the burning EM in Figs. 6.8 a and (6.8 b, 6.8 c), are equal to 0.46 and 0.48, correspondingly. It means that the stability of self-sustaining combustion of these EM is expected to be high and observed transient combustion behavior is governed mainly by the heat sink in the subsurface layer of EM. Figure 6.8 c shows that the increase in melting temperature leads to increase in stability of transition to self-sustaining combustion after ceasing the irradiation. This effect is qualitatively similar to that in case of combustion response to oscillating heat flux.

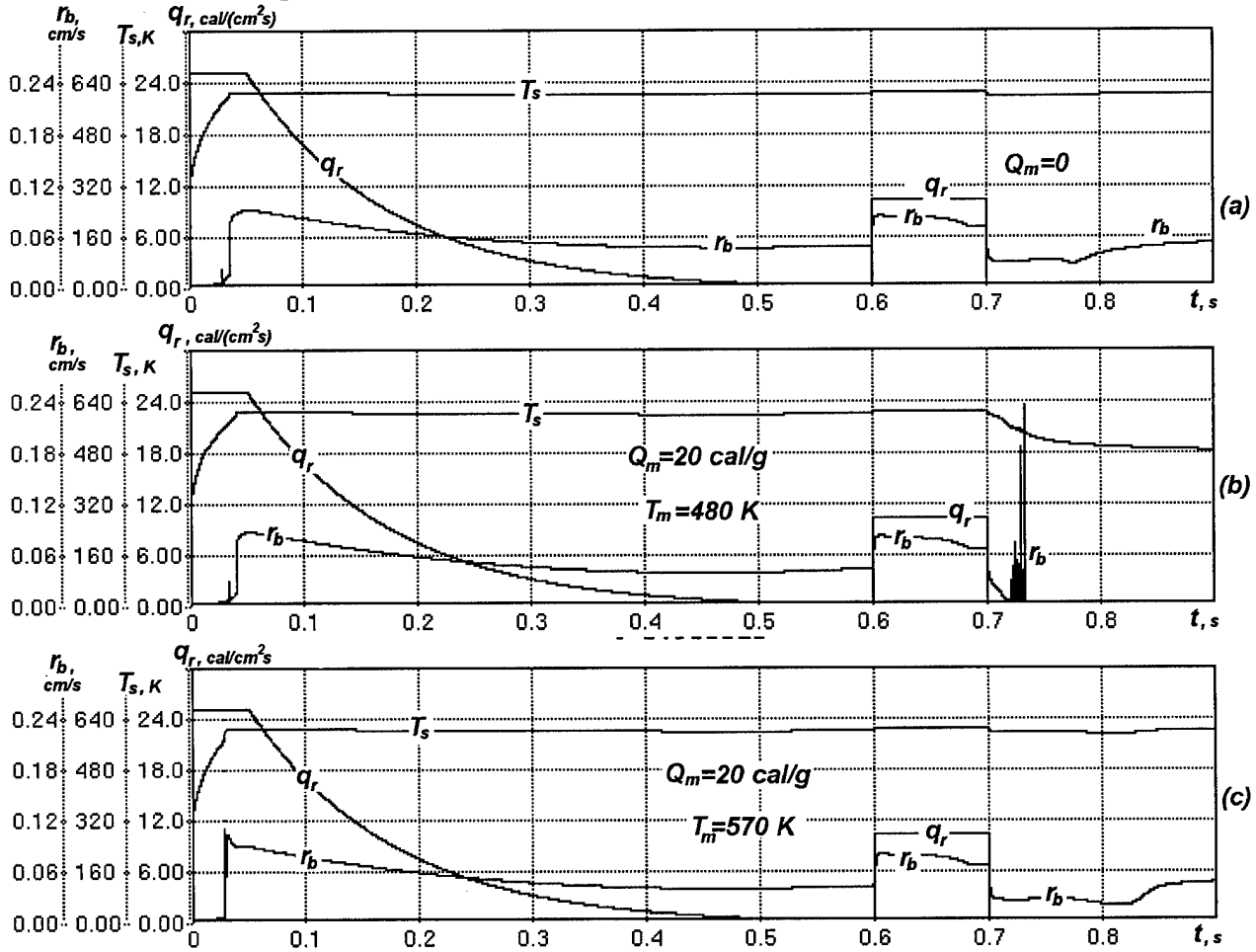

Fig.6.8. Radiation-driven burning rate behavior for EM with Q_m=0 (a); Q_m=20 cal/g, T_m=480 K (b); Q_m=20 cal/g, T_m=570 K (c).

6.3.5. Ignition peculiarities.

The ignition of EM by thermal radiation was modeled as follows. For semi-transparent EM (α = 1000 cm^{-1} in terms of the Beer law) we assumed time-dependent irradiation by flux $q_r(t)$ which is constant $q_r=q_0$ within the time interval $0<t<t_1$, linearly decreases to zero with $t_1<t<t_2$ and at last vanishes. It appears that depending on the value of parameters q_0, t_1, t_2 and kinetic parameters (for the gas phase, first of all) possible are one-, two- or even three-stage ignition regimes. All

regimes have the same beginning phase, i.e. "inert" heating when all reactions can be neglected. This phase continues until the surface temperature reaches the EM boiling (a bit lower) temperature T_b. When T_s approaches T_b, noticeable are the rates of evaporation from the surface and reactions in the liquid and gas.

To demonstrate the effects of multi-stage ignition the calculations were conducted with following reference parameters: Q_{liq} = 102 cal/g, $E_1 = E_2$ = 35400 cal/ mol, Q_1 = 250 cal/g, Q_2 = 716 cal/g, $A_{g1} = 10^{14}$ g/(cm^3 s atm$^{1.6}$) and $A_{g2} = 10^{13.5}$ g/(cm^3 s atm$^{1.6}$) for Figure 6.9; $A_{g1} = A_{g2} = 10^{13.5}$ g/(cm^3 s atm$^{1.6}$) for Figure 6.10; $A_{g1} = 10^{13.5}$ g/(cm^3 s atm$^{1.6}$) and $A_{g2} = 10^{12.3}$ g/(cm^3 s atm$^{1.6}$) for Figure 6.11.

One-stage ignition is realized with sufficiently strong heat release of reactions in the gas phase, in the time interval $0 < t \sim t_1$ (Figure 6.9). The gas flame is stabilized in close vicinity of surface and provides heating and evaporation of the condensed phase. When the q_r gradually vanishes, the steady-state regime of self-sustaining combustion can be established, if the deradiation time (t_2-t_1) is not much shorter than the characteristic relaxation time of preheat layer in this regime (in opposite case the flame quenches). In self-sustaining regime a regression rate is relatively high, conversion degree in liquid is small.

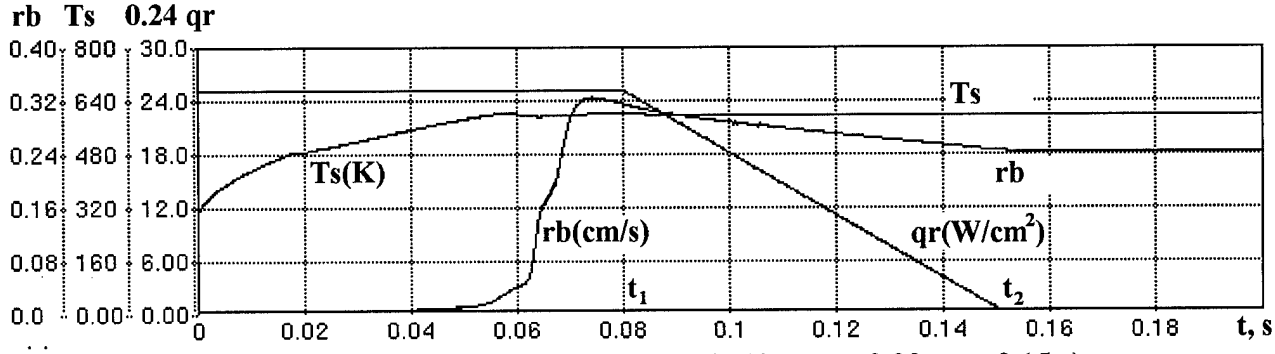

Figure 6.9. One-stage ignition (q_0=105 W/cm$_2$, t_1=0.08 s, t_2=0.15 s).

Two-stage regime is possible (Figure 6.10) with relatively slow kinetics of the first gas phase reaction. The gas flame arises when the $T_s \approx T_b$ and evaporation starts. However, the flame is realized in the "zone separation regime", i.e. far from the surface at a distance $h \approx V_g t_{ign}$. In this case $V_g \sim q_r$ is the velocity of gas flowing from the surface; t_{ign} is the time of thermal explosion in gas at characteristic temperature T_s. When $h > \lambda/(c\rho V_g)$, the heat from gas flame does not effectively feed to the surface. In these conditions the gasification regime is observed presumably under the action of the external heat flux q_r. When q_r decreases, the degree of conversion in the condensed phase increases (for used reference parameters it reaches ~ 0.2), and r_b decreases too. With $q_r(t)$ decreasing, the gas velocity and distance h also decrease and the flame approaches the surface. When q_r vanishes, the flame provides the heat flux to the surface that is necessary for the steady-state self-sustaining regime (if deradiation was not too fast). In this case, the mass fraction of vapor above the surface y_{1s}, which in the zone separation regime of combustion or in gasification regime coincides with y_{cs}, becomes smaller due to the diffusion dilution of vapor by combustion products that leads to a small drop in T_s. As a result, the value of $(1-y_{cs})$ decreases compared to gasification regime.

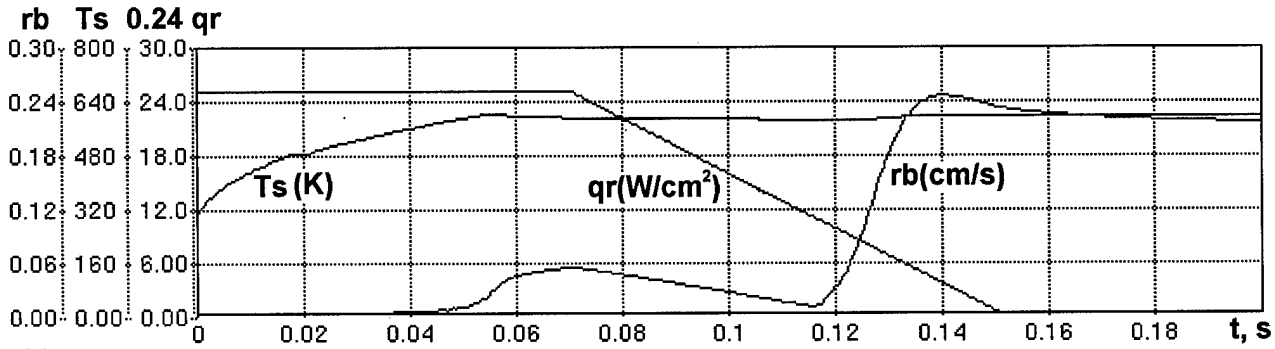

Fig.6.10. Two-stage ignition (q_0=105 W/cm$_2$, t_1=0.07 s, t_2=0.15 s).

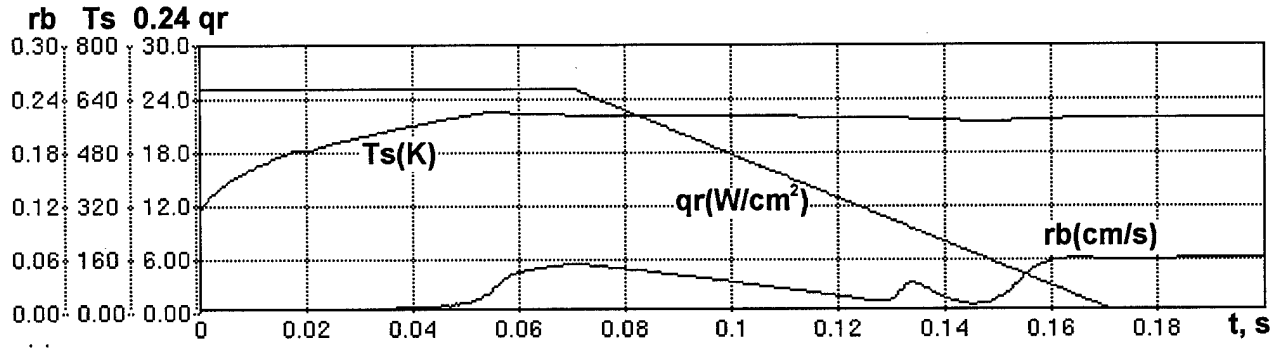

Figure 6.11. Three-stage ignition (q_0=105 W/cm$_2$, t_1=0.07 s, t_2=0.17 s).

Three-stage regime is possible (Figure 6.11) with fairly "slow" kinetics of the second reaction in the gas phase (burning in a far zone). In this case, at the first stage in the gasification regime the gas flame of the first reaction is separated from the surface and from the flame of the second reaction in a far zone. As q_r decreases, the flame in a far zone approaches the first flame and merges with it. Finally, the merged flame approaches the surface.

It should be noted that the regime of the flameless gasification under irradiation by Nd-YAG laser was experimentally observed in combustion under atmospheric pressure of pressed RDX samples. Experiments were conducted in 1998 in the Institute of Chemical Kinetics and Combustion, Novosibirsk.

6.3.6. Concluding remarks

The above results show that the effect of melting on the combustion behavior of EM can be qualitatively explained from the point of view of classic thermal theory of combustion. If one assumes that increase in absolute value of the melting heat is equivalent to decrease of initial temperature of EM, the observed decrease of intrinsic combustion stability in response to small or finite pulse perturbations of heat flux is the result of lowering the effective initial temperature. The influence of initial temperature on the combustion stability limit is determined by the closeness of calculated value of the parameter $k = (T_s - T_o)\ (\partial ln r_b/\partial T_o)_p$ to its critical value corresponding to the boundary of stable combustion regimes. In the case of gas phase reactions con-

trolling the propellant burning rate the coefficient $\partial ln r_b/\partial T_o \sim E_g/RT_g^2$ has a weak dependence on T_o and parameter k increases when initial temperature T_o decreases. Thus, with T_o decreasing the combustion stability becomes lower due to increase of parameter k. Such statement works in case of small perturbations and may work in case of finite amplitude perturbations.

The effect of the magnitude of melting temperature on the combustion stability can be qualitatively treated through the analysis of interaction of thermal disturbances with melting surface. When the thermal wave penetrates deep in the bulk of EM and reaches the melting surface, the interaction with the heat sink caused by the EM melting leads to the weakening (dissipation) of thermal disturbance as it follows from the Le Chatelier principle. Therefore, the higher the melting temperature (closer to the burning surface temperature), the higher the stability of self-sustaining and transient combustion both in the regimes of pressure drop and irradiation pulse.

Calculations within the framework of the proposed mathematical model for combustion of melted and evaporated EM showed that variations of the surface temperature are effectively reduced by the surface heat sink created by EM evaporation. This leads to relatively small magnitude of parameter $r = (\partial T_s/\partial T_o)_p$ and to relatively weak frequency dependence of burning rate response to pressure oscillations. It should be noted that such theoretical predictions still have no actual confirmation in experiments.

6.4. NONSTEADY-STATE COMBUSTION OF METALLESS HETEROGENEOUS COMPOUNDS

6.4.1. Combustion of coarse grain oxidizer in active binder.

In view of the extraordinary variety of heterogeneous condensed systems (HCS) and their combustion conditions it is only possible to describe the combustion of HCS plausibly by a system of the models. While in steady-state combustion several elements of this system are known, in nonsteady-state combustion, where the variety of combustion conditions is much higher, in different variants mainly a model is used assuming that $d << \kappa/u$ (d is the particle size; κ is the condensed phase thermal diffusivity; u is HCS burning rate). Another important assumption used is about one-dimensional heat propagation process. At the same time, it is clear that with $d \geq \kappa/u$, when burnout time d/u for a single particle and the time κ/u^2 for thermal relaxation of the preheated HCS layer are comparable, combustion of a system may be locally nonstationary [126, 127]. The nature of disturbances caused by heterogeneity may be different.

If gasification products of one of the components (dispersed filler or binder), issued with a velocity v from the surface, flows around projections of the other less volatile component rising by ~d above it, then with $Re = \rho vd/\mu \sim 10$ it is possible for pulsations to occur as a result of the detachment of Karman vortices with the frequency ~v/d. If the binder burns independently and more rapidly than the filler, the role of the latter for a broad class of HCS is reduced to heat transfer from the combustion zone of the binder [128]. With a reduction in thickness h of the binder layer between filler grains (with an increase in its volume fraction ς, in HCS or with a reduction in d) combustion of the binder slows down, and on reaching a critical thickness h* it ceases as a result of extinction of the gas flame, as demonstrated in tests in [129] with DB propellant specimens. In many cases according to [91] homogeneous DB propellant specimens with a thickness close to

the critical value burn in oscillating regime. The same behavior may also be expected for layers of rapidly burning binder in HCS.

Finally, with h » h*, when the greater part of the binder and filler surfaces burn in dependently of each other, nonstationary combustion of HCS under transient pressure is determined by the evolution of the filler surface area that leads to variation of the mass flow rate of the system components. Let pressure changes system with the fast burning filler components.

Combustion under fast changing ambient pressure. Let pressure changes with a high rate. If the time for change in pressure $t_p << d/u_m$ ($u_m = \max(u_H, u_b)$; u_H and u_b are linear combustion rate for the filler and binder, respectively), then it is possible to ignore the change in HCS surface structure during interval time t_p. According to [11], a HCS specimen of cross section S burns as two independently burning specimens (of solid filler and of binder) with a plane combustion surface ($S_{ox} = S^o_{ox}$, $S_b = S^o_b$), with the "steady-state" relationships being met:

$$S^o_{ox}\, u^o_{ox} = \varsigma\, S\, u^o, \quad S^o_b\, u^o_b = (1-\varsigma)\, S\, u^o,$$

where u^o is the steady-state (before the start of change in pressure) burning rate for the whole specimen. The only difference consists of the fact that the mass flow rates calculated by formulas

$$M_{ox} = S^o_{ox}\, \rho_{ox}\, u_{ox}(t), \quad M_b = S^o_b\, \rho_b\, u_b(t)$$

for the two components should assume instantaneously mixing at the HCS surface. The variability of $M_{ox}(t)/M_b(t)$ causes a change in temperature of the combustion products. These variations (by hundreds of degrees) have been recorded in experiments [11, 13, 130].

System with fast burning filler component. Some predictions for relatively nonsteady-state combustion may also be carried out for the case $d/u_{ox} << t_p$, $u_{ox} >> u_b$ when the corresponding steady-state regime is described by models of a relay the type [131-134]. For such a steady-state regime from a model in [133] it follows that $u \approx u_b/(1 - \varsigma_{eff})$. Here $\varsigma_{eff} = \varsigma/\varsigma_1$ is the effective volume fraction of rapidly burning component considering that with each filler particle there is a certain volume of binder, adjacent to it, that also burns out rapidly. The condition adopted $d/u_{ox} << t_p$ means that a change in the process parameters (in particular composition of the combustion products) is only considered in intervals of time essentially exceeding the time for burn out of a single filler grain. Filler gasification products issuing from the surface of a HCS specimen in such time intervals depend on the slow gasification-rate for binder layers between particles. This statement is a basis for deriving a "steady-state" equation $u \approx u_b/(1 - \varsigma_{eff})$. In other words, if it is possible to ignore the effect of non-uniformity in the gas phase and assume that the value of ς_1 is constant, in the nonsteady-state regime described the ratio M_{ox}/M_b does not change (and T depending upon it), and the overall mass flow rate $M_{ox}+M_b$ is proportional to non-steady-state burning rate $u_b(t)$ of the binder.

It should mean that steady-state models of a relay race type, used extensively in the case of $u_{ox}>u_b$, are unsuitable with a quite high volume fraction $\varsigma > \varsigma^*$ for the filler when it may form continuous solid chains in the HCS [135, 136]. For example, this limitation may be applied to an equation provided from [133] if it is assumed that in it $\varsigma_1 = \varsigma^*$. Then $u \approx u_{ox}$ and combustion propagates along chains of the filler in a similar way to that along binder layers in HCS with rapidly burning binder, and simple conclusions about nonsteady-state combustion can only be made as before for rapidly oscillating pressure ($t_p << d/u_m$).

In the general case, when times t_p, d/u_{ox} and d/u_b; are comparable, the synchronizing effect of changing external conditions on local nonsteady-state phenomena around individual grains weakens as compared with the case $t_p << \max(d/u_{ox}, d/u_b)$. It requires consideration of the change in time t_p of surface structure in the region of an individual grain. These attempts made in models in [137, 59, 62], however, can be considered only for HCS with an ordered structure. Nonetheless, developed in [137, 59, 62] approach may be useful if according to [138] a highly loaded HCS, consisting of randomly located and orientated elements with correctly (hexagonal and cubic) placed particles in these elements, is considered.

Combustion under periodically oscillating pressure. Consider now in more detail the situation when filler particle location in the HCS is completely disordered; particle dimensions are quite large so that combustion of almost the whole particle surface and almost the whole surface of the binder may be assumed to be independent ($h >> h^*$). Let response functions exist, found theoretically or experimentally, for pure filler and binder in the form

$$f_{ox}(\omega) = (\Delta u_{ox}/ u_{ox})/(\Delta P/P), \qquad f_b(\omega) = (\Delta u_b/ u_b)/(\Delta P/P), \tag{6.20}$$

for harmonic change in pressure $\Delta P = |\Delta P| \exp(i\omega t)$. In this way the binder burns faster than the filler, $u_{ox} < u_b$ (grains burn out in gas phase), but values of $t_p \sim 2\pi/\omega$, d/ u_{ox} and d/u_b are comparable so that a change in grain shape in the pressure pulsation time should be considered. In the bulk of HCS a filler grain is assumed to be spherical and identical everywhere. It is necessary to obtain in a linear approximation response functions for mass velocity M for HCS specimen combustion

$$f_M(\omega) = (\Delta M/M)/(\Delta P/P) \tag{6.21}$$

and for combustion product temperature

$$f_{RT}(\omega) = (\Delta RT/RT)/(\Delta P/P) \tag{6.22}$$

In order to find both of these values it is sufficient to know current values of mass velocities of gas formation for the filler and binder at the specimen surface:

$$M = M_{ox} + M_b, \quad \Delta M/M = (\Delta M_{ox}/M_{ox})(M_{ox}/M) + (\Delta M_b/M_b)(1 - M_{ox}/M) \tag{6.23}$$

The dependence of flame temperature on M_{OX}/M is assumed to be known from a test or calculation, then taking account of (4) one obtains

$$f_{RT}(\omega) \approx \{d \ln RT/d(M_{ox}/M)\}\, \Delta(M_{ox}/M)/(\Delta P/P), \tag{6.24}$$
$$\Delta(M_{ox}/M) = (M_{ox}M_b/M^2)\,[\Delta M_{ox}/M_{ox} - \Delta M_b/M_b]$$

In order to find the variation of mass flow rates $M_{ox}(t)$ and $M_b(t)$ it is convenient to present them in the form

$$M_b = \rho_b S_b u_b, \quad (\Delta M_b/M_b)/(\Delta P/P) = (\Delta S_b/S_b)/(\Delta P/P) + f_b(\omega); \quad M_{ox} = \rho_{ox} \int(-\partial w/\partial t)dN \tag{6.25}$$

Here w is the as yet unburned volume of filler particles; N is the number of burning particles (also including those flying off). Thus, with known $f_{ox}(\omega)$, $f_{ox}(\omega)$ the problem is reduced to geometry, i.e., to calculation of $\Delta S_b(t)$ and the integral (6.25).

The binder surface in contact with gas is assumed to be plane and having area

$$S_b \approx (1-\varsigma)S = \text{const}, \quad \Delta S_b(t) = 0. \tag{6.26}$$

This assumption reflects reality very conditionally. Actually, the binder surface is curved every-

where (see in Fig. 6.12a evolution of the plane front at first enveloping a single particle), and the area of it is less than the value (1-ς)S corresponding to a plane front. In fact, steady-state velocity $u< u_b$ due to curvature. On the other hand, the geometric relationship $uS(1 - \varsigma) = S_b u_b$ is fulfilled, and whence with $u < u_b$ it follows that $S_b < S(1 - \varsigma)$. Considering curvature the behavior of function $u/u_b < 1$ versus ς may be obtained by experiment or theoretically, for example, by assuming the HCS consists of arbitrarily orientated elements with a correct structure for particles. However, it is noted that for linear nonsteady-state analysis the left-hand pert of equality (6.26) is not so important as the right-hand part, and the latter is accurately fulfilled. This follows from the fact that the leading combustion of the binder in this arrangement in no way depends on the nature of filler burn out (the movement of a curved binder combustion front is the same as if the filler was inert). Since normal velocity $u_b(t)$ is identical everywhere, the shape and area of the local binder surface elements depends only on the thickness of the burning layer $\int u_b dt$ and it does not depend on how velocity changes during its combustion. Whence it follows that for the whole specimen S_b does not depend on time with $p = p(t)$.

Consider now the filler combustion. If with pressure variations there is also variation of ratio u_{ox}/u_b, toward the center of a burning surface of each grains waves propagate of the change in surface shape from the contact line with the binder, which serves as a source of disturbances. A similar process was considered in [139]. The phenomenon is described by an equation in first order partial derivatives. However, if it is considered that actual particles have an irregular shape and they are in contact with the disordered curved surface of the binder, then the simplification introduced in the BDP model [140] is valid. It is assumed that emerging from the HCS surface a particle burns at its tip at rate $u_{ox}(t)$, and the rest of the surface in contact with gas (Fig. 6.12b) changes, remaining by part of a sphere bounded with the plane surface of the binder moving at a rate of $u_b(t)$. By calculating integral (6) with these assumptions for HCS with randomly distributed particles throughout the volume, it is possible to obtain (see Appendix 6.4.1)

$$(\Delta M_{os}/M_{ox})/(\Delta P/P) = f_b(\omega)+3(f_{ox}(\omega)-f_b(\omega))\delta F(\Omega,\delta) \tag{6.27}$$

$$F(\Omega,\delta)=[1/6+(1-\delta)^2/(3\delta)+i(1-\delta)^2/\Omega+(1-(1-\delta)4\delta)/\Omega^2+2i\delta(2-5\delta)/\Omega^3] - $$
$$- [(1-2\delta^2)/\Omega^2+2i\delta(2+3\delta)/\Omega^3] \exp(-i\Omega) + (16i\delta^2/\Omega^3) \exp(-i\Omega/2\delta) \cos(\Omega/2), \tag{6.28}$$
$$\delta = u_{ox}/u_b, \ \Omega = \omega d/u_b.$$

It is possible to show that in (6.28) with $\omega\to 0$, $F(\Omega, \delta)\to 0$, so that $(\Delta M_{ox}/M_{ox})\to \Delta u_b/ u_b$. This corresponds to a physical meaning: With slow pressure variations the specimen burns in a quasi - steady way at a rate of $u_b(P)$. According to [11] with high frequencies there should be $(\Delta M_{ox}/M_{ox})\to\Delta u_{ox}/u_{ox}$, i.e., in (6.27) there should be $3\delta F(\Omega,\delta)\to 1$. However, from (6.28) it follows that $F(\infty, \delta)=(1/3\delta)-1/2+\delta/3$, which complies in fact only with $\delta = u_{ox}/u_b << 1$. The reason for the divergence is use of a simplifying assumption about always spherical shape for the part of the particle projecting above the binder. According to this assumption it is necessary that in order to retain a spherical shape the particle surface responses instantaneously as much as necessary to rapid variation of the boundary with the binder, which contradicts the physical meaning. A more accurate mathematical statement without using assumptions for spherical shape leads to a quite cumbersome calculation algorithm and it is out of place while taking account of the roughness of other adopted idealizations. Instead of F let we use a "corrected" function

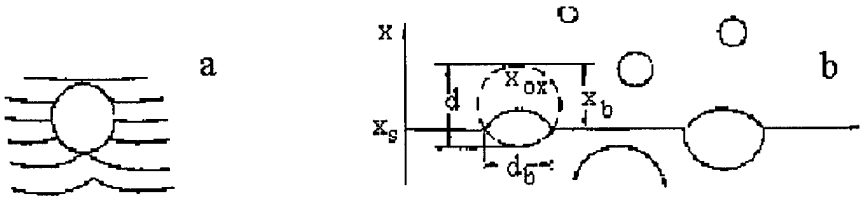

Fig. 6.12. Curvature of the plane combustion front around an inert particle (a) and HCS surface geometry (b).

$$F_1 = F + (1/2 - \delta/3)\{1 - [1 - \exp(-i\Omega\gamma)]/(i\Omega\gamma)\}, \tag{6.29}$$

where γ is matching factor (probably, it is of the order of 1). According to (6.28), (6.29), $F_1 \to 0$ with $\Omega \to 0$; $F_1 \to 1/3\delta$ with $\Omega \to \infty$. By assuming $F_1 = F_2 + iF_3$, we have from (6.28) and (6.29)

$$\begin{aligned} F_2 &= (1-2\delta)^2/(3\delta\Omega^2) - (1-2\delta^2)\Omega^{-2}\cos\Omega - 2\delta(2+3\delta)\Omega^{-3}\sin\Omega + \\ &+ 16\,\delta^2\Omega^{-3}\sin(\Omega/2\delta)\cos(\Omega/2) - (3-2\delta)(6\gamma\Omega)^{-1}\sin(\gamma\Omega), \\ F_3 &= (1-\delta)^2/\Omega + 2\delta(2-5\delta)/\Omega^3 + (1-2\delta^2)\Omega^{-2}\sin\Omega - 2\delta(2+3\delta)\Omega^{-3}\cos\Omega + \\ &+ 16\,\delta^2\Omega^{-3}\cos(\Omega/2\delta)\cos(\Omega/2) + (3-2\delta)(6\gamma\Omega)^{-1}[1-\cos(\gamma\Omega)]. \end{aligned} \tag{6.30}$$

Other forms of "corrected" function F are possible apart from (6.29). Now by substituting in (6.27) function F_1 according to (6.27)-(6.30), it is possible to obtain from (1)-(8) the $f_M(\omega), f_{RT}(\omega)$ sought.

Let we discuss the form of $f_{RT}(\omega)$. From (6.24)-(6.27) it follows that

$$f_{RT} = (\Delta RT/RT)/(\Delta P/P) =$$

$$= [d\ln RT/d(M_{ox}/M)](M_{ox}/M)(1 - M_{ox}/M)3[f_{ox}(\omega) - f_b(\omega)]\delta F_1(\Omega,\delta) \tag{6.31}$$

Shown in Fig. 6.13 are the values of modulus A (ascending curves) and argument (descending curves) for the value $3\delta F_1$ depending on $\Omega = \omega d/u_b$ with different $\delta = u_{ox}/u_b$ and γ;

$$A = 3\delta(F^2_2 + F^2_3)^{1/2}, \qquad \vartheta = \operatorname{arctg}(F_3/F_2). \tag{6.32}$$

It can be seen that the dependence on the matching factor $\gamma = 0.5$-2 is small, it weakens with an increase in the ratio $1/\delta = u_b/u_{ox}$, and in any case it does not qualitatively change the shape of curves.

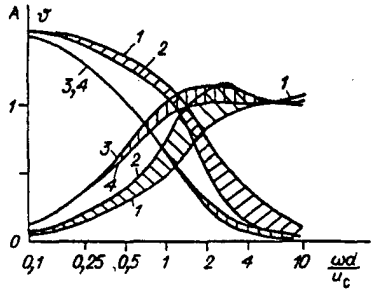

Fig. 6.13. Modulus and argument of value $3\delta F_1$. u_{ox}/u_b: 1) 0.3, 2) 0.3, 3) 0.1, 4) 0.1; γ: 1) 0.5, 2) 2, 3) 2, 4) 0.5.

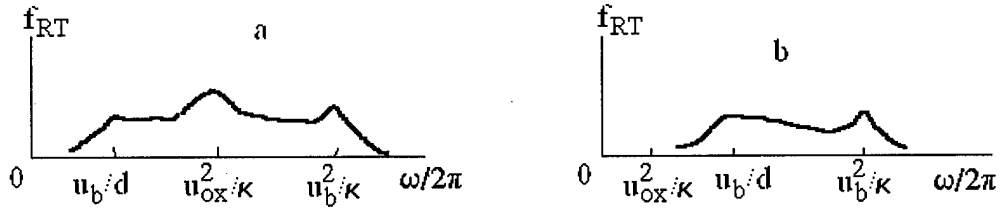

Fig. 6.14. Qualitative dependence of response modulus for product temperature on frequency, a) $u^2_{ox}/\kappa \geq u_b/d$; b) $u^2_{ox}/\kappa \leq u_b/d$;.

Now it is possible to draw some conclusions about the nature of the relationship $f_{RT}(\omega)$ according to (6.31) (Fig. 6.14). It is well known [20] that for a homogeneous composition with a linear combustion rate u at low frequencies ($\omega << 2\pi u^2/\kappa$) the response function $f = (\Delta u/u)/(\Delta p/p)$ is close to the index in the burning law $\nu = d\ln u/d\ln p$, and with $\omega \sim 2\pi u^2/\kappa$ modulus f normally has a maximum and then it decreases. Taking account of $\delta = u_{ox}/u_b < 1$, the dependence of product modulus $(f_{ox} - f_b)3\delta F_1$ on ω may have a zero slope "shelf" starting at $\omega/2\pi \sim u_b/d$ and two maximums at $\omega/2\pi \sim u^2_{ox}/\kappa$ and $\omega/2\pi \sim u^2_b/\kappa$ (see Fig. 6.14a). If $u^2_{ox}/\kappa < u_b/d$, the "shelf" and the maximum, connected with the response of the filler, degenerate into a maximum with $\omega/2\pi \sim u_b/d$ (see Fig. 6.14b).

APPENDIX 6.4.1.

According to (6.25) in order to obtain the relationship $M_{ox}(t)$ at first it is necessary to find the unburned volume of grain partly emerging at the surface. We take as origin x = 0 at the cold end of the specimen, and at the burning surface $x = x_s$. At instant t we consider the geometry of a particle with a center (without considering combustion) in plane x. The still unburned particle consists of two segments with heights h_B and h_{OX} with a common base, i.e., a circle of diameter d_b and with total volume

$$w = (\pi h_B/6)[3(d_b/2)^2 + h^2_B] + (\pi h_{OX}/6)[3(d_b/2)^2 + h^2_{OX}]. \qquad (I)$$

We express h_B and h_{OX} in terms of x_{OX} and x_b, which indicate at what distance at instant t combustion has propagated through the particle (from the tip) and through the binder, i.e., with appearance of particle tip at the burning surface (see Fig. 6.12b)

$$h_B = x_b - x_{OX}, \qquad h_{OX} = d - x_b, \qquad (II)$$

We use the geometric relationship

$$(d_b/2)^2 = x_b\,(d - x_b). \; l) \qquad (III)$$

If the center of the particle (without considering combustion) lies in plane x, then

$$x_b = x - x_s + d/2, \qquad -dx_s/dt = u_b \qquad (IV)$$

Particle combustion started with

$$x_s = x_s^* = x + d/2 \qquad (V)$$

and particle separated from the surface with $x_s = x_s^{**} = x - d/2$.

For x_{OX}, there is fulfillment of

$$x_H = \int^t u_{ox}\, dt = \int_{x_s(t)}^{x_s^*(t)} \delta\, dx_S, \qquad \delta = u_{ox}/u_b$$

From (I)-(III) it follows that

$$w/(\pi d^3/6) = (\xi_b-\xi_{OX})[3\xi_b(1-\xi_b)+(\xi_b-\xi_{OX})^2]+(1-\xi_b)^2(1+2\xi_b), \qquad (VI)$$
$$\xi_b < 1, \quad \xi = x/d.$$

Further instead of time we will use a value of $\xi_s = x_s(t)/d$. Then for the period after particle separation we have

$$w/(\pi d^3/6) = \max[0, (1+\xi_{OX}^{**}-2\xi_{OX})^3], \qquad \xi_s < \xi_s^{**}(\xi) \qquad (VII)$$
$$\bar{w}(\xi, \xi_s) = w/(\pi d^3/6) \qquad (VIII)$$

$$\bar{w}(\xi, \xi_s) = \psi(\xi_b, \xi_{OX}), \qquad \text{if } \xi - \xi_s < \tfrac{1}{2};$$
$$\bar{w}(\xi, \xi_s) = \varphi(\xi_{OX}^{**}, \xi_{OX}), \qquad \text{if } \xi - \xi_s > \tfrac{1}{2}.$$

where ψ and φ are given by (VI) and (VII),

$$\xi_H^{**}(\xi) = \int_{\xi-1/2}^{\xi+1/2} \delta(\xi_S)\, d\xi_S, \quad \xi_H(\xi, \xi_S) = \int_{\xi_S}^{\xi+1/2} \delta(\xi_S)\, d\xi_S, \qquad (IX)$$

In calculating integral (6) the number of particle centers dN in a layer of thickness dx is found as the product of volume Sdx for this layer for average volume concentration $\xi/(\pi d^3/6)$ of particle centers in the specimen. Then (6) takes the form

$$M_{OX} = \rho_{OX} S \zeta u_b(t) \int \frac{\partial \bar{w}(\xi, \xi_S)}{\partial \xi_S} d\xi. \qquad (X)$$

According to (V) and (VII) for the integration limits there is fulfillment of $\xi = \xi_s - 1/2$ and $1 + \xi_{OX}^{**} - 2\xi_{OX} = 0$, respectively (start and end of combustion). Now we place in integral (X) expression (VIII) for $\bar{w}$

$$\int \frac{\partial \bar{w}(\xi, \xi_S)}{\partial \xi_S} d\xi. = \int_{\xi_S - 1/2}^{\xi_S + 1/2} \left[\frac{\partial \psi}{\partial \xi_c} \frac{\partial \xi_c}{\partial \xi_S} - \frac{\partial \psi}{\partial \xi_H} \frac{\partial \xi_H}{\partial \xi_S} \right] d\xi \quad + \int_{\xi=\xi_S+1/2}^{1+\xi_H^{**}-2\xi_H=0} \frac{\partial \varphi}{\partial \xi_H} \frac{\partial \xi_H}{\partial \xi_S} d\xi \qquad (XI)$$

From (IV) and (IX) it follows that

$$\frac{\partial \xi_c}{\partial \xi_S} = -1, \quad \frac{\partial \xi_c}{\partial \xi} = 1, \quad \frac{\partial \xi_H}{\partial \xi_S} = -\delta(\xi_S),$$

$$\frac{\partial \xi_H}{\partial \xi} = \delta(\xi + 1/2), \quad \frac{\partial \xi_H^{**}}{\partial \xi} = \delta(\xi + 1/2) - \delta(\xi - 1/2),$$

so that (XI) takes the form

$$\int \frac{\partial \bar{w}}{\partial \xi_S} d\xi. = \int_{\xi_S - 1/2}^{\xi_S + 1/2} \left[\frac{\partial \psi}{\partial \xi_c}(-1) + \frac{\partial \psi}{\partial \xi_H}(-\delta(\xi_S)) \right] d\xi \quad + \int_{\xi=\xi_S+1/2}^{1+\xi_H^{**}-2\xi_H=0} \frac{\partial \varphi}{\partial \xi_H}(-\delta(\xi_S))\, d\xi \qquad (XII)$$

For comparison it is useful to write the expression

$$1=\int -\frac{\partial w}{\partial \xi_S}d\xi. = \int_{\xi_S-1/2}^{\xi_S+1/2}\left[-\frac{\partial \psi}{\partial \xi_C}1-\frac{\partial \psi}{\partial \xi_H}\delta(\xi+1/2)\right]d\xi +$$

$$+\int_{\xi=\xi_S+1/2}^{1+\xi_H{}^{**}-2\xi_H=0}\left[-\frac{\partial \varphi}{\partial \xi_H}\delta(\xi+1/2)-\frac{\partial \varphi}{\partial \xi_H{}^{**}}(\delta(\xi+1/2)-\delta(\xi-1/2))\right]d\xi \qquad \text{(XIII)}$$

From comparison of (XII) and (XIII) it follows {taking account of (VI), (VII), (XI)} that

$$\frac{M_{OX}}{\rho_{OX}S\,\xi u_b(t)}-1=-3\int_{\xi_S-1/2}^{\xi_S+1/2}\{\xi_C(1-\xi_C)+(\xi_C-\xi_H)^2\}[\delta(\xi+1/2)-\delta(\xi_S)]d\xi +$$

$$+\int_{\xi=\xi_S+1/2}^{1+\xi_H{}^{**}-2\xi_H=0}(1+\xi_H{}^{**}-2\xi_H)^2[-\delta(\xi+1/2)-\delta(\xi-1/2)+2\delta(\xi_S)]d\xi \qquad \text{(XIV)}$$

$$\xi_C=\xi-\xi_S+1/2, \qquad \xi_S=const-(1/d)\int_0^t u_b(t)dt \qquad \text{(XV)}$$

In a steady-state regime the left and right-hand parts of (XIV) revert to zero. By calculating deviation from a steady-state regime, referred to $\Delta p/p$, for the left-hand part we obtain $(\Delta M_{ox}/ M_{ox})/(\Delta p/p)$ — $f_b(\omega)$. In the right hand side of (XIV), the expressions in square brackets in a steady-state regime revert to zero, and therefore for a linear approximation the rest of the multipliers beneath the integral and the limits of the integral may be given steady-state values by taking there according to (IX) and (XV) that

$$\xi_{OX}=\xi_b\,\delta,\ \xi_{OX}{}^{**}=\delta,\ \xi_s=\text{const}-u_bt/d.$$

For disturbance of value $\delta = u_{ox}(t)/u_b(t)$ we obtain

$$\Delta\delta(\xi_s)/(\Delta p(t)/p)=(f_{ox}-f_b)\,\delta$$

[see designations in (1)]. If instead of ξ_s we give to value δ the argument $\xi+1/2=\xi_s+\xi_b$, then (in accordance with the relationship $\xi_s = \text{const} - u_bt/d$) this will be equivalent to substituting t by $t - \xi_b d/u_b$.

Then taking account of $\Delta p \sim \exp(i\omega t)$, we obtain

$$\frac{\Delta\delta(\xi+1/2)}{\Delta p(t)/p}=\frac{\Delta\delta(\xi_S+\xi_C)}{\Delta p(t-\xi_C d/u_b)/p}\frac{\Delta p(t-\xi_C d/u_b)}{\Delta p(t)}=(f_{OX}-f_b)\delta e^{-i\Omega\xi_C}.$$

Similarly $$\frac{\Delta\delta(\xi-1/2)}{\Delta p(t)/p}==(f_{OX}-f_b)\delta e^{-i\Omega(\xi_C-1)}, \quad \Omega=\omega d/u_b.$$

By introducing under integral (XIV) a new variable $\xi_b = \xi - \xi_s + 1/2$, we obtain

$$(\Delta M_{OX}/M_{OX})/(\Delta P/P)=f_b(\omega)+3(f_{OX}(\omega)-f_b(\omega))\delta F(\Omega,\delta),$$

$$F(\Omega,\delta)=[1/\delta+(1-\delta)^2/(3\delta)+i(1-\delta)^2/\Omega+(1-(1-\delta)4\delta)/\Omega^2+2i\delta(2-5\delta)/\Omega^3]-$$

$$-[(1-2\delta^2)/\Omega^2+2i\delta(2+3\delta)/\Omega^3]\exp(-i\Omega)+(16i\delta^2/\Omega^3)\exp(-i\Omega/2\delta)\cos(\Omega/2).$$

From integral expression $F(\Omega,\delta)$ it can be seen that $F(0, \delta) = 0$.

6.4.2. Possibility of synchronization of burning rate fluctuations over the burning surface.

The possibility of synchronizing the fluctuations was first mentioned in [I41]. Fluctuations in the

burning rate of localized parts of the fuel surface can arise, even at constant pressure, in combustion of non-homogeneous compositions [60] and common quasi-homogeneous solid propellants, by the accumulation and periodic loss of the less volatile components from the surface [142]. Randomness, when pressure is constant, is provided for commercial propellants by manufacturing process whereas for double base propellants some "disordering" process on the surface may play role. The transition from chaotic to organized structures occurs because of the totally nonlinear interaction is one of the effects of synergy [143].

Let us consider a composite solid propellant comprising a fast-burning matrix with inert additions. The experimental data [128] shows that if the matrix contains a catalyst, then the particles of metal and even oxidizing agents could remain inert (i.e. the rate of burning was not influenced by the nature of these particles, but only by their ability to extract heat from the condensed phase of the substrate). Such a situation is possible only if the rate control stage is located in the condensed phase and if it is possible to neglect the solid phase chemical interaction between the matrix and the foreign particles. Burning in such a system will spread along the layers of matrix of varying thickness and complexity of form, between the inert particles. Because of the heat transfer to the particles, which is dependent on the thickness and form of the layer, the rate of burning also varies. It is a maximum in the pockets (expansions of the binder layer) between several particles. It may be assumed that the propagation of the flame will follow some crooked route by the widest- interconnecting path between particles. Burning spreads to the narrowest layers later, without influencing the speed of propagation of the flame along the other paths. Let us neglect the intersection of the separate paths. In other words, the propagation of the flame along each path is independent of the situation in the other paths. Further, assuming that the thickness, h, of a layer along each path is a periodic function of its length, x, then:

$$h/h_o = 1+|\Delta h/h_0| \sin(\varphi+2\pi x/a). \qquad (6.33)$$

Some justification for these assumptions follows from [135], where local "close order" in highly loaded mixtures, similar to that in the molecular structure of liquids, was observed. Total order does not exist in real systems, and its use in the model leads to complete anisotropy and reduces the applicability of the model (e.g., [137]). In order to avoid this problem, assume that identical paths leading from the surface exist and that disorder is introduced: the paths move haphazardly along normalize to the surface and then, still randomly, become distorted, (Fig. 6.15). The surface of such a propellant, under constant pressure, would burn at randomly fluctuating local rates, and the surface would also be randomly distorted.

Consider now the burning along a single path. It may be assumed that the burning rate will depend on the ratio of the burnout time of the preheated (without lateral heat transfer) layer $t_1 \sim \kappa / u^2$ to the time of transverse heating of a interlayer of thickness h, $t_2 \sim h^2/\kappa$, then:

$$t_2 / t_1 = (uh/\kappa)^2, \; u/u_m = z(t_2 / t_1). \qquad (6.34)$$

where κ is the thermal conductivity of the matrix, u_m is the burning rate of solid propellant without particles (pure matrix). The relation (6.34) has a stepped form. The upper value ($u/u_o \sim 1$ at $uh/\kappa > 1$) reflects the insignificant lateral heat loss for interlayers which are wide in comparison with preheated layer thickness. The lower value ($u/u_o \approx$ const < 1 at $uh/\kappa << 1$) reflects the burning of a solid propellant with finely dispersed inert particles. According to [128, 144], in this system, the action of the inert particles can be equivalent to a reduction in the initial temperature. T_o. Note that the inert particles may act in other ways, e.g., by the absorption of the active centers

in the condensed phase. The opposite effect is also possible [131]. To describe the transition between the extreme cases, it is necessary to consider the multidimensional [145] and unstable temperature field and, the effect of the hot gaseous phase on the particles, which are protruding from the surface. Another approach is to apply a correction coefficient to Eq.(6.34). For example, in [128], the following ratio (for some mean thickness, h) was used:

$$z = u/u_m = 1 - const_1 \, (1 - \exp(-const_2 / uh)). \tag{6.35}$$

This approximation has been used to describe a wide range of 'stationary' experiments. The analytical form (6.35), derived in [128] was based on physical considerations, but the acceptance of idealization raised rather more doubts than simple approximation based on dimensional analysis. Since the aim is only to demonstrate a possible mechanism for synchronization, instead of Eq. (6.35), the simpler expression can be proposed

$$u/u_m = \exp(-const / uh),$$

is adequate and is used in the convenient form:

$$z = \exp(-B/z), \; B = B_1 \, (h_o/h) \, (u_0/u_m). \tag{6.36}$$

If $B > B^* = 1/e$, Eq. (6.36) gives only zero value for z. If $B < B^*$, two additional solutions appear, of which the greater has to be taken. The burning law for a pure matrix under variable pressure takes the form:

$$u_m = u_0 \; (p/p_0)^{\nu} = 1 + |\Delta p/p_0| \sin(2\pi nt). \tag{6.37}$$

Using the relations:

$$dx/dt = u; \;\; x(0) = 0, \tag{6.38}$$

we get a closed system (6.33), (6.36) – (6.38), in which x is the flame propagation path along a particular route, the uniqueness of which is set by the initial lag Φ in Eq. (6.36). Theoretical results are presented in Fig. 6.16, for the dimensionless size $D = uh^2 / u_o h_0^2$ with $\nu = 0.5$, $|\Delta p/p_0| = |\Delta h/h_0| = 0.75$, $B_1 = 0.1$, $na/u_0 = 0.5$ for paths having lags of $\Phi = 0$ and $\Phi = \pi$, at the start of burning. Calculations for any other value of φ also showed the complete synchronization of the gas release on all paths after some oscillations. It seems that, for the group of parameters used, $n = u_o / 2a$ is the natural frequency of the system. At different of the natural frequencies of the pressure fluctuations there is no complete synchronization and the mean gas release from the unit surface area is taken as the arithmetic mean of the 25 paths with lags of $2\pi i/25$ ($0 \le i \le 24$). The examples of the fluctuations are shown in Fig. 6.17. It is seen that the maximum amplitude of the total gas release from the sample, based on the used simplified model of burning, is almost independent of the frequency. Loss of synchronization leads only to a complicated relation between the total gas release and time.

Let us consider a simplified model for the burning of a solid propellant when a carbon skeleton

forms on the surface and periodically collapses. Assume that after gasification of the volatile components and up to the next break-off, the skeleton is not deformed. Then, the rate of widening of the layer, x_{sk}, of the skeleton is equal to the linear rate of gasification:

$$d\,x_{sk} / dt = u. \tag{6.39}$$

By analogy with [I46], assume that the break-off occurs when and where the local strength of the skeleton, related to its local temperature by the function exp(E/RT), becomes less than the rupture force, created by the infiltration of gases into the skeleton. Using Fick's law of diffusion, in the form $dp/dx \sim v \sim mT/p$, then we have for the section $0 < x < x_{sk}$ the condition for strength of material:

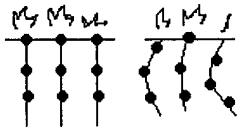

Fig. 6.15 Scheme of the solid propellant with flame propagation paths.

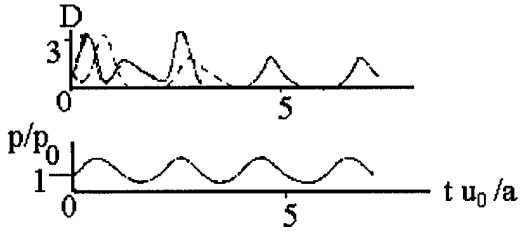

Fig. 6.16. Temporal behavior of gas release rate from two flame propagation paths, $\nu = 0.5$, $|\Delta p/p_0| = |\Delta h/h_0| = 0.75$, $B_1 = 0.1$, $na/u_0 = 0.5$ (solid line, $\Phi = 0$; dotted line, $\Phi = \pi$).

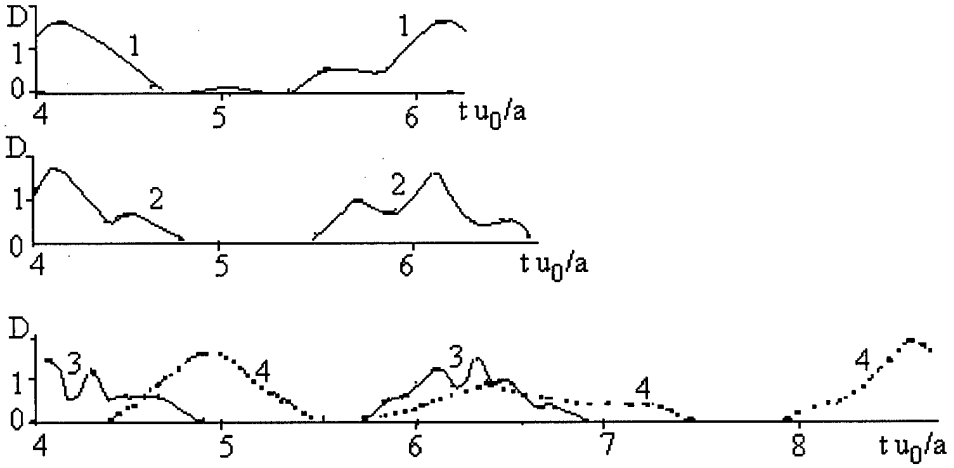

Fig. 6.17. Temporal behavior of the total gas release from the surface of solid propellant, for $\nu = 0.5$, $|\Delta p/p_0| = |\Delta h/h_0| = 0.75$, $B_1 = 0.1$, with frequencies, n, of fluctuations in p differing from natural frequency of composition, na/u_0 1 = 1, 2 = 2, 3 = 4, 4= 1/4.

$$const \cdot e^{E/RT} > \frac{m}{p} \int_{X}^{Xsk} T dx \tag{6.40}$$

In deriving Eq. (6.40), the small relative change in p with the thickness of the skeleton is ignored.

If p = const, a small heterogeneity in the solid propellant means that the next skeleton break-off do not always occur simultaneously over the entire surface. Close to the boundary with the zone in which there is only partial break-off of the layer, multidimensional filtration (Fig. 6.18a) reduces the break-away force. This causes a delay in the break-off of that part of the zone (Fig. 6.18b). Thus, the synchronization of the break-off can be unstable. However, it should be remembered that the purely mechanical bond of the skeleton along the burning surface could lead, on the contrary, to synchronization.

Consider further the situation with a random distribution of skeleton zones on the surface, with different times of existence after a break-off. It is seen from Fig. 6.18, that due to the interaction between zones, there can be changes in the boundaries between the zones, during successive break-off of the skeleton. This is almost independent of the conditions and time of the subsequent break-off, which will occur initially in the center of the zone under of one-dimensional strength condition (6.40). Let us examine the nature of burning along the axis of one zone.

Let the solid propellant contains particles of catalyst or metal, which after gasification of the surrounding volatile components remain at a carbon skeleton (such a phenomenon has been described in [147]). Assume that an exothermic reaction occurs, under diffusion conditions, on the particles and that until break-off of the skeleton, the carry-away of agglomerated particles from skeleton can be ignored. Then, the heat release will have a uniform distribution along the skeleton layer, with a certain volumetric density (cal/cm^{3}s). If we ignore the heat entering the skeleton layer from the gas phase, and assume that this layer has homogeneous thermal properties, then the temperature distribution over the layer thickness will be parabolic:

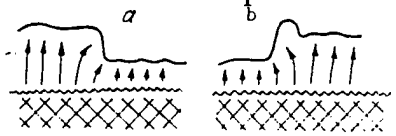

Fig. 6.18. Effect of heterogeneous filtration on change of boundaries with time for different times of skeleton break-off.

$$T = T_{sk}(t) - C(t)[x_{sk}(t)-x]^2. \tag{6.41}$$

C(t) is found from the heat balance at the boundary between the condensed phase and the skeleton

$$x = 0,\ \lambda_{sk}\,\partial T/\partial x = 2\lambda_{sk}\,x_{sk}C = mc(T_s - T_0 - Q/c), \tag{6.42}$$
$$C = (T_s - T_0 - Q/c)\,m(t)c/(2\lambda_{sk}\,x_{sk}),$$

where Q is the heat of gasification. In Eqs. (6.41) and (6.42), it was assumed that a quasistationary thermal profile existed in the condensed phase and skeleton, which is true if the pressure change is sufficiently small. Assuming the temperature of gasification of the volatile components, T_s, is constant, then from Eqs. (6.41) and (6.42):

$$T_{sk} - T_s = (T_s - T_0 - Q/c)\,mc\,x_{sk}/2\lambda_{sk}, \tag{6.43}$$

The heat balance for the entire skeleton layer gives (using Eq. (6.41))

$$Q_M x_{sk} - mc\left(T_s - T_0 - \frac{Q}{c}\right) = (c\rho)_{sk}\frac{d}{dt}\int_0^{Xsk} T(x,t)dx = (c\rho)_{sk}\frac{d}{dx}\left[x_{sk}(2T_{sk} - T_s)\right] \tag{6.44}$$

Let us denote

$$m_M = \sqrt{\frac{2Q_M\lambda_{sk}/c^2}{T_s - T_0 - Q/c}},\quad x_M = \frac{2\lambda_{sk}}{cm_M},\quad t_M = \frac{x_M\rho_p}{m_M} = \frac{c\rho_p(T_s - T_0 - Q/c)}{Q_M} \tag{6.45}$$

where ρ_p is the propellant density. Then we get from Eqs. (6.39), (6.43), and (6.44)

$$d\xi/d\tau = \mu,\quad \mu\xi = \vartheta,\quad \xi - \mu = 2b\, d[\xi(\vartheta + (3/2)\,\vartheta_s)]/d\tau \tag{6.46}$$

Furthermore, assume b = 1.

The geometric condition for break-off is a tangent to the graph of the right and left hand parts of Eq. (6.40), relative to the coordinate x. From Eqs. (6.41)-(6.46), we get:

$$e^{A/y} = C_1\frac{A^{-3/2}(2+y)\sqrt{\mu\xi(1-y)}}{1+|\Delta p/p|\sin(2\pi N\tau)}, \tag{6.47}$$

$$A = E/RT_{sk} = \alpha/(1+\mu\xi/\vartheta_s),\ y = 1-3y^3/[2A(2+y)],\ C_1 = \text{const.}$$

The term $\Delta p/p$ in the denominator of Eq. (6.47) indicate the relative change in pressure. The value of y is related to T / T_{sk}, where T is the temperature at the place of rupture. From Eq. (6.41), the intermittent change in the skeleton thickness during break-off is found using the formula:

$$x/x_{sk} = 1-[(1-y)(1+\vartheta_s/\mu\xi)]^{1/2}. \tag{6.48}$$

The theoretical results from Eqs. (6.46)-(6.48) are shown in Fig.6.19. Initially, with $|\Delta p/p_0| = 0$, for the arbitrary assumed initial values of ξ_0 and μ_0 the calculations were conducted until establishment of sustaining fluctuations with period $\Delta\tau = 7$. Then, for $|\Delta p/p_0| = 0.75$, $N = 1/\Delta\tau = 1/7$, two calculations were made, using the initial values calculated for the case $|\Delta p/p_0| = 0$ at moments of time, separated by approximately one half period. Synchronization was achieved after five periods. Fluctuations caused by the break-off of the skeleton from different zones of the solid fuel surface, independently of heating as described in the above model, became coherent if the frequency of pressure fluctuations coincided with the natural frequency (break-off of localized zones when p = const). At other pressure fluctuation frequencies, the surface processes were not synchronized.

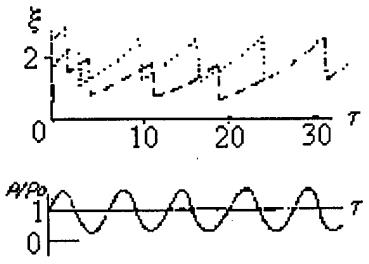

Fig. 6.19. Change in skeleton layer thickness for two surface zones: $C_1 = 5000$, $\alpha = 7$, $\vartheta_s = 2, 0.75$, $N = |\Delta p/p_0| = 1.7$. (dotted line, $\xi_0 = 1.84$, $\mu_0 = 0.20$, dashed line, $\xi_0 = 2.67$, $\mu_0 = 0.25$).

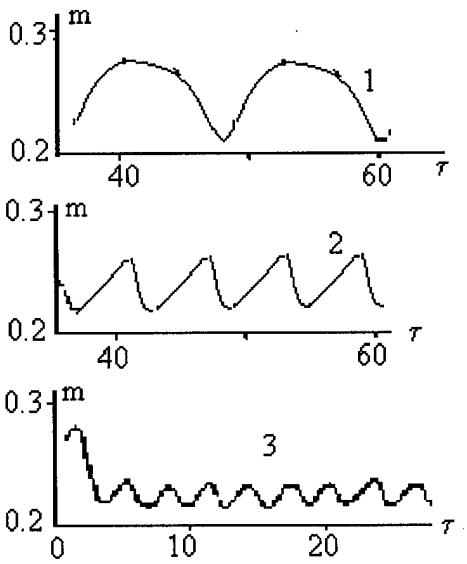

Fig. 6.20. Fluctuation of mean surface speed of gas release rate: C_1= 5000, α = 8, ϑ_s = 2, $|\Delta p/p_0|$ = 0.75., Frequency of break-off in local zone (equal to the frequency of pressure fluctuations) N=0.0788 (1), N=0.1576 (2), N=3153 (3), for $|\Delta p/p_0|$ = 0 N=0.1576.

The relation between the average time on surface and the dimensionless rate of gas release is shown in Fig. 6.20. The value of m was taken as the arithmetic mean of the value for 25 independently burning local zones , with initial values ξ , μ uniformly distributed over the phase fluctuations (for p = const.) of the local zone. In particular, for $|\Delta p/p_0|$ = 0, the average value of m for 25 zones varied with time only in the fourth figure. It is seen that in the proposed model, an increase in the frequency of pressure fluctuations with $|\Delta p/p_0|$ = const, simply leads to a reduction in $|\Delta m/m|$, and the transition through the natural frequency, associated with synchronization of the different surface zones, does not cause any characteristic features in the mean fluctuations of the gas release rate.

6.4.3. Possible mechanism of nonstationary erosion combustion

Only a small part of the studies on nonsteady-state combustion of composite solid propellants (CSP) has been devoted to nonsteady-state erosion combustion. In [148], for a homogeneous solid propellant, a function relating the burning rate response to changes in the cross-flow velocity has been obtained. To this end, a double base propellant specimen was fired at the center of a T-chamber (where pressure oscillations form a node, i.e., have zero amplitude, but flow velocity oscillations display bunching, i.e., are maximal). It was mentioned [144] that the phenomenological ZeI'dovich-Novozhilov model holds for the nonsteady-state erosion combustion of quasi-homogeneous propellants. In particular, it follows from this model that a propellant whose stationary burning rate is independent of the cross-flow of gases is also insensitive to it in the nonsteady-state combustion regime. However, as it was underlined in [149], the theoretical basis of this phenomenon is not sufficiently developed.

No experimental studies on the nonsteady-state erosion combustion of heterogeneous compositions are known to the authors. Nevertheless, there is a great need for such investigations since upon transition of CSP combustion into the nonsteady-state regime the probability of erosion ef-

fects increases. Thus, they can arise in transient combustion of propellants, which did not manifest them in stationary combustion.

As follows from [150, 151], for some propellants the propagation of the leading edges corresponding to gasification of less thermostable components determines (see, e.g., [128]).the value of the stationary burning rate and can be weakly affected or even unaffected by blowing of the CSP surface. However, the nonstationary blowing is sure to substantially change the gas generation by the branched protruding surface of a thermostable component. Changes will also occur in the ratio of the gas phase components and in the temperature of combustion products. This possibility is thought to stimulate the experimental and theoretical studies on the nonsteady-state CSP erosion combustion.

The magnitude of the effect (i.e. the changes in the gas phase component composition) depends on the structure of the protruding thermostable component regions. When a heterogeneous component is thermostable and there are no processes keeping it on the surface, the ejected particles burn out in the combustion chamber volume and this is determined not only by the instantaneous gas velocity near the CSP surface but also by the whole hydrodynamics of the combustion chamber.

When a thermostable component forms a sufficiently strong framework on the surface, the cross-flow effect depends on the character of framework destruction, which can be either a local or quasi-homogeneous. In the latter case, knowing the empirical dependence of the framework mass M per 1 cm^2 of the surface on the stationary flow velocity v, one can readily estimate the nonstationary addition to the burning rate dM/dt = (dM/dv)(dv/dt) (for details see [152]). Obviously, there are certain problems in measuring M. Experiments involving no surface cross-flow have been described in [147].

If a thermostable component forms separate protrusions, empirical data on their size as a function of v can be useful. In this case, one also needs information on changes in the protrusion form in the nonsteady-state regime. The information can easily be obtained in particular by approximate methods [150, 151].

Let us describe a possible semiempirical method [153] for determining the response function for a propellant with thermostable component protrusions. To this end, we restrict ourselves to the simplest approximation with CSP modeled by a composite "sandwich" type system, the flat cross section of which consists of alternating rectangles of (1cm·b) for nonvolatile, slow burning and of (1cm·a) for fast burning components.

Assume that in experiments with combustion gases flowing over the burning surface of a model laminated specimen (across the layers) in the steady-state regime it is found that the linear burning rate и is actually independent of the flow velocity v. We have mentioned above the most probable reason for this phenomenon. The burn-out of the less thermostable component in the leading edges, which determines the stationary burning rate of the whole system, is protected from the influence of combustion product flow by protrusions of the thermostable component. The protrusions are subjected to this influence in all respects, i.e., as v changes, the form and

height of the protrusions also change. It is quite probable that intensifying heat and mass transfer causes a decrease in the protrusion height. Needless to say, at a fairly high critical flow velocity the protrusions cease to play a protective role and the stream will influence the leading edges. This range of parameters is beyond the limits of our study.

Assume that the "stationary" empirical v-dependence of the protrusion height h_{st} on the surface is known. In the steady-state regime, the propagation rates of protrusions $u_l \equiv - dx_l / dt$ and edges $u_f \equiv -dx_f/dt$ coincide. Under conditions of transient blowing, the maximum gas velocity is believed to be not higher than the critical one. Hence, $u_f = const = u_{st}$ and for u_l the following relation holds:

$$u_l = u_{l,\,st} + A[h - h_{st}(v(t))],$$

hence,

$$dh/dt = -A[h - h_{st}(v(t))]. \tag{6.49}$$

Here - $h_{st}(v)$ is a "quasi-stationary" dependence, e.g.,

$$h_{st} \equiv x_l - x_f = h_o - kv^2 \tag{6.50}$$

Here x is the coordinate of the surface in the system related to CSP; the indices st, l, f, 0 mean the steady-state, slow and fast burning components, and the absence of blowing, respectively. Note that the only data obtained by measuring the roughness of quenched specimens burning without any blowing are presented in [91]. The photo- and radiographs of CSP-modeling laminated specimens may be useful for obtaining h(v). The quadratic dependence (6.50) is taken as the simplest one to satisfy the requirement for the independence of the whole erosion combustion pattern from the sign of the flow velocity. The meaning of (6.49) is as follows. The more the slow burning component protrudes outside the quasistationary level, the faster it burns out due to the action of the cross-flow, and vice versa. The constant A can be determined from either the "nonstationary" experiment or theory. Solution (6.49) limited at $t \rightarrow - \infty$ (more precisely, obeying the condition $\lim_{t \rightarrow -\infty} [h \exp(At)] = 0$) has the form

$$h(t) = A \int_{-\infty}^{t} h_{st}(v(t)) e^{-A(t-\tau)} d\tau \tag{6.51}$$

In particular, with sign-alternating variations in the stream velocity (e.g., for the developed tangential gas flow oscillations in cylindrical bore of the burning CSP charge) with frequency ω, when $v = v_a \cos(\omega t)$, Eqs. (6.50) and (6.51) give

$$h = h_o - kv_a^2 \{0.5 + [0.5A \cos(2\omega t) + \omega \sin(2\omega t)] A/(A^2+4\omega^2)\} \tag{6.52}$$

The changes in the ratio of the components products of gasification in the gas phase can be estimated with the use of the law of change in the shape of protrusions with change in their height (e.g., similarly to [4, 5]). Assuming a triangle form of protrusions, the leading points of which at

the boundary with an easily gasified component propagate throughout CSP with a constant speed u_f and the height h can vary with time, we obtain the mass flow rate of the slow burning solid component (calculated for one layer):

$$M_l^* = \rho_l . b(u_f - 0.5\ dh/dt) \tag{6.53}$$

The mass flow rate of one layer of the fast burning component is time-independent and amounts to $M_f^* = \rho_f a u_f$,. Here ρ_l and ρ_f are the component densities. Hence, taking into account (6.52), we obtain

$$\frac{M_l^*}{M_f^*} = \frac{\alpha}{1-\alpha}\left(1 - \frac{k v_a^2}{2u_{st}} \frac{\omega}{\sqrt{1+(2\omega/A)^2}} sin(2\omega t - \varphi)\right), \tag{6.54}$$

$\varphi = \arctan(2\omega/A)$. With $\omega \to \infty$, this yields

$$\frac{M_l^*}{M_f^*} = \frac{\alpha}{1-\alpha}\left(1 + \frac{Ak v_l^2}{4u_{st}} cos(2\omega t)\right).$$

In (6.54) the $(\rho_l b) / (\rho_f a) = \alpha/(1 - \alpha)$ relation is used, which holds true for the above composite system where α is the mass fraction of the slow burning (thermostable) component in the system.

Relation (6.54) determines the variable composition of combustion products. For composite systems (not necessarily for the sandwich ones) consisting of the two above-mentioned components, when the "stationary" dependence of the temperature of the combustion products on the composition $T_p(\alpha)$ is known from either thermodynamic calculations or experiment, relation (6.54) can be used for calculating the variable $T_p(\alpha(t))$ with $\alpha(t) = (M_l^* / M_f^*)/(1 + M_l^* / M_f^*)$ for given non-steady-state regime of the laminated system.

Thus, the above analysis shows that a laminated system with combustion characteristics that are almost insensitive to stationary cross-flow can display nonstationary effects under transient blowing.

CHAPTER 6 REFERENCES

1. **Zeldovich Ya. B.**, "On the theory of combustion for powders and explosives", *Journal of Experimental and Theoretical Physics* (Russian), 1942, vol.12, 498.
2. **Novozhilov B.V.**, Journal Prikladnoi Matematiki i Teknicheskoi Fiziki, 1965, 4, 157
3. **Denison M.R. and Baum E.,** ARS Journal, 1961, 31, No. 2
4. **Lavrentiev M.A. and Shabat V.V.,** Hydrodynamics problems and its mathematical models, Moscow, Nauka, 1977
5. **Vilyunov V.N. and Rudnev A.P.,** Fizika Gorenia i Vzryva (Combustion, Explosion, and Shock Waves), 1977, N 1

6. **Gostintsev Yu.A., Pokhil P.F. and Sukhanov L.A.**, Doklady AN SSSR, 1970, 195, N 1
7. **Gusachenko L.K.**, Inzhenerno-Fizicheskii Journal, 1966, N 4
8. **Novozhilov B.V.**, *Khimicheskaya Fizika*, 1988, 7, 388
9. **Maximov E.I.**, *Journal Fizicheskoi Khimii*, 1963, 37, 5
10. **Buldakov V.F., Romanov O.Ya. and Shelukhin G.G.**, *Fizika Aerodispersnykh System*, Odessa, 1973, N 8
11. **Iljukhin V.S., Margolin A.D. and Sverchkov Yu.E.**, In: Gorenie Kondensirovannykh Sistem, Chernogolovka, 1977
11 a. **Bukharov V.N., Gusachenko L.K.**, *Fizika Gorenia i Vzryva (Combustion, Explosion, and Shock Waves)*, 1989, 25, N 2
12. **Shelukhin G.G., Buldakov V.F. and Belov V.P.**, *Combustion, Explosion, and Shock Waves*, 1969, 5, N 1
13. **Iljukhin V.S., Margolin A.D., Valeev I.N. et al.**, *Fizika Gorenia i Vzryva (Combustion, Explosion, and Shock Waves)*, 1987, 23, N 3
14. **Gusachenko L.K.**, *Fizika Gorenia i Vzryva (Combustion, Explosion, and Shock Waves)*, 1990, 26, N 4
15. **Belyaev A.F.**, *Zhurnal Fizicheskoi Khimii*, 1938, 12, 1, 93.
16. **Zeldovich Ya. B., Leipunskii O.I., Librovich V.B.**, Theory of the Unsteady Combustion of Powder. Nauka, Moscow, 1975.
17. **Istratov A.G., Librovich B.V.**, *Zhurnal Prikladnoi Mekhaniki i Tekhnicheskoi Fiziki*, 1964,5, 38.
18. **Novikov S.S., Ryazantsev Yu. S.**, *Zhurnal Prikladnoi Mekhaniki i Technicheskoi Fiziki*, 1965,1,59.
19. **Novozhilov B.V.**, *Zhurnal Prikladnoi Mekhaniki i Tekhnicheskoi Fiziki*, 1965, 6, 141.
20. **Novozhilov B.V.**, Nonstationary Combustion of Solid Rocket Propellants. Nauka, Moscow, 1973. Translation AFSC FTD-MT-24-317-74.
21. **Frost V.A., Yumashev V.L.**, *Combustion, Explosion, and Shock Waves*, 1976, 12, 496.
22. **Kiskin A.B.**, *Combustion, Explosion, and Shock Waves*, 1983, 19, 3, 295.
23. **Zenin A.A, Nefedova O.I.**, *Combustion, Explosion, and Shock Waves*, 1967, 3, 1, 26.
24. **Kovalskii A.A., Konev E.V., Krasilnikov B.V.**, *Combustion, Explosion, and Shock Waves*, 1967,3, 4,547.
25. **ZarkoV.E.**, Dr.Sci. Dissertation, Institute Chem. Kinetics and Combustion, Novosibirsk,1985.
26-**Zarko V.E., Simonenko V.N., Kiskin A.B.**, *Progress in Astronautics and Aeronautics* (De Luca L., Price E.W., Summerfield M., Eds.), 1992, 143, Ch.10, 363.
27. **Simonenko V.N., ZarkoV.E., Koutzenogii K.P.**, *Combustion, Explosion, and Shock Waves*, 1980,15,3,298.
28. **Novikov S.S., Pokhil P.F., et al.**, *Doklady AN SSSR*, 1968, 180, 6.
29. **Novikov S.S., Ryazantsev Yu. S.**, *Zhurnal Prikladnoi Mekhaniki i Technicheskoi Fiziki*, 1969,10, 2, 93.
30. **Dik I.G., ZurerA.B., Kuznetsov V.T.**, *Combustion, Explosion, and Shock Waves*, 1980, 15, 3,351.
31. **Khlevnoi S.S.**, *Combustion, Explosion, and Shock Waves*, 1971, 7, 147.
32. **Summerfield M., Caveny L.H., et al.**, *Journal of Spacecraft and Rockets*, 1971, 8, 251. (see also AIAA Paper 1970, 70).

33. **Frost V.A., Yumashev V.L.,** *Zhurnal Prikladnoi Mekhaniki i Technicheskoi Fiziki*, 1973, 14,371.
34. **De Luca L.**, *Progress in Astronautics and Aeronautics* (Kuo K.K., Summerfield M., Eds), 1984,90, Ch 12, 661
35. **Zarko V.E., KnyazevaA.G.**, *AIAA Paper* , 1994,94-0790
36 **.Librovich V.B.**, *Zhurnal Prikladnoi Mekhaniki i Technicheskoi Fiziki*, 1963, 6,74.
37 **Novozhilov B.V.**, *Progress in Astronautics and Aeronautics* (De Luca L., Price E.W., Summerfield M., Eds.), 1992, 143, Ch.15, 601.
38. **Kiskin A.B.**, Cand. Sci.Dissertation. Institute of Chem. Kinetics and Combustion, Novosibirsk, 1989.
39. **Zarko V.E., Simonenko V.N., Kiskin A.B.**, : Book of Abstracts, XIII ICDERS, 1991, Nagoya.
40. **Hart W. R., McClure F.T.,** *J. Chem. Phys.*, 1959, 30, 1501.
41. **Geckler R. D.**, *Fifth Symposium (International) on Combustion*, Reinhold, New York, 1955,35.
42. **Green L.,** *Jet Propulsion*, 1954, 24, 252.
43.**ChengSin-I**, *Jet Propulsion*, 1954, 24, 28.
44. **Horton M. D.**, *ARS Journal*, April 1962, 644 .
45. **Price E. W.**, *Tenth Symposium (International) on Combustion*, The Combustion Institute, 1965,1067.
46. **Hart R. W., Farrell R.A., Cantrell R.H.,** *Comb. and Flame*, 1966, 10, 367.
47. **Culick F. E. C.**, *AIAA J.*, 1968, 6, 12, 2241.
48. **Zenin A. A., Novozhilov B. V.**, *Combustion, Explosion & Shock Waves*, 1973, 9, 2, 246.
49. **Renie J. P., Osborn J.R.**, *AFRPL-TR*-79-21, 1979.
50. **Condon J. A., Osborn J.R., Glick R.L.**, *13th JANNAF Combustion Meeting*, 1976, II, 209.
51. **King M. K.**, *Nineteenth Symposium (International) on Combutsion*, Pittsburgh, Pa, 1982, 707.
52. **Zarko V. E., Simonenko V.N., Kiskin A.B.**, *Combustion, Explosion & Shock Waves,* 1987, 23,5,16.
53. **Beckstead M. W.**, *13th JANNAF Combustion Meeting*, 1976, CPIA #281, II, 299.
54. **Butcher A. G., Beckstead M.W.**, *16th JANNAF Combustion Meeting*, 1979, III, CPIA #308, 527.
55. **CohenN.S.**, *21st Joint Propulsion Conference*, 1985, AIAA-85-111 4.
56. **Beckstead M.W.**, *28th JANNAF Combustion Meeting*, 1991, III, CPIA #573, 369.
57. **Cohen N. S., Bowyer J.M., et al**, *14th JANNAF Combustion Meeting*, 1977,1, CPIA # 292, 55.
58. **Cohen N. S., Strand L.D.**, *18th JANNAF Combustion Meeting*, 1981, III, CPIA # 347, 7.
59. **Boggs T. L., Beckstead M.W.**, *AIAA J.*, 1970, 8, 4, 626.
60. **Ilyukhin V.S., Margolin A.D., et.al.,** *Combustion,Explosion & Shock Waves*, 1975, 11, 3, 498.
61. **Cohen N. S.**, *AIAA J.*, 1981, 19, 7, 907.
62. **Cohen N. S., Strand L.D.**, *AIAA J.*, 1985, 23, 5, 760.
63. **Cohen N. S.**, *AFRPL TR*-86-048, 1987.
64. **Simonenko V.N., Chertishchev V.V.**, *Combustion, Explosion & Shock Waves*, 1993, 29,3,304

65. **Margolis S.B., Armstrong R.C.**, *23rd JANNAF Combustion Meeting*, 1986, 1, CPIA #457, 65.
66. **Margolis S.B.,Wmiams F.A.**, *24th JANNAF Combustion Meeting*, 1987, 1, CPIA #476, 61.
67. **Margolis S.B., Williams F.A.**, *Combust. Sci. and Tech,*. 1988, 59, 27.
68. Deur J.M., Price E.W., *23rd Joint Propulsion Conference*, 1987, AIAA- 87-1875.
69. **Deur J.M., Price E.W.**, 24th Joint Propulsion Conference, 1988, AIAA- 88-2938.
70. **Clavin P., Lazimi D.**, *Combust. Sci. and Tech.*, 1992, 82, 1.
71. **Huang I.T., Micci M.M.**, *Combust. Sci. and Tech.*, 1991, 75, 73.
72.**YangV., Tseng I.S.**, Final Report, PL-TR-91-3041, Feb. 1992, Penn State University (see also **Tseng I.S., Yang V.**, *Comb. Flame*, 1994, 96, 4, 325)
73.**Williams F.A.**, Combustion Theory. 2nd Ed., Princeton Univ., Princeton, 1984
74. **Zeldovich Ya.B., Barenblatt G.I., et al**. The Mathematical Theory of Combustion and Explosions. Moscow. Nauka.1980 (English Translation: New York, Consultants Bureau, 1985)
75. **Vilyunov V.N. , Sidonskii O.B.**, *Combustion, Explosions, and Shock Waves*, 1965, 1, 4, 39.
76. **Baklan S.I., Vilyunov V.N.,Dik I.G.**, *Combustion, Explosions, and Shock Waves*, 1985, 22, 6, 722.
77. **Vilyunov V.N., Zarko V.E.**, Ignition of Solids. Amsterdam, Elsevier, 1989.
78. **Armstrong R.S.,Koszykowski M.L.**, *Comb. Flame*, 1988, 72, 13.
79. **Dik I.G., Sazhenova E.A., Selikhovkin A.M.**, *Combustion, Explosions, and Shock Waves*, 1990,27,4,396.
80. **Price C.F., Boggs T.L.**, *Progress in Astronautics and Aeronautics* (De Luca L., Price E. W., Summerfield M.,Eds.) 1992, 143, Ch. 12,441
81. **Knyazeva A.G., Zarko V.E.**, *Combustion, Explosions, and Shock Waves*, 1993, 29, 3, 266.
82. **Zarko V.E.**, *Combustion, Explosions, and Shock Waves*, 1990, 26, 6, 623.
83. **Mikheev V.F., Levashev Yu.V.**, *Combustion, Explosions, and Shock Waves*, 1973,9,438
84. **Ohiemiller T.J., Caveny L.H., et al.**, *XIV Symposium (International) on Combustion*, Pittsburgh.Pa., 1972, 1297
85. **Zenin A.A.**, *Progress in Astronautics and Aeronautics* (De Luca L., Price E.W., Summerfield M., Eds.), 1992, 143, Ch. 6, 197.
86. **Parr T., Hanson-Parr D.**, *Progress in Astronautics and Aeronautics* (De Luca L, Price E.W., Summerfield M., Eds.) 1992, 143, Ch. 8, 261.
87. **Novozhilov B.V.**,*Khim.phisika.*1988, N3
88. **Kiskin A.B**. Ph. D. Thesis, 1990.
89 **Assovskii I.G., Istratov A.G.**, *Zhurnal priklad.mechaniki i teoret.phisiki*, 1971, N5.
90. **Margolin A.D., Fogelsang A.E**, *Combustion, Explosion, and Shock Waves*, 1966, N2.
91. **Zenin A.A.**, Physical processes with combustion and explosion. "Atomizdat", Moskow, 1980 (in Russian).
92. **Novozhilov B.V.**, *Khim.phisika.*1988, V.8, N1.
93. **Vilyunov B.N., Rudnev A.P.**, *Zhurnal priklad.mechaniki i teoret.phisiki*, 1973, N5.
94. **Romanov O.Ya.**, *Combustion, Explosion, and Shock Waves*, 1975, N2.
95. **Romanov O.Ya.**, *Combustion, Explosion, and Shock Waves*, 1975, N3.
96. **Buldakov B.F., Romanov O.Ya., Tarchov V.C.**, *Combustion, Explosion, and Shock Waves*, 1980, N3.
97. **Bucharov V.N., Gusachenko L.K.**, *Combustion, Explosion, and Shock Waves*, 1989, N2.
98. **Romanov O.Ya.**, *Combustion, Explosion, and Shock Waves*, 1976, N3.

99. **T'ien J.S.,** *Combust.Sci.and Tech.*, 1972, V.5, pp.47-54.
100. **Allison C.B., Faeth G.M.**, *AIAA J.*, 1975, N10.
101. **Novozhilov B.V.**, *Khim.phisika.*1988, V.7, N5.
102. **Belous V.L., Novozhilov B.V.**, *Proceedinds of IX russian symposium on combustion and explosion, issue "Condensed system combustion"*, pp.44-47, Chernogolovka, 1989.
103. **Vilyunov B.N., Sabdenov K.O.**, *Chim.phisika.*1992, V.11, N3.
104. **Zel'dovich Ya.B., Barenblatt G.I., Librovich V.B.,and Makhviladze G.M.,** The mathematical theory of combustion and explosion, "Nauka", Moscow, 1980.
105. **V. Ya Zyryanov**. Author's abstracts of PhD thesis. Novosibirsk: Institute of Chemical Kinetics and Combustion, Siberian Division of the Academy of Sciences of the SSSR, 1980. (R)
106. **Zarko V.E., Gusachenko L.K., and Rychkov A.D.**, "Simulation of combustion of melting energetic materials", *Defence Science Journal* (India), Vol. 46, No. 5, 1996, pp. 425-433.
107. **Gusachenko L.K.**, "Effect of melting on combustion stability of quasihomogeneous compositions. The Zeldovich - Novozhilov method", *Combustion, Explosion, and Shock Waves*, Vol. 34, No. 4, 1998, pp. 26-29.
108. **Cozzi F., De Luca L., and Novozhilov B.V.** "Linear stability and pressure-driven response function of energetic solid materials with phase transition", *Journal of Propulsion and Power*, No. 6, 1999.
109. **Bizot A., and Beckstead M.W**, "Role of carbon/carbonageous matter formation in the combustion of double base rocket propellants", *Flame Structure (Proc. of the III Int. Seminar on Flame Structure).* Novosibirsk, Nauka, Vol.1, 1991, pp. 230-235.
110. **Kuo K.K., and Lu Y.-C.**, "Modeling of physicochemical processes of RDX monopropellant with detailed treatments for surface reaction zone". Challenges in Propellants and Combustion 100 Years after Nobel, edited by K.K. Kuo, et al, Bergel House, 1997, pp. 583-600.
111. **Rogers R.N. and Daub G.W.** (1973), *Anal. Chem.*, Vol. 45, 1973, pp. 596--600.
112. **Melius C.F.**, "Thermochemical Modeling, II. Application to Ignition and Combustion of Energetic Materials", Chemistry and Physics of Energetic Materials, edited by Bulusu S.N., NATO ASI Series, Kluwer Academic Publishers, 1990, pp.51-78.
113. **Liau Y.--C., and Yang V.**, "Analysis of RDX monopropellant combustion with two--phase subsurface reactions", *Journal of Propulsion and Power*, Vol.11, No.4, 1995, pp. 729-739.
114. **Davidson J. and Beckstead M.**, "Improvements to RDX combustion modeling", *AIAA Paper*, 96-0885 (34th Aerospace Sciences Meeting, Reno, 1996).
115. **Ermolin N.E., and Zarko V.E.**, "Reduction of kinetic mechanism for RDX combustion", submitted in *Combustion, Explosion, and Shock Waves*, 2000.
116. **Margolin A.D., and Pokhil P.F.,** *Doklady Akademii Nauk SSSR*, Vol. 150, No. 6, 1963.
117. **Yakusheva O.B., Maksimov E.I., and Merzhanov A.G.**, "The effect of gaseous decomposition products solubility on the condensed substances burning regularity", *Combustion, Explosion, and Shock Waves*, 1966, No. 3, pp.125-129.
118. **Maksimov E.I., and Merzhanov A.G.**, "To the theory of the condensed systems combustion", *Combustion, Explosion, and Shock Waves*, 1966, No. 1, pp. 47-58.
119. **Margolis S.B., Williams F.A., and Armstrong R.C.**, "Influences of two-phase flow in the deflagration of homogeneous solids", *Combustion and Flame*, Vol. 67, No. 3, 1987, pp. 249 -- 258.
120. **Li S.C., Williams F.A., and Margolis S.B.**, "Effects of two-phase flow in a model for nitramine deflagration", *Combustion and Flame*, Vol. 80, No. 3, 1990, pp. 329 -- 349.

121. **Margolis S.B., and Williams F.A.**, "Effect of two-phase flow on the deflagration of porous energetic materials", *Journal of Propulsion and Power*, Vol. 11, No. 4, 1995, pp. 759-768.
122. **Zarko V.E., Zyryanov V.Ya., and Chertischev V.V.**, "Dispersion of the Surface Layer during Combustion of Homogeneous Propellants", *AIAA Paper* 96-0814 (34th Aerospace Sciences Meeting, Reno, 1996)
123. **Ben-Reuven M., and Caveny L.H.**, "Nitramine flame chemistry and deflagration interpreted in terms of a flame model", *AIAA Journal*, Vol. 19, 1981, pp. 1276-1285.
124. **Brill T.B.**, "Multiphase Chemistry Considerations at the Surface of Burning Nitramine Monopropellants", *Journal of Propulsion and Power*, Vol. 11, No. 4, 1995, pp.740-751.
125. **Gusachenko L.K., Zarko V.E. and Rychkov A.D**. "Instability of a combustion model with evaporating and overheat in the condensed phase", *Combustion, Explosion, and Shock Waves*, 1997, No. 1.
126. **N. N. Bakhman,** *Dokl. Akad. Nauk SSSR*, 129, No. 5, (1959).
127. **S. S. Novikov, P. F. Pokhil, Yu. S. Ryazantsev, et al.**, *Zh. Prike. Mekh. Tekh. Fiz.*, No. 3 (1968).
128. **S. S. Novikov, V. Yu. Potulov, and S. V. Chuiko**, "On interaction of the combustion front of the condensed system with heterogeneous inclusions" in: Combustion of Condensed Systems [in Russian], Chernogolovka (1977).
129. **I. Ya. Vishnevetskii, A. P. Denisyuk, and E. A. Fogelzang**, *Combustion, Explosion, and Shock Waves*, 15. No. 1 (1979).
130. **A. D. Baer, N. D. Raien, and E. V. Shultz**, *AIAA J.*, No. 5 (1971).
131. **N. N. Bakhman and A. F. Belaev**, Combustion of Heterogeneous Condensed Systems [in Russian], Nauka, Moscow (1967).
132. **M. W. Beckstead, K. P. McCarty,** "Modeling calculations for HMX composite propellants". *AIAA Journal,* 1982, V. 20, No 1, pp. 106-115.
133. **N. Kubota and T. Masamoto**, *16th Symp. (Int.) on Combustion* (1976).
134. **M. W. Beckstead**, *18th Symp. (Int.) on Combustion* (1981).
135. **J. Gurland**, in: Planses Proc., S. Benesovsky (ed.), Vienna (1962).
136. **D. Seetharamacharyulu, V. P. Pai Verneder, K. M. Mailya, et al.,** *Combust. Sci. Technol., 25_*, No. 1 (1981).
137. **M. K. King**, *AIAA Paper* 78-216 (1978).
138. **E. H. Blum and R. H. Wilhelm**, *AlChE-IChE Symp.* Series A (1965).
139. **L. K. Gusachenko**, in: Combustion and Explosion [in Russian], Nauka, Moscow (1972).
140. **M. W. Beckstead, R. L. Derr, C. F. Price**. "A model of composite solid-propellant combustion based on multiple flames". *AIAA Journal*, 1970, V. 8, No 12, pp. 2200-2207.
141. **I. B. Svetlichnyi, A. D. Margolin, and P. F. Pokhil**, *Combustion, Explosion, and Shock Wave*, 7, No. 2 (1971).
142. **E. I. Maksimov**, *Zh. Fiz. Khim.*, N6, 5 (1963).
143. **I. Prigozhin**, From Existing to Developing [in Russian] Nauka, Moscow (1985).
144. **Ya. B. Zel'dovich, O. I. Leipunskii, and V. B. Librovich**, in: Theory of Unstable Burning of Gunpowder [in Russian], Nauka, Moscow (1967).
145. **S. S. Rybanin**, Multidimensional Theory of Burning in Macroheterogeneous Systems [in Russian], Author's abstract of Dr.Sci. Dissertation, Chernogolovka (1988).
146. **V. Ya. Zyryanov**, in: Burning in Condensed Systems (in Russian], Chernogolovka (1988)
147. **V. A. Babuk, V. P. Belov, V. V. Khodosov, et al.**, *Combustion, Explosion, and Shock*

Waves, No. 3 (1985),
148. **Yu. I. Medvedev and L. N. Revyagin**, "On nonstationary powder erosion," *Combustion, Explosion, and Shock Waves,* 10, No. 5, 341-345 (1974).
149. **E. W. Price and G. A. Flandro**, "Status and prospects for future developments," in, *Non-steady Burning and Combustion Stability of Solid Propellants, Progress in Astronautics and Aeronautics,*143, Washington, 849-873 (1992).
150. **L. K. Gusachenko**, "Nonsteady-state combustion of nonmetalized heterogeneous compositions," *Combustion, Explosion, and Shock Waves,* 24, No. 4, pp. (R) 47-54 (1988).
151. **L. K. Gusachenko and I. F. Sadykov**, "Model for the nonsteady-state combustion of a composite system," *Combustion, Explosion, and Shock Waves,* 27, No. 5, pp. (R) 81-84 (1991).
152. **L. K. Gusachenko**, "Phenomenological model of nonsteady-state SP combustion with a component accumulated on the surface," *Combustion, Explosion, and Shock Waves,* 25, No. 2, pp. (R) 38-42 (1989).
153. **L. K. Gusachenko and V. E. Zarko**, "Possible mechanism of nonsteady state erosion combustion of composite solid propellants", *Combustion, Explosion, and Shock Waves,* Vol. 31, No. 4, 1995.

CONCLUDING COMMENTS

The aim of the mathematical modeling of energetic materials combustion is prediction of the combustion characteristics under given external conditions that provides opportunity for diminishing a number of costly firing tests with different kind gas generators. In fact, at the present time combustion modeling of energetic materials became mature scientific discipline starting from pioneer works of Ya. B. Zeldovich performed in the beginning of 1940's. Great progress has been achieved now in developing of detailed kinetic schemes and sophisticated numerical methods for solving the combustion problems. However, the importance of these novel approaches should not be overestimated because, as it was already mentioned in Preface, simple comparison of theoretical and restricted experimental data does not give enough evidences for the validity of theoretical model. This idea was also formulated in several works including excellent paper by M. Miller [1] and published later exhaustive review by F. A. Williams [2]. The latter wrote: "So many phenomena are included in typical computational results that agreement between experiment and computation no longer explains experimental results" [2].

This means that analytical approaches and physically substantiated theory are needed for explaining both experimental observations and computational results. At the same time, to provide background for existing and newly developed combustion models there is a great need of development of novel research techniques, which may give space– and time – resolved information about processes in the combustion wave. Actually, to make comparison with contemporary theoretical models one needs experimental data not only on temperature profile and stationary burning rate but also on species distribution and transient burning rate. Partially these data became available now from the measurements in the gas phase mainly with various spectroscopy techniques and with recoil force and ultra sound techniques. However, it remains difficult obtaining data under high pressures and high frequency fluctuations of external conditions.

At present time most difficult technical task is getting detailed information about processes in the bulk and on the surface of the condensed phase of energetic materials. Obviously, the data on thermal decomposition obtained in conditions of slow heating rates (tens of K/min in classical DTA methods) can not be used directly in the modeling of processes running in the combustion waves (typically thousands of K/s). More appropriate is use of data derived from experiments on ignition or high temperature pyrolysis that simulate more closely the conditions of high temperature and relatively thin preheated layer inherent for combustion process.

Another problem is a description of physical state of a subsurface layer in burning energetic material. It is known fact that majority of new effective oxidizers like ADN, HNF as well as classical AP, HMX and RDX form melted layer at the surface that may lead to appearance of bubbles and two-phase flow of decomposition products. Existing theoretical models [3,4] are still based on arbitrary assumptions on the origination and growth of the bubbles. Therefore, reliable experimental observations are strongly needed for substantiation of such kind models. It should be also mentioned the lack of information on behavior of typical and newly developed binders under fast heating conditions. Totally it takes appropriate efforts and resources in order to develop experimental means to measure parameters in the condensed phase. Combination of fresh experimental results and modern theoretical approaches will allow formulating the comprehensive combustion models of energetic materials that meet demands of engineering design.

CONCLUSION- REFERENCES.

1. **M.C. Miller**, " In search of idealized combustion model for homogeneous solid propellant", Comb. Flame, 1982, **46**, pp. 51-73.
2. **F. A. Williams**, "The role of theory in combustion science", 24th Symposium (Intern.) on Combustion, The Combustion Institute, 1992, pp. 1-17.
3. **E. I. Maksimov, A. G. Merzhanov**. To the theory of the combustion of condensed substances. *Combustion, Explosion, and Shock Waves*, 1966, Vol. 2, pp.(R) 47-58.
4. **K. K. Kuo and Y. C. Ling,** "Modeling of physicochemical processes of burning RDX monopropellants," in: Proc. 20th Int. Pyrotechnics Seminar, 1994, pp. 583-600.